frontiers | Research Topics

The role of thyroid hormones in vertebrate development, volume II

Edited by
Marco António Campinho and Laurent M. Sachs

Published in
Frontiers in Endocrinology

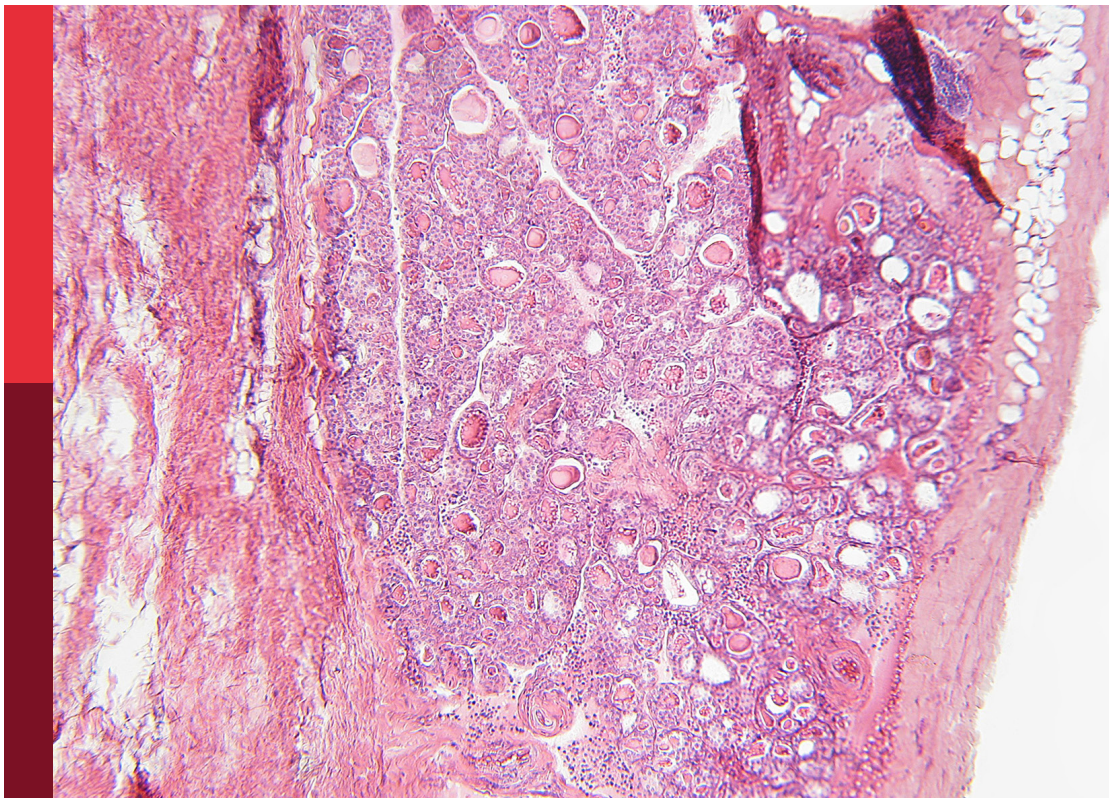

FRONTIERS EBOOK COPYRIGHT STATEMENT

The copyright in the text of individual articles in this ebook is the property of their respective authors or their respective institutions or funders. The copyright in graphics and images within each article may be subject to copyright of other parties. In both cases this is subject to a license granted to Frontiers.

The compilation of articles constituting this ebook is the property of Frontiers.

Each article within this ebook, and the ebook itself, are published under the most recent version of the Creative Commons CC-BY licence. The version current at the date of publication of this ebook is CC-BY 4.0. If the CC-BY licence is updated, the licence granted by Frontiers is automatically updated to the new version.

When exercising any right under the CC-BY licence, Frontiers must be attributed as the original publisher of the article or ebook, as applicable.

Authors have the responsibility of ensuring that any graphics or other materials which are the property of others may be included in the CC-BY licence, but this should be checked before relying on the CC-BY licence to reproduce those materials. Any copyright notices relating to those materials must be complied with.

Copyright and source acknowledgement notices may not be removed and must be displayed in any copy, derivative work or partial copy which includes the elements in question.

All copyright, and all rights therein, are protected by national and international copyright laws. The above represents a summary only. For further information please read Frontiers' Conditions for Website Use and Copyright Statement, and the applicable CC-BY licence.

ISSN 1664-8714
ISBN 978-2-8325-4845-5
DOI 10.3389/978-2-8325-4845-5

About Frontiers

Frontiers is more than just an open access publisher of scholarly articles: it is a pioneering approach to the world of academia, radically improving the way scholarly research is managed. The grand vision of Frontiers is a world where all people have an equal opportunity to seek, share and generate knowledge. Frontiers provides immediate and permanent online open access to all its publications, but this alone is not enough to realize our grand goals.

Frontiers journal series

The Frontiers journal series is a multi-tier and interdisciplinary set of open-access, online journals, promising a paradigm shift from the current review, selection and dissemination processes in academic publishing. All Frontiers journals are driven by researchers for researchers; therefore, they constitute a service to the scholarly community. At the same time, the *Frontiers journal series* operates on a revolutionary invention, the tiered publishing system, initially addressing specific communities of scholars, and gradually climbing up to broader public understanding, thus serving the interests of the lay society, too.

Dedication to quality

Each Frontiers article is a landmark of the highest quality, thanks to genuinely collaborative interactions between authors and review editors, who include some of the world's best academicians. Research must be certified by peers before entering a stream of knowledge that may eventually reach the public - and shape society; therefore, Frontiers only applies the most rigorous and unbiased reviews. Frontiers revolutionizes research publishing by freely delivering the most outstanding research, evaluated with no bias from both the academic and social point of view. By applying the most advanced information technologies, Frontiers is catapulting scholarly publishing into a new generation.

What are Frontiers Research Topics?

Frontiers Research Topics are very popular trademarks of the *Frontiers journals series*: they are collections of at least ten articles, all centered on a particular subject. With their unique mix of varied contributions from Original Research to Review Articles, Frontiers Research Topics unify the most influential researchers, the latest key findings and historical advances in a hot research area.

Find out more on how to host your own Frontiers Research Topic or contribute to one as an author by contacting the Frontiers editorial office: frontiersin.org/about/contact

The role of thyroid hormones in vertebrate development, volume II

Topic editors

Marco António Campinho — University of Algarve, Portugal

Laurent M. Sachs — Muséum National d'Histoire Naturelle, France

Citation

Campinho, M. A., Sachs, L. M., eds. (2024). *The role of thyroid hormones in vertebrate development, volume II*. Lausanne: Frontiers Media SA.

doi: 10.3389/978-2-8325-4845-5

Table of contents

frontiers | Frontiers in Endocrinology

TYPE Editorial
PUBLISHED 17 April 2024
DOI 10.3389/fendo.2024.1408070

Check for updates

OPEN ACCESS

EDITED AND REVIEWED BY
Terry Francis Davies,
Icahn School of Medicine at Mount Sinai, United States

*CORRESPONDENCE
Laurent M. Sachs
sachs@mnhn.fr
Marco António Campinho
macampinho@ualg.pt

RECEIVED 27 March 2024
ACCEPTED 05 April 2024
PUBLISHED 17 April 2024

CITATION
Campinho MA and Sachs LM (2024) Editorial: The role of thyroid hormones in vertebrate development, volume II.
Front. Endocrinol. 15:1408070.
doi: 10.3389/fendo.2024.1408070

COPYRIGHT
© 2024 Campinho and Sachs. This is an open-access article distributed under the terms of the Creative Commons Attribution License (CC BY). The use, distribution or reproduction in other forums is permitted, provided the original author(s) and the copyright owner(s) are credited and that the original publication in this journal is cited, in accordance with accepted academic practice. No use, distribution or reproduction is permitted which does not comply with these terms.

Editorial: The role of thyroid hormones in vertebrate development, volume II

Marco António Campinho[1,2]* and Laurent M. Sachs[3]*

[1]Algarve Biomedical Center-Research Institute, University of the Algarve, Faro, Portugal, [2]Faculty of Medicine and Biomedical Sciences, University of the Algarve, Faro, Portugal, [3]Unité Mixte de Recherche 7221, Département Adaptation du Vivant, Centre National de la Recherche Scientifique, Muséum National d'Histoire Naturelle, Alliance Sorbonne Universités, Paris, France

KEYWORDS

thyroid hormones, development, vertebrates, teleosts, Amphibians, mammals

Editorial on the Research Topic
The role of thyroid hormones in vertebrate development, volume II

The thyroid hormone is an important signaling molecule system involved in vertebrate development, acting at the embryonic and post-embryonic levels (1). Although this has long been established, a detailed understanding of the thyroid hormone's developmental action still needs to be fully understood. The present Frontiers in Endocrinology Research Topic aims to close this knowledge gap by bringing together a collection of papers addressing what is known and the challenges ahead on the role of thyroid hormones in vertebrate development, from teleosts to humans. The published manuscripts highlight the pivotal action of thyroid hormones in vertebrate neurodevelopment (Lee at al.; Ng et al.; O'Shaughnessy et al.; Richard et al.; Silva and Campinho; Valcárcel-Hernández et al.), post-natal development in amphibians (8–10) and how thyroid disorders can affect human development (Ru et al.; SeyedAlinaghi et al.).

Thyroid hormone signaling plays an essential role in neurodevelopment. Puzzling out the mechanisms of action of thyroid hormones in the developing brain will help contribute to progress in the prevention and treatment of several neurological disorders. Using data obtained in animal models, Richard et al. first review the adverse effects of thyroid hormone signaling disruption in the central nervous system before recalling how GABAergic neurons were found to be a major target of TH signaling during development and highlighting the difficulties in analyzing the mechanisms by which TH act on brain development. In mice, O'Shaughnessy et al. bring new data. They show how congenital hypothyroidism affects neurodevelopment at the ventricular zone, limiting glial cells, tight junctions, extracellular matrix, and blood-brain and blood-cerebrospinal barrier development. Moreover, this work suggests that the action of thyroid hormones in mice brain development likely occurs by genomic and non-genomic mechanisms. The action of thyroid hormones is not limited to the brain. The retina is also a target of thyroid hormones affecting cones, the photoreceptors that mediate color vision. Ng et al. previously reported the functions for thyroid hormone receptor TRb2 in mice, encoded by the gene *Thrb*. Here, they provide new knowledge investigating TRb1, another thyroid hormone receptor b isoform also expressed in the retina, suggesting novel functions in retinal and non-neural ocular tissues. Zebrafish is another animal model relevant to address the role of thyroid

hormones in neurodevelopment. In this teleost fish, Silva and Campinho study the effect of functional impairment of T_3 membrane transporter Mct8 (monocarboxylic acid transporter 8) that leads to the Allan-Herndon-Dudley syndrome when mutated in humans (2). The findings show that *mct8* gene deletion in zebrafish phenocopies many symptoms observed in patients, thus contributing to the understanding of the cellular and molecular mechanism underlying the severe underdevelopment of the central nervous system. The effect of thyroid hormones is also necessary for neurodevelopment throughout life. Valcárcel-Hernández et al. discuss the latest advances in the role of thyroid hormones in regulating adult neurogenesis in rodents and their potential implication in human health and therapeutical approaches in neurodegenerative diseases.

Another action controlled by thyroid hormones in vertebrates is the developmental change coming from a need to adapt to a change in habitat during post-embryonic development events. Amphibian metamorphosis is such transition from the larval state to the adult state, when the tadpole undergoes physiological and anatomical changes. This biological process resembles mammalian postembryonic development (3), with many organs mature into their adult forms. Using Xenopus, an anuran amphibian, Tanizaki et al. review the roles of thyroid hormones in larval epithelial cell death and *de novo* formation of adult intestinal stem cells, suggesting that T_3-induced activation of cell cycle program. Still, in the Xenopus model, the work by Tribondeau et al. shows that T_4 and T_3 have similar actions and are involved in regulating the expression of genes involved in cell proliferation during early larval stages. Because these developmental stages are not normally subject to a physiological action of thyroid hormones, these data highlight the potential molecular actors that could be involved in the adverse effects of thyroid hormones during the larval period. The modalities of metamorphosis can be very diverse in amphibians, the latter also being paedomorphic by maintaining larval characteristics in reproductive adults and rarely, if ever, metamorphose in nature. This is the case of the Axolotl, the model used by Lazcano et al. Further expanding our knowledge on how different thyroid hormone metabolites are involved in post-natal development, they demonstrate bioactivity of 3,5-T_2 inducing gill retraction, which is reversible following treatment withdrawal and at high concentration irreversible metamorphosis. These contrasting effects are explained by 3,5-T_2 regulation of different genetic responses.

Finally, in human, Lee at al. investigate the iodine status and its association with thyroid function in South Korean children. Adequate iodine intake is essential because this trace element, is a necessary and limiting substrate for thyroid hormone synthesis and both deficient and excessive iodine status can result in thyroid dysfunction. They show that excess iodine was prevalent in Korean children and associated with a decrease in FT_4 or T_3 levels and an increase in TSH levels. In a different context, Ru et al. explore the association of maternal anti-thyroid peroxidase antibody (TPOAb) on placenta morphology and potential pathophysiologic inflammatory and oxidative stress responses in this organ and discuss the potential consequences for the developing embryo. Meta-analysis of previously published datasets by SeyedAlinaghi et al. reveals a close association between thyroid hormone disorders and later incidence of hip fractures in both men and women, shedding light on the effects of thyroid action through an individual lifespan.

With this Research Topic, we provide a diversified developmental and evolutionary picture of how thyroid hormones are important in vertebrate development. There is no doubt that further studies are required to fully understand the role of thyroid hormones during development not only in humans but also in many classes of vertebrates in order to better characterize and treat thyroid hormone-associated pathologies or anthropomorphic disruption of thyroid hormone signaling in humans (4) and ecosystems (5).

Author contributions

MC: Writing – original draft, Writing – review & editing. LS: Writing – original draft, Writing – review & editing.

Funding

The author(s) declare financial support was received for the research, authorship, and/or publication of this article. LS work are supported by the "Centre National la Recherche Scientifique" and the "Muséum National d'Histoire Naturelle." ABC-RI internal grant NeuRare supports MC work.

Acknowledgments

The editors wish to thank all authors and reviewers for their outstanding contributions to this Frontiers Research Topic.

Conflict of interest

The authors declare that the research was conducted in the absence of any commercial or financial relationships that could be construed as a potential conflict of interest.

The author(s) declared that they were an editorial board member of Frontiers, at the time of submission. This had no impact on the peer review process and the final decision.

Publisher's note

All claims expressed in this article are solely those of the authors and do not necessarily represent those of their affiliated organizations, or those of the publisher, the editors and the reviewers. Any product that may be evaluated in this article, or claim that may be made by its manufacturer, is not guaranteed or endorsed by the publisher.

References

1. Rousseau K, Dufour S, Sachs LM. Interdependence of thyroid and corticosteroid signaling in vertebrate developmental transitions. *Front Ecol Evol*. (2021) 9:735487. doi: 10.3389/fevo.2021.735487

2. van Geest FS, Gunhanlar N, Groeneweg S, Visser WE. Monocarboxylate transporter 8 deficiency: from pathophysiological understanding to therapy development. *Front Endocrinol*. (2021) 12:723750. doi: 10.3389/fendo.2021.723750

3. Paris M, Laudet V. The history of a developmental stage: metamorphosis in chordates. *Genesis*. (2008) 46:657–72. doi: 10.1002/dvg.20443

4. Pearce EN. Endocrine disruptors and thyroid health. *Endocr Pract*. (2024) 30 (2):172–6. doi: 10.1016/j.eprac.2023.11.002

5. Zwahlen J, Gairin E, Vianello S, Mercader M, Roux N, Laudet V. The ecological function of thyroid hormones. *Philos Trans R Soc Lond B Biol Sci*. (2024) 379 (1898):20220511. doi: 10.1098/rstb.2022.0511

frontiers | Frontiers in Endocrinology

TYPE Original Research
PUBLISHED 10 February 2023
DOI 10.3389/fendo.2023.1090081

Check for updates

OPEN ACCESS

EDITED BY
Laurent M. Sachs,
Muséum National d'Histoire Naturelle, France

REVIEWED BY
Frédéric Flamant,
Université de Lyon, France
Thomas Bastian,
University of Minnesota Twin Cities, United States
Robert Opitz,
Charity University Medicine Berlin, Germany

*CORRESPONDENCE
Katherine L. O'Shaughnessy
oshaughnessy.katie@epa.gov

SPECIALTY SECTION
This article was submitted to Thyroid Endocrinology, a section of the journal Frontiers in Endocrinology

RECEIVED 04 November 2022
ACCEPTED 09 January 2023
PUBLISHED 10 February 2023

CITATION
O'Shaughnessy KL, McMichael BD, Sasser AL, Bell KS, Riutta C, Ford JL, Stoker TE, Grindstaff RD, Pandiri AR and Gilbert ME (2023) Thyroid hormone action controls multiple components of cell junctions at the ventricular zone in the newborn rat brain.
Front. Endocrinol. 14:1090081.
doi: 10.3389/fendo.2023.1090081

COPYRIGHT
© 2023 O'Shaughnessy, McMichael, Sasser, Bell, Riutta, Ford, Stoker, Grindstaff, Pandiri and Gilbert. This is an open-access article distributed under the terms of the Creative Commons Attribution License (CC BY). The use, distribution or reproduction in other forums is permitted, provided the original author(s) and the copyright owner(s) are credited and that the original publication in this journal is cited, in accordance with accepted academic practice. No use, distribution or reproduction is permitted which does not comply with these terms.

Thyroid hormone action controls multiple components of cell junctions at the ventricular zone in the newborn rat brain

Katherine L. O'Shaughnessy[1]*, Benjamin D. McMichael[1,2], Aubrey L. Sasser[1,2], Kiersten S. Bell[1,2], Cal Riutta[1,2], Jermaine L. Ford[3], Tammy E. Stoker[1], Rachel D. Grindstaff[1], Arun R. Pandiri[4] and Mary E. Gilbert[1]

[1]United States Environmental Protection Agency, Public Health Integrated Toxicology Division, Center for Public Health and Environmental Assessment, Research Triangle Park, NC, United States, [2]Oak Ridge Institute for Science Education, Oak Ridge, TN, United States, [3]Chemical Characterization and Exposure Division, Center for Computational Toxicology and Exposure, United States Environmental Protection Agency, Research Triangle Park, NC, United States, [4]Comparative and Molecular Pathogenesis Branch, Division of Translational Toxicology, National Institute of Environmental Health Sciences, Research Triangle Park, NC, United States

Thyroid hormone (TH) action controls brain development in a spatiotemporal manner. Previously, we demonstrated that perinatal hypothyroidism led to formation of a periventricular heterotopia in developing rats. This heterotopia occurs in the posterior telencephalon, and its formation was preceded by loss of radial glia cell polarity. As radial glia mediate cell migration and originate in a progenitor cell niche called the ventricular zone (VZ), we hypothesized that TH action may control cell signaling in this region. Here we addressed this hypothesis by employing laser capture microdissection and RNA-Seq to evaluate the VZ during a known period of TH sensitivity. Pregnant rats were exposed to a low dose of propylthiouracil (PTU, 0.0003%) through the drinking water during pregnancy and lactation. Dam and pup THs were quantified postnatally and RNA-Seq of the VZ performed in neonates. The PTU exposure resulted in a modest increase in maternal thyroid stimulating hormone and reduced thyroxine (T4). Exposed neonates exhibited hypothyroidism and T4 and triiodothyronine (T3) were also reduced in the telencephalon. RNA-Seq identified 358 differentially expressed genes in microdissected VZ cells of hypothyroid neonates as compared to controls (q-values $\leq$0.05). Pathway analyses showed processes like maintenance of the extracellular matrix and cytoskeleton, cell adhesion, and cell migration were significantly affected by hypothyroidism. Immunofluorescence also demonstrated that collagen IV, F-actin, radial glia, and adhesion proteins were reduced in the VZ. Immunohistochemistry of integrin $\alpha v\beta 3$ and isoforms of both thyroid receptors (TRα/TRβ) showed highly overlapping expression patterns, including enrichment in the VZ. Taken together, our results show that TH action targets multiple components of cell junctions in the VZ, and this may be mediated by both genomic and nongenomic mechanisms. Surprisingly, this work also suggests that the blood-brain and blood-cerebrospinal fluid barriers may also be affected in hypothyroid newborns.

KEYWORDS

thyroid hormone action, hypothyroidism, brain development, ventricular zone, cell migration, radial glia, cell adhesion, cell junctions

1 Introduction

Thyroid hormone (TH) action controls multiple developmental pathways in the brain (reviewed in 1). These thyroid-dependent processes all exhibit striking spatiotemporal activity, with subcompartments of the brain exhibiting differing sensitivities to THs, which also varies with developmental time (1, 2).

Highlighting these spatiotemporal dynamics, we previously reported that a transient maternal exposure to the propylthiouracil (PTU) resulted in the formation of a periventricular heterotopia in the developing rat brain (3, 4). This malformation is not only inducible by anti-thyroid pharmaceuticals, but also by environmental thyroid disrupting chemicals in multiple strains of rats (3–9). The heterotopia is predominantly comprised of ectopic neurons and can be detected in 100% of pups following a 5-day perinatal exposure (gestational day 19 – postnatal day 2, GD19 – PN2) (4). In addition to a clear temporal susceptibility, we also identified a spatial sensitivity to TH action. The heterotopia reproducibly occurs in the posterior telencephalon, directly medial to the lateral ventricular epithelium as this region extends into the corpus callosum (3, 5–8). Given these data, we hypothesized that the developing ventricular epithelium is acutely sensitive to reduced TH action during the perinatal period in the rat. We postulated that this may be due in part to its anatomical location. The most luminal cells come in direct contact the cerebrospinal fluid (CSF), one source of brain THs (10). The ventricular epithelium also possesses an enriched vascular network, and as THs are also actively transported across the blood-brain barrier (BBB), the microvasculature represents a second source of brain T4/T3 (4, 11). Thus, the cells of the ventricular epithelium reside at the intersection of TH transport.

In addition to being a potential target of TH action, the neonatal ventricular epithelium is also one of two stem cell niches that supports neurogenesis. The most apical proliferative population is the ventricular zone (VZ), and houses multipotent stem cells, namely radial glia (12–14). Importantly, while radial glia are progenitors, they also act as migratory scaffolding to mediate the travel of neuroblasts into regions like the cortex (14). The next most basal cell layer is called the subventricular zone (SVZ), which also possesses undifferentiated cells including intermediate progenitors (14–16). Unlike the SVZ, which supports neurogenesis throughout life, the VZ is only present during embryonic and early postnatal development in rodents (13). The VZ appears as the pseudostratified ventricular epithelium due to the cell bodies of numerous radial glia (13). By approximately 2-weeks of age, the pseudostratified epithelium remodels to simple columnar as radial glia cells differentiate, leaving the SVZ with only limited proliferative capacity (13). These dynamics between VZ/SVZ transition during the postnatal period, in addition to the VZ's anatomical location, may also contribute to TH susceptibility.

Here we investigated the hypothesis that the posterior VZ is a target of TH action during the neonatal period in rats. We exposed pregnant animals to a low dose of propylthiouracil (PTU) beginning in early pregnancy. Using laser capture microdissection (LCM), we isolated cells of the posterior VZ in pups during a known period of hormone sensitivity (PN2) (4). We then employed RNA-Sequencing (RNA-Seq) and pathway analyses to investigate the molecular pathways disturbed in affected neonates. Next, we performed immunohistochemistry to garner further support of our RNA-Seq findings, which includes mediators of TH action.

2 Materials and methods

2.1 Animal husbandry and exposure

All experiments were conducted with prior approval from the United States Environmental Protection Agency's (US EPA's) Institutional Animal Care and Usage Committee and were carried out in an Association for Assessment and Accreditation of Laboratory Animal Care approved facility. N=16 timed pregnant Long Evans rats were purchased from Charles River (Morrisville, NC) and delivered on gestational day (GD) 2; sperm positive was considered GD0 and pup birth postnatal day 0 (PN0). Dams were single housed in polycarbonate cages, maintained a 12:12 light cycle and offered chow (Purina 5008) and deionized water ad libitum. Animals were weight ranked and then randomly allocated to two treatment groups. N=8 dams were exposed to 3 ppm (0.0003%) 6-propyl-2-thiouracil (PTU, purity ≥98%, Sigma) dissolved in deionized drinking water; N=8 control dams were administered vehicle only (deionized drinking water). The maternal exposure was initiated on GD6 and continued through PN14. This PTU exposure was not expected to induce overt toxicity in dams, but was sufficient to induce a periventricular heterotopia in their offspring (3). N=8 controls and N=7 PTU exposed dams gave birth.

2.2 Serum thyroid hormone quantification

To evaluate serum total thyroxine (T4), triiodothyronine (T3), and thyroid stimulating hormone (TSH), pups on PN2 and dams on PN14 were euthanized by rapid decapitation and trunk blood collected in serum separator tubes with clot activating gel (BD Vacutainer). Serum hormones were quantified from N=8 vehicle control and N=7 PTU exposed dams and litters. Pup blood was pooled from two littermates, taking one male and one female from each litter when possible. Previous work has shown that PTU exposure similarly reduces serum T4 and T3 in both sexes of rats (17, 18). Blood samples were allowed to clot on ice for at least 30 minutes before centrifugation at 1300 x g (4° C). Serum was then aliquoted in sterile, nonstick tubes and stored at -80°C until analysis. Pups were analyzed on PN2 due to our previous work demonstrating that TH dysfunction at this stage is associated with periventricular heterotopia development (4). The dams were euthanized at the conclusion of this animal exposure on PN14; other data collected from this animal cohort will be published elsewhere. For further information on dam serum TH profiles over the perinatal period following a 3 ppm PTU exposure, see (3).

Serum T4 and T3 were analyzed by liquid chromatography with tandem mass spectrometry using an AB Sciex (Framingham,

Massachusetts) Exion AC UHPLC-Qtrap 6500+ Linear Ion Trap LC/MS/MS system as previously described (19). The lower limit of quantitation (LLOQ) for each analyte was set to the concentration of the lowest calibration standard that gave an acceptable ion ratio, and acceptable recovery of ±30% of the spike amount; the lower limit of quantification (LLOQ) for both T4/T3 were 0.1 ng/ml (100 pg/ml). Each sample batch consisted of a method blank, a laboratory control sample (blank spike), and a continuing calibration verification sample prepared in the solvent. Serum TSH was analyzed on using a Milliplex Rat Thyroid Hormone Magnetic Bead Panel (Millipore Sigma, RTHYMAG-30K-01) according to the manufacturer's protocol. The curve fit R^2 was >0.99 and the sum of residuals was -0.004. Unpaired, two-tailed Welch's t-tests with an α=0.05 were performed for each measured analyte using GraphPad Prism 9.1.2 (GraphPad Software, San Diego, CA).

2.3 Brain hormone quantification

Following rapid decapitation, the brain from one female pup per litter was extracted from the skull and the telencephalon (forebrain) isolated in sterile 0.01 M phosphate buffered saline (PBS). Tissue was blotted to remove excess buffer, weighed, placed in sterile tubes, and frozen in liquid nitrogen. All samples were stored at -80°C until analysis. THs were isolated by solid phase extraction and analyzed by LC/MS/MS as previously described (19) for N=5 control and N=5 PTU exposed samples. The LLOQ for total T4 and reverse T3 (rT3) were 0.01 ng/g and total T3 0.05 ng/g. Unpaired, two-tailed Welch's t-tests with an α=0.05 were performed for each TH measured using GraphPad Prism 9.1.2 (GraphPad Software, San Diego, CA). Previous work has shown no differences in heterotopia incidence or severity between the sexes, suggesting that sex not a significant variable in determination of this phenotype (3). Hence, only female brain hormones were assessed.

2.4 Laser capture microdissection

One male pup was selected from each of N=7 control and N=6 PTU exposed litters on PN2 for laser capture microdissection (LCM) and sequencing. Pups were administered an overdose of Euthasol® and transcardiac perfusion performed with 30% sucrose in sterile 0.01 M PBS pH 7.4. Following sucrose perfusion, the brain was immediately dissected from the skull, embedded in Tissue Freezing Medium™ (Fisher Scientific, 15-183-13), and frozen on a slurry of dry ice and isopentane. The brains were cryosectioned coronally at 10 µm thickness and collected directly onto MicroDissect polyethylene terephthalate membrane single frame slides (ASEE, FS-LMD-M-50r); slides were placed on dry ice immediately after section pickup and stored -80°C. Immediately before microdissection slides were stained with 2% cresyl violet in 75% ethanol, dehydrated, and cleared. Laser capture of the posterior ventricular epithelium was then performed using a MMI CellCut LCM System (Molecular Machines and Industries). The epithelium as identified by its pseudostratified appearance, consistent with reports that this morphology represents the VZ (13). Isolated cells were then collected using 0.5 ml MicroDissect stick-cap tubes (ASEE, ST-LMD-M-500). The ventricular epithelium from both hemispheres of ~20 sections was collected from each animal.

2.5 RNA isolation

RNA was isolated using Qiagen's RNeasy® Micro kit (Qiagen, 74004). Immediately after cells from each slide were collected as described, 10 µl of RLT lysis buffer was added directly on to the cap for 5 minutes. RNA was isolated from lysed cells according to the manufacturer's protocol, including on-column DNA digestion. RNA concentrations were determined using Qubit (RNA HS, Q32852) and quality using Agilent Bioanalyzer (Nano, 5067-1511). The average RNA concentration across biological replicates was 15 ng/µl and RNA Integrity Number was (RIN) 5.3. While this indicates some RNA degradation, slide control cells (microdissected CA1/CA3 of the hippocampus) revealed consistently intact RNA with RIN ≥8 across all biological replicates (Supplementary Figure 1). Therefore, we attributed the lower RINs of our microdissected VZ to the long, narrow shape of this region, which likely resulted in an increased amount of burned cellular debris relative to intact cells following microdissection.

2.6 Library preparation and RNA-Sequencing (RNA-Seq)

Total RNA-Sequencing libraries were prepared using the SMARTer® Stranded Total RNA-Seq Kit v3 - Pico Input Mammalian kit (Takara, 634485) according to the manufacturer's protocol. This included sample barcoding and rRNA depletion. Library quantities were evaluated using Qubit (dsDNA, Q32851) and library size and quality evaluated using Agilent Bioanalyzer (DNA HS, 5067-4626). Libraries were pooled and sequenced on two lanes of Illumina HiSeq 4000 and paired end sequenced to an average depth of 58 million reads/sample.

2.7 Identifying differentially expressed genes (DEGs)

Samples were demultiplexed and trimmed using Trimmomatic (20). Downstream processing of RNA-Seq data was performed in Partek Flow Bioinformatics Software (Chesterfield, MO). Samples were aligned to the *Rattus norvegicus* reference genome (mRatBN7.2/rn7) using STAR 2.7.8a. Counts were quantified using the Partek Expectation/Maximization (E/M) model and the rat RefSeq annotation (GCF_015227675.2) and normalized using median ratio. Differential expression was identified by comparing N=6 PTU exposed samples to N=7 controls using DESeq2 (21), and multiple testing corrected using the Benjamini–Hochberg step-up procedure to control the False Discovery Rate (FDR). DEGs were identified by an FDR (q-value) ≤0.05. A volcano plot was generated using the ggplot2 R package (22), and a heatmap of normalized count values using the Pheatmap (23) and Viridis R packages (24).

2.8 Gene ontology and pathway analyses

For preliminary investigation of the RNA-Seq data, all differentially expressed genes (DEGs) with a q-value ≤0.05 were analyzed using Gene Ontology (GO) in STRING (25). Results within the sub-ontologies of Cellular Components and Biological Function are reported here, with an adjusted p-value (q) ≤0.05 considered significant. Next, significant DEGs (q ≤ 0.05) were analyzed in Ingenuity Pathway Analysis (IPA) (Qiagen, Hilden, Germany) and used to generate predicted canonical and disease and function pathway analyses between control and PTU exposure.

2.9 Immunohistochemistry and imaging

A subset of PN2 pups of both sexes were euthanized for immunohistochemistry. Pups were administered an overdose of Euthasol® and perfused with sterile 0.01 M PBS pH 7.4, and then 4% paraformaldehyde. Brains were isolated and cryoprotected in 30% sucrose in PBS before embedding in Tissue Freezing Medium™ (Fisher Scientific, 15-183-13). Blocks were frozen on a slurry of dry ice and isopentane. The brains were cryosectioned coronally at 35 µm and collected in PBS for free-floating immunohistochemistry (IHC). All primary and secondary antibody combinations can be found in Supplementary Table 1. For fluorescent IHC, nonspecific binding was blocked in a mixture of 10% horse and goat serum in PBS with 0.1% triton-X for 2 hours. Primary antibodies were then diluted in block buffer and incubated overnight at 4°C. The sections were then washed in PBS and incubated with appropriate Alexa Fluor antibodies and counterstained with DAPI. For visualization of filamentous actin (F-actin), sections were incubated in 0.5% triton for 15 minutes before incubation in Alexa Fluor 647 phalloidin according to manufacturer's protocol (Abcam, ab176759). Fluorescent sections were then mounted on SuperFrost Plus (Fisher Scientific, 12-550-15) slides and coverslipped using ProLong Diamond (Thermo Fisher Scientific, P36965). Imaging was performed using a Nikon A1 laser scanning confocal microscope fitted with an Eclipse Ti inverted microscope base and a T-P2 Nikon polarizer slider. Control sections were imaged first and PTU exposed animals analyzed using the same parameters (see laser line information in Supplementary Table 1). For calorimetric detection background staining was reduced by incubating in 0.3% hydrogen peroxide diluted in methanol for 30 minutes. Nonspecific binding was reduced in block as stated above, and the signal amplified by avidin-biotin complex (ABC kit, Vector PK-4001 and PK-4002); the color reaction was developed with 3,3′-Diaminobenzidine (Sigma, D8001). Slides were then mounted, dehydrated, cleared, and cover slipped before imaging using an Aperio slide scanner (Leica). For all immunohistochemistry experiments at least N=3 control and N=3 PTU exposed pups were analyzed, and all images are representative of repeated findings.

2.10 Figure preparation

Microscopy images were prepared in Adobe Photoshop and figures assembled in Adobe Illustrator, with the same settings applied across control and PTU exposed images.

3 Results

3.1 PTU exposure perturbed the maternal thyroid axis

Following the drinking water exposure beginning on GD6, PTU significantly reduced dam T4 by 53% as compared to vehicle controls on PN14 (Figure 1A, p<0.0001). In contrast, there was no significant change in serum T3 (Figure 1B, p=0.33). Serum TSH was increased by 72% (Figure 1C, p=0.01). Together, the T4/T3/TSH results shows that PTU exposed dams exhibited thyroid axis perturbation.

3.2 Neonatal pups exhibited hypothyroidism and decreased brain T4/T3

On PN2, a known day of hormone susceptibility (4), serum T4 was reduced in neonates by 80% (p<0.0001) (Figure 1D) and serum T3 by 39% (p=0.03) (Figure 1E). Serum TSH was increased by 243% (p<0.0001) (Figure 1F). In the telencephalon, T4 was significantly reduced by 80% (p=0.001) and T3 by 38% (p=0.02) (Figures 2A, B). Reverse T3 (rT3) was not significantly different following PTU exposure in the neonatal telencephalon (p=0.16) but showed more biological variability than T4/T3 (Figure 2C). Together, these serum and brain data show that the pups exhibited overt hypothyroidism and decreased brain tissue T4/T3 concentrations.

3.3 TH action regulates gene expression at the neonatal ventricular epithelium

To confirm that the posterior ventricular epithelium is the VZ, we performed SRY-Box 2 (SOX2) immunofluorescence. SOX2 is expressed in multipotent neural stem cells, and is enriched in the VZ (26). Results show that in the posterior telencephalon, strong SOX2 expression was observed in the PN2 ventricular epithelium, which appears pseudostratified when observed by DAPI nuclear staining (Figure 3A). Following laser capture microdissection of this region and RNA-Seq (Figure 3B), 358 DEGs with FDR ≤0.05 were identified in male pups (172 downregulated, 186 upregulated) (Figures 3B–D, see Supplementary File 1 for full results). Preliminary examination of the dataset revealed a subset of DEGs related to extracellular matrix composition. This included 4 collagen genes with a q<0.05 (*Col8a2*, *Col2a1*, *Col12a1*, *Col4a6*), and 3 approaching statistical significance (q ≤ 0.07, *Col9a3*, *Col25a1*, *Col4a5*) (Table 1, which includes full gene names). All of these collagen transcripts were downregulated except for *Col25a1*. Several other genes encoding extracellular matrix proteins were also significantly downregulated, including a glypican, syndecan, and dystroglyan (*Glp4*, *Sdc2*, *Dag1*). Another subset of DEGs were also related to cytoskeleton formation and/or dynamics. Four genes related to actin or tubulin formation were upregulated (*Actg1*, *Tbcb*, *Tpgs2*, *Tubb2b*, and *Tubb4a*, Table 1); three unconventional myosins, which bind F-actin, were all downregulated (*Myo1d*, *Myo1e*, *Myo7a*). A third subgroup of DEGs related to cell adhesion and/or cell junctions were downregulated, including *Cldn1* and *Jam3* (Table 1). Further, genes related to Wnt/Planar cell polarity (*Vangl1*, *Vangl2*), hedgehog

10.3389/fendo.2023.1090081

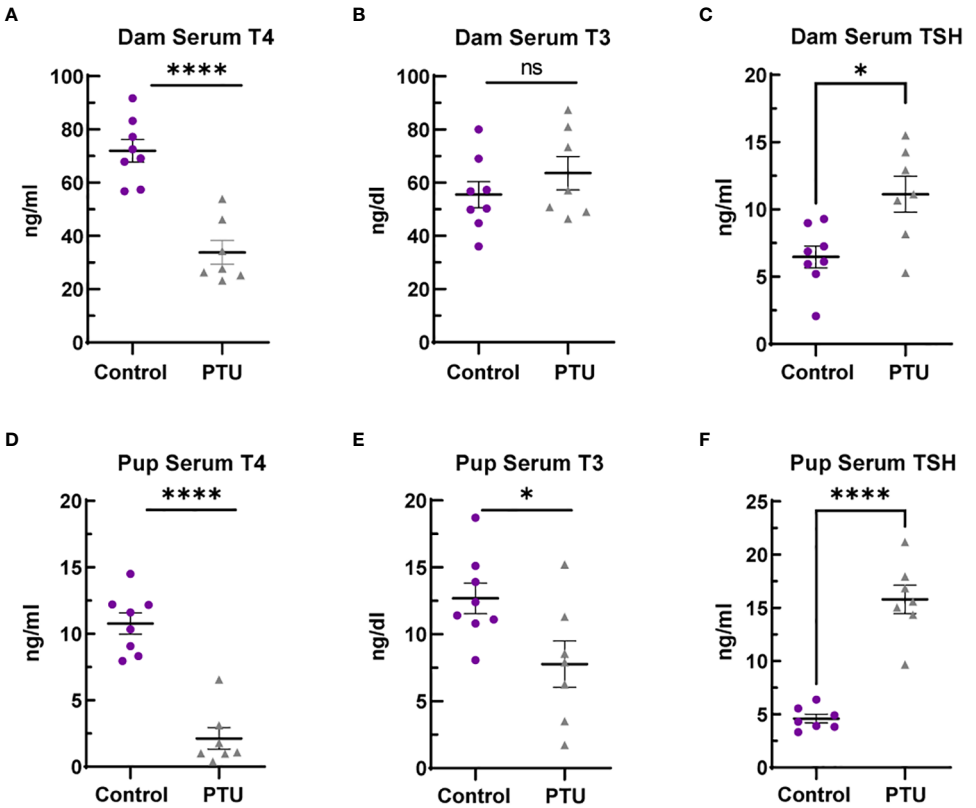

FIGURE 1
Serum thyroid hormones in dams and pups. **(A)** Dam serum T4 is reduced in dams on PN14, whereas **(B)** total T3 was not significantly different. **(C)** TSH was increased by 72% in PTU exposed dams on PN14. **(D)** Pup serum T4 and **(E)** T3 were reduced in pups on PN2. **(F)** TSH was increased in PN2 neonates. In all presented data, N=8 control and N=7 PTU exposed dams or litters were assayed. For all pup data, each biological replicate represents serum pooled from multiple littermates of mixed sex. The data were then analyzed by t-test and each graph shows the value of each biological replicate and the SEM; ****$p \leq 0.0001$, *$p \leq 0.05$, ns, not significant.

signaling (*Gli2*, *Gli3*), and bone morphogenetic protein (BMP) signaling (*Rgma*, *Bmp1*, *Bmper*) were also all downregulated in PTU exposed VZ cells (Table 1). Downregulation of *Spred1* was also detected, a gene we previously implicated in heterotopia development (4). Surprisingly, only 3 genes were identified as known mediators of TH transport and/or action, including *Slc16a2*, *Tshr*, and *Thrsp*, all of which were downregulated (Table 1); no deiodinase enzymes (i.e., *Dio2*) or known T4/T3 receptors (i.e., *Thra*, *Thrb*) were differentially expressed in the VZ (Supplementary File 1). Genes known to respond to lowered brain T4/T3, like *Klf9* and *Hr*, were also not amongst the DEGs (Supplementary File 1). We acknowledge that downregulation of *Slc16a2* (MCT8) was a

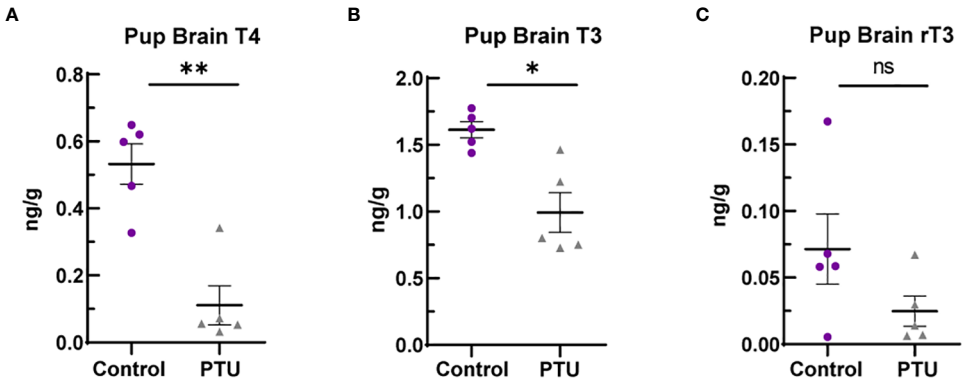

FIGURE 2
Telencephalon thyroid hormones in PN2 pups. **(A)** Brain T4 was significantly reduced on PN2, as was **(B)** T3. **(C)** Reverse T3 (rT3) was reduced in PTU exposed animals when comparing group means, but this was not statistically significant. In all presented data, N=8 control and N=7 PTU exposed female pups were assayed (1 pup/litter). The data were then analyzed by t-test and each graph shows the value of each biological replicate and the SEM; **$p \leq 0.001$, *$p \leq 0.05$, ns, not significant.

10.3389/fendo.2023.1090081

counterintuitive finding. Given that our brain hormone measures show a significant reduction in T3, one would expect upregulation of *Slc16a2* to increase T3 availability at the VZ. While we do not understand why *Slc16a2* is downregulated, it is important to consider if this signal is originating from specific cell types, or is similar across all *Slc16a2* expressing cells. As the apical VZ abuts TH containing CSF and the VZ possesses an enriched BBB, there may be complex mechanisms of regulating TH economy in this region that we cannot discern by bulk RNA-Seq. The lack of transcriptional signal for deiodinases and thyroid receptors is less surprising, as previous gene expression studies of mild/moderate developmental hypothyroidism in the postnatal rat brain have reported similar data (4, 27, 28).

We next investigated the signaling pathways with overrepresentation amongst the DEGs. Gene Ontology (GO) Cellular Component analysis showed most gene products will localize intracellularly, within the cytoplasm, and at the cell junction (Figure 4A and Supplementary File 2). Among the most significant Biological Processes identified include nervous system development (q<0.001), cellular component organization (q=0.002), fiber organization (q=0.002), actin filament organization (q=0.02), lateral sprouting from an epithelium (q=.03), adhesion (q=0.03), and cytoskeletal organization (q=0.03) (Figure 4B and Supplementary File 3). A transcriptional signal for circulatory system development was also detected (q=0.03). Ingenuity Pathway Analysis showed similar results as GO Biological Processes. The top Molecular and Cellular

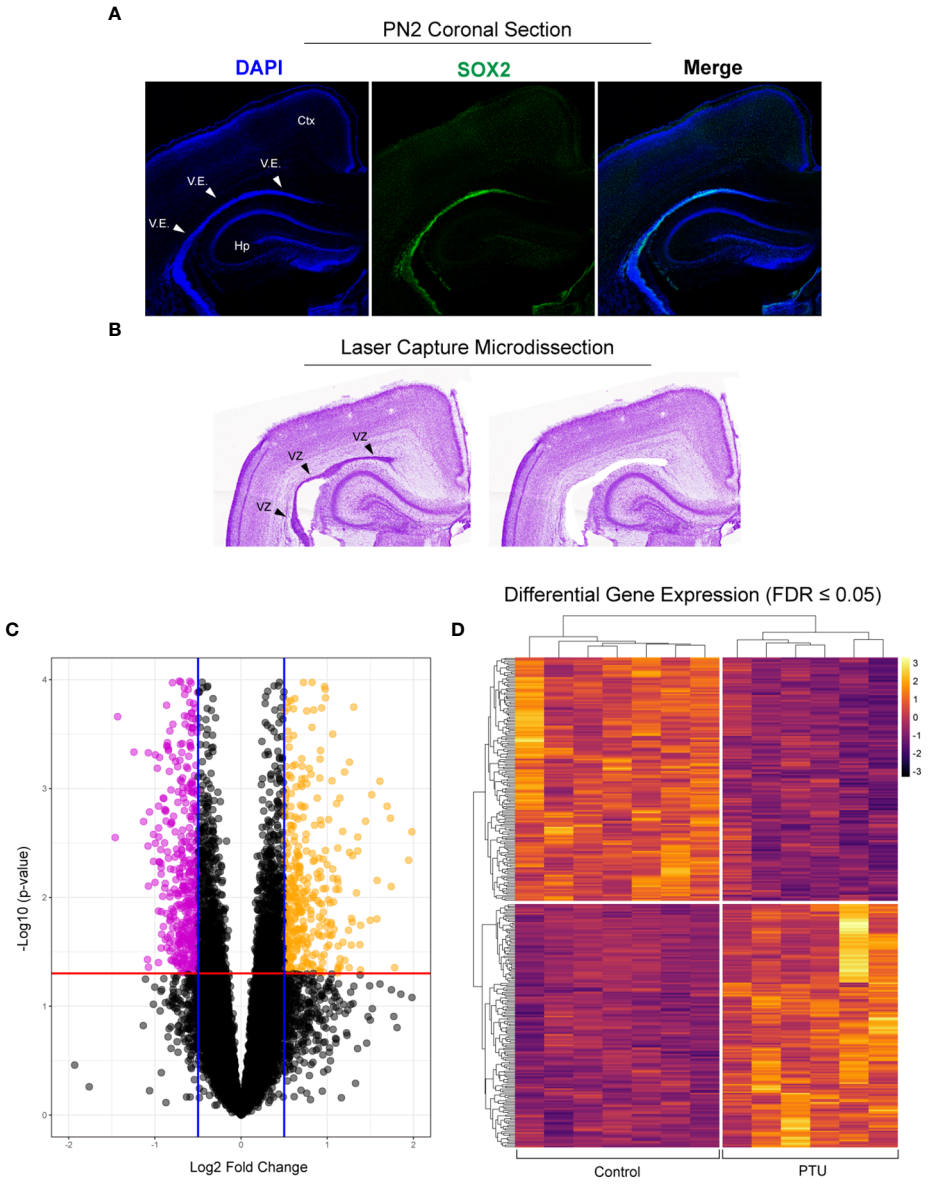

FIGURE 3
Laser capture microdissection and RNA-Seq of the neonatal ventricular zone (VZ). **(A)** Fluorescent immunostaining in control animals demonstrates that the ventricular epithelium (V.E.) of the posterior telencephalon is highly enriched for SOX2, demonstrating that this is the VZ (ventricular zone, progenitor cell niche) on postnatal day 2 (PN2). **(B)** Example of laser capture microdissection of the VZ. **(C)** Volcano plot of resulting RNA-Seq data obtained from microdissected VZ from PN2 male pups, with downregulated (pink) and upregulated (yellow) genes highlighted (q ≤ 0.05). **(D)** These differentially expressed genes (DEGs) were then visualized by a heatmap, which shows clear differences between the control (euthyroid) and PTU exposed (hypothyroid) neonates. Each column of the heatmap represents a biological replicate (N=7 control and N, 6 PTU exposed pups).

10.3389/fendo.2023.1090081

TABLE 1 Genes of interest from RNA-Seq dataset.

Gene Name	Ensembl ID	Description	p-value	q-value	Fold change
Gpc4	ENSRNOG00000002413	glypican 4	<0.001	0.00	-1.71
Sdc2	ENSRNOG00000004936	syndecan 2	<0.001	0.02	-1.42
Frem2	ENSRNOG00000021670	FRAS1 related extracellular matrix 2	<0.001	0.04	-1.35
Dag1	ENSRNOG00000019400	dystroglycan 1	<0.001	0.04	-1.24
Col8a2	ENSRNOG00000010841	collagen type VIII alpha 2 chain	<0.001	0.02	-1.80
Col2a1	ENSRNOG00000058560	collagen type II alpha 1 chain	<0.001	0.02	-1.93
Col12a1	ENSRNOG00000058470	collagen type XII alpha 1 chain	<0.001	0.04	-1.36
Col4a6	ENSRNOG00000056772	collagen type IV alpha 6 chain	<0.001	0.04	-1.45
Col9a3	ENSRNOG00000009531	collagen type IX alpha 3 chain	<0.01	0.06	-1.45
Col25a1	ENSRNOG00000050706	collagen type XXV alpha 1 chain	<0.01	0.06	2.45
Col4a5	ENSRNOG00000018951	collagen, type IV, alpha 5	<0.01	0.07	-1.37
Tbcb	ENSRNOG00000020781	tubulin folding cofactor B	<0.001	0.01	1.47
Tpgs2	ENSRNOG00000054118	tubulin polyglutamylase complex subunit 2	<0.001	0.02	1.38
Tubb2b	ENSRNOG00000017445	tubulin, beta 2B class Iib	<0.001	0.04	1.22
Actg1	ENSRNOG00000036701	actin, gamma 1	<0.001	0.02	1.21
Myo1d	ENSRNOG00000003276	myosin ID	<0.001	0.02	-1.61
Myo1e	ENSRNOG00000061928	myosin IE	<0.001	0.02	-1.39
Myo7a	ENSRNOG00000013641	myosin VIIA	<0.001	0.04	-1.55
Ajap1	ENSRNOG00000050137	adherens junctions associated protein 1	<0.001	0.02	2.71
Jam3	ENSRNOG00000009149	junctional adhesion molecule 3	<0.001	0.02	-1.29
Celsr1	ENSRNOG00000021285	Cadherin EGF LAG seven-pass receptor 1	<0.001	0.02	-1.37
Cldn1	ENSRNOG00000001926	claudin 1	<0.01	0.05	-1.81
Hepacam	ENSRNOG00000009219	hepatic and glial cell adhesion molecule	<0.01	0.05	-1.32
Vangl1	ENSRNOG00000016477	VANGL planar cell polarity protein 1	<0.001	0.02	-1.53
Vangl2	ENSRNOG00000004889	VANGL planar cell polarity protein 2	<0.001	0.02	-1.30
Gli2	ENSRNOT00000009963	GLI family zinc finger 2	<0.001	0.03	-1.34
Gli3	ENSRNOT00000019396	GLI family zinc finger 3	<0.001	0.05	-1.35
Bmp1	ENSRNOG00000010890	bone morphogenetic protein 1	<0.001	0.04	-1.35
Bmper	ENSRNOG00000015357	BMP-binding endothelial regulator	<0.01	0.05	-1.38
Slc16a2	ENSRNOG00000002832	monocarboxylic acid transporter 8	<0.001	0.02	-1.49
Tshr	ENSRNOG00000003972	thyroid stimulating hormone receptor	<0.001	0.02	-1.41
Thrsp	ENSRNOG00000012404	thyroid hormone responsive	<0.001	0.04	-1.42
Spred1	ENSRNOG00000070996	sprouty-related EVH1 domain containing 1	<0.001	0.02	-1.25

Functions include Cellular Assembly and Organization (54 DEGs associated, p-values <0.001) as well as Cell-to-Cell Signaling and Interaction (36 DEGs, p-values <0.001). Between these two categories, there were 68 unique DEGs (Figure 5). Highly significant processes within this curated data include cell-cell contact, organization of cytoplasm, organization of cytoskeleton, formation of cellular protrusions, microtubule dynamics, neuritogenesis, formation of actin, and cell migration (Figure 5, all p-values <0.001). Ingenuity Pathway Analysis's Canonical Pathways also revealed both different and overlapping signals in our DEGs. The most significant Canonical Pathways were oxidative phosphorylation, mitochondrial dysfunction, and protein kinase A signaling; cell-cell junction as well as endothelin-1 signaling were also significant in our data set (all p-values <0.001) (see Supplementary File 4).

10.3389/fendo.2023.1090081

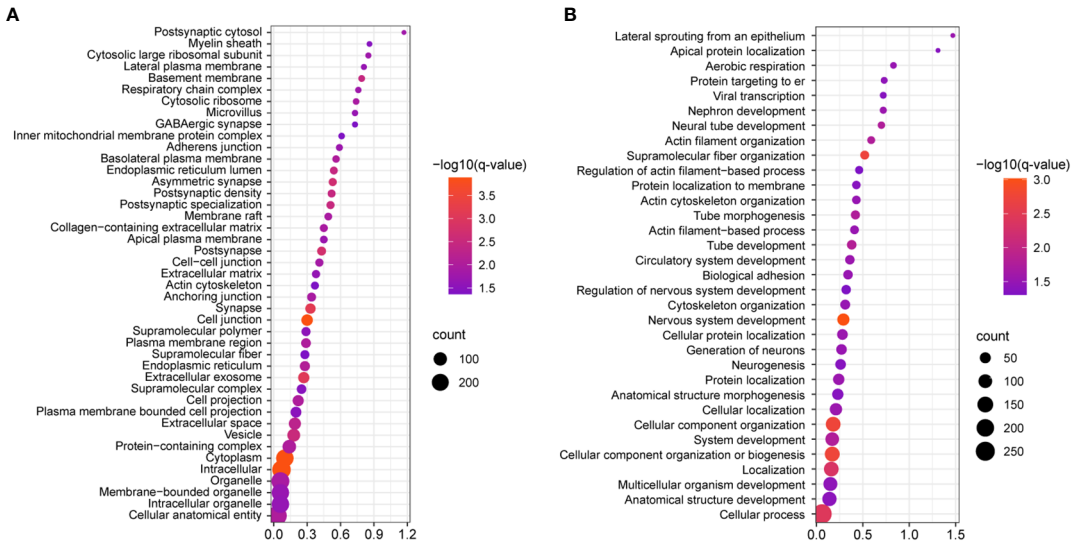

FIGURE 4
Statistically significant gene ontology (GO) analyses of the identified DEGs, as visualized by bubble plots. **(A)** Cell component GO reveals that the most statistically significant categories include intracellular, cytoplasm, and cell junction (q=0.00013 for each); this shows that most protein products DEGs will localize to these cellular compartments. **(B)** Biological processes analysis shows that cell component organization, nervous system development, cytoskeletal organization, and supramolecular fiber organization are amongst the most statistically significant processes (q≤0.0018), while more specific categories like cytoskeletal organization, biological adhesion, actin filament-based processes, were also identified. In both panels all categories listed are supported by q≤0.05.

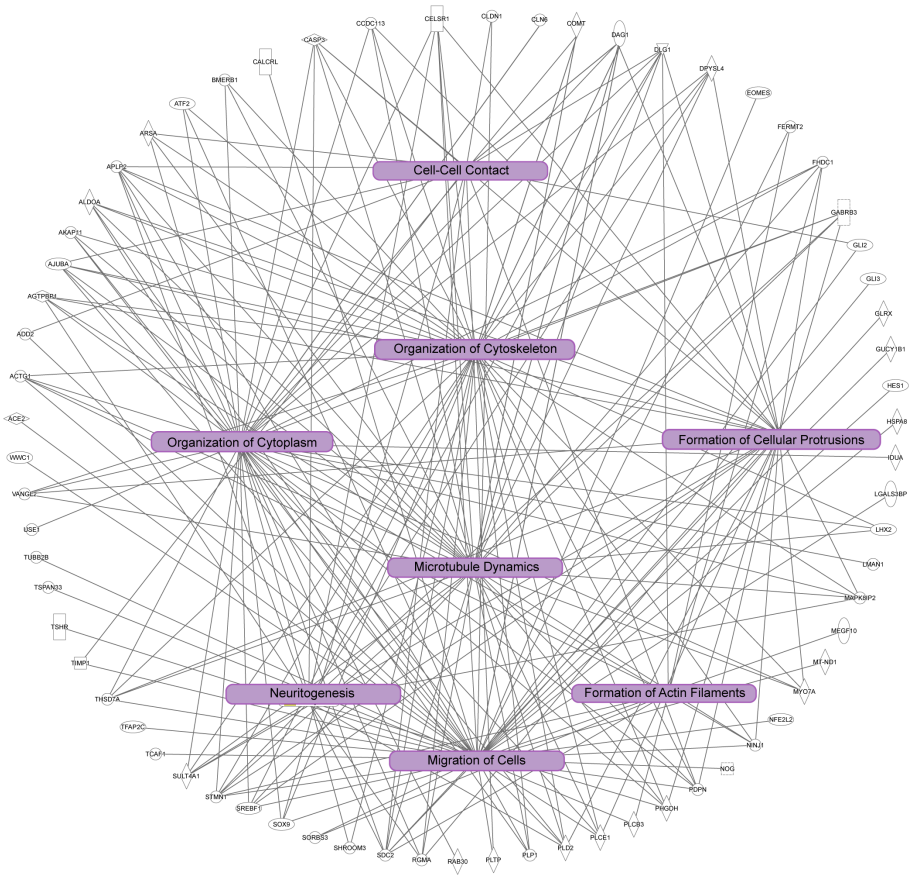

FIGURE 5
Ingenuity pathway analysis of significant cellular pathways. In this diagram unique genes identified are the outside of the circle, and connected to statistically significant processes (p<0.001). Note the overlap of the biological processes highlighted in purple boxes, which are correlated to dynamics of the cytoskeleton and cytoplasm, cell adhesion, cell morphology, and cell migration.

10.3389/fendo.2023.1090081

3.4 Immunofluorescence demonstrates thyroid-dependent changes in cell junction components of the VZ

To corroborate the RNA-Seq findings, we next performed immunofluorescence to visualize components of the extracellular matrix, cytoskeleton, and cell junctions at the VZ in PN2 littermates. We first investigated collagen IV (COL IV), a critical extracellular matrix protein that maintains the basement membrane in brain endothelial cells. One collagen IV subunit was downregulated in our RNA-Seq data (*Col4a6*), and another was downregulated and approaching statistical significance (*Col4a5*, see Table 1 and Supplementary File 1). Our results in control pups show COL IV is highly expressed at the brain barriers, including in the choroid plexus (blood-cerebrospinal fluid barrier) and in the blood vessels of the VZ (Figures 6A, B, D, for colorblind compatible images see Supplementary Figure 2). Expression was also observed near the apical surface of the inferior VZ (Figure 6B). In contrast to euthyroid controls, PTU exposed pups show pronounced differences in the pattern of COL IV expression, specifically a notable reduction in the vasculature throughout the VZ (Figures 6C, E and Supplementary Figures 3A–C, see white arrows). Next, we visualized components of the cytoskeleton, given the RNA-Seq signal related to its formation and function. Filamentous actin (F-actin) was visualized by phalloidin staining in PN2 littermates. In euthyroid controls, F-actin is normally distributed throughout the brain, including in the VZ and its associated blood vessels (Figures 6F, H and Supplementary Figure 3D). In hypothyroid neonates, F-actin expression appeared globally reduced, and with a more punctate staining patterns as compared to controls (Figures 6G, I and Supplementary Figure 3E). This was apparent along the entire VZ (inferior, superior, and medial) and in the surrounding parenchyma (Figures 6G, I and Supplementary Figures 3D, E). This change in F-actin is reminiscent of the T4 and rT3-dependent change in actin polymerization, which has been reported in neurons and astrocytes *in vitro* and *ex vivo* by others (29–34). We next examined vimentin (VIM) immunostaining, another component of the cytoskeleton. Vimentin is an intermediate filament and used to visualize radial glial progenitor cells. Radial glia progenitors originate from neuroepithelial cells of the VZ, and anchor endfeet to this region (13). In our RNA-Seq dataset *Vim* was reduced in PTU exposed pups and this change was approaching statistical significance (q=0.06); *Pax6*, a transcription factor expressed by radial glia, was also downregulated (q=0.06, Supplementary File 1). Our results show that VIM is highly expressed in the PN2 control brain, with pronounced staining of radial glia cells as expected (Figure 7A). At high magnification, the spindle-like morphology of radial glial cells is clearly observed, including their attachment to the VZ (Figure 7A). In hypothyroid pups, VIM was still observed throughout the brain, although the apicobasal polarity of radial glial cells was abnormal (Figure 7B). This was clear at high magnification (Figure 7B).

As our data suggested that hypothyroid animals exhibited differences in the components that comprise cell junctions, we next asked whether adhesive proteins were also affected. Adherens junctions are the primary cell junction type of the VZ and are responsible for maintaining normal adhesion of the epithelium, including radial glia. This is supported by our results, where N-cadherin expression is strongly expressed in the VZ, especially along its apical border (Figure 7C, for colorblind compatible images see Supplementary Figure 4). In contrast, a loss of both basal and apical N-cadherin staining is observed in PTU exposed pups, including amongst the most luminal cells (Figure 7D and Supplementary Figure 4D, see arrows). In addition to adherens junctions, tight (occluding) junctions are crucial for polarization of epithelial cells, and for the normal functioning of the brain barriers. To visualize tight junctions, we examined the distribution of claudin 5 (CLD5). We did not observe any overt changes in the expression patterns of CLD5 in the brain parenchyma of the VZ, except along the apical surface; these changes were not as pronounced as N-cadherin (Figures 7E, F). CLD5 was also expressed in the CSF-facing epithelial cells of the choroid plexus (Figure 7E); interestingly, CLD5 expression appeared disorganized in the choroid plexus of PTU exposed neonates.

Next, as our bioinformatic analyses suggested that vascular patterning and/or function may be implicated in our RNA-Seq data, we analyzed the endothelial cell marker platelet endothelial cell adhesion molecule 1 (PECAM-1). PECAM-1 was observed in the vascular component of the choroid plexus, as well as in the brain's blood vessels (Figure 7E). The PECAM-1 pattern at the VZ appeared less complex in PTU exposed pups as compared to controls, which was most apparent at the transition between the VZ-SVZ (Figure 7F). We did not observe any notable changes in the co-labeling of PECAM-1 and CLD5 between hypothyroid and euthyroid pups in the VZ parenchyma. However, the disorganization of normal CLD5/PECAM-1 expression was appreciable in the plexus of PTU exposed neonates (compare merge images of 7E and F, see C.P.). In total, these results showed differences in the expression patterns of extracellular matrix, cytoskeletal, and adhesive proteins within the posterior VZ. Surprisingly, during imaging we also observed clear differences in markers of the BBB (cerebral microvasculature, COL IV, PECAM-1, F-actin), as well as the blood-cerebrospinal fluid barrier (choroid plexus, COL IV, F-actin, PECAM-1, CLD5). It is noted that the choroid plexus data were gathered incidentally during imaging, and the RNA-Seq experiment did not include these cells.

3.5 TH action at the VZ may be mediated by both nongenomic and genomic mechanisms

While we found that thyroid stimulating hormone receptor (*Tshr*) was differentially expressed in the posterior VZ (Table 1), the potential role of TSH in the VZ is unknown. However, it is expressed in the adult SVZ, suggesting it may be of importance in this region (35). No known receptor for T4 or T3 was identified as a DEG (Supplementary File 1). Given this lack of transcriptional signal, we chose to evaluate the localization of known T4/T3 receptors *in vivo*. Specifically, we hypothesized that the T4 receptor integrin αvβ3 would be highly expressed in the VZ. Integrins are transmembrane adhesion proteins that anchor intracellular F-actin to the extracellular matrix, serving as a cell-matrix junction (36). They are implicated in not only cell adhesion, but are critical to cell migration. Consistent with this hypothesis, we observed robust immunostaining of integrin αvβ3 in the VZ of both control and PTU exposed pups. (Figures 8A, B). We also detected its expression in the choroid plexus as well as in

10.3389/fendo.2023.1090081

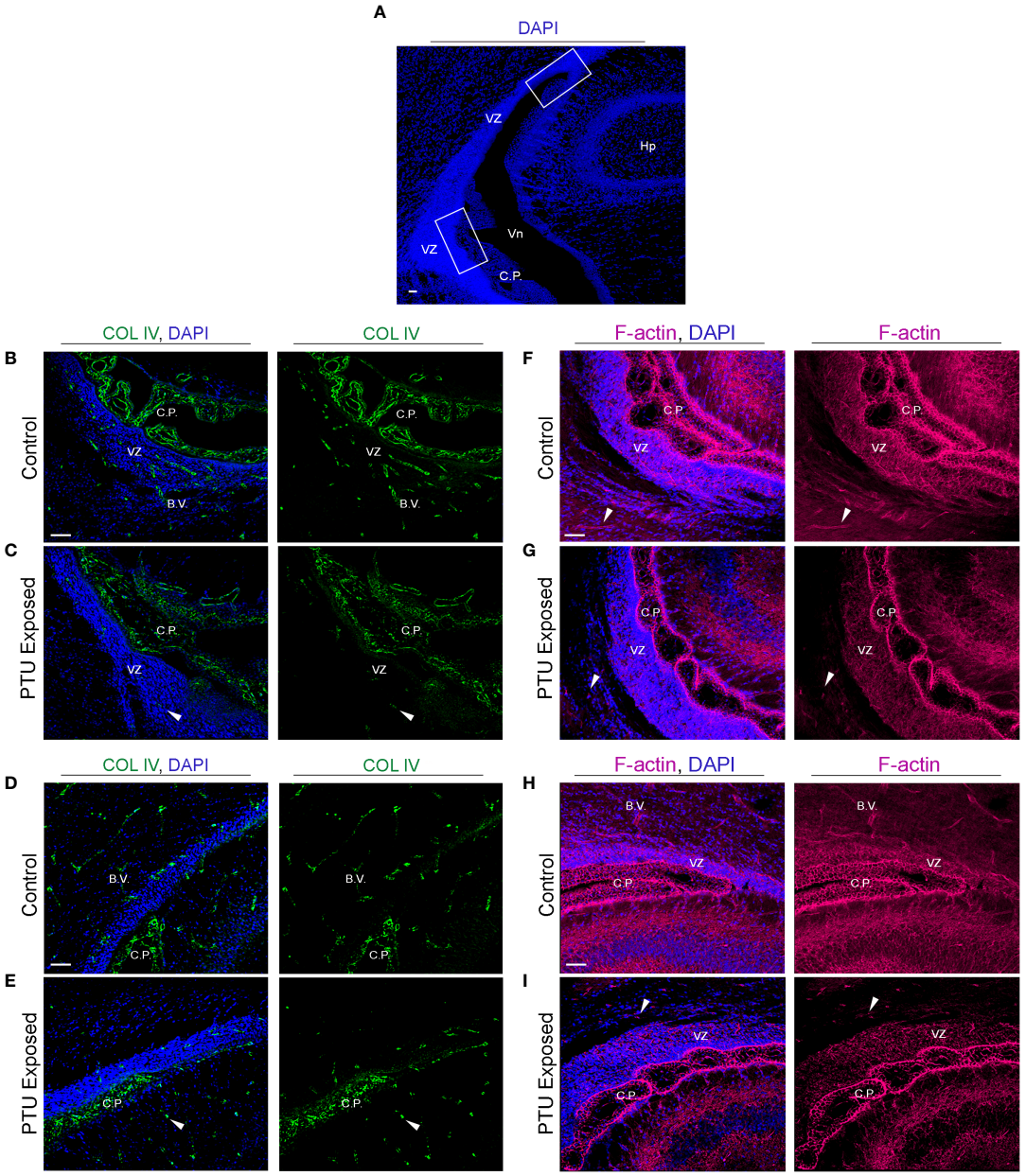

FIGURE 6
Developmental hypothyroidism affects collagen IV (COL IV) and filamentous actin (F-actin) in PN2 neonates **(A)** Representative regions of the posterior telencephalon. The white bonding boxes represent the inferior and superior portions of the VZ, and represent where the images were captured. Note that the choroid plexus (C.P., blood-cerebrospinal fluid barrier) is in proximity to the VZ and thus often imaged simultaneously. **(B)** Collagen IV (COL IV) is an extracellular matrix protein that is critical to basement membrane maintenance in cerebral endothelial and in some epithelial cells, and was implicated by RNA-Seq. In control pups, COL IV is enriched in blood vessels (B.V.) of the inferior VZ, as well as the vascular component of the choroid plexus. Less pronounced staining is also observed in the more luminal area of the VZ. **(C)** In PTU exposed pups, there was a clear disorganization of COL IV in the blood vessels, the choroid plexus, and in the inferior VZ parenchyma (see arrows). **(D)** COL IV is expressed in the blood vessels and choroid plexus of the superior VZ. **(E)** In PTU exposed pups COL IV also appears reduced in the superior VZ. **(F)** Visualization of F-actin by phalloidin shows strong signal throughout the brain, including in the blood vessels of the inferior VZ. F-actin was also highly enriched surrounding the nuclei of cells (blue DAPI staining) in the VZ, as expected. **(G)** In the PTU exposed animals, staining appeared globally reduced, which was especially notable in the parenchymal cells surrounding the VZ as well as in blood vessels (see arrows). **(H)** F-actin is highly expressed in the superior VZ and its associated blood vessels in control animals. **(I)** The PTU-associated changes in F-actin are apparent in the VZ and the surrounding parenchna. In all panels VZ, ventricular zone; C.P., choroid plexus; Hp, hippocampus; B.V., blood vessel; Vn, ventricle and scale bars are 50 μm.

other brain compartments (Figures 8A, B). We next examined the expression of thyroid receptor isoforms, thyroid receptor alpha 2 and beta 1/2 (TRα2 and TRβ1/2). TRα2 and TRβ1/2 mediate genomic (nuclear initial action) and nongenomic (extranuclear initial action) TH signaling (see 37), and in addition to integrin αvβ3 in the VZ, could explain this region's hormone sensitivity. Both *Thra* and *Thrb* were expressed in microdissected VZ cells although they were not differentially expressed between exposure groups; *Thra* exhibited higher expression as compared to *Thrb* (Supplementary File 1). Using an antibody that recognizes TRα2, the dominant negative isoform highly expressed in the developing rat brain (38), we showed that TRα2 is expressed in the VZ of both control and PTU exposed

10.3389/fendo.2023.1090081

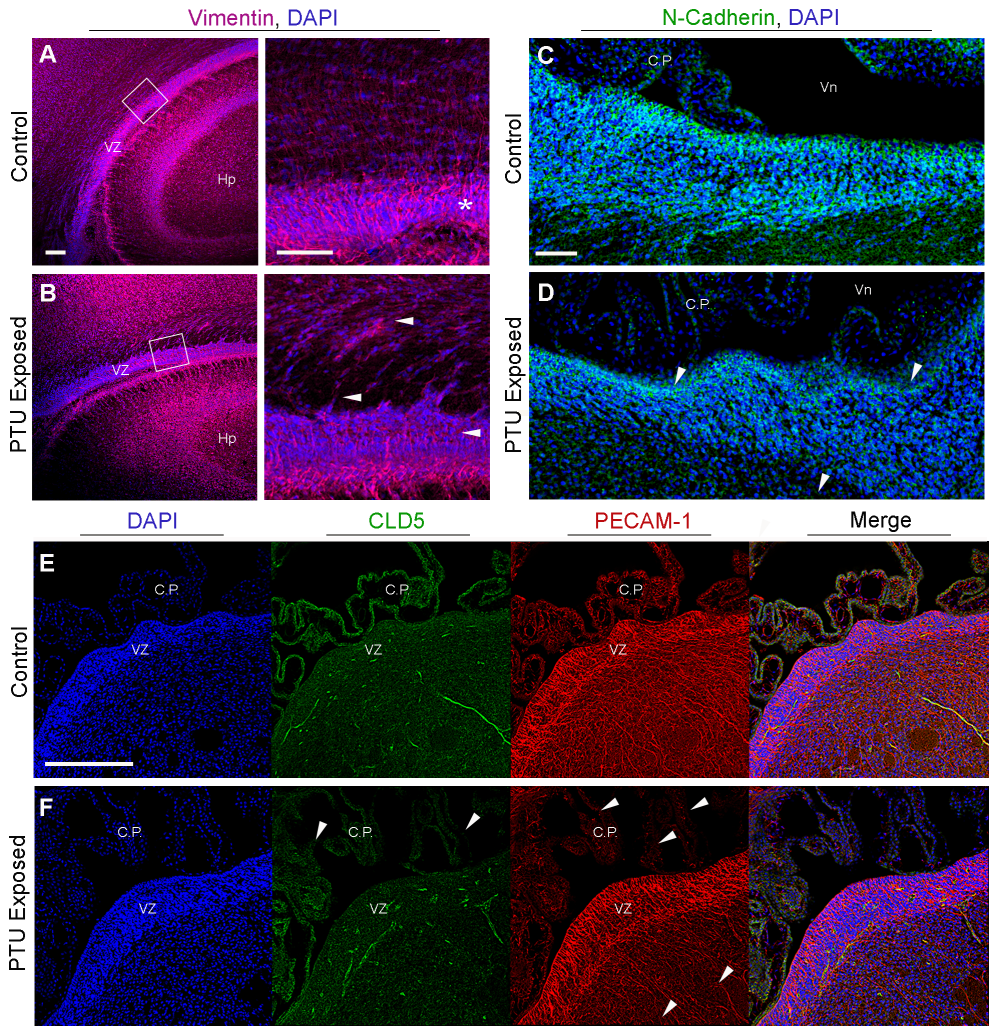

FIGURE 7
Radial glia cells and cell adhesion are affected in the newborn VZ. **(A)** Vimentin immunohistochemistry highlights radial glia cells. In control animals radial glia endfeet anchor these cells to the ventricular zone (VZ), as seen at high magnification (see asterisk). **(B)** In PTU exposed pups, there is a loss of the apicobasal polarity of radial glia, which is especially prominent at high magnification (see white arrows). Note that the high magnification image was rotated so that the VZ was viewed horizontally. **(C)** Visualization of adherens junctions by N-cadherin. N-cadherin expression is observed in the VZ, notably along the apical border which faces cerebrospinal fluid. **(D)** In PTU exposed pups on PN2 there is a disorganization of N-Cadherin, especailly along the apical border (see arrows). **(E)** Examination of tight junctions by claudin 5 (CLD5) and endothelial cell by PECAM-1. CLD5 is normally expressed in endothelial cells and is a critical compoenent of the blood-brain and blood-cerebrospinal fluid barriers. It is also expressed along the apical surface of the VZ, similar to N-Cadherin. **(F)** In hypothyroid (PTU exposed) neontates, there was a pronounced reduction and disorganization in CLD5 staining in the choroid plexus (see arrows). There was also subtle changes in CLD5 along the apical surface of the VZ. Interestingly, PECAM-1 was also affected in the choroid plexus, and at the more basal region of the VZ as it transitions to the SVZ (see arrows). In all panels VZ, ventricular zone; C.P., choroid plexus; Hp, hippocampus; B.V., blood vessel; Vn, ventricle, and scale bars are 50 µm.

pups on PN2 (Figures 8C, D). TRα2 was also observed in the hippocampus, as well as in the choroid plexus (Figures 8C, D, Hp and C.P.). Next, using an antibody that recognizes TRβ1/2, robust expression was also observed in the VZ of both control and PTU exposed animals; the hippocampus, and choroid plexus also showed signal (Figures 8E, F). Strikingly, integrin αvβ3, TRα2, and TRβ1/2 show highly similar distribution in the PN2 telencephalon, including enrichment in the VZ (see Supplementary Figure 5 for antibody control experiments). Taken together, this suggests that the VZ may be a "hotspot" of TH action in the developing brain.

4 Discussion

Neurodevelopment requires tightly coordinated spatiotemporal signaling processes, including those controlled by THs. Here we addressed the hypothesis that the posterior VZ is sensitive to TH action during the neonatal period in the rat. While the anterior and/or entire VZ/SVZ has been studied at different developmental stages including adulthood (39–44), the posterior VZ has not been investigated in isolation during an established time of TH dependency.

10.3389/fendo.2023.1090081

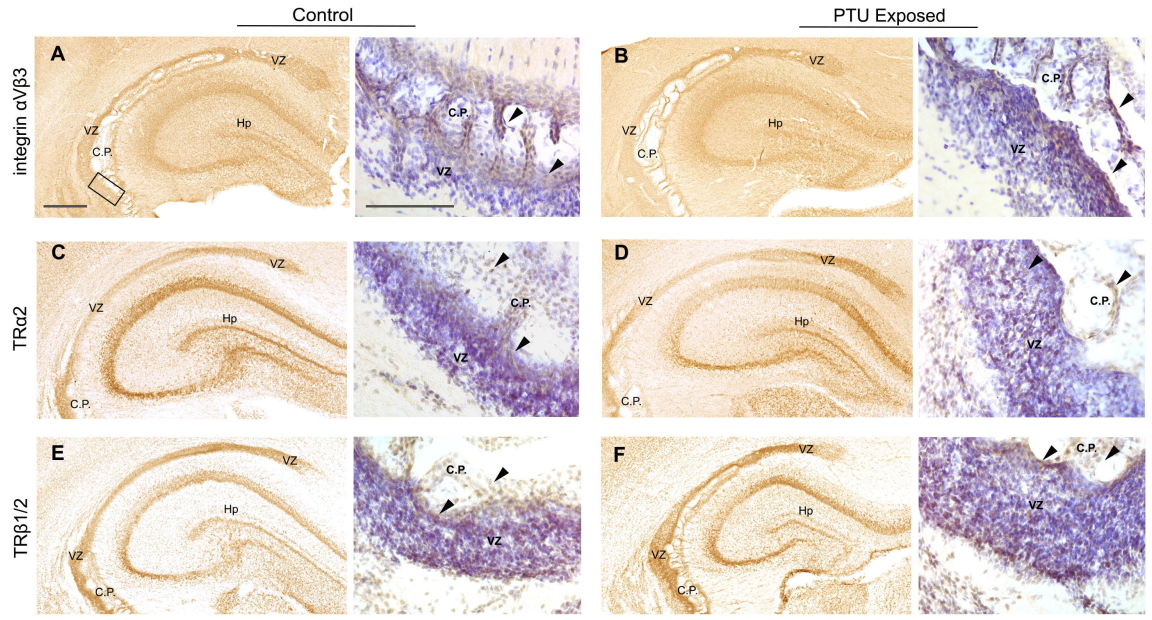

FIGURE 8
Mediators of TH action in PN2 pups. All receptors are visualized by diaminobenzidine (DAB) staining; at low magnification DAB is used alone and high magnification images were taken from sections counterstained with Cresyl violet. **(A)** Integrin $\alpha_V\beta3$ is expressed in the VZ of control and **(B)** PTU exposed pups. Signal was also detected in the hippocampus and choroid plexus. High magnification images of the inferior VZ (see bounding box in panel A) demonstrates enriched expression of integrin αVβ3 along the apical border of the VZ and in the choroid plexus (see arrows). **(C)** Thyroid receptor alpha 2 (TRα2) was detected in the VZ of both euthyroid control pups and **(D)** PTU exposed pups. High magnification images show TRα2 staining throughout the VZ and in the choroid plexus (arrows). **(E)** Thyroid receptor beta 1/2 (TRβ1/2) was also expressed in the VZ of both control and **(F)** PTU exposed pups, in similar brain compartments as integrin $\alpha_V\beta3$ and TRα2. At high magnification TRβ1/2 is also expressed in throughout the VZ and in choroid plexus cells (arrows). In all panels VZ, ventricular zone; C.P., choroid plexus; Hp, hippocampus; B.V., blood vessel; Vn, ventricle and scale bars are 50 μm. Low magnification images are stained with DAB alone, and high magnification images counterstained with Cresyl violet.

4.1 TH action affects components of cell junctions in the ventricular zone

Cell–cell junctions link cells to maintain tissue homeostasis, and regulate critical processes like tissue barrier function, cell proliferation, and cell migration. Tight and adherens junctions are two different multiprotein complexes that require similar components: adhesion proteins to physically connect cells, anchoring proteins that link the intercellular cytoskeleton, and an extracellular matrix that supports cell shape and contacts (45). Perturbation of any of these components can disrupt the structure and function of cell junctions. For example, disruption of CLD5 (adhesion molecule), actin (cytoskeleton), or COL IV (basement membrane, extracellular matrix) in tight junctions of brain endothelial cells will disturb the occluding activity of the BBB (46–48). In this study we show that various adhesion, cytoskeletal, and extracellular matrix proteins are simultaneously disturbed by moderate developmental hypothyroidism *in vivo*. While these findings may have several implications for the development and function of the brain, it is clear that cell migration is affected.

Our previous work to understand the cellular etiology of the periventricular heterotopia showed that radial glia cells were abnormal in hypothyroid rat pups (4). We correlated this observation to downregulation of *Spred1*, as detected by qRT-PCR in a hand-dissected region of the brain that included the cortex, hippocampus, and VZ (2, 4). Here, using a lower dose of PTU and laser capture microdissection to isolate the VZ in newborn rats, we again demonstrate downregulation of *Spred1* and loss of radial glia apicobasal polarity. Phoenix and Temple (49) showed that *Spred1* knockdown in the embryonic mouse brain caused reduced cell adhesion at the VZ/SVZ, abnormal morphology of radial glia cells, and disordered neuroblast migration. The authors also detected periventricular heterotopia in the posterior telencephalon of postnatal mice (49). In patients, periventricular heterotopia are often attributed to mutations in cytoskeletal proteins. The most commonly associated are within filamin A (FLNA), but other genes encoding cytoskeletal, adhesive, and extracellular matrix proteins are also implicated (reviewed in 50). Intriguingly, various COL IV mutations cause not only heterotopia, but also small vessel disease of the brain in affected individuals (50). Here we also show that TH action affects expression of *Col4a6* (q=*0.04*), *Col4a5* (q=*0.07*), and COL IV at the rat VZ. Regardless of the molecular etiology, it is established across species that heterotopia are caused by abnormalities in radial glia-mediated cell migration (49–52). These observations, coupled with our repeatable findings, strengthens the interpretation that TH action affects radial glia form and function, which then leads to heterotopia formation in the rat.

The conclusion that radial glial cells and/or cell migration can be affected by TH action has been supported by others (8, 53–60). There are several hypotheses about why this occurs, including TH-mediated loss of cell adhesion at the VZ, which normally anchors radial glia endfeet (4, 59). Other hypotheses include direct changes in the cytoskeleton of radial glia, as F-actin in particular is responsive to T4 and rT3 in the brain (29–34, 61). Given the data presented here, we

cannot determine whether abnormalities in adherens junctions of the VZ cause loss of radial glial cell morphology, or if this is a secondary effect of cytoskeletal changes in radial glia themselves. Regardless, loss of adherens junctions in the VZ is associated with loss of radial glia apicobasal polarity, which results in abnormal cell migration in other models (62). Interestingly, despite the VZ's function as a stem cell niche, we did not detect a robust transcriptional signal related to neurogenesis and/or cell differentiation. For example, we did not detect a downregulation of genes related to oligodendrocyte progenitors (i.e., *Ng2*, *Olig1*, *Olig2*) in PTU exposed animals, even though reduced myelination is well established consequence of hypothyroidism (1). We acknowledge that bulk RNA-Seq may make such determinations regarding cell population changes difficult (63). But overall, the RNA-Seq data are supportive of our previous work, where we did not find a significant difference in Ki67+ cells at the ventricular epithelium in PN2 hypothyroid neonates (4). Neurogenesis in the developing and adult VZ-SVZ has been shown to be affected by THs (39, 42, 44, 64, 65), but the majority of published work has examined the anterior or entire VZ and/or SVZ in rodents older than this study. Some cellular biology studies have shown that abnormal cell junctions in the brain precede neurogenesis and cellular differentiation deficits, due to a breakdown in intercellular communication (reviewed in 66). We also show by pathway analysis that oxidative phosphorylation was significantly represented in our RNA-Seq data, and that it was estimated to be activated. Neural progenitor cells switch primarily from glycolysis to oxidative phosphorylation upon differentiation (67), so it is possible that this transcriptional signal may be another early indicator of abnormal neurogenesis in hypothyroid animals. In the future it would be interesting to determine if and how TH-action may affect cell differentiation in this model of moderate hypothyroidism, but developmental stages later than PN2 should be included.

TH action may influence the cytoskeleton and extracellular matrix of brain tissue by multiple mechanisms (29, 31–33, 61). With respects to *in vivo* models, Morte et al. reported differential expression of cytoskeletal genes in the brains of hypothyroid rat pups; however, maternal TH function was abolished by thyroidectomy as well as methamizole exposure 68. In a series of *ex vivo* experiments, Farwell et al. showed that deficiency in T4 and rT3 reduced F-actin in rat cerebellar cells, which attenuated neurite migration (33). This migration phenotype could be recapitulated by blocking the integrin β1 subunit, even in the presence of sufficient T4/rT3 concentrations. This suggests that that the hormonal regulation of F-actin is necessary for normal integrin β1-mediated cell migration (33). With respects to this study, brain T4 was significantly reduced although rT3 was more variable between rat pups across litters. Integrin αvβ3 protein was also expressed in the developing rat VZ. Similar to *in vitro* and *ex vivo* reports, we demonstrated that F-actin appeared reduced and our model suffers from abnormal cell migration as evidenced by periventricular heterotopia formation (3, 5–8). Thus, the similarities between experimental models are compelling and suggests the brain cytoskeleton can be perturbed by moderate hypothyroidism *in vivo*. In the future, additional studies are needed to fully elucidate the TH signaling mechanism(s) at the VZ and how this translates to the observed cellular abnormalities. This could include rescue experiments where T4/T3 are each supplemented to hypothyroid pups and gene expression measured at the VZ, chromatin immunoprecipitation of thyroid receptors, and/or pharmacological manipulation of integrin αvβ3.

4.2 TH action and the blood-brain and blood-cerebrospinal fluid barriers

We previously hypothesized that the VZ was susceptible to TH action, due to its juxtaposition between two sources of brain THs: the CSF and an enriched vascular network (4). The VZ itself also represents the developmentally transient CSF-brain barrier (69, 70). What we did not expect to discover was that the TH-dependent changes in the VZ parenchyma may also extended to cerebral endothelial cells.

The blood-brain and blood-CSF barriers develop in parallel with the brain tissue, and these fluid interfaces are functional during fetal development (71, 72). These mechanical and physiological barriers are comprised of tight and adherens junctions that line endothelial cells of the central nervous system, expression and activity of influx and efflux transporters, and fluid flux-flow dynamics (73). However, tight junctions are the hallmark of their occluding activity. In our RNA-Seq experiment, we sequenced all cell types within microdissected VZ, which represents a heterogeneous population. We subsequently identified several DEGs that are critical to brain barrier function (Table 1); microscopy also revealed pronounced effects in endothelial cells of the brain vasculature and/or choroid plexus, in addition to changes in VZ parenchyma. Specifically, COL IV, F-actin, CLD5, and PECAM-1 are associated with endothelial cell patterning and/or function of the BBB *in vivo* (46, 74, 75), and we discovered clear effects in their localization between euthyroid and hypothyroid neonates. These preliminary findings pose the new question – could brain barrier development and/or function be an underappreciated target of TH action?

Several studies in adult and canines demonstrate that hypothyroidism is associated with increased permeability of the brain barriers (76–81). Clinically, this manifests as increased protein concentrations in the CSF. In one study, necropsy of affected hypothyroid dogs suggested cerebrovascular disease in this species (80). More than half a century ago, Thompson et al. studied 17 adult patients with myxedema, who also presented with increased CSF protein concentrations (76). Amazingly, after supplementation with thyroid extract all but 2 patients had a marked reduction in CSF protein content, and achieved normal levels once euthyroidism was established (76). This rescue to a normal phenotype demonstrates that brain barrier function directly responds to TH action. While the mechanisms of these observations are unknown, TH signaling can affect vascular function and patterning in different tissues. This has been shown *in vitro* and *in vivo* with regards to T4/rT3 action on integrin αvβ3 (reviewed in Davis et al., 2020), as well as TSH activity *via* TSHR in primary human cultures (82). Both pathways appear to be proangiogenic, where both excess T4 or TSH can induce angiogenesis (36, 82). It has also been shown in rats exposed to PTU from birth to PN21 that brain angiogenesis was reduced, including in the complexity and density of microvessels (83). Taken together, there is evidence that THs control the morphogenesis and function of endothelial cells, and this is likely mediated by multiple complex mechanisms. While there is convincing evidence that

thyroid-mediated brain barrier disruption in adults is transient and corrects following TH supplementation, this may not occur during development. If TH action controls patterning of cells that comprise the brain barriers, then it is possible that developmental hypothyroidism could lead to permanent changes in the way the barriers are formed and/or function. Future studies should determine if TH action can affect brain barrier activity, and if so, determine its persistence. There is accumulating evidence that both neurodevelopmental and neurodegenerative disorders are associated with increased permeability of the BBB (84), so any TH-mediated effects could have significant consequences.

4.3 The human health implications of this study

This study extends our previous observations and reinforces that TH action targets multiple components of normal cell junctions in the developing brain. These abnormalities can converge to affect downstream processes like cell migration and potentially brain barrier function. While previous *in vivo* work has demonstrated that radial glia morphology and/or cell migration is affected by developmental hypothyroidism, these conclusions were drawn from experiments that induced severe TH disturbances (e.g., maternal thyroidectomy and/or high doses of TH modulators) (53–57, 59, 60). While these studies are critical to our understanding of mechanisms, it can be difficult to translate these findings to patients. Our PTU exposed dams exhibited a relatively minor 72% increase in TSH, with no significant change in serum T3. The American Thyroid Association advises that normal TSH in pregnant patients during the second trimester is 0.2-3.0 mIU/L in absence of a laboratory-established reference range (85). Given the biological variability of TSH in human populations and our presented data, we consider our experiment representative of moderate maternal hypothyroidism. The pronounced effects we observed at the neonatal VZ, with the knowledge that a 3 ppm PTU exposure will induce a periventricular heterotopia in offspring (3, 5, 6), emphasizes that euthyroidism throughout pregnancy is critical. The mammalian brain undergoes protracted development, so processes like cell migration occur over many weeks in both human and rodents (13, 86).

In conclusion, this study provides evidence that the posterior VZ is sensitive to THs in newborn rats, even under conditions of moderate maternal hypothyroidism. Specifically, components of normal cell junctions including adhesive, cytoskeletal, and extracellular matrix transcripts were differentially expressed as detected by RNA-Seq and pathway analyses. Immunofluorescence reinforced these results, and supports that cell migration is a target of TH action. In addition, this work led to the unexpected finding that components of both the blood-brain and blood-cerebrospinal fluid barrier may also be affected by hypothyroidism. While we acknowledge our study's limitations, namely that there are multiple cell types in this the developing VZ and we performed bulk RNA-Seq, these findings support previous hypotheses that cell adhesion and radial glia cell polarity are affected in this critical region. In the future, single cell RNA-Seq to differentiate between various cell types in the VZ (i.e., radial glia versus endothelia cells), and functional studies of brain barrier function could further illuminate mechanisms of TH action.

Data availability statement

All raw data for hormone analyses can be found in the public repository Science Hub. The sequencing data discussed in this publication have been deposited in NCBI's Gene Expression Omnibus (87) and are accessible through GEO Series accession number GSE218930 (https://www.ncbi.nlm.nih.gov/geo/query/acc.cgi?acc= GSE218930).

Ethics statement

All experiments were conducted with prior approval from the United States Environmental Protection Agency's (US EPA's) Institutional Animal Care and Usage Committee and were carried out in an Association for Assessment and Accreditation of Laboratory Animal Care approved facility.

Author contributions

KO conceived and executed the study, performed sectioning, laser capture microdissection, library preparations, bioinformatics, microscopy, prepared figures, and wrote the article. AS performed sectioning and immunohistochemistry. BM assisted with bioinformatics. KB and MG assisted with the animal exposure. CR, JF, and RG measured thyroid hormones. TS provided equipment, and AP also provided equipment and training for laser capture microdissection. All authors contributed to the article and approved the submitted version.

Funding

This work was supported by US EPA's Office of Research and Development and Division of the National Toxicology Program at the National Institute of Environmental Health Sciences.

Acknowledgments

The authors thank Drs. Andrew Johnstone and Emily Pitzer for their comments on previous versions of this manuscript.

Conflict of interest

The authors declare that the research was conducted in the absence of any commercial or financial relationships that could be construed as a potential conflict of interest.

Publisher's note

All claims expressed in this article are solely those of the authors and do not necessarily represent those of their affiliated organizations, or those of the publisher, the editors and the reviewers. Any product

that may be evaluated in this article, or claim that may be made by its manufacturer, is not guaranteed or endorsed by the publisher.

Author disclaimer

This document has been subjected to review by the Center for Public Health and Environmental Assessment and approved for publication. Approval does not signify that the contents reflect the views of the Agency, nor does mention of trade names or commercial products constitute endorsement or recommendation for use.

Supplementary material

The Supplementary Material for this article can be found online at: https://www.frontiersin.org/articles/10.3389/fendo.2023.1090081/full#supplementary-material

References

1. Bernal J. Thyroid hormones in brain development and function. In: De Groot LJ, Beck-Peccoz GCP, Dungan K, Grossman A, Hershman JM, C. Koch R, McLachlan MN, Rebar R, Singer F, Vinik A, Weickert MO, editors. *Endotext*. South Dartmouth (MA: MDText.com, Inc (2015).

2. O'Shaughnessy KL, Gilbert ME. Thyroid disrupting chemicals and developmental neurotoxicity - new tools and approaches to evaluate hormone action. *Mol Cell Endocrinol* (2019) 518:110663, 110663. doi: 10.1016/j.mce.2019.110663

3. O'Shaughnessy KL, Kosian PA, Ford JL, Oshiro WM, Degitz SJ, Gilbert ME. Developmental thyroid hormone insufficiency induces a cortical brain malformation and learning impairments: A cross-fostering study. *Toxicol Sci* (2018) 163(1):101–15. doi: 10.1093/toxsci/kfy016

4. O'Shaughnessy KL, Thomas SE, Spring SR, Ford JL, Ford RL, Gilbert ME. A transient window of hypothyroidism alters neural progenitor cells and results in abnormal brain development. *Sci Rep* (2019) 9(1):4662. doi: 10.1038/s41598-019-40249-7

5. Goodman JH, Gilbert ME. Modest thyroid hormone insufficiency during development induces a cellular malformation in the corpus callosum: A model of cortical dysplasia. *Endocrinology* (2007) 148(6):2593–7. doi: 10.1210/en.2006-1276

6. Gilbert ME, Ramos RL, McCloskey DP, Goodman JH. Subcortical band heterotopia in rat offspring following maternal hypothyroxinaemia: Structural and functional characteristics. *J Neuroendocrinol* (2014) 26(8):528–41. doi: 10.1111/jne.12169

7. Spring SR, Bastian TW, Wang Y, Kosian P, Anderson GW, Gilbert ME. Thyroid hormone-dependent formation of a subcortical band heterotopia (SBH) in the neonatal brain is not exacerbated under conditions of low dietary iron (FeD). *Neurotoxicol Teratol* (2016) 56:41–6. doi: 10.1016/j.ntt.2016.05.007

8. Ramhoj L, Fradrich C, Svingen T, Scholze M, Wirth EK, Rijntjes E, et al. Testing for heterotopia formation in rats after developmental exposure to selected *in vitro* inhibitors of thyroperoxidase. *Environ pollut* (2021) 283:117135. doi: 10.1016/j.envpol.2021.117135

9. Minami K, Suto H, Sato A, Ogata K, Kosaka T, Hojo H, et al. Feasibility study for a downsized comparative thyroid assay with measurement of brain thyroid hormones and histopathology in rats: Case study with 6-propylthiouracil and sodium phenobarbital at high dose. *Regul Toxicol Pharmacol* (2022) 137:105283. doi: 10.1016/j.yrtph.2022.105283

10. Hansen JM, Siersbaek-Nielsen K. Cerebrospinal fluid thyroxine. *J Clin Endocrinol Metab* (1969) 29(8):1023–6. doi: 10.1210/jcem-29-8-1023

11. Bernal J. The significance of thyroid hormone transporters in the brain. *Endocrinology* (2005) 146(4):1698–700. doi: 10.1210/en.2005-0134

12. Noctor SC, Flint AC, Weissman TA, Wong WS, Clinton BK, Kriegstein AR. Dividing precursor cells of the embryonic cortical ventricular zone have morphological and molecular characteristics of radial glia. *J Neurosci* (2002) 22(8):3161–73. doi: 20026299

13. Tramontin AD, Garcia-Verdugo JM, Lim DA, Alvarez-Buylla A. Postnatal development of radial glia and the ventricular zone (VZ): A continuum of the neural stem cell compartment. *Cereb Cortex* (2003) 13(6):580–7. doi: 10.1093/cercor/13.6.580

14. Noctor SC, Martinez-Cerdeno V, Ivic L, Kriegstein AR. Cortical neurons arise in symmetric and asymmetric division zones and migrate through specific phases. *Nat Neurosci* (2004) 7(2):136–44. doi: 10.1038/nn1172

15. Wu SX, Goebbels S, Nakamura K, Nakamura K, Kometani K, Minato N, et al. Pyramidal neurons of upper cortical layers generated by NEX-positive progenitor cells in the subventricular zone. *Proc Natl Acad Sci U S A* (2005) 102(47):17172–7. doi: 10.1073/pnas.0508560102

16. Petros TJ, Bultje RS, Ross ME, Fishell G, Anderson SA. Apical versus basal neurogenesis directs cortical interneuron subclass fate. *Cell Rep* (2015) 13(6):1090–5. doi: 10.1016/j.celrep.2015.09.079

17. Mellert W, Deckardt K, Walter J, Gfatter S, van Ravenzwaay B. Detection of endocrine-modulating effects of the antithyroid acting drug 6-propyl-2-thiouracil in rats, based on the "Enhanced OECD test guideline 407. *Regul Toxicol Pharmacol* (2003) 38 (3):368–77. doi: 10.1016/j.yrtph.2003.07.003

18. Bansal R, Zoeller RT. CLARITY-BPA: Bisphenol a or propylthiouracil on thyroid function and effects in the developing Male and female rat brain. *Endocrinology* (2019) 160(8):1771–85. doi: 10.1210/en.2019-00121

19. Gilbert ME, Hassan I, Wood C, O'Shaughnessy KL, Spring S, Thomas S, et al. Gestational exposure to perchlorate in the rat: Thyroid hormones in fetal thyroid gland, serum, and brain. *Toxicol Sci* (2022) 188(1):117–30. doi: 10.1093/toxsci/kfac038

20. Bolger AM, Lohse M, Usadel B. Trimmomatic: A flexible trimmer for illumina sequence data. *Bioinformatics* (2014) 30(15):2114–20. doi: 10.1093/bioinformatics/btu170

21. Love MI, Huber W, Anders S. Moderated estimation of fold change and dispersion for RNA-seq data with DESeq2. *Genome Biol* (2014) 15(12):550. doi: 10.1186/s13059-014-0550-8

22. Wickham H. *ggplot2: Elegant graphics for data analysis*. New York: Springer-Verlag (2016).

23. Kolde R. Pheatmap: pretty heatmaps. *R Package version* (2012) 1(2):726.

24. Garnier S, Noam R, Rudis R, Sciaini M, Pedro Camargo A, Scherer C. *Viridis - colorblind-friendly color maps for r* (2021). Available at: https://sjmgarnier.github.io/viridis/.

25. Szklarczyk D, Gable AL, Lyon D, Junge A, Wyder S, Huerta-Cepas J, et al. STRING v11: protein-protein association networks with increased coverage, supporting functional discovery in genome-wide experimental datasets. *Nucleic Acids Res* (2019) 47(D1):D607–13. doi: 10.1093/nar/gky1131

26. Hutton SR, Pevny LH. SOX2 expression levels distinguish between neural progenitor populations of the developing dorsal telencephalon. *Dev Biol* (2011) 352 (1):40–7. doi: 10.1016/j.ydbio.2011.01.015

27. Royland JE, Parker JS, Gilbert ME. A genomic analysis of subclinical hypothyroidism in hippocampus and neocortex of the developing rat brain. *J Neuroendocrinol* (2008) 20(12):1319–38. doi: 10.1111/j.1365-2826.2008.01793.x

28. O'Shaughnessy KL, Wood CR, Ford RL, Kosian PA, Hotchkiss MG, Degitz SJ, et al. Thyroid hormone disruption in the fetal and neonatal rat: Predictive hormone measures and bioindicators of hormone action in the developing cortex. *Toxicol Sci* (2018) 166 (1):163–79. doi: 10.1093/toxsci/kfy190

29. Farwell AP, Lynch RM, Okulicz WC, Comi AM, Leonard JL. The actin cytoskeleton mediates the hormonally regulated translocation of type II iodothyronine 5'-deiodinase in astrocytes. *J Biol Chem* (1990) 265(30):18546–53. doi: 10.1016/S0021-9258(17)44786-7

30. Siegrist-Kaiser CA, Juge-Aubry C, Tranter MP, Ekenbarger DM, Leonard JL. Thyroxine-dependent modulation of actin polymerization in cultured astrocytes. a novel, extranuclear action of thyroid hormone. *J Biol Chem* (1990) 265(9):5296–302. doi: 10.1016/S0021-9258(19)34121-3

31. Farwell AP, Leonard JL. Dissociation of actin polymerization and enzyme inactivation in the hormonal regulation of type II iodothyronine 5'-deiodinase activity in astrocytes. *Endocrinology* (1992) 131(2):721–8. doi: 10.1210/endo.131.2.1322280

32. Farwell AP, Tranter MP, Leonard JL. Thyroxine-dependent regulation of integrin-laminin interactions in astrocytes. *Endocrinology* (1995) 136(9):3909–15. doi: 10.1210/endo.136.9.7649099

33. Farwell AP, Dubord-Tomasetti SA, Pietrzykowski AZ, Stachelek SJ, Leonard JL. Regulation of cerebellar neuronal migration and neurite outgrowth by thyroxine and 3,3',5'-triiodothyronine. *Brain Res Dev Brain Res* (2005) 154(1):121–35. doi: 10.1016/j.devbrainres.2004.07.016

34. Farwell AP, Dubord-Tomasetti SA, Pietrzykowski AZ, Leonard JL. Dynamic nongenomic actions of thyroid hormone in the developing rat brain. *Endocrinology* (2006) 147(5):2567–74. doi: 10.1210/en.2005-1272

35. Crisanti P, Omri B, Hughes E, Meduri G, Hery C, Clauser E, et al. The expression of thyrotropin receptor in the brain. *Endocrinology* (2001) 142(2):812–22. doi: 10.1210/endo.142.2.7943

36. Davis PJ, Mousa SA, Lin HY. Nongenomic actions of thyroid hormone: The integrin component. *Physiol Rev* (2021) 101(1):319–52. doi: 10.1152/physrev.00038.2019

37. Flamant F, Cheng SY, Hollenberg AN, Moeller LC, Samarut J, Wondisford FE, et al. Thyroid hormone signaling pathways: Time for a more precise nomenclature. *Endocrinology* (2017) 158(7):2052–7. doi: 10.1210/en.2017-00250

38. Strait KA, Schwartz HL, Perez-Castillo A, Oppenheimer JH. Relationship of c-erbA mRNA content to tissue triiodothyronine nuclear binding capacity and function in developing and adult rats. *J Biol Chem* (1990) 265(18):10514–21. doi: 10.1016/S0021-9258(18)86977-0

39. Lopez-Juarez A, Remaud S, Hassani Z, Jolivet P, Pierre Simons J, Sontag T, et al. Thyroid hormone signaling acts as a neurogenic switch by repressing Sox2 in the adult neural stem cell niche. *Cell Stem Cell* (2012) 10(5):531–43. doi: 10.1016/j.stem.2012.04.008

40. Stenzel D, Wilsch-Brauninger M, Wong FK, Heuer H, Huttner WB. Integrin alphavbeta3 and thyroid hormones promote expansion of progenitors in embryonic neocortex. *Development* (2014) 141(4):795–806. doi: 10.1242/dev.101907

41. Remaud S, Ortiz FC, Perret-Jeanneret M, Aigrot MS, Gothie JD, Fekete C, et al. Transient hypothyroidism favors oligodendrocyte generation providing functional remyelination in the adult mouse brain. *Elife* (2017) 6. doi: 10.7554/eLife.29996

42. Vancamp P, Gothie JD, Luongo C, Sebillot A, Le Blay K, Butruille L, et al. Gender-specific effects of transthyretin on neural stem cell fate in the subventricular zone of the adult mouse. *Sci Rep* (2019) 9(1):19689. doi: 10.1038/s41598-019-56156-w

43. Luongo C, Butruille L, Sebillot A, Le Blay K, Schwaninger M, Heuer H, et al. Absence of both thyroid hormone transporters MCT8 and OATP1C1 impairs neural stem cell fate in the adult mouse subventricular zone. *Stem Cell Rep* (2021) 16(2):337–53. doi: 10.1016/j.stemcr.2020.12.009

44. Vancamp P, Le Blay K, Butruille L, Sebillot A, Boelen A, Demeneix BA, et al. Developmental thyroid disruption permanently affects the neuroglial output in the murine subventricular zone. *Stem Cell Rep* (2022) 17(3):459–74. doi: 10.1016/j.stemcr.2022.01.002

45. Adil MS, Narayanan SP, Somanath PR. Cell-cell junctions: structure and regulation in physiology and pathology. *Tissue Barriers* (2021) 9(1):1848212. doi: 10.1080/21688370.2020.1848212

46. Nitta T, Hata M, Gotoh S, Seo Y, Sasaki H, Hashimoto N, et al. Size-selective loosening of the blood-brain barrier in claudin-5-deficient mice. *J Cell Biol* (2003) 161(3):653–60. doi: 10.1083/jcb.200302070

47. Lai CH, Kuo KH, Leo JM. Critical role of actin in modulating BBB permeability. *Brain Res Brain Res Rev* (2005) 50(1):7–13. doi: 10.1016/j.brainresrev.2005.03.007

48. Xu L, Nirwane A, Yao Y. Basement membrane and blood-brain barrier. *Stroke Vasc Neurol* (2019) 4(2):78–82. doi: 10.1136/svn-2018-000198

49. Phoenix TN, Temple S. Spred1, a negative regulator of ras-MAPK-ERK, is enriched in CNS germinal zones, dampens NSC proliferation, and maintains ventricular zone structure. *Genes Dev* (2010) 24(1):45–56. doi: 10.1101/gad.1839510

50. Vriend I, Oegema R. Genetic causes underlying grey matter heterotopia. *Eur J Paediatr Neurol* (2021) 35:82–92. doi: 10.1016/j.ejpn.2021.09.015

51. Carabalona A, Beguin S, Pallesi-Pocachard E, Buhler E, Pellegrino C, Arnaud K, et al. A glial origin for periventricular nodular heterotopia caused by impaired expression of filamin-a. *Hum Mol Genet* (2012) 21(5):1004–17. doi: 10.1093/hmg/ddr531

52. Watrin F, Manent JB, Cardoso C, Represa A. Causes and consequences of gray matter heterotopia. *CNS Neurosci Ther* (2015) 21(2):112–22. doi: 10.1111/cns.12322

53. Rami A, Rabie A. Effect of thyroid deficiency on the development of glia in the hippocampal formation of the rat: An immunocytochemical study. *Glia* (1988) 1(5):337–45. doi: 10.1002/glia.440010506

54. Gould E, Frankfurt M, Westlind-Danielsson A, McEwen BS. Developing forebrain astrocytes are sensitive to thyroid hormone. *Glia* (1990) 3(4):283–92. doi: 10.1002/glia.440030408

55. Berbel P, Guadano-Ferraz A, Martinez M, Quiles JA, Balboa R, Innocenti GM. Organization of auditory callosal connections in hypothyroid adult rats. *Eur J Neurosci* (1993) 5(11):1465–78. doi: 10.1111/j.1460-9568.1993.tb00214.x

56. Berbel P, Auso E, Garcia-Velasco JV, Molina ML, Camacho M. Role of thyroid hormones in the maturation and organisation of rat barrel cortex. *Neuroscience* (2001) 107(3):383–94. doi: 10.1016/s0306-4522(01)00368-2

57. Martinez-Galan JR, Escobar del Rey F, Morreale de Escobar G, Santacana M, Ruiz-Marcos A. Hypothyroidism alters the development of radial glial cells in the term fetal and postnatal neocortex of the rat. *Brain Res Dev Brain Res* (2004) 153(1):109–14. doi: 10.1016/j.devbrainres.2004.08.002

58. Berbel P, Navarro D, Auso E, Varea E, Rodriguez AE, Ballesta JJ, et al. Role of late maternal thyroid hormones in cerebral cortex development: An experimental model for human prematurity. *Cereb Cortex* (2010) 20(6):1462–75. doi: 10.1093/cercor/bhp212

59. Pathak A, Sinha RA, Mohan V, Mitra K, Godbole MM. Maternal thyroid hormone before the onset of fetal thyroid function regulates reelin and downstream signaling cascade affecting neocortical neuronal migration. *Cereb Cortex* (2011) 21(1):11–21. doi: 10.1093/cercor/bhq052

60. Mohan V, Sinha RA, Pathak A, Rastogi L, Kumar P, Pal A, et al. Maternal thyroid hormone deficiency affects the fetal neocorticogenesis by reducing the proliferating pool, rate of neurogenesis and indirect neurogenesis. *Exp Neurol* (2012) 237(2):477–88. doi: 10.1016/j.expneurol.2012.07.019

61. Zamoner A, Funchal C, Jacques-Silva MC, Gottfried C, Barreto Silva FR, Pessoa-Pureur R. Thyroid hormones reorganize the cytoskeleton of glial cells through gfap phosphorylation and rhoa-dependent mechanisms. *Cell Mol Neurobiol* (2007) 27(7):845–65. doi: 10.1007/s10571-006-9084-2

62. Veeraval L, O'Leary CJ, Cooper HM. Adherens junctions: Guardians of cortical development. *Front Cell Dev Biol* (2020) 8:6. doi: 10.3389/fcell.2020.00006

63. Thind AS, Monga I, Thakur PK, Kumari P, Dindhoria K, Krzak M, et al. Demystifying emerging bulk RNA-seq applications: The application and utility of bioinformatic methodology. *Brief Bioinform* (2021) 22(6). doi: 10.1093/bib/bbab259

64. Lemkine GF, Raj A, Alfama G, Turque N, Hassani Z, Alegria-Prevot O, et al. Adult neural stem cell cycling *in vivo* requires thyroid hormone and its alpha receptor. *FASEB J* (2005) 19(7):863–5. doi: 10.1096/fj.04-2916fje

65. Gothie JD, Sebillot A, Luongo C, Legendre M, Nguyen Van C, Le Blay K, et al. Adult neural stem cell fate is determined by thyroid hormone activation of mitochondrial metabolism. *Mol Metab* (2017) 6(11):1551–61. doi: 10.1016/j.molmet.2017.08.003

66. Rodriguez E. M., Guerra M. M., Vio K., Gonzales C., Ortloff A., Batiz L. F., et al. A cell junction pathology of neural stem cells leads to abnormal neurogenesis and hydrocephalus. *Biol Res* (2012) 45(3):231–242. doi: 10.4067/S0716-97602012000300005

67. Zheng X, Boyer L, Jin M, Mertens J, Kim Y, Ma L, et al. Metabolic reprogramming during neuronal differentiation from aerobic glycolysis to neuronal oxidative phosphorylation. *Elife* (2016) 5. doi: 10.7554/eLife.13374

68. Morte B, Diez D, Auso E, Belinchon MM, Gil-Ibanez P, Grijota-Martinez C, et al. Thyroid hormone regulation of gene expression in the developing rat fetal cerebral cortex: prominent role of the Ca2+/calmodulin-dependent protein kinase IV pathway. *Endocrinology* (2010) 151(2):810–20. doi: 10.1210/en.2009-0958

69. Mollgard K, Balslev Y, Lauritzen B, Saunders NR. Cell junctions and membrane specializations in the ventricular zone (germinal matrix) of the developing sheep brain: a CSF-brain barrier. *J Neurocytol* (1987) 16(4):433–44. doi: 10.1007/BF01668498

70. Whish S, Dziegielewska KM, Mollgard K, Noor NM, Liddelow SA, Habgood MD, et al. The inner CSF-brain barrier: developmentally controlled access to the brain *via* intercellular junctions. *Front Neurosci* (2015) 9:16. doi: 10.3389/fnins.2015.00016

71. Johansson PA, Dziegielewska KM, Liddelow SA, Saunders NR. The blood-CSF barrier explained: when development is not immaturity. *Bioessays* (2008) 30(3):237–48. doi: 10.1002/bies.20718

72. Ek CJ, Dziegielewska KM, Habgood MD, Saunders NR. Barriers in the developing brain and neurotoxicology. *Neurotoxicology* (2012) 33(3):586–604. doi: 10.1016/j.neuro.2011.12.009

73. Saunders NR, Dziegielewska KM, Mollgard K, Habgood MD. Physiology and molecular biology of barrier mechanisms in the fetal and neonatal brain. *J Physiol* (2018) 596(23):5723–56. doi: 10.1113/JP275376

74. Shi Y, Zhang L, Pu H, Mao L, Hu X, Jiang X, et al. Rapid endothelial cytoskeletal reorganization enables early blood-brain barrier disruption and long-term ischaemic reperfusion brain injury. *Nat Commun* (2016) 7:10523. doi: 10.1038/ncomms10523

75. Pong S, Karmacharya R, Sofman M, Bishop JR, Lizano P. The role of brain microvascular endothelial cell and blood-brain barrier dysfunction in schizophrenia. *Complex Psychiatry* (2020) 6(1-2):30–46. doi: 10.1159/000511552

76. Thompson WO, Thompson PK, Silveus E, Dailey ME. The protein content of the cerebrospinal fluid in myxedema. *J Clin Invest* (1928) 6(2):251–5. doi: 10.1172/JCI100196

77. Schacht RA, Tourtellotte WW, Frame B, Nickel SN. Distribution of protein, lipid and administered bromide between serum and CSF in myxedema. *Metabolism* (1968) 17(9):786–93. doi: 10.1016/0026-0495(68)90028-0

78. Nystrom E, Hamberger A, Lindstedt G, Lundquist C, Wikkelso C. Cerebrospinal fluid proteins in subclinical and overt hypothyroidism. *Acta Neurol Scand* (1997) 95(5):311–4. doi: 10.1111/j.1600-0404.1997.tb00216.x

79. Frost N, Lee MS, Sweeney P. Myxedema, papilledema, and elevated CSF protein. *Neurology* (2004) 63(4):754–5. doi: 10.1212/01.wnl.0000134655.40360.ab

80. Pancotto T, Rossmeisl JHJr., Panciera DL, Zimmerman KL. Blood-brain-barrier disruption in chronic canine hypothyroidism. *Vet Clin Pathol* (2010) 39(4):485–93. doi: 10.1111/j.1939-165X.2010.00253.x

81. Pancotto TE, Rossmeisl JHJr., Huckle WR, Inzana KD, Zimmerman KL. Evaluation of endothelin-1 and MMPs-2, -9, -14 in cerebrospinal fluid as indirect indicators of blood-brain barrier dysfunction in chronic canine hypothyroidism. *Res Vet Sci* (2016) 105:115–20. doi: 10.1016/j.rvsc.2016.01.021

82. Tian L, Ni J, Guo T, Liu J, Dang Y, Guo Q, et al. TSH stimulates the proliferation of vascular smooth muscle cells. *Endocrine* (2014) 46(3):651–8. doi: 10.1007/s12020-013-0135-4

83. Zhang L, Cooper-Kuhn CM, Nannmark U, Blomgren K, Kuhn HG. Stimulatory effects of thyroid hormone on brain angiogenesis *in vivo* and *in vitro*. *J Cereb Blood Flow Metab* (2010) 30(2):323–35. doi: 10.1038/jcbfm.2009.216

84. Stolp HB, Dziegielewska KM. Review: Role of developmental inflammation and blood-brain barrier dysfunction in neurodevelopmental and neurodegenerative diseases. *Neuropathol Appl Neurobiol* (2009) 35(2):132–46. doi: 10.1111/j.1365-2990.2008.01005.x

85. Alexander EK, Pearce EN, Brent GA, Brown RS, Chen H, Dosiou C, et al. 2017 guidelines of the American thyroid association for the diagnosis and management of thyroid disease during pregnancy and the postpartum. *Thyroid* (2017) 27(3):315–89. doi: 10.1089/thy.2016.0457

86. Howard BM, Zhicheng M, Filipovic R, Moore AR, Antic SD, Zecevic N. Radial glia cells in the developing human brain. *Neuroscientist* (2008) 14(5):459–73. doi: 10.1177/1073858407313512

87. Edgar R, Domrachev M, Lash AE. Gene expression omnibus: NCBI gene expression and hybridization array data repository. *Nucleic Acids Res* (2002) 30(1):207–10. doi: 10.1093/nar/30.1.207

frontiers | Frontiers in Endocrinology

TYPE Original Research
PUBLISHED 13 February 2023
DOI 10.3389/fendo.2023.1099824

Check for updates

OPEN ACCESS

EDITED BY
Laurent M. Sachs,
Muséum National d'Histoire Naturelle, France

REVIEWED BY
Patricia Rannaud-bartaire,
Muséum National d'Histoire Naturelle, France
Wenxing Guo,
Tianjin Medical University, China

*CORRESPONDENCE
Young Ah Lee
nina337@snu.ac.kr

SPECIALTY SECTION
This article was submitted to Thyroid Endocrinology, a section of the journal Frontiers in Endocrinology

RECEIVED 16 November 2022
ACCEPTED 01 February 2023
PUBLISHED 13 February 2023

CITATION
Lee YJ, Cho SW, Lim Y-H, Kim B-N, Kim JI, Hong Y-C, Park YJ, Shin CH and Lee YA (2023) Relationship of iodine excess with thyroid function in 6-year-old children living in an iodine-replete area. *Front. Endocrinol.* 14:1099824. doi: 10.3389/fendo.2023.1099824

COPYRIGHT
© 2023 Lee, Cho, Lim, Kim, Kim, Hong, Park, Shin and Lee. This is an open-access article distributed under the terms of the Creative Commons Attribution License (CC BY). The use, distribution or reproduction in other forums is permitted, provided the original author(s) and the copyright owner(s) are credited and that the original publication in this journal is cited, in accordance with accepted academic practice. No use, distribution or reproduction is permitted which does not comply with these terms.

Relationship of iodine excess with thyroid function in 6-year-old children living in an iodine-replete area

Yun Jeong Lee[1,2], Sun Wook Cho[3,4], Youn-Hee Lim[5,6,7], Bung-Nyun Kim[8], Johanna Inhyang Kim[9], Yun-Chul Hong[6,7,10], Young Joo Park[3,4], Choong Ho Shin[1,2] and Young Ah Lee[1,2]*

[1]Department of Pediatrics, Seoul National University Children's Hospital, Seoul, Republic of Korea, [2]Department of Pediatrics, Seoul National University College of Medicine, Seoul, Republic of Korea, [3]Department of Internal Medicine, Seoul National University Hospital, Seoul, Republic of Korea, [4]Department of Internal Medicine, Seoul National University Hospital College of Medicine, Seoul, Republic of Korea, [5]Section of Environmental Health, Department of Public Health, University of Copenhagen, Copenhagen, Denmark, [6]Institute of Environmental Medicine, Seoul National University Medical Research Center, Seoul, Republic of Korea, [7]Environmental Health Center, Seoul National University College of Medicine, Seoul, Republic of Korea, [8]Division of Children and Adolescent Psychiatry, Department of Psychiatry, Seoul National University Hospital, Seoul, Republic of Korea, [9]Department of Psychiatry, Hanyang University Medical Center, Seoul, Republic of Korea, [10]Department of Preventive Medicine, Seoul National University College of Medicine, Seoul, Republic of Korea

Background: Adequate iodine intake is essential for growing children, as both deficient and excessive iodine status can result in thyroid dysfunction. We investigated the iodine status and its association with thyroid function in 6-year-old children from South Korea.

Methods: A total of 439 children aged 6 (231 boys and 208 girls) were investigated from the Environment and Development of Children cohort study. The thyroid function test included free thyroxine (FT4), total triiodothyronine (T3), and thyroid-stimulating hormone (TSH). Urine iodine status was evaluated using urine iodine concentration (UIC) in morning spot urine and categorized into iodine deficient (< 100 μg/L), adequate (100–199 μg/L), more than adequate (200–299 μg/L), mild excessive (300–999 μg/L), and severe excessive (≥ 1000 μg/L) groups. The estimated 24-hour urinary iodine excretion (24h-UIE) was also calculated.

Results: The median TSH level was 2.3 μIU/mL, with subclinical hypothyroidism detected in 4.3% of patients without sex differences. The median UIC was 606.2 μg/L, with higher levels in boys (684 μg/L vs. 545 μg/L, $p = 0.021$) than girls. Iodine status was categorized as deficient (n = 19, 4.3%), adequate (n = 42, 9.6%), more than adequate (n = 54, 12.3%), mild excessive (n = 170, 38.7%), or severe excessive (n = 154, 35.1%). After adjusting for age, sex, birth weight, gestational age, body mass index z-score, and family history, both the mild and severe excess groups showed lower FT4 ($\beta = -0.04$, $p = 0.032$ for mild excess; $\beta = -0.04$, $p = 0.042$ for severe excess) and T3 levels ($\beta = -8.12$, $p = 0.009$ for mild excess; $\beta = -9.08$, $p = 0.004$ for severe excess) compared to the adequate group. Log-transformed estimated 24h-UIE showed a positive association with log-transformed TSH levels ($\beta = 0.04$, $p = 0.046$).

Conclusion: Excess iodine was prevalent (73.8%) in 6-year-old Korean children. Excess iodine was associated with a decrease in FT4 or T3 levels and an increase in TSH levels. The longitudinal effects of iodine excess on later thyroid function and health outcomes require further investigation.

KEYWORDS

iodine, thyroid hormone, urine, thyroid function test, child, Republic of Korea

1 Introduction

Iodine is an essential micronutrient for the synthesis of thyroid hormone synthesis (1). Both iodine deficiency and excess can result in thyroid dysfunction, with a U-shaped association between iodine exposure and the risk of thyroid disease (2). Considering the critical role of thyroid function in childhood growth and development, children need an optimal iodine intake. The global health program has focused on intervention for iodine deficiency through salt iodization (3). However, with effective iodine fortification, concerns about iodine excess and its health impact have also been raised (4, 5). Iodine excess-induced hypothyroidism, resulting from failure to escape from the acute Wolff-Chaikoff effect in susceptible individuals has been reported (5) in addition to iodine-induced hyperthyroidism after iodine supplementation in iodine-deficient areas (6).

The association between iodine excess and thyroid dysfunction has been studied in the pediatric population (7–9), with some supporting results showing elevated thyroid stimulating hormone (TSH) levels in children exposed to iodine excess (8, 9). South Korea is an iodine-replete area (10) characterized by high seaweed consumption (11). According to the 2013–2015 Korean National Health and Nutrition Examination Survey, a high prevalence (64.9%) of iodine excess has been reported in Korean children and adolescents (8, 12).

In this study, we aimed to investigate the iodine status, using urine iodine measurements, and its association with thyroid function in 6-year-old Korean children.

2 Methods

2.1 Study population

This study was performed as a part of the Environment and Development of Children cohort study investigating the effects of early-life environmental risk factors on physical and neurobehavioral development (13). Among the 574 children who were examined at 6-years of age during 2015–2017 study period, 477 were evaluated for thyroid function and iodine status. Thirty-six children with multiple births and two diagnosed with thyroid disease (congenital hypothyroidism and Hashimoto's thyroiditis, respectively) were excluded. Finally, 439 children were included in this study (Supplementary Figure 1). Informed consent was waived in accordance with the institutional review board of Seoul National University Hospital (IRB no. 1704-118-848).

2.2 Anthropometric assessments and questionnaires

Height, weight, and BMI z-scores were calculated using the 2007 Korean National Growth Charts, with overweight or obesity was defined as a body mass index (BMI) above the 85th percentile (14). Data on personal and parental medical history, socioeconomic status (monthly household income and parental educational status), dietary supplement intake, and dairy product consumption were collected using structured questionnaires.

2.3 Evaluation of iodine status

Single spot urine samples were collected in the morning, after 8-hour of fasting, to measure the levels of UIC (μg/L) and urinary creatinine (Cr, mg/dL). UIC was measured by inductively coupled plasma mass spectrometry (ICP-MS), using a 7900 ICP-MS apparatus (Agilent Technologies, Santa Clara, CA, USA), and urinary Cr levels were measured by the kinetic alkaline picrate method (Architect TBA-C16000, Abbott, Abbott Park, IL, USA). The range of intra- and inter-assay coefficients of variation (CV) for UIC was 1.6-2.0% and 1.6-1.9%, respectively. The iodine status of the participants was assessed using the UIC (μg/L), iodine/Cr ratio (μg/g), and estimated 24-hour urine iodine excretion (24 h-UIE, μg/day). Children were categorized into four iodine status groups using the UIC, based on World Health Organization (WHO) recommendations: iodine deficiency (UIC < 100 μg/L), adequate (UIC 100–199 μg/L), more than adequate (UIC 200–299 μg/L), and excessive (UIC ≥ 300 μg/L) (3). The excessive group was further divided into the mild excessive (UIC 300–999 μg/L) and severe excessive (UIC ≥ 1000 μg/L) groups. The estimated 24 h-UIE (μg/day) was calculated from the iodine/Cr ratio using the following equation: estimated 24 h-UIE (μg/day) = iodine/Cr (μg/g) × predicted 24 h-Cr excretion (g/day). The predicted 24 h-Cr excretion (g/day) was determined using age- and anthropometry-based reference values (15).

2.4 Measurement of thyroid function

Thyroid function tests, including assays for free thyroxine (FT4), total triiodothyronine (T3), and TSH, were performed using a chemiluminescent microparticle immune assay on an ARCHITECT i2000 System (Abbott Korea, Seoul, Korea). The normal range was defined as 0.70–1.48 ng/dL (9.01–19.05 pmol/L) for FT4, 58–159 ng/

dL (0.89–2.44 nmol/L) for T3, and 0.38–4.94 μIU/mL for TSH, respectively. The range of CVs for FT4, T3, and TSH was 2.0-2.6%, 3.0-4.4%, and 2.6-2.9%, respectively. Subclinical hypothyroidism was defined as TSH levels between 4.94–10 μIU/mL with normal FT4 levels.

2.5 Statistical analysis

All continuous variables were tested for normality and expressed as mean ± standard deviation or median with interquartile range (IQR). Iodine parameters and TSH levels were log-transformed for analysis. The participants' characteristics were analyzed using the Student's t-test or Mann–Whitney *U*-test for continuous variables, and the chi-squared test was used for categorical variables. Clinical characteristics and thyroid function were compared among the four iodine status groups (each group vs. the iodine-adequate group as a reference group), and a Bonferroni-corrected *p*-value of 0.017 was applied when performing multiple comparisons. The linear trend in thyroid function in the UIC categories was evaluated. We used generalized additive models (GAMs) to test the nonlinear relationship between iodine measurements and thyroid hormone levels. Linear and logistic regression analyses were used to evaluate the relationship between iodine status, thyroid hormone levels, and subclinical hypothyroidism. A directed acyclic graph (DAG) was used to visualize the causal relationships among variables and to identify potential confounding variables (Supplementary Figure 2) (16). The following variables were included in the multivariate model: age, sex, gestational age, birth weight, BMI z-scores, and parental history of thyroid disease. The R Statistical Software package (version 3.6.0; R Foundation for Statistical Computing, Vienna, Austria) was used for the statistical analyses, and the statistical significance was determined as $p < 0.05$.

3 Results

3.1 Clinical characteristics

Table 1 shows the clinical characteristics of 439 children (231 boys) included in the analysis. The mean age was 5.9 ± 0.1 years and the mean BMI z-score was -0.1 ± 1.0. Twenty-one patients (4.8%) had a history of thyroid disease. Most parents (82.9% of mother and 85.2% of father) had high educational levels. The mean FT4 and T3 levels were 1.16 ± 0.11 ng/dL and 148.1 ± 18.5 ng/dL, respectively. The median TSH level was 2.29 μIU/mL (range, 0.53–8.59 μIU/mL). None of the patients showed overt hypothyroidism and 19 (4.3%) had subclinical hypothyroidism. No sex-related differences in thyroid function were observed. All children with subclinical hypothyroidism had a normal stature, with three children (15.8%)

TABLE 1 Clinical characteristics of study participants.

Variables	Total (N = 439)	Boys (n = 231)	Girls (n = 208)
Age, years	5.9 ± 0.1	5.9 ± 0.1	5.9 ± 0.1
Gestational age, weeks	39.3 ± 1.3	39.3 ± 1.3	39.3 ± 1.3
Birth weight, kg	3.3 ± 0.4	3.3 ± 0.4*	3.2 ± 0.4*
Height, cm	115.9 ± 4.5	116.5 ± 4.6*	115.2 ± 4.2*
Weight, kg	21.4 ± 3.3	21.6 ± 3.2	21.1 ± 3.3
Body mass index, kg/m^2	15.9 ± 1.8	15.9 ± 1.7	15.9 ± 2.0
Body mass index z-score	−0.06 ± 1.03	−0.14 ± 0.99	0.02 ± 1.07
Parental history of thyroid disease, n (%)	21 (4.8)	13 (5.6)	8 (3.9)
Monthly household income (> 4,000K KRW), n (%)	303 (69.0)	151 (65.4)	152 (73.1)
Paternal education level ≥ college, n (%)	374 (85.2)	197 (85.3)	177 (85.1)
Maternal education level ≥ college, n (%)	364 (82.9)	191 (82.7)	173 (83.2)
FT4, ng/dL	1.16 ± 0.11	1.17 ± 0.11	1.16 ± 0.11
T3, ng/dL	148.1 ± 18.5	147.6 ± 18.9	148.7 ± 18.0
TSH, μIU/mL	2.29 (1.71–2.98)	2.29 (1.63–2.98)	2.30 (1.76–2.99)
Subclinical hypothyroidism, n (%)	19 (4.3)	11 (4.8)	8 (3.9)
UIC, μg/L	606.2 (292.4–1446.4)	683.6 (317.1–1570.8) *	554.8 (236.8–1272.7) *
Iodine status group[a], n (%)	19/42/54/324 (4.3/9.6/12.3/73.8)	6/17/29/179 (2.6/7.4/12.6/77.5)	13/25/25/145 (6.3/12.0/12.0/69.7)
Iodine/Cr ratio, μg/g	826.1 (427.6–1856.1)	825.3 (434.2–2079.7)	838.2 (417.8–1690.8)
Estimated 24 h-UIE, μg/day	313.4 (155.9–646.3)	333.4 (166.2–802.4)	284.4 (145.4–590.8)

Data are expressed as the mean ± standard deviation, median (interquartile range), or number (%).
*$p < 0.05$ between boys and girls.
[a]Iodine status groups were as follows: iodine deficient (UIC < 100 μg/L), adequate (UIC 100 to 199 μg/L), more than adequate (UIC 200 to 299 μg/L), and excessive (UIC ≥ 300 μg/L).
UIC, urine iodine concentration; Cr, creatinine; 24h-UIE, 24-hour urinary iodine excretion; FT4, free thyroxine; T3, total triiodothyronine; TSH, thyroid stimulating hormone.

being overweight and two (10.5%) obese. None of these children showed clinical signs of hypothyroidism.

3.2 Comparison among iodine status categories

The median UIC was 606.2 μg/L (IQR, 292.4–1446.4 μg/L), with a between-sex difference (683.6 μg/L in boys vs. 554.8 μg/L in girls, p = 0.021, Table 1). The distribution of iodine status categories was as follows: iodine deficient (n = 19, 4.3%), adequate (n = 42, 9.6%), more than adequate (n = 54, 12.3%), or excessive (n = 324, 73.8%). The median iodine/Cr and estimated 24 h-UIE levels were 826.1 μg/g and 313.4 μg/day, respectively, with no between-sex difference. There were no differences in clinical characteristics among the four iodine categories (Supplementary Table 1). In addition, dietary supplement intake or proportion of high dairy product consumption (≥ 2 cups/day) did not differ among the four groups.

As shown in Table 2, we compared the three iodine status categories (iodine deficient, more than adequate, and excessive groups) with the reference category (iodine adequate group). The iodine excessive group showed lower T3 levels (147.2 vs. 155.1 mg/dL, p = 0.010), as revealed by the Bonferroni correction (p = 0.017). Interestingly, 17 (89.5%) of the 19 children with subclinical hypothyroidism had excessive iodine. However, FT4 and log-transformed TSH (log-TSH) levels and the risk of subclinical hypothyroidism did not differ among the four iodine categories.

3.3 Relationship between iodine status and thyroid function

Due to the high prevalence of iodine excess, iodine status was classified into five categories [deficient, adequate, more than adequate, mild excessive (UIC of 300–999 μg/L, n = 170, 38.7%), and severe excessive (UIC ≥ 1000 μg/L, n = 154, 35.1%)]. The results of the univariate analysis are described in Supplementary Tables 2, 3. After adjusting for age, sex, gestational age, birth weight, BMI z-scores, and parental history of thyroid disease, a multivariate-adjusted model was constructed to compare thyroid function among the five iodine categories. Compared to the reference category (iodine adequate group), the more than adequate group showed lower T3 levels (β = −8.62, p = 0.021, Figure 1B) and log-TSH levels (β = −0.19, p = 0.035, Figure 1C), and both mild and severe excessive groups showed lower FT4 (β = −0.04, p = 0.032; mild excessive group: β = −0.04, p = 0.042 for the severe excessive group; Figure 1A) and T3 levels (β = −8.12, p = 0.009, for the mild excessive group; β = −9.08, p = 0.004 for the severe excessive group; Figure 1B). In a sex-stratified analysis, these associations for iodine excess were significant in girls but not in boys (Figure 1; Table 3). In girls, FT4 and T3 levels were lower in the iodine-deficient group than in the iodine-adequate group with marginal significance. Due to the small number of children with adequate and more than adequate group, we performed a sensitivity analysis by combining the two groups as a reference category. The results showed the similar trends of lower FT4 and T3 and higher TSH levels among the iodine excess group compared to reference group (Supplementary Table 4).

We investigated the nonlinear relationship between iodine measurements and thyroid hormone levels using GAM but did not reveal clear nonlinear relationships (Supplementary Figure 3). To focus on the association between iodine excess and thyroid function, we analyzed iodine-sufficient or-excessive children (n = 420) after excluding iodine-deficient children (n = 19). Results of the univariate analysis are reported in Supplementary Table 5, showing positive associations between continuous iodine variables and log-TSH levels in girls. After adjusting for covariates, log-transformed iodine/Cr (log-iodine/Cr) and log-transformed estimated 24 h-UIE (log-estimated 24 h-UIE) levels were significantly associated with log-TSH levels (β = 0.05, p = 0.035 for log-iodine/Cr; β = 0.04, p = 0.046 for log-estimated 24 h-UIE, Table 4). In a sex-stratified analysis, a positive relationship between log-iodine/Cr and log-estimated 24 h-UIE and log-TSH levels was found only in girls (p < 0.05, Table 4) but

TABLE 2 Thyroid function status according to iodine status.

	Deficient (UIC < 100 μg/L)	Adequate (UIC 100 to 199 μg/L)	More than adequate (UIC 200 to 299 μg/L)	Excessive (UIC ≥ 300 μg/L)	*P* for trend	*P* for between group comparison[a] (each group vs. adequate group as reference)		
						Pa	*Pb*	*Pc*
Total, n	19	42	54	324		–	–	–
FT4, ng/dL	1.16 ± 0.09	1.20 ± 0.10	1.18 ± 0.12	1.16 ± 0.11	0.125	0.147	0.412	0.032
T3, ng/dL	150.7 ± 17.0	155.1 ± 20.4	147.2 ± 18.1	147.2 ± 18.2	0.034	0.414	0.048	0.010
Log-transformed TSH, μIU/mL	0.72 ± 0.39	0.87 ± 0.37	0.67 ± 0.47	0.84 ± 0.45	0.213	0.155	0.028	0.740
Subclinical hypothyroidism, n (%)	0 (0.0)	1 (2.4)	1 (1.9)	17 (5.3)	0.127	0.999	0.999	0.668

Pa, adequate vs. deficient; *Pb*, adequate vs. more than adequate; *Pc*, adequate vs. excessive.
[a]Bonferroni correction was applied for multiple comparisons and the significance level was set at p < 0.017.
Data are expressed as the mean (standard deviation) or number (%).
UIC, urine iodine concentration, FT4, free thyroxine; T3, total triiodothyronine; TSH, thyroid stimulating hormone.

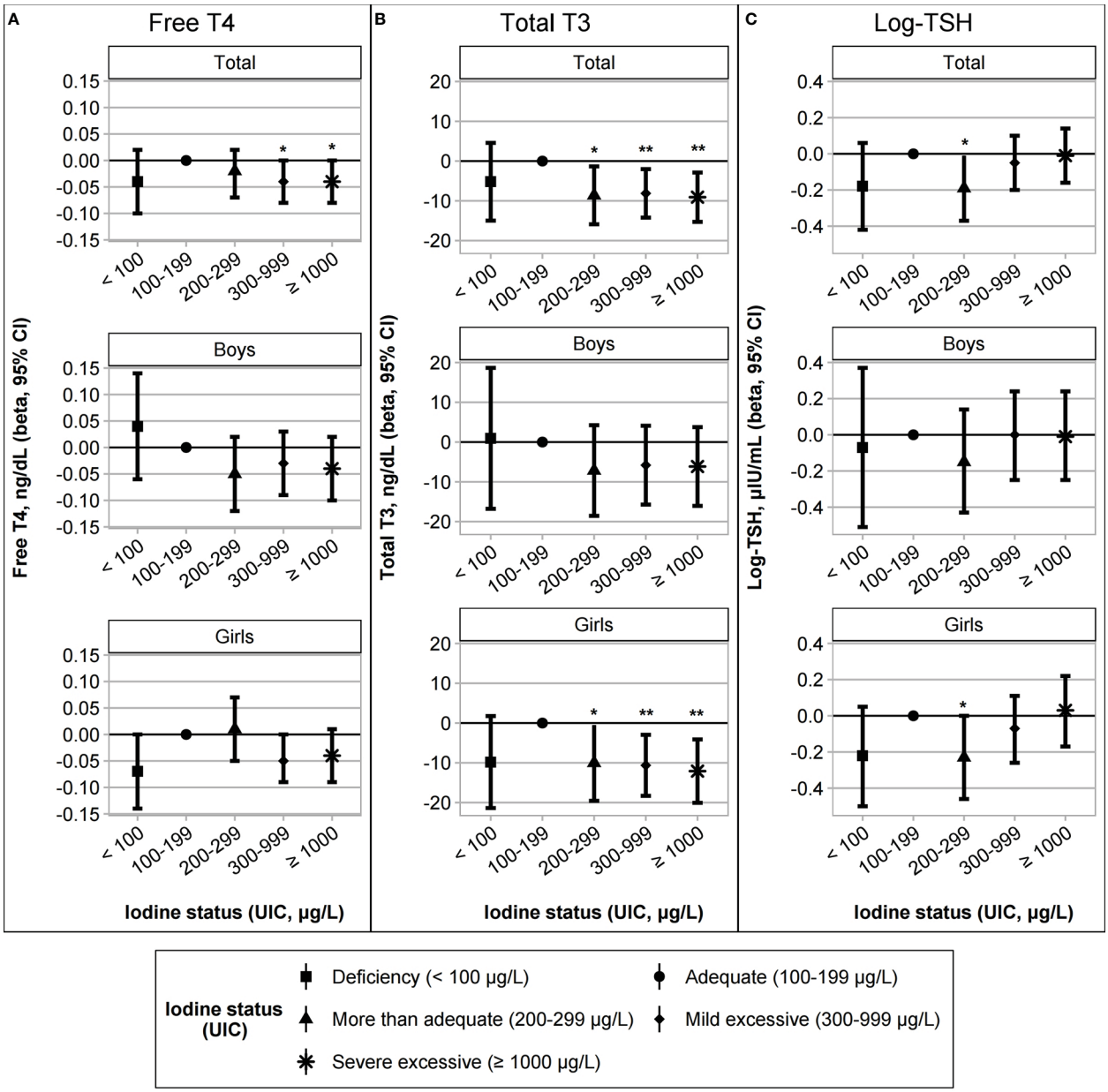

FIGURE 1
Association between iodine status and thyroid function **(A)** free T4, **(B)** total T3, and **(C)** log-transformed TSH levels. The iodine status groups were categorized as deficient (UIC < 100 μg/L, n = 19), adequate (UIC 100–199 μg/L, n = 42), more than adequate (UIC 200–299 μg/L, n = 54), mild excessive (UIC 300–999 μg/L, n = 170), or severe excessive (UIC ≥ 1000 μg/L, n = 154). Regression models for the total group were adjusted for age, sex, gestational age, birth weight, body mass index z-scores, and a parental history of thyroid disease. The sex-stratified models were adjusted for age, gestational age, birth weight, body mass index z-scores, and parental history of thyroid disease. *$p < 0.05$; **$p < 0.01$.

not in boys. FT4 and T3 levels were not associated with log-transformed UIC, iodine/Cr, nor estimated 24 h-UIE levels in either sex. The risk of subclinical hypothyroidism was not associated with continuous iodine variables (Supplementary Table 6).

4 Discussion

Among 6-year-old children living in South Korea, iodine excess was prevalent (73.8%), with a median UIC level of 606 μg/L. Only 9.6% of the children showed adequate iodine status, with a low frequency (4.3%) of iodine deficiency. Compared to the iodine adequate group, the iodine excessive group exhibited lower FT4 and T3 levels, and the log-estimated 24 h-UIE showed a positive association with log-TSH levels. In a sex-stratified analysis, this trend was only significant in girls. Although iodine excess was reported to be prevalent in Korean children, 6 to 19 years of age, this is the first study showing a decreasing trend of FT4 and T3 levels within the normal range in the iodine excess group and an increasing trend of log-TSH levels, with higher urine iodine excretion in Korean prepubertal children.

TABLE 3 Association between the iodine status and thyroid hormone levels after adjusting for covariates (multivariate models).

Category	UIC, μg/L	N	FT4, ng/dL (β, 95% CI)			T3, ng/dL (β, 95% CI)			Log-transformed TSH, μIU/mL (β, 95% CI)		
			Total (n = 439)	Boys (n = 231)	Girls (n = 208)	Total (n = 439)	Boys (n = 231)	Girls (n = 208)	Total (n = 439)	Boys (n = 231)	Girls (n = 208)
Deficient	<100	19	−0.04 (−0.10, 0.02)	0.04 (−0.06, 0.14)	−0.07 (−0.14, 0.00)	−5.21 (−14.98, 4.57)	0.94 (−16.78, 18.65)	−9.81 (−21.37, 1.75)	−0.18 (−0.42, 0.06)	−0.07 (−0.51, 0.37)	−0.22 (−0.50, 0.05)
Adequate	100–199	42	0 [Ref]			0 [Ref]			0 [Ref]		
More than adequate	200–299	54	−0.02 (−0.07, 0.02)	−0.05 (−0.12, 0.02)	0.01 (−0.05, 0.07)	−8.62 (−15.89, −1.34)*	−7.16 (−18.56, 4.24)	−10.02 (−19.55, −0.49)*	−0.19 (−0.37,−0.01)*	−0.15 (−0.43, 0.14)	−0.23 (−0.46, 0.00)*
Mild excessive	300–999	170	−0.04 (−0.08, 0.00)*	−0.03 (−0.09, 0.03)	−0.05 (−0.09, 0.00)	−8.12 (−14.22, −2.03)**	−5.81 (−15.72, 4.10)	−10.63 (−18.30, −2.96)**	−0.05 (−0.20, 0.10)	0.00 (−0.25, 0.24)	−0.07 (−0.26, 0.11)
Severe excessive	≥ 1000	154	−0.04 (−0.08, 0.00)*	−0.04 (−0.10, 0.02)	−0.04 (−0.09, 0.01)	−9.08 (−15.29, −2.88)**	−6.15 (−16.05, 3.75)	−12.09 (−20.06, −4.12)**	−0.01 (−0.16, 0.14)	−0.01 (−0.25, 0.24)	0.03 (−0.17, 0.22)

UIC, urine iodine concentration, FT4, free thyroxine; T3, total triiodothyronine; TSH, thyroid stimulating hormone; N, number; CI, confidence interval; Ref, Reference.
Regression models for the total group were adjusted for age, sex, gestational age, birth weight, body mass index z-scores, and parental history of thyroid disease. Sex-stratified models were adjusted for age, gestational age, birth weight, body mass index z-scores, and parental history of thyroid disease.
*$p < 0.05$; **$p < 0.01$.

The high levels of the median UIC (606 μg/L (IQR, 292.4–1466.4]) and the high prevalence of iodine excess (73.8%) in 6-year-old children were comparable to previous pediatric reports in children 6 to 19 years of age (median UIC of 449 μg/L and 64.9% of iodine excess) (8). This was higher than the UIC of 274 ug/L in the adult population, according to the same database from the Korean National Health and Nutrition Examination Survey from 2013–2015 (17). Excessive iodine status has been reported in Korean children, ranging from 54.9% to 76.7% prevalence of iodine excess and 328 to 458 μg/L median UIC (18–20). Common dietary sources of iodine in Korea include seaweeds, such as sea mustard, laver, kelp, as well as pickled vegetables, milk, and dairy products (11). However, there were no significant differences in dairy product consumption among iodine status groups in this study. Higher UIC levels in boys than in girls may result from higher consumption of iodine-rich food and higher energy intake in boys (21). Considering the absence of sex differences in Cr-adjusted iodine variables, sex differences in UIC may be due to differences in urine volume or hydration status (12, 17).

The decreasing trend in FT4 and T3 levels with increasing TSH levels in the iodine excess group suggests a possible risk for iodine excess-associated hypothyroidism. Although the prevalence of subclinical hypothyroidism was not significantly different among the iodine groups (2.4% in the adequate and 5.3% in the excess group), 89.5% (17 of 19 children) of children with subclinical hypothyroidism had an iodine excess. Several pediatric studies have supported the effect of iodine excess on a shift in FT4 or T3 to lower levels (8), TSH towards higher levels (8, 9, 22), and an increased risk of subclinical hypothyroidism (23). However, some studies have reported no significant associations (7, 24). The prevalence of subclinical hypothyroidism among iodine groups also varied according to the geographic region and age group. A previous nationwide Korean study showed significantly different frequencies of subclinical hypothyroidism: 3.9% in the iodine adequate and 6.6% in the excess group (8). A Chinese study also reported similar results, with a higher prevalence of subclinical hypothyroidism in high iodine area (6.7%, median UIC of 1030 μg/L) than in adequate iodine area (0.7%, median UIC of 123 μg/L) (23). However, an international study performed in 12 countries showed similar rates of subclinical hypothyroidism in the iodine adequate (0.5%) and excess (0.6%) group (9). A meta-analysis found that chronic exposure to excess iodine increased the odds ratio for subclinical and overt hypothyroidism in adults but not children, possibly due to the high heterogeneity of the included pediatric studies (4). Previous pediatric studies were limited by reporting the crude differences in thyroid hormone levels among UIC groups (8, 9, 22, 24). Only a few pediatric studies have performed the adjusted relationship between iodine status and thyroid function (7, 23). The use of multivariate-adjusted regression models strengthened the findings in our study.

We found lower FT4 levels in girls in the iodine-deficient group than in the adequate group. However, our results were limited by the small number of participants in iodine-deficient groups. Iodine deficiency is associated with hypothyroidism and goiter in children (25). Thus, both iodine deficiency and excess can lead to impaired thyroid hormone production, suggesting a U-shaped correlation (2). A recent nationwide study in Korean children and adolescents (10–19 years of age) also showed a U-shape and an inverted U-shape correlation between serum TSH and FT4 levels and UIC, respectively (8).

TABLE 4 Association between continuous iodine variables and thyroid hormone levels after adjusting for covariates.

Variables	FT4, ng/dL (β, 95% CI)			T3, ng/dL (β, 95% CI)			Log-transformed TSH, μIU/mL (β, 95% CI)		
	Total (n = 420)	Boys (n = 225)	Girls (n = 195)	Total (n = 420)	Boys (n = 225)	Girls (n = 195)	Total (n = 420)	Boys (n = 225)	Girls (n = 195)
Log-transformed UIC, μg/L	−0.01 (−0.02, 0.00)	−0.01 (−0.02, 0.01)	0.00 (−0.02, 0.01)	−1.49 (−3.18, 0.19)	−0.60 (−2.99, 1.79)	−2.38 (−4.79, 0.04)	0.03 (−0.01, 0.07)	0.01 (−0.05, 0.07)	0.05 (0.00, 0.11)
Log-transformed iodine/Cr, μg/g	−0.01 (−0.02, 0.01)	−0.01 (−0.02, 0.01)	−0.01 (−0.02, 0.01)	−1.23 (−2.98, 0.52)	−0.57 (−3.01, 1.88)	−1.85 (−4.46, 0.76)	0.05 (0.00, 0.09)*	0.03 (−0.03, 0.09)	0.08 (0.02, 0.14)**
Log-transformed estimated 24 h-UIE, μg/day	−0.01 (−0.02, 0.00)	−0.01 (−0.02, 0.01)	−0.01 (−0.02, 0.01)	−1.23 (−2.98, 0.51)	−0.56 (−2.98, 1.85)	−1.89 (−4.51, 0.74)	0.04 (0.00, 0.09)*	0.03 (−0.04, 0.09)	0.08 (0.02, 0.14)*

UIC, urine iodine concentration; Cr, creatinine; 24h-UIE, 24-hour urinary iodine excretion; FT4, free thyroxine; T3, total triiodothyronine; TSH, thyroid stimulating hormone.
The iodine-deficient group (n = 19) was excluded from analysis. Regression models for the total group were adjusted for age, sex, gestational age, birth weight, body mass index z-scores, and parental history of thyroid disease. The sex-stratified models were adjusted for age, gestational age, birth weight, body mass index z-scores, and parental history of thyroid disease.
*$p < 0.05$; **$p < 0.01$.

The mechanisms underlying iodine-induced thyroid dysfunction include failure to escape Wolff-Chaikoff effects or iodine-induced thyroid autoimmunity (5), although there is a possibility of additional mechanisms. Acute iodine excess can cause a transient decrease in thyroid hormone production by inhibiting thyroid peroxidase activity or intrathyroidal deiodinase activity, called the Wolff-Chaikoff effect (5). Healthy individuals can maintain normal thyroid function by escaping the Wolff-Chaikoff effect within several days, through a decrease in sodium iodine symporter expression. However, failure of this adaptation can lead to iodine-induced hypothyroidism in susceptible populations, such as infants, the elderly, or those with thyroid diseases (5, 26, 27). In addition, high iodine levels may induce thyroid autoimmunity, leading to elevated TSH levels and hypothyroidism (26). As this study included healthy children, iodine-induced thyroid dysfunction was not definite in our study population. However, a decreasing trend in thyroid hormone levels was observed in the iodine-excessive group.

Only girls showed a significant association between iodine status and thyroid function in this study. A Korean adult study reported that the correlation between iodine status and the thyroid disease was only significant in women, suggesting that women may be more susceptible to excessive iodine exposure (28). Estrogen, directly and indirectly, affects thyroid gland proliferation and function, including iodine uptake through the sodium-iodine symporter and thyroid peroxidase activity (29). However, because this study included prepubertal children, the mechanisms underlying sex differences remain unclear.

In this study, a higher BMI z-score and lower gestational age were associated with higher serum T3 levels in our sample of 6-year-old children. With regard to childhood obesity, the positive relationship between BMI and T3 levels can be explained by an adaptation process to increase resting energy expenditure or elevated deiodinase activity (30–32). The relationship between prematurity and childhood thyroid function has previously been reported, showing trends towards decrease in free T4 and an increase in T3 and TSH levels (33, 34), although the underlying mechanisms remains to be determined.

We used UIC, iodine/Cr ratio, and the estimated 24h-UIE as iodine variables in this study. Although measurement of 24h-UIE is the most reliable method to evaluate iodine status, it is difficult to apply in field studies (35, 36). UIC from spot urine has been the most widely used biomarker for iodine status in populations as >90% of dietary iodine is excreted by urine, although UIC is influenced by urine volume and hydration status (35). UIC related to urinary Cr has been used to overcome this limitation to determine iodine status. In children, anthropometry-based 24-h urinary Cr reference values can be used to estimate the 24h-UIE from spot urine (15). Several pediatric studies have reported that the estimated 24h-UIE better reflects measured 24h-UIE than UIC, providing a valid and reliable alternative to measured 24h-UIE (37, 38). In this study, we used the estimated 24h-UIE to complement UIC and identified a significant positive association between the estimated 24h-UIE and TSH levels.

The limitations of our study need to be acknowledged in the interpretation of findings to practice. Foremost is the cross-sectional design and relatively small sample size, including the small proportion of participants in the non-iodine excess group, which did not allow us to evaluate the relationship between iodine deficiency and thyroid function. Further studies using a prospective design and

focusing on environmental sources of iodine excess are needed to generalize the adverse effects of iodine excess on health outcomes and to suggest preventive strategies for iodine excess. Second, the single-spot urine collection used in this study to assess UIC for iodine status could not reflect within-day and day-to-day variations in urine iodine excretion. Although we could not collect 24 h urine samples or repeatedly collect spot urine samples, an ideal way to provide a valid estimate of iodine status (39), spot urine samples collected in the morning after overnight fasting can eliminate within-day variations. In addition, we obtained similar results regardless of which iodine variables (UIC or urinary Cr-adjusted iodine status) used to examine the association between iodine status and thyroid function (35). Third, we could not evaluate thyroid autoantibodies in all study populations. However, thyroid autoantibodies were not detected in our children with subclinical hypothyroidism. Considering the low prevalence of positive thyroid autoantibodies (2.3%) in Korean children and adolescents (8), the modifying effect of thyroid autoimmunity is insignificant in our 6-year-old children. Fourth, potential confounders, such as exposure to endocrine disrupting chemicals (EDCs) or heavy metals that can affect thyroid dysfunction, were not considered in this study. The mixed effects of various thyroid disrupting chemicals, including both iodine and other EDCs, need further investigation.

In conclusion, iodine was deficient in 4.3%, adequate in 21.9%, and excessive in 73.8% of 6-year-old children living in South Korea during 2015–2017. Furthermore, excess iodine was associated with decreased FT4 or T3 levels and increased TSH levels, particularly in girls. The long-term health effects of iodine excess remain to be determined, considering the high prevalence of iodine excess in Korean children. Further studies to determine the optimal iodine intake are required.

Data availability statement

The datasets presented in this article are not readily available because the fundamental results of the study are reported in the paper and supporting information. The raw data cannot be shared publicly due to ethical restrictions because they contain potentially sensitive information. The data are available upon reasonable request from the Scientific Research Committee. Requests to access the datasets should be directed to YJL, yjlee103@naver.com.

Ethics statement

The studies involving human participants were reviewed and approved by Institutional Review Board of Seoul National University Hospital (IRB no. 1704-118-848). Written informed consent from the participants' legal guardian/next of kin was not required to participate in this study in accordance with the national legislation and the institutional requirements.

Author contributions

YJL carried out the initial analyses, drafted the initial manuscript, and reviewed and revised the manuscript. SWC, Y-HL, B-NK, JIK, Y-CH, YJP, and CHS conceptualized and designed the study, coordinated and supervised data collection, and critically reviewed the manuscript for important intellectual content. YAL conceptualized and designed the study, collected data, and reviewed and revised the manuscript. All authors contributed to the article and approved the submitted version.

Funding

The EDC study was initially supported by grants from the Environmental Health Center funded by the Korean Ministry of Environment, a grant from the Ministry of Food and Drug Safety in 2018 (18162MFDS121), and the Center for Environmental Health through the Ministry of Environment. This study was supported by a National Research Foundation of Korea (NRF) grant funded by the Ministry of Education, Science, and Technology (MEST) of the Korean government (No. 2021R1A2C1011241). This research was supported by the Research Program 2017, funded by the Seoul National University College of Medicine Research Foundation (No. 800-20170140). This study was supported by a grant from the SNUH Research Fund (no. 04-2016-3020).

Acknowledgments

The authors thank Kyung-shin Lee, Jin-A Park, Ji-Young Lee, and Yumi Choi for their assistance with data collection. The Biospecimens and data used in this study were provided by the Biobank of Seoul National Univrsity Hospital, a member of the Korea Biobank Network.

Conflict of interest

The authors declare that the research was conducted in the absence of any commercial or financial relationships that could be construed as a potential conflict of interest.

Publisher's note

All claims expressed in this article are solely those of the authors and do not necessarily represent those of their affiliated organizations, or those of the publisher, the editors and the reviewers. Any product that may be evaluated in this article, or claim that may be made by its manufacturer, is not guaranteed or endorsed by the publisher.

Supplementary material

The Supplementary Material for this article can be found online at: https://www.frontiersin.org/articles/10.3389/fendo.2023.1099824/full#supplementary-material

References

1. Chung HR. Iodine and thyroid function. *Ann Pediatr Endocrinol Metab* (2014) 19 (1):8–12. doi: 10.6065/apem.2014.19.1.8

2. Laurberg P, Pedersen IB, Carlé A, Knudsen N, Andersen S, Ovesen L, et al. The U-shaped curve of iodine intake and thyroid disorders. In: Preedy VR, Burrow GN, Watson R, editors. *Comprehensive handbook of iodine*. San Diego: Elsevier (2009). p. 449–55.

3. World Health Organization. *Assessment of iodine deficiency disorders and monitoring their elimination: a guide for programme managers* ([amp]]lrm;2007). World Health Organization. Available at: https://apps.who.int/iris/handle/10665/43781 (Accessed May 15, 2022).

4. Katagiri R, Yuan X, Kobayashi S, Sasaki S. Effect of excess iodine intake on thyroid diseases in different populations: A systematic review and meta-analyses including observational studies. *PloS One* (2017) 12(3):e0173722. doi: 10.1371/journal.pone.0173722

5. Leung AM, Braverman LE. Consequences of excess iodine. *Nat Rev Endocrinol* (2014) 10(3):136–42. doi: 10.1038/nrendo.2013.251

6. Stanbury JB, Ermans AE, Bourdoux P, Todd C, Oken E, Tonglet R, et al. Iodine-induced hyperthyroidism: Occurrence and epidemiology. *Thyroid* (1998) 8(1):83–100. doi: 10.1089/thy.1998.8.83

7. Chen W, Zhang Y, Hao Y, Wang W, Tan L, Bian J, et al. Adverse effects on thyroid of Chinese children exposed to long-term iodine excess: Optimal and safe tolerable upper intake levels of iodine for 7- to 14-y-old children. *Am J Clin Nutr* (2018) 107(5):780–8. doi: 10.1093/ajcn/nqy011

8. Kang MJ, Hwang IT, Chung HR. Excessive iodine intake and subclinical hypothyroidism in children and adolescents aged 6-19 years: Results of the sixth Korean national health and nutrition examination survey, 2013-2015. *Thyroid* (2018) 28(6):773–9. doi: 10.1089/thy.2017.0507

9. Zimmermann MB, Aeberli I, Andersson M, Assey V, Yorg JA, Jooste P, et al. Thyroglobulin is a sensitive measure of both deficient and excess iodine intakes in children and indicates no adverse effects on thyroid function in the UIC range of 100-299 mug/L: a UNICEF/ICCIDD study group report. *J Clin Endocrinol Metab* (2013) 98 (3):1271–80. doi: 10.1210/jc.2012-3952

10. Iodine Global Network. *Global scorecard of iodine nutrition in 2017 in the general population and in pregnant women (PW)* (2017). Iodine Global Network. Available at: https://www.ign.org/cm_data/IGN_Global_Scorecard_AllPop_and_PW_May2017.pdf (Accessed May 15, 2022).

11. Choi JY, Ju DL, Song YJ. Revision of an iodine database for Korean foods and evaluation of dietary iodine and urinary iodine in Korean adults using 2013-2015 Korea national health and nutrition examination survey. *J Nutr Health* (2020) 53(3):271–87. doi: 10.4163/jnh.2020.53.3.271

12. Choi YC, Cheong JI, Chueh HW, Yoo JH. Iodine status and characteristics of Korean adolescents and their parents based on urinary iodine concentration: A nationwide cross-sectional study. *Ann Pediatr Endocrinol Metab* (2019) 24(2):108–15. doi: 10.6065/apem.2019.24.2.108

13. Kim KN, Lim YH, Shin CH, Lee YA, Kim BN, Kim JI, et al. Cohort profile: The environment and development of children (EDC) study: A prospective children's cohort. *Int J Epidemiol* (2018) 47(4):1049–50f. doi: 10.1093/ije/dyy070

14. Moon JS, Lee SY, Nam CM, Choi JM, Choi BK, Seo JW, et al. 2007 Korean National growth chart: review of developmental process and an outlook. *Korean J Pediatr* (2008) 51(1):1–25. doi: 10.3345/kjp.2008.51.1.1

15. Remer T, Neubert A, Maser-Gluth C. Anthropometry-based reference values for 24-h urinary creatinine excretion during growth and their use in endocrine and nutritional research. *Am J Clin Nutr* (2002) 75(3):561–9. doi: 10.1093/ajcn/75.3.561

16. Textor J, van der Zander B, Gilthorpe MS, Liskiewicz M, Ellison GT. Robust causal inference using directed acyclic graphs: The r package 'dagitty'. *Int J Epidemiol* (2016) 45 (6):1887–94. doi: 10.1093/ije/dyw341

17. Kim HI, Oh HK, Park SY, Jang HW, Shin MH, Kim SW, et al. Urinary iodine concentration and thyroid hormones: Korea national health and nutrition examination survey 2013-2015. *Eur J Nutr* (2019) 58(1):233–40. doi: 10.1007/s00394-017-1587-8

18. Choi YS, Ock S, Kwon S, Jung SB, Seok KH, Kim YJ, et al. Excessive iodine status among school-age children in Korea: A first report. *Endocrinol Metab (Seoul)* (2017) 32 (3):370–4. doi: 10.3803/EnM.2017.32.3.370

19. Lee J, Kim JH, Lee SY, Lee JH. Iodine status in Korean preschool children as determined by urinary iodine excretion. *Eur J Nutr* (2014) 53(2):683–8. doi: 10.1007/s00394-013-0558-y

20. Lee JH. Analysis of urine iodine concentration by inductively coupled plasma-mass spectrometry method in normally developed children aged less than 7 years in masan city (Korea). *J Korean Child Neurol Soc* (2011) 19(3):199–207.

21. Vila L, Donnay S, Arena J, Arrizabalaga JJ, Pineda J, Garcia-Fuentes E, et al. Iodine status and thyroid function among Spanish schoolchildren aged 6-7 years: the tirokid study. *Br J Nutr* (2016) 115(9):1623–31. doi: 10.1017/S0007114516000660

22. Medani AM, Elnour AA, Saeed AM. Excessive iodine intake, water chemicals and endemic goitre in a Sudanese coastal area. *Public Health Nutr* (2013) 16(9):1586–92. doi: 10.1017/S1368980012004685

23. Sang Z, Chen W, Shen J, Tan L, Zhao N, Liu H, et al. Long-term exposure to excessive iodine from water is associated with thyroid dysfunction in children. *J Nutr* (2013) 143(12):2038–43. doi: 10.3945/jn.113.179135

24. Nepal AK, Suwal R, Gautam S, Shah GS, Baral N, Andersson M, et al. Subclinical hypothyroidism and elevated thyroglobulin in infants with chronic excess iodine intake. *Thyroid* (2015) 25(7):851–9. doi: 10.1089/thy.2015.0153

25. Zimmermann MB, Boelaert K. Iodine deficiency and thyroid disorders. *Lancet Diabetes Endocrinol* (2015) 3(4):286–95. doi: 10.1016/s2213-8587(14)70225-6

26. Laurberg P, Cerqueira C, Ovesen L, Rasmussen LB, Perrild H, Andersen S, et al. Iodine intake as a determinant of thyroid disorders in populations. *Best Pract Res Clin Endocrinol Metab* (2010) 24(1):13–27. doi: 10.1016/j.beem.2009.08.013

27. Farebrother J, Zimmermann MB, Andersson M. Excess iodine intake: Sources, assessment, and effects on thyroid function. *Ann N Y Acad Sci* (2019) 1446(1):44–65. doi: 10.1111/nyas.14041

28. Kim S, Kwon YS, Kim JY, Hong KH, Park YK. Association between iodine nutrition status and thyroid disease-related hormone in Korean adults: Korean national health and nutrition examination survey VI (2013-2015). *Nutrients* (2019) 11(11):2757. doi: 10.3390/nu11112757

29. Santin AP, Furlanetto TW. Role of estrogen in thyroid function and growth regulation. *J Thyroid Res* (2011) 2011:875125. doi: 10.4061/2011/875125

30. Metwalley KA, Farghaly HS. Subclinical hypothyroidism in children: updates for pediatricians. *Ann Pediatr Endocrinol Metab* (2021) 26(2):80–5. doi: 10.6065/apem.2040242.121

31. Reinehr T. Thyroid function in the nutritionally obese child and adolescent. *Curr Opin Pediatr* (2011) 23(4):415–20. doi: 10.1097/MOP.0b013e328344c393

32. Marras V, Casini MR, Pilia S, Carta D, Civolani P, Porcu M, et al. Thyroid function in obese children and adolescents. *Horm Res Paediatr* (2010) 73(3):193–7. doi: 10.1159/000284361

33. Radetti G, Fanolla A, Pappalardo L, Gottardi E. Prematurity may be a risk factor for thyroid dysfunction in childhood. *J Clin Endocrinol Metab* (2007) 92(1):155–9. doi: 10.1210/jc.2006-1219

34. Posod A, Odri Komazec I, Pupp Peglow U, Meraner D, Griesmaier E, Kiechl-Kohlendorfer U. Former very preterm infants show alterations in thyroid function at a preschool age. *BioMed Res Int* (2017) 2017:3805370. doi: 10.1155/2017/3805370

35. Rohner F, Zimmermann M, Jooste P, Pandav C, Caldwell K, Raghavan R, et al. Biomarkers of nutrition for development–iodine review. *J Nutr* (2014) 144(8):1322S–42S. doi: 10.3945/jn.113.181974

36. Vejbjerg P, Knudsen N, Perrild H, Laurberg P, Andersen S, Rasmussen LB, et al. Estimation of iodine intake from various urinary iodine measurements in population studies. *Thyroid* (2009) 19(11):1281–6. doi: 10.1089/thy.2009.0094

37. Montenegro-Bethancourt G, Johner SA, Stehle P, Neubert A, Remer T. Iodine status assessment in children: Spot urine iodine concentration reasonably reflects true twenty-four-hour iodine excretion only when scaled to creatinine. *Thyroid* (2015) 25 (6):688–97. doi: 10.1089/thy.2015.0006

38. Chen W, Li X, Guo X, Shen J, Tan L, Lin L, et al. Urinary iodine excretion (UIE) estimated by iodine/creatinine ratio from spot urine in Chinese school-age children. *Clin Endocrinol (Oxf)* (2017) 86(4):628–33. doi: 10.1111/cen.13282

39. Konig F, Andersson M, Hotz K, Aeberli I, Zimmermann MB. Ten repeat collections for urinary iodine from spot samples or 24-hour samples are needed to reliably estimate individual iodine status in women. *J Nutr* (2011) 141(11):2049–54. doi: 10.3945/jn.111.144071

frontiers | Frontiers in Endocrinology

TYPE Original Research
PUBLISHED 23 March 2023
DOI 10.3389/fendo.2023.1174600

Check for updates

OPEN ACCESS

EDITED BY
Laurent M. Sachs,
Muséum National d'Histoire Naturelle, France

REVIEWED BY
Frédéric Flamant,
Université de Lyon, France
Pieter Vancamp,
Essen University Hospital, Germany

*CORRESPONDENCE
Douglas Forrest
forrestd@niddk.nih.gov

SPECIALTY SECTION
This article was submitted to Thyroid Endocrinology, a section of the journal Frontiers in Endocrinology

RECEIVED 26 February 2023
ACCEPTED 08 March 2023
PUBLISHED 23 March 2023

CITATION
Ng L, Liu H, Liu Y and Forrest D (2023) Biphasic expression of thyroid hormone receptor TRβ1 in mammalian retina and anterior ocular tissues.
Front. Endocrinol. 14:1174600.
doi: 10.3389/fendo.2023.1174600

COPYRIGHT
© 2023 Ng, Liu, Liu and Forrest. This is an open-access article distributed under the terms of the Creative Commons Attribution License (CC BY). The use, distribution or reproduction in other forums is permitted, provided the original author(s) and the copyright owner(s) are credited and that the original publication in this journal is cited, in accordance with accepted academic practice. No use, distribution or reproduction is permitted which does not comply with these terms.

Biphasic expression of thyroid hormone receptor TRβ1 in mammalian retina and anterior ocular tissues

Lily Ng, Hong Liu, Ye Liu and Douglas Forrest*

National Institute of Diabetes and Digestive and Kidney Diseases, Laboratory of Endocrinology and Receptor Biology, National Institutes of Health, Bethesda, MD, United States

The retina is increasingly recognized as a target of thyroid hormone. We previously reported critical functions for thyroid hormone receptor TRβ2, encoded by *Thrb*, in cones, the photoreceptors that mediate color vision. TRβ1, another *Thrb* receptor isoform, is widely expressed in other tissues but little studied in the retina. Here, we investigate these N-terminal isoforms by RNA-sequencing analysis and reveal a striking biphasic profile for TRβ1 in mouse and human retina. In contrast to the early TRβ2 peak, TRβ1 peaks later during retinal maturation or later differentiation of human retinal organoids. This switch in receptor expression profiles was confirmed using *lacZ* reporter mice. TRβ1 localized in cones, amacrine cells and ganglion cells in contrast to the restricted expression of TRβ2 in cones. Intriguingly, TRβ1 was also detected in the retinal pigmented epithelium and in anterior structures in the ciliary margin zone, ciliary body and iris, suggesting novel functions in non-retinal eye tissues. Although TRβ1 was detected in cones, TRβ1-knockout mice displayed only minor changes in opsin photopigment expression and normal electroretinogram responses. Our results suggest that strikingly different temporal and cell-specific controls over TRβ1 and TRβ2 expression may underlie thyroid hormone actions in a range of ocular cell types. The TRβ1 expression pattern suggests novel functions in retinal and non-neural ocular tissues.

KEYWORDS

thyroid hormone receptor, *THRB* gene, retina, anterior eye, neurodevelopment

Introduction

A growing body of evidence indicates the sensitivity of the mammalian retina to thyroid hormone and the potential for retinal dysfunction in thyroid disorders. Genetic studies have revealed particularly critical functions in cone photoreceptors, the specialized cells that mediate color vision and daylight vision. Color vision is mediated by cone populations with opsin photopigments for response to different regions of the light spectrum, usually medium-long (M, "green") or short (S, "blue") wavelength regions in

mammals (1, 2). Mice deleted for thyroid hormone receptor TRβ2, encoded by *Thrb*, lack M opsin resulting in a form of monochromatic color-blindness (3). These findings reflect a key role for TRβ2 in promoting M and S cone diversity from cone precursors with a default S opsin identity (4, 5). Mutations of the *THRB* gene in human resistance to thyroid hormone have been associated with monochromacy and impaired responses to medium-long wavelength light (6–8). Mutation of *THRB* in human retinal organoids impairs expression of opsins for medium-long wavelength responses (9), suggesting conserved functions for the *Thrb* gene in the mammalian retina.

Thyroid hormone also influences photoreceptor differentiation and survival. Hypothyroidism in rodents impairs M opsin expression (10–12) and responses to green wavelength light (13). Hyperthyroidism can alter opsin expression (14) but excesses cause cone cell death in mice (15, 16). Human population studies suggest an association of high levels of thyroxine (T4), the major circulating form of thyroid hormone, with age-related macular degeneration (17, 18), a disorder of the retinal pigmented epithelium that leads to deterioration of photoreceptors. Inhibition of thyroid hormone signaling can reduce the loss of photoreceptors in mouse models of retinal degeneration (15, 19) or macular degeneration (20). Accordingly, studies to elucidate the receptor-mediated basis for thyroid hormone action in the retina might suggest new therapeutic approaches for retinal disease.

Mapping of receptor expression patterns has been instrumental in identifying cellular targets for thyroid hormone. TRβ2 and TRβ1 isoforms encoded by *Thrb* differ in their N-termini but share common DNA binding and ligand binding domains. TRβ1 is widely expressed including in the pituitary, brain, liver and cochlea (21–23) but has been little studied in the retina. Differential expression of isoforms in the retina was first indicated in the chick embryo by *in situ* hybridization with specific N-terminal probes: TRβ2 localized in the outer nuclear (photoreceptor) layer whereas a TRβ1-like isoform appeared later in the outer nuclear layer and inner nuclear (interneuron) layer (24). However, previous *in situ* hybridization analyses lacked cell type resolution. Subsequently, TRβ2 expression was localized in cones using knockin or transgenic reporters in mice (3, 25) and transgenic reporters in avian and fish species (26, 27). The TRβ1 cellular expression pattern is undefined. RNA-sequencing (RNA-seq) is now common for gene expression studies of the retina or retinal organoid cultures as a model system [e.g., see refs (9, 28, 29).]. However, standard RNA-seq analyses yield reads for the total *Thrb* gene and do not distinguish TRβ1- and TRβ2-specific 5' exons, which lie > 6 kb upstream in the mRNA (30). In single cell analyses, the limitations are compounded by the very small amounts of input RNA (4, 31).

We have tested the hypothesis that TRβ1 has a role in cones or other retinal cell types by determination of the TRβ1 expression profile in mouse and human retina using customized RNA-seq analysis. We localized cellular expression of TRβ1 using a knockin *lacZ* reporter (23) and investigated cone phenotypes in TRβ1-knockout mice. The results show a unique pattern of TRβ1 expression that differs strikingly from that of TRβ2, and suggest versatile roles for the *Thrb* gene in the retina and other non-neural tissues of the eye.

Materials and methods

Mouse strains

Tissue expression of TRβ1 was investigated in $Thrb^{b1}$ lacZ reporter mice (23) that express β-galactosidase instead of TRβ1 and which in the homozygous state represent a knockout of TRβ1. TRβ2 expression was investigated using a $Thrb^{b2}$ lacZ knockin (3); homozygotes ($Thrb^{b2/b2}$) were used to enhance detection of signals. Phenotypic analyses were performed on homozygotes of each strain representing knockouts of TRβ1 and TRβ2, respectively. Both strains were back-crossed to a C57BL/6J background for ~10 generations. Genotyping was performed by PCR as described (3, 23). Experiments followed approved protocols at NIDDK at the National Institutes of Health.

Library construction and RNA-seq analysis

Total RNA was prepared from pooled retinas of C57BL/6J mice (The Jackson Lab, cat # 000664). Each pool represented 4 - 6 embryos (8 - 12 retinas) or ≥ 3 postnatal mice (≥ 6 retinas), except at P60, two samples represented pools of 3 mice (6 retinas) and four samples represented individual mice (both retinas per mouse). At postnatal ages, males were selected to provide datasets of a defined sex. For practical reasons, for embryos and P1 neonates, when sex could not be determined visually at time of collection, samples included mixed sexes; larger pools were required at these early stages as tissue amounts were smaller. RNA was prepared using TRIzol (ThermoFisher) and RNeasy Micro kit (Qiagen, cat# 74004) isolation. Each RNA-seq library was constructed from ~250 ng of purified RNA using SMARTer total RNA Sample Prep kit (TakaraBio, cat# 634874). Libraries were sequenced on an Illumina HiSeq-2500 instrument at the NIDDK Genomics Facility. For each library, ~20 million single-end 50 base reads were collected, then converted using bcl2fastq (version 2) into fastq files and aligned on (GRCm38/mm10) with STAR (version 2.7.3a).

Dataset analyses: Transcripts were analyzed in bam files using STAR (v2.6.0c, https://github.com/alexdobin/STAR) as counts per million reads (cpm), or quantified in fastq files using Kallisto (version 0.46.1, https://pachterlab.github.io/kallisto/) as transcript per million reads (TPM). Samples at a given age were highly consistent as shown by a principal component analysis, in which the major source of variance was contributed by developmental age (87.9% for the first principal component). To analyze TRβ1 and TRβ2 isoforms, customized reference indices were created for four defined TRβ1-specific exons (see Figure 1A) and the single TRβ2-specific exon after removal of the total *Thrb* gene exons from the reference genome index. The isoform-specific indices were analyzed in STAR or Kallisto programs. Total *Thrb* reads were calculated for a standard *Thrb* whole gene reference index based on NCBI or ENSEMBL databases using STAR or Kallisto. Gene expression heatmaps were generated using gplots in R version 4.2.1 (https://cran.r-project.org/) for these retinal datasets and previously reported isolated cone datasets (groups of 21 - 30 cells/age) (4).

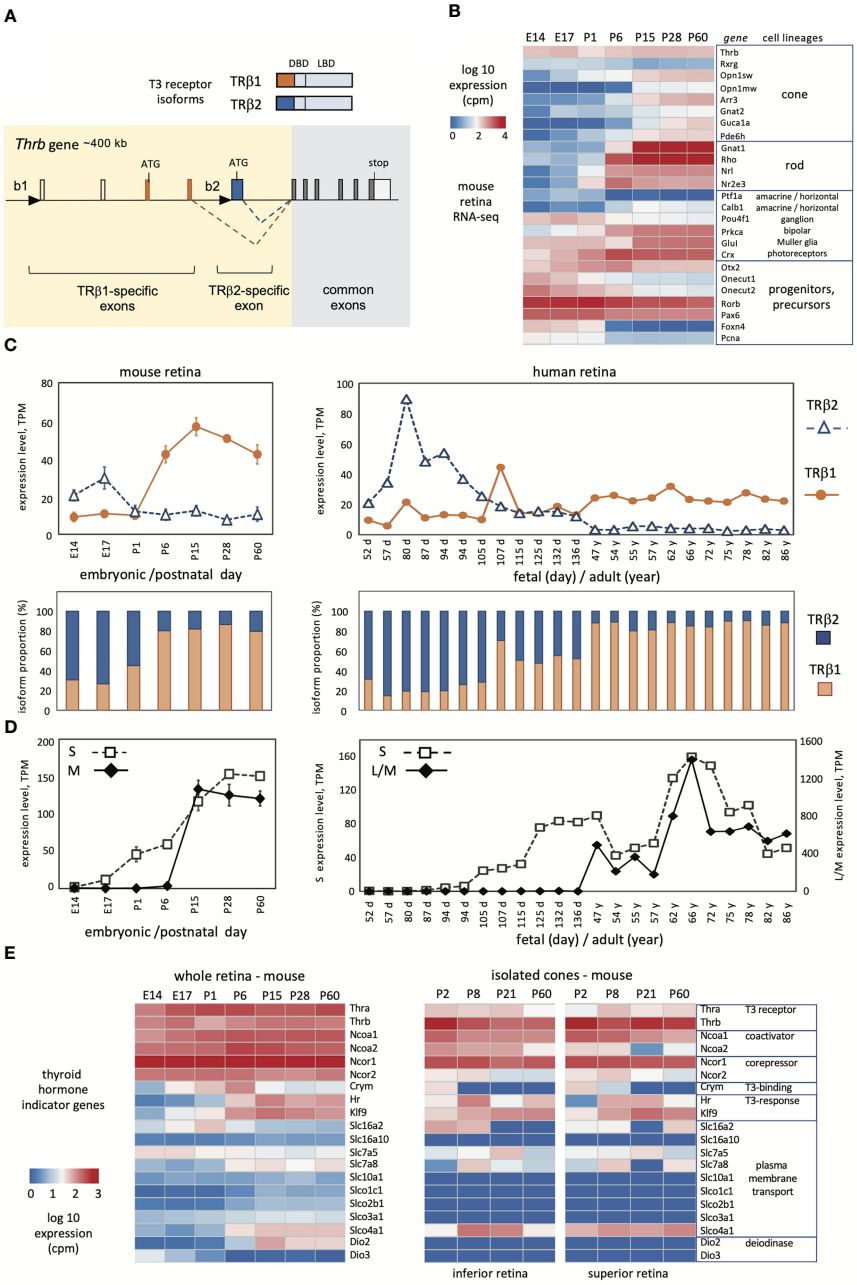

FIGURE 1
Developmental profiles of TRβ1 and TRβ2 in mouse and human retina. **(A)**, Mouse *Thrb* gene showing TRβ1- and TRβ2-specific 5'-exons and promoters (black triangles) and receptor products above. DBD, DNA binding domain, LBD, ligand binding domain. **(B)**, Overview of retinal lineage markers in RNA-seq datasets in mice. Groups, n = 3 to 6; mean ± S.D., cutoff average = 10 cpm. **(C)**, Developmental profiles of TRβ1 and TRβ2 in mouse (*left*) and human retina (*right*). Mouse RNA-seq datapoints represent groups, mean ± S.D.; human datapoints, individual samples. **(D)**, Cone opsin expression in the same RNA-seq datasets; S opsin and M opsin (mouse) or L/M opsins (human). The human L/M opsin curve represents reads from both genes in the *OPN1LW-OPN1MW* gene cluster. **(E)**, Representative indicator genes for thyroid hormone signaling in mouse whole retina (*left*) or isolated cones (*right*; cones from superior or inferior regions).

Human retinal RNA-seq analysis

Fetal datasets provided by Drs. A. Swaroop and T. Reh (32) were obtained from the NEI-Commons at the National Eye Institute (https://neicommons.nei.nih.gov/#/dataSearch) (GEO accession GSE104827). Adult retina datasets representing peripheral retinal punches provided by Drs. A. Swaroop, M.J. Brooks and K. Kaya (33) were obtained from GEO (GSE115828). For PEN8E iPSC-derived retinal organoids (NEI-001 control A) (34), groups included 2 or 3 samples (GSE129104). The "60 day"

stage represents 2 samples at 60 days and one at 67 days in culture. For H9 retinal organoids (35), groups included two samples per stage. For analyses of human *THRB* isoforms, customized indices were created for the TRβ1- and TRβ2-specific exons equivalent to the exons used for the mouse gene, and separately for *THRB* common exons, using STAR or Kallisto programs. Gene expression heatmaps were generated from human retinal and retinal organoid datasets using R version 4.2.1 (https://cran.r-project.org/).

TRβ1 and TRβ2 cDNA isolation

Total RNA from PEN8E retinal organoids (34) was kindly provided by Anand Swaroop and Zepeng Qu (National Eye Institute, NIH). RNA pooled from organoids at 90 and 120 day stages was reverse-transcribed into cDNA using the SMARTer RACE 5'/3' kit (TakaraBio, Cat# 634858). Specific primers for PCR-amplification of full-length TRβ1 or TRβ2 coding cDNAs were based on *THRB* genomic exon sequences. Specific 5' primer for TRβ1: Fb1, TTG CAT GAA TAA TGT GAG TGC; specific 5' primer for TRβ2: Fb2, TAT GCT TCT CTG CGT ATA TGC CCA GC; common 3'-end reverse primer, Rc, CCA AAT AAT CCC TCC CAA CAC.

Quantitative PCR analysis

Analysis of gene expression followed described procedures (4). Briefly, total RNA was extracted using RNeasy Plus mini kit (Qiagen, Cat #74136) from whole retina or sub-dissected pieces of superior or inferior retina. First-strand cDNA was synthesized using Superscript IV Reverse Transcriptase kit with oligo dT primers (Thermofisher, Cat #18091050). The qPCR reaction was performed with FastStart Universal SYBR Green Master-Mix (Roche; Cat #04913914001) on a StepOne or QuantStudio 3 instrument with analysis using software provided by the manufacturer (ThermoFisher). Relative gene expression levels were quantified using the $2^{-\Delta\Delta}C_T$ method (36) and normalized to Hprt (for photoreceptor gene analysis) or Actb (for TRβ1 and TRβ2 isoform analysis) as internal controls.

Primer pairs for photoreceptor genes: Opn1mw-F: CTG GTG AAC TTG GCA GTT GC; Opn1mw-R: AAA TGA TGG CCA GGG ACC AG; Opn1sw-F: ATG CAC TGA TGG TGG TCC TG; Opn1sw-R: CAG ACT CTT GCT GCT GAG CT; Rho-F: TTG GCT GGT CCA GGT ACA TC; Rho-R: GAA TGG TGA AGT GGA CCA CG; Arr3-F: TCA GTA ACA CTG CAG CCT GG; Arr3-R: CAT CCA GGC CTG CAG TTG TA;

Ccdc136-F: TGA GAT GGA GAT TGC CTC GC; Ccdc136-R: TCG TAC TCC GTA GCA GGT GA; Gucy2e-F: AGT CCA CTG GAC TGC CTT AC; Gucy2e-R: CGT GTC CTC AAT ACC CTT GC; Pgc-F: TAG CCT GCC TAC CCT CAC TT; Pgc-R: CCC ACC CTG TTA TTG CCC AT; Kcne2-F: AGG TCT CCT GCA TTG CTC AC; Kcne2-R: TGC CGA TCA TCA CCA TGA GG; Grk1-F: GAG GAG AGA AGG TAG AGA AC; Grk1-R: CCA ACA GCT GCT CAC AGA AG; Hprt-F: TAC CTC ACT GCT TTC CGG AG, Hprt-R: ATC GCT AAT CAC GAC GCT GG;

Primer pairs for TRβ1 and TRβ2: Trb1-F: AAT AAG AAG GTC AGA GGG AAT GCC; Trb1-R: CCT GGA TAA GGT GTG GGG AAG TC; Trb2-F: CCT GTA GTT ACC CTG GAA ACC TG; Trb2-R: TAC CCT GTG GCT TTG TCC C; Actb-F: CAC AGC TTC TTT GCA GCT CC; Actb-R: ACC CAT TCC CAC CAT CAC AC;

Histochemistry and immunostaining

Experiments followed previously described procedures (5). Retinas were fixed in 1% PFA for 1 hour for β-galactosidase histochemistry or 3 hours for immunostaining. Twelve µm-thick cryosections were incubated with 5-bromo-4-chloro-3-indolyl-D-galactopyranoside (xgal)(1 mg/mL) using a β-Galactosidase Reporter Gene Staining kit (Sigma). Images were obtained using a Nikon 80i microscope. At each stage, at least 6 eyes (n ≥ 3 mice) were examined. For immunostaining, sections were incubated with primary antibodies overnight then with secondary antibodies for 1 hour. Images were obtained using a Leica TCS SPE confocal microscope and processed using ImageJ software.

Primary antibodies (*target antigen, type, dilution, source, RRID*): TRβ2, rabbit polyclonal, 1:2,000 (37) (RRID : AB_2927439); β-galactosidase, chicken polyclonal, 1:500 (Abcam ab9361, RRID : AB_307210); Arr3, rabbit polyclonal, 1:1,000 (Millipore, AB15282, RRID : AB_1163387); Calbindin, rabbit polyclonal, 1:500 (Millipore, AB 1778, RRID : AB_2068336); RBPMS, rabbit polyclonal, 1:500 (PhosphoSolutions, 1830-RBPMS, RRID : AB_2492225); Calretinin, rabbit polyclonal, 1:500 (Millipore AB 5054, RRID : AB_2068506); S opsin, rabbit polyclonal, 1:500 (Millipore, AB 5407, RRID : AB_177457); M opsin, rabbit polyclonal, 1:1,000 (Millipore AB 5405, RRID : AB_177456); Rho, rabbit polyclonal, 1:500 (Abcam AB40673, RRID : AB_777706). *Secondary antibodies*: Alexa Fluor 488-conjugated anti-chicken IgY, goat polyclonal, 1:500 (Invitrogen, A11039, RRID : AB_2534096); Alexa Fluor 568-conjugated anti-rabbit IgG, goat polyclonal, 1:500 (Invitrogen, A11011, RRID : AB_143157). *Lectin*: Rhodamine Peanut Agglutinin (PNA), 10 µg/ml (Vector Lab, RL-1072, RRID : AB_2336642);

Electroretinogram analysis

Electroretinogram (ERG) analysis was performed as described (5) on 6 - 8 week old mice anesthetized with ketamine and xylazine (25 and 10 microgram per g body weight, respectively). The ERG was recorded using an Espion Electrophysiology System (Diagnosys LLC) for groups (6 - 8 mice) with approximately equal numbers of males and females.

Statistical analyses

Statistical significance was evaluated using unpaired two-tailed Student's t-tests, with significance set at $p < 0.05$. Analyses were

performed with GraphPad Prism version 9 (GraphPad Software). Experimental design was based on previous studies (16, 38). Column graphs for cell counts and qPCR analyses were plotted using GraphPad Prism. The ERG b-wave graphs were plotted using Microsoft XL (version 16.69.1).

Data availability

RNA-seq datasets of mouse retina generated in this work are available at GEO (GSE224863).

RNA-seq datasets of mouse single photoreceptors are available at GEO (GSE 203481).

Human RNA-seq datasets are available at NEI-Commons (https://neicommons.nei.nih.gov) and at GEO: fetal retinal datasets, GSE104827; adult retinal datasets, GSE115828. Datasets for H9 and PEN8E retinal organoids are at GEO (GSE129104). Human TRβ2 and TRβ1 cDNA sequences are available at GenBank access OQ406274 and OQ406275.

Results

TRβ1 and TRβ2 profiles in mouse retinal development

The mammalian *Thrb* gene spans > 400 kb of genomic DNA and includes a complex 5' region with distinct promoters and exons encoding the specific N-termini of TRβ1 and TRβ2 (Figure 1A) (39, 40). The common exons encoding the DNA binding and ligand binding domains, and the TRβ2-specific and TRβ1-specific 5' coding exons are highly conserved in mammalian species (41). We derived RNA-seq datasets to investigate expression of TRβ isoforms in mouse retina from embryonic day 14 (E14) to adulthood (postnatal day 60, P60). This period spans the neurogenesis of retinal cell types, postnatal differentiation and eye opening (~P13), then functional maturation, as verified by a summary heatmap of selected marker genes for retinal cell lineages (Figure 1B). This period encompasses the differentiation of cone photoreceptors. The generation of cone precursors begins by ~E12, and is complete by around birth in mice (42). Cones then mature postnatally and express markers including opsin (*Opn1sw*, *Opn1mw*) and phototransduction genes (e.g., *Arr3*, *Guca1a*).

To distinguish TRβ1 and TRβ2 reads, we created customized reference indices for analysis of TRβ1- and TRβ2-specific exons. The TRβ2 index represented the single TRβ2-specific exon. The TRβ1 index represented four exons: the two TRβ1-specific coding exons, the non-coding exon at the TRβ1 promoter region and the next downstream, non-coding exon consistently found in TRβ1-specific cDNAs (depicted in Figure 1A). RNA-sequencing was performed with substantial depth to improve detection of low level mRNAs (~18 million reads/library). We detected TRβ1 at very low levels in embryonic retina, then a postnatal increase and plateau at ~P15 with levels maintained into adulthood (Figure 1C, first and second row plots). In contrast, TRβ2 was high at embryonic stages then declined postnatally, consistent with northern (3) and western blot (37) analyses. Analyses of *Thrb* total reads (using a standard *Thrb* whole gene index) was incapable of revealing this striking developmental switch of TRβ2 and TRβ1 expression (see *Thrb* in the heatmap in Figure 1B).

We investigated these retinal datasets for other genes that serve as indicators of thyroid hormone signaling (Figure 1D). The *Thra* thyroid hormone receptor gene displayed modest increases in development. Previous northern blot analysis showed that the TRα1 receptor and a non-receptor splice variant α2 were both expressed with α2 in greater abundance in retina (3) as in other tissues (21, 22). Certain transporters that convey thyroid hormones across the plasma membrane, including *Slc16a2* (*Mct8*), *Slc7a5* and *Slc7a8* (43, 44) showed shifting patterns, suggesting that the control of ligand uptake or release may change during retinal maturation. Type 3 (*Dio3*) and type 2 (*Dio2*) deiodinases inactivate and activate thyroid hormone, respectively. The expression of *Dio3* and *Dio2* decreased and increased, respectively, consistent with previous findings, supporting the view that the retina progresses from a protected to a T3-sensitive state during maturation (45).

Given the sensitivity of cones to thyroid hormone, we analyzed these indicator genes in high resolution datasets for isolated cones (4), which suggested cell type selectivity compared to whole retina. For example, transcriptional coactivators (*Ncoa1*, *Ncoa2*) and corepressors (*Ncor1*, *Ncor2*) for thyroid hormone receptors were generally expressed in retina but in cones were more selective with *Ncoa1* and *Ncor1* being more prominently expressed. Expression of thyroid hormone transporters was more restricted in cones than whole retina although some were enriched such as the organic anion transporter *Slco4a1*. *Dio2* and *Dio3* expression was undetected in cones, supporting previous evidence that these genes are primarily expressed in surrounding cell types rather than the cone itself (45). In summary, the results show that TRβ1 expression rises during a phase of retinal maturation when sensitivity to thyroid hormone is acquired or refined and when systemic thyroid hormone levels rise in development (45).

TRβ1 and TRβ2 profiles in human retinal development

To investigate similarities in mouse and human retina, we analyzed TRβ1 and TRβ2 expression using published human RNA-seq resources (Figure 1C, columns on *right*). Previous studies of human retina have reported general *THRB* reads without distinguishing TRβ1 and TRβ2 (9, 29, 31). We analyzed datasets representing fetal days 52 to 136 (~8 to ~20 fetal weeks) (32) and adults at 47 to 86 years of age (33). Cones are generated during the first trimester of human gestation and express S opsin (encoded by *OPN1SW*) by ~10 fetal weeks followed by L/M opsins (encoded by the *OPN1LW-OPN1MW* locus) (46). The onset of S then L/M opsin expression resembles that of S followed by M opsin in mouse development (Figure 1D). The maturation of opsin patterning may continue at least until birth (~40 weeks) and eye opening in humans (29, 32, 46). Morphological and functional maturation of cones continues into infancy in humans (47, 48).

10.3389/fendo.2023.1174600

Analysis of TRβ2- and TRβ1-specific exons identified a peak of TRβ2 expression at human fetal weeks ~8 to 18 (days 52 - 136) then low levels at postnatal, adult ages. In contrast, TRβ1 mRNA levels rose as TRβ2 declined during later fetal development. At adult ages, expression of TRβ1 was maintained whereas TRβ2 remained low. Although the time course is prolonged in human development, the overall trend resembled that in the mouse or chick (24) with sequential peaks of TRβ2 followed by TRβ1.

Given the interest in retinal organoids as a model for human retina, we investigated *THRB* isoform expression using RNA-seq datasets from human retinal organoids derived from iPSC line PEN8E (34, 35) and H9 embryonic stem cells (28, 35) over a period of ~37 to 200 days in culture (Figure 2A). During differentiation in culture, retinal organoids produce both rod- and cone-like cells and acquire a partly laminated retinal-like structure. These organoids also express opsins although the lag between onset of S and L/M opsins is short compared to human or mouse retinal tissue (Figure 2B). We found that both lines of retinal organoids displayed an early peak of TRβ2 at ~60 - 90 days and a lagging peak of TRβ1 at ~90 - 200 days in culture. This biphasic pattern of isoform expression resembled that in retinal tissue, suggesting that the organoid model recapitulates *THRB* expression patterns that occur in the retina.

Analysis of indicator genes for thyroid hormone signaling revealed a broadly similar pattern of dynamic developmental changes correlating with the switch of *THRB* isoforms in human

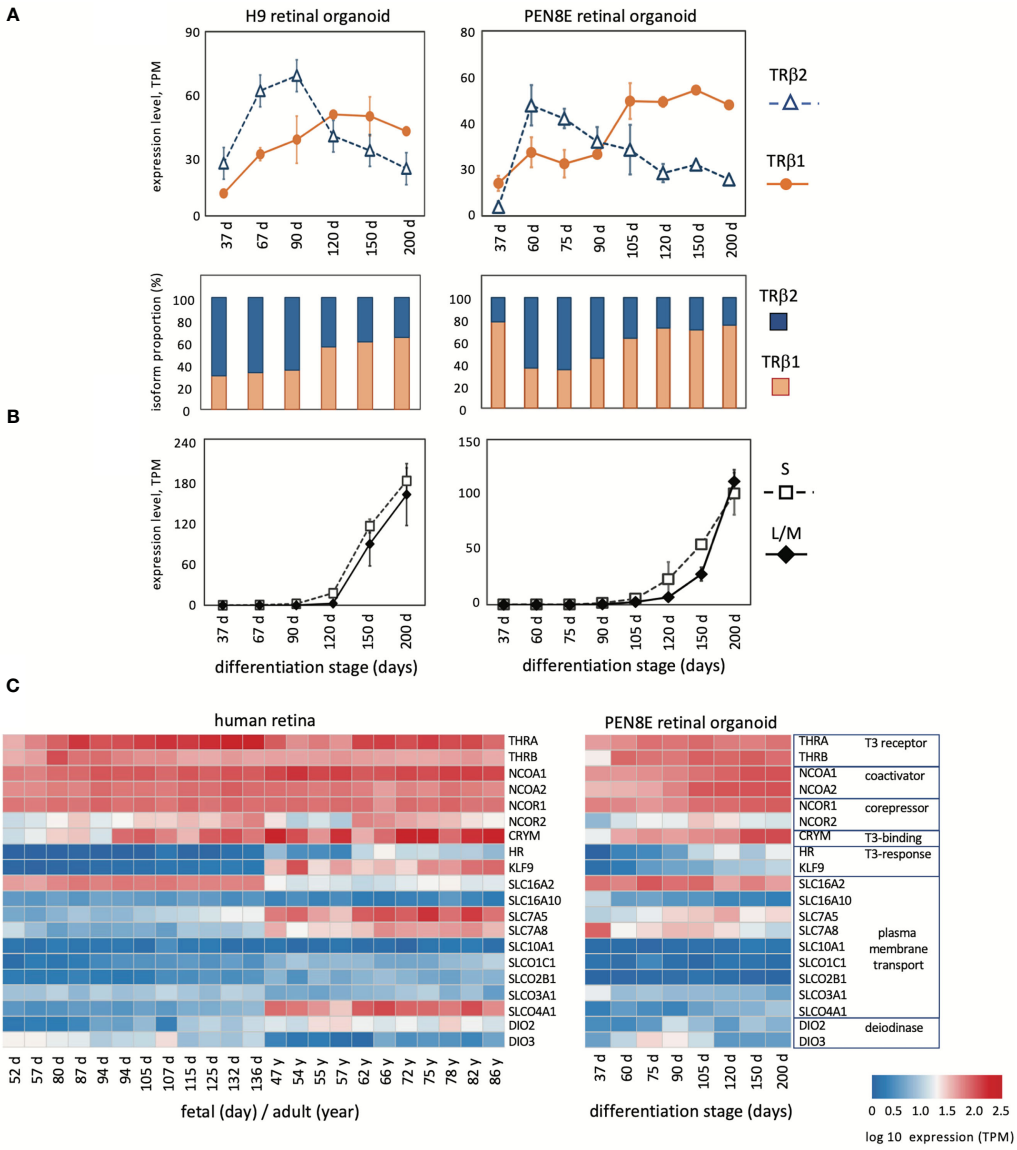

FIGURE 2
Expression of *THRB* and other genes in human retinal organoids and retina. **(A)**, RNA-seq analysis of TRβ1 and TRβ2 in H9 organoids and PEN8E organoids, derived from embryonic stem cells and iPSC lines, respectively. Mean ± S.D. The relative proportion of each isoform is indicated in the column graph, below. **(B)**, Cone opsin expression in the same RNA-seq datasets. *OPN1SW*, blue (S) opsin and *OPN1LW-OPN1MW*, red/green (L/M) opsins; the L/M curve represents reads from both genes in the *OPN1LW-OPN1MW* gene cluster. **(C)**, Heatmaps of expression of indicator genes for thyroid hormone signaling in human retina and PEN8E retinal organoids.

retina as in mouse retina (Figure 2C). Retinal organoids also showed general similarities, although for some genes, such as transporter genes, expression was more restricted than in retinal tissue. The results suggest that TRβ1 expression rises in the retina and in organoid model systems during a period when sensitivity to thyroid hormone signaling is acquired or refined during tissue maturation.

Isolation of coding cDNAs for human TRβ2 and TRβ1

To confirm the expression of coding mRNAs for TRβ2 and TRβ1 in human retinal-like tissue, we isolated full-length cDNA clones from PEN8E retinal organoids. The TRβ1 cDNA sequence encodes a protein of 461 amino acids and aligns with multiple human TRβ1 sequences in the GenBank database (49). TRβ2 is a rare isoform and is absent in most tissues. The human sequence is represented in GenBank by a single, partial 5'-fragment (471 base cDNA, pituitary adenoma origin, GenBank X74497) but no full-length cDNA or published reference. In rodent models, TRβ2 is detected in very few tissues (e.g. pituitary, cochlea, retina) (21, 41). The full-length human TRβ2 cDNA we isolated encodes a 476 amino acid protein as predicted from the human *THRB* gene exons and aligns with the mouse TRβ2 cDNA (30).

Localization of TRβ1 in the neural retina

To corroborate the expression profiles revealed by RNA-seq analysis and to localize TRβ1 in the retina, we analyzed *Thrb*^{b1} reporter mice with a *lacZ* knockin at a TRβ1-specific exon in the endogenous *Thrb* gene (23). In the embryonic retina, we detected only occasional, weakly *lacZ*-positive cells in the outer neuroblastic layer where newly-generated, immature cones reside (Figures 3A, B). After P3, signals rose in this outer zone of the outer nuclear layer (ONL) during retinal maturation. By P15, shortly after eye-opening, signals increased, filling the cone soma, pedicles that contact inner retinal interneurons and the light-detecting segments. We also detected signals in sub-populations of neurons in the inner nuclear layer (INL) and ganglion cell/displaced amacrine cell layer at postnatal ages. In contrast, TRβ2, detected using *Thrb*^{b2} *lacZ* reporter mice, was restricted to cones and peaked at late embryonic stages as reported (3). The biphasic peaks of TRβ2 and TRβ1 correlated closely with the RNA-seq results.

During postnatal maturation, very weak signals for TRβ1 were detected over the width of the ONL which is composed primarily of rods, the photoreceptors that mediate vision in dim light. In mice, rods outnumber cones ~30-fold and occupy most of the ONL whereas the sparser cone nuclei reside at the outer edge of the ONL (50). Further analysis of RNA-seq data from isolated rods and cones (4) detected only low *Thrb* reads in rods (Figure 3C), consistent with very low TRβ1 expression in rods compared to cones.

We confirmed expression of TRβ1 (as β-galactosidase protein encoded by *lacZ*) in cones by double-staining with cone markers in *Thrb*$^{+/b1}$ lacZ reporter mice (Figure 4A). Immunofluorescence at P15 identified β-galactosidase-positive cones that co-stained for TRβ2, indicating co-expression of both TRβ isoforms during cone maturation. The cone identity was further confirmed by co-staining for cone arrestin (Arr3).

The *lacZ* staining pattern in the inner retina in *Thrb*$^{+/b1}$ mice suggested expression in amacrine cells which are involved in processing signals relayed from the photoreceptors to the ganglion cells. Amacrine cells exist as many sub-types based on staining with markers such as calbindin and laminar location (51). β-galactosidase-positive cells detected in both the inner zone of the INL and the displaced amacrine cell zone (in the ganglion cell layer) co-stained with calbindin (Figure 4B) indicating TRβ1 expression in amacrine cell populations. Calbindin also stains horizontal cells. β-galactosidase-positive cells in the horizontal cell layer of the INL stained with calbindin, indicating TRβ1 expression in horizontal cells. We investigated if β-galactosidase signals in the ganglion/displaced amacrine cell layer also localized in ganglion cells by staining with RBPMS, a ganglion cell marker (52). β-galactosidase-positive cells co-stained with RBPMS, indicating expression of TRβ1 in ganglion cells.

TRβ1 in the ciliary margin zone, ciliary body, iris and retinal pigmented epithelium

TRβ1 is undetectable in most embryonic tissues but was identified in the early ciliary margin zone (CMZ) and associated anterior structures of the eye in *Thrb*$^{+/b1}$ reporter mice at E14.5 (Figures 5A–I). The CMZ gives rise to non-neural epithelia of the ciliary body (CB) and iris (53) and has been reported to have a potential to generate some neurons that contribute to the neural retina (54). The expression of TRβ1 in the early CMZ was in striking contrast to TRβ2 in newly-generated cone precursors (Figures 5C, D), indicating radically different control of the TRβ1 and TRβ2-specific promoters of the *Thrb* gene by different cell types in retinal development.

The ciliary body, which supports lens focusing, acquires a folded morphology in mouse postnatal development (53) (Figures 5F, I). TRβ1 was detected in the pigmented epithelia of the ciliary body as well as the non-pigmented cells that produce the aqueous humor of the eye. The iris expressed TRβ1 in both the sphincter pupillae and dilator pupillae, muscles that control the aperture opening of the pupil (Figures 5J, K). TRβ1 was also detected in the retinal pigmented epithelium (RPE), which provides support for photoreceptors (Figures 5G, H). These results suggest wider roles for TRβ1 in non-neural ocular tissues as well as in photoreceptors and neurons of the inner retinal layers.

Cone gene expression in TRβ1-deficient mice

The expression of TRβ1 in cones led us to test a role for TRβ1 in opsin regulation by investigation of TRβ1-KO mice. In mice at mature ages, M and S opsins are expressed in counter-gradients over the superior-inferior plane of the retina. M opsin has a

10.3389/fendo.2023.1174600

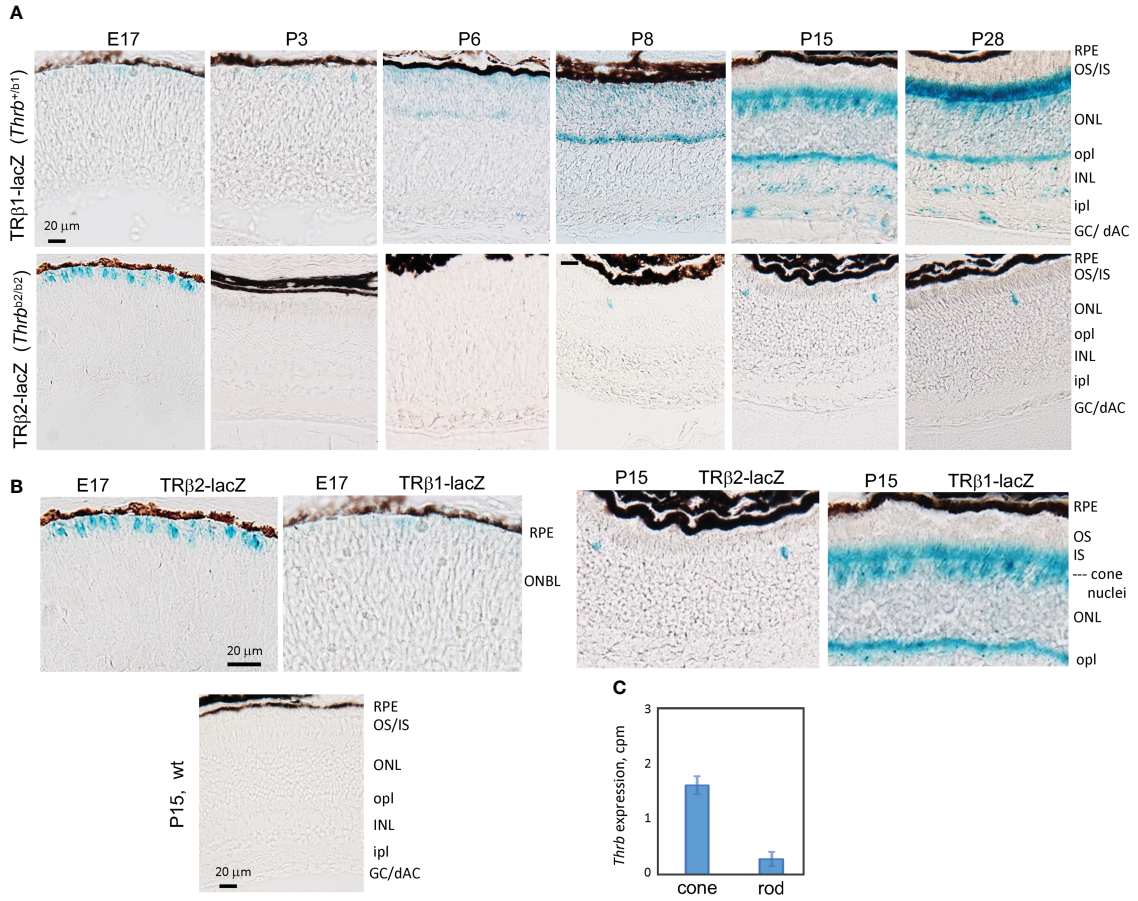

FIGURE 3
Developmental expression of TRβ1 in the retina detected in *Thrb*^{b1} lacZ reporter mice. **(A)**, TRβ1 detected as β-galactosidase activity using x-gal substrate (blue) in cryosections from *Thrb*$^{+/b1}$ reporter mice. TRβ2 was detected using *Thrb*$^{b2/b2}$ lacZ mice. X-gal color reaction times were overnight (~16 hr) except at P28 for *Thrb*$^{+/b1}$, with a time of 6 hr to avoid saturation of signal. At least 6 retinas (n ≥ 3 mice) analyzed per stage. **(B)**, Higher magnification showing the shift from TRβ2 to TRβ1 expression in cone differentiation. Wild type (wt) sections gave little or no background. **(C)**, RNA-seq detection of *Thrb* (total gene) expression in isolated cones and rods; mean ± S.D., 34 cones, 29 rods; 2 month old mice. GC/dAC, ganglion cell/displaced amacrine cell layer; INL, inner nuclear layer; ipl, inner plexiform layer; IS, inner segments; ONBL, outer neuroblastic layer; ONL, outer nuclear layer; opl, outer plexiform layer; OS, outer segments, RPE, retinal pigmented epithelium.

modest gradient biased to the superior and S opsin has a more marked gradient biased to the inferior (Figures 6A, B) (1). Opsin expression changes, if pronounced, may be detected by immunostaining on retinal sections. TRβ1-KO adult mice (~2 months old) displayed only marginal decreases of M opsin-positive cones in inferior regions and no obvious change of S opsin-positive cones (Figure 6C). In comparison, TRβ2-KO mice have severe loss of M opsin in all regions and S opsin expression extends to all cones (example in Figure 6A) (3). TRβ1-KO mice retained normal total cone numbers, indicated by staining with peanut agglutinin (PNA), a pan-cone marker (Figure 6C). These results were corroborated by qPCR analysis of *Opn1mw* (M) and *Opn1sw* (S) mRNA in isolated pieces of superior and inferior retina (Figure 6D). Expression of *Opn1mw* was slightly decreased in inferior regions whereas *Opn1sw* was moderately increased in superior regions. These minor changes in TRβ1-KO mice resemble in a minimal way the extreme phenotypes in TRβ2-KO mice, suggesting that TRβ1 may influence some similar transcriptional pathways as TRβ2 in cones.

Other TRβ2-regulated cone genes (4) displayed only limited changes in TRβ1-KO mice. Expression of cone arrestin (*Arr3*), which has an M opsin-like superior bias, was slightly decreased in the inferior retina, partly resembling the defect in TRβ2-KO mice (4). Other TRβ2-dependent genes including *Pgc*, *Ccdc136* and *Kcne2* showed no obvious change in TRβ1-KO mice. These results suggest that TRβ1 has a limited contribution to the control of TRβ2-dependent genes. No obvious changes were detected in expression of rhodopsin, the rod photopigment, by immunostaining or by qPCR analysis of *Rho* mRNA in TRβ1-KO mice. Selected phototransduction genes common to cones and rods showed little (*Grk1*) or no (*Gucy2e*) change in expression.

We investigated TRβ2 mRNA in retina by qPCR to assess if elevation of TRβ2 levels might compensate for loss of TRβ1 in TRβ1-KO mice (Figure 6E). As expected TRβ1 levels were severely depleted in TRβ1-KO mice at P19 or P30. However, TRβ2 mRNA levels were similar in wild type and TRβ1-KO mice. If there is compensation by TRβ2, this would presumably be accomplished by TRβ2 levels in the normal range. In a similar analysis, we found

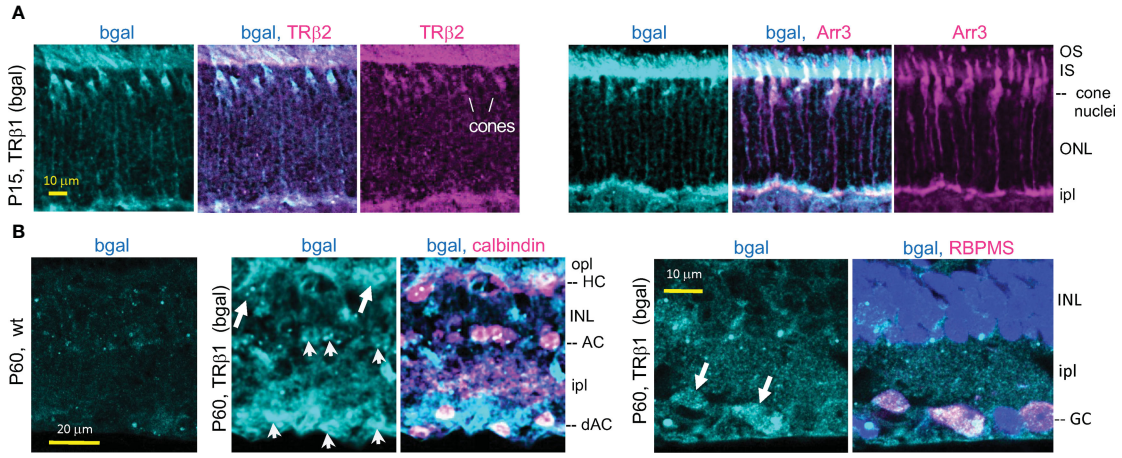

FIGURE 4
TRβ1 localization in cones and inner retinal neurons detected in *Thrb*^{b1} lacZ reporter mice. **(A)**, TRβ1 (β-galactosidase, bgal protein immunofluorescence) co-staining with cone markers (TRβ2, Arr3) in *Thrb*$^{+/b1}$ mice. **(B)**, TRβ1 (bgal) in amacrine (arrowheads) and horizontal cells (arrows) shown by staining for calbindin (*left*). Staining was sometimes weak and appeared punctate. TRβ1 was also detected in ganglion cells (arrowheads) by staining for RBPMS (*right*). In panel **(B)**, *Thrb*$^{b1/b1}$ homozygotes were analyzed to enhance detection of bgal. For RBPMS, a general nuclear stain (DAPI, blue) shows tissue background. AC, amacrine cell; dAC, displaced AC; GC, ganglion cell; HC, horizontal cell; INL, inner nuclear layer; ipl, inner plexiform layer; IS/OS, inner/outer segments; ONL, outer nuclear layer; opl, outer plexiform layer.

no obvious distortion of TRβ1 expression in TRβ2-KO mice (Figure 6F).

Electroretinogram analysis

To investigate cone function, we analyzed the photopic electroretinogram in TRβ1-KO adult mice. Responses to light stimuli at 516 nm and 368 nm, optimal wavelengths for stimulation of M and S opsins, respectively in mice (55), were in the normal ranges in TRβ1-KO mice (Figure 7). The b-wave magnitudes were in the normal range in TRβ1-KO mice. Rod responses in scotopic, dark-adapted electroretinogram analyses, lacked obvious defects in TRβ1-KO mice. These results indicate that unlike deletion of TRβ2 (3), deletion of TRβ1 in mice does not result in obvious defects in cone function.

Discussion

We report a novel pattern of TRβ1 expression in ocular tissues, suggesting remarkably diverse roles for thyroid hormone in cones, other retinal neurons and non-neural cell types. The findings indicate the importance of specific analyses of individual receptor isoforms encoded by *Thrb* rather than general analyses of *Thrb* expression in total. Our results suggest that the *Thrb* gene accomplishes diverse functions in the eye by independent regulation of two promoters that drive differential expression of the TRβ1 and TRβ2 receptor isoforms. The similar temporal switches of TRβ1 and TRβ2 in mouse and human retina suggest conserved functions during maturational periods when sensitivity to thyroid hormone is determined.

Biphasic expression of TRβ isoforms in the neural retina

In mice, cones mature into M and S opsin-expressing populations during postnatal development (42). Surprisingly, although TRβ1 is expressed in cones, only subtle opsin changes were detected in TRβ1-KO mice unlike the extreme loss of M opsin and gain of S opsin in TRβ2-KO mice (3). It is possible that the persistent low levels of TRβ2 at mature ages suffice to minimize cone phenotypes in TRβ1-KO mice. However, the converse is not true; i.e., TRβ1 cannot compensate for deletion of TRβ2. This might be explained if TRβ2 primes gene expression in immature cones in a way that cannot be achieved by the later expression of TRβ1 when the epigenetic status of the cone lineage may be less pliable (4). In support of this proposal, we recently demonstrated that an intronic enhancer in the *Thrb* gene determines the appropriate timing and level of expression of endogenous TRβ2 protein and consequently, levels of M opsin and the spectral sensitivity of cones (38). The timing and cell-specificity of TRβ2 expression suggest that a threshold level of receptor at a sensitive developmental time is required for normal maturation and function of cone photoreceptors.

Mutations of the human *THRB* gene have been associated with monochromacy and impaired spectral sensitivity in the syndrome of resistance to thyroid hormone (6–8). All known *THRB* mutations in this syndrome occur in common regions of the gene and interfere with both TRβ1 and TRβ2 (56). Mutation of the *THRB* common region in human retinal organoids impairs expression of the *OPN1LW-OPN1MW* locus (9). In the organoid model study, the possibility was raised that TRβ1 activates the *OPN1LW-OPN1MW* locus although a specific deletion of TRβ1 has not been reported. The sequential peaks of TRβ2 then TRβ1, first observed in the chick, are broadly similar in human and mouse development and in

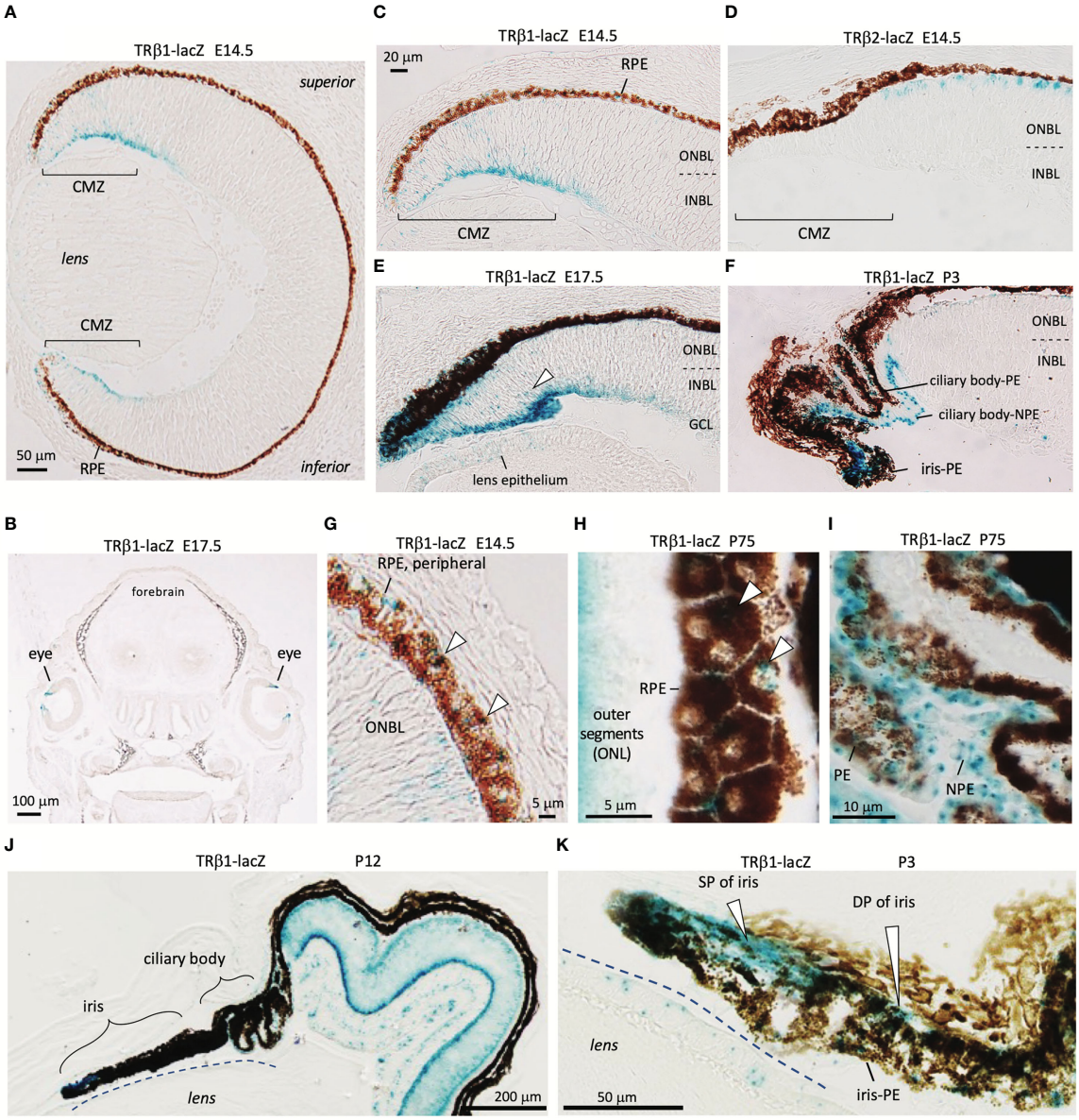

FIGURE 5
TRβ1 in the ciliary margin zone, iris and associated tissues detected in *Thrb*^{b1} lacZ reporter mice. **(A, B)**, TRβ1 in the ciliary margin zone (CMZ) (x-gal staining, blue) in *Thrb*$^{+/b1}$ embryos. Otherwise, expression is rare in embryonic tissues (coronal head section in *B*). **(C, D)**, Expression of TRβ1 in the CMZ contrasts with TRβ2 in cone precursors shown in *Thrb*$^{b2/b2}$ lacZ reporter mice. **(E)**, TRβ1 in the late embryonic CMZ. Arrowhead, positive progenitor cells in the neuroblastic layers of the CMZ. Weak signals are detected in the lens epithelium. **(F)**, TRβ1 in the non-pigmented (NPE) and pigmented epithelia (PE) of the ciliary body at P3. **(G, H)**, TRβ1 in the retinal pigmented epithelium (RPE) (arrowheads) at embryonic **(G)** and mature **(H)** stages. Oblique section in *H* shows the planar polygonal shape of RPE cells. **(I)**, TRβ1 expression in NPE and PE of the ciliary body in the adult. **(J, K)**, Iris and ciliary body at P12 in overview **(J)** and iris at P3 at higher magnification **(K)**. TRβ1 is detected in the sphincter pupillae (SP) and dilator pupillae (DP) and pigmented epithelium of the iris (iris-PE). CMZ, ciliary margin zone; GCL, ganglion cell layer; INBL, inner neuroblastic layer; NPE, non-pigmented epithelium of ciliary body; ONBL, outer neuroblastic layer; ONL, outer nuclear layer; PE, pigmented epithelium of ciliary body; RPE, retinal pigmented epithelium.

human retinal organoids (Figure 1). However, the full course of cone differentiation in the context of the human lifespan is prolonged over many months and extends into infancy (46, 47). It is unclear if the TRβ2 and TRβ1 peaks might overlap during this period to a greater extent in human than mouse retinal development. Further insights may be gained by localization of TRβ1 in human retinal cell types. Immunostaining previously detected TRβ2 in human fetal cones and in human retinoblastomas, which arise from cone-like L/M opsin-positive cells (57).

It is not excluded that TRβ1 might modify responses to challenge or stress at adult or aging stages. Prolonged hypothyroidism when induced in adult rodents over months can reversibly alter M and S opsin patterning (58). This residual

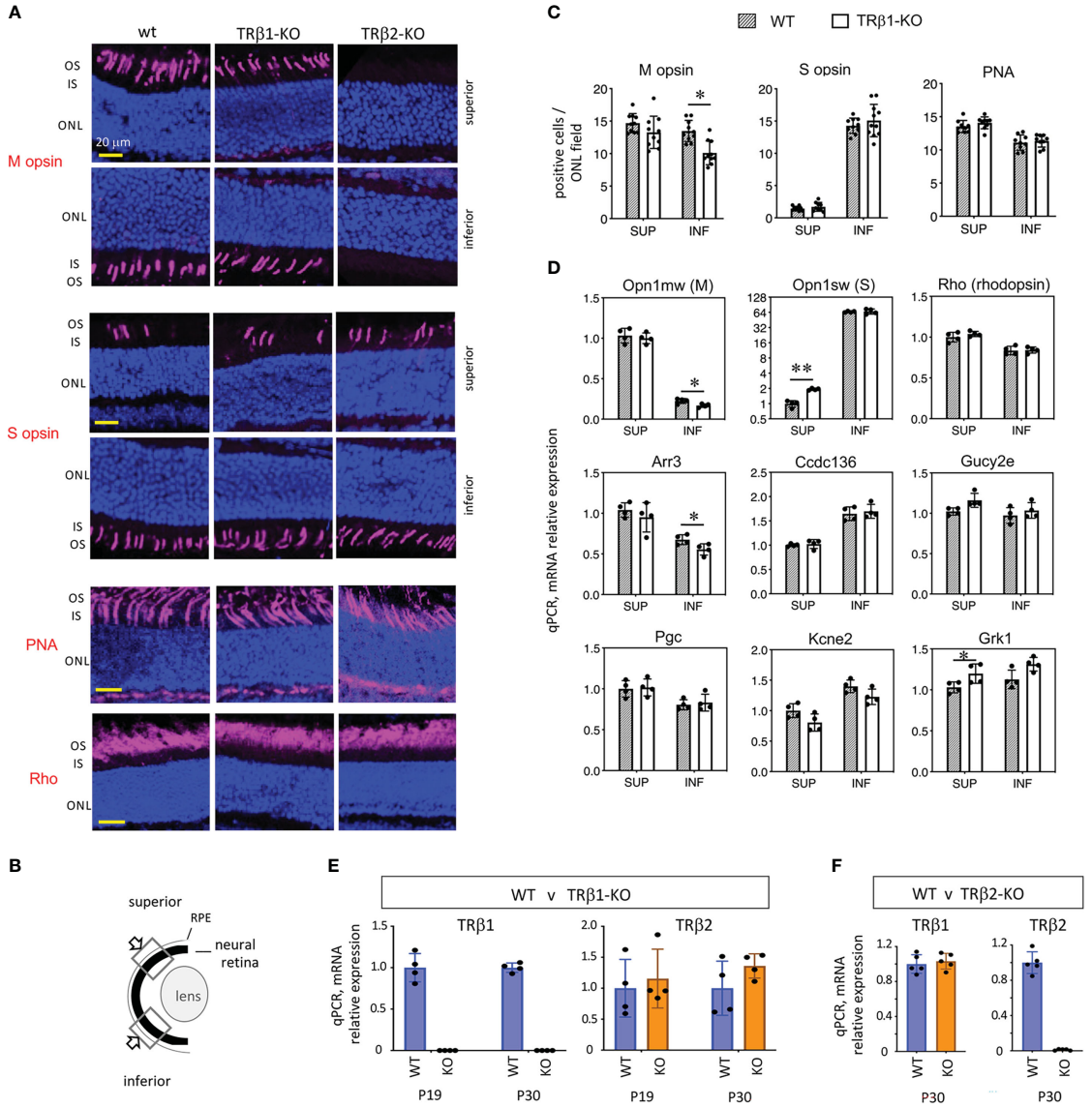

FIGURE 6
Cone gene expression in TRβ1-KO mice. **(A, B)**, Opsin immunostaining (magenta, in outer segments) in retinal cryosections showing superior and inferior views in control (wt) and TRβ1-KO (*Thrb*$^{b1/b1}$) adult mice (~2 months old). Fields of view represent 100 μm lengths of ONL (for locations see *B)*. For comparison, a representative TRβ2-KO displays severe loss of M opsin and extended expression of S opsin in all areas. PNA, peanut agglutinin, pan-cone marker. Rho, rod photopigment, rhodopsin. Dark blue, nuclear (DAPI) stain, shows tissue background. **(C)**, Counts of opsin- and PNA-positive cones. Mean ± S.D., adult mice; 10 views from the superior and 10 from the inferior retina in the vertical plane around the mid-retinal region obtained from 6 retinas from 3 mice; *p < 0.05, unpaired t-test. **(D)**, Cone and rod gene mRNA expression analyzed by qPCR. Control mice display counter-gradients of M (*Opn1mw*) and S (*Opn1sw*) opsin mRNA over the superior - inferior plane. In TRβ1-KO mice, *Opn1mw* and *Arr3* are marginally decreased in the inferior retina and *Opn1sw* modestly elevated in the superior. Most genes show little or no change. Groups, n = 4 mice, with 2 retinas pooled per mouse per region; mean ± S.D., *p < 0.05; **p < 0.001, unpaired t-test on log transformed expression data. **(E)**, TRβ2 mRNA expression is unchanged in TRβ1-KO mice shown at 2 ages (mean ± S.D., p = 0.58 (P19) and p = 0.16 (P30), unpaired t-test, log transformed expression data); n = 4 retinas representing at least one retina from each of 3 mice. TRβ1-KO lacks TRβ1 mRNA as expected. **(F)**, TRβ1 mRNA expression is unchanged in TRβ2-KO mice, shown at P30 (mean ± S.D., p = 0.61, unpaired t-test on log transformed expression data); n = 5 retinas representing at least one retina from each of 3 mice. ONL, outer nuclear layer; OS/IS, outer/inner segments.

plasticity of patterning might reflect latent function of the normal developmental program and could involve TRβ1, the predominant TRβ isoform at mature ages. TRβ1 might also contribute to cone loss caused by thyroid hormone excesses (15, 16). Deletion of the *Thrb* gene diminishes cone loss in models of retinal degeneration (19) and reduces loss of RPE and photoreceptors in a chemically-induced model of macular degeneration (20), which might involve TRβ1 at mature ages.

The detection of TRβ1 in the inner retina suggests possible roles for thyroid hormone in amacrine cells, which process visual information transmitted from the photoreceptors, and in the ganglion cells that relay these signals through the optic nerve (51,

10.3389/fendo.2023.1174600

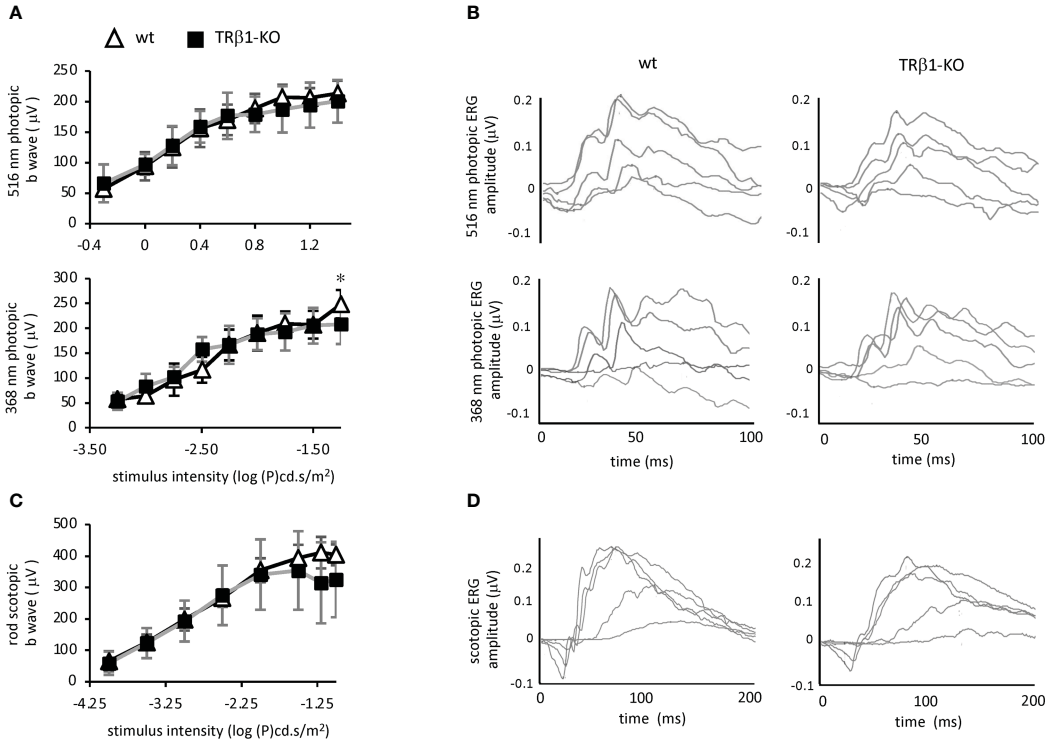

FIGURE 7
Electroretinogram analysis of TRβ1-KO mice. **(A)**, Photopic, light-adapted responses to optimal wavelengths for stimulation of cone M opsin (516 nm) and S opsin (368 nm) in mice. Curve plots show b-wave magnitudes, mean ± S.D. Groups, 6 wild type and 8 TRβ1 KO mice, ~2 months of age. * $p < 0.05$, unpaired t-test for each stimulus intensity. **(B)**, Example waveforms in response to varying stimulus intensities in single representative mice; intensities of 1.26, 3.16, 10, 19.95 and 32 cd.s/m^2 for 516 nm; 0.0001, 0.001, 0.0031, 0.01 and 0.0316 cd.s/m^2 for 368 nm. **(C)**, Scotopic, dark-adapted responses indicating rod function, showing b wave magnitudes, mean ± S.D. Groups, 8 wt and 7 TRβ1 KO mice, 6 - 8 weeks old. **(D)**, Example waveforms for varying stimulus intensities of 0.0001, 0.001, 0.01, 0.0316 and 0.1 cd.s/m^2 for scotopic responses.

59). Consistent with our results, studies of a mouse reporter model (FIND-T3) for thyroid hormone activity suggested amacrine and ganglion cells as targets in the postnatal retina (60). This may suggest a role for thyroid hormone in visual processing in the inner retina but this remains to be explored. It has been reported that hypothyroidism impairs visual-evoked potentials in central pathways in rats (13, 61).

TRβ1 in the ciliary body, iris and retinal pigmented epithelium

TRβ1 is undetected in most embryonic tissues but is detected in the ciliary margin zone and anterior tissues that give rise to the ciliary body and iris of the eye (53). The iris controls the aperture of the pupil and entry of light whereas the ciliary body focuses the lens and also produces aqueous humor. The ciliary margin zone can also generate some neurons that contribute to the neural retina (54, 62). There has been little study of thyroid hormone action in these tissues but the TRβ1 expression pattern suggests possible functions in anterior structures of the eye.

We also detected TRβ1 in the RPE, which provides crucial support for the photoreceptors. Other studies have reported thyroid hormone receptor gene expression in human RPE cells in culture (63) and in the RPE of zebrafish (64). The RPE mediates transepithelial transport and is involved in the renewal of outer segment discs, the opsin-packed structures of photoreceptors. Material from disc shedding is phagocytosed by the RPE. Hypothyroidism in adult rats has been reported to reduce the rate of disc renewal (65). It is noteworthy that deletion of *Thrb* can protect RPE cells and photoreceptors from damage in a chemically-induced model of macular degeneration (20). Our findings suggest that this susceptibility to damage might reflect TRβ1 functions in both RPE and cone cells. In amphibian and fish species, a function of thyroid hormone is to induce cyp27c1 in the RPE, which produces vitamin A2, a specialized chromophore for enhanced sensitivity to red light (66).

Severe developmental hypothyroidism in rats retards craniofacial features such as width of the eye-nose axis, eyeball mass, opening of the eyelids and thickening of retinal layers (67–69). Although this retardation has undefined cellular etiology, it is possible that TRβ1 underlies some of these functions in the eye. The *Thra* gene is also expressed in the retina (24) and RPE (64) suggesting that the TRα1 receptor mediates functions in the eye that remain to be discovered. In summary, our finding of differential expression of TRβ1 and TRβ2 reinforces the view that ocular development is coordinated in part by thyroid hormone acting on specific retinal and non-neural cell types in the eye.

Data availability statement

The original contributions presented in the study are included in the article/supplementary material. Further inquiries can be directed to the corresponding author.

Ethics statement

The animal study was reviewed and approved by NIH/NIDDK Animal Care and Use Committee.

Author contributions

LN, HL, YL and DF designed research. LN, HL and YL performed research. LN, HL, YL and DF analyzed data. DF, LN wrote the paper with input from all authors. All authors contributed to the article and approved the submitted version.

Funding

LN, HL, YL and DF are supported by the intramural research program at NIDDK at the National Institutes of Health.

Acknowledgments

We thank Harold Smith and Sijung Yun at the NIDDK Genomics sequencing facility. We thank Anand Swaroop, Matthew J Brooks and Koray Kaya at the National Eye Institute at NIH for the retinal and retinal organoid RNA-seq datasets available at the NEI-Commons site; and Anand Swaroop and Dr. Zepeng Qu for RNA samples.

Conflict of interest

The authors declare that the research was conducted in the absence of any commercial or financial relationships that could be construed as a potential conflict of interest.

Publisher's note

All claims expressed in this article are solely those of the authors and do not necessarily represent those of their affiliated organizations, or those of the publisher, the editors and the reviewers. Any product that may be evaluated in this article, or claim that may be made by its manufacturer, is not guaranteed or endorsed by the publisher.

References

1. Hunt DM, Peichl L. S cones: Evolution, retinal distribution, development, and spectral sensitivity. *Vis Neurosci* (2014) 31(2):115–38. doi: 10.1017/S0952523813000242

2. Nathans J. The evolution and physiology of human color vision: Insights from molecular genetic studies of visual pigments. *Neuron* (1999) 24(2):299–312. doi: 10.1016/S0896-6273(00)80845-4

3. Ng L, Hurley JB, Dierks B, Srinivas M, Saltó C, Vennström B, et al. A thyroid hormone receptor that is required for the development of green cone photoreceptors. *Nat Genet* (2001) 27(1):94–8. doi: 10.1038/83829

4. Aramaki M, Wu X, Liu H, Liu Y, Cho YW, Song M, et al. Transcriptional control of cone photoreceptor diversity by a thyroid hormone receptor. *Proc Natl Acad Sci USA* (2022) 119(49):e2209884119. doi: 10.1073/pnas.2209884119

5. Ng L, Lu A, Swaroop A, Sharlin DS, Swaroop A, Forrest D. Two transcription factors can direct three photoreceptor outcomes from rod precursor cells in mouse retinal development. *J Neurosci* (2011) 31(31):11118–25. doi: 10.1523/JNEUROSCI.1709-11.2011

6. Campi I, Cammarata G, Bianchi Marzoli S, Beck-Peccoz P, Santarsiero D, Dazzi D, et al. Retinal photoreceptor functions are compromised in patients with resistance to thyroid hormone syndrome (RTHbeta). *J Clin Endocrinol Metab* (2017) 102(7):2620–7. doi: 10.1210/jc.2016-3671

7. Newell FW, Diddie KR. [Typical monochromacy, congenital deafness, and resistance to intracellular action of thyroid hormone (author's transl)]. *Klin Monbl Augenheilkd* (1977) 171(5):731–4.

8. Weiss AH, Kelly JP, Bisset D, Deeb SS. Reduced l- and m- and increased s-cone functions in an infant with thyroid hormone resistance due to mutations in the THRbeta2 gene. *Opht Genet* (2012) 33(4):187–95. doi: 10.3109/13816810.2012.681096

9. Eldred KC, Hadyniak SE, Hussey KA, Brenerman B, Zhang PW, Chamling X, et al. Thyroid hormone signaling specifies cone subtypes in human retinal organoids. *Science* (2018) 362(6411):6411–8. doi: 10.1126/science.aau6348

10. Glaschke A, Glosmann M, Peichl L. Developmental changes of cone opsin expression but not retinal morphology in the hypothyroid Pax8 knockout mouse. *Invest Ophthalmol Vis Sci* (2010) 51(3):1719–27. doi: 10.1167/iovs.09-3592

11. Lu A, Ng L, Ma M, Kefas B, Davies TF, Hernandez A, et al. Retarded developmental expression and patterning of retinal cone opsins in hypothyroid mice. *Endocrinology* (2009) 150(3):1536–44. doi: 10.1210/en.2008-1092

12. Pessoa CN, Santiago LA, Santiago DA, Machado DS, Rocha FA, Ventura DF, et al. Thyroid hormone action is required for normal cone opsin expression during mouse retinal development. *Invest Ophthalmol Vis Sci* (2008) 49(5):2039–45. doi: 10.1167/iovs.07-0908

13. Boyes WK, Degn L, George BJ, Gilbert ME. Moderate perinatal thyroid hormone insufficiency alters visual system function in adult rats. *Neurotoxicology* (2018) 67:73–83. doi: 10.1016/j.neuro.2018.04.013

14. Roberts MR, Srinivas M, Forrest D, Morreale de Escobar G, Reh TA. Making the gradient: thyroid hormone regulates cone opsin expression in the developing mouse retina. *Proc Natl Acad Sci USA* (2006) 103(16):6218–23. doi: 10.1073/pnas.0509981103

15. Ma H, Thapa A, Morris L, Redmond TM, Baehr W, Ding XQ. Suppressing thyroid hormone signaling preserves cone photoreceptors in mouse models of retinal degeneration. *Proc Natl Acad Sci USA* (2014) 111(9):3602–7. doi: 10.1073/pnas.1317041111

16. Ng L, Lyubarsky A, Nikonov SS, Ma M, Srinivas M, Kefas B, et al. Type 3 deiodinase, a thyroid-hormone-inactivating enzyme, controls survival and maturation of cone photoreceptors. *J Neurosci* (2010) 30(9):3347–57. doi: 10.1523/JNEUROSCI.5267-09.2010

17. Chaker L, Buitendijk GH, Dehghan A, Medici M, Hofman A, Vingerling JR, et al. Thyroid function and age-related macular degeneration: a prospective population-based cohort study–the Rotterdam study. *BMC Med* (2015) 13:94. doi: 10.1186/s12916-015-0329-0

18. Gopinath B, Liew G, Kifley A, Mitchell P. Thyroid dysfunction and ten-year incidence of age-related macular degeneration. *Invest Ophthalmol Vis Sci* (2016) 57 (13):5273–7. doi: 10.1167/iovs.16-19735

19. Ma H, Yang F, Butler MR, Belcher J, Redmond TM, Placzek AT, et al. Inhibition of thyroid hormone receptor locally in the retina is a therapeutic strategy for retinal degeneration. *FASEB J* (2017) 31(8):3425–38. doi: 10.1096/fj.201601166RR

20. Ma H, Yang F, Ding XQ. Deficiency of thyroid hormone receptor protects retinal pigment epithelium and photoreceptors from cell death in a mouse model of age-related macular degeneration. *Cell Death Dis* (2022) 13(3):255. doi: 10.1038/s41419-022-04691-2

21. Hodin RA, Lazar MA, Chin WW. Differential and tissue-specific regulation of the multiple rat c-erbA messenger RNA species by thyroid hormone. *J Clin Invest* (1990) 85(1):101–5. doi: 10.1172/JCI114398

22. Strait KA, Schwartz HL, Perez-Castillo A, Oppenheimer JH. Relationship of c-erbA mRNA content to tissue triiodothyronine nuclear binding capacity and function in developing and adult rats. *J Biol Chem* (1990) 265:10514–21. doi: 10.1016/S0021-9258(18)86977-0

23. Ng L, Cordas E, Wu X, Vella KR, Hollenberg AN, Forrest D. Age-related hearing loss and degeneration of cochlear hair cells in mice lacking thyroid hormone receptor beta1. *Endocrinology* (2015) 156(10):3853–65. doi: 10.1210/en.2015-1468

24. Sjoberg M, Vennstrom B, Forrest D. Thyroid hormone receptors in chick retinal development: Differential expression of mRNAs for alpha and n-terminal variant beta receptors. *Development* (1992) 114(1):39–47. doi: 10.1242/dev.114.1.39

25. Jones I, Ng L, Liu H, Forrest D. An intron control region differentially regulates expression of thyroid hormone receptor beta2 in the cochlea, pituitary, and cone photoreceptors. *Mol Endocrinol* (2007) 21(5):1108–19. doi: 10.1210/me.2007-0037

26. Emerson MM, Surzenko N, Goetz JJ, Trimarchi J, Cepko CL. Otx2 and Onecut1 promote the fates of cone photoreceptors and horizontal cells and repress rod photoreceptors. *Dev Cell* (2013) 26(1):59–72. doi: 10.1016/j.devcel.2013.06.005

27. Suzuki SC, Bleckert A, Williams PR, Takechi M, Kawamura S, Wong RO. Cone photoreceptor types in zebrafish are generated by symmetric terminal divisions of dedicated precursors. *Proc Natl Acad Sci USA* (2013) 110(37):15109–14. doi: 10.1073/pnas.1303551110

28. Kaewkhaw R, Kaya KD, Brooks M, Homma K, Zou J, Chaitankar V, et al. Transcriptome dynamics of developing photoreceptors in three-dimensional retina cultures recapitulates temporal sequence of human cone and rod differentiation revealing cell surface markers and gene networks. *Stem Cells* (2015) 33(12):3504–18. doi: 10.1002/stem.2122

29. Welby E, Lakowski J, Di Foggia V, Budinger D, Gonzalez-Cordero A, Lun ATL, et al. Isolation and comparative transcriptome analysis of human fetal and iPSC-derived cone photoreceptor cells. *Stem Cell Rep* (2017) 9(6):1898–915. doi: 10.1016/j.stemcr.2017.10.018

30. Wood WM, Ocran KW, Gordon DF, Ridgway EC. Isolation and characterization of mouse complementary DNAs encoding alpha and beta thyroid hormone receptors from thyrotrope cells: The mouse pituitary-specific beta 2 isoform differs at the amino terminus from the corresponding species from rat pituitary tumor cells. *Mol Endocrinol* (1991) 5(8):1049–61. doi: 10.1210/mend-5-8-1049

31. Peng YR, Shekhar K, Yan W, Herrmann D, Sappington A, Bryman GS, et al. Molecular classification and comparative taxonomics of foveal and peripheral cells in primate retina. *Cell* (2019) 176(5):1222–37.e22. doi: 10.1016/j.cell.2019.01.004

32. Hoshino A, Ratnapriya R, Brooks MJ, Chaitankar V, Wilken MS, Zhang C, et al. Molecular anatomy of the developing human retina. *Dev Cell* (2017) 43(6):763–79.e4. doi: 10.1016/j.devcel.2017.10.029

33. Ratnapriya R, Sosina OA, Starostik MR, Kwicklis M, Kapphahn RJ, Fritsche LG, et al. Retinal transcriptome and eQTL analyses identify genes associated with age-related macular degeneration. *Nat Genet* (2019) 51(4):606–10. doi: 10.1038/s41588-019-0351-9

34. Kruczek K, Qu Z, Gentry J, Fadl BR, Gieser L, Hiriyanna S, et al. Gene therapy of dominant CRX-leber congenital amaurosis using patient stem cell-derived retinal organoids. *Stem Cell Rep* (2021) 16(2):252–63. doi: 10.1016/j.stemcr.2020.12.018

35. Kaya KD, Chen HY, Brooks MJ, Kelley RA, Shimada H, Nagashima K, et al. Transcriptome-based molecular staging of human stem cell-derived retinal organoids uncovers accelerated photoreceptor differentiation by 9-cis retinal. *Mol Vis* (2019) 25:663–78. doi: 10.1101/733071

36. Livak KJ, Schmittgen TD. Analysis of relative gene expression data using real-time quantitative PCR and the 2(-delta delta C(T)) method. *Methods* (2001) 25(4):402–8. doi: 10.1006/meth.2001.1262

37. Ng L, Ma M, Curran T, Forrest D. Developmental expression of thyroid hormone receptor β2 protein in cone photoreceptors in the mouse. *Neuroreport* (2009) 20(6):627–31. doi: 10.1097/WNR.0b013e32832a2c63

38. Liu H, Lu A, Kelley KA, Forrest D. Noncoding mutations in a thyroid hormone receptor gene that impair cone photoreceptor function. *Endocrinology* (2023) 164(3). doi: 10.1210/endocr/bqad006

39. Frankton S, Harvey CB, Gleason LM, Fadel A, Williams GR. Multiple messenger ribonucleic acid variants regulate cell-specific expression of human thyroid hormone receptor β1. *Mol Endocrinol* (2004) 18(7):1631–42. doi: 10.1210/me.2003-0346

40. Wood WM, Dowding JM, Haugen BR, Bright TM, Gordon DF, Ridgway EC. Structural and functional characterization of the genomic locus encoding the murine β2 thyroid hormone receptor. *Mol Endocrinol* (1994) 8(12):1605–17.

41. Jones I, Srinivas M, Ng L, Forrest D. The thyroid hormone receptor β gene: structure and functions in the brain and sensory systems. *Thyroid* (2003) 13(11):1057–68. doi: 10.1089/105072503770867228

42. Carter-Dawson LD, LaVail MM. Rods and cones in the mouse retina. II. autoradiographic analysis of cell generation using tritiated thymidine. *J Comp Neurol* (1979) 188(2):263–72. doi: 10.1002/cne.901880205

43. Groeneweg S, van Geest FS, Peeters RP, Heuer H, Visser WE. Thyroid hormone transporters. *Endocr Rev* (2020) 41(2):146–201. doi: 10.1210/endrev/bnz008

44. Schweizer U, Kohrle J. Function of thyroid hormone transporters in the central nervous system. *Biochim Biophys Acta* (2013) 1830(7):3965–73. doi: 10.1016/j.bbagen.2012.07.015

45. Hernandez A, Martinez ME, Ng L, Forrest D. Thyroid hormone deiodinases: Dynamic switches in developmental transitions. *Endocrinology* (2021) 162(8). doi: 10.1210/endocr/bqab091

46. Xiao M, Hendrickson A. Spatial and temporal expression of short, long/medium, or both opsins in human fetal cones. *J Comp Neurol* (2000) 425(4):545–59. doi: 10.1002/1096-9861(20001002)425:4<545::AID-CNE6>3.0.CO;2-3

47. Hansen RM, Fulton AB. Development of the cone ERG in infants. *Invest Ophthalmol Vis Sci* (2005) 46(9):3458–62. doi: 10.1167/iovs.05-0382

48. Hendrickson A, Possin D, Vajzovic L, Toth CA. Histologic development of the human fovea from midgestation to maturity. *Am J Ophthalmol* (2012) 154(5):767–78 e2. doi: 10.1016/j.ajo.2012.05.007

49. Weinberger C, Thompson CC, Ong ES, Lebo R, Gruol DJ, Evans RM. The c-erb-A gene encodes a thyroid hormone receptor. *Nature* (1986) 324(6098):641–6. doi: 10.1038/324641a0

50. Carter-Dawson LD, LaVail MM. Rods and cones in the mouse retina. i. structural analysis using light and electron microscopy. *J Comp Neurol* (1979) 188(2):245–62. doi: 10.1002/cne.901880204

51. Masland RH. The fundamental plan of the retina. *Nat Neurosci* (2001) 4(9):877–86. doi: 10.1038/nn0901-877

52. Rodriguez AR, de Sevilla Muller LP, Brecha NC. The RNA binding protein RBPMS is a selective marker of ganglion cells in the mammalian retina. *J Comp Neurol* (2014) 522(6):1411–43. doi: 10.1002/cne.23521

53. Smith RS, Sundberg JP, John SWM. The anterior segment and ocular adnexae. In: Smith RS, John SWM, Nishina PM, Sundberg JP, editors. *Systematic evaluation of the mouse eye*. Boca Raton: CRC Press (2002). p. 3–23.

54. Belanger MC, Robert B, Cayouette M. Msx1-positive progenitors in the retinal ciliary margin give rise to both neural and non-neural progenies in mammals. *Dev Cell* (2017) 40(2):137–50. doi: 10.1016/j.devcel.2016.11.020

55. Lyubarsky AL, Falsini B, Pennesi ME, Valentini P, Pugh ENJr. UV- and midwave-sensitive cone-driven retinal responses of the mouse: A possible phenotype for coexpression of cone photopigments. *J Neurosci* (1999) 19(1):442–55. doi: 10.1523/JNEUROSCI.19-01-00442.1999

56. Refetoff S, Weiss RE, Usala SJ. The syndromes of resistance to thyroid hormone. *Endocr Rev* (1993) 14:348–99. doi: 10.1210/edrv-14-3-348

57. Xu XL, Fang Y, Lee TC, Forrest D, Gregory-Evans C, Almeida D, et al. Retinoblastoma has properties of a cone precursor tumor and depends upon cone-specific MDM2 signaling. *Cell* (2009) 137(6):1018–31. doi: 10.1016/j.cell.2009.03.051

58. Glaschke A, Weiland J, Del Turco D, Steiner M, Peichl L, Glosmann M. Thyroid hormone controls cone opsin expression in the retina of adult rodents. *J Neurosci* (2011) 31(13):4844–51. doi: 10.1523/JNEUROSCI.6181-10.2011

59. Sanes JR, Zipursky SL. Design principles of insect and vertebrate visual systems. *Neuron* (2010) 66(1):15–36. doi: 10.1016/j.neuron.2010.01.018

60. Arbogast P, Flamant F, Godement P, Glosmann M, Peichl L. Thyroid hormone signaling in the mouse retina. *PloS One* (2016) 11(12):e0168003. doi: 10.1371/journal.pone.0168003

61. Takeda M, Onoda N, Suzuki M. Characterization of thyroid hormone effect on the visual system of the adult rat. *Thyroid* (1994) 4(4):467–74. doi: 10.1089/thy.1994.4.467

62. Marcucci F, Murcia-Belmonte V, Wang Q, Coca Y, Ferreiro-Galve S, Kuwajima T, et al. The ciliary margin zone of the mammalian retina generates retinal ganglion cells. *Cell Rep* (2016) 17(12):3153–64. doi: 10.1016/j.celrep.2016.11.016

63. Duncan KG, Bailey KR, Baxter JD, Schwartz DM. The human fetal retinal pigment epithelium: A target tissue for thyroid hormones. *Opht Res* (1999) 31(6):399–406. doi: 10.1159/000055564

64. Volkov LI, Kim-Han JS, Saunders LM, Poria D, Hughes AEO, Kefalov VJ, et al. Thyroid hormone receptors mediate two distinct mechanisms of long-wavelength vision. *Proc Natl Acad Sci USA* (2020) 117(26):15262–9. doi: 10.1073/pnas.1920086117

65. Takeda M, Kakegawa T, Suzuki M. Effect of thyroidectomy on photoreceptor cells in adult rat retina. *Life Sci* (1996) 58(7):631–7. doi: 10.1016/0024-3205(95)02331-3

66. Enright JM, Toomey MB, Sato SY, Temple SE, Allen JR, Fujiwara R, et al. Cyp27c1 red-shifts the spectral sensitivity of photoreceptors by converting vitamin A1 into A2. *Curr Biol CB* (2015) 25(23):3048–57. doi: 10.1016/j.cub.2015.10.018

67. Gamborino MJ, Sevilla-Romero E, Munoz A, Hernandez-Yago J, Renau-Piqueras J, Pinazo-Duran MD. Role of thyroid hormone in craniofacial and eye development using a rat model. *Opht Res* (2001) 33(5):283–91. doi: 10.1159/000055682

68. Pinazo-Duran MD, Iborra FJ, Pons S, Sevilla-Romero E, Gallego-Pinazo R, Munoz A. Postnatal thyroid hormone supplementation rescues developmental abnormalities induced by congenital-neonatal hypothyroidism in the rat retina. *Opht Res* (2005) 37(4):225–34. doi: 10.1159/000086863

69. Sevilla-Romero E, Munoz A, Pinazo-Duran MD. Low thyroid hormone levels impair the perinatal development of the rat retina. *Opht Res* (2002) 34(4):181–91. doi: 10.1159/000063885

frontiers | Frontiers in Endocrinology

TYPE Original Research
PUBLISHED 04 May 2023
DOI 10.3389/fendo.2023.1157685

Check for updates

OPEN ACCESS

EDITED BY
Liezhen Fu,
National Institutes of Health (NIH),
United States

REVIEWED BY
Soledad Bárez-López,
Spanish National Research Council (CSIC),
Spain
Hong Liu,
National Institute of Diabetes and Digestive and Kidney Diseases (NIH), United States

*CORRESPONDENCE
Marco António Campinho
macampinho@ualg.pt

SPECIALTY SECTION
This article was submitted to Thyroid Endocrinology, a section of the journal Frontiers in Endocrinology

RECEIVED 02 February 2023
ACCEPTED 04 April 2023
PUBLISHED 04 May 2023

CITATION
Silva N and Campinho MA (2023) In a zebrafish biomedical model of human Allan-Herndon-Dudley syndrome impaired MTH signaling leads to decreased neural cell diversity.
Front. Endocrinol. 14:1157685.
doi: 10.3389/fendo.2023.1157685

COPYRIGHT
© 2023 Silva and Campinho. This is an open-access article distributed under the terms of the Creative Commons Attribution License (CC BY). The use, distribution or reproduction in other forums is permitted, provided the original author(s) and the copyright owner(s) are credited and that the original publication in this journal is cited, in accordance with accepted academic practice. No use, distribution or reproduction is permitted which does not comply with these terms.

In a zebrafish biomedical model of human Allan-Herndon-Dudley syndrome impaired MTH signaling leads to decreased neural cell diversity

Nádia Silva[1,2] and Marco António Campinho[1,2,3]*

[1]Centre for Marine Sciences of the University of the Algarve, Faro, Portugal, [2]Algarve Biomedical Center-Research Institute, University of the Algarve, Faro, Portugal, [3]Faculty of Medicine and Biomedical Sciences, University of the Algarve, Faro, Portugal

Background: Maternally derived thyroid hormone (T3) is a fundamental factor for vertebrate neurodevelopment. In humans, mutations on the thyroid hormones (TH) exclusive transporter monocarboxylic acid transporter 8 (*MCT8*) lead to the Allan-Herndon-Dudley syndrome (AHDS). Patients with AHDS present severe underdevelopment of the central nervous system, with profound cognitive and locomotor consequences. Functional impairment of zebrafish T3 exclusive membrane transporter Mct8 phenocopies many symptoms observed in patients with AHDS, thus providing an outstanding animal model to study this human condition. In addition, it was previously shown in the zebrafish *mct8* KD model that maternal T3 (MTH) acts as an integrator of different key developmental pathways during zebrafish development.

Methods: Using a zebrafish Mct8 knockdown model, with consequent inhibition of maternal thyroid hormones (MTH) uptake to the target cells, we analyzed genes modulated by MTH by qPCR in a temporal series from the start of segmentation through hatching. Survival (TUNEL) and proliferation (PH3) of neural progenitor cells (*dla*, *her2*) were determined, and the cellular distribution of neural MTH-target genes in the spinal cord during development was characterized. In addition, *in-vivo* live imaging was performed to access NOTCH overexpression action on cell division in this AHDS model. We determined the developmental time window when MTH is required for appropriate CNS development in the zebrafish; MTH is not involved in neuroectoderm specification but is fundamental in the early stages of neurogenesis by promoting the maintenance of specific neural progenitor populations. MTH signaling is required for developing different neural cell types and maintaining spinal cord cytoarchitecture, and modulation of NOTCH signaling in a non-autonomous cell manner is involved in this process.

Discussion: The findings show that MTH allows the enrichment of neural progenitor pools, regulating the cell diversity output observed by the end of embryogenesis and that Mct8 impairment restricts CNS development. This work contributes to the understanding of the cellular mechanisms underlying human AHDS.

KEYWORDS

maternal thyroid hormone, monocarboxylic acid transporter 8, neurodevelopment, spinal cord, zebrafish, Allan-Herndon-Dudley syndrome (AHDS)

1 Introduction

During the early stages of vertebrate development, the embryonic naïve system cannot endogenously produce thyroid hormones (TH), thus depending on a precise supply of maternal-derived TH, which is essential for proper central nervous system (CNS) development. Maternally produced prohormone thyroxine (T4) must be converted locally into the active form triiodothyronine (T3) by deiodinase 2. T3 acts in target cells by binding to thyroid hormone receptors (TRs), which regulates target gene expression (1). TH importantly influences neurodevelopment during the fetal period and regulates processes involved in the formation of the cytoarchitecture of the brain, such as proliferation, migration and myelination and neuronal and glial cell differentiation (2–6). Maternal TH (MTH) deprivation outcomes in offspring are various and mainly depend on the timing and severity of the deficiency (3, 7).

The genetic responses to T3 in specific cellular contexts have been identified (8, 9), and several phenotypic outcomes arising from inappropriate levels of TH supply were found (7, 10). However, the underlying cellular and developmental mechanisms of action are less understood. Furthermore, a key feature of TH developmental action is the strict windows of time when the hormone acts, which determine the biological outcome (11, 12).

The importance of MTH transport by monocarboxylate transporter 8 (MCT8, SLC16A2), in human neurodevelopment is highlighted by the severe global neurological impairment observed in subjects with the rare human disease Allan-Herndon-Dudley-Syndrome (AHDS) (13, 14). This disease is characterized by developmental delay, reduced myelination, intellectual disability, poor language and walking skills, hypotonia, and a reduced life span (15), and histopathological outcomes can be identified from fetal stages (16). The severeness of the phenotypic outcome varies among patients (17–20), and could be related to the residual functionality of the mutant MCT8 protein and, consequently, the efficiency of TH transport into the target cells (21).

In the fetal and adult human brains, MCT8 is expressed in the blood-brain barrier (BBB) and blood-cerebrospinal fluid barrier (BCSFB). In fetal stages, MCT8 localizes in ependymal cells, tanycytes, neurons, and cells of the ventricular (VZ) and subventricular (SVZ) zones, the proliferative areas of the brain (22, 23).

The consequences of AHDS highlight the fundamental role of MTH on vertebrate neurodevelopment. Until recently, postnatal treatment of these patients with TH supplementation, with the TH analogs, TRIAC (24) or DITPA that do not require transport by MCT8 results in better thyroid function tests, improving hypermetabolism. However, no motor or cognitive skills improvement was observed (25). Very recently, prenatal treatment using levothyroxine (LT4) ameliorated the neuromotor and neurocognitive function of an AHDS patient (26)

Zebrafish is an established model for AHDS study (27–30). High concentrations of maternally deposited TH have been found in fish eggs (31). Also present in unfertilized eggs are many transcripts of components of the thyroid axis (32). Virtually all known components of the thyroid axis have been characterized in zebrafish, and these are structurally and functionally comparable with higher vertebrates (33, 34). The high degree of conservation between zebrafish *mct8* and its mammalian orthologs (35), points to a conservation of function, albeit zebrafish Mct8 specifically transports T3 at physiological temperature (26°C) and T3 and T4 at human physiological temperature (37°C) (36). Expression of *mct8* in zebrafish is detected from 3hpf with expression increasing through larval stages peaking at 48-96hpf (36, 37). Another advantage of zebrafish to model AHDS is that until 60hpf, there is no endogenous production of TH (38). In the zebrafish model, the developmental action of MTH through Mct8 can be examined without major compensatory mechanisms such as maternal TH compensation, endogenous TH production, or increased uptake by co-expressed TH transporters, as occurs in the mouse model (39), where a similar model of AHDS was only achieved after double KO of *Mct8* and *Oatp1c1* (40–42) or *Mct8* and *D2* (43). More recently, it has been reported the generation of a new mouse model with a human AHDS patient-derived *MCT8* mutation that presents brain hypothyroidism alongside neuro-architectural changes (44). This new mouse model presents similarities to already available zebrafish AHDS models where suppressing Mct8 function (27–29) makes it possible to reproduce many pre-natal neurological consequences observed in human patients with AHDS (16). Previous evidence from zebrafish Mct8 loss of function studies showed that several neural progenitors and neurons depend on MTH for development (27, 45). The spinal cord appears significantly reliant on MTH action for its normal development since, in the absence of functional Mct8, dorsal and medial neurons are mostly lost or show an

abnormal morphology and positioning (27). In contrast, ventral spinal cord neurons are favored and increase their number (27). Transcriptomic analysis of zebrafish *mct8* morphant embryos revealed that MTH modulates several critical developmental networks, like Notch, Wnt, and Hh signaling, thus working as an integrative signal (45). Nonetheless, fundamental questions on the action of MTH in zebrafish embryonic development and AHDS remain unanswered. In the present work, we focused on zebrafish spinal cord development and aimed to elucidate three fundamental questions: 1) the developmental time window where MTH action occurs, 2) the types of neural cell populations dependent on MTH signaling, 3) the cellular mechanisms of MTH action.

2 Materials and methods

2.1 Zebrafish husbandry and spawning

Adult wild-type (AB strain) zebrafish were maintained in standard conditions in the CCMAR fish facility at the University of Algarve (Portugal). Adult fish were kept at a 14 h/10 h light/dark cycle and 28°C. Breeding stock feeding twice daily with granulated food (Tetra granules, Germany) and once with Artemia sp. nauplii. One female and one male zebrafish were isolated in mating tanks the night before egg collection. After the lights were turned on in the morning, the separator was removed to allow fertilization.

2.2 Morpholino injection

Upon spawning, embryos were immediately collected and microinjected within 45 min, at the 1-2-cell stage, with 1nL of morpholino solution containing either 0.8pmol CTRLMO (control morpholino) or MCT8MO (*mct8* morpholino) as described (27). The diffusion process of the morpholino compound is immediate and ubiquitous throughout the embryo, and the blocking effect over *mct8* lasts robustly up to 72hpf.

Then, embryos were randomly distributed into plastic plates containing E3 medium (5 mM NaCl, 0.17 mM KCl, 0.33 mM CaCl, 0.33 mM MgSO4) and incubated until sampling time at 28.5°C (Sanyo, Germany) under 12h:12h light: dark cycles.

2.3 Analysis of gene expression

Embryos were manually dechorionated, snap-frozen in liquid nitrogen, and stored at -80°C. Embryo staging was performed by observing control embryos' developmental landmarks (46). Eight independent biological replicates (pools of 20 embryos) were sampled at 10, 12, 18, 22, and 25 hpf (hours post fertilization), and eight biological replicates (pool of 15 embryos) were sampled at 30, 36, and 48hpf. Total RNA was extracted from the embryos with an OMEGA Total RNA extraction kit I (Omega Biotek, USA), followed by treatment with Ambion Turbo DNA-free kit (Life Sciences, USA), according to the manufacturer's instructions. RNA concentration was determined by spectrophotometry using NanoDrop ND-1000 (NanoDrop Technologies Inc., USA), and integrity was determined by visualization in an agarose gel stained with SYBR Green (ThermoFisher Scientific). Only total RNA samples with a 2:1 ratio of 28s:18s rRNA were used in the analysis.

Synthesis of cDNA with 500ng of purified total RNA was reverse transcribed using RevertAid First Strand cDNA Synthesis and Random Hexamer Primers (Thermo Fisher Scientific, USA). cDNA was diluted 1/5 in ultrapure water and stored at -20°C. The quantification method used with the RT-QPCR method was the absolute quantification method, which determines the number of mRNA copies in the sample from a standard curve. Primers were designed using Primer 3 Plus using RNA-seq data (45). Supplementary Table 1 provides primer sequences amplicon size and RefSeq for each gene included in the analysis. The gene's target sequence was amplified by PCR, purified (EZNA Gel Extraction Kit, Omega Biotek), quantified (NanoDrop Technologies Inc., USA), and sequenced by Dye-termination to confirm identity. Quantitative real-time PCR (qPCR) was performed in a CFX-384 well (Biorad) with 6 µL of total volume. Final concentrations of PCR mix consisted of 1X SensiFASTTM SYBR, No-ROX Kit (Bioline, USA), 150nM forward primer, 150nM reverse primer, and 1 µL cDNA (1/5). The PCR amplification protocol was 95°C for 3 min, and 44 cycles of 95°C for 10 sec and 60°C for 15 sec, followed by a denaturation step from 60 to 95°C, 5 sec in 0.5°C increment, to obtain product specificity. Each cDNA sample was run as two technical replicates and averaged for expression analysis. Samples were discarded for quantification if the difference between replicates was over 0.5 cycles. No commonly used reference gene (*18S* and *gapdh*) presented invariable expression during the embryonic stages analyzed. Therefore, total RNA input was used as a normalizer according to the criteria for qPCR quantification in such cases (47).

2.4 Immunohistochemistry

One-cell stage embryos microinjected with either 0.8pmol of either CTRLMO (GeneTools) or MCT8MO (27) were fixed at selected stages in ice-cold 4%PFA/PBS overnight at 4°C. Samples were washed, depigmented when needed with PBS/0.3%H2O2/0.5% KOH, transferred into 100% methanol, and stored at -20°C until use. Samples in 100% MeOH were brought to room temperature and washed using a MeOH : PBS series (100% MeOH to 100% PBS). Embryos were hydrated, washed in PBS with 0.1% Triton X-100 (PBTr), and blocked with the addition of 10% sheep serum (Sigma-Aldrich Aldrich). Primary antibodies used were: 1:500 rabbit anti-HuC/D (16A11 - Invitrogen), 1:100 CF594 mouse anti-Zrf1 (ZDB-ATB-081002-46, ZIRC) and 1:50 mouse anti-Nkx6.1 (F55A10 DSHB). Samples were washed, and secondary antibody fluorescent labelling was carried out using 1:400 of goat anti-mouse IgG-CF594 (SAB4600321, Sigma-Aldrich), goat anti-rabbit IgG- Alexa 488 (111-545-047, Jackson Labs) or anti-mouse IgG-CF488 (SAB4600388, Sigma-Aldrich). Imaging was carried out in a Zeiss Z.1 light-sheet microscope. Images were imported into Fiji, and a region of interest was selected in a two-somite area (8800µm^2) between somites 8-12. For neuron number determination, the 3D

object counter in Fiji was used. Glial cell abundance was measured by determining the stained area after maximum intensity projection.

2.5 Riboprobe preparation and colorimetric whole-mount *in situ* hybridization (WISH)

Riboprobe synthesis, hybridization, and imaging of colorimetric *WISH* were performed as described in detail (27). To prepare *neurog1, fabp7a, slc1a2b, and olig2* riboprobes for *in-situ* hybridization, primers (Supplementary Table 2) were designed using as a template the sequences from the zebrafish assembled transcriptome (45). Analysis of cell distribution pattern (*her2*, *fabp7a*, *neurog1* and *slc1a2b*) on transverse sections of the spinal cord, *WISH* embryos were re-fixed in PFA 4%, dehydrated in MeOH/PBS and embedded in paraffin by isopropanol/paraffin gradient. Paraffin blocks were sectioned at 8µm and mounted on Poly-L-Lysine covered slides. Sections of interest were dewaxed, and coverslips were mounted with glycerol-gelatine (Sigma-Aldrich). Images of whole mounts and sections were acquired using a Leica LM2000 microscope coupled to a digital color camera DS480 (Leica).

2.6 Double fluorescent whole-mount *in situ* hybridization WISH

Riboprobes were generated as described in the previous section and labeled with either digoxigenin (Dig) (*mct8*, *thraa*, and *thrab*) or fluorescein (Fluo) (*her2*, *dla*, and *fabp7a*). A double hybridization procedure combining one Dig and one Fluo probe was performed in zebrafish embryos (10, 12, 18, 25, 30, 36, 48hpf) following (27). Antibody detection and development of the signal were carried out sequentially using a combination of antibody/Tyramide signal amplification (Perkin-Elmer, USA).WISH was carried out identically to (27) except hybridization was performed in the presence of 0.5 ng/mL of both Dig- and Fluo-labelled cRNA probes in HybMix. Stringency washes were performed as previously described (27). For the first probe detection, embryos were incubated overnight at 4°C in blocking solution MABTr/10% sheep serum (Sigma-Aldrich-Aldrich)/2% Blocking solution (Roche, Switzerland) with anti-DIG-POD Fab fragments serum (1:500, Roche, Switzerland). Embryos were washed in PBSTw and incubated for fluorescent color development in Alexa Fluor-594 Tyramide Reagent (ThermoFisher, USA), 1:100 in amplification reagent (Perkin Elmer), followed by several washes in PBSTw. To detect the second probe, *the* peroxidase activity of POD conjugated anti-serum was quenched by incubating samples for 1h in 3% H_2O_2 in PBS. Samples were washed in PBSTr and incubated overnight at 4°C MABTr/10% sheep serum (Sigma-Aldrich-Aldrich)/2% Blocking solution (Roche, Switzerland) with anti-Fluorescein-POD Fab fragments serum (1:500, Roche, Switzerland). Embryos were washed in PBSTw and then incubated in FITC-Tyramide (Perkin-Elmer) 1:100 in amplification reagent (Perkin Elmer), followed by several washes in PBSTw. Samples were stored in PBS containing 0.1% Dabco (CarlRoth, Germany).

2.7 Mitosis detection

Immediately after single fluorescent *WISH*, embryos were subject to immunohistochemistry to detect mitotic cells. The primary antibody used was rabbit anti-PH3 1:500 (06-570 Sigma-Aldrich-Aldrich), and the secondary antibody was goat anti-rabbit IgG-CF594 (SAB4600388, Sigma-Aldrich-Aldrich). Antibody incubation and blocking steps were performed in 1xPBS:10% Sheep serum.

2.8 Apoptosis detection (TUNEL assay)

Immediately after the single fluorescent *WISH* of *dla* and *her2*, cell death detection in embryos was determined by TUNEL assay using the *in-situ* cell death detection kit – TMR red (12156792910, Roche). According to the manufacturer's instructions, including experimental controls. Briefly, samples were washed for 15 minutes at RT with 1xPBS/0.1% TritonX 100 (Sigma-Aldrich)/0.1 M Sodium Acetate pH6. Embryos were further treated for 15 minutes at RT with 1ug/mL Proteinase K (Sigma-Aldrich-Aldrich) followed by four 5 minutes of washes in 1xPBT.

2.9 Image acquisition and analysis of double *WISH, WISH*-mitosis and *WISH*-apoptosis

Light-sheet Z.1 (ZEISS) microscope was used to acquire images of double *WISH*, *WISH*-mitosis, and *WISH* apoptosis. Samples were mounted in 1% low melting agarose (CarlRoth, Germany). The total depth of the medial spinal cord was acquired using a 10x lens with 2.5x or 1x optical zoom, according to the developmental stage, using dual illumination and a z step of 1,69µm or 1,813 µm, according to the optical zoom in use. In addition, dual illumination image volumes from the Z.1 were merged by Dual Side Fusion (Zen Black, Zeiss), and imaging and colocalization analysis were performed in Fiji (48).

Colocalization Colormap plugin (49) was used to determine the colocalization of Dig and Fluo cRNA probes. Briefly, ROI was selected in a two-somite area (8800µm^2) between somite 8-12. Next, the threshold was adjusted and fixed for each gene pair for the double WISH, and 3-8 individuals per condition were analyzed. The resulting stack of the colocalization channel was then superimposed into the original Z.1 image to create the final figures. When necessary, stacks were resliced in y orientation to enable lateral views.

For the *WISH*-mitosis and *WISH* apoptosis, the image threshold was adjusted and fixed for each target pair, and a total of 5-13 individuals per condition were analyzed. Colocalization Colormap plugin (49) was used to determine the colocalization of cRNA probes with mitotic marker PH3 and apoptotic marker

TMR-red. Co-localized cells were counted manually with Fiji's "3D object counter" tool.

2.10 NICD overexpression

In this experiment, a variant of zebrafish notch1a, notch1a-intracellular domain (NICD), was used, which encodes a Notch receptor that is constitutively active in neurogenesis (50). A pCS2+ plasmid containing the cDNA coding for CAAX-GFP (membrane label) and the Notch-intracellular domain (NICD) (50) were linearized, and mRNAs synthesized using the mMessage Machine SP6 transcription kit from Ambion, following the manufacturer's instructions. The mRNAs were phenol: chloroform purified, diluted in RNAse-free water, and frozen at -80°C until use. The effects of this NICD mRNA injection are attributed to high NOTCH activity in general (50). The pCS2+ GFP-CaaX was generated after subcloning the GFP-CaaX construct from a Tol2 kit plasmid (51).

2.11 Live imaging

Zebrafish Tg(*elav3:LY-mCherry*) (52) x WT AB previously injected with CTRL or MCT8MO were used for mRNA injection. This transgenic line allows for the visualization of mature neurons, *elav3*, allowing us to distinguish them from neural progenitor cells. For mosaic overexpression of NICD, 100 pg of *nicd* mRNA and 50pg of *gfp-caax* mRNA were injected into one blastomere dorsal right 1 - DRA1 or dorsal right 2 -DRA2, between the 16- to 32-cell stages, which will contribute to brain and spinal cord cell fates (53). *gfp-caax* mRNA was used to allow the individual cell visualization of the cell-autonomous response to NICD in CTRL and MCT8MO injected embryos. Hence, four groups were prepared, GFP-CaaX injection in MCT8MO and CTRLMO; NICD and GFP-CaaX injection in MCT8MO and CTRLMO. Embryos were left to develop at 28°C until 22hpf when sorting and mounting for imaging were performed.

Imaging was carried out by light-sheet microscopy, Lightsheet Z.1 (ZEISS, Germany), as described previously (54), with minor alterations. Briefly, embryos were anesthetized with 0.08% tricaine pH7.4 buffered, mounted alive in 0.3% (w/v) low-melting agarose (LMA) in E3 medium containing tricaine (0.08%) into FEP tubes closed with a 1% LMA. Three animals per group, CTRLMO and MCT8MO, were imaged in the same tube. Two independent experiments were carried out. Time lapses images were taken from 23 until 26hpf. Z-stacks ranging from the full depth of the medial spinal cord were acquired every 15 min for 3h. The spinal cord was imaged with an x20 lens, 2x zoom with a z-step of 1.56 µm with single angle and dual illumination. For image analysis, dual illumination images from the Z.1 were merged using Dual side Fusion (Zen Black, Zeiss). Next, images were imported into Fiji, and a region of interest was selected in a two-somite area (8800µm^2) between somite 8-12. Analysis of cell divisions was performed manually in FIJI. Only Huc(-) cells expressing GFP were tracked for analysis. In brief, symmetric divisions of GFP+ cells in any group were considered if the cell division plane was 0-<30° to the ventricular side of the spinal cord. Asymmetric divisions were considered if the cell division plane was ≥30-90° to the ventricular side of the spinal cord (55, 56).

2.12 Generation of Mct8 loss-of-function mutant

CRISPRScan (57) was used to design two adjacent guide RNAs (gRNAs) against the first exon of the zebrafish *mct8* gene (GGCTGGTGGGACGCCCGGCT and GGAGCGCAAG CTGGCCCCGG). gRNAs were purified after phenol-chloroform extraction and were precipitated overnight at -20°C in 10uL of 3.5M sodium acetate pH3.5 and 250uL of 100% ethanol. After centrifugation, gRNA was purified, dried, resuspended in DEPC-treated water, and kept at -80°C until use. The oligos for each gRNAs were acquired (STABvida) and used for direct *in vitro* transcription as described (57). On the injection day, the two gRNAs were diluted to 300ng/uL in a 600ng/uL Cas9 protein (Champalimaud Foundation) solution.

Adult zebrafish were made to spawn in natural conditions, and embryos were immediately collected. 1-cell stage embryos were used to inject 1nL of gRNAs+Cas9 (300ng/uL+600ng/uL). At 24hpf, eight embryos per injection clutch were collected for genotyping by PCR. Genomic DNA extraction was carried out after overnight digestion at 50°C in genomic extraction buffer (10mM Tris pH8.2, 10mM EDTA, 20mM NaCl, 0.5% SDS, 200ng/mL Proteinase K), followed by centrifugation and washing with 70% ethanol, air dried, and resuspended in 20uL of TE pH8. PCR was carried out with primers (0.2uM) flanking the gRNAs binding sites (Fw – ATGCACTCGGAAAGCGATGA; Rv – AGCAGCGAACAC CACGACCCA) using the DreamTaq polymerase kit (Thermo). Thermocycling was carried out as follows: 95°C for 30 seconds, 35 cycles of 95°C for 30 seconds, 60°C for 15 seconds, and 72°C for 15 seconds, followed by a 5-minute extension at 72°C. PCR products were resolved in a 3.5% agarose/1xTAE gel. Afterwards, bands were isolated from the gel and extracted with a gel extraction band kit (OMEGA), followed by Sanger sequencing using the Big-dye termination method.

The isolated band sequence was confirmed after BLAST analysis and alignment to the zebrafish mct8 locus. That ensured that injected clutches had embryos carrying the desired genetic lesions on the mct8 locus. Injected embryos were reared until adulthood. After isolation, adult-inject PCR genotyped fish after fin-clipping to identify carriers of genetic lesions on the *mct8* locus. After sequencing, only carriers of mutations that induced an early STOP codon or a frameshift in the *mct8* ORF were allowed to cross with wild-type siblings to give rise to non-mosaic F1 carrier lines. Adult F1 carriers were genotyped by PCR after fin-clipping and sequenced. In-crosses were carried out to generate F2 homozygous mutants for the mct8 locus. Identified lines with embryos with expected phenotypes were collected, genomic DNA extracted, genotyped by PCR, and sequenced. Identified lines were crossed to wild-type siblings. Only F3 adult carriers were used to generate homozygous *mct8* mutant embryos. That was done to mitigate any possible non-specific genomic lesions other than in the *mct8* locus.

2.13 Statistical analysis

All statistical analyses were carried out in GraphPad Prism v6.01 (San Diego, USA). Values are represented as means ± SD. The datasets' normality was previously accessed using D'Agostino & Pearson omnibus normality test. The levels of statistical significance were expressed as p-values, *$p < 0.05$; **$p < 0.01$; ***$p < 0.001$; ns: non-significant.

Due to the role played by the genes analyzed in embryonic development, the present work did not intend to determine their temporal expression patterns, only the effect of MCT8 knockdown on their expression at specific time points. To determine gene expression differences between CTRLMO and MCT8MO embryos, statistical significance was determined by unpaired Students t-test: two-sample, assuming equal variances. For image analysis quantification, One-way analysis of variance (ANOVA) followed by Dunnett's multiple comparison tests or an unpaired Student's t-test was used when data sets presented a normal distribution. Otherwise, a Kruskal-Wallis test followed by Dunn's multiple comparison tests was used. Distribution differences in symmetric/asymmetric divisions between experimental groups were determined by $\chi 2$ analysis. Statistical difference in symmetric or asymmetric divisions between experimental groups was determined by one-way ANOVA followed by Holm-Sidak's multiple comparison *post hoc* analysis.

3 Results

To further guarantee the validity of our MCT8 knockdown approach using morpholinos, its specific effects, and the lack of unspecific morpholino effects, we developed a CRISPR/Cas9 loss-of-function mct8 mutant (-/-) (Supplementary Figure 1). The mutant *mct8* (-/-) has an early STOP codon in the sixth codon, missense mutations, and a 9-bp insertion (Supplementary Figures S1A, B). After injection of the MCT8 morpholino at 0.8pmol in mct8 (-/-) embryos, we did not observe any additional effects different from control morpholino injected 24hpf mct8 (-/-) embryos (Supplementary Figure 1C). Complying with the best practices for using morpholinos (58, 59), our morpholino-based approach has shown to be highly specific and fully recapitulates the loss of function in the newly developed *mct8* (-/-) embryos without non-specific effects. Together with our previous validations (27, 45), these two converging models fully recapitulate the loss of MTH-impaired signaling during embryonic development.

3.1 Timing of MTH action in zebrafish embryogenesis

To determine the developmental time window of MTH action in zebrafish embryogenesis, we analyzed genes already known from previous transcriptomic data to have altered expression in 25hpf MCT8MO embryos (45) (Supplementary Figure 2A). Genes shown to be regulated by MTH involved in the early neural specification, NOTCH signaling pathway, and neurogenesis (Supplementary Figure 2A) were analyzed.

Genes belonging to the SoxB1 family (*sox3*, *sox19a*, and *sox19b*) are recognized for their role in the specification and development of the embryonic ectoderm into the neuroectoderm lineage (60, 61). These candidate genes were downregulated at 25hpf in the MCT8MO RNA-seq data (Supplementary Figure 2A), indicating a possible role for MTH in maintaining the neuroectodermal progenitor pool. Analysis by qPCR (Figure 1 and Supplementary Figure 2B-D) revealed that the expression of these genes did not change in MCT8MO embryos during early neurodevelopment

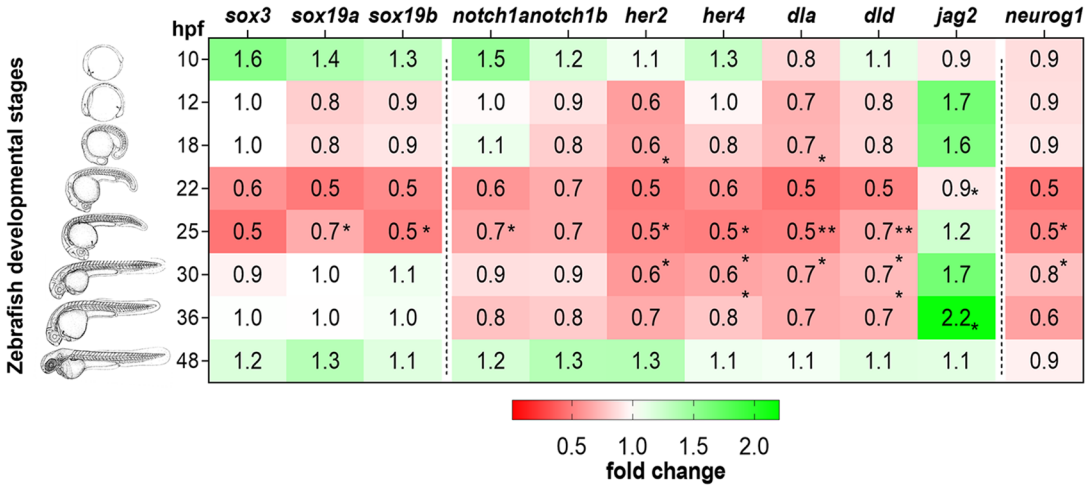

FIGURE 1
Expression of MTH-responsive genes reveals 22-31hpf as the developmental time more sensitive to MTH. Zebrafish developmental stages analyzed by qPCR are depicted by camera lucida drawings adapted from (46). Heatmap representation of gene expression levels of *sox3*, *sox19a*, *sox19b*, *notch1a*, *notch1b*, *her2*, *her4*, *dla*, *dld*, *jag2a*, and *neurog1*, determined after RT-qPCR in MCT8MO and CTRLMO during embryonic development. Data are represented as fold change of MCT8MO expression relative to the CTRLMO. Statistical differences were evaluated between MCT8MO and CTRLMO for each time point using a t-test after normal distribution was confirmed (D'Agostino & Pearson test). N = 8 (*p<0.05; **p<0.01).

(10hpf-18hpf). The results suggest that MTH does not play a role in maintaining B1 Sox gene expression during neural plate establishment and neural induction. However, expression of *sox19a* and *sox19b* is significantly lower in MCT8MO embryos at 22hpf (t-test, $p<0.05$), while *sox3* and *sox19b* show a decreased expression also at 25hpf (Figure 1), in accordance with RNA-seq data (45), although this change does not reach statistical significance in the qPCR assay (t-test, $p=0.083$, and $p=0.079$, respectively).

Notch ligand-receptor combinations that coincide during development in zebrafish are essential for adequate brain development and cell diversity (62). Gene expression analysis by qPCR revealed that only *notch1a* was significantly downregulated in MCT8MO at 22hpf (Figure 1; Supplementary Figure 2E; t-test, $p<0.05$) and continues to be lower than CTRLMO, in MCT8MO embryos until 36hpf, although not statistically significant (Figure 1; Supplementary Figure 2E). A similar trend occurs for the expression of the *notch1b* receptor; however, this decrease between 22-36hpf is not statistically significant (Figure 1; Supplementary Figure 2F, t-test, $p>0.05$).

The expression of NOTCH direct targets *her2* and *her4*, which are involved in the maintenance and proliferation of neuroprogenitor cells (63–65), was analyzed (Figure 1). Expression of *her2* is downregulated in MCT8MO embryos at 12, 22 and 25hpf (Figure 1; Supplementary Figure 2G, t-test, $p<0.05$).In zebrafish, *her4* is involved in primary neuron development under Notch 1 signaling (65). *Her4* downregulation at 22, 25, and 30hpf in MCT8MO suggests the involvement of MTH in regulating the development of some primary neurons (Figure 1; Supplementary Figure 2H, t-test, $p<0.05$).

Notch ligands *dla* and *dld*, which are expressed in differentiating neural cells and are involved in the specification of progenitor pool size domains (66), showed a significant decrease in expression in MCT8MO embryos at 25hpf (Figure 1; Supplementary Figures 2I, J, respectively, t-test, $p<0.05$). The downregulation of *dla* is observable by 12hpf (Figure 1; Supplementary Figure 2I, t-test, $p<0.05$) during primary neurogenesis and occurs at 22 and 25hpf (Figure 1; Supplementary Figure 2I, t-test, $p<0.001$ and $p<0.05$, respectively). On the other hand, the decrease in *dld* expression (Figure 1; Supplementary Figure 2J) only occurs later in neurogenesis at 22 (t-test, $p<0.01$), 25 (t-test, $p<0.05$), and 30hpf (t-test, $p<0.05$).

In contrast with *dla* and *dld*, the Notch ligand *jag2a* is upregulated in MCT8MO embryos (Figure 1; Supplementary Figure 2K, t-test, $p<0.05$). The temporal pattern of expression of *jag2a* was opposite to the delta ligands, *dla*, and *dld*, since it was upregulated at 18hpf (Figure 1 $p<0.05$) and again at 36hpf (t-test, $p<0.05$).

To further understand how MTH is involved in neuron progenitor specification, we analyzed the expression of *neurog1*, a pro-neural gene expressed by intermediate neuronal precursors and neuron-committed cells. No differences in *neurog1* expression occur from 10-18hpf between CTRL and MCT8MO embryos suggesting MTH is not involved in the differentiation of these cells (Figure 1 and Figure 1 and Supplementary Figure 2L). However, at 22 and 25hpf (Figure 1 and Supplementary Figure 2L, t-test, $p<0.05$), *neurog1* expression decreased, suggesting a possible role for MTH in the maintenance/differentiation of neuron progenitor populations from these stages of neurogenesis while no differences in expression were found at later stages (Figure 1 and Supplementary Figure 2L, t-test, $p>0.05$).

3.2 Impaired MTH action has a time-dependent effect on spinal cord neural development

We interrogated if gene expression changes are paralleled with neurogenesis and gliogenesis changes, focusing on the spinal cord since it provides a simplified version of neural development. Immunostaining for Elav3 (HuC/D) of CTRLMO and MCT8MO zebrafish, which labels all post-mitotic neurons from 15-48hpf, revealed a time-dependent topology and abundance of neurons (Figure 2). Notably, in all developmental stages analyzed, the distribution of neurons in the three regions of the spinal cord (dorsal, medial, and ventral) present different HuC/D staining profiles between CTRLMO and MCT8MO embryos (Figure 2A). From as early as 15hpf, neurogenesis was impaired, as can be seen by the decrease in post-mitotic neurons in MCT8MO (Figure 2B; t-test, $p<0.05$). The most affected spinal cord neuron population in MCT8MO embryos is medial, as can be observed in lateral and transversal sections (Figure 2A). As development progresses, at 22hpf, there are fewer neurons, and the distribution is different in MCT8MO embryos (Figures 2A, B; t-test, $p<0.05$). That is especially evident in the lateral view, where medial and ventral neurons seem to be particularly affected. By 25hpf, and although neuron numbers have recovered (Figure 2B; t-test, $p>0.05$), MCT8MO neuron distribution is more compact (Figure 2A transversal view) with an apparent accumulation of dorsally located neurons, some of which appear to be out of the spinal cord scaffold (Supplementary Figure 3). The different distribution of the cells between CTRLMO and MCT8MO embryos is exacerbated at 36hpf, where dorsal neurons seem to increase with a simultaneous decrease in medial and ventral neurons. Additionally, at 36hpf, neurons are decreased in MCT8MO (Figure 2; t-test, $p<0.0001$). By 48hpf, the distribution of neurons in any view of the spinal cord is different in CTRLMO and MCT8MO embryos, especially evident dorso-ventrally (Figure 2A lateral and transversal views), but there is no difference in the neuron number (Figure 2B; t-test, $p>0.05$).

We also interrogated how spinal cord gliogenesis was affected by impaired MTH signaling (Figure 3). To this end, embryos were immunostained with an anti-GFAP serum, and the stained volume of a 2 myotome section of the spinal cord was determined. We observed a time-dependent effect of impaired MTH action on gliogenesis up to 25hpf in MCT8MO (Figure 3). At 15hpf, there is a noticeable reduction of GFAP staining in MCT8MO embryos (Figure 3, t-test, $p<0.001$) with a very restricted GFAP signal (Figure 3A). In contrast to CTRLMO embryos, in MCT8MO morphants, the ventral signal of GFAP at 15hpf was spread along the left-right axis of the spinal cord. In contrast, medial and dorsal staining was mostly lost (Figure 3A, transversal). By 22hpf, the topology of GFAP staining was different between groups (Figure 3A), and the overall stain by GFAP was lower in MCT8MO (Figure 3B, t-test, $p<0.01$). By this time, the GFAP signal in MCT8MO embryos increased in the lateral basal edge of the

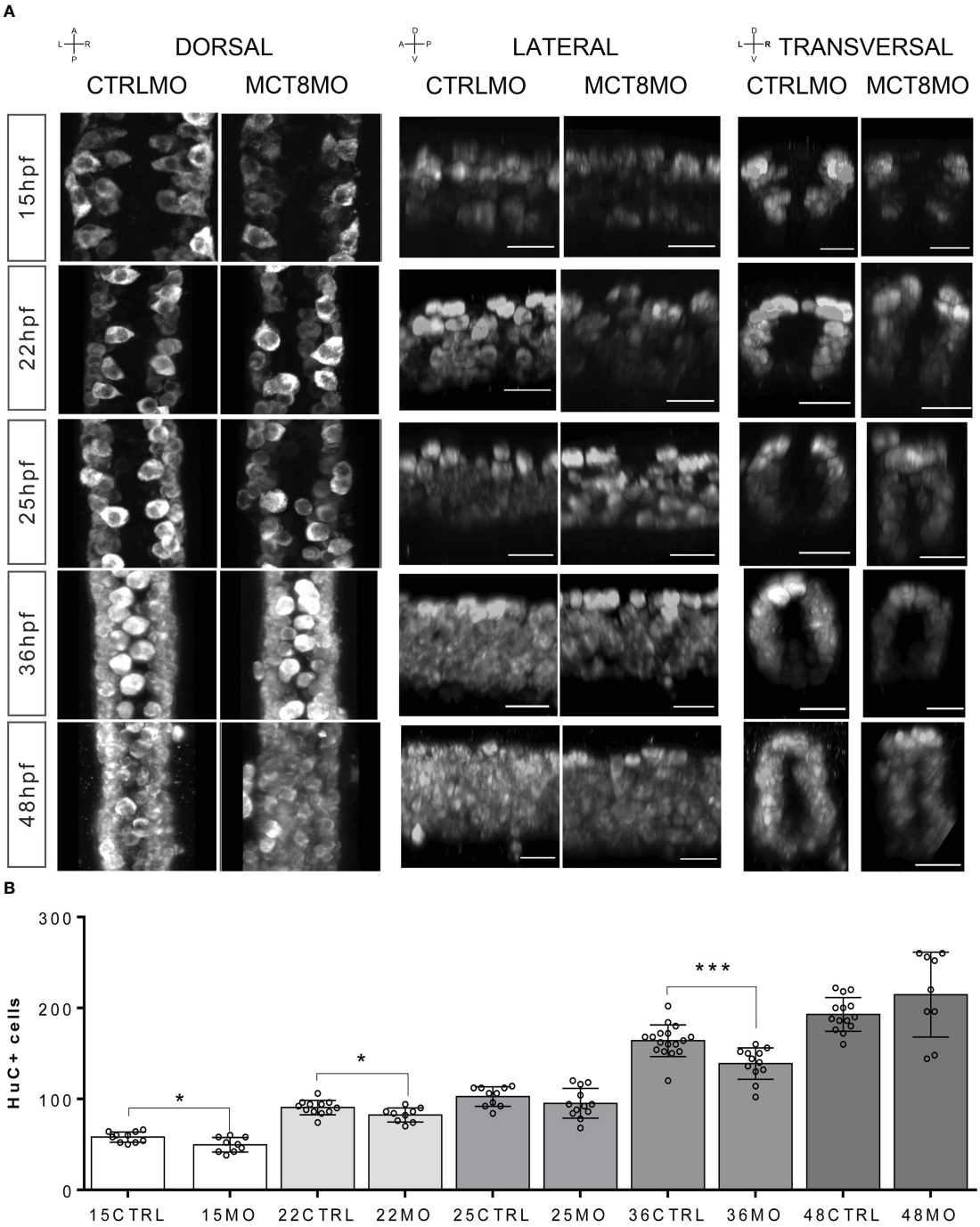

FIGURE 2
Compromised number and distribution of HuC/D neurons in MCT8MO embryos at specific stages of development. **(A)** Representative maximum projection images of the pan-neuronal marker HuC/D immunostaining (white) in the spinal cord between somite 8-12. Comparison of the pattern of neuron distribution in the spinal cord between CTRLMO and MCT8MO embryos at different stages of development. Red highlight - dorsal views, anterior spinal cord up. Blue highlight - lateral view, anterior spinal cord right. Green highlight -transversal view, dorsal spinal cord up. Scale bars represent 25 µm. **(B)** Quantification of the number of HuC/D single positive cells in a 2-myotome length of the spinal cord. n=9-17. CTRL (CTRLMO); MO (MCT8MO). Results are presented as mean ± SD; Statistical significance determined by t-test: two-sample, assuming equal variances: *p<0.05; ***p<0.001.

spinal cord, and little to no signal was found in the apical region. At 25hpf, the signal distribution in any axis differs between the two experimental groups (Figure 3A). In contrast, in CTRLMO, GFAP staining lined the basal edge of the spinal cord, while in MCT8MO embryos, it was scattered throughout the basal-apical orientation (Figure 3, transversal). However, the stained volume of GFAP in the spinal cord is similar in both groups (Figure 3B, t-test, p>0.05). The observation argues that MTH modulates gliogenesis, determining the position of glial cells and likely the cell diversity generated in this neural population.

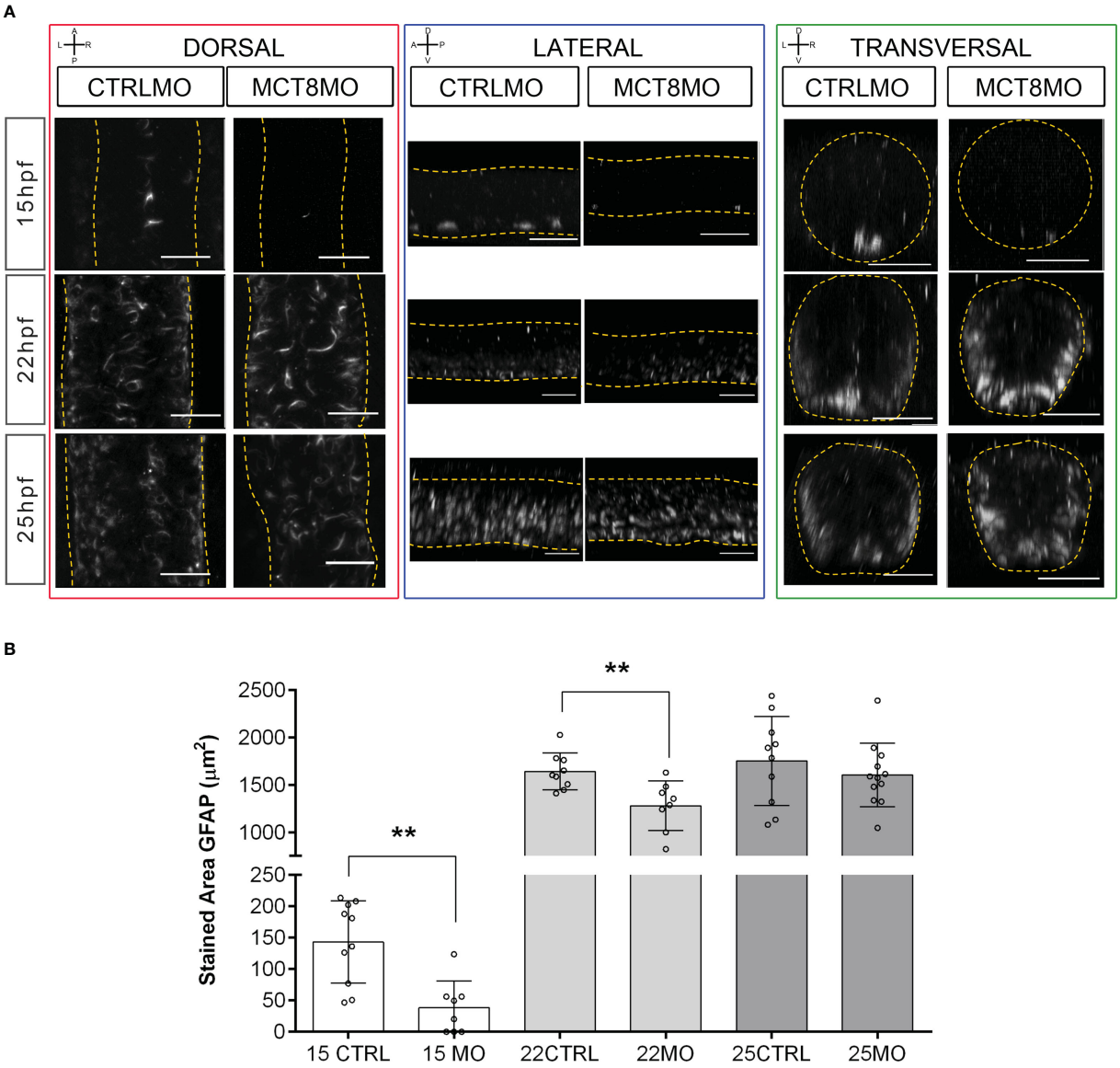

FIGURE 3
MCT8MO embryos have altered glial cell development during early neurogenesis. **(A)** Representative maximum intensity projection images of the spinal cord between somite 8-12 after glial cell labelling with ZRF-1 immunostaining (white, labelling GFAP fibers). In control embryos, at 15hpf glial cell fibers are organized in the developing ventral spinal cord; in MCT8MO embryos, the development of these cells is delayed, and only some scattered GFAP fibers are detected in the ventral-most neural tube. At 22hpf, the neural tube is closed, and glial cells can be detected throughout the spinal cord of CTRLMO and MCT8MO embryos; at 25hpf, the patterning of glial cells is altered in MCT8MO embryos. Red highlight - dorsal views, anterior spinal cord up. Blue highlight - lateral view, anterior spinal cord right. Green highlight - transversal view dorsal spinal cord up. All scale bars represent 25 µm. Dashed yellow lines denote spinal cord boundaries. **(B)** Quantification of the area of GFAP staining in a 2-myotome length of the spinal cord. n=9-17. CTRL (CTRLMO); MO (MCT8MO). Results are presented as mean ± SD; Statistical significance determined by t-test: two-sample, assuming equal variances: **p<0.01.

To further dissect which cell populations in the spinal cord are affected by lack of MTH, we analyzed the expression of genes involved in neural progenitor specification (*her2*, Figure 4A), neuron committed progenitors (*neurog1*, Figure 4B), radial glial cells (*fabp7a*, Figure 4C), astrocyte-like cells (*slc1a2b*, Figure 4D), oligodendrocytes (*olig2*, Figure 4E) and motorneurons (Nkx6.1, Figure 4F).

her2+ neural progenitors are lost from as early as 18hpf in MCT8MO, and dorsal populations are most affected (Figure 4A). Cells expressing *her2* become more spaced, suggesting that some but not all *her2*+ progenitors are more susceptible to impaired MTH signaling than others (Figure 4A).

A similar situation is observed for *neurog1*+ neuron committed progenitors (Figure 4B). At 18hpf, there are significantly fewer *neurog1* + cells in MCT8MO (Figure 4B), leading to a primarily complete loss of dorsal *neurog1*+ cells by 25hpf s (Figure 4B). This pattern continues at 32hpf. Additionally, gaps are observed in *neurog1*+ cell staining (green asterisk in Figure 4B). That observation suggests that specific *neurog1*+ progenitors at specific spinal cord locations depend more on MTH

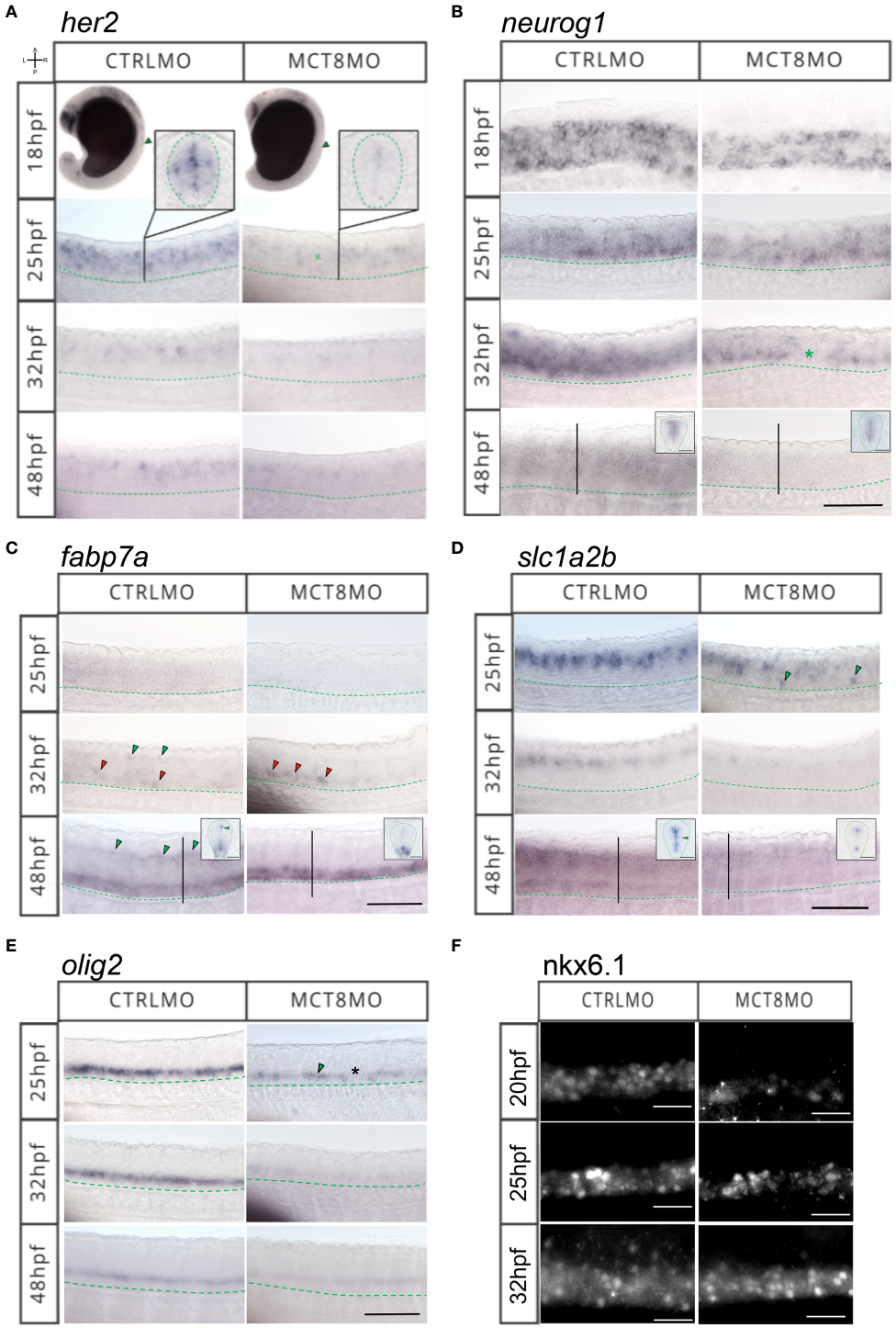

FIGURE 4
MTH is necessary for developing and correctly positioning neural cells in the spinal cord. WISH expression pattern of **(A)** *her2*, **(B)** *neurog1*, **(C)** *fabp7a*, **(D)** *slc1a2b*, **(E)** *olig2*, **(F)** IHC for Nkx6.1 in the spinal cord (SC) of zebrafish during embryonic development in MCT8MO and CTRLMO embryos. **(A)** Green asterisk in 25hpf MCT8MO represents absence of *her2* expression. **(B)** Green asterisk in 32hpf MCT8MO highlights absence of *neurog1* expression. **(C)** Green arrowheads at 32hpf CTRLMO, indicate the dorsal *fabp7a*+ cells which are lost in MCT8MO. Red arrowheads indicate increased *fabp7a* staining in the ventral domain in MCT8MO. At 48hpf, green arrowheads indicate *fabp7a*+ cells in the CTRLMO SC dorsal domain, which are less evident in MCT8MO. **(D)** At 25hpf, green arrowheads indicate misplaced *slc1a2b*+ cells in the ventral SC of MCT8MO. At 32hpf, the expression of *slc1a2b* is less abundant in MCT8MO. At 48hpf MCT8MO display reduced *slc1a2b* signal in cells at the most ventral and dorsal regions of the neurocoelom. The green arrowhead in the CTRLMO inset indicates an area where *slc1a2b* expression is less abundant in MCT8MO. **(E)** In CTRLMO, *olig2*+ cells were present in the most ventral region of the SC. At 25hpf, the green arrowhead indicates the position of *olig2*+ cell clusters, and the asterisk denotes the absence of cells in MCT8MO. **(F)** Nkx6.1 immunofluorescence detection at 20, 25, and 32hpf. A minimum of 10 individuals/conditions/gene or protein were analyzed. Images represent a lateral view of the SC (unless specified) between somites 8-12 with rostral orientation located to the left; Green dashed line represents the ventral limit of the SC; Scale bars represent 50 µm. Insets in **(B–D)** at 48hpf are transverse sections; Green dashed line represents the outermost boundary of the SC; Scale bars represent 20 µm.

than others. By 48hpf, *neurog1*+ progenitors in MCT8MO embryos are restricted to the more ventricular region of the spinal cord surrounding the neurocoelom (inserts in Figure 4B).

At 25hpf *fabp7a*+ radial glial cells seem to be highly dependent on MTH for their development, given their almost absence in MCT8MO embryos (Figure 4C). By 32hpf, some *fabp7a*+ cells are found; however, these are primarily ventral (red arrowheads in Figure 4C). In contrast, dorsal *fabp7a*+ cells are lost (green arrowheads in CTRLMO embryos in Figure 4C). This effect is accentuated at 48hpf where no dorsal *fabp7a*+ cells (green arrowheads in CRTLMO embryos in Figure 4C) are found in MCT8MO embryos. However, the ventral expression field of *fabp7a*+ in MCT8MO embryos is more extensive and presents a different spatial distribution than in CTRLMO embryos (inserts in Figure 4C).

Astrocyte-like cells expressing *slc1a2b*+ are also affected in MCT8MO embryos (Figure 4D). Already by 25hpf, there is a decrease in expression of *slc1a2b* in the dorsal spinal cord of MCT8MO embryos (Figure 4D) with a less dense row of cells present, while concomitantly with the development of ventral located *slc1a2b*+ cells (green arrowheads in Figure 4D) which are absent in control embryos. By 32hpf and 48hpf, there is a general decrease of *slc1a2b*+ cells in MCT8MO embryos' spinal cord (Figure 4D), which at 48hpf is accompanied by a restriction of the expression field, which confines to the most dorsal and ventral regions of the spinal cord canal (inserts in Figure 4D).

In MCT8MO embryos, *olig2*+ cells in the spinal cord decrease from as early as 25hpf (Figure 4E). This reduction is even more apparent at 32hpf but slightly recovers by 48hpf (Figure 4E). Nonetheless, *olig2*+ staining is always lower in MCT8MO than in control embryos (Figure 4E), suggesting the loss of some cells.

The Nkx6.1+ motorneuron cells are strongly decreased in MCT8MO embryos as early as 20hpf. That is still noticeable at 25hpf, but at 32hpf, there is an expansion of the Nkx6.1+ domain in MCT8MO embryos that is broader than in control embryos (Figure 4F). Moreover, a medial to a dorsal expansion of Nkx6.1 cells occurs in MCT8MO embryos, while in control embryos these are primarily concentrated in a ventral position (Figure 4F), suggesting that the identity of these Nkx6.1+ cells may not be identical in CTRL and MCT8MO embryos.

3.3 MTH is essential for a subset of neural progenitor cells to survive and proliferate

The previous results suggest that MTH is involved in specifying distinct neural populations. The decrease in *her2, neurog1*, and *fabp7a* expression in *mct8* morphants suggest that the function of MTH in the generation of cell diversity in the zebrafish spinal cord arises already at the progenitor level, either by restricting the fate of daughter cells or restricting the diversity within the progenitor pool itself.

All components of T3 cellular signaling (i.e. *mct8*, *thraa*, and *thrab*) are already present in the zebrafish neuro-epithelium from as early as 12hpf and widely expressed in the spinal cord up until 48hpf (Supplementary Figure 4). At 25hpf, several MTH sensitive (*mct8*+) *her2*+ neural progenitors are present in a scattered pattern more frequently in the ventral half of the spinal cord (Figure 5A). In a receptor-specific pattern, *thraa* is mostly co-expressed with *her2* dorsally (arrow) and continuously expressed anterior-posteriorly (Figure 5A). *thrab/her2* co-expression also appears anterior-posteriorly; however, it is present in bands separated by regions of no co-expression (Figure 5A). These *thrab/her2* co-expression bands spawn the dorsal-ventral axis but are more frequent in the medial region of the spinal cord. In MCT8MO embryos, co-expression of *her2* with the receptors is not lost. However, it decreases and presents different distributions (Figure 5A). In MCT8MO embryos, *thraa/her2* co-expression becomes more ventral (arrowhead) and medial, even though some dorsal co-expression is visible (Figure 5A). *thrab/her2* co-expression loses the anterior-posterior pattern of defined bands, becoming continuous and more restricted to the medial region of the spinal cord (Figure 5A).

These findings indicate the existence of at least six *her2*+ neural populations dependent at some point on MTH signaling components during spinal cord development: MTH+/*thraa*/+*thrab*+, MTH+/*thraa*+/*thrab*-, MTH+/*thraa*-/*thrab*+, MTH-/*thraa*+/*thrab*+, MTH-/*thraa*+/*thrab*- and MTH-/*thraa*-/*thrab*+.

At 25hpf, MTH sensitive cells (*mct8*+) *dla*+ cells are restricted to the medial region of the spinal cord. No *mct8/dla* co-expressing cells are detected in the spinal cord's most dorsal and ventral regions (Figure 5B). At this time, spinal cord *thraa/dla* co-expression has a very defined anterior-posterior expression pattern in bands that spawns dorso-ventrally but is more frequent medially (Figure 5B). In contrast, *thrab/dla* co-expression has an anterior-posterior decrease in frequency (asterisks) but is uniformly distributed dorso-ventrally and in large clusters (Figure 5B). At 25hpf, *mct8* morphant embryos' co-expression of *dla* with *thraa* or *thrab* is severely decreased, and its distribution changed compared to control siblings (Figure 5B). In these embryos, *thraa/dla* colocalization loses the pattern found in control siblings and is scattered with some larger clusters found in discrete dorsal, medial and ventral regions of the spinal cord (Figure 5B). In turn, *thrab/dla* colocalization still presents a decreased anterior-posterior expression (asterisk) but is almost lost dorsally and medially (Figure 5B). Although decreased compared to CTRLMO embryos, the co-expression of *thrab/dla* is more frequent at a ventral position (arrowheads in Figure 5B). These observations indicate that only a fraction of the *dla*+ cells depend on MTH, since most *thraa*+/*dla*+ co-expression is lost in MCT8MO. In the MTH-sensitive, *mct8*+/*dla*+ population cells, *thraa* is likely the primary receptor mediating the genomic action of the hormone. In MCT8MO a similar situation occurs for *thrab*+/*dla*+ co-expression, although not so widespread. Moreover, comparing the co-expression patterns between groups indicates that: i) in most dorsal and ventral regions of the spinal cord, *thrab/dla*+ cells are likely mostly irresponsive to MTH and ii) most MTH sensitive *thrab*+/*dla*+ cells have a medial localization (Figure 5B).

We further looked at *fabp7a* colocalization with *mct8*, *thraa*, and *thrab* at 48hpf, a time of extreme sensitivity of radial glial cells (RGC) to MTH (Figure 4C). In CTRLMO, colocalization of *mct8*+/*fabp7a*+, is primarily located on the most dorsal (arrow) and ventral (arrowhead) regions of the spinal cord (Figure 5C). Most

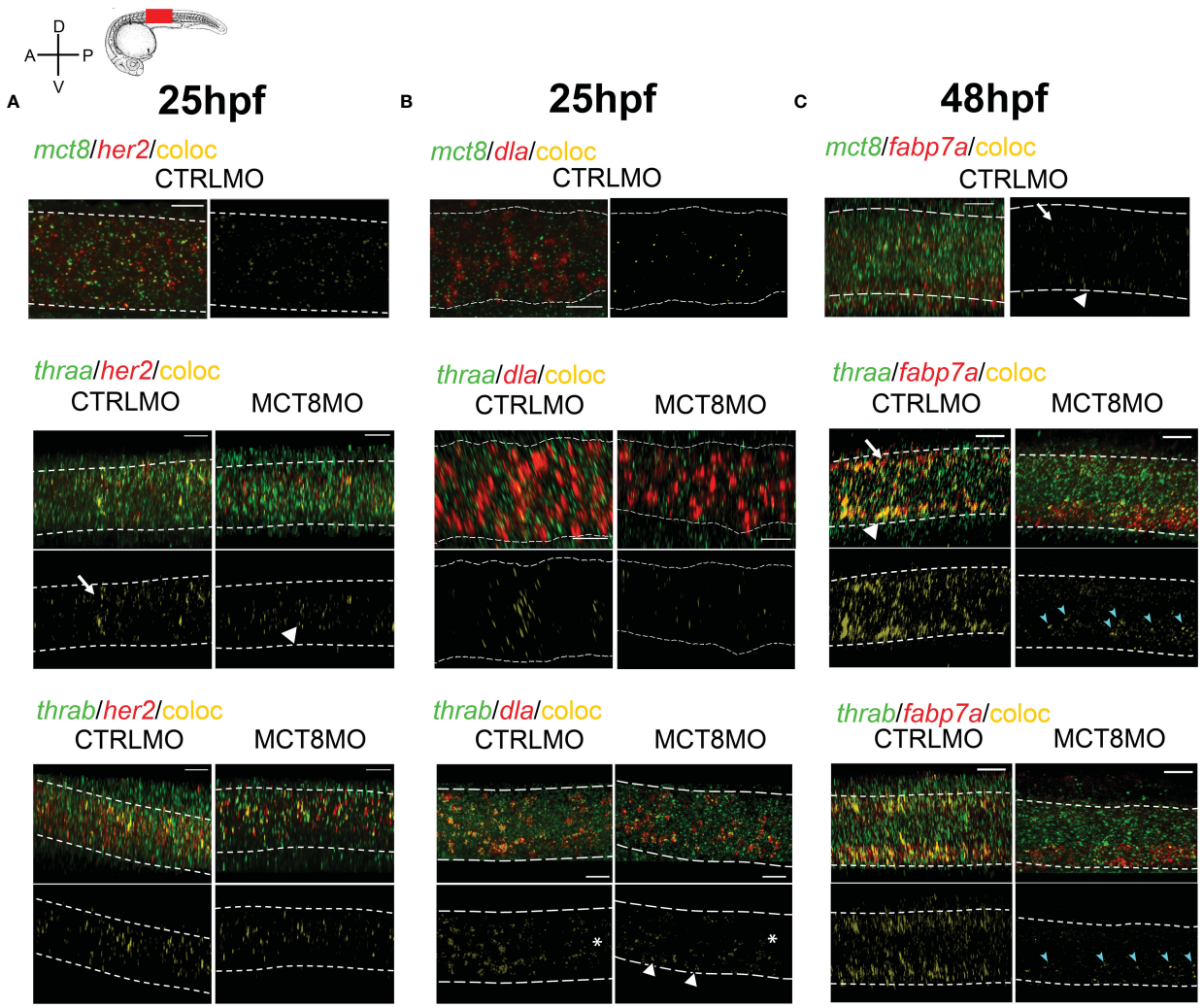

FIGURE 5
MTH is directly involved in the development of discrete *her2*, *dla*, and *fabp7a* cells. Colocalization of zebrafish *thraa*, *thrab*, and *mct8* with *her2* and *dla* expressing cells at after double WISH. *thraa*, *thrab* and *mct8* (green); *her2*, *dla* and *fabp7a* (red) and colocalization (yellow). **(A)** At 25hpf, *thraa*/*her2* colocalization in CTRLMO embryos (arrow) is increased in the apical spinal cord, while in MCT8MO *thraa*/*her2* colocalization has a more medial distribution in the spinal cord (arrowhead). **(B)** At 25hpf, *thrab*/*dla* colocalization is less predominant in MCT8MO embryos, and asterisks denote decreased colocalization along the anterior-posterior axis of the spinal cord. Arrowheads indicate the increased colocalization of *thrab*/*dla*+ in cells of the ventral spinal cord in MCT8MO embryos. **(C)** At 48hpf, *mct8*/*fabp7a* colocalization in CTRLMO occurs scattered through the spinal cord with an arrow indicating colocalization in the dorsal spinal cord and arrowhead colocalization in the ventral spinal cord. Colocalization of *fabp7a* with *thraa* and *thrab* in MCT8MO embryos is more restricted to the ventrally located *fabp7a*+ cells (blue arrowheads). All images depict a spinal cord section between somite 8-12; rostral is left and dorsal up. White dashed lines show the boundary of the spinal cord. A minimum of 3 individuals/conditions was analyzed. The scale bar represents 20μm.

fabp7a+ cells co-express *thraa* and or *thrab* (Figure 5C), indicating that RGCs are highly dependent on MTH regulated transcription. That becomes even more evident when we look at MCT8MO embryos, where there is a drastic decrease in the frequency of *fabp7*a co-expression with *thraa* and *thrab* (Figure 5C). In fact, dorsal co-expression of *fabp7a* and thrab is almost entirely lost (Figure 5C). Ventrally, in the MCT8MO, a different scenario is found. Although most co-expression of *fabp7a* with *thraa* and *thrab* is lost, *fabp7a* expression increases (Figure 5C). Notably, the remaining co-expression fields of *fabp7a* with either *thraa* or *thrab* are in clusters on the dorsal portion of the most ventral third of the spinal cord (cyan arrows in Figure 5C). Nonetheless, the superimposition of the two co-expression fields does not retire the possibility that in some *fabp7a*+ cells, MTH action occurs *via* both receptors (Figure 5C). Together these observations indicate that: i) dorsal developing *fabp7a*+ RGC rely more on MTH to differentiate than ventral RGC; ii) ventrally MTH action might be more important in RGC fate decisions and diversity (specialization) generation than general RGC *fabp7a*+ development; iii) most *fabp7a*+ RGC are dependent on MTH genomic action, but a small portion of RGC depend on thyroid receptor aporeceptor function to develop.

To further understand how MTH acts on spinal cord *her2*+ and *dla*+ neural progenitors' development, we carried out assays to understand if these cells stop proliferating or undergo apoptosis when MTH uptake by MCT8 is blocked (Figures 6, 7). We analyzed

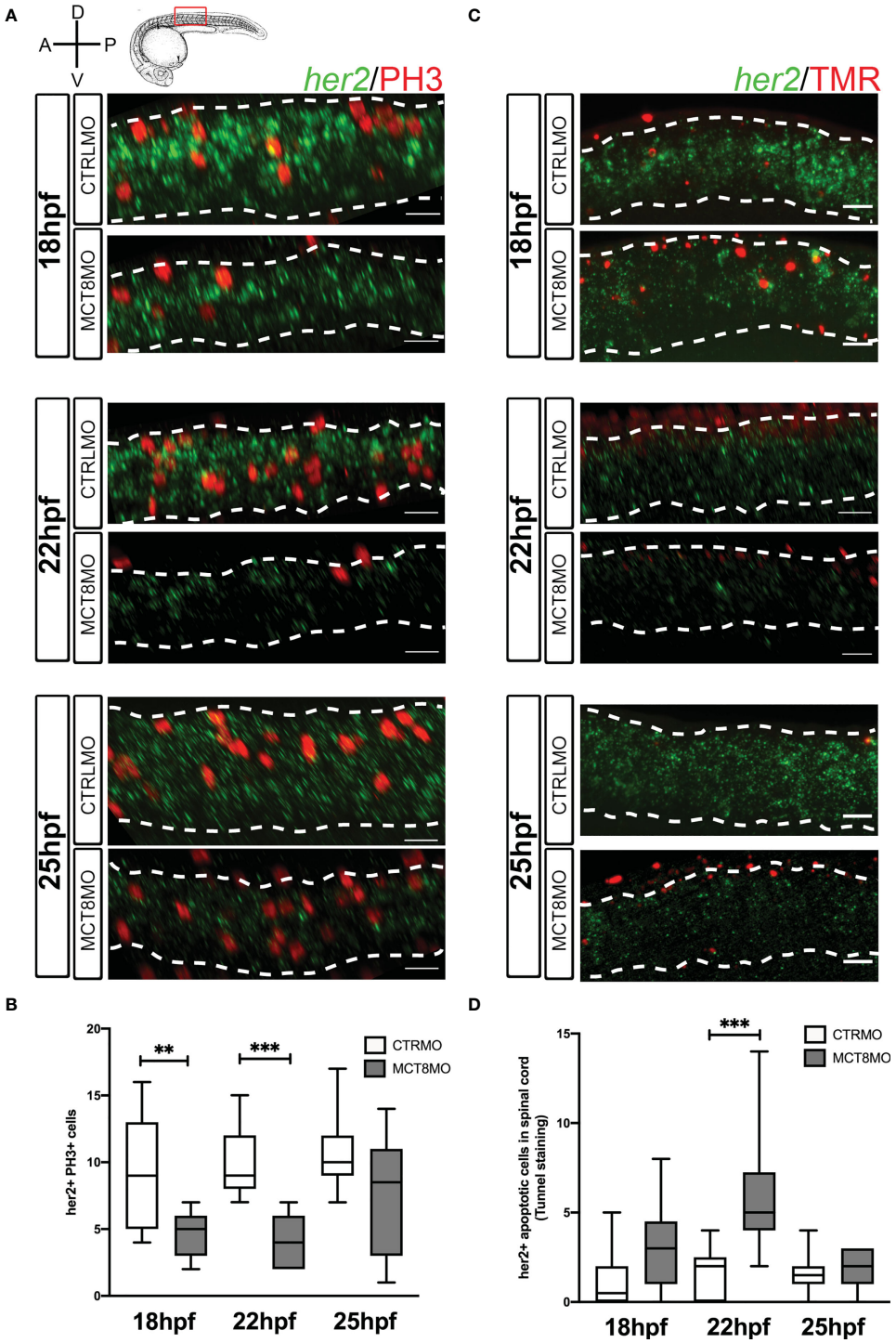

FIGURE 6
Impaired MTH signaling decreases *her2+* neural progenitor cells undergoing mitosis in the spinal cord. **(A)** Analysis of *her2* expression by fluorescent *in situ* hybridization (green) and mitotic cells (phosphohistone 3 antibody; red) in CTRLMO) and MCT8MO embryos. **(B)** Box-and-whiskers plot depicting quantification of the number of *her2+* mitotic cells (*her2+*/PH3+) in the spinal cord at 18, 22, and 25hpf. **(C)** Analysis of *her2* expression by fluorescent *in situ* hybridization (green) and colocalization with apoptotic cell detected using a TUNEL assay (red). **(D)** Box-and-whiskers plot depicting the quantification of the number of *her2+* apoptotic cells in the spinal cord. The images represent a lateral view of the spinal cord between somite 8-12; rostral is to the left in all images; the scale bar represents 50 µm. Colocalization was quantified in the volume of 2 myotomes within this spinal cord region. n=10-15. Statistical significance determined by t-test: two-sample, assuming equal variances. **p<0.01; *** p<0.001.

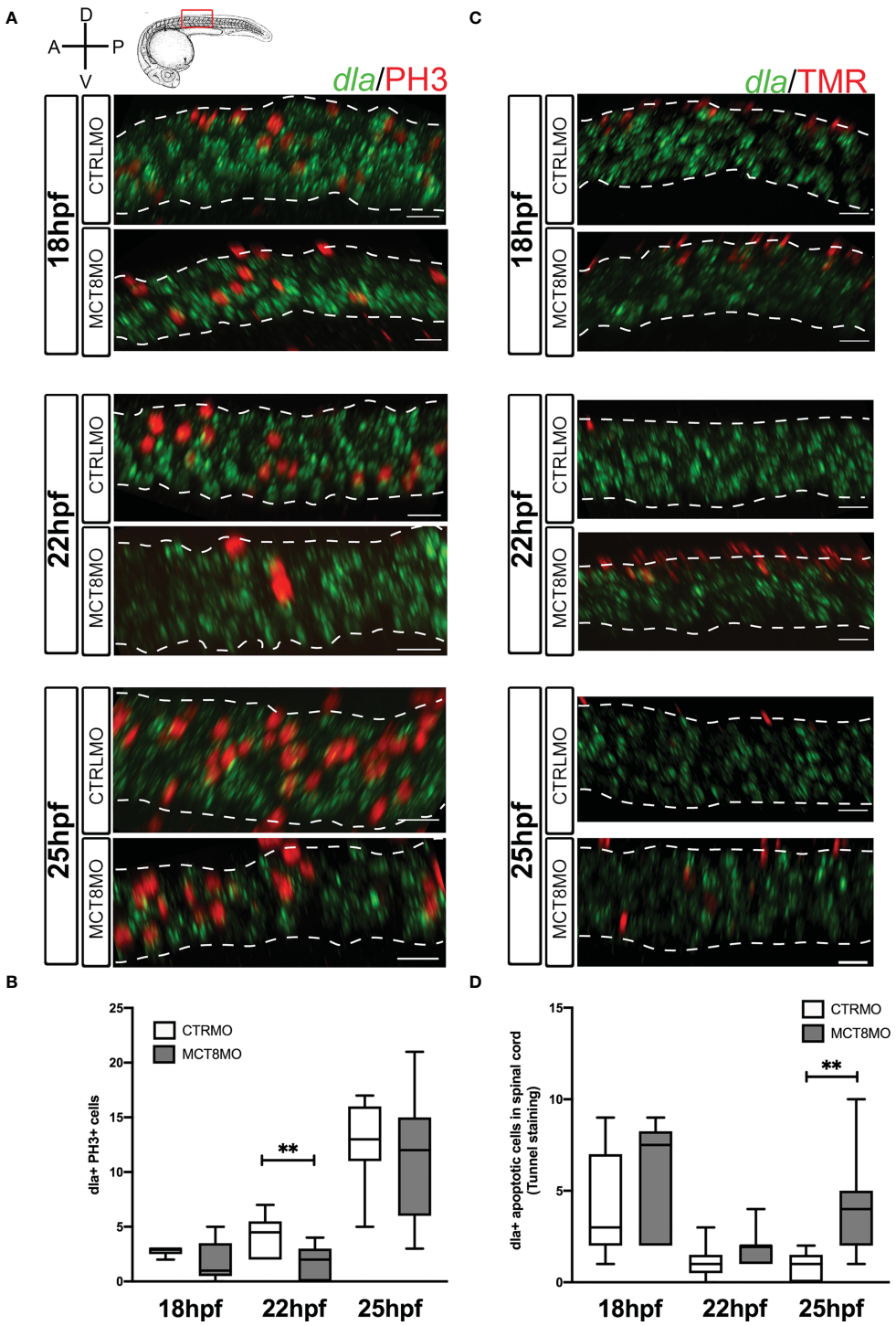

FIGURE 7
Impaired MTH signaling affects proliferation and apoptosis of *dla+* spinal cord cells in a time-restricted manner. **(A)** Analysis of *dla* expression by fluorescent *in situ* hybridization (green) and colocalization with cell mitosis (phosphohistone 3 immunostaining, red) in CTRLMO) andMCT8MO embryos. **(B)** – Box-and-whiskers plot of quantification of the number of *dla+* mitotic cells in the spinal cord at 18, 22, and 25hpf in control and MCT8MO injected embryos. **(C)** Analysis of *dla* expression by fluorescent *in situ* hybridization (green) and colocalization with apoptotic cell detected using a TUNEL assay (red). **(D)** Box-and-whiskers plot quantifying the number of *dla+* apoptotic cells in the spinal cord at 18, 22, and 25hpf in control and MCT8MO injected embryos. The images present a lateral view of the spinal cord between somite 8-12, rostral is to the left, and dorsal up in all images. The scale bar represents 50 µm. Colocalization was analyzed in 2 myotome volume sections within this spinal cord region (n=10-15). Statistical significance determined by t-test: two-sample, assuming equal variances. **p<0.01.

embryos between 18hpf and 25hpf when qPCR analysis showed that *her2* and *dla* expression was more responsive to MTH (Figure 1). In general, cell proliferation (as measured from mitotic index labeling PH3) is decreased by ~50% on average at 18 to 25hpf in MCT8MO (Supplementary Figure 5A, p<0.0001). On the other hand, in all developmental stages analyzed, apoptosis is increased 2-fold in MCT8MO relative to CTRLMO embryos (Supplementary Figure 5B, p<0.001). As previously reported (27), this increase in apoptosis is specific to the lack of MTH and cannot be rescued by p53 signaling abrogation, thus indicating a specific effect of impaired MTH.

At 18 and 22hpf, *her2*+ mitotic cells decreased ~50% in MCT8MO embryos (Figures 6A, B, p<0.01; Supplementary Figures 6A-a"). At 25hpf, there are no differences between the two groups. These results parallel the data obtained for general PH3 staining and suggest that about one-quarter of *her2*+ mitotic cells depend on MTH to proliferate (Figure 6B; Supplementary Figure 5A). Loss of *her2*+ mitotic cells in *mct8* morphants occurs more frequently in medium and ventral regions of the spinal cord at 18 and 22hpf (Figure 6A). By 25hpf, there is an evident increase in *her2*+ mitotic cells in these regions of the spinal cord in *mct8* morphants (Figure 6A; Supplementary Figures 6A-a").

Apoptosis of *her2*+ cells in MCT8MO is only higher at 22hpf (p<0.001) but not at 18 and 25hpf (Figures 6C, D; Supplementary Figure 6B-b"). The divergence of *her2*+ apoptotic cells from general spinal cord apoptosis indicates that only a small subset of *her2*+ arising at 22hpf are likely dependent on MTH to develop. Irrespective of any experimental group, apoptotic *her2*+ cells are more frequent dorsally, especially at 22 and 25hpf (Figure 6C). Together, these observations indicate that from 18 until 22hpf, about one-quarter of *her2*+ progenitors depend on MTH to survive. The evidence argues that the major role of MTH on *her2*+ progenitors is likely involved in cell fate decisions and cellular diversity generation.

The proliferation of *dla*+ cells depends on MTH only at 22hpf (Figures 7A, B, p<0.01). At that time, only one-sixth of *dla*+ cells are proliferating; of these, only half seem dependent on MTH (Figure 7B; Supplementary Figure 7A-a"). Notably, *dla*+ proliferating cells do not follow the same frequency observed for general proliferation in the spinal cord for CTRLMO and MCT8MO embryos (Figures 7A, B; Supplementary Figure 5A). At 22hpf, dla+ MTH-dependent proliferating cells in control embryos are mostly ventrally localized and mostly lost in the MCT8MO (Figure 7A).

In contrast to cell proliferation, *dla*+ apoptotic cells in the MCT8MO are increased only at 25hpf (Figures 7C, D, p<0.01; Supplementary Figure 7B-b"), accounting for twice as much as those found in control embryos. Moreover, *dla*+ apoptotic cells in control embryos only represent about 20% of all apoptotic cells in the spinal cord at 25hpf, thus suggesting that in MCT8MO, apoptotic *dla*+ cells might represent a different *dla*+ population than the one found in control siblings (Figure 7D and Supplementary Figure 5B). Notably, *dla*+ cell death does not follow the same distribution for overall spinal cord apoptosis (Figure 7D and Supplementary Figure 5B). In both control and MCT8MO embryos, most *dla*+ cells are found in the most dorsal region of the spinal cord at 18 and 22hpf (Figure 7C). In contrast, to control embryos, at 25hpf in *mct8* morphants, *dla*+ apoptotic cells locate mainly in the medial and ventral regions of the spinal cord. The results indicate that only a small subset of *dla*+ cells depend on MTH for proliferation and survival. Moreover, this dependence seems restricted to dorsally located cells and well-defined developmental times (Figure 7).

The previous evidence further supports that NOTCH signaling mediates MTH action in zebrafish spinal cord neural progenitor cells. Furthermore, our evidence supports that the dependence of NOTCH signaling on MTH is highest between 18-30hpf. To further understand if this action of MTH can be cell-autonomously rescued by activated NOTCH signaling, each morpholino group was injected with either GFP mRNA or NICD+GFP mRNA, live imaging of the spinal cord was carried out between 23-26hpf (Figure 8A) and quantified symmetric and asymmetric GFP+ cells divisions in that period (Figures 8B–F). The NICD construct will activate the Notch signaling (50). No differences in the overall cell division of GFP-expressing cells between any of the experimental groups were observed (Figure 8C). However, there were significant differences in the proportion of symmetric/asymmetric divisions in control embryos with other experimental groups (Figure 8D; $\chi 2$, $p \leq 0.05$). Nonetheless, symmetric divisions occurred more frequently in NICD+CTRLMO, MCT8MO, and NICD+MCT8MO experimental groups, although these were not statistically significant from the CTRLMO (Figure 8E, t-test p>0.05). In contrast, asymmetric divisions in MCT8MO and NICD +MCT8MO experimental groups were significantly less frequent compared to the CTRLMO group (Figure 8F, One-way ANOVA p<0.01, Sidak, p<0.05) but not the NICD+CTRLMO or between themselves. These results argue that NOTCH overexpression cannot rescue the lack of MTH signaling in these progenitor cells in a cell-autonomous manner.

4 Discussion

In the present work, we use an established zebrafish AHDS, MCT8 knockdown model and provide further evidence of a critical developmental time of MTH action. We reveal that in zebrafish, the period between 18-30hpf (~pharyngeal stage) is the most dependent on MTH based on the T3-responsive gene expression. This zebrafish developmental period corresponds to 8-24 weeks of human gestation, where MTH action in human embryonic development is essential for neurodevelopment (2, 3). Together, this data establishes a parallel action of MTH on neurodevelopment in humans and zebrafish.

Our analysis strongly supports that MTH action on target cells depends on tissue/cellular context. In zebrafish, as in mammalian systems, T3 is involved in the differentiation and proliferation of a wide variety of cell types, and this action depends on the cell identity, developmental state, and cellular context (27, 45, 67).

The data argue that MTH is not involved in neuroectoderm induction *via* B1Sox genes. However, at 12hpf, there a decrease in expression of Notch ligands *dla* and *her2* in the *mct8* morphants is observed, pointing out that a subset of neural progenitor cells

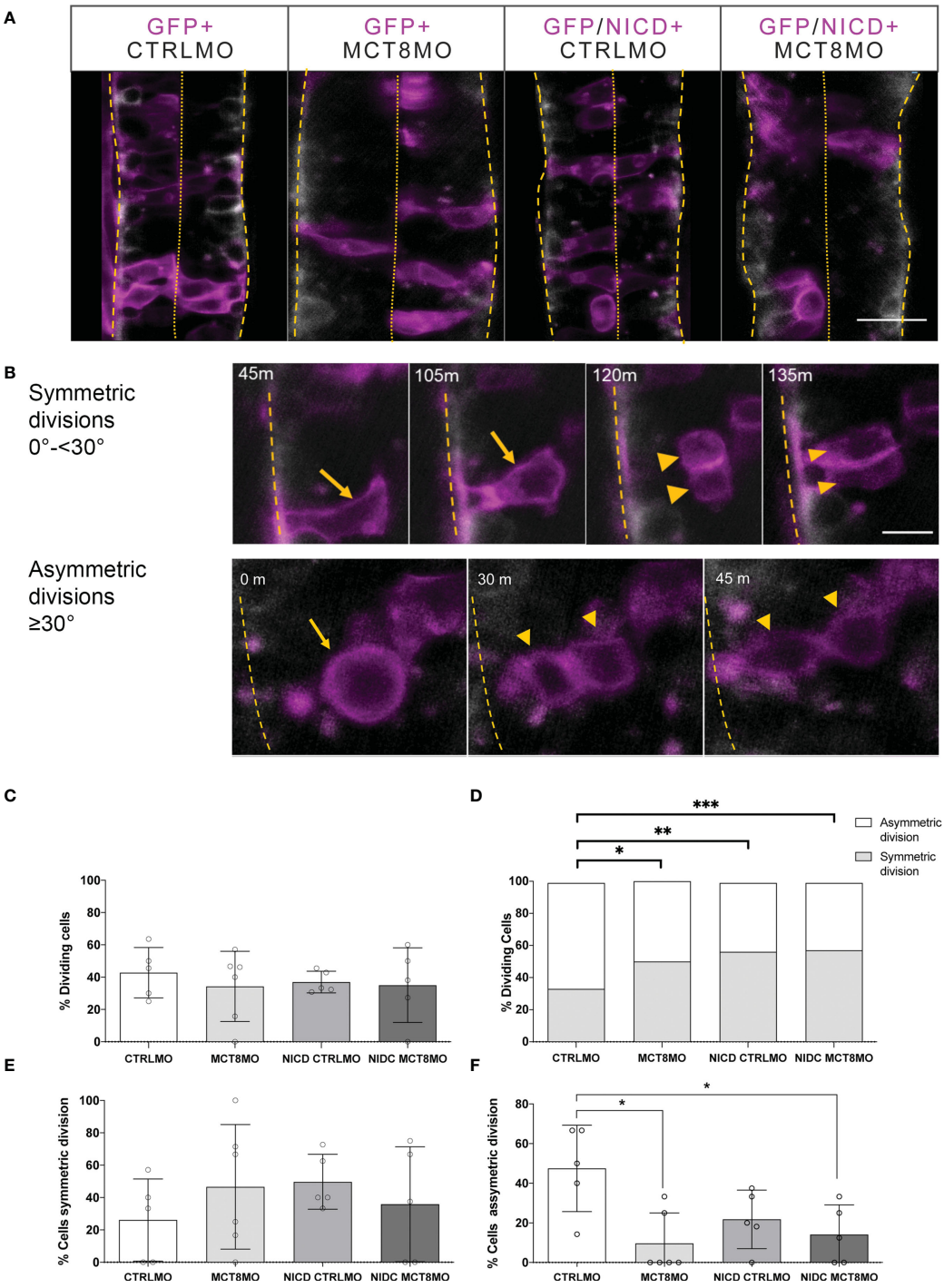

FIGURE 8
Effect of impaired MTH signaling and NICD overexpression on progenitor cell division. **(A)** At the start of imaging, representative images of the spinal cord of experimental Tg(elav3:LY-mCherry) embryos at 23hpf. Neurons (mCherry) are shown in white. Embryos were injected at the one-cell stage with either CTRLMO or MCT8MO followed by injection at the 16-cell stage in one blastomere with *gfp* mRNA only or *nicd* and *gfp* mRNA. Cells overexpressing NICD (and GFP) are labelled in magenta. Dorsal views of single slices between somite 8-15 are shown, anterior spinal cord up. The scale bar represents 50 µm. **(B)** Upper panel: Detail of symmetric division originating 2 morphologically similar GFP+ cells. A cell undergoing symmetric mitosis (yellow arrow), and the originating daughter cells (yellow arrowheads); Lower panel: Representative images of asymmetric division. A dividing cell (yellow arrow) originates two daughter cells (yellow arrowheads). Scale bar in B represent 20 µm. In all panels, the spinal cord basal limit is indicated by a dashed yellow line and the pial limit by dotted yellow lines. **(C–F)** **(C)** Percentage of analyzed GFP+ cells that underwent division. **(D)** Distribution of GFP+ dividing cells relative to all GFP+ cells observed in the period from 23-26hpf. $\chi 2$ analysis showed differences in the distribution of the number of cells undergoing symmetric or asymmetric divisions amongst experimental groups and CTRLMO ($p<0.05$). **(E)** Percentage of a cell undergoing symmetric division. **(F)** Percentage of cells undergoing asymmetric division. The results in C, D, and F are presented as the mean ± SD; results in D depict the ratio of cell division type in all GFP+ dividing cells analyzed. N =5-6 individuals per group (number of cells evaluated by group: CTRLMO/GFP=56; MCT8MO/GFP=77; CTRLMO/NICD/GFP=93; MCT8MO/NICD/GFP=46); Statistical significance in **(C, E, F)** was determined by a one-way ANOVA followed by a Holm-Sidak's multiple comparison *post hoc* analysis, *p<0.05, **p<0.01, ***p<0.001.

already responds to MTH early in neurodevelopment. The identity of these early MTH-responsive cells and their progeny remains to be confirmed.

We demonstrate that MTH is essential for the proliferation and survival of both neural stem cells, *her 2*+, and committed neuron and glial progenitors, *dla*+. That argues that MTH regulation of neural diversity is likely achieved by modulation of the output from various progenitor cells. Inhibition of MTH uptake *via* mct8 transporter during zebrafish spinal cord neurodevelopment mainly affects the expression of dorsal *her2* + neural stem cells, *neurog1*+ intermediate neuron progenitors, *fabp7a*+ and *pax6a*+ (45) radial glial progenitors, and *olig2*+ motoneuron and oligodendrocyte progenitor cells. Cells arising from these progenitors, such as *slc1a2*+ astrocyte-like cells, Nkx6.1+ motoneurons, and *gad1b*+ inhibitory interneurons (45), also show restricted development in their dorsal domains. The action of T3 on neuron development and survival has been described in chickens where mct8 knockdown leads to impaired optic tectum development, depletion of neuroprogenitors, and impaired neurogenesis with reduced neuron numbers and diversity (68). In *in vitro* mammalian cells, T3 is directly involved in the development of granule neurons by, on the one hand affecting the survival and differentiation of these cells (69) but also by preventing their apoptosis (70). Impaired maternal thyroid hormone signaling during mammalian neurodevelopment caused by mutations in thyroid hormone receptors giving resistance to T3 (71–74), congenital hypothyroid athyroid pax8 mutants, or double-knockdown *Mct8*/*Oatp1c1* (40, 75, 76), present similar cellular effects to the ones observed in zebrafish *mct8* morphant embryos ((27, 45), present study). In the developing cortex of *Mct8*/*Octp1c1* double-KO embryonic mice (40, 41, 76), *Hr* and *gad67* (respectively, homologs of zebrafish *her2* and *gad1b*) expressing cells are mostly lost in the dorsal region, suggesting that in vertebrates MTH is an essential factor for dorsal specification of neuronal cell identities. Most notably, inhibitory neuron development seems particularly dependent on MTH action in mice (41, 76) and zebrafish (27, 45). In rat embryos, T3 deficiency decreases the proliferation and delays the maturation of the precursors of cerebellar GABAergic interneurons, with effects on the number of mature GABAergic neurons and GABAergic terminals (76, 77). A similar situation is found in a new mice AHDS model. Here a human AHDS-related mutation was introduced in the *Mct8* gene (P253L) and presented altered neuroarchitecture and impaired GABAergic neuron development, but no TH-target genes expression change is found at P90 (44). Notably, in zebrafish *mct8* morphants, a decrease in dorsal spinal cord neurons was observed simultaneously with an increase in ventral motoneurons (27). These suggest that the increase in excitatory neurons and depletion of GABAnergic interneurons contribute to the cellular basis of impaired locomotion observed in *mct8* morphants (27, 28) and human AHDS patients (78–80). Above all, a key observation in zebrafish *mct8* morphants is the recovery of spinal cord neuron numbers at 25 and 48hpf. However, these neurons' identity, topology, and morphology are not identical to control morphants. That indicates that other neuron types assume their positions/locations in the loss of MTH-dependent neuron development, thus anticipating a compensatory mechanism. A similar compensatory mechanism was observed in Xenopus neurodevelopment. Here impaired NOTCH signaling leads to delayed neurogenesis, which is later compensated at the expense of impaired cell diversity (81). In human AHDS patients, microcephaly is rarely observed (79), strongly suggesting that impaired development of some neuron types leads to overgrowth from other types. The increased distribution domain of Nkx6.1+ neurons in MCT8MO suggests an alternate nature of Nkx6.1+ neurons. Indeed, in chicken embryonic retinal development, mct8 knockdown leads to a shift towards increased blue cones at the expense of green/red cones (82), confirming that in vertebrates, MTH is involved in generating neural cell diversity and the adequate balance between neuron types, in order to develop a fully functional central nervous system. In the adult mouse cortex SVZ, a similar role for T3 was found and mediated by TRa1,where the hormone balances the maintenance of the neurogenic progenitor pool and neuron differentiation (83).

The cellular mechanisms of TH action during neurodevelopment were also approached by determining the expression of TH machinery in neural spinal cord cells. In CTRLMO zebrafish embryos, co-expression of *her2* with *mct8* resembles mostly *her2* co-expression with *thraa*, suggesting that in *her2*+ progenitors, effectuation of MTH signaling is *thraa* driven. Indeed, in *mct8* morphants, *thraa* co-expression with *her2* is mainly lost in dorsal spinal cord cells, whereas it is maintained chiefly ventrally. That argues that *her2*+ dorsal NSC populations depend on MTH action *via* thraa, whereas ventral populations rely on thraa unliganded aporeceptor function to differentiate. A similar but not predominant situation appears with *thrab* since medial spinal cord co-expression with *her2*+ is mainly maintained in *mct8* morphants but lost dorsally. From our analysis, the loss of dorsal *her2*+ MTH-dependent progenitors is likely due to apoptosis since TUNEL staining strongly co-localizes with *her2*+ cells in *mct8* morphants. A similar situation is found in the embryonic mouse cortex, where impaired MTH supply leads to decreased cell cycle length and apoptosis of progenitor cells (9, 84, 85). Moreover, in cultured rat pituitary tumor granule cells, T3-induced cell proliferation is mediated by changes in G1 cyclin/cyclin-dependent kinase levels and activity (86).

Previous transcriptomic analysis in zebrafish *mct8* morphants shows a steep decrease in the expression of cell-cycle genes (45), further strengthening this possibility. However, from our analysis, one cannot discard that decreased *her2*+MTH-dependent cells diminished their numbers after reduced proliferation due to precocious differentiation and exit from the cell cycle. Therefore, another possibility is that the lack of MTH leads these progenitors into senescence. That was previously observed in the neural stem cells of adult *Mct8*/*Octp1c1* double-KO mice mutants (87).

Our data also suggest that different progenitor populations respond to MTH differently. Although co-expression of *her2* and *dla* was previously observed by single-cell analysis in wild-type zebrafish embryos (88), the effect of MTH absence on proliferation and apoptosis of *her2* and *dla* expressing cells is unequal. *dla* is expressed in neural precursors and transiently in post-mitotic neurons at 11.5hpf (89). The increased cell death of progenitor cells, especially at an early stage of neurogenesis, can contribute to

reducing progenitor pools leading to compromised neurogenesis. That is the case for oligodendrocyte progenitor populations in the zebrafish spinal cord development (90). In the case of *dla*+ cells, regulation by MTH seems to depend on two different mechanisms where *thraa* and *thrab* have different roles in different spinal cord locations, suggesting the existence of at least three different *dla*+ populations: one dependent on MTH and relies on *thraa*, one dorsal *thrab*+ population dependent on MTH, and a ventral population that is positive to *thrab* but likely irresponsive to MTH. Nonetheless, and a limitation of this study, it is not yet possible to determine the identity and the progeny arising from these different *dla*+ cell populations, and cell lineage studies are required to elucidate this aspect fully.

Interestingly, our data suggest that in zebrafish development, *fabp7a*+ radial glial cells are highly dependent on MTH and that both *trhaa* and *thrab* are fundamental for the response of these cells to MTH. A similar situation occurs in the developing mouse hippocampus and cerebellum, wherein the hypothyroid embryo's GFAP expression was markedly reduced in a time-dependent manner (91). Again, in MCT8MO, dorsal localized *fabp7a*+ RGC are almost entirely lost while an expansion of *fabp7a*+ RGC cells in the ventral domain occurs. In this ventral *fabp7a*+ domain, colocalization with *thraa* or *thrab* is maintained in MCT8MO. Interestingly, in *mct8* morphants, *pax6a*+ is also lost dorsally but less ventrally (45), further arguing for a differential dorsal-ventral role of MTH in RGCs development. From these observations, MTH is involved in the specification of different *fabp7a*+ RGCs in the spinal cord, which is then reflected in the restricted development of *slc1a2b*+ astrocyte-like cells in *mct8* morphant embryos. Our data indicate that MTH is essential to establish the correct combination of glial cell types that allow the development of adequate cytoarchitecture of the spinal cord. The observation further supports the finding that in zebrafish *mct8* morphants, neurons develop outside of the dorsal spinal cord, a region where the most significant loss of RGCs is observed.

The developmental genetic mechanisms underlying MTH control of development are poorly understood. Notwithstanding, our previous findings indicate that MTH regulates zebrafish neurodevelopment by modulating critical genetic signaling pathways, most notably WNT, SHH, and NOTCH (45). In zebrafish neurodevelopment, the NOTCH pathway appears especially responsive to MTH signaling, as major system components respond time-dependently to the hormone (Figure 1, present study). NOTCH plays a fundamental role in regulating animal neurodevelopment (revised in (92)), most notably by lateral inhibition, where it promotes cell fate specification of neural progenitors and daughter cells. However, the only examples of T3 control of the NOTCH pathway come from studies in mice (93) and Xenopus (94) postnatal intestinal development. In these models, T3 regulates several components of the NOTCH pathway, including receptors and ligands, in intestinal progenitor cells in a time and cell-context-dependent manner, hence functioning as a cell fate determinant (93, 94). Our findings point to a similar mode of action of MTH on the NOTCH pathway by regulating neural progenitor proliferation, survival, and developmental output during zebrafish neurodevelopment (discussed above). We use live imaging to show impaired MTH signaling decreases asymmetric divisions during zebrafish spinal cord development while symmetric divisions are unaffected. In the developing nervous system, symmetric divisions are associated with progenitor pool amplification or terminal differentiation of progenitors (55, 56). In contrast, asymmetric divisions are related to the acquisition of new cell fates by daughter cells or asymmetric terminal differentiation giving rise to different daughter cells and, in this way, increasing cell diversity (55). An excellent example is the lack of development of inhibitory *pax8* neurons that are lost in the spinal cord of *mct8* morphants (27). Furthermore, cell-autonomous activation of the NOTCH pathway, accomplished by mosaic overexpression of NICD, cannot rescue the consequences of impaired MTH signaling in neural progenitor cells. This observation reinforces the hypothesis that MTH likely functions in neurodevelopment as an integrative signal that allows for balanced NOTCH signaling that gives rise to the different neural cell types in a time and cell-context-dependent manner and that cannot be rescued in a cell-autonomous manner. The observation that impaired T3 signaling impacts delta and jagged ligands expression in opposing manners ((45), present study) suggests that the hormone functions as a balance and integrator that enables the appropriate input from NOTCH ligands and the developmental outcome that arises from that. That is of extreme significance given that new studies indicate that NOTCH ligand dynamics are fundamental for mice multipotent pancreatic progenitor cell output and the fate of daughter cells arising from the division of these progenitors (95). Such an integrative function of MT3 in neurodevelopment supports the observations that both excess and impaired hormone signaling have profound effects on central nervous system development and function.

Nonetheless, new studies are necessary to further dissect MTH's role on NOTCH signaling modulation and neural progenitor output in zebrafish and human neurodevelopment. Another important aspect of this evidence is that MTH action is modulated by tissue and cellular context. Engraftment of human patient-derived *MCT8*(-/-) iPSCs cells into euthyroid neonatal mice corpus callosum and cerebellum can differentiate into oligodendrocytes and myelinate adjacent fibers. In contrast, if these patient-derived cells are injected into an *Mct8*(-/-);*Oatp1c1*(-/-);*Rag2*(-/-) hypothyroid neonatal mice corpus callosum and cerebellum human *MCT8*(-/-) iPSCs cells remain in an undifferentiated progenitor state (96). That is reminiscent of our present results with NOTCH and argues that MTH action in neurodevelopment depends highly on cell and tissue context.

The implications of present findings for the comprehension of ADHS, and the development of putative therapies, are significant. It has been suggested that the pathogenesis associated with MCT8 deficiency arises from impaired TH transport across the blood-brain barrier (97, 98). Here we show that the effect over neural cell progenitors occurs before blood-brain-barrier development in zebrafish, suggesting that MTH entering through Mct8 of CNS-residing cells regulates their development.

In conclusion, our data support that the restricted temporal action of MTH is critical for vertebrate neurodevelopment. MTH acting through Mct8 is essential to sustain neural progenitor cells' survival and proliferation, allowing them to reach the full potential of cell

diversity during neurogenesis and gliogenesis. That is likely achieved by MTH regulation of particular neural progenitors' developmental output (i.e. fate decisions) reflecting neuronal and glial cell populations. In zebrafish *mct8* morphant embryos, the overall neurodevelopmental effects of MTH impairment arise from the lack of a direct action of MTH on target gene transcription and relief of gene expression repression by unliganded thyroid receptors. In both cases, the likely cause behind this impaired development is decreased differentiated neural cell diversity due to the loss of lineage-committed progenitors. Given this evidence, two non-mutually exclusive hypotheses arise to explain how MTH regulates vertebrate neurodevelopment: 1) MTH acts in neural progenitors to allow particular cellular states that enable the generation of the full potential cell fates arising from these progenitors, and 2) MTH acts by allowing final differentiation and survival of neural progenitors committed to a given cell fate generation.

Data availability statement

The raw data supporting the conclusions of this article will be made available by the authors, without undue reservation.

Ethics statement

Fish husbandry was conducted by trained scientists according to the EU Directive (2010/63/EU) and followed the Portuguese legislation for the use of laboratory animals (DL n°113/2013, 7 August). All experimental animals are younger than 5-dpf, and no ethical approval is required accordingly to Portuguese (DL n°113/2013, 7 August) and EU (2010/63/EU) law.

Author contributions

NS: Methodology, Visualization, Writing - Original Draft, Review and Editing. MC: Conceptualization, Methodology, Writing - Original Draft, Review and Editing, Supervision. All authors contributed to the article and approved the submitted version.

Funding

This study received Portuguese national funds from FCT - Foundation for Science and Technology through project PTDC/EXPL/MAR-BIO/0430/2013 and FCT UIDB/04326/2020 COMPETE 2020, through project EMBRC.PT ALG-01-0145-FEDER-022121. ABC-RI CRESC Algarve 2020. NS was a recipient of an FCT Ph.D. grant SFRH/BD/111226/2015. MC received an FCT-IF Starting Grant (IF/01274/2014). Support of ABC and Camara Municipal de Loulé.

Acknowledgments

The authors thank Susana Santos Lopes for the Notch-intracellular domain (NICD) construct and Michael Orger for the zebrafish Tg(*elav3:LY-mCherry*) line.

Conflict of interest

The authors declare that the research was conducted in the absence of any commercial or financial relationships that could be construed as a potential conflict of interest.

Publisher's note

All claims expressed in this article are solely those of the authors and do not necessarily represent those of their affiliated organizations, or those of the publisher, the editors and the reviewers. Any product that may be evaluated in this article, or claim that may be made by its manufacturer, is not guaranteed or endorsed by the publisher.

Supplementary material

The Supplementary Material for this article can be found online at: https://www.frontiersin.org/articles/10.3389/fendo.2023.1157685/full#supplementary-material

SUPPLEMENTARY FIGURE 1
MCT8 morpholino KD is a valid strategy to generate a zebrafish AHDS biomedical model.

SUPPLEMENTARY FIGURE 2
Expression of MTH-responsive genes reveals 22-31hpf as the developmental time more sensitive to MTH.

SUPPLEMENTARY FIGURE 3
Impairment of MTH signaling leads to altered spinal cord cytoarchitecture at the end of embryogenesis.

SUPPLEMENTARY FIGURE 4
Spatio-temporal expression of MTH cellular signaling genes mct8, thraa, and thrab during zebrafish spinal cord neurodevelopment.

SUPPLEMENTARY FIGURE 5
Impaired MTH signaling affects mitosis and apoptosis in the spinal cord.

SUPPLEMENTARY FIGURE 6
Colocalization analysis of *her 2* expression by wish with cell mitosis by immunohistochemistry with phosphohistone 3 (PH3) and apoptotic cell labelling (TUNEL) of a 22hpf CTRLMO zebrafish.

SUPPLEMENTARY FIGURE 7
Colocalization analysis of *dla* expression by wish with cell mitosis by immunohistochemistry with phosphohistone 3 (PH3) and apoptotic cell labeling (TUNEL) of a 22hpf CTRLMO zebrafish.

References

1. Yen PM, Ando S, Feng X, Liu Y, Maruvada P, Xia X. Thyroid hormone action at the cellular, genomic and target gene levels. *Mol Cell Endocrinol* (2006) 246:121–7. doi: 10.1016/j.mce.2005.11.030

2. Williams GR. Neurodevelopmental and neurophysiological actions of thyroid hormone. *J Neuroendocrinol* (2008) 20:784–94. doi: 10.1111/j.1365-2826.2008.01733.x

3. Morreale de Escobar G, Obregon MJ, Escobar del Rey F. Role of thyroid hormone during early brain development. *Eur J Endocrinol* (2004) 151:U25–37. doi: 10.1530/eje.0.151u025

4. Morreale de Escobar G, Obregón MAJ, Escobar del Rey F. Is neuropsychological development related to maternal hypothyroidism or to maternal hypothyroxinemia? *J Clin Endocrinol Metab* (2000) 85:3975–87. doi: 10.1210/jc.85.11.3975

5. De Escobar GM, Calvo R, Obregon MJ, Del Rey FE. Contribution of maternal thyroxine to fetal thyroxine pools in normal rats near term. *Endocrinology* (1990) 126:2765–7. doi: 10.1210/endo-126-5-2765

6. Obregon MJ, Mallol J, Pastor R, Escobar GMD, Rey FED. L-thyroxine and 3,5,3'-trii000-l-thyronine in rat embryos before onset of fetal thyroid function. *Endocrinology* (1984) 114:305–7. doi: 10.1210/endo-114-1-305

7. Zoeller RT, Rovet J. Timing of thyroid hormone action in the developing brain: clinical observations and experimental findings. *J Neuroendocrinol* (2004) 16:809–18. doi: 10.1111/j.1365-2826.2004.01243.x

8. Chatonnet F, Flamant F, Morte B. A temporary compendium of thyroid hormone target genes in brain. *Biochim Biophys Acta (BBA) - Gene Regul Mech* (2015) 1849:122–9. doi: 10.1016/j.bbagrm.2014.05.023

9. Gil-Ibañez P, García-García F, Dopazo J, Bernal J, Morte B. Global transcriptome analysis of primary cerebrocortical cells: identification of genes regulated by triiodothyronine in specific cell types. *Cereb Cortex* (2015) 27:706–17. doi: 10.1093/cercor/bhv273

10. Salazar P, Cisternas P, Martinez M, Inestrosa NC. Hypothyroidism and cognitive disorders during development and adulthood: implications in the central nervous system. *Mol Neurobiol* (2019) 56:2952–63. doi: 10.1007/s12035-018-1270-y

11. Vancamp P, Darras VM. From zebrafish to human: a comparative approach to elucidate the role of the thyroid hormone transporter MCT8 during brain development. *Gen Comp Endocrinol* (2018) 265:219–29. doi: 10.1016/j.ygcen.2017.11.023

12. Bernal J. Thyroid hormones in brain development and function. in: De Groot LJ, Chrousos G, and D. K, (Eds.), Endotext, MDText.com, Inc, South Dartmouth, 2015.

13. Friesema ECH, Ganguly S, Abdalla A, Fox JEM, Halestrap AP, Visser TJ. Identification of monocarboxylate transporter 8 as a specific thyroid hormone transporter. *J Biol Chem* (2003) 278:40128–35. doi: 10.1074/jbc.M300909200

14. Dumitrescu AM, Liao XH, Best TB, Brockmann K, Refetoff S. A novel syndrome combining thyroid and neurological abnormalities is associated with mutations in a monocarboxylate transporter gene. *Am J Hum Genet* (2004) 74:168–75. doi: 10.1086/380999

15. Remerand G, Boespflug-Tanguy O, Tonduti D, Touraine R, Rodriguez D, Curie A, et al. Expanding the phenotypic spectrum of Allan–Herndon–Dudley syndrome in patients with SLC16A2 mutations. *Dev Med Child Neurol* (2019) 61:1439–47. doi: 10.1111/dmcn.14332

16. Lopez-Espindola D, Morales-Bastos C, Grijota-Martinez C, Liao XH, Lev D, Sugo E, et al. Mutations of the thyroid hormone transporter MCT8 cause prenatal brain damage and persistent hypomyelination. *J Clin Endocrinol Metab* (2014) 99:E2799–804. doi: 10.1210/jc.2014-2162

17. Boccone L, Dessì V, Meloni A, Loudianos G. Allan–Herndon–Dudley syndrome (AHDS) in two consecutive generations caused by a missense MCT8 gene mutation. phenotypic variability with the presence of normal serum T3 levels. *Eur J Med Genet* (2013) 56:207–10. doi: 10.1016/j.ejmg.2013.02.001

18. Azzolini S, Nosadini M, Balzarin M, Sartori S, Suppiej A, Mardari R, et al. Delayed myelination is not a constant feature of Allan-Herndon-Dudley syndrome: report of a new case and review of the literature. *Brain Dev* (2014) 36:716–20. doi: 10.1016/j.braindev.2013.10.009

19. Rodrigues F, Grenha J, Ortez C, Nascimento A, Morte B, M-Belinchón M, et al. Hypotonic male infant and MCT8 deficiency - a diagnosis to think about. *BMC Pediatr* (2014) 14:252. doi: 10.1186/1471-2431-14-252

20. Matheus MG, Lehman RK, Bonilha L, Holden KR. Redefining the pediatric phenotype of X-linked monocarboxylate transporter 8 (MCT8) Deficiency: Implications for diagnosis and therapies. *J Child Neurol* (2015) 30:1664–8. doi: 10.1177/0883073815578524

21. Novara F, Groeneweg S, Freri E, Estienne M, Reho P, Matricardi S, et al. Clinical and molecular characteristics of SLC16A2 (MCT8) mutations in three families with the Allan–Herndon–Dudley syndrome. *Hum Mutat* (2017) 38:260–4. doi: 10.1002/humu.23140

22. Chan SY, Hancox LA, Mart√≠n-Santos A, Loubi√®re LS, Walter MNM, Gonz√°lez A-M, et al. MCT8 expression in human fetal cerebral cortex is reduced in severe intrauterine growth restriction. *J Endocrinol* (2014) 220:85–95. doi: 10.1530/JOE-13-0400

23. López-Espíndola D, García-Aldea Á, Gómez de la Riva I, Rodríguez-García AM, Salvatore D, Visser TJ, et al. Thyroid hormone availability in the human fetal brain: novel entry pathways and role of radial glia. *Brain Struct Funct* (2019) 224:2103–19. doi: 10.1007/s00429-019-01896-8

24. Groeneweg S, Peeters RP, Moran C, Stoupa A, Auriol F, Tonduti D, et al. Effectiveness and safety of the tri-iodothyronine analogue triac in children and adults with MCT8 deficiency: an international, single-arm, open-label, phase 2 trial. *Lancet Diabetes Endocrinol* (2019) 7:695–706. doi: 10.1016/S2213-8587(19)30155-X

25. Grijota-Martínez C, Montero-Pedrazuela A, Hidalgo-Álvarez J, Bárez-López S, Guadaño-Ferraz A. Intracerebroventricular high doses of TRIAC at juvenile stages improve peripheral hyperthyroidism and mediate thyromimetic effects in limited brain regions in a mouse model of MCT8 deficiency. *Thyroid* (2022) 4:501–10. doi: 10.1089/thy.2022.0562

26. Refetoff S, Pappa T, Williams MK, Matheus MG, Liao XH, Hansen K, et al. Prenatal treatment of thyroid hormone cell membrane transport defect caused by MCT8 gene mutation. *Thyroid* (2021) 31:713–20. doi: 10.1089/thy.2020.0306

27. Campinho MA, Saraiva J, Florindo C, Power DM. Maternal thyroid hormones are essential for neural development in zebrafish. *Mol Endocrinol* (2014) 28:1136–44. doi: 10.1210/me.2014-1032

28. de Vrieze E, van de Wiel SMW, Zethof J, Flik G, Klaren PHM, Arjona FJ. Knockdown of monocarboxylate transporter 8 (mct8) disturbs brain development and locomotion in zebrafish. *Endocrinology* (2014) 155:2320–30. doi: 10.1210/en.2013-1962

29. Vatine GD, Zada D, Lerer-Goldshtein T, Tovin A, Malkinson G, Yaniv K, et al. Zebrafish as a model for monocarboxyl transporter 8-deficiency. *J Biol Chem* (2013) 288:169–80. doi: 10.1074/jbc.M112.413831

30. Zada D, Tovin A, Lerer-Goldshtein T, Vatine GD, Appelbaum L. Altered behavioral performance and live imaging of circuit-specific neural deficiencies in a zebrafish model for psychomotor retardation. *PloS Genet* (2014) 10:e1004615. doi: 10.1371/journal.pgen.1004615

31. Chang J, Wang M, Gui W, Zhao Y, Yu L, Zhu G. Changes in thyroid hormone levels during zebrafish development. *Zool Sci* (2012) 29:181–4. doi: 10.2108/zsj.29.181

32. Vergauwen L, Cavallin JE, Ankley GT, Bars C, Gabriëls IJ, Michiels EDG, et al. Gene transcription ontogeny of hypothalamic-pituitary-thyroid axis development in early-life stage fathead minnow and zebrafish. *Gen Comp Endocrinol* (2018) 266:87–100. doi: 10.1016/j.ygcen.2018.05.001

33. Blanton ML, Specker JL. The hypothalamic-pituitary-thyroid (HPT) axis in fish and its role in fish development and reproduction. *Crit Rev Toxicol* (2007) 37:97–115. doi: 10.1080/10408440601123529

34. Porazzi P, Calebiro D, Benato F, Tiso N, Persani L. Thyroid gland development and function in the zebrafish model. *Mol Cell Endocrinol* (2009) 312:14–23. doi: 10.1016/j.mce.2009.05.011

35. Kinne A, Kleinau G, Hoefig CS, Groters A, Kahrle J, Krause G, et al. Essential molecular determinants for thyroid hormone transport and first structural implications for monocarboxylate transporter 8. *J Biol Chem* (2010) 285:28054–63. doi: 10.1074/jbc.M110.129577

36. Arjona FJ, de Vrieze E, Visser TJ, Flik G, Klaren PHM. Identification and functional characterization of zebrafish solute carrier Slc16a2 (Mct8) as a thyroid hormone membrane transporter. *Endocrinology* (2011) 152:5065–73. doi: 10.1210/en.2011-1166

37. Walter KM, Miller GW, Chen X, Harvey DJ, Puschner B, Lein PJ. Changes in thyroid hormone activity disrupt photomotor behavior of larval zebrafish. *NeuroToxicology* (2019) 74:47–57. doi: 10.1016/j.neuro.2019.05.008

38. Opitz R, Maquet E, Huisken J, Antonica F, Trubiroha A, Pottier Gl, et al. Transgenic zebrafish illuminate the dynamics of thyroid morphogenesis and its relationship to cardiovascular development. *Dev Biol* (2012) 372:203–16. doi: 10.1016/j.ydbio.2012.09.011

39. Roberts LM, Woodford K, Zhou M, Black DS, Haggerty JE, Tate EH, et al. Expression of the thyroid hormone transporters monocarboxylate transporter-8 (SLC16A2) and organic ion transporter-14 (SLCO1C1) at the blood-brain barrier. *Endocrinology* (2008) 149:6251–61. doi: 10.1210/en.2008-0378

40. Mayerl S, Müller J, Bauer R, Richert S, Kassmann CM, Darras VM, et al. Transporters MCT8 and OATP1C1 maintain murine brain thyroid hormone homeostasis. *J Clin Invest* (2014) 124:1987–99. doi: 10.1172/JCI70324

41. Maity-Kumar G, Ständer L, DeAngelis M, Lee S, Molenaar A, Becker L, et al. Validation of Mct8/Oatp1c1 dKO mice as a model organism for the Allan-Herndon-Dudley syndrome. *Mol Metab* (2022) 66:101616. doi: 10.1016/j.molmet.2022.101616

42. Trajkovic-Arsic M, Muller J, Darras VM, Groba C, Lee S, Weih D, et al. Impact of monocarboxylate transporter-8 deficiency on the hypothalamus-Pituitary-Thyroid axis in mice. *Endocrinology* (2010) 151:5053–62. doi: 10.1210/en.2010-0593

43. Bárez-López S, Grijota-Martínez C, Ausó E, Fernández-de Frutos M, Montero-Pedrazuela A, Guadaño-Ferraz A. Adult mice lacking Mct8 and Dio2 proteins present alterations in peripheral thyroid hormone levels and severe brain and motor skill impairments. *Thyroid* (2019) 29:1669–82. doi: 10.1089/thy.2019.0068

44. Valcárcel-Hernández V, Guillén-Yunta M, Bueno-Arribas M, Montero-Pedrazuela A, Grijota-Martínez C, Markossian S, et al. A CRISPR/Cas9-engineered avatar mouse model of monocarboxylate transporter 8 deficiency displays distinct neurological alterations. *Neurobiol Dis* (2022) 174:105896. doi: 10.1016/j.nbd.2022.105896

45. Silva N, Louro B, Trindade M, Power DM, Campinho MA. Transcriptomics reveal an integrative role for maternal thyroid hormones during zebrafish embryogenesis. *Sci Rep* (2017) 7:16657. doi: 10.1038/s41598-017-16951-9

46. Kimmel CB, Ballard WW, Kimmel SR, Ullmann B, Schilling TF. Stages of embryonic development of the zebrafish. *Dev Dyn* (1995) 203:253–310. doi: 10.1002/aja.1002030302

47. Bustin SA, Benes V, Garson JA, Hellemans J, Huggett J, Kubista M, et al. The MIQE guidelines: minimum information for publication of quantitative real-time PCR experiments. *Clin Chem* (2009) 55:611–22. doi: 10.1373/clinchem.2008.112797

48. Schindelin J, Arganda-Carreras I, Frise E, Kaynig V, Longair M, Pietzsch T, et al. Fiji: An open-source platform for biological-image analysis. *Nat Methods* (2012) 9:676–82. doi: 10.1038/nmeth.2019

49. Gorlewicz A, Krawczyk K, Szczepankiewicz AA, Trzaskoma P, Mulle C, Wilczynski GM. Colocalization colormap -an ImageJ plugin for the quantification and visualization of colocalized signals. *Neuroinformatics* (2020) 18:661–4. doi: 10.1007/s12021-020-09465-9

50. Takke C, Campos-Ortega JA. her1, a zebrafish pair-rule like gene, acts downstream of notch signalling to control somite development. *Development* (1999) 126:3005–14. doi: 10.1242/dev.126.13.3005

51. Kwan KM, Fujimoto E, Grabher C, Mangum BD, Hardy ME, Campbell DS, et al. The Tol2kit: a multisite gateway-based construction kit for <I>Tol2</I> transposon transgenesis constructs. *Dev Dyn* (2007) 236:3088–99. doi: 10.1002/dvdy.21343

52. Bianco IH, Ma L-H, Schoppik D, Robson DN, Orger MB, Beck JC, et al. The tangential nucleus controls a gravito-inertial vestibulo-ocular reflex. *Curr Biol* (2012) 22:1285–95. doi: 10.1016/j.cub.2012.05.026

53. Strehlow D, Heinrich G, Gilbert W. The fates of the blastomeres of the 16-cell zebrafish embryo. *Development* (1994) 120:1791–8. doi: 10.1242/dev.120.7.1791

54. Kaufmann A, Mickoleit M, Weber M, Huisken J. Multilayer mounting enables long-term imaging of zebrafish development in a light sheet microscope. *Development* (2012) 139:3242–7. doi: 10.1242/dev.082586

55. Götz M, Huttner WB. The cell biology of neurogenesis. *Nat Rev Mol Cell Biol* (2005) 6:777–88. doi: 10.1038/nrm1739

56. Taverna E, Magdalena G, Wieland BH. The cell biology of neurogenesis: toward an understanding of the development and evolution of the neocortex. *Annu Rev Cell Dev Biol* (2014) 30:465–502. doi: 10.1146/annurev-cellbio-101011-155801

57. Moreno-Mateos MA, Vejnar CE, Beaudoin J-D, Fernandez JP, Mis EK, Khokha MK, et al. CRISPRscan: designing highly efficient sgRNAs for CRISPR-Cas9 targeting in vivo. *Nat Meth* (2015) 12:982–8. doi: 10.1038/nmeth.3543

58. Rossi A, Kontarakis Z, Gerri C, Nolte H, Holper S, Kruger M, et al. Genetic compensation induced by deleterious mutations but not gene knockdowns. *Nature* (2015) 524:230–3. doi: 10.1038/nature14580

59. Stainier DYR, Raz E, Lawson ND, Ekker SC, Burdine RD, Eisen JS, et al. Guidelines for morpholino use in zebrafish. *PloS Genet* (2017) 13:e1007000. doi: 10.1371/journal.pgen.1007000

60. Okuda Y, Ogura E, Kondoh H, Kamachi Y. B1 SOX coordinate cell specification with patterning and morphogenesis in the early zebrafish embryo. *PloS Genet* (2010) 6 (5):e1000936. doi: 10.1371/journal.pgen.1000936

61. Schmidt R, Strahle U, Scholpp S. Neurogenesis in zebrafish - from embryo to adult. *Neural Dev* (2013) 8. doi: 10.1186/1749-8104-8-3

62. Okigawa S, Mizoguchi T, Okano M, Tanaka H, Isoda M, Jiang Y-J, et al. Different combinations of notch ligands and receptors regulate V2 interneuron progenitor proliferation and V2a/V2b cell fate determination. *Dev Biol* (2014) 391 (2):196–206. doi: 10.1016/j.ydbio.2014.04.011

63. Cheng Y-C, Chiang M-C, Shih H-Y, Ma T-L, Yeh T-H, Huang Y-C, et al. The transcription factor hairy/E(spl)-related 2 induces proliferation of neural progenitors and regulates neurogenesis and gliogenesis. *Dev Biol* (2015) 397:116–28. doi: 10.1016/j.ydbio.2014.10.018

64. Gao H, Bu Y, Wu Q, Wang X, Chang N, Lei L, et al. Mecp2 regulates neural cell differentiation by suppressing the Id1 to Her2 axis in zebrafish. *J Cell Sci* (2015) 128:2340–50. doi: 10.1242/jcs.167874

65. Takke C, Dornseifer P, Weizs√§cker VE, Campos-Ortega JA. her4, a zebrafish homologue of the drosophila neurogenic gene e(spl), is a target of NOTCH signalling. *Development* (1999) 126:1811–21. doi: 10.1242/dev.126.9.1811

66. Mahler J, Filippi A, Driever W. DeltaA/DeltaD regulate multiple and temporally distinct phases of notch signaling during dopaminergic neurogenesis in zebrafish. *J Neurosci* (2010) 30:16621–35. doi: 10.1523/JNEUROSCI.4769-10.2010

67. Puzianowska-Kuznicka M, Damjanovski S, Shi YB. Both thyroid hormone and 9-cis retinoic acid receptors are required to efficiently mediate the effects of thyroid hormone on embryonic development and specific gene regulation in xenopus laevis. *Mol Cell Biol* (1997) 17:4738–49. doi: 10.1128/MCB.17.8.4738

68. Vancamp P, Deprez M-A, Remmerie M, Darras VM. Deficiency of the thyroid hormone transporter monocarboxylate transporter 8 in neural progenitors impairs cellular processes crucial for early corticogenesis. *J Neurosci* (2017) 37:11616–31. doi: 10.1523/JNEUROSCI.1917-17.2017

69. Heisenberg CP, Thoenen H, Lindholm D. Tri-iodothyronine regulates survival and differentiation of rat cerebellar granule neurons. *Neuroreport* (1992) 3:685–8. doi: 10.1097/00001756-199208000-00008

70. Muller Y, Rocchi E, Lazaro JB, Clos J. Thyroid hormone promotes BCL-2 expression and prevents apoptosis of early differentiating cerebellar granule neurons. *Int J Dev Neurosci* (1995) 13:871–85. doi: 10.1016/0736-5748(95)00057-7

71. Hashimoto K, Curty FH, Borges PP, Lee CE, Abel ED, Elmquist JK, et al. An unliganded thyroid hormone receptor causes severe neurological dysfunction. *Proc Natl Acad Sci* (2001) 98:3998–4003. doi: 10.1073/pnas.051454698

72. Yu L, Iwasaki T, Xu M, Lesmana R, Xiong Y, Shimokawa N, et al. Aberrant cerebellar development of transgenic mice expressing dominant-negative thyroid hormone receptor in cerebellar purkinje cells. *Endocrinology* (2015) 156:1565–76. doi: 10.1210/en.2014-1079

73. Fauquier T, Romero E, Picou F, Chatonnet F, Nguyen X-N, Quignodon L, et al. Severe impairment of cerebellum development in mice expressing a dominant-negative mutation inactivating thyroid hormone receptor alpha1 isoform. *Dev Biol* (2011) 356:350–8. doi: 10.1016/j.ydbio.2011.05.657

74. Fauquier T, Chatonnet F, Picou F, Richard S, Fossat N, Aguilera N, et al. Purkinje cells and bergmann glia are primary targets of the TRα1 thyroid hormone receptor during mouse cerebellum postnatal development. *Development* (2014) 141:166–75. doi: 10.1242/dev.103226

75. Harder L, Dudazy-Gralla S, Müller-Fielitz H, Hjerling Leffler J, Vennström B, Heuer H, et al. Maternal thyroid hormone is required for parvalbumin neurone development in the anterior hypothalamic area. *J Neuroendocrinol* (2018) 30:e12573. doi: 10.1111/jne.12573

76. Mayerl S, Chen J, Salveridou E, Boelen A, Darras VM, Heuer H. Thyroid hormone transporter deficiency in mice impacts multiple stages of GABAergic interneuron development. *Cereb Cortex* (2021) 32:329–41. doi: 10.1093/cercor/bhab211

77. Manzano J, Cuadrado M, Morte B, Bernal J. Influence of thyroid hormone and thyroid hormone receptors in the generation of cerebellar γ-aminobutyric acid-ergic interneurons from precursor cells. *Endocrinology* (2007) 148:5746–51. doi: 10.1210/en.2007-0567

78. Masnada S, Sarret C, Antonello CE, Fadilah A, Krude H, Mura E, et al. Movement disorders in MCT8 deficiency/Allan-Herndon-Dudley syndrome. *Mol Genet Metab* (2022) 135:109–13. doi: 10.1016/j.ymgme.2021.12.003

79. Friesema ECH, Visser WE, Visser TJ. Genetics and phenomics of thyroid hormone transport by MCT8. *Mol Cell Endocrinol* (2010) 322:107–13. doi: 10.1016/j.mce.2010.01.016

80. Groeneweg S, van Geest FS, Abacı A, Alcantud A, Ambegaonkar GP, Armour CM, et al. Disease characteristics of MCT8 deficiency: an international, retrospective, multicentre cohort study. *Lancet Diabetes Endocrinol* (2020) 8:594–605. doi: 10.1016/S2213-8587(20)30153-4

81. Solini GE, Pownall ME, Hillenbrand MJ, Tocheny CE, Paudel S, Halleran AD, et al. Xenopus embryos show a compensatory response following perturbation of the notch signaling pathway. *Dev Biol* (2020) 460:99–107. doi: 10.1016/j.ydbio.2019.12.016

82. Vancamp P, Bourgeois NMA, Houbrechts AM, Darras VM. Knockdown of the thyroid hormone transporter MCT8 in chicken retinal precursor cells hampers early retinal development and results in a shift towards more UV/blue cones at the expense of green/red cones. *Exp Eye Res* (2019) 178:135–47. doi: 10.1016/j.exer.2018.09.018

83. López-Juárez A, Remaud S, Hassani Z, Jolivet P, Pierre Simons J, Sontag T, et al. Demeneix, thyroid hormone signaling acts as a neurogenic switch by repressing Sox2 in the adult neural stem cell niche. *Cell Stem Cell* (2012) 10:531–43. doi: 10.1016/j.stem.2012.04.008

84. Mohan V, Sinha RA, Pathak A, Rastogi L, Kumar P, Pal A, et al. Maternal thyroid hormone deficiency affects the fetal neocorticogenesis by reducing the proliferating pool, rate of neurogenesis and indirect neurogenesis. *Exp Neurol* (2012) 237:477–88. doi: 10.1016/j.expneurol.2012.07.019

85. Morte B, Ceballos A, Diez D, Grijota-Martinez C, Dumitrescu AM, Di Cosmo C, et al. Thyroid hormone-regulated mouse cerebral cortex genes are differentially dependent on the source of the hormone: a study in monocarboxylate transporter-8- and deiodinase-2-Deficient mice. *Endocrinology* (2010) 151:2381–7. doi: 10.1210/en.2009-0944

86. Barrera-Hernandez G, Park KS, Dace A, Zhan Q, Cheng S-y. Thyroid hormone-induced cell proliferation in GC cells is mediated by changes in G1 Cyclin/Cyclin-dependent kinase levels and activity. *Endocrinology* (1999) 140:5267–74. doi: 10.1210/endo.140.11.7145

87. Luongo C, Butruille L, Sébillot A, Le Blay K, Schwaninger M, Heuer H, et al. Absence of both thyroid hormone transporters MCT8 and OATP1C1 impairs neural stem cell fate in the adult mouse subventricular zone. *Stem Cell Rep* (2021) 16(2):337–53. doi: 10.1016/j.stemcr.2020.12.009

88. Farrell JA, Wang Y, Riesenfeld SJ, Shekhar K, Regev A, Schier AF. Single-cell reconstruction of developmental trajectories during zebrafish embryogenesis. *Science* (2018) 360:eaar3131. doi: 10.1126/science.aar3131

89. Appel B, Eisen JS. Regulation of neuronal specification in the zebrafish spinal cord by delta function. *Development* (1998) 125:371–80. doi: 10.1242/dev.125.3.371

90. Scott K, O'Rourke R, Winkler CC, Kearns CA, Appel B. Temporal single-cell transcriptomes of zebrafish spinal cord pMN progenitors reveal distinct neuronal and glial progenitor populations. *Dev Biol* (2021) 479:37–50. doi: 10.1016/j.ydbio.2021.07.010

91. Faivre-Sarrailh C, Rami A, Fages C, Tardy M. Effect of thyroid deficiency on glial fibrillary acidic protein (GFAP) and GFAP-mRNA in the cerebellum and hippocampal formation of the developing rat. *Glia* (1991) 4:276–84. doi: 10.1002/glia.440040305

92. Breunig JJ, Nelson BR. Chapter 13 - notch and neural development. In: Rubenstein J, Rakic P, Chen B, Kwan KY, editors. *Patterning and cell type*

specification in the developing CNS and PNS, 2nd ed. London, UK: Academic Press (2020). p. 285–310.

93. Sirakov M, Boussouar A, Kress E, Frau C, Lone IN, Nadjar J, et al. The thyroid hormone nuclear receptor TRα1 controls the notch signaling pathway and cell fate in murine intestine. *Development* (2015) 142:2764–74. doi: 10.1242/dev.121962

94. Hasebe T, Fujimoto K, Kajita M, Fu L, Shi Y-B, Ishizuya-Oka A. Thyroid hormone-induced activation of notch signaling is required for adult intestinal stem cell development during xenopus laevis metamorphosis. *Stem Cells* (2017) 35:1028–39. doi: 10.1002/stem.2544

95. Seymour PA, Collin CA, Egeskov-Madsen A, Jørgensen MC, Shimojo H, Imayoshi I, et al. Jag1 modulates an oscillatory Dll1-Notch-Hes1 signaling module to coordinate growth and fate of pancreatic progenitors. *Dev Cell* (2020) 52:731–747.e8. doi: 10.1016/j.devcel.2020.01.015

96. Vatine GD, Shelest O, Barriga BK, Ofan R, Rabinski T, Mattis VB, et al. Oligodendrocyte progenitor cell maturation is dependent on dual function of MCT8 in the transport of thyroid hormone across brain barriers and the plasma membrane. *Glia* (2021) 69:2146–59. doi: 10.1002/glia.24014

97. Ceballos A, Belinchon MM, Sanchez-Mendoza E, Grijota-Martinez C, Dumitrescu AM, Refetoff S, et al. Importance of monocarboxylate transporter 8 for the blood-brain barrier-dependent availability of 3,5,3'-Triiodo-L-Thyronine. *Endocrinology* (2009) 150:2491–6. doi: 10.1210/en.2008-1616

98. Vatine GD, Al-Ahmad A, Barriga BK, Svendsen S, Salim A, Garcia L, et al. Modeling psychomotor retardation using iPSCs from MCT8-deficient patients indicates a prominent role for the blood-brain barrier. *Cell Stem Cell* (2017) 20:831–843.e5. doi: 10.1016/j.stem.2017.04.002

frontiers | Frontiers in Endocrinology

TYPE Correction
PUBLISHED 31 May 2023
DOI 10.3389/fendo.2023.1228183

Check for updates

OPEN ACCESS

APPROVED BY
Frontiers Editorial Office,
Frontiers Media SA, Switzerland

*CORRESPONDENCE
Marco António Campinho
macampinho@ualg.pt

RECEIVED 24 May 2023
ACCEPTED 25 May 2023
PUBLISHED 31 May 2023

CITATION
Silva N and Campinho MA (2023) Corrigendum: In a zebrafish biomedical model of human Allan-Herndon-Dudley syndrome impaired MTH signaling leads to decreased neural cell diversity.
Front. Endocrinol. 14:1228183.
doi: 10.3389/fendo.2023.1228183

COPYRIGHT
© 2023 Silva and Campinho. This is an open-access article distributed under the terms of the Creative Commons Attribution License (CC BY). The use, distribution or reproduction in other forums is permitted, provided the original author(s) and the copyright owner(s) are credited and that the original publication in this journal is cited, in accordance with accepted academic practice. No use, distribution or reproduction is permitted which does not comply with these terms.

Corrigendum: In a zebrafish biomedical model of human Allan-Herndon-Dudley syndrome impaired MTH signaling leads to decreased neural cell diversity

Nádia Silva[1,2] and Marco António Campinho[1,2,3]*

[1]Centre for Marine Sciences of the University of the Algarve, Faro, Portugal, [2]Algarve Biomedical Center-Research Institute, University of the Algarve, Faro, Portugal, [3]Faculty of Medicine and Biomedical Sciences, University of the Algarve, Faro, Portugal

KEYWORDS

maternal thyroid hormone, monocarboxylic acid transporter 8, neurodevelopment, spinal cord, zebrafish, Allan-Herndon-Dudley syndrome (AHDS)

A corrigendum on

In a zebrafish biomedical model of human Allan-Herndon-Dudley syndrome impaired MTH signaling leads to decreased neural cell diversity

by Silva N and Campinho MA (2023) *Front. Endocrinol.* 14:1157685. doi: 10.3389/fendo.2023.1157685

In the published article, the Funding statement was missing. The correct Funding statement appears below.

"This study received Portuguese national funds from FCT - Foundation for Science and Technology through project PTDC/EXPL/MAR-BIO/0430/2013 and FCT UIDB/04326/2020 COMPETE 2020, through project EMBRC.PT ALG-01-0145-FEDER-022121. ABC-RI CRESC Algarve 2020. NS was a recipient of an FCT Ph.D. grant SFRH/BD/111226/2015. MC received an FCT-IF Starting Grant (IF/01274/2014). Support of ABC and Camara Municipal de Loulé".

The authors apologize for this error and state that this does not change the scientific conclusions of the article in any way. The original article has been updated.

Publisher's note

All claims expressed in this article are solely those of the authors and do not necessarily represent those of their affiliated organizations, or those of the publisher, the editors and the reviewers. Any product that may be evaluated in this article, or claim that may be made by its manufacturer, is not guaranteed or endorsed by the publisher.

frontiers | Frontiers in Endocrinology

TYPE Mini Review
PUBLISHED 17 May 2023
DOI 10.3389/fendo.2023.1184013

Check for updates

OPEN ACCESS

EDITED BY
Marco António Campinho,
University of Algarve, Portugal

REVIEWED BY
Yoshio Yaoita,
Hiroshima University, Japan
Nicolas Buisine,
Muséum National d'Histoire Naturelle, France

*CORRESPONDENCE
Yun-Bo Shi
Shi@helix.nih.gov

RECEIVED 10 March 2023
ACCEPTED 03 May 2023
PUBLISHED 17 May 2023

CITATION
Tanizaki Y, Shibata Y, Na W and Shi Y-B (2023) Cell cycle activation in thyroid hormone-induced apoptosis and stem cell development during *Xenopus* intestinal metamorphosis.
Front. Endocrinol. 14:1184013.
doi: 10.3389/fendo.2023.1184013

COPYRIGHT
© 2023 Tanizaki, Shibata, Na and Shi. This is an open-access article distributed under the terms of the Creative Commons Attribution License (CC BY). The use, distribution or reproduction in other forums is permitted, provided the original author(s) and the copyright owner(s) are credited and that the original publication in this journal is cited, in accordance with accepted academic practice. No use, distribution or reproduction is permitted which does not comply with these terms.

Cell cycle activation in thyroid hormone-induced apoptosis and stem cell development during *Xenopus* intestinal metamorphosis

Yuta Tanizaki, Yuki Shibata, Wonho Na and Yun-Bo Shi*

Section on Molecular Morphogenesis, Eunice Kennedy Shriver National Institute of Child Health and Human Development (NICHD), National Institutes of Health (NIH), Bethesda, MD, United States

Amphibian metamorphosis resembles mammalian postembryonic development, a period around birth when many organs mature into their adult forms and when plasma thyroid hormone (T3) concentration peaks. T3 plays a causative role for amphibian metamorphosis. This and its independence from maternal influence make metamorphosis of amphibians, particularly anurans such as pseudo-tetraploid *Xenopus laevis* and its highly related diploid species *Xenopus tropicalis*, an excellent model to investigate how T3 regulates adult organ development. Studies on intestinal remodeling, a process that involves degeneration of larval epithelium via apoptosis and *de novo* formation of adult stem cells followed by their proliferation and differentiation to form the adult epithelium, have revealed important molecular insights on T3 regulation of cell fate during development. Here, we review some evidence suggesting that T3-induced activation of cell cycle program is important for T3-induced larval epithelial cell death and *de novo* formation of adult intestinal stem cells.

KEYWORDS

programmed cell death, metamorphosis, *Xenopus laevis*, *Xenopus tropicalis*, postembryonic development, intestine, thyroid hormone receptor, stem cell

Introduction

The development of vertebrate intestine, like many other organs, takes place in two phases, the initial formation of a neonatal/juvenile form and subsequent maturation into the adult form. This second phase often occurs during postembryonic development, a perinatal period when plasma thyroid hormone (T3) level peaks (1–3). This period corresponds the first 2-3 weeks after birth in mouse and metamorphosis in amphibians such as the highly related anurans pseudo-tetraploid *Xenopus laevis* and diploid *Xenopus tropicalis* (Note that due to the conservations between the two species, we will simply refer to both as *Xenopus* unless specified, although earlier studies on anuran metamorphosis were mainly on *Xenopus laevis* while more recent ones, particularly gene knockout studies,

10.3389/fendo.2023.1184013

have been on *Xenopus tropicalis*). Importantly, maturation of the intestine during this second phase appears to be highly conserved (4–10). For example, the mouse intestine has villi but no crypts, where adult stem cells reside, at birth and develop crypts during the first 3 weeks after birth when T3 levels are high. Similarly, the intestine in a premetamorphic *Xenopus* tadpole, when there is little or no T3, is also simple in structure, consisting of mostly a single layer of epithelial cells, surrounded by thin layers of connective tissue and muscles (Figure 1A) (12–17). As T3 levels rises after stage 54 (about 4 weeks of age) (18, 19), metamorphosis begins and larval epithelial cells undergo programmed cell death (12, 13, 20). Some larval epithelial cells undergo dedifferentiation during metamorphosis to form clusters of cells that proliferate rapidly and express well-known adult intestinal stem cell markers such as Lgr5 by climax of metamorphosis, e.g., stage 61 (about 6-7 weeks of age) (Figure 1A) (11, 21, 22). By the end of metamorphosis or stage 66 (about 2 months after fertilization), these proliferating stem cells differentiate to form a multi-folded epithelium surrounded by elaborate connective tissue and muscles (4, 16, 17, 23, 24). In the adult frog, the intestinal stem cells are localized at the bottom of the epithelial fold while cell death occurs mainly at the crest of the fold, similar to those taking place in the crypt-villus unit in adult mammalian intestine (16, 25).

T3 not only has peak levels during postembryonic development but also plays critical roles during this period, with T3 deficiency causing severely developmental problems in all vertebrates including human (1, 2, 26, 27). T3 is both necessary and sufficient for anuran metamorphosis. Thus, preventing the synthesis of endogenous T3 allows *Xenopus* tadpoles to remain in tadpole form for years while wild type animals typically finish metamorphosis by around 2 months of age (1, 2, 15). Conversely, treating premetamorphic *Xenopus* tadpoles with physiological levels of T3 in the rearing water causes precociously metamorphosis. Making use of the ability to easily manipulate anuran metamorphosis by controlling the availability of T3 to tadpoles or even organ or primary cell cultures and the advancement in genetic technologies, especially gene-editing for knockout studies in the diploid *Xenopus tropicalis* (28–35), we and others have been studying the molecular mechanism by which T3 regulates cell fate and tissue transformation during metamorphosis. Here, we review some recent studies on intestinal remodeling, with an emphasis on the potential role of cell cycle activation in larval epithelial cell death and adult stem cell development.

T3 induces larval epithelial cell death and adult stem cell development in an organ autonomous manner via T3 receptor

Intestinal remodeling, just like any other events during metamorphosis, requires T3. Treatment of premetamorphic *Xenopus* tadpoles with T3 leads to premature intestinal metamorphosis (16). The most noticeable changes during intestinal metamorphosis are the nearly 90% reduction in the length of the small intestine, while the most dramatic tissue transformation occurs in the epithelium with the larva epithelial cells induced to undergo apoptosis by T3, followed by rapid proliferation of newly formed cell clusters in the epithelium

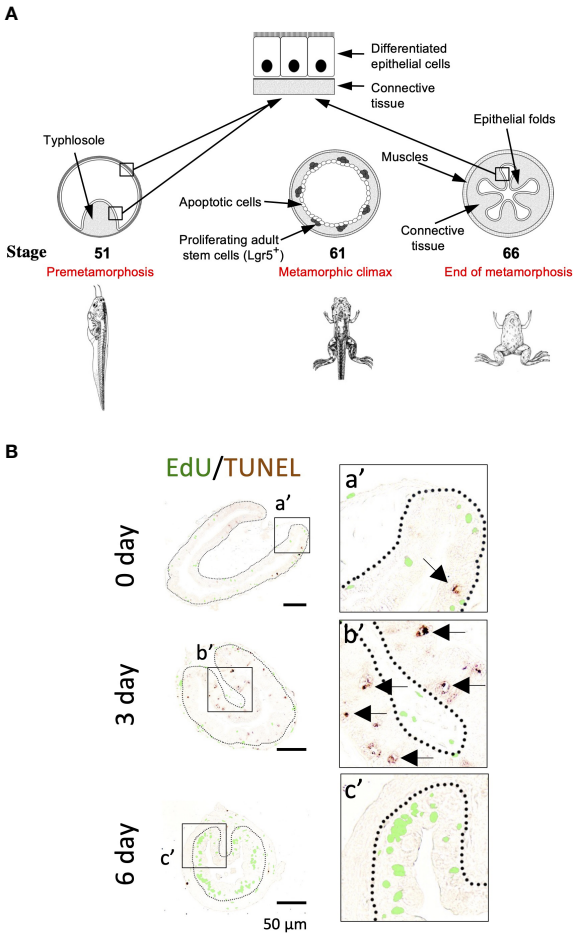

FIGURE 1
(A). Schematic diagram of *Xenopus* intestinal metamorphosis. Both tadpole and frog intestine are structurally simple, consisting of mainly three tissue layers: inner epithelium, connective tissue, and outer muscle layers. The tadpole intestine is much simpler, with only a single epithelial fold, the typhlosole. In contrast, the frog intestine has multiple epithelial folds with elaborate connective tissue and muscle layers. The major events underlying the change from tadpole to frog intestine during metamorphosis include the apoptosis of essentially all larval epithelial cells, as indicated by circles. Concurrently, the adult epithelial stem cells, with high level expression of known stem cell markers such as Lgr5, are formed *de novo* through dedifferentiation of some larval epithelial cells and rapidly proliferate at the climax metamorphosis, as indicated by the dots. The connective tissue and muscle cells also develop extensively during metamorphosis. **(B)**. Apoptotic and proliferating cells are non-overlapping epithelial cells during T3-induced intestinal metamorphosis. Premetamorphic *Xenopus laevis* tadpoles at stage 54 were treated with 10 nM T3 for 0, 3, or 6 days and sacrificed one hour after injection with EdU to label proliferating cells. Intestinal cross-sections were double stained for EdU and by TUNEL for apoptotic cells. A higher magnification of the boxed areas labeled with a'-c' is shown on the right. The dotted lines depict the epithelium-mesenchyme boundary. Note that apoptosis as shown by the TUNEL signal in the epithelium occurred prior to the appearance of the clusters (islets) of EdU-labeled cells and in distinct epithelial cells during T3 treatment (c'). Arrows point to some apoptotic cells. See (11) for more details.

(Figure 1B) (11). Importantly, these proliferating cells express high levels of known markers of adult mammalian intestinal stem cells such as Lgr5 (Figure 1B) (11), suggesting that T3 induces the formation of adult stem cells during metamorphosis.

Importantly, T3-treatment of intestinal organ cultures from premetamorphic tadpoles also leads to larval epithelial cell death and *de novo* formation of adult stem cells, indicating that the adult stem cells develop organ-autonomously in an T3-dependent manner. More importantly, by using recombinant organ cultures generated from isolated intestinal epithelium and non-epithelial tissues (the rest of the intestine after separating the epithelium) from premetamorphic wild type tadpoles and transgenic tadpoles expressing GFP ubiquitously, we have shown that T3-induced stem cells originate from larval epithelium, likely due to dedifferentiation of some larval epithelial cells (23) since there has been no evidence of pre-existing epithelial stem cells in the tadpole intestine and that the differentiated larval epithelial cells are capable of proliferation (16, 36). These findings also indicate that T3 is both necessary and sufficient for larval intestinal cell death and adult stem cell development during metamorphosis.

T3 functions mainly by binding to T3 receptors (TRs) to regulate target gene transcription (37–40). There are two types of TR genes, TRα and TRβ, in all vertebrates. TRs can activate or repress target gene transcription in the presence or absence of T3, respectively, by binding, as heterodimers with 9-cis retinoic acid receptors (RXRs), to specific DNA sequences called T3-response elements (TREs) within target genes (41–45). Earlier studies on the expression patterns and molecular properties of TRs in *Xenopus laevis* have led to a dual function model for TRs during *Xenopus* metamorphosis (46). According to the model, TRs are mainly unliganded in premetamorphic tadpoles when there is little or no T3 and thus repress target genes to prevent precocious metamorphosis. During metamorphosis when T3 level is high, T3 binds to TR to activate target genes, thus leading to tadpole metamorphosis. Extensive molecular and transgenic studies in *Xenopus laevis* and gene knockout studies in *Xenopus tropicalis* have provided strong support for this model (47–58).

A critical role of TR in intestinal metamorphosis was demonstrated by studies with recombinant organ cultures made of intestinal epithelium and non-epithelial tissues from premetamorphic wild type tadpoles or transgenic ones containing a heat shock-inducible dominant positive TR (dpTR) that cannot bind to T3 but functions like a constitutively liganded TR (59, 60). In these recombinant organ cultures, T3 signaling can be activated in either the epithelium or non-epithelial tissues or both by heat shock treatment of the organ cultures without the presence of T3. Such studies have revealed that dpTR expression in both epithelium and non-epithelium can induce intestinal metamorphosis, including larval epithelial apoptosis and adult intestinal stem cell formation and their subsequent proliferation and differentiation, in the absence of T3 (60). These findings indicate that TR is sufficient for mediating all effects of T3 for intestinal metamorphosis, including larval epithelial cell death and adult stem cell development. Interestingly, activating T3-signaling by expressing dpTR in either the epithelium or non-epithelial tissues alone can induce larval epithelial degeneration, indicating that larval epithelial apoptosis can be induced by T3-signaling both cell autonomously and via cell-cell interaction. However, dpTR expression in either the epithelium or the non-epithelial tissues alone fails to induce the formation of adult stem cells, although dpTR expression in the epithelium alone results in dedifferentiation of some larval epithelial cells (60). These findings suggest that epithelial T3-signaling induces larval epithelial cell dedifferentiation while T3-signaling in the non-epithelial tissues is required to help such dedifferentiated cells to develop into stem cells, likely via the formation of a proper stem cell niche through cell-cell and/or cell-ECM (extracellular matrix) interactions (60–63).

TR is not needed for adult intestinal morphogenesis but is essential for larval epithelial cell death and adult intestinal stem cell development during metamorphosis

The role of endogenous TR in regulating intestinal metamorphosis was first suggested by transgenic studies with dominant negative mutant TRs that cannot bind to T3. The expression of such dominant negative TRs was found to inhibits *Xenopus laevis* metamorphosis, including intestinal remodeling (50, 61, 64, 65). Since the dominant negative TRs compete functionally against endogenous wild type TR that can bind T3, the findings are not surprising given the causative role of T3 in all aspects of metamorphosis but demonstrate an essential role for TR to mediate the metamorphic effects of T3, including larval intestinal cell death and adult stem cell development.

With the advancement of gene editing technologies, it became possible to knock out endogenous TR genes in *Xenopus*. Indeed, individual TRα and TRβ genes or both have been knocked out recently in the diploid *Xenopus tropicalis* and found to have distinct tissue-dependent effects during metamorphosis (52, 55–58, 66–70). Consistent with the high but relatively constant expression of TRα during intestinal metamorphosis (71), knocking out TRα delayed intestinal remodeling (66, 69, 72). Surprisingly, knocking out TRβ had relatively subtle effect on intestinal remodeling during natural metamorphosis (52, 55), although TRβ expression, which is very low in premetamorphic tadpole intestine, is dramatically upregulated during intestinal metamorphosis (71). On the other hand, when premetamorphic wild type and TRβ knockout tadpoles were induced to metamorphose with exogenous T3 treatment, both larval epithelial cell death and adult intestinal stem cell formation, which occurred within 2-3 days in wild type tadpoles after the treatment, were delayed or inhibited in the TRβ knockout tadpoles (55). These findings suggest that TRα and TRβ have distinct but compensatory roles during intestinal metamorphosis. As T3-induced metamorphosis occurs much faster than the 2-3 weeks required for the premetamorphic tadpoles at stage 54 to develop to the climax (stages 60-62, when larval cell death and adult epithelial stem cell formation occur) during the natural metamorphosis, the compensation by TRα may be too slow to prevent the effects of TRβ knockout on intestinal remodeling during T3-induced metamorphosis but fast enough to prevent any major defect in

10.3389/fendo.2023.1184013

intestinal remodeling during natural metamorphosis in TRβ knockout animals.

When both TRα and TRβ genes were knocked out in *Xenopus tropicalis*, the tadpoles could develop to the climax stage 61 and died after about 2 weeks at stage 61, in contrast to wild type tadpoles that develop from stage 61 to the end of metamorphosis in a week (56). While the wild type intestine at stage 61 had extensive larval epithelial cell death and proliferation of new formed adult epithelial stem cells, TR double knockout tadpoles at stage 61 had little larval cell death or adult stem cell proliferation (Figure 2A) (73). In addition, as predicted, T3 treatment of premetamorphic TR double knockout animals had no effect on the intestine (56, 73), in contrast to the wild type animals (Figure 1B). Surprisingly, the intestine of TR double knockout tadpoles developed adult morphology (with numerous epithelial folds and thick layers of connective tissue and muscles) precociously, by as early as stage 58, mimicking the wild type intestine at the end of metamorphosis (stage 66) (Figure 2A) (73). These findings indicate that TR is required for T3-induced larval epithelial cell death and adult epithelial stem cell development but not for adult intestinal morphogenesis during metamorphosis.

Cell cycle activation by liganded TR is involved in larval epithelial cell death and adult stem cell development

As a transcription factor, TR regulates target gene transcription in a T3-dependent manner. Toward understanding how T3 regulates intestinal remodeling, various approaches have been used to isolate and characterize T3-response genes during *Xenopus* intestinal metamorphosis (74–78). These studies have revealed, perhaps expectedly, that many genes in signaling pathways known to be important for stem cell proliferation and function are induced by T3 during intestinal remodeling. These pathways include hedgehog pathway (21, 79–82), Wnt signaling (83–85), Notch pathway (86), and BMP signaling (87, 88), etc. In addition, many other genes, such as the methyl-CpG binding domain protein 3 (MBD3) (89) and tRNA methyltransferase-like 1 (Mettl1) (90), that were not previously known to associated with cell death or stem cells, were found to be highly upregulated by T3 during intestinal metamorphosis, suggesting that they may be novel regulators of cell death or stem cells during development.

When global gene expression analyses with RNA-seq were carried out on wild type and TR knockout intestine during metamorphosis, it was revealed that many more genes in gene ontology (GO) terms related to stem cells, cell proliferation, and apoptosis were upregulated in the wild type tadpole intestine at the climax of metamorphosis (stage 61) compared to premetamorphic stage 54 than in the TR double knockout intestine (73), consistent with the massive larval epithelial cell death and formation/proliferation of adult stem cells at the climax of metamorphosis in the wild type but not TR double knockout intestine. In addition, GO and KEGG pathway analyses of the genes that were regulated between stage 54 and stage 61 in the intestine of wild type and TR double knockout animals showed that many GO terms and KEGG pathways, particularly cell cycle/proliferation-related ones, were enriched among the upregulated genes in the wild type but not TR double knockout intestine. In fact, several cell cycle/proliferation-related GO terms were even enriched among genes downregulated at stage 61 compared to stage 54 in the TR double knockout intestine. Furthermore, when GO and KEGG pathway analyses were performed on the genes expressed at higher levels in the intestine of wild type than TR double knockout tadpoles at stage 61, it was again found that many cell cycle-related GO terms/

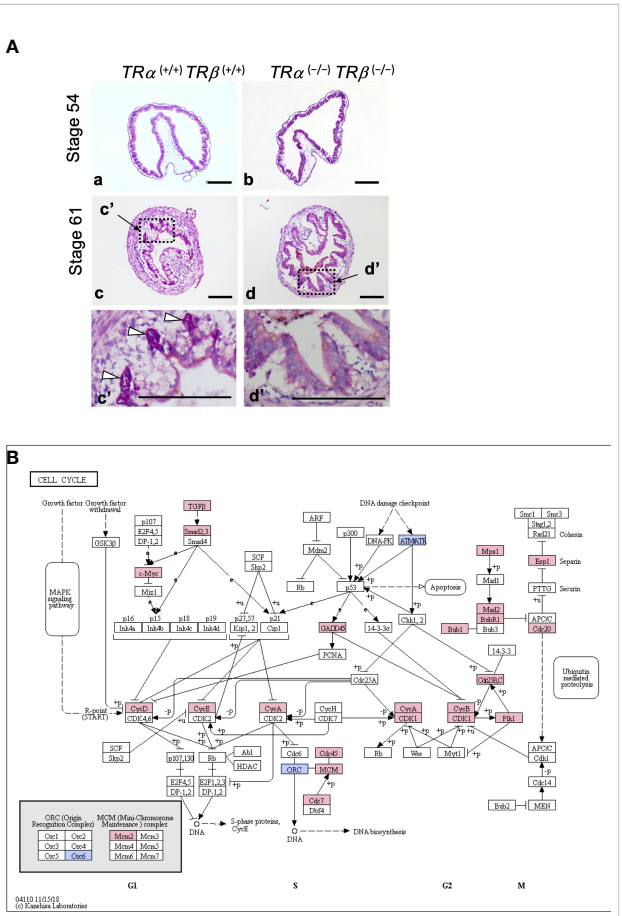

FIGURE 2
(A) TR double knockout tadpoles have abnormal intestinal morphology with premature adult type epithelial folding. Cross-sections of the intestine of indicated genotypes stages were stained with methyl green-pyronin Y. (a, c): Wild type $TR\alpha^{(+/+)}TR\beta^{(+/+)}$; and (b, d): TR double knockout $TR\alpha^{(-/-)}TR\beta^{(-/-)}$. Dashed boxes in c and d are shown in higher magnification in c' and d', respectively. White arrowheads point to the clusters of proliferating adult epithelial stem cells adjacent to/underneath the degenerating larval epithelium (vacuole-like, poorly stained) at the climax of metamorphosis (stage 61) in wild type tadpoles. Note that the knockout tadpoles lacked such clusters at stage 61 and the epithelium appeared to be uniform without any obvious degeneration, but with numerous folds. Bars: 100 μm. See (73) for details. **(B)** TRα is required for the activation of many cell cycle genes during early phase of T3-induced intestinal remodeling. Genes regulated by at least 2.0-fold after 18 hours of T3 treatment in stage 54 wild type but not TRα knockout tadpoles were mapped onto the KEGG pathway for cell cycle. Pink boxes indicate upregulation and blue boxes indicate downregulation. Note that most of the regulated genes were upregulated by T3. See (72) for more details.

pathways were enriched among these genes (73). These findings suggest that T3-bound TR activates cell cycle programs to facilitate intestinal metamorphosis. Given the rapid proliferation of adult stem cells at the climax of intestinal metamorphosis in the wild type (Figure 1) but not TR double knockout tadpoles, it is not surprising to find the upregulation of genes in the cell cycle program in the wild type intestine compared to the TR double knockout ones at the climax of metamorphosis.

A recent RNA-seq analysis of intestinal gene expression in premetamorphic wild type and TRα knockout tadpoles at stage 54 after 18 hours of T3 treatment suggests that activation of cell cycle program may also be important for T3-induced larval epithelial cell death during metamorphosis (72). During T3-induced metamorphosis, larval epithelial cell death is induced dramatically after 2 days while epithelial cell proliferation is increased significantly only after 3 days, due to the formation of adult epithelial stem cells (Figure 1) (11, 91). Thus, it was expected that T3 would not induce cell proliferation program, e.g., cell cycle activation, in the first 2 days of treatment. Surprisingly, GO and KEGG pathway analyses of the genes regulated by 18 hour T3 treatment of wild type tadpoles showed significant enrichment of GO terms and KEGG pathways related to cell cycle (72). This raises a possibility that the activation of the cell cycle program by T3 is an important early step for T3 to induced larval epithelial cell death (11, 72, 91). Furthermore, when the gene expression in the intestine of wild type and TRα knockout tadpoles with or without 18 hour T3-treatment were compared, it was found that the endogenous TRα was important for the regulation of the cell cycle program (72), including the KEGG cell cycle pathway, where many genes were upregulated by T3 in the wild type but not TRα knockout tadpoles (Figure 2B). This important role of TRα in gene regulation by T3 during the early phase of T3-induced metamorphosis is consistent with the fact that there is little TRβ expression in premetamorphic tadpole intestine (71). Thus, T3 likely activates the cell cycle program via TRα early during metamorphosis to facilitate epithelial cell fate determination in the intestine: apoptosis *vs.* dedifferentiation into adult stem cells.

Whether cell cycle activation leads to larval epithelial cell death and adult stem cell development remains to be elucidated. As cell cycle activation is typically associated with cell proliferation in development, the discovery of a role of cell cycle activation in developmental cell death was surprising. On the other hand, there has been evidence for involvement of cell cycle regulators in apoptosis. For example, c-Myc, a well-known oncogene that activate target gene transcription and promote cell proliferation, can induce cell death when overexpressed, at least in cell cultures (92–102). It is possible that that over activation of cell cycle pathways may lead to apoptosis in some cells. As the larval intestinal epithelial cells are mitotically active, even though differentiated sufficiently to function in the tadpole (16), T3-induced further activation of the cell cycle/proliferation pathways in such mitotically active yet differentiated cells may force to them to change their fate, either death via apoptosis or dedifferentiation to become adult stem cells to accommodate the faster proliferation needed for intestinal metamorphosis. Such a mechanism may explain why cell cycle/proliferation pathways are activated in the larval epithelium prior to and throughout the two major epithelial transformations, apoptotic larval epithelial degeneration, and *de novo* formation of the adult epithelium, during T3 intestinal remodeling.

Conclusion

The ability of vertebrate intestinal epithelium for self-renewal throughout adulthood has made the intestine a well-studied model for analyses of the properties and regulation of adult organ-specific stem cells (4–10). The formation of the adult intestinal stem cells during vertebrate development is much less known but appears to be conserved in vertebrates. In both mouse and *Xenopus*, the formation of the adult intestinal stem cells occurs during postembryonic development (the neonatal period in mouse and metamorphosis in *Xenopus*) when plasma T3 level peaks, and T3-signaling is important for the development and/or maintenance of the adult intestine (6, 103–111). These suggest a conservation in T3-regulation of adult intestinal development.

Studies on intestinal metamorphosis in *Xenopus laevis* and *Xenopus tropicalis* have revealed important and novel insights on how T3 regulates the development of the adult intestine. First, T3 induces *de novo* formation of adult intestinal epithelial stem cells via larval epithelial cell dedifferentiation. Second, T3-signaling in both the epithelium and non-epithelial tissues are required for adult stem cell development, likely involving the formation of adult stem cell niche. Third, TR is essential to mediate T3 signaling for both larval epithelial cell death and the formation of adult stem cells while adult intestinal morphogenesis does not require TR. Finally, and importantly, global gene expression studies on intestinal development in wild type and TR knockout tadpoles have not only revealed the regulation of diverse GO terms and pathways by T3 during intestinal metamorphosis but also implicate a surprising and novel role of cell cycle activation by T3 in cell fate determination. It would be interesting to test whether the activation of cell cycle by T3 is indeed a prerequisite for larval epithelial cells to choose between apoptosis or dedifferentiation into stem cells during intestinal metamorphosis. Future studies on the potentially conserved functions of the T3-induced GO terms and pathways in the development of the adult intestine in other species should improve our understanding of the development and function of adult stem cells in human intestinal homeostasis and diseases.

Author contributions

All authors contributed to the article and approved the submitted version.

Funding

This work was supported by the intramural Research Program of NICHD, NIH. YS and YT were supported in part by the Japan

Society for the Promotion of Science (NIH) Fellowship (No. 29-71715 and 28-71606).

Conflict of interest

The authors declare that the research was conducted in the absence of any commercial or financial relationships that could be construed as a potential conflict of interest.

Publisher's note

All claims expressed in this article are solely those of the authors and do not necessarily represent those of their affiliated organizations, or those of the publisher, the editors and the reviewers. Any product that may be evaluated in this article, or claim that may be made by its manufacturer, is not guaranteed or endorsed by the publisher.

References

1. Shi Y-B. *Amphibian metamorphosis: from morphology to molecular biology*. New York: John Wiley & Sons, Inc. (1999).

2. Tata JR. Gene expression during metamorphosis: an ideal model for post-embryonic development. *Bioessays* (1993) 15:239–48. doi: 10.1002/bies.950150404

3. Atkinson BG. Metamorphosis: model systems for studying gene expression in postembryonic development. *Dev Genet* (1994) 15:313–9. doi: 10.1002/dvg.1020150402

4. Shi YB, Hasebe T, Fu L, Fujimoto K, Ishizuya-Oka A. The development of the adult intestinal stem cells: insights from studies on thyroid hormone-dependent amphibian metamorphosis. *Cell Biosci* (2011) 1:30. doi: 10.1186/2045-3701-1-30

5. van der Flier LG, Clevers H, Cells S. Self-renewal, and differentiation in the intestinal epithelium. *Annu Rev Physiol* (2009) 71:241–60. doi: 10.1146/annurev.physiol.010908.163145

6. Sun G, Shi Y-B. Thyroid hormone regulation of adult intestinal stem cell development: mechanisms and evolutionary conservations. *Int J Biol Sci* (2012) 8:1217–24. doi: 10.7150/ijbs.5109

7. Sun G, Fu L, Shi Y-B. Epigenetic regulation of thyroid hormone-induced adult intestinal stem cell development during anuran metamorphosis. *Cell Biosci* (2014) 4:73. doi: 10.1186/2045-3701-4-73

8. Sirakov M, Kress E, Nadjar J, Plateroti M. Thyroid hormones and their nuclear receptors: new players in intestinal epithelium stem cell biology? *Cell Mol Life Sci* (2014) 71:2897–907. doi: 10.1007/s00018-014-1586-3

9. Clevers H. The intestinal crypt, a prototype stem cell compartment. *Cell* (2013) 154:274–84. doi: 10.1016/j.cell.2013.07.004

10. Bao L, Shi B, Shi YB. Intestinal homeostasis: a communication between life and death. *Cell Biosci* (2020) 10:66. doi: 10.1186/s13578-020-00429-9

11. Okada M, Wen L, Miller TC, Su D, Shi YB. Molecular and cytological analyses reveal distinct transformations of intestinal epithelial cells during xenopus metamorphosis. *Cell Biosci* (2015) 5:74. doi: 10.1186/s13578-015-0065-3

12. McAvoy JW, Dixon KE. Cell proliferation and renewal in the small intestinal epithelium of metamorphosing and adult xenopus laevis. *J Exp Zool* (1977) 202:129–38. doi: 10.1002/jez.1402020115

13. Marshall JA, Dixon KE. Cell specialization in the epithelium of the small intestine of feeding xenopus laevis tadpoles. *J Anat* (1978) 126:133–44.

14. Ishizuya-Oka A, Shimozawa A. Development of the connective tissue in the digestive tract of the larval and metamorphosing xenopus laevis. *Anat Anz* (1987) 164:81–93.

15. Dodd MHI, Dodd JM. The biology of metamorphosis. In: Lofts B, editor. *Physiology of the amphibia*. New York: Academic Press (1976). p. 467–599.

16. Shi Y-B, Ishizuya-Oka A. Biphasic intestinal development in amphibians: embryogensis and remodeling during metamorphosis. *Curr Topics Dev Biol* (1996) 32:205–35. doi: 10.1016/S0070-2153(08)60429-9

17. Sterling J, Fu L, Matsuura K, Shi Y-B. Cytological and morphological analyses reveal distinct features of intestinal development during xenopus tropicalis metamorphosis. *PloS One* (2012) 7:e47407. doi: 10.1371/journal.pone.0047407

18. Leloup J, Buscaglia M. La triiodothyronine: hormone de la métamorphose des amphibiens. *C.R. Acad Sci* (1977) 284:2261–3.

19. Nieuwkoop PD, Faber J. Normal table of xenopus laevis. *North Holland Publishing Amsterdam* (1965).

20. Ishizuya-Oka A, Shimozawa A. Programmed cell death and heterolysis of larval epithelial cells by macrophage-like cells in the anuran small intestine *in vivo* and in vitro. *J Morphol* (1992) 213:185–95. doi: 10.1002/jmor.1052130205

21. Wen L, Hasebe T, Miller TC, Ishizuya-Oka A, Shi YB. A requirement for hedgehog signaling in thyroid hormone-induced postembryonic intestinal remodeling. *Cell Biosci* (2015) 5:13. doi: 10.1186/s13578-015-0004-3

22. Ishizuya-Oka A, Shimizu K, Sakakibara S, Okano H, Ueda S. Thyroid hormone-upregulated expression of musashi-1 is specific for progenitor cells of the adult epithelium during amphibian gastrointestinal remodeling. *J Cell Sci* (2003) 116:3157–64. doi: 10.1242/jcs.00616

23. Ishizuya-Oka A, Hasebe T, Buchholz DR, Kajita M, Fu L, Shi YB. Origin of the adult intestinal stem cells induced by thyroid hormone in xenopus laevis. *FASEB J* (2009) 23:2568–75. doi: 10.1096/fj.08-128124

24. Schreiber AM, Cai L, Brown DD. Remodeling of the intestine during metamorphosis of xenopus laevis. *Proc Natl Acad Sci U.S.A.* (2005) 102:3720–5. doi: 10.1073/pnas.0409868102

25. Ishizuya-Oka A, Shi YB. Evolutionary insights into postembryonic development of adult intestinal stem cells. *Cell Biosci* (2011) 1:37. doi: 10.1186/2045-3701-1-37

26. Hetzel BS. *The story of iodine deficiency: an international challenge in nutrition*. Oxford: Oxford University Press (1989).

27. Porterfield SP, Hendrich CE. The role of thyroid hormones in prenatal and neonatal neurological development–current perspectives. *Endocr Rev* (1993) 14:94–106. doi: 10.1210/edrv-14-1-94

28. Young JJ, Cherone JM, Doyon Y, Ankoudinova I, Faraji FM, Lee AH, et al. Efficient targeted gene disruption in the soma and germ line of the frog xenopus tropicalis using engineered zinc-finger nucleases. *Proc Natl Acad Sci U.S.A.* (2011) 108:7052–7. doi: 10.1073/pnas.1102030108

29. Lei Y, Guo X, Liu Y, Cao Y, Deng Y, Chen X, et al. Efficient targeted gene disruption in xenopus embryos using engineered transcription activator-like effector nucleases (TALENs). *Proc Natl Acad Sci U.S.A.* (2012) 109:17484–9. doi: 10.1073/pnas.1215421109

30. Lei Y, Guo X, Deng Y, Chen Y, Zhao H. Generation of gene disruptions by transcription activator-like effector nucleases (TALENs) in xenopus tropicalis embryos. *Cell Biosci* (2013) 3:21. doi: 10.1186/2045-3701-3-21

31. Blitz IL, Biesinger J, Xie X, Cho KW. Biallelic genome modification in F(0) xenopus tropicalis embryos using the CRISPR/Cas system. *Genesis* (2013) 51:827–34. doi: 10.1002/dvg.22719

32. Nakayama T, Fish MB, Fisher M, Oomen-Hajagos J, Thomsen GH, Grainger RM. Simple and efficient CRISPR/Cas9-mediated targeted mutagenesis in xenopus tropicalis. *Genesis* (2013) 51:835–43. doi: 10.1002/dvg.22720

33. Nakade S, Tsubota T, Sakane Y, Kume S, Sakamoto N, Obara M, et al. Microhomology-mediated end-joining-dependent integration of donor DNA in cells and animals using TALENs and CRISPR/Cas9. *Nat Commun* (2014) 5:5560. doi: 10.1038/ncomms6560

34. Shi Z, Wang F, Cui Y, Liu Z, Guo X, Zhang Y, et al. Heritable CRISPR/Cas9-mediated targeted integration in xenopus tropicalis. *FASEB J* (2015) 29:4914–23. doi: 10.1096/fj.15-273425

35. Wang F, Shi Z, Cui Y, Guo X, Shi YB, Chen Y. Targeted gene disruption in xenopus laevis using CRISPR/Cas9. *Cell Biosci* (2015) 5:15. doi: 10.1186/s13578-015-0006-1

36. Ishizuya-Oka A, Shi YB. Thyroid hormone regulation of stem cell development during intestinal remodeling. *Mol Cell Endocrinol* (2008) 288:71–8. doi: 10.1016/j.mce.2008.02.020

37. Lazar MA. Thyroid hormone receptors: multiple forms, multiple possibilities. *Endocr Rev* (1993) 14:184–93. doi: 10.1210/edrv-14-2-184

38. Yen PM. Physiological and molecular basis of thyroid hormone action. *Physiol Rev* (2001) 81:1097–142. doi: 10.1152/physrev.2001.81.3.1097

39. Tsai MJ, O'Malley BW. Molecular mechanisms of action of steroid/thyroid receptor superfamily members. *Ann Rev Biochem* (1994) 63:451–86. doi: 10.1146/annurev.bi.63.070194.002315

40. Laudet V, Gronemeyer H. *The nuclear receptor FactsBook*. San Diego: Academic Press (2002).

41. Jones PL, Shi Y-B. N-CoR-HDAC corepressor complexes: roles in transcriptional regulation by nuclear hormone receptors. In: Workman JL, editor. *Current topics in microbiology and immunology: protein complexes that modify chromatin*. Berlin: Springer-Verlag (2003). p. 237–68.

42. Perissi V, Jepsen K, Glass CK, Rosenfeld MG. Deconstructing repression: evolving models of co-repressor action. *Nat Rev Genet* (2010) 11:109–23. doi: 10.1038/nrg2736

43. O'Malley BW, Malovannaya A, Qin J. Minireview: nuclear receptor and coregulator proteomics–2012 and beyond. *Mol Endocrinol* (2012) 26:1646–50. doi: 10.1210/me.2012-1114

44. Bulynko YA, O'Malley BW. Nuclear receptor coactivators: structural and functional biochemistry. *Biochemistry* (2011) 50:313–28. doi: 10.1021/bi101762x

45. Shi YB, Matsuura K, Fujimoto K, Wen L, Fu L. Thyroid hormone receptor actions on transcription in amphibia: the roles of histone modification and chromatin disruption. *Cell Biosci* (2012) 2:42. doi: 10.1186/2045-3701-2-42

46. Sachs LM, Damjanovski S, Jones PL, Li Q, Amano T, Ueda S, et al. Dual functions of thyroid hormone receptors during xenopus development. *Comp Biochem Physiol B Biochem Mol Biol* (2000) 126:199–211. doi: 10.1016/S0305-0491(00)00198-X

47. Grimaldi A, Buisine N, Miller T, Shi YB, Sachs LM. Mechanisms of thyroid hormone receptor action during development: lessons from amphibian studies. *Biochim Biophys Acta* (2013) 1830:3882–92. doi: 10.1016/j.bbagen.2012.04.020

48. Buchholz DR, Paul BD, Fu L, Shi YB. Molecular and developmental analyses of thyroid hormone receptor function in xenopus laevis, the African clawed frog. *Gen Comp Endocrinol* (2006) 145:1–19. doi: 10.1016/j.ygcen.2005.07.009

49. Shi Y-B. Dual functions of thyroid hormone receptors in vertebrate development: the roles of histone-modifying cofactor complexes. *Thyroid* (2009) 19:987–99. doi: 10.1089/thy.2009.0041

50. Nakajima K, Yaoita Y. Dual mechanisms governing muscle cell death in tadpole tail during amphibian metamorphosis. *Dev Dyn* (2003) 227:246–55. doi: 10.1002/dvdy.10300

51. Denver RJ, Hu F, Scanlan TS, Furlow JD. Thyroid hormone receptor subtype specificity for hormone-dependent neurogenesis in xenopus laevis. *Dev Biol* (2009) 326:155–68. doi: 10.1016/j.ydbio.2008.11.005

52. Nakajima K, Tazawa I, Yaoita Y. Thyroid hormone receptor alpha- and beta-knockout xenopus tropicalis tadpoles reveal subtype-specific roles during development. *Endocrinology* (2018) 159:733–43. doi: 10.1210/en.2017-00601

53. Sachs LM. Unliganded thyroid hormone receptor function: amphibian metamorphosis got TALENs. *Endocrinology* (2015) 156:409–10. doi: 10.1210/en.2014-2016

54. Nakajima K, Tazawa I, Shi YB. A unique role of thyroid hormone receptor beta in regulating notochord resorption during xenopus metamorphosis. *Gen Comp Endocrinol* (2019) 277:66–72. doi: 10.1016/j.ygcen.2019.03.006

55. Shibata Y, Tanizaki Y, Shi YB. Thyroid hormone receptor beta is critical for intestinal remodeling during xenopus tropicalis metamorphosis. *Cell Biosci* (2020) 10:46. doi: 10.1186/s13578-020-00411-5

56. Shibata Y, Wen L, Okada M, Shi YB. Organ-specific requirements for thyroid hormone receptor ensure temporal coordination of tissue-specific transformations and completion of xenopus metamorphosis. *Thyroid* (2020) 30:300–13. doi: 10.1089/thy.2019.0366

57. Buchholz DR, Shi YB. Dual function model revised by thyroid hormone receptor alpha knockout frogs. *Gen Comp Endocrinol* (2018) 265:214–8. doi: 10.1016/j.ygcen.2018.04.020

58. Shi YB. Life without thyroid hormone receptor. *Endocrinology* (2021) 162: bqab028, 1–12. doi: 10.1210/endocr/bqab028

59. Buchholz DR, Tomita A, Fu L, Paul BD, Shi Y-B. Transgenic analysis reveals that thyroid hormone receptor is sufficient to mediate the thyroid hormone signal in frog metamorphosis. *Mol Cell Biol* (2004) 24:9026–37. doi: 10.1128/MCB.24.20.9026-9037.2004

60. Hasebe T, Buchholz DR, Shi YB, Ishizuya-Oka A. Epithelial-connective tissue interactions induced by thyroid hormone receptor are essential for adult stem cell development in the xenopus laevis intestine. *Stem Cells* (2011) 29:154–61. doi: 10.1002/stem.560

61. Schreiber AM, Mukhi S, Brown DD. Cell-cell interactions during remodeling of the intestine at metamorphosis in xenopus laevis. *Dev Biol* (2009) 331:89–98. doi: 10.1016/j.ydbio.2009.04.033

62. Ishizuya-Oka A, Shimozawa A. Connective tissue is involved in adult epithelial development of the small intestine during anuran metamorphosis in vitro. *Roux's Arch Dev Biol* (1992) 201:322–9. doi: 10.1007/BF00592113

63. Ishizuya-Oka A, Hasebe T. Establishment of intestinal stem cell niche during amphibian metamorphosis. *Curr Top Dev Biol* (2013) 103:305–27. doi: 10.1016/B978-0-12-385979-2.00011-3

64. Schreiber AM, Das B, Huang H, Marsh-Armstrong N, Brown DD. Diverse developmental programs of xenopus laevis metamorphosis are inhibited by a dominant negative thyroid hormone receptor. *PNAS* (2001) 98:10739–44. doi: 10.1073/pnas.191361698

65. Buchholz DR, Hsia VS-C, Fu L, Shi Y-B. A dominant negative thyroid hormone receptor blocks amphibian metamorphosis by retaining corepressors at target genes. *Mol Cell Biol* (2003) 23:6750–8. doi: 10.1128/MCB.23.19.6750-6758.2003

66. Choi J, Ishizuya-Oka A, Buchholz DR. Growth, development, and intestinal remodeling occurs in the absence of thyroid hormone receptor alpha in tadpoles of xenopus tropicalis. *Endocrinology* (2017) 158:1623–33. doi: 10.1210/en.2016-1955

67. Choi J, Suzuki KI, Sakuma T, Shewade L, Yamamoto T, Buchholz DR. Unliganded thyroid hormone receptor alpha regulates developmental timing via gene repression as revealed by gene disruption in xenopus tropicalis. *Endocrinology* (2015) 156:735–44. doi: 10.1210/en.2014-1554

68. Wen L, Shi YB. Unliganded thyroid hormone receptor alpha controls developmental timing in xenopus tropicalis. *Endocrinology* (2015) 156:721–34. doi: 10.1210/en.2014-1439

69. Wen L, Shibata Y, Su D, Fu L, Luu N, Shi Y-B. Thyroid hormone receptor α controls developmental timing and regulates the rate and coordination of tissue specific metamorphosis in xenopus tropicalis. *Endocrinology* (2017) 158:1985–98. doi: 10.1210/en.2016-1953

70. Wen L, Shi YB. Regulation of growth rate and developmental timing by xenopus thyroid hormone receptor alpha. *Dev Growth Differ* (2016) 58:106–15. doi: 10.1111/dgd.12231

71. Wang X, Matsuda H, Shi Y-B. Developmental regulation and function of thyroid hormone receptors and 9-cis retinoic acid receptors during xenopus tropicalis metamorphosis. *Endocrinology* (2008) 149:5610–8. doi: 10.1210/en.2008-0751

72. Tanizaki Y, Shibata Y, Zhang H, Shi YB. Analysis of thyroid hormone receptor alpha-knockout tadpoles reveals that the activation of cell cycle program is involved in thyroid hormone-induced larval epithelial cell death and adult intestinal stem cell development during xenopus tropicalis metamorphosis. *Thyroid* (2021) 31:128–42. doi: 10.1089/thy.2020.0022

73. Shibata Y, Tanizaki Y, Zhang H, Lee H, Dasso M, Shi YB. Thyroid hormone receptor is essential for larval epithelial apoptosis and adult epithelial stem cell development but not adult intestinal morphogenesis during xenopus tropicalis metamorphosis. *Cells* (2021) 10:536. doi: 10.3390/cells10030536

74. Shi Y-B, Brown DD. The earliest changes in gene expression in tadpole intestine induced by thyroid hormone. *J Biol Chem* (1993) 268:20312–7. doi: 10.1016/S0021-9258(20)80730-3

75. Amano T, Yoshizato K. Isolation of genes involved in intestinal remodeling during anuran metamorphosis. *Wound Repair Regener* (1998) 6:302–13. doi: 10.1046/j.1524-475X.1998.60406.x

76. Buchholz DR, Heimeier RA, Das B, Washington T, Shi Y-B. Pairing morphology with gene expression in thyroid hormone-induced intestinal remodeling and identification of a core set of TH-induced genes across tadpole tissues. *Dev Biol* (2007) 303:576–90. doi: 10.1016/j.ydbio.2006.11.037

77. Heimeier RA, Das B, Buchholz DR, Fiorentino M, Shi YB. Studies on xenopus laevis intestine reveal biological pathways underlying vertebrate gut adaptation from embryo to adult. *Genome Biol* (2010) 11:R55. doi: 10.1186/gb-2010-11-5-r55

78. Fu L, Das B, Matsuura K, Fujimoto K, Heimeier RA, Shi YB. Genome-wide identification of thyroid hormone receptor targets in the remodeling intestine during xenopus tropicalis metamorphosis. *Sci Rep* (2017) 7:6414. doi: 10.1038/s41598-017-06679-x

79. Hasebe T, Kajita M, Fu L, Shi YB, Ishizuya-Oka A. Thyroid hormone-induced sonic hedgehog signal up-regulates its own pathway in a paracrine manner in the xenopus laevis intestine during metamorphosis. *Dev Dyn* (2012) 241:403–14. doi: 10.1002/dvdy.23723

80. Hasebe T, Kajita M, Shi YB, Ishizuya-Oka A. Thyroid hormone-up-regulated hedgehog interacting protein is involved in larval-to-adult intestinal remodeling by regulating sonic hedgehog signaling pathway in xenopus laevis. *Dev Dyn* (2008) 237:3006–15. doi: 10.1002/dvdy.21698

81. Ishizuya-Oka A, Ueda S, Inokuchi T, Amano T, Damjanovski S, Stolow M, et al. Thyroid hormone-induced expression of sonic hedgehog correlates with adult epithelial development during remodeling of the xenopus stomach and intestine. *Differentiation* (2001) 69:27–37. doi: 10.1046/j.1432-0436.2001.690103.x

82. Stolow MA, Shi YB. Xenopus sonic hedgehog as a potential morphogen during embryogenesis and thyroid hormone-dependent metamorphosis. *Nucleic Acids Res* (1995) 23:2555–62. doi: 10.1093/nar/23.13.2555

83. Shi YB. Thyroid hormone and intestinal tumor: a wnt connection. *Oncotarget* (2018) 9:31941. doi: 10.18632/oncotarget.25822

84. Hasebe T, Fujimoto K, Kajita M, Ishizuya-Oka A. Thyroid hormone activates wnt/beta-catenin signaling involved in adult epithelial development during intestinal remodeling in xenopus laevis. *Cell Tissue Res* (2016) 365:309–18. doi: 10.1007/s00441-016-2396-8

85. Ishizuya-Oka A, Kajita M, Hasebe T. Thyroid hormone-regulated Wnt5a/Ror2 signaling is essential for dedifferentiation of larval epithelial cells into adult stem cells in the xenopus laevis intestine. *PloS One* (2014) 9:e107611. doi: 10.1371/journal.pone.0107611

86. Hasebe T, Fujimoto K, Kajita M, Fu L, Shi YB, Ishizuya-Oka A. Thyroid hormone-induced activation of notch signaling is required for adult intestinal stem cell development during xenopus laevis metamorphosis. *Stem Cells* (2017) 35:1028–39. doi: 10.1002/stem.2544

87. Ishizuya-Oka A, Hasebe T, Shimizu K, Suzuki K, Ueda S. Shh/BMP-4 signaling pathway is essential for intestinal epithelial development during xenopus larval-to-adult remodeling. *Dev Dyn* (2006) 235:3240–9. doi: 10.1002/dvdy.20969

88. Ishizuya-Oka A, Ueda S, Amano T, Shimizu K, Suzuki K, Ueno N, et al. Thyroid-hormone-dependent and fibroblast-specific expression of BMP-4 correlates with adult epithelial development during amphibian intestinal remodeling. *Cell Tissue Res* (2001) 303:187–95. doi: 10.1007/s004410000291

89. Fu L, Li C, Na W, Shi YB. Thyroid hormone activates xenopus MBD3 gene via an intronic TRE in vivo. *Front Biosci (Landmark Ed)* (2020) 25:437–51. doi: 10.2741/4812

90. Na W, Fu L, Luu N, Shi YB. Direct activation of tRNA methyltransferase-like 1 (Mettl1) gene by thyroid hormone receptor implicates a role in adult intestinal stem cell

development and proliferation during xenopus tropicalis metamorphosis. *Cell Biosci* (2020) 10:60. doi: 10.1186/s13578-020-00423-1

91. Okada M, Miller TC, Wen L, Shi YB. A balance of mad and myc expression dictates larval cell apoptosis and adult stem cell development during xenopus intestinal metamorphosis. *Cell Death Dis* (2017) 8:e2787. doi: 10.1038/cddis.2017.198

92. Shi Y, Glynn JM, Guilbert LJ, Cotter TG, Bissonnette RP, Green DR. Role for c-myc in activation-induced apoptotic cell death in T cell hybridomas. *Science* (1992) 257:212–4. doi: 10.1126/science.1378649

93. Koskinen PJ, Alitalo K. Role of myc amplification and overexpression in cell growth, differentiation and death. *Semin Cancer Biol* (1993) 4:3–12.

94. Amati B, Land H. Myc-Max-Mad: a transcription factor network controlling cell cycle progression, differentiation and death. *Curr Opin Genet Dev* (1994) 4:102–8. doi: 10.1016/0959-437X(94)90098-1

95. McMahon SB. MYC and the control of apoptosis. *Cold Spring Harb Perspect Med* (2014) 4:a014407. doi: 10.1101/cshperspect.a014407

96. Nieminen AI, Partanen JI, Klefstrom J. C-myc blazing a trail of death: coupling of the mitochondrial and death receptor apoptosis pathways by c-myc. *Cell Cycle* (2007) 6:2464–72. doi: 10.4161/cc.6.20.4917

97. Packham G, Cleveland JL. C-myc and apoptosis. *Biochim Biophys Acta* (1995) 1242:11–28. doi: 10.1016/0304-419X(94)00015-T

98. Kuchino Y, Asai A, Kitanaka C. Myc-mediated apoptosis. *Prog Mol Subcell Biol* (1996) 16:104–29. doi: 10.1007/978-3-642-79850-4_7

99. Thompson EB. The many roles of c-myc in apoptosis. *Annu Rev Physiol* (1998) 60:575–600. doi: 10.1146/annurev.physiol.60.1.575

100. Dang CV. C-myc target genes involved in cell growth, apoptosis, and metabolism. *Mol Cell Biol* (1999) 19:1–11. doi: 10.1128/MCB.19.1.1

101. Pelengaris S, Rudolph B, Littlewood T. Action of myc *in vivo* - proliferation and apoptosis. *Curr Opin Genet Dev* (2000) 10:100–5. doi: 10.1016/S0959-437X(99)00046-5

102. Okada M, Shi YB. The balance of two opposing factors mad and myc regulates cell fate during tissue remodeling. *Cell Biosci* (2018) 8:51. doi: 10.1186/s13578-018-0249-8

103. Muncan V, Heijmans J, Krasinski SD, Buller NV, Wildenberg ME, Meisner S, et al. Blimp1 regulates the transition of neonatal to adult intestinal epithelium. *Nat Commun* (2011) 2:452. doi: 10.1038/ncomms1463

104. Harper J, Mould A, Andrews RM, Bikoff EK, Robertson EJ. The transcriptional repressor Blimp1/Prdm1 regulates postnatal reprogramming of intestinal enterocytes. *Proc Natl Acad Sci U.S.A.* (2011) 108:10585–90. doi: 10.1073/pnas.1105852108

105. Matsuda H, Shi YB. An essential and evolutionarily conserved role of protein arginine methyltransferase 1 for adult intestinal stem cells during postembryonic development. *Stem Cells* (2010) 28:2073–83. doi: 10.1002/stem.529

106. Plateroti M, Gauthier K, Domon-Dell C, Freund JN, Samarut J, Chassande O. Functional interference between thyroid hormone receptor alpha (TRalpha) and natural truncated TRDeltaalpha isoforms in the control of intestine development. *Mol Cell Biol* (2001) 21:4761–72. doi: 10.1128/MCB.21.14.4761-4772.2001

107. Flamant F, Poguet AL, Plateroti M, Chassande O, Gauthier K, Streichenberger N, et al. Congenital hypothyroid Pax8(-/-) mutant mice can be rescued by inactivating the TRalpha gene. *Mol Endocrinol* (2002) 16:24–32. doi: 10.1210/mend.16.1.0766

108. Kress E, Rezza A, Nadjar J, Samarut J, Plateroti M. The frizzled-related sFRP2 gene is a target of thyroid hormone receptor alpha1 and activates beta-catenin signaling in mouse intestine. *J Biol Chem* (2009) 284:1234–41. doi: 10.1074/jbc.M806548200

109. Plateroti M, Chassande O, Fraichard A, Gauthier K, Freund JN, Samarut J, et al. Involvement of T3Ralpha- and beta-receptor subtypes in mediation of T3 functions during postnatal murine intestinal development. *Gastroenterology* (1999) 116:1367–78. doi: 10.1016/S0016-5085(99)70501-9

110. Bao L, Roediger J, Park S, Fu L, Shi B, Cheng SY, et al. Thyroid hormone receptor alpha mutations lead to epithelial defects in the adult intestine in a mouse model of resistance to thyroid hormone. *Thyroid* (2019) 29:439–48. doi: 10.1089/thy.2018.0340

111. Plateroti M, Kress E, Mori JI, Samarut J. Thyroid hormone receptor alpha1 directly controls transcription of the beta-catenin gene in intestinal epithelial cells. *Mol Cell Biol* (2006) 26:3204–14. doi: 10.1128/MCB.26.8.3204-3214.2006

frontiers | Frontiers in Endocrinology

TYPE Original Research
PUBLISHED 10 July 2023
DOI 10.3389/fendo.2023.1208182

Check for updates

OPEN ACCESS

EDITED BY
Liezhen Fu,
National Institutes of Health (NIH),
United States

REVIEWED BY
Fernando Faunes,
Andres Bello University, Chile
Takashi Hasebe,
Nippon Medical School, Japan

*CORRESPONDENCE
I. Lazcano
ivanlazcano@comunidad.unam.mx
A. Orozco
aureao@unam.mx

RECEIVED 18 April 2023
ACCEPTED 01 June 2023
PUBLISHED 10 July 2023

CITATION
Lazcano I, Olvera A, Pech-Pool SM, Sachs L, Buisine N and Orozco A (2023) Differential effects of 3,5-T2 and T3 on the gill regeneration and metamorphosis of the *Ambystoma mexicanum* (axolotl). *Front. Endocrinol.* 14:1208182. doi: 10.3389/fendo.2023.1208182

COPYRIGHT
© 2023 Lazcano, Olvera, Pech-Pool, Sachs, Buisine and Orozco. This is an open-access article distributed under the terms of the Creative Commons Attribution License (CC BY). The use, distribution or reproduction in other forums is permitted, provided the original author(s) and the copyright owner(s) are credited and that the original publication in this journal is cited, in accordance with accepted academic practice. No use, distribution or reproduction is permitted which does not comply with these terms.

Differential effects of 3,5-T2 and T3 on the gill regeneration and metamorphosis of the *Ambystoma mexicanum* (axolotl)

I. Lazcano[1]*, A. Olvera[1], S. M. Pech-Pool[1], L. Sachs[2], N. Buisine[2] and A. Orozco[1,3]*

[1]Instituto de Neurobiología, Universidad Nacional Autónoma de México (UNAM), Querétaro, Mexico, [2]UMR PhyMA CNRS, Muséum National d'Histoire Naturelle, Paris, France, [3]Escuela Nacional de Estudios Superiores, Unidad Juriquilla, Universidad Nacional Autónoma de México (UNAM), Querétaro, Mexico

Thyroid hormones (THs) regulate tissue remodeling processes during early- and post-embryonic stages in vertebrates. The Mexican axolotl (*Ambystoma mexicanum*) is a neotenic species that has lost the ability to undergo metamorphosis; however, it can be artificially induced by exogenous administration of thyroxine (T4) and 3,3′,5-triiodo-L-thyronine (T3). Another TH derivative with demonstrative biological effects in fish and mammals is 3,5-diiodo-L-thyronine (3,5-T2). Because the effects of this bioactive TH remains unexplored in other vertebrates, we hypothesized that it could be biologically active in amphibians and, therefore, could induce metamorphosis in axolotl. We performed a 3,5-T2 treatment by immersion and observed that the secondary gills were retracted, similar to the onset stage phenotype; however, tissue regeneration was observed after treatment withdrawal. In contrast, T4 and T3 immersion equimolar treatments as well as a four-fold increase in 3,5-T2 concentration triggered complete metamorphosis. To identify the possible molecular mechanisms that could explain the contrasting reversible or irreversible effects of 3,5-T2 and T3 upon gill retraction, we performed a transcriptomic analysis of differential expression genes in the gills of control, 3,5-T2–treated, and T3-treated axolotls. We found that both THs modify gene expression patterns. T3 regulates 10 times more genes than 3,5-T2, suggesting that the latter has a lower affinity for TH receptors (TRs) or that these hormones could act through different TR isoforms. However, both TH treatments regulated different gene sets known to participate in tissue development and cell cycle processes. In conclusion, 3,5-T2 is a bioactive iodothyronine that promoted partial gill retraction but induced full metamorphosis in higher concentrations. Differential effects on gill retraction after 3,5,-T2 or T3 treatment could be explained by the activation of different clusters of genes related with apoptosis, regeneration, and proliferation; in addition, these effects could be initially mediated by TRs that are expressed in gills. This study showed, for the first time, the 3,5,-T2 bioactivity in a neotenic amphibian.

KEYWORDS

***Ambystoma mexicanum*, thyroid hormones, metamorphosis, transcriptomics, 3,5-T2, gills**

Introduction

Metamorphosis is a fascinating phenomenon that occurs in some vertebrate and invertebrate animal species that involves spectacular post-embryonic transition and changes in the morphology, physiology, behavior, and ecology of the individual. Available data suggest that this post-embryonic remodeling is governed by thyroid hormones (THs), at least in chordates (1). A well-studied example is amphibian metamorphosis, in which tadpoles experience a peak of TH plasma levels prior to its onset that triggers tissue remodeling by hierarchically controlling the expression of a complex cascade of target genes (1, 2). The diversity of molecular and cellular processes that convey this life transition involves cell-specific expression and regulation of TH nuclear receptor (TR) genes, THRA and THRB, which act as TH-dependent transcription factors (3–5).

In contrast to frogs, some salamanders like the Mexican axolotl (*Ambystoma mexicanum*) have lost the ability to undergo metamorphosis under natural conditions (6), retaining juvenile characteristics in the mature breeding stage (paedomorphosis) (7). In this neotenic species, plasma TH concentrations are much lower than those found in other premetamorphic anurans, but their tissues possess functional deiodinases and TRs, the molecular components that are essential to decode the TH signal (7). In fact, exogenous exposure to the prohormone T4 or the bioactive T3 experimentally triggers axolotl metamorphosis, confirming the TH involvement in amphibian metamorphosis. However, a more precise characterization of these TH actions is *unclear* given that the protocols used, thus far, have been inconsistent, differing in the method and frequency of hormone administration (immersion or *intra peritoneal (i.p.)* injection), in the developmental stage of the axolotl at the time of induction, among others (8–10).

Recently, 3,5-diiodo-L-thyronine (3,5-T2), an active metabolite of T3, has been shown to act as an endogenous alternative TR ligand with demonstrative biological actions that mimic those of the recognized bioactive T3. For example, 3,5-T2 decreases body weight and serum thyroid- stimulating hormone and regulates lipid metabolism in mammals (11, 12). In fish, both, T3 and 3,5-T2 promote growth (13), and each hormone regulates the expression of specific genes in the tilapia brain and liver (14). Possible thyromimetic effects of 3,5-T2 in other vertebrate species are still unknown. Thus, the aim of the present study was to gain a deeper understanding of TH actions upon axolotl metamorphosis induction, as well as prompted the hypothesis that, as an alternative TR ligand, 3,5-T2 could also induce metamorphosis in this species and/or differentially regulate some aspects of the tissue remodeling involved in this life transition.

Material and methods

Animals

Juvenile axolotls were kindly donated by Marco Terrones (Axolkali) and Dr. Jesus Chimal (Instituto de Investigaciones Biomédicas, UNAM). All axolotls were maintained and handled in accordance with protocols approved by the Ethics for Research Committee of the Instituto de Neurobiología, UNAM; the guidelines for use of live amphibians and reptiles in field and laboratory research of the American Society of Ichthyologists and Herpetologists; and the ARRIVE guidelines. Animals of around 8 – 10 months after hatching and weighing between 9 and 12 g were maintained at our local housing for at least 20 days prior to experiments at 18°C in a 14-h/10-h light/dark cycle and fed with small pieces of meat and live brine shrimp.

Metamorphosis induction with thyroid hormone treatment

The immersion protocol allows adding hormones at a desired concentration in the rearing water of aquatic species, eliminating the manipulation stress factor. In the present study, nanomolar concentrations of THs were added to the rearing water and replaced every 3 days. With this TH administration protocol, the onset of metamorphosis at around day 26 post-treatment with T4 was reported (8, 10). Initial experiments to analyze whether 3,5-T2 could induce metamorphosis consisted in treating groups of axolotls (female or male axolotls) with 50 nM of this TH derivative. Control animals were immersed in vehicle (0.001 M NaOH). In further experiments, axolotls were treated with 500 nM of thyroxine (T4), 3,3′,5-L-triiodothyronine (T3) and 3,3′,5′-triiodothyronine (rT3) (Sigma-Aldrich). These treatments were extended for 12 days, a time point at which the rearing water was changed every 3 days for at least 45 days post- withdrawal (dpw). In a second protocol, we immersed axolotls with a higher dose (2 μM) of 3,5-T2 or rT3, and these solutions were replaced with hormone-containing rearing water on Mondays, Wednesdays, and Fridays. The onset of metamorphosis was determined when reabsorption of the external gills and dorsal fin was observed. Climax was established when gills and dorsal fin were completely absorbed. Full metamorphosis was reached when the axolotls became salamanders. Once reaching this state, we observed a 30% increase in lethality, which was unrelated to the hormone used for metamorphosis induction. Phenotype changes in T3-treated axolotls can be observed in Supplementary Video 1.

Semi-quantification of secondary gills length

Secondary gills were measured during the experiments. To this end, we captured microphotographs (dorsal view) of the secondary gills in free moving axolotls by using a stereomicroscope (SteREO Discovery.V12, Zeiss). Subsequently, we measured (software ZEN) at least 10 secondary gill filaments and averaged the length to get a value for each animal. Cases when the first and secondary gills were completely absorbed were reported as “not detected” (n.d.).

Immunohistochemistry of thyroid hormone receptors in axolotl gill

The complete gill was dissected from a young axolotl previously anesthetized with 0.4% tricaine during 12–14 min. Immediately, the gill was transferred into 4% paraformaldehyde for 24 h, and, then, the tissue was cryoprotected in sucrose (30%) for 12 h and freeze mounted onto aluminum sectioning blocks using Tissue-Tek® O.C.T (Sakura Finetek, Torrance, CA, USA). Sections of ~ 14 µm were obtained using a cryostat (Leica CM3050, Buffalo Grove, IL, USA) and mounted on Superfrost ™ microscope slides from Fisher Scientific. Gill sections were hydrated in Phosphate Buffered Saline (PBS) during 15 min and then permeated with 2 M HCl during 20 min, and, then, the slides were washed in Tris Buffered Saline (TBS) (3 × 10 min) and treated with citrate buffer 100 mM, pH 6, at 80°C for 30 min, after which free binding sites were blocked with 5% non-fat dry milk (Bio-Rad, Hercules, CA, USA) for 2 h. After blocking, the slides were washed with Tween-Tris Buffered Saline (TTBS) (0.1% Triton X-100 in TBS) three times, and the tissues were incubated for 24 h with the primary anti-thyroid hormone receptor (Abcam, ab42565) in a 1:500 dilution. All the slides were washed (3 × 10 min) and incubated with goat anti-rabbit Immunoglobulin G (IgG) H & L (Alexa Fluor® 488) from Abcam (ab150077) in a 1:1,000 dilution during 12 h. DAPI (4′,6-diamidino-2-phenylindole) was used to label cell nuclei. All the slides were mounted with vectashield (Vector Laboratories Inc., Burlingame, CA, USA), and micrographs were captured with a Zeiss LSM 780 DUO confocal microscope (Carl Zeiss AG, Oberkochen, Germany) and image software ZEN. Image post-processing was performed using ImageJ software (developed by NIH, freeware).

Differential gene expression analysis

We performed high-throughput sequencing with a differential transcriptomic analysis on the gills of control, 3,5-T2–treated, and T3-treated juvenile axolotls. The animals were submitted to an immersion protocol with vehicle, 500 nM of 3,5-T2 or T3 of by 6 days. At this time point, the gills were dissected in axolotls anesthetized with 0.4% tricaine. Immediately, the gill was transferred into RNA later (Invitrogen), manually homogenized, and processed for total RNA extraction using TRIzol (Invitrogen).

Libraries were generated using the Illumina TruSeq RNA Sample Preparation Kit according to the manufacturer's instructions. Transcriptome sequencing was conducted using Genome Analyzer GAIIx (Illumina) at the genome sequencing facility of our university located at "Instituto de Biotecnología, UNAM". A configuration for pair-end reads with a 72-bp read length was used. Sequence Read Archive data are available as BioProject ID: PRJNA957439.

Reads quality control were generated with FastQC (www.bioinformatics.babraham.ac.uk/projects/fastqc/) and mapped on axolotl genome (GCA_002915635.3_AmbMex60DD) with bowtie2 (15) ran with sensitive parameters (–sensitive). Differential analysis and clustering followed the same procedure as previously described (16).

Enrichment analysis of biological processes and pathways are based on the GORILLA website (17) and Kyoto Encyclopedia of Genes and Genomes (KEGG) pathways databases (18). The protein–protein interaction network was modeled from the BIOGRID database (19).

RT-qPCR verification of transcriptomic data

The mRNA was reversed -transcribed (RT) (RevertAid First Strand, Thermo Fisher) from 0.5 µg of total RNA using an oligo(dT) primer (final volume of 20 µl). Quantitative $2^{-\Delta\Delta CT}$ qPCR was carried out in duplicates in two independent assays with three samples per group using the geometric mean of Gapdh and Eif5a as an internal standard in reactions that contained 2 µl of the diluted 1:10 RT reaction, 3.3 µl of Maxima SYBR Green/ROX qPCR Master Mix (Fermentas, Waltham, MA, USA), and 250 nM forward and reverse primers in a final volume of 8 µl. PCR protocol of 95°C for 10 s, 60°C for 10 s, and 72°C for 10 s were used. Oligonucleotides used are enlisted in Supplementary Data 2.

Data analysis

Results of the length of secondary gills are presented as the mean ± S.E.M. Data were analyzed using one-way ANOVA followed by a Tukey *post -hoc* test. Values of $p < 0.05$ were considered statistically significant.

Results

Effect of the different THs on axolotl metamorphosis

As an initial approach to test whether 3,5-T2 could induce axolotl metamorphosis, we used an immersion protocol previously characterized for T4 (8, 10), but no induction was observed with the 50 nM 3,5-T2 treatment (data not shown). After a 10-fold increase in 3,5-T2 concentration (500 nM), secondary gill retraction (~ 50%) was observed 6 days after the onset of the treatment (Figures 1A, B). As time progressed, no further morphological changes that indicated metamorphosis progression were observed in the treated axolotl, but secondary gill retraction was more evident, prompting withdrawal at day 25 post- treatment to avoid the possible death of the individuals. Unexpectedly, progressive secondary gill regeneration was observed, recovering their full-length around 45 dpw (Figures 1C, D). The reversible gill phenotypic transition promoted by the 3,5-T2 treatment withdrawal raised the possibility that these effects were also elicited by the prohormone T4 and the bioactive T3. Therefore, we replicated experiments treating

10.3389/fendo.2023.1208182

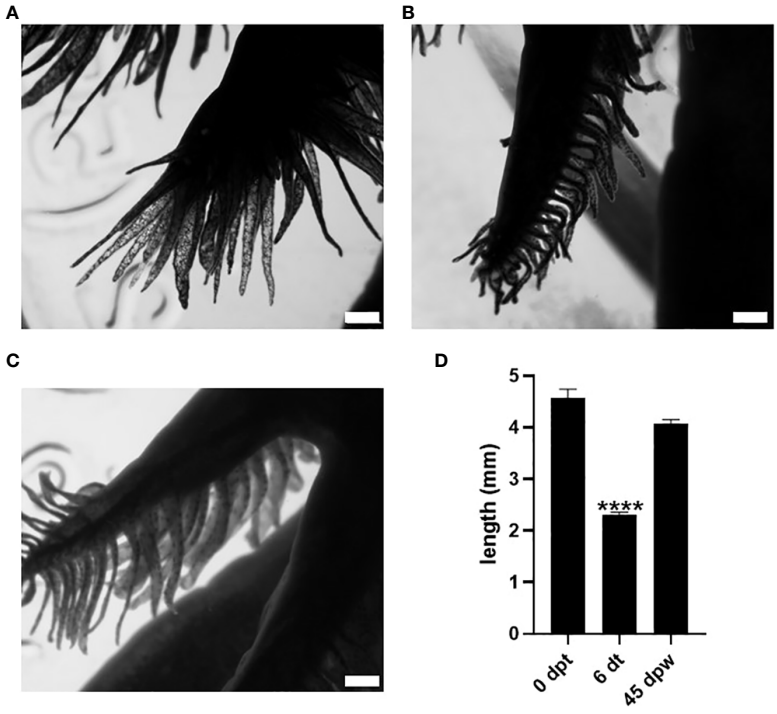

FIGURE 1
Effect of 50 nM 3,5-T2 exposure upon the length and morphology of axolotl secondary gills. Dorsal view photomicrographs of axolotl secondary gill were taken to analyze the effect of the 3,5-T2 immersion treatments upon the length of the gill at 0 dpt. **(A)** Six days after the onset of 3,5-T2 treatment (6 dt). **(B)** Forty-five days post-withdrawal (dpw) of 3,5-T2 exposure. **(C)** The semi-quantification of secondary gill lengths from **(A)** to **(C)** is shown in **(D)**; data are represented as the mean ± S.E.M. (n = 4) and were analyzed using one-way ANOVA followed by a Tukey *post -hoc* test. Asterisks indicate statistical difference when compared to 0 dpt. **** $p < 0.01$. Scale bar, 1 mm.

axolotls with equimolar concentrations of 500 nM of T4, T3, or 3,5-T2 for 12 days, when visible changes in gill retraction were evident in the 3,5-T2–treated group. At this time point, we withdrew all hormone treatments and close monitored the axolotl for phenotypic changes for 23 dpw (Figure 2A). For this experiment, a more systematic characterization of the TH-specific effects upon axolotl metamorphosis was achieved, identifying pre-metamorphic, onset, climax, and post-metamorphic stages (Supplementary Figure 1; Supplementary Video 1). As shown in Figures 2B, D, only 3,5-T2 treatment elicited secondary gill retraction by 6 days post-treatment (dpt), whereas exposure to T3 elicited this retraction after 12 dpt and T4 effects were only observed after 3 dpw. Furthermore, as previously observed, suspension of 3,5-T2 treatment elicited secondary gill regeneration, whereas an irreversible metamorphic progression resulted from T4 or T3 withdrawal (Figures 2B, D). The T3-treated group exhibited a full post-metamorphic (salamander) phenotype by 23 dpw, whereas that of T4 presented a climax stage phenotype at this same time point (Figure 2C).

3,5-T2 can induce axolotl metamorphosis

Given that some of the TH-related effects observed in mammals generally require higher concentrations of 3,5-T2 than those of T3 (11), we tested whether a higher 3,5-T2 concentration (2 µM) could induce axolotl metamorphosis using the same immersion protocol (Figure 3A). In addition, we included a negative control group treated with equimolar concentrations of the inactive reverse T3 (rT3) (20). Interestingly, 3,5-T2 was able to induce complete metamorphosis, evidencing that, for the first time, this alternative ligand is bioactive also in the axolotl, whereas rT3 lacked metamorphic effects, further confirming its inactive nature in this species, at least in this experimental paradigm (Figures 3B, C). Unexpectedly, and although 3,5-T2 and T3 were able to induce full metamorphosis, the resulting phenotypes of the salamanders were different, particularly regarding the skin color pattern. 3,5-T2–triggered metamorphosis produced salamanders with intense and abundant yellow spots, whereas the skin of the T3-treated group was darker and almost spotless (Supplementary Figure 2).

Axolotl gill expresses thyroid hormone receptors

The observed reversible gill phenotypic transition elicited by 3,5-T2 treatment withdrawal raised the question of whether 3,5-T2 effects were indeed mediated by canonical TRs. To investigate this, we first explored secondary gill cyto-architecture and observed the presence of a large number of filaments along the tissue, a gill mesenchyme, followed by a layer of undetermined cells and of gill

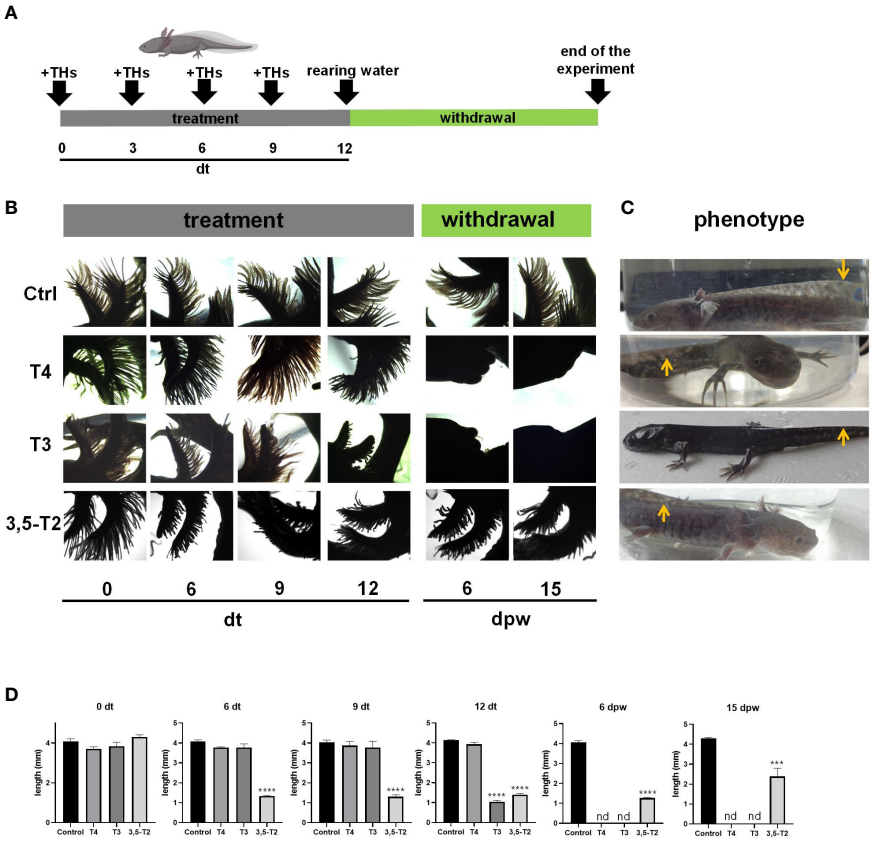

FIGURE 2
Effects of different iodothyronines on the length and morphology of axolotl secondary gills. **(A)** Graphical representation of the experimental protocol, including TH treatment and withdrawal. **(B)** Dorsal view photomicrographs of axolotl secondary gill treated with vehicle (Ctrl) or 500 nM of T4, T3, or 3,5-T2. Days of treatment (dt) or post- withdrawal (dpw) are indicated. **(C)** Phenotype of the treated axolotl. After 45 dpw, control and 3,5-T2– treated animals showed the classical neotenic phenotype; T4 treatment only reached a climax phenotype, and T3- treated animals were post-metamorphic. Arrows indicate the similarities and differences of the dorsal fin. **(D)** The semi-quantification of secondary gill lengths from **(B)**. Pictures show the morphology of the axolotls under different treatments at 23 dpw. Data are shown as mean ± S.E.M. (n = 3 per group). In **(D)**, data were analyzed using one-way ANOVA followed by a Tukey *post- hoc* test. Asterisks indicate statistical differences between treatment and control groups. ***$p < 0.01$; **** $p < 0.001$; n.d., not detected.

muscle (Figure 4A). In addition, we employed a specific antibody, which is predicted to bind to axolotl TRα and TRβ isoforms (Supplementary Figure 3). The immunohistochemistry revealed the presence of TRs mainly in the secondary gills and in the tissue opposite to these filaments (Figures 4B, C). While exploring in more detail the subcellular TR distribution, we detected a strong immunoreactivity signal co-localizing with the nuclei of these receptors in both structure samples [Figures 4D–I (1), I (2)], suggesting that 3,5-T2 could be signaling through canonical TRs.

3,5-T2 and T3 regulate different gene networks in the gill

With the aim of analyzing the possible molecular pathways involved in secondary gill remodeling after 3,5-T2 or T3 exposure, we treated axolotl with 500 nM of either hormone for 6 days, and gill total RNA was extracted to perform a high-throughput transcriptome sequencing followed by differential analysis. An illustrative example of quality control as well as sequencing and mapping statistics are shown in the Supplementary Data 1. Independent RT-qPCR measures of gene expression changes on a selected number of target genes were in very good agreement with RNA- seq data (Supplementary Data 2), thus illustrating the robustness of our analyses. We next conducted a cluster analysis on normalized expression levels (Figure 5A) to derive groups of synexpression and compared T3- or 3,5-T2–treated axolotl versus controls. As discussed previously (16, 21), the direct comparison of differential analysis results (e.g., with Venn diagrams) often fails because it relies too much on p-values set in an unfavorable statistical setting (low number of biological replicates and high number of observables). On the basis of this analysis, we found a total of 138 and 277 genes regulated by 3,5-T2 and T3, respectively. Note that nine genes are regulated by 3,5-T2 alone and 148 genes by T3, thereby readily identifying specific components of gene regulatory responses (Figure 5B). The full list of gene clusters is provided in Supplementary Data 3. It is interesting that the cluster of T3 exclusively upregulated genes is the largest, comprising 120

10.3389/fendo.2023.1208182

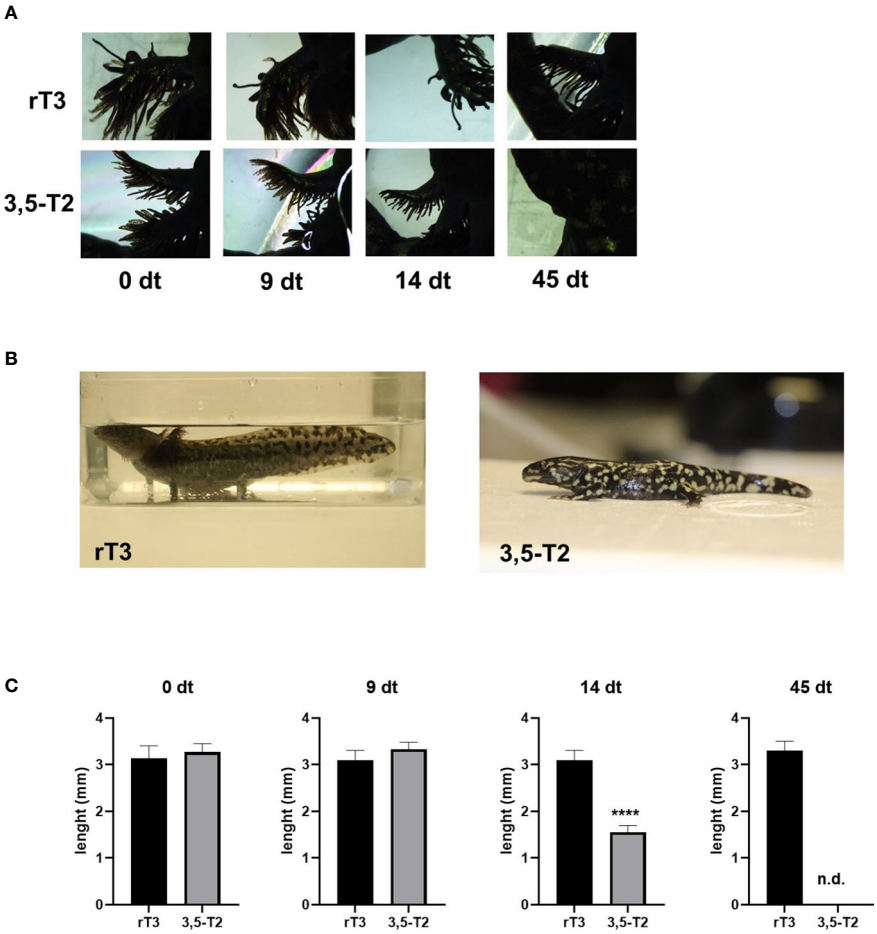

FIGURE 3
3,5-T2 induces metamorphosis in axolotls. **(A)** Dorsal view photomicrographs of secondary gill from axolotls treated with 2 μM of 3,5-T2 or rT3. Days of treatment (dt) are indicated. **(B)** Axolotl phenotypes at the end of the experiment (45 dpt), showing a 3,5-T2 but not by rT3 metamorphosis induction. **(C)** Semi-quantification of the length of secondary gills from **(A)**; data were analyzed using one-way ANOVA followed by a Tukey *post- hoc* test and are shown as the mean ± S.E.M. (n = 3 per group). Asterisks indicate statistical differences between groups. ****$p < 0.001$. n.d., not detected.

genes, almost three times more than those upregulated by both iodothyronines (45 genes).

We performed a gene ontology analysis to explore the physiological implications of T3 and 3,5-T2 treatments upon gill remodeling (Figure 6). The most enriched biological process found for genes regulated by both hormones belonged to three principal categories: metabolism, cell cycle, and stress. The lists of genes regulated exclusively by 3,5-T2 or T3 did not show significant enrichment of biological processes, as often found when the number of genes is low (22). Nevertheless, some of the genes exclusively regulated by T3 have been associated with developmental processes. The analysis of KEGG revealed that metabolism, cell signaling, and cell cycle are pathways activated by genes regulated by both iodothyronines (Figure 6B). Interestingly, the p53 pathway was identified in the pool of genes exclusively regulated by T3; this gene network could be participating either in cell cycle arrest or in apoptosis. This made us think that the differences observed in metamorphosis induction, that is, reversible (+ 3,5-T2) or full secondary gill absorption (+ T3), could be operated by an interplay of tissue remodeling, proliferation, and apoptosis. This idea was further supported by the manual identification of other 3,5-T2– and T3-differentially regulated genes, all of which are known to participate in processes that are key for life transition events, like metamorphosis (Table 1).

We also explored whether 3,5-T2 or T3 differentially regulated genes engaged in particular known protein–protein interactions within biological networks (BioGRID analysis). We found a major component constituted of highly interconnected nodes (i.e., gene

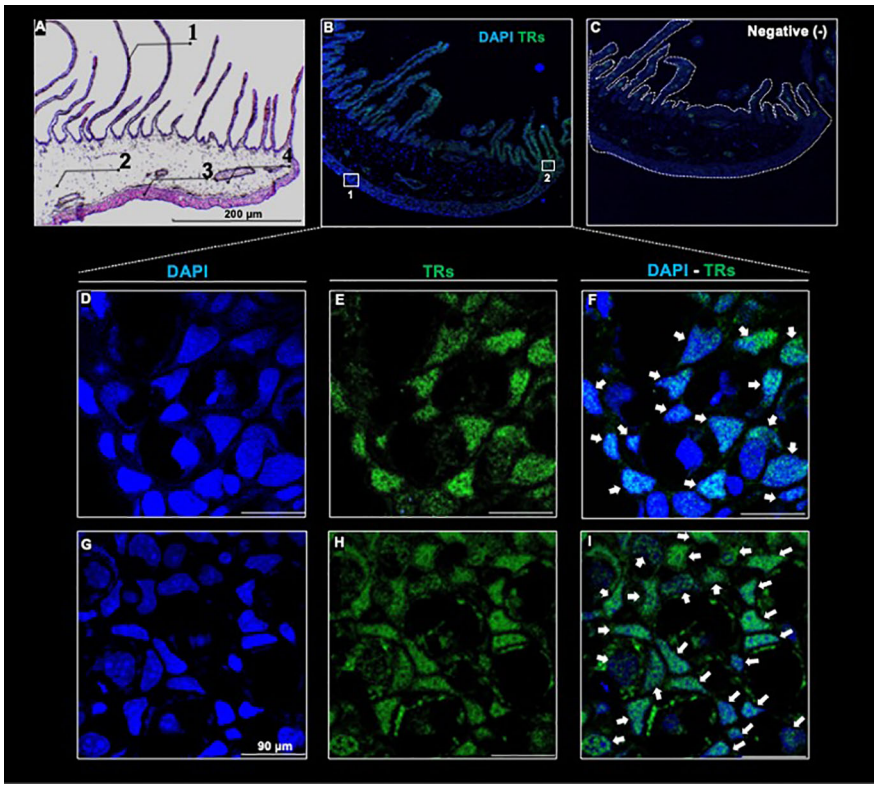

FIGURE 4
Thyroid hormone receptor immunodetection in a full-length transversal axolotl gill **(A)** Hematoxylin/eosin staining. Numbers indicate gill filament (1); gill mesenchyme (2); external portion of the gill (3), and gill muscle (4). **(B)** Co-localization of anti - TR/DAPI. **(C)** Negative control. **(D–F)**: amplification of the external gill, **(G–I)**: amplification of the filament base. White arrows indicate anti - TR immunoreactive cells. Scale bar = 90 µm

products) mostly involved in DNA replication, cell cycle control, and chromatin dynamics, further illustrating TH functional input in these cellular processes (Figure 7).

Discussion

In the present study, we describe that, for the first time, 3,5-T2 can induce axolotl metamorphosis and that this alternative TR ligand elicits transient and reversible gill remodeling that involves the regulation of specific gene clusters.

3,5-T2 has been well recognized as an alternate TR ligand (Mendoza et al., 2013); it regulates TH canonical actions like growth (13, 23) and lipid metabolism (12, 24), as well as elicits differential effects upon the expression of TH-regulated genes in fish (23, 25) and mammals (11, 12, 24). Other TH alternative ligands had been shown to induce metamorphosis in several species that emerged in different timepoints of evolution. For example, Triiodothyroacetic acid (TRIAC) has been shown to promote amphioxus metamorphosis (26, 27). However, whether 3,5-T2 had postembryonic remodeling effects in any amphibian had never been explored. In this context, the paedomorphic axolotl is a fascinating model because, in contrast to anurans, they can undergo metamorphosis only after T4 or T3 exogenous treatment (8–10). When treating axolotl with equimolar concentrations (500 nM) of T4, T3, and 3,5-T2, only T4 and T3 were capable of inducing full metamorphosis. Interestingly, T4 induction occurred around 20 days later than that with T3. This highlights the prohormone nature of T4, which requires a biotransformation into the bioactive form of the hormone, possibly catalyzed by deiodinase type II (28). T4 could act as a partial TR agonist (29), resulting in a full but time extended transformation. In contrast, exogenous administration of T3 directly promotes cellular actions and induces a faster metamorphosis.

Interestingly, immersion in 500 nM 3,5-T2 only affected the size of the secondary gills without inducing a true metamorphosis, whereas treatment withdrawal resulted in progressive secondary gill regeneration. This suggests differential effects of 3,5-T2 at least in this remodeling process. The lack of metamorphosis induction at this concentration could be either a reflection of deficient intracellular TH transport and/or a lower 3,5-T2 affinity for TRs as has been described for mammals (11). Neither of these mechanisms have been studied in amphibians for any TH or their derivatives, leaving these hypotheses still unresolved. Full axolotl metamorphosis was attained when the 3,5-T2 treatment was scaled four-fold. As compared with T3, 3,5-T2 has a higher affinity for L-TRβ1 in fish and lower affinity for TRβ1 in humans, respectively (30), and thus preferentially binds to the beta isoform. Al though we do not know whether 3,5-T2 is binding to canonical axolotl TRs, our results show that the secondary gill expresses these receptors abundantly, which could explain the early effects on gill retraction with all tested iodothyronines. Gaining insight of 3,5-T2 and

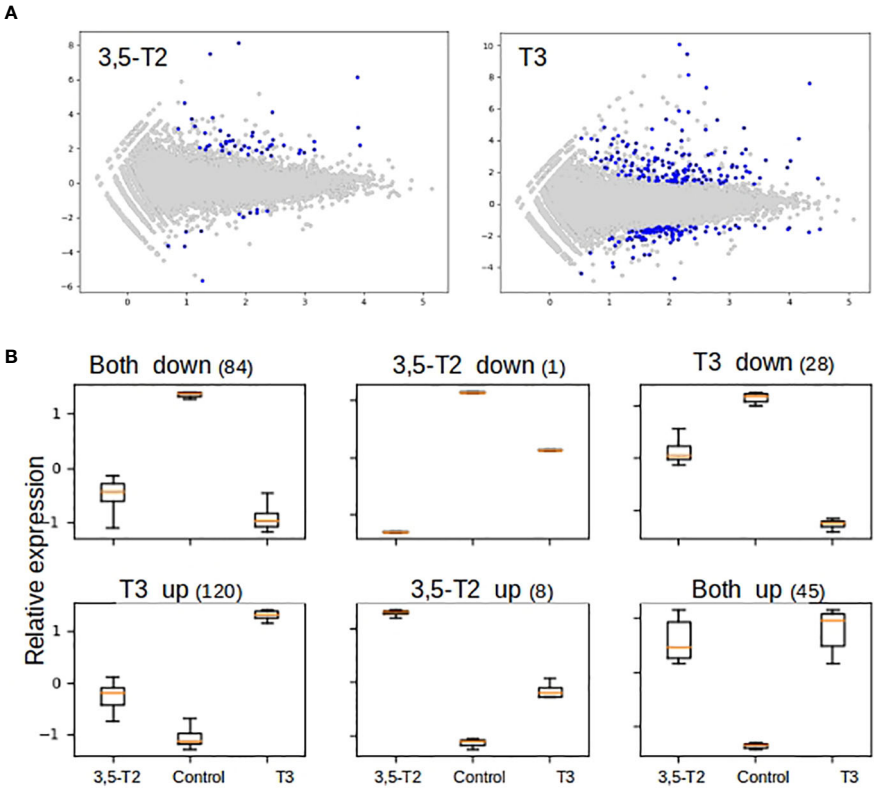

FIGURE 5
Differential gene expression and cluster analysis in the axolotl gill after 3,5-T2 or T3 treatment. **(A)** MA plot of differentially regulated genes by 3,5-T2 or T3. Data represent individual gene responses plotted as logarithmic fold-change vs. total counts of mRNA, False Discovery Rate (FDR) < 0.05. **(B)** Cluster analysis of logarithmic fold change of gene expression normalized and scaled (*y*-axis), comparing TH treatments vs. controls (*x*-axis). Number above represents the total number of genes in each cluster.

T3 binding affinity for axolotl TR isoforms would be necessary to analyze these hypotheses.

A T3- or 3,5-T2–treated gill transcriptomic analysis was performed to further decipher if the expression of different gene clusters could explain the observed effects upon secondary gill remodeling processes. Our results showed that both iodothyronines induced a change in gene expression; these findings, together with the notion that TRs are being expressed in the gill, allow the hypothesis that 3,5-T2 and T3 are acting through canonic TR isoforms to modulate tissue remodeling. 3,5-T2-exclusively regulated genes were 10 times lower than those T3-exclusively regulated, suggesting that these hormones could be acting through different TR isoforms that have divergent outcomes. Furthermore, T3 seems to be irreversibly involved in tissue remodeling, regulating genes such as metalloproteinases like the matrix metalloproteinase 11 (MMP11) and the ADAM metallopeptidase with thrombospondin type 1 motif 17 (ADAMT17). MMP11has been shown to be a T3 target in the Xenopus laevis metamorphosis, essential for the degradation of the extracellular matrix during tissue remodeling and ADAMT17 involved on tissue morphogenesis in Xenopus development (31, 32). Another possibility to explain the more pronounced effects elicited by T3 is that this hormone is regulating the expression of other transcription modulators that, in turn, regulate the expression of different gene sets, as the *HR lysine demethylase* and *nuclear receptor corepressor* as well as *the Bcl6 corepressor* (BCOR), found in the T3 upregulated gene cluster.

The fact that 3,5-T2 withdrawal results in gill regeneration is puzzling and suggests that this hormone does not fully engage with the irreversible gill remodeling program triggered by equimolar concentrations of T3. This is certainly enigmatic and, at the moment, difficult to elucidate. Indeed, a smaller number of gene clusters are regulated by this hormone; some of these genes are still not fully annotated, leaving the possibility that they could participate in proliferative or mitogenic processes.

Protein–protein interaction differences within biological networks after 3,5-T2 or T3 treatments also reflect the transcriptomic analysis outcomes. Indeed, TH functional input is mostly involved in DNA replication, cell cycle control, and chromatin dynamics. Interestingly, among the additional small subnetworks, two transcription factors, Bcl6 and Zbtb16, display a differential regulation after T3 or 3,5-T2 treatments, a thought-provoking result, given that Zbtb16 is a repressor of Bcl6 (33, 34), suggesting opposing TH-regulating cell fate mechanisms.

Understanding the molecular mechanisms that underlay the pleiotropic effects exerted by THs is a current challenge in thyroid physiology. The combination of tissue-specific expression TR isoforms and the bioavailability of different TH derivatives are some of the events that have explained, in part, this pleiotropy.

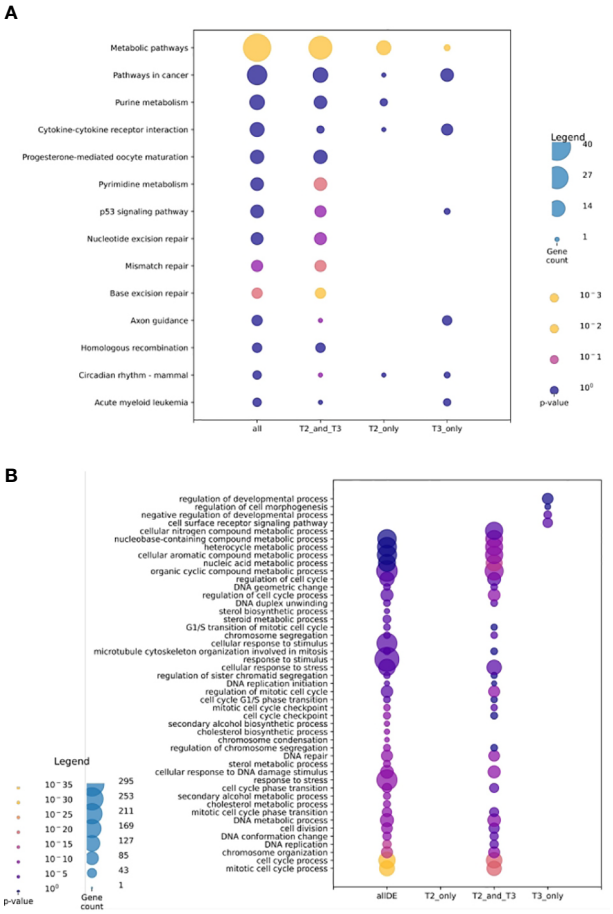

FIGURE 6
Gene ontology analysis for transcriptomic data. **(A)** Gene ontology UniProt–Gene Ontology most enriched biological processes. **(B)** Analysis of KEGG most enriched pathways. Sets **(A, B)** show all transcriptomic data; 3,5-T2 and T3 regulated transcripts, and 3,5-T2– or T3-exclusively regulated transcripts. The size of the circle represents the transcript abundance as gene count and color represents the *p*- value.

TABLE 1 Genes implicated in tissue remodeling regulated specifically by 3,5-T2 or T3.

3,5-T2 regulated genes		
FGF23	Fibroblast growth factor 23; this gene encodes a member of the fibroblast growth factor family of proteins, which possess broad mitogenic and cell survival activities. (2)	Upregulated
KY	Kyphoscoliosis peptidase; this protein is involved in the function, maturation, and stabilization of the neuromuscular junction and may be required for normal muscle growth. (2)	Downregulated
T3 regulated genes		
Gene symbol	*Function summary*	*Regulation*
NOXO1	NADPH oxidase (NOX) organizer; the *knockout* increases of the proliferative capacity in colon epithelial cells. (1)	Upregulated
MMP11	Matrix metalloproteinase 11; this protein family is involved in the breakdown of extracellular matrix in normal physiological processes, such as embryonic development, reproduction, and tissue remodeling. (2)	
SORBS3	This gene encodes an SH3 domain–containing adaptor protein. The presence of SH3 domains play a role in this protein's ability to bind other cytoplasmic molecules and contribute to cystoskeletal organization, cell adhesion and migration, signaling, and gene expression. (2)	
ADAMTS17	A disintegrin-like and metalloprotease; this has diverse roles in tissue morphogenesis in xemopus development. (3)	
CDKN1B	This gene encodes a cyclin-dependent kinase inhibitor and controls the cell cycle progression at G1. (2)	

(Continued)

TABLE 1 Continued

3,5-T2 regulated genes		
NGFR	Nerve growth factor receptor; this plays an important role in differentiation and survival of specific neuronal populations. (2)	
BCOR	BCL6-interacting corepressor; a POZ/zinc finger transcription repressor is required for germinal center formation and may influence apoptosis. (2)	
APCDD1L	Adenomatosis polyposis coli down-regulated 1 protein-like; this predicted to be involved in negative regulation of Wnt signaling pathway. (2)	
MMP28	Matrix metalloproteinase 23B; this family is involved in the breakdown of extracellular matrix. (2)	Downregulated
FAM107A	Family with sequence similarity 107 member A; this is involved in several processes, including negative regulation of G1/S transition of mitotic cell cycle; negative regulation of focal adhesion assembly; and regulation of cytoskeleton organization. (2)	
PITX1	Paired-like homeodomain transcription factor 1; this transcriptional regulator is involved in organ development. (2)	
CARD10	Caspase recruitment domain–containing protein 10; this participates in apoptosis signaling through highly specific protein-protein homophilic interactions. (2)	
MELK	Maternal embryonic leucine zipper kinase; this is involved in apoptotic process, cell population proliferation, and protein autophosphorylation. (2)	

(1) Moll et al., 2018 (https://doi.org/10.3389/fimmu.2018.00973)
(2) GeneCards.
(3) Desanilis et al., 2018.

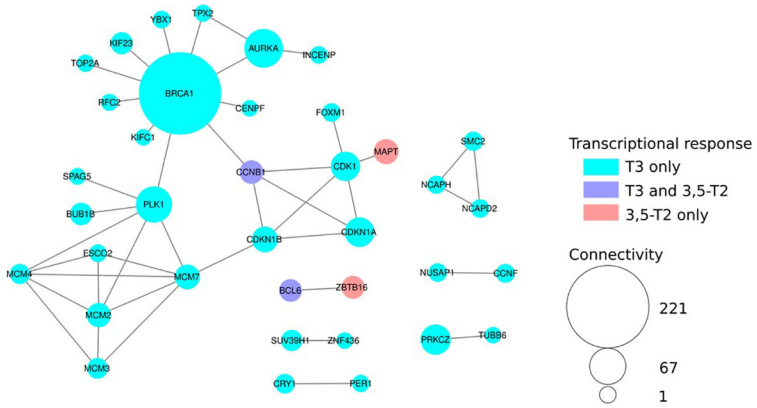

FIGURE 7
Network analysis of Differentially Expressed (DE) genes reveals hot spots of THs action. Protein–protein interaction network build from the BIOGRID database. Nodes colored in cyan are DE only after T3 treatment and red only with 3,5-T2. Violet nodes are DE with both T3 and 3,5-T2. Node size is proportional to its connectivity, i.e., the number of known protein partners it interacts with. Large nodes (hubs, connectivity > 20) are major sensors and controllers of biological networks. For clarity, only DE genes connected to other DE genes are shown.

This is clearly illustrated by the very specific effects (i.e., reversible gill absorption and different skin phenotype in post-metamorphic axolotl) elicited by 3,5-T2 in a very complex developmental phenomenon. From a translational viewpoint, our observations add further support to the notion that alternative TR ligands could be used to pharmacologically target specific actions in illness.

Data availability statement

The datasets presented in this study can be found in online repositories. The names of the repository/repositories and accession number(s) can be found in the article/Supplementary Material.

Ethics statement

All axolotls were maintained and handled in accordance with protocols approved by the Ethics for Research Committee of the Instituto de Neurobiología at the Universidad Nacional Autónoma de México (UNAM).

Author contributions

AOr: Conceptualization, Planning, Writing, Funding, Review and Discussion. IL; Conceptualization, Planning, Writing, Experimentation, Funding, Review and Discussion. AOl: Transcriptomic analysis and validation, Review and Discussion. SP-P: Immunohistochemical analysis, Review and Discussion. LS: Manuscript Review. NB: Transcriptomic analysis, Review and Discussion. All authors contributed to the article and approved the submitted version.

Funding

UNAM PAPIIT IA201122 UNAM PAPIIT IN210823 Ciencias de Frontera CONACyT 319880.

Acknowledgments

We want to thank Marco Terrones (Axolkali), Alejandra Castilla León, Nuri Aranda López, and Ing. Ramón Martínez Olvera.

Conflict of interest

The authors declare that the research was conducted in the absence of any commercial or financial relationships that could be construed as a potential conflict of interest.

Publisher's note

All claims expressed in this article are solely those of the authors and do not necessarily represent those of their affiliated organizations, or those of the publisher, the editors and the reviewers. Any product that may be evaluated in this article, or claim that may be made by its manufacturer, is not guaranteed or endorsed by the publisher.

Supplementary material

The Supplementary Material for this article can be found online at: https://www.frontiersin.org/articles/10.3389/fendo.2023.1208182/full#supplementary-material

References

1. Laudet V. The origins and evolution of vertebrate metamorphosis. *Curr Biol* (2011) 21(18):R726–37. doi: 10.1016/j.cub.2011.07.030

2. Buchholz DR, Shi YB. Dual function model revised by thyroid hormone receptor alpha knockout frogs. *Gen Comp Endocrinol* (2018) 265:214–8. doi: 10.1016/j.ygcen.2018.04.020

3. Yaoita Y, Brown DD. A correlation of thyroid hormone receptor gene expression with amphibian metamorphosis. *Genes Dev* (1990) 4(11):1917–24. doi: 10.1101/gad.4.11.1917

4. Huang H, Cai L, Remo BF, Brown DD. Timing of metamorphosis and the onset of the negative feedback loop between the thyroid gland and the pituitary is controlled by type II iodothyronine deiodinase in xenopus laevis. *Proc Natl Acad Sci* (2001) 98 (13):7348–53. doi: 10.1073/pnas.131198998

5. Darras VM, Van Herck SLJ, Heijlen M, De Groef B. Thyroid hormone receptors in two model species for vertebrate embryonic development: chicken and zebrafish. *J Thyroid Res* (2011) 2011:1–8. doi: 10.4061/2011/402320

6. Wakahara M. Heterochrony and neotenic salamanders: possible clues for understanding the animal development and evolution. *Zoological Sci* (1996) 13 (6):765–76. doi: 10.2108/zsj.13.765

7. De Groef B, Grommen SVH, Darras VM. Forever young: endocrinology of paedomorphosis in the Mexican axolotl (Ambystoma mexicanum). *Gen Comp Endocrinol* (2018), 266:194–201. doi: 10.1016/j.ygcen.2018.05.016

8. Page RB, Voss SR. Induction of metamorphosis in axolotls *(Ambystoma mexicanum). Cold Spring Harb Protoc* (2009) 2009(8):pdb.prot5268. doi: 10.1101/pdb.prot5268

9. Khattak S, Murawala P, Andreas H, Kappert V, Schuez M, Sandoval-Guzmán T, et al. Optimized axolotl (Ambystoma mexicanum) husbandry, breeding, metamorphosis, transgenesis and tamoxifen-mediated recombination. *Nat Protoc* (2014) 9(3):529–40. doi: 10.1038/nprot.2014.040

10. Coots PS, Seifert AW. Thyroxine-induced metamorphosis in the axolotl (Ambystoma mexicanum). In: Kumar A, Simon A, editors. *Salamanders in regeneration research*. New York, NY: Springer New York (2015). p. 141–5. Available at: http://link.springer.com/10.1007/978-1-4939-2495-0_11. Methods in Molecular Biology; vol. 1290.

11. Jonas W, Lietzow J, Wohlgemuth F, Hoefig CS, Wiedmer P, Schweizer U, et al. 3,5-Diiodo-L-Thyronine (3,5-T_2) exerts thyromimetic effects on hypothalamus-Pituitary-Thyroid axis, body composition, and energy metabolism in Male diet-induced obese mice. *Endocrinology* (2015) 156(1):389–99. doi: 10.1210/en.2014-1604

12. Senese R, de Lange P, Petito G, Moreno M, Goglia F, Lanni A. 3,5-diiodothyronine: a novel thyroid hormone metabolite and potent modulator of energy metabolism. *Front Endocrinol* (2018) 9:427. doi: 10.3389/fendo.2018.00427

13. Navarrete-Ramírez P, Luna M, Valverde-R C, Orozco A. 3,5-di-iodothyronine stimulates tilapia growth through an alternate isoform of thyroid hormone receptor β1. *J Mol Endocrinol* (2014) 52(1):1–9. doi: 10.1530/JME-13-0145

14. Olvera A, Martyniuk CJ, Buisine N, Jiménez-Jacinto V, Sanchez-Flores A, Sachs LM, et al. Differential transcriptome regulation by 3,5-T2 and 3′,3,5-T3 in brain and liver uncovers novel roles for thyroid hormones in tilapia. *Sci Rep* (2017) 7(1):15043. doi: 10.1038/s41598-017-14913-9

15. Langmead B, Salzberg SL. Fast gapped-read alignment with bowtie 2. *Nat Methods* (2012) 9(4):357–9. doi: 10.1038/nmeth.1923

16. Rigolet M, Buisine N, Scharwatt M, Duvernois-Berthet E, Buchholz DR, Sachs LM. Crosstalk between thyroid hormone and corticosteroid signaling targets cell proliferation in xenopus tropicalis tadpole liver. *IJMS* (2022) 23(22):13715. doi: 10.3390/ijms232213715

17. Eden E, Navon R, Steinfeld I, Lipson D, Yakhini Z. GOrilla: a tool for discovery and visualization of enriched GO terms in ranked gene lists. *BMC Bioinf* (2009) 10 (1):48. doi: 10.1186/1471-2105-10-48

18. Kanehisa M, Sato Y, Kawashima M, Furumichi M, Tanabe M. KEGG as a reference resource for gene and protein annotation. *Nucleic Acids Res* (2016) 44(D1): D457–62. doi: 10.1093/nar/gkv1070

19. Oughtred R, Rust J, Chang C, Breitkreutz B, Stark C, Willems A, et al. The BioGRID database: a comprehensive biomedical resource of curated protein, genetic, and chemical interactions. *Protein Sci* (2021) 30(1):187–200. doi: 10.1002/pro.3978

20. Halsall DJ, Oddy S. Clinical and laboratory aspects of 3,3′,5′-triiodothyronine (reverse T3). *Ann Clin Biochem* (2021) 58(1):29–37. doi: 10.1177/0004563220969150

21. Buisine N, Grimaldi A, Jonchere V, Rigolet M, Blugeon C, Hamroune J, et al. Transcriptome and methylome analysis reveal complex cross-talks between thyroid

hormone and glucocorticoid signaling at xenopus metamorphosis. *Cells* (2021) 10 (9):2375. doi: 10.3390/cells10092375

22. Tribondeau A, Sachs LM, Buisine N. Tetrabromobisphenol a effects on differentiating mouse embryonic stem cells reveals unexpected impact on immune system. *Front Genet* (2022) 13:996826. doi: 10.3389/fgene.2022.996826

23. Orozco A, Navarrete-Ramírez P, Olvera A, García-G C. 3,5-diiodothyronine (T2) is on a role. a new hormone in search of recognition. *Gen Comp Endocrinol* (2014) 203:174–80. doi: 10.1016/j.ygcen.2014.02.014

24. Köhrle J, Lehmphul I, Pietzner M, Renko K, Rijntjes E, Richards K, et al. 3,5-T2–a janus-faced thyroid hormone metabolite exerts both canonical T3-mimetic endocrine and intracrine hepatic action. *Front Endocrinol* (2020) 10:787. doi: 10.3389/fendo.2019.00787

25. Hernández-Linares Y, Olvera A, Villalobos P, Lozano-Flores C, Varela-Echavarría A, Luna M, et al. 3,5-T2 and 3,3′,5-T3 regulate cerebellar thyroid hormone signalling and myelin molecular dynamics in tilapia. *Sci Rep* (2019) 9 (1):7359. doi: 10.1038/s41598-019-43701-w

26. Paris M, Escriva H, Schubert M, Brunet F, Brtko J, Ciesielski F, et al. Amphioxus postembryonic development reveals the homology of chordate metamorphosis. *Curr Biol* (2008) 18(11):825–30. doi: 10.1016/j.cub.2008.04.078

27. Klootwijk W, Friesema ECH, Visser TJ. A nonselenoprotein from amphioxus deiodinates triac but not T3: is triac the primordial bioactive thyroid hormone? *Endocrinology* (2011) 152(8):3259–67. doi: 10.1210/en.2010-1408

28. Orozco A, Valverde-R C, Olvera A, García-G C. Iodothyronine deiodinases: a functional and evolutionary perspective. *J Endocrinol* (2012) 215(2):207–19. doi: 10.1530/JOE-12-0258

29. Schroeder A, Jimenez R, Young B, Privalsky ML. The ability of thyroid hormone receptors to sense T4 as an agonist depends on receptor isoform and on cellular cofactors. *Mol Endocrinol* (2014) 28(5):745–57. doi: 10.1210/me.2013-1335

30. Mendoza A, Navarrete-Ramírez P, Hernández-Puga G, Villalobos P, Holzer G, Renaud JP, et al. 3,5-T2 is an alternative ligand for the thyroid hormone receptor β1. *Endocrinology* (2013) 154(8):2948–58. doi: 10.1210/en.2013-1030

31. Mathew S, Fu L, Hasebe T, Ishizuya-Oka A, Shi YB. Tissue-dependent induction of apoptosis by matrix metalloproteinase stromelysin-3 during amphibian metamorphosis. *Birth Defect Res C* (2010) 90(1):55–66. doi: 10.1002/bdrc.20170

32. Desanlis I, Felstead HL, Edwards DR, Wheeler GN. ADAMTS9, a member of the ADAMTS family, in xenopus development. *Gene Expression Patterns* (2018), 29:72–81. doi: 10.1016/j.gep.2018.06.001

33. He J, Wu M, Xiong L, Gong Y, Yu R, Peng W, et al. BTB/POZ zinc finger protein ZBTB16 inhibits breast cancer proliferation and metastasis through upregulating ZBTB28 and antagonizing BCL6/ZBTB27. *Clin Epigenet* (2020) 12(1):82. doi: 10.1186/s13148-020-00867-9

34. Cheng ZY, He TT, Gao XM, Zhao Y, Wang J. ZBTB transcription factors: key regulators of the development, differentiation and effector function of T cells. *Front Immunol* (2021) 12:713294. doi: 10.3389/fimmu.2021.713294

frontiers | Frontiers in Endocrinology

TYPE Original Research
PUBLISHED 22 September 2023
DOI 10.3389/fendo.2023.1182049

Check for updates

OPEN ACCESS

EDITED BY
Marco António Campinho,
University of Algarve, Portugal

REVIEWED BY
Silvia Martina Ferrari,
University of Pisa, Italy
Luigi Carbone,
University of Naples Federico II, Italy

*CORRESPONDENCE
Kun Huang
ahmuhuangk@163.com

RECEIVED 08 March 2023
ACCEPTED 05 September 2023
PUBLISHED 22 September 2023

CITATION
Ru X, Yang M, Teng Y, Han Y, Hu Y, Wang J, Tao F and Huang K (2023) Association of maternal thyroid peroxidase antibody during pregnancy with placental morphology and inflammatory and oxidative stress responses.
Front. Endocrinol. 14:1182049.
doi: 10.3389/fendo.2023.1182049

COPYRIGHT
© 2023 Ru, Yang, Teng, Han, Hu, Wang, Tao and Huang. This is an open-access article distributed under the terms of the Creative Commons Attribution License (CC BY). The use, distribution or reproduction in other forums is permitted, provided the original author(s) and the copyright owner(s) are credited and that the original publication in this journal is cited, in accordance with accepted academic practice. No use, distribution or reproduction is permitted which does not comply with these terms.

Association of maternal thyroid peroxidase antibody during pregnancy with placental morphology and inflammatory and oxidative stress responses

Xue Ru[1], Mengting Yang[1], Yuzhu Teng[1], Yan Han[1], Yabin Hu[1], Jianqing Wang[1], Fangbiao Tao[1] and Kun Huang[1,2]*

[1]Department of Maternal, Child & Adolescent Health, School of Public Health, Key Laboratory of Population Health Across Life Cycle, Anhui Medical University (AHMU), Ministry of Education of the People's Republic of China, National Health Commission Key Laboratory of Study on Abnormal Gametes and Reproductive Tract, Anhui Provincial Key Laboratory of Population Health and Aristogenics, Hefei, China, [2]Scientific Research Center in Preventive Medicine, School of Public Health, Anhui Medical University (AHMU), Hefei, China

Background: Studies suggest that thyroid peroxidase antibody (TPOAb) positivity exposure during pregnancy may contribute to changes in placental morphology and pathophysiology. However, little is known about the association of maternal TPOAb during pregnancy with placental morphology and cytokines. This study focuses on the effect of repeated measurements of maternal TPOAb during pregnancy on the placental morphology and cytokines.

Methods: Based on Ma'anshan Birth Cohort (MABC) in China, maternal TPOAb levels were retrospectively detected in the first, second and third trimesters. Placental tissues were collected 30 minutes after childbirth, placental morphological indicators were obtained by immediate measurement and formula calculation, and cytokine mRNA expression was detected by real-time quantitative polymerase chain reaction (RT-qPCR) afterward. Generalized linear models and linear mixed models were analyzed for the relationships of maternal TPOAb in the first, second and third trimesters with placental indicators.

Results: Totally 2274 maternal-fetal pairs were included in the analysis of maternal TPOAb levels and placental morphology, and 2122 pairs were included in that of maternal TPOAb levels and placental cytokines. Maternal TPOAb levels in early pregnancy were negatively associated with placental length, thickness, volume, weight and disc eccentricity, while positively correlated with placental IL-6, TNF-α, CRP, CD68, MCP-1, IL-10, HO-1, HIF-1α and GRP78. In mid-pregnancy, maternal TPOAb levels were negatively correlated with placental length, width and area. In late pregnancy, maternal TPOAb levels were negatively correlated with placental length, area, volume and weight. Repeated measures analysis showed that maternal TPOAb positivity tended to increase placental TNF-α, CD68 and MCP-1 while decreasing placental length, width and area than TPOAb negativity. Repeated measures analysis showed that maternal TPOAb levels were positively correlated with

placental IL-6, TNF-α, CD68, MCP-1, IL-10, HO-1, HIF-1α and GRP78, while negatively correlated with placental length, area, volume, weight, and disc eccentricity.

Conclusion: There may be trimester-specific associations between maternal TPOAb levels and placental morphology and inflammatory and oxidative stress responses. The effect of maternal TPOAb levels on placental morphology is present throughout pregnancy. Early pregnancy may be the critical period for the association between maternal TPOAb levels and placental inflammatory and oxidative stress responses.

KEYWORDS

TPOAb, placental morphology, inflammation, oxidative stress, pregnancy, cytokines, cohort

Introduction

Thyroid peroxidase (TPO) is the primary enzyme involved in producing thyroid hormones (1). Thyroid peroxidase antibody (TPOAb) acts as a competitive inhibitor of the action of TPO and is responsible for thyroid inflammation (2, 3). TPOAb is the most common anti-thyroid autoantibody. TPOAb is a marker of autoimmune thyroid disease (AITD) and would cause thyroid cell damage by activating complement-mediated cytotoxicity and antibody-dependent cell-mediated cytotoxicity (ADCC) (4, 5). TPOAb positivity is frequently present in women of reproductive age. The prevalence of TPOAb positivity observed in pregnant women ranges from 2% to 17%, with a higher prevalence in iodine-deficient populations (6). TPOAb positivity enhances the risk of adverse pregnancy outcomes, including developing thyroid disease during pregnancy, miscarriage, preterm birth, placental abruption, premature rupture of membranes and fetal neurodevelopmental delay (7).

Successful pregnancy maintenance depends on immune homeostasis, immune tolerance and relative cytokines levels (2). Studies have demonstrated that the expression of the inflammatory cytokines tumor necrosis factor-α (TNF-α), interleukin-1β (IL-1β), IL-6, IL-8 and monocyte chemoattractant protein-1 (MCP-1) was elevated in the fetal membranes, cervix, amniotic fluid and placenta (8). TPOAb positivity may lead to failure of immune tolerance at the maternal-fetal interface, severely compromising placental-fetal development (4, 9). Elevated TPOAb levels may modulate immune activity at the cellular level, leading to preterm birth (10). Animal studies indicated extremely preterm birth and fetal intrauterine growth restriction (IUGR) were associated with placental injury and inflammation, as evidenced by the upregulation of inflammatory cytokine and chemokine genes in placenta, including TNF-α, IL-1β, IL-6, MCP-1, macrophage inflammatory peptide-2 (MIP-2) and keratinocyte-derived chemokine (KC) (11). In addition, TPOAb may diffuse through the placental barrier at all stages of pregnancy, increasing immune responses and affecting placental development and pregnancy progression (9, 12). Therefore, it is speculated that maternal TPOAb levels may influence the immune status at the maternal-fetal interface by altering the expression of cytokines in the placenta.

The existence of thyroid autoimmune could indicate a decrease in the ability of the thyroid gland to adapt to the necessary changes related to pregnancy adequately. Hypothyroidism affects fetal-placental development by impairing placental decidualization and vascularization, increasing apoptosis and reducing trophoblast proliferation (13). This may be linked to inflammatory mediators in the placenta. At present, there is only evidence from animal studies suggesting that hypothyroidism affects maternal immune function by interfering with the development of an anti-inflammatory environment, and that maternal hypothyroidism is associated with hypoxia and activation of inflammatory and oxidative stress at the maternal-fetal interface (14, 15). Hypothyroidism reduced the expression of placental interferon-γ (IFN-γ), IL-10 and migration inhibitory factor (MIF) in rats (14), which stimulates the expression of a wide variety of pro-inflammatory cytokines (16). Furthermore, even in the absence of thyroid dysfunction, many studies have linked the presence of TPOAb to adverse maternal-fetal outcomes during pregnancy (9). However, there are no population studies of the association between maternal TPOAb levels and placental cytokines, and it is unclear whether the effect on the placenta is independent or mediated by thyroid hormones.

Abbreviations: MABC, Ma'anshan Birth Cohort; TPO, thyroid peroxidase; TPOAb, thyroid peroxidase antibody; AITD, autoimmune thyroid disease; ADCC, antibody-dependent cell-mediated cytotoxicity; IFN-γ, interferon-γ; MCP-1, monocyte chemoattractant protein-1; IL, interleukin; IUGR, intrauterine growth restriction; MIP-2, macrophage inflammatory peptide-2; KC, keratinocyte-derived chemokine; TNF-α, tumor necrosis factor α; MIF, migration inhibitory factor; HO-1, heme oxygenase 1; GRP78, glucose regulated protein 78 kda; GDM, gestational diabetes mellitus; HDCP, hypertensive disorder complicating pregnancy; CRP, C-reactiveprotein; HIF-1α, hypoxia-inducible factor 1α; TSH, thyroid-stimulating hormone; FT_4, free thyroxine; PE, pre-eclampsia; CHOP, C/EBP homologous protein; NRF2, nuclear factor erythroid 2-related factor 2.

Placental morphology was significantly associated with placental function, and abnormal placental morphological indicators were related with the increased risk of pregnancy complications (17, 18). In previous studies, limited studies have focused on the effect of maternal TPOAb presence on placental morphology during pregnancy and findings were controversial (19–21). A study from Japan found that placental weight was significantly lower among TPOAb-positive subjects compared with controls mothers (20). However, a cohort study showed that significantly higher placental weights were observed among TPOAb-positive mothers (21). Moreover, evidence from population studies was absent regarding the association of maternal TPOAb levels with placental inflammatory and oxidative stress responses.

In the current study, based on a prospective birth cohort study, we had repeatedly measured maternal TPOAb in the first, second and third trimester of pregnancy. We aimed to examine the relationship of maternal TPOAb levels with placental morphology and inflammatory and oxidative stress responses and to identify the potential critical period.

Materials and methods

Participants

This study was based on Ma'anshan Birth Cohort (MABC) in China. Pregnant women who had their first antenatal checkup from May 2013 to September 2014 were invited to join the study. The inclusion criteria were as follows: 1) permanent residents in Ma'anshan City; 2) within 14 weeks of gestation; 3) planning to have pregnancy checkups and delivery at Ma'anshan Maternal and Child Health Center; 4) able to understand and complete the questionnaires (22). Further exclusion criteria were set in the current study as 1) twin pregnancy and adverse pregnancy outcomes (spontaneous abortion, therapeutic abortion, ectopic pregnancy, and stillbirth); 2) having a family history of thyroid diseases and/or those who suffered from thyroid conditions (including hypothyroidism, hyperthyroidism, thyroiditis, thyroid tumor/cancer) before/during pregnancy and received treatment; 3) missing data on maternal TPOAb concentrations; 4) missing data on placental morphology or cytokines.

The current study was a retrospective cohort study from prospectively collected data. Women had been prospectively followed up during pregnancy. After delivery, their children were continuously followed up in the cohort. Maternal thyroid function was determined retrospectively during childhood follow up. Women were not aware of their thyroid function from assays of biological samples collected in this study.

All participants provided written informed consent. The study protocol was approved by the Biomedical Ethics Committee of the Anhui Medical University (No. 20131401).

Evaluation of maternal thyroid function

Fasting venous blood from women was collected in the first (before 13 weeks), second (14-27 weeks) and third (28 weeks and beyond) trimester of pregnancy, respectively. After centrifugation, the serum was stored at -80°C. During the children's follow-up period, thyroid-stimulating hormone (TSH), free thyroxine (FT_4) and TPOAb levels were determined retrospectively by electrochemical immunoassay (Cobas E411 analyzer; Roche Company, Germany). The detection limit of TPOAb was 5.0 IU/mL, and the coefficient of variation between the reagent batches was<10% (22). Women with TPOAb positivity were defined as TPOAb >34.0 IU/mL, otherwise were defined as TPOAb negative controls.

Measurement of placental indicators

Placenta tissues were collected 30 minutes after delivery, and the placental length, width and thickness were measured immediately. Placental area, volume, weight and disc eccentricity were calculated using the following formulas (23–26).

$$Placental\ area = \pi/4 \times placental\ length \times placental\ width$$

$$Placental\ volume = 4\pi/3 \times (placental\ length \times placenta\ width \times placenta\ thickness)/2^3$$

$$Placental\ weight = \pi/4 \times placental\ length \times placental\ width \times placenta\ thickness$$

$$Disc\ eccentricity = placental\ length/placental\ width$$

Then, the placental lobule without calcification was taken and cut smaller into ≤0.5 cm pieces, and placed in RNAlater solution to allow the solution to thoroughly penetrate the tissue. After removing the supernatant, the tissues were stored at -80°C. Placental cytokines mRNA expression was detected by real-time quantitative polymerase chain reaction (RT-qPCR), including IL-1β, IL-6, TNF-α, IFN-γ, C-reactive protein (CRP), CD68, MCP-1, IL-4, IL-10, heme oxygenase 1 (HO-1), hypoxia-inducible factor 1α (HIF-1α), glucose regulated protein 78 kda (GRP78). The detailed procedures could be found elsewhere in our previous studies (27, 28).

Covariates

Based on the previous literature and directed acyclic graph (Supplementary Figure 1), maternal age, education level, gestational weight gain, monthly income, parity, fetal gender, smoking and drinking during pregnancy were identified as potential confounders. Data on maternal age, education level, monthly income, parity, smoking and drinking during pregnancy were collected questionnaires during recruitment. Information on fetal gender and gestation weight gain was obtained from medical notes.

In addition, TSH and FT_4 levels, gestational diabetes mellitus (GDM), hypertensive disorder complicating pregnancy (HDCP),

maternal infection or inflammation during pregnancy, and gestational age at birth were included in the sensitivity analyses, respectively. Maternal infection or inflammation during pregnancy covered bronchitis, influenza, gastroenteritis, cholecystitis, vaginitis, chorioamnionitis, and pelvic inflammatory disease.

Statistical analysis

SPSS 26.0 was adopted for statistical analyses and Graphpad Prism 8.0.2 was used for figure drawing. Statistical significance was declared at $P<0.05$.

Compared to the differences between the included and excluded, T-test was used for continuous variables, and chi-square test was performed for categorical variables. Since the distributions of TSH, FT_4, TPOAb concentrations and placental indicators were right-skewed, they were all ln-transformed. Generalized linear models were analyzed for the relationships of maternal TPOAb exposure in three trimesters with placental indicators, respectively. Linear mixed models, a powerful and robust statistical methods for addressing mixed relationships with the same exposure at different times, were fitted to determine the effect of the repeated measurements of maternal TPOAb on placental indicators.

Five sensitivity analyses were conducted. 1) TPOAb positivity may be related to an increased risk of clinical or subclinical hypothyroidism (29, 30), and maternal hypothyroidism further affects placental growth and development (9, 31). Therefore, thyroid hormone levels may be potential mediators. When analyzing TPOAb in a single trimester, FT_4 and TSH levels in that trimester and TPOAb levels in the other trimesters were further adjusted. FT_4 and TSH data during pregnancy were further adjusted when performing repeated measure analysis. 2) Maternal TPOAb may be related to GDM (32). Maternal obesity could influence placental inflammatory status and morphology in human term placenta (33). Maternal GDM was further adjusted. 3) Maternal TPOAb may be related to HDCP (34). HDCP may decrease placental blood flow and oxidative stress (35). Maternal HDCP was further adjusted. 4) Maternal infection or inflammation may cause placental maladjustment (36, 37). Maternal infection or inflammation was further adjusted. 5) The effect of thyroid hormones on placental formation and development varies with gestational age (4). Maternal gestational age was further adjusted.

Results

Basic characteristics of participants

A total of 3474 women were recruited as the initial study population. Totally 2274 maternal-fetal pairs were included in the analysis of maternal TPOAb levels and placental morphology, and 2122 pairs were included in that of maternal TPOAb levels and placental cytokines (Figure 1). Baseline characteristics of 2639 included and 835 excluded participants were shown in Table 1. Compared with the excluded participants, the included mothers had a higher level of education, a higher gestational age at birth, a lower TSH concentration in the first trimester, a higher percentage of primiparas, a higher prevalence of HDCP and GDM.

Distribution of maternal TPOAb levels and placental indicators

Maternal TPOAb concentrations during three trimesters, placental morphological indicators and inflammatory and oxidative stress cytokines mRNA expression are presented in Table 2. The geometric means of maternal TPOAb concentrations were 19.35, 13.12 and 15.48 IU/mL in the first, second and third trimester of pregnancy, respectively. The positive rates of TPOAb in early, mid, and late pregnancy were 11.6%, 6.7%, and 7.2%, respectively. The overall rate of maternal TPOAb positivity during pregnancy was 12.6%.

Association between maternal TPOAb and placental morphology

In early pregnancy, TPOAb levels were negatively correlated with placental length (β -0.006, 95%CI -0.011 to -0.001), thickness (β -0.010, 95%CI -0.020 to -0.0004), volume (β -0.016, 95%CI -0.029 to -0.002), weight (β -0.016, 95%CI -0.029 to -0.002) and disc eccentricity (β -0.007, 95%CI -0.012 to -0.002). In the second trimester, TPOAb levels were negatively correlated with placental length (β -0.007, 95%CI -0.013 to -0.001), width (β -0.007, 95%CI -0.014 to -0.00001) and area (β -0.014, 95%CI -0.025 to -0.002). In late pregnancy, TPOAb levels were negatively correlated with placental length (β -0.011, 95%CI -0.018 to -0.003), area (β -0.017, 95%CI -0.030 to -0.005), volume (β -0.019, 95%CI -0.038 to -0.0002) and weight (β -0.019, 95%CI -0.038 to -0.0002) (Table 3).

In the repeated measures analysis, maternal TPOAb positivity during pregnancy tended to reduce placental length (β -0.012, 95% CI -0.021 to -0.003), width (β -0.011, 95%CI -0.021 to -0.002), and area (β -0.023, 95%CI -0.039 to -0.007) (Figure 2).

In the repeated measures analysis, maternal TPOAb levels during pregnancy were negatively correlated with placental length (β -0.007, 95%CI -0.010 to -0.004), area (β -0.010, 95%CI -0.016 to -0.004), volume (β -0.012, 95%CI -0.021 to -0.003), weight (β -0.012, 95%CI -0.021 to -0.003) and disc eccentricity (β -0.004, 95%CI -0.007 to -0.0004) (Figure 2).

Association between maternal TPOAb and placental cytokines

In early pregnancy, TPOAb levels were positively correlated with placental IL-6 (β 0.193, 95%CI 0.127-0.259), TNF-α (β 0.161, 95%CI 0.086-0.236), CRP (β 0.167, 95%CI 0.055-0.279), CD68 (β 0.370, 95%CI 0.276-0.464), MCP-1 (β 0.198, 95%CI 0.131-0.265), IL-10 (β 0.143, 95%CI 0.065-0.221), HO-1 (β 0.169, 95%CI 0.098-0.240), HIF-1α (β 0.176, 95%CI 0.105-0.246), GRP78 (β 0.286, 95% CI 0.189-0.383) mRNA expression (Table 4).

10.3389/fendo.2023.1182049

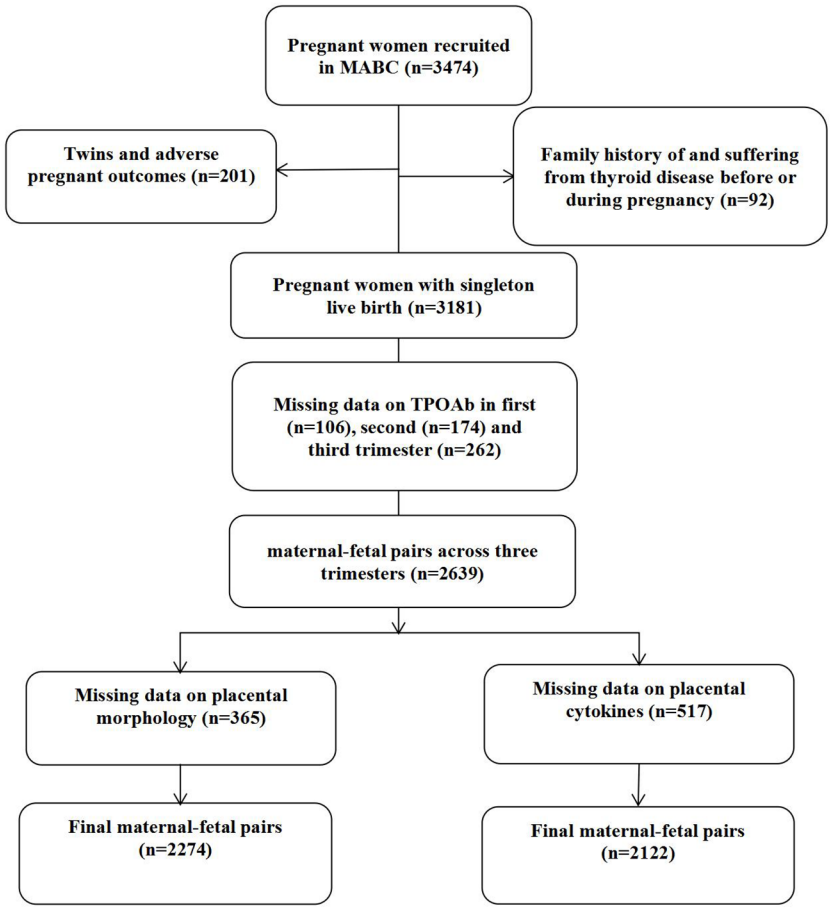

FIGURE 1
Flowchart of Participants recruitment.

TABLE 1 Basic Characteristics of Included and Excluded Participants (n=3474).

Characteristics	Included (n=2639)	Excluded (n=835)	Missing	p-value
Maternal age, year	26.6 ± 3.6	26.9 ± 4.1	0(0)	0.088
Maternal education level,year	13.4 ± 3.1	13.1 ± 3.2	0(0)	0.007
Gestational weight gain, kg	17.9 ± 5.0	17.7 ± 5.3	255(7.3)	0.545
Gestational age at birth, week	39.1 ± 1.2	38.6 ± 1.9	200(5.8)	0.000
Maternal concentrations of TSH during pregnancy, μIU/mL				
In 1st trimester	1.9 ± 2.2	2.4 ± 5.4	143(4.1)	0.047
In 2nd trimester	2.7 ± 1.5	2.8 ± 1.6	346(10.0)	0.298
In 3rd trimester	2.5 ± 1.4	2.5 ± 1.4	520(15.0)	0.652
Maternal concentrations of FT_4 during pregnancy, pmol/L				
In 1st trimester	17.1 ± 3.3	17.1 ± 5.0	143(4.1)	0.793
In 2nd trimester	12.0 ± 1.7	12.0 ± 1.9	346(10.0)	0.859
In 3rd trimester	13.4 ± 2.4	13.6 ± 2.7	520(15.0)	0.133
Monthly income, yuan			0(0)	0.826

(Continued)

10.3389/fendo.2023.1182049

TABLE 1 Continued

Characteristics	Included (n=2639)	Excluded (n=835)	Missing	p-value
≤2500	703(26.6)	215(25.7)		
2500~4000	1127(42.7)	366(43.8)		
>4000	809(30.7)	254(30.4)		
Parity			0(0)	0.000
Nulliparous	2356(89.3)	707(84.7)		
Multiparous	283(10.7)	128(15.3)		
Maternal smoking			0(0)	0.282
No	2531(95.9)	793(95.0)		
Yes	108(4.1)	42(5.0)		
Maternal drinking			0(0)	0.883
No	2428(92.0)	770(92.2)		
Yes	211(8.0)	65(7.8)		
GDM			153(4.4)	0.000
No	2318(87.8)	561(82.3)		
YES	321(12.2)	121(17.7)		
HDCP			208(6.0)	0.003
No	2489(94.5)	577(91.3)		
YES	145(5.5)	55(8.7)		
Maternal infection or inflammation during pregnancy			201(5.8)	0.628
No	2426(91.9)	579(91.3)		
Yes	213(8.1)	55(8.7)		
Fetal gender			206(5.9)	0.859
Boy	1345(51.0)	325(51.4)		
Girl	1291(49.0)	307(48.6)		

Data are given as Mean ± standard deviations (SD) or n (%). TSH, thyroid stimulating hormone; FT_4, free thyroxine; GDM, gestational diabetes mellitus; HDCP, hypertensive disorder complicating pregnancy.

TABLE 2 Distribution of maternal TPOAb concentrations, placental morphological indicators, inflammatory and oxidative stress cytokines in the participants.

	GM	P25	P50	P75
TPOAb concentration (IU/mL, n=2639)				
First trimester	19.35	12.97	19.29	24.66
Second trimester	13.12	9.00	12.42	17.01
Third trimester	15.48	11.19	14.78	19.63
Placental size (n=2274)				
Placental length (cm)	18.87	17.60	18.50	20.00
Placental width (cm)	16.52	15.50	16.50	17.80
Placental thickness (cm)	2.31	2.00	2.30	2.60
Placental area (cm^2)	244.72	219.80	240.20	275.54

(Continued)

TABLE 2 Continued

	GM	P25	P50	P75
Placental volume (cm^3)	376.21	315.62	377.26	456.44
Placental weight (g)	564.32	473.43	565.89	684.65
Disc eccentricity	1.14	1.06	1.11	1.19
Placental cytokines mRNA expression (n=2122)				
IL-1β	2.46	0.93	2.45	6.74
IL-6	2.22	0.98	2.20	5.67
TNF-α	4.26	1.56	4.52	12.70
IFN-γ	3.16	0.95	3.43	11.08
CRP	3.62	0.83	4.09	20.27
CD68	6.92	1.57	7.92	30.56
MCP-1	1.68	0.70	1.78	4.25
IL-4	2.43	0.93	2.18	6.61
IL-10	2.84	1.00	2.55	8.27
HO-1	2.75	1.16	2.82	6.54
HIF-1α	1.69	0.69	1.65	4.31
GRP78	3.57	0.90	3.80	18.07

GM, geometric mean.

In the repeated measures analysis, maternal TPOAb positivity tended to increase placental TNF-α (β 0.137, 95%CI 0.002-0.272), CD68 (β 0.270, 95%CI 0.098-0.442) and MCP-1 (β 0.144, 95%CI 0.022-0.266) mRNA expression (Figure 3).

In the repeated measures analysis, maternal TPOAb levels during pregnancy were positively correlated with placental IL-6 (β 0.103, 95%CI 0.059-0.147), TNF-α (β 0.099, 95%CI 0.049-0.148), CD68 (β 0.215, 95%CI 0.152-0.278), MCP-1 (β 0.093, 95%CI 0.048-0.138), IL-10 (β 0.074, 95%CI 0.022-0.126), HO-1 (β 0.067, 95%CI 0.020-0.114), HIF-1α (β 0.054, 95%CI 0.007-0.101), GRP78 (β 0.101, 95%CI 0.036-0.166) mRNA expression (Figure 3).

Sensitivity analyses did not fundamentally change the results of the main analyses, and details of the repeated measures and sensitivity analyses are provided in the Supplementary Tables 1–6.

Discussion

In this prospective cohort study, maternal TPOAb levels were found to be negatively related to placental morphology in the first, second and third trimester of pregnancy. Maternal TPOAb positivity tended to decrease placental length, width and area. The

TABLE 3 Association (β and 95% confidence intervals) of maternal TPOAb exposure (IU/mL) and placental morphological indicators (n=2274).

	Placental Length	Placental Width	Placental Thickness	Placental Area	Placental Volume	Placental Weight	Disc Eccentricity
TPOAb_a	-0.006 (-0.011,-0.001)*	0.001 (-0.005,0.006)	-0.010 (-0.020,-0.0004)*	-0.005 (-0.015,0.004)	-0.016 (-0.029,-0.002)*	-0.016 (-0.029,-0.002)*	-0.007 (-0.012,-0.002)*
TPOAb_b	-0.007 (-0.013,-0.001)*	-0.007 (-0.014,-0.00001)*	0.010 (-0.002,0.022)	-0.014 (-0.025,-0.002)*	-0.004 (-0.021,0.013)	-0.004 (-0.021,0.013)	-0.00007 (-0.007,0.007)
TPOAb_c	-0.011 (-0.018,-0.003)**	-0.007 (-0.015,0.001)	-0.002 (-0.015,0.012)	-0.017 (-0.030,-0.005)**	-0.019 (-0.038,-0.0002)*	-0.019 (-0.038, -0.0002)*	-0.004 (-0.011,0.004)

Adjusted for maternal age, maternal education level, gestational weight gain, monthly income, parity, smoking, drinking and fetal gender.
a: First Trimester; b: Second Trimester; c: Third Trimester.
*: P< 0.05. **: P< 0.01.

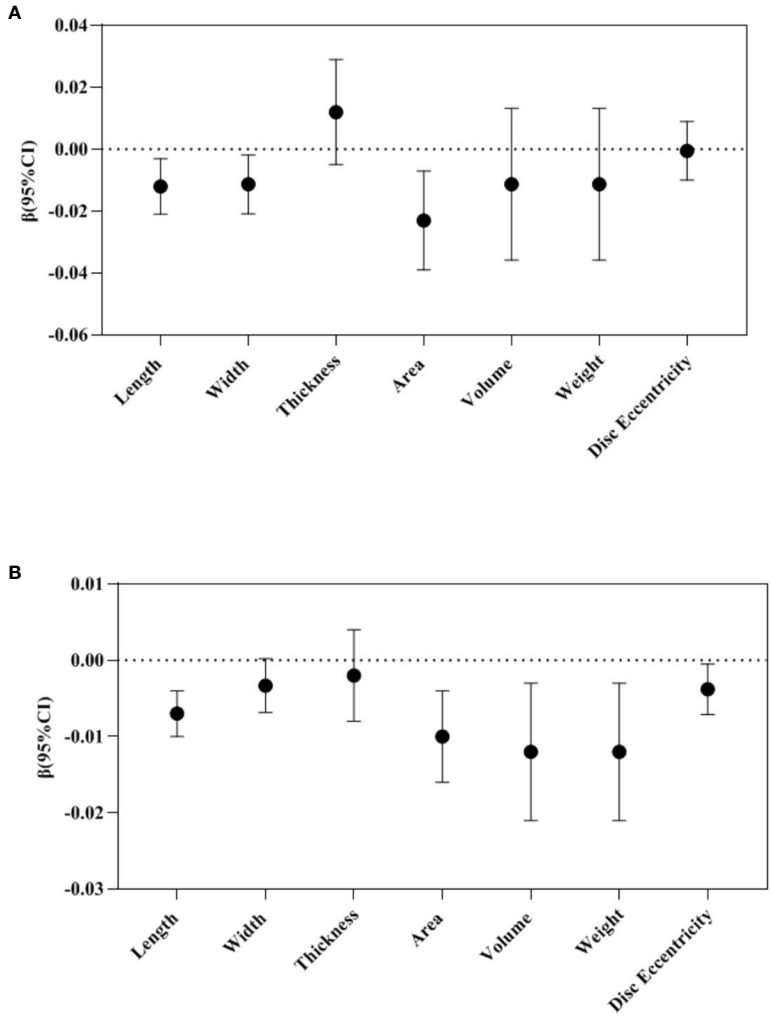

FIGURE 2
Repeated measure analysis: Association between maternal TPOAb exposure and placental morphology (n=2274). **(A)** Maternal TPOAb positive (vs TPOAb negative) increased placental length, width and area. **(B)** Maternal TPOAb levels throughout pregnancy were negatively associated with placental length, area, volume, weight and disc eccentricity. Adjusted for maternal age, maternal education years, gestational weight gain, monthly income, parity, smoking, drinking and fetal gender.

current study also provides longitudinal evidence that maternal exposure to TPOAb during pregnancy may be an important risk factor for maternal-placental immune activation. Significant positive associations between maternal TPOAb levels and placental mRNA expression of IL-6, TNF-α, CRP, CD68, MCP-1, IL-10, HO-1, HIF-1α and GRP78 in early pregnancy were observed. Maternal TPOAb positivity tended to increase TNF-α, CD68 and MCP-1 mRNA expression.

Altered placental morphology may reflect its responses to intrauterine stress during early placental development (38). Our results are consistent with previous studies showing lower placental morphological indicators in TPOAb-positive mothers than in control women. Spinillo et al. found that TPOAb-positive women with TSH ≥2.5 mU/L had lower placental volume and area than euthyroid TPOAb-negative women (19). Tissues growing along the length and width of the placenta have different functions and are influenced by different factors. Tissues growing across the width could be involved in maternal-fetal nutrient transport. However, the tissues along the length have different functions but remain to be studied (39, 40). Placental thickness is the main dimension of placental growth in late pregnancy and may reflect the vascularization of the chorionic villi. Placental surface area is mainly established before late pregnancy and may indicate the number of spiral arteries supplying the placenta (38, 41).

Placental weight can be used as a proxy for fetal metabolic rate. In our study, maternal TPOAb levels were negatively correlated with placental weight. Recently, there have been conflicting studies on the association between TPOAb levels and placental weight. A small retrospective study from Japan showed that placental weight was lower in TPOAb-positive women (20). Männistö et al. found that significantly higher placental weights were observed in TPOAb-positive mothers as well as women with high TSH and low FT_4 levels in early pregnancy based on the Northern Finland Birth Cohort (21). An animal study showed that hypothyroidism reduced placental weight in rats (42). Placental weight and disc eccentricity were reported to be directly related to placental stress

TABLE 4 Association (β and 95% confidence intervals) of maternal TPOAb exposure (IU/mL) and placental inflammatory and oxidative stress cytokines (n=2122).

	IL-1β	IL-6	TNF-α	IFN-γ	CRP	CD68	MCP-1	IL-4	IL-10	HO-1	HIF-1α	GRP78
TPOAb_a	0.066 (-0.005, 0.138)	0.193 (0.127, 0.259)**	0.161 (0.086, 0.236)**	0.034 (-0.053, 0.121)	0.167 (0.055, 0.279)**	0.370 (0.276, 0.464)**	0.198 (0.131, 0.265)**	0.002 (-0.074, 0.077)	0.143 (0.065, 0.221)**	0.169 (0.098, 0.240)**	0.176 (0.105, 0.246)**	0.286 (0.189, 0.383)**
TPOAb_b	-0.051 (-0.139, 0.036)	0.049 (-0.033, 0.131)	0.058 (-0.034, 0.150)	0.080 (-0.027, 0.187)	-0.033 (-0.170, 0.105)	0.106 (-0.011, 0.223)	-0.002 (-0.085, 0.081)	0.047 (-0.045, 0.139)	-0.009 (-0.105, 0.087)	-0.032 (-0.119, 0.055)	-0.074 (-0.161, 0.013)	-0.078 (-0.198, 0.043)
TPOAb_c	-0.050 (-0.149, 0.048)	0.020 (-0.072, 0.112)	0.049 (-0.054, 0.153)	0.043 (-0.077, 0.163)	-0.004 (-0.159, 0.151)	0.096 (-0.035, 0.228)	0.030 (-0.063, 0.123)	0.052 (-0.051, 0.156)	0.062 (-0.047, 0.170)	0.011 (-0.087, 0.109)	-0.007 (-0.105, 0.090)	-0.007 (-0.142, 0.129)

Adjusted for maternal age, maternal education level, gestational weight gain, monthly income, parity, smoking, drinking and fetal gender.
a: First Trimester; b: Second Trimester; c: Third Trimester.
**: P< 0.01.

(43). This suggests maternal TPOAb levels may directly affect placentation and impair placental growth and development.

The negative correlation between maternal TPOAb levels and placental morphology in our study was present in all three trimesters, suggesting that maternal TPOAb levels during pregnancy may be an essential risk factor for placental development. Variation in placental morphology is common, but this variation must be limited to a specific range to ensure adequate placental function. The greater the degree of variability in placental morphology, the more severe the decline in function.

Abnormal expression of placental inflammatory and oxidative stress cytokines may respond to high levels of maternal TPOAb. In this study, rising maternal TPOAb levels correlated with an upward trend in inflammatory cytokines. Early pregnancy is the critical period for this association. Increased numbers of Th1 and decreased frequencies of Th2 in the endometrial leukocyte of women with autoimmune thyroid disease would lead to hypersecretion of IFN-γ and reduced production of IL-4 and IL-10 (44). Related studies have also shown that the ratio of TNF-α/IL-10 produced by CD3+/CD4+ cells is significantly higher in women with AITD compared to normal controls (45). This suggests that the maternal TPOAb levels moderately aggravate placental inflammatory status and interfere with placental immune tolerance.

There is a unique immunologic state during successful pregnancy, the balance between the anti-inflammatory and pro-inflammatory environments changes to facilitate the establishment and maintenance of immune tolerance and promote placental development, but excessive inflammation can affect placental function (2, 46). Abnormal expression of placental cytokines may lead to insufficiency and increase the risk of adverse pregnancy outcomes, such as pre-eclampsia (PE) and preterm birth (47, 48). Ma et al. found higher expression of placental pro-inflammatory cytokines IL-1β, IL-6 and MCP-1 in pregnant women with PE (49). Animal studies have shown that exacerbated levels of IL-6 and TNF-α contribute to placental dysfunction (50). Excessive TNF-α in the placenta may impair trophoblast fusion and hormone production and promote apoptosis (51, 52). CD68, primarily localized to lysosomes and endosomes, could be significantly upregulated in macrophages in response to inflammatory stimuli (53). Kim et al. found that maternal CRP was deposited in the human placenta, and its elevated level was related to chorioamnionitis, PE and preterm birth (54).

The maintenance of immune tolerance during pregnancy depends on the expression of anti-inflammatory cytokines, which is critical to prevent fetal immune rejection (55). In our study, TPOAb levels were found to be positively correlated with placental IL-10 mRNA expression in early pregnancy. IL-10 suppresses the production of many pro-inflammatory cytokines, such as IL-6 and TNF-α. IL-10 promotes trophoblast differentiation, inhibits trophoblast invasion and indirectly stimulates angiogenesis (46). It is suggested that increased IL-10 expression may be involved in regulating the adverse effects of inflammation and oxidative stress, which may be a protective mechanism of the placenta against high TPOAb levels.

This study firstly reported that high levels of TPOAb may be associated with elevated placental oxidative stress cytokines. An animal study had shown that hypothyroidism decreased the expression of HO-1, GRP78 and C/EBP homologous protein (CHOP) genes/proteins in the mid-gestation while increased the expression of HIF-1α, CHOP and nuclear factor erythroid 2-related factor 2 (NRF2) genes/proteins (15). HO-1 is a crucial cytokine for immune tolerance and promotes the establishment of an anti-inflammatory environment (56). HO-1 expression is induced under hypoxic conditions and modulates IL-10 signaling (57). HIF-1α is a key regulator of the cellular response to the hypoxic environment and plays a critical role in regulating trophoblast differentiation and invasion and in spiral artery remodeling (58). CHOP and GRP78 are known endoplasmic reticulum stress markers, and their elevation promotes trophoblast fusion, syncytialization and invasion (59–61). Spinillo et al. found that in women with positive TPOAb in early pregnancy, the presence of multiple placental pathological features suggested placental hypoxic/ischemic injury (38, 62). This suggests that high levels of TPOAb may activate oxidative stress at the maternal-fetal interface.

This study has several strengths. To the best of our knowledge, this is the first study to systematically investigate the potential effect of maternal TPOAb levels in the first, second and third trimester of pregnancy on placental morphology and inflammatory and oxidative stress responses based on a prospective birth cohort study. All information about exposures, outcomes and potential

10.3389/fendo.2023.1182049

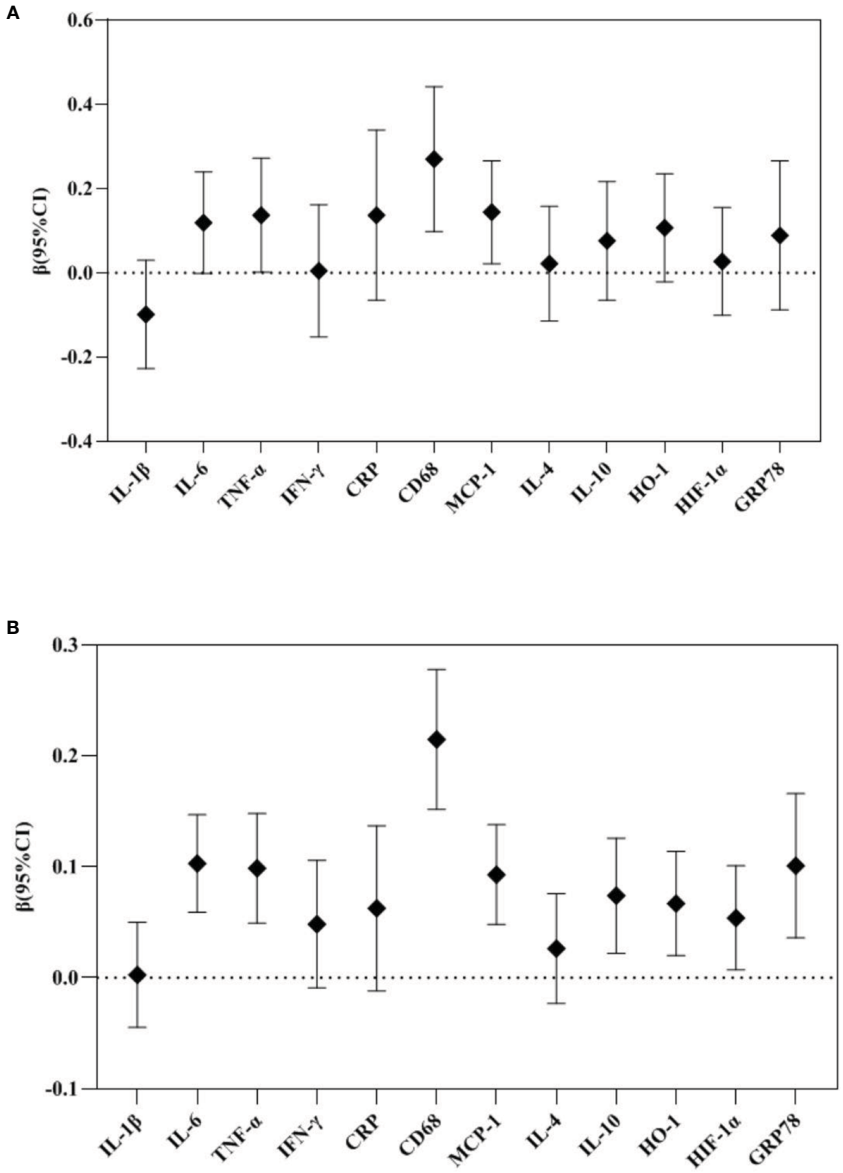

FIGURE 3
Repeated measure analysis: Association between maternal TPOAb exposure and placental cytokines (n=2122). **(A)** Maternal TPOAb positive (vs TPOAb negative) increased placental TNF-α, CD68 and MCP-1. **(B)** Maternal TPOAb levels throughout pregnancy were negatively associated with placental IL-6, TNF-α, CD68, MCP-1, IL-10, HO-1, HIF-1α and GRP78. Adjusted for maternal age, maternal education years, gestational weight gain, monthly income, parity, smoking, drinking and fetal gender.

confounding factors was collected prospectively, effectively avoiding recall and confounding bias. Second, thyroid indicators, including TPOAb levels, were measured retrospectively during childhood follow-up period. Women did not know their thyroid function from our biological samples. Except for those who might have had interventions during routine antenatal checkups (and those women were actually excluded from the current study), women did not have any interventions or medications relevant to thyroid function. This would provide natural and real data on the thyroid function of the participants during pregnancy. Actually, studies had revealed that levothyroxine supplementation in TPO euthyroid women was not associated with adverse perinatal outcomes in TPO-positive women with normal thyroid function (63). Third, multidimensional placental indicators were used to provide a comprehensive measurement of placental morphology and inflammatory and oxidative stress responses. This allowed a wide understanding on the effect of maternal TPOAb levels on placental morphology and function. Furthermore, multiple sensitivity analyses were performed, fully considering maternal conditions, including GDM, HDCP and systemic inflammation. After further adjusting for these variables, the main findings remained unchanged. It highly increases the robustness and precision of the findings, and indicates that the potential effect of maternal TPOAb exposure on placental morphology and inflammation and oxidative stress may be independent of maternal systemic endocrinal or inflammatory conditions.

Some limitations must be recognized. Firstly, only data on the expression of placental transcriptional biomarkers are available in this study, which only indirectly reflects protein translation. But mRNA assay is more feasible than protein levels in a large sample studies measuring multiple cytokines. Secondly, human placenta samples can usually be collected after childbirth. Dynamic placental monitoring can better reflect placental temporal and spatial characteristics, which could be observed by antenatal ultrasound scan. However, in the current study, we did not have data on maternal ultrasound scan. Thirdly, information on local basic iodine levels needed to be in this study, as it would be an important factor related to individual thyroid function. However, Ma'anshan City has yet to be reported as an iodine area. Finally, although many potential confounders were considered in the current study, residual confounding factors could not be ruled out, such as maternal exposure to selenium (64), heavy metals (11, 65), and environmental endocrine disruptors (66).

Conclusions

In conclusion, there may be trimester-specific associations between maternal TPOAb levels and placental morphology and inflammatory and oxidative stress responses. The effect of maternal TPOAb levels on placental morphology is present throughout pregnancy. Early pregnancy may be the critical period for the association between maternal TPOAb levels and placental inflammatory and oxidative stress responses. This study provides evidence for the potentially independent effect of maternal TPOAb on placental morphology and function, which act as the pathway to pregnancy outcomes. Close monitoring of women's TPOAb levels during pregnancy is believable to be important for placental development and subsequent fetal health.

Data availability statement

The original contributions presented in the study are included in the article/Supplementary Material, further inquiries can be directed to the corresponding author.

Ethics statement

The studies involving humans were approved by Biomedical Ethics Committee of the Anhui Medical University (No. 20131401). The studies were conducted in accordance with the local legislation and institutional requirements. The participants provided their written informed consent to participate in this study

Author contributions

XR and KH performed data analysis and wrote the paper. MY and YT conceived study design and performed data analysis. YH, YBH and JW conducted data acquisition and interpretation and laboratory testing. FT provided project administration and resource support. KH obtained funding for this research. All authors contributed to the article and approved the submitted version.

Funding

This work was supported by the National Natural Science Foundation of China (82273639), the National Key Research and Development Program of China (2022YFC27022901) and Research Fund of Anhui Institute of translational medicine (ZHYX2020A001).

Acknowledgments

We appreciate all the children and mothers who agreed to participate in our study. We also are grateful to all Ma'anshan Maternal and Child Health Hospital for their assistance and support.

Conflict of interest

The authors declare that the research was conducted in the absence of any commercial or financial relationships that could be construed as a potential conflict of interest.

Publisher's note

All claims expressed in this article are solely those of the authors and do not necessarily represent those of their affiliated organizations, or those of the publisher, the editors and the reviewers. Any product that may be evaluated in this article, or claim that may be made by its manufacturer, is not guaranteed or endorsed by the publisher.

Supplementary material

The Supplementary Material for this article can be found online at: https://www.frontiersin.org/articles/10.3389/fendo.2023.1182049/full#supplementary-material

References

1. Trbojević B, Djurica S. Srp arh celok lek. *Srpski arhiv za celokupno lekarstvo* (2005) 133(Suppl 1):25–33. doi: 10.2298/sarh05s1025t

2. Löb S, Amann N, Kuhn C, Schmoeckel E, Wöckel A, Zati Zehni A, et al. Interleukin-1 beta is significantly upregulated in the decidua of spontaneous and recurrent miscarriage placentas. *J Reprod Immunol* (2021) 144:103283. doi: 10.1016/j.jri.2021.103283

3. Ferrari SM, Paparo SR, Ragusa F, Elia G, Mazzi V, Patrizio A, et al. Chemokines in thyroid autoimmunity. *Best Pract Res Clin Endocrinol Metab* (2023) 37(2):101773. doi: 10.1016/j.beem.2023.101773

4. Springer D, Jiskra J, Limanova Z, Zima T, Potlukova E. Thyroid in pregnancy: From physiology to screening. *Crit Rev Clin Lab Sci* (2017) 54(2):102–16. doi: 10.1080/10408363.2016.1269309

5. Chardès T, Chapal N, Bresson D, Bès C, Giudicelli V, Lefranc MP, et al. The human anti-thyroid peroxidase autoantibody repertoire in Graves' and Hashimoto's autoimmune thyroid diseases. *Immunogenetics* (2002) 54(3):141–57. doi: 10.1007/s00251-002-0453-9

6. Moreno-Reyes R, Glinoer D, Van Oyen H, Vandevijvere S. High prevalence of thyroid disorders in pregnant women in a mildly iodine-deficient country: a population-based study. *J Clin Endocrinol Metab* (2013) 98(9):3694–701. doi: 10.1210/jc.2013-2149

7. Dhillon-Smith RK, Coomarasamy A. TPO antibody positivity and adverse pregnancy outcomes. *Best Pract Res Clin Endocrinol Metab* (2020) 34(4):101433. doi: 10.1016/j.beem.2020.101433

8. Chen CY, Chen CP, Lin KH. Biological functions of thyroid hormone in placenta. *Int J Mol Sci* (2015) 16(2):4161–79. doi: 10.3390/ijms16024161

9. Vissenberg R, Manders VD, Mastenbroek S, Fliers E, Afink GB, Ris-Stalpers C, et al. Pathophysiological aspects of thyroid hormone disorders/thyroid peroxidase autoantibodies and reproduction. *Hum Reprod Update* (2015) 21(3):378–87. doi: 10.1093/humupd/dmv004

10. Kyrilli A, Unuane D, Poppe KG. Thyroid autoimmunity and pregnancy in euthyroid women. *Best Pract Res Clin Endocrinol Metab* (2023) 37(2):101632. doi: 10.1016/j.beem.2022.101632

11. Zhu YD, Liang CM, Hu YB, Li ZJ, Wang SF, Xiang HY, et al. Repeated measures of prenatal thallium exposure and placental inflammatory cytokine mRNA expression: The Ma'anshan birth cohort (MABC) study. *Chemosphere* (2020) 246:125721. doi: 10.1016/j.chemosphere.2019.125721

12. Abdolmohammadi-Vahid S, Samaie V, Hashemi H, Mehdizadeh A, Dolati S, Ghodrati-Khakestar F, et al. Anti-thyroid antibodies and underlying generalized immunologic aberrations in patients with reproductive failures. *J Reprod Immunol* (2022) 154:103759. doi: 10.1016/j.jri.2022.103759

13. Silva JF, Ocarino NM, Serakides R. Thyroid hormones and female reproduction. *Biol Reprod* (2018) 99(5):907–21. doi: 10.1093/biolre/ioy115

14. Silva JF, Ocarino NM, Serakides R. Maternal thyroid dysfunction affects placental profile of inflammatory mediators and the intrauterine trophoblast migration kinetics. *Reproduction* (2014) 147(6):803–16. doi: 10.1530/REP-13-0374

15. Dos Anjos Cordeiro JM, Santos LC, de Oliveira LS, Santos BR, Santos EO, Barbosa EM, et al. Maternal hypothyroidism causes oxidative stress and endoplasmic reticulum stress in the maternal-fetal interface of rats. *Free Radic Biol Med* (2022) 191:24–39. doi: 10.1016/j.freeradbiomed.2022.08.033

16. Cardaropoli S, Paulesu L, Romagnoli R, Ietta F, Marzioni D, Castellucci M, et al. Macrophage migration inhibitory factor in fetoplacental tissues from preeclamptic pregnancies with or without fetal growth restriction. *Clin Dev Immunol* (2012) 2012:639342. doi: 10.1155/2012/639342

17. Takemoto R, Anami A, Koga H. Relationship between birth weight to placental weight ratio and major congenital anomalies in Japan. *PloS One* (2018) 13(10):e0206002. doi: 10.1371/journal.pone.0206002

18. Frayne J, Nguyen T, Hauck Y, Liira H, Keelan JA. The relationship between pregnancy exposure to antidepressant and atypical antipsychotic medications and placental weight and birth weight ratio: A retrospective cohort study. *J Clin Psychopharmacol* (2018) 38(6):563–9. doi: 10.1097/JCP.0000000000000964

19. Spinillo A, De Maggio I, Ruspini B, Bellingeri C, Cavagnoli C, Giannico S, et al. Placental pathologic features in thyroid autoimmunity. *Placenta* (2021) 112:66–72. doi: 10.1016/j.placenta.2021.07.287

20. Ushijima J, Furukawa S, Sameshima H. The presence of thyroid peroxidase antibody is associated with lower placental weight in maternal thyroid dysfunction. *Tohoku J Exp Med* (2019) 249(3):231–6. doi: 10.1620/tjem.249.231

21. Männistö T, Vääräsmäki M, Pouta A, Hartikainen AL, Ruokonen A, Surcel HM, et al. Perinatal outcome of children born to mothers with thyroid dysfunction or antibodies: a prospective population-based cohort study. *J Clin Endocrinol Metab* (2009) 94(3):772–9. doi: 10.1210/jc.2008-1520

22. Li P, Teng Y, Ru X, Liu Z, Han Y, Tao F, et al. Sex-specific effect of maternal thyroid hormone trajectories on preschoolers' Behavioral development: A birth cohort study. *J Clin Endocrinol Metab* (2022) 107(5):e2037–46. doi: 10.1210/clinem/dgab887

23. Burton GJ, Fowden AL, Thornburg KL. Placental origins of chronic disease. *Physiol Rev* (2016) 96(4):1509–65. doi: 10.1152/physrev.00029.2015

24. Barker DJP, Eriksson JG, Kajantie E, Alwasel SH, Fall CHD, Roseboom TJ, et al. The maternal and placental origins of chronic disease. In: Burton GJ, Barker DJP, Moffett A, Thornburg K, editors. *The Placenta and Human Developmental Programming*. Cambridge: Cambridge University Press (2010). p. 5–16.

25. Barker DJ, Bull AR, Osmond C, Simmonds SJ. Fetal and placental size and risk of hypertension in adult life. *BMJ* (1990) 301(6746):259–62. doi: 10.1136/bmj.301.6746.259

26. Punshon T, Li Z, Jackson BP, Parks WT, Romano M, Conway D, et al. Placental metal concentrations in relation to placental growth, efficiency and birth weight. *Environ Int* (2019) 126:533–42. doi: 10.1016/j.envint.2019.01.063

27. Hu Y, Huang K, Sun Y, Wang J, Xu Y, Yan S, et al. Placenta response of inflammation and oxidative stress in low-risk term childbirth: the implication of delivery mode. *BMC Pregnancy Childbirth* (2017) 17(1):407. doi: 10.1186/s12884-017-1589-9

28. Zhou J, Teng Y, Zhang F, Ru X, Li P, Wang J, et al. Sex-specific association between placental inflammatory cytokine mRNA expression and preschoolers' behavioral development: The Ma'anshan birth cohort study. *Brain Behav Immun* (2022) 104:110–21. doi: 10.1016/j.bbi.2022.05.017

29. Sieiro Netto L, Medina Coeli C, Micmacher E, Mamede Da Costa S, Nazar L, Galvão D, et al. Influence of thyroid autoimmunity and maternal age on the risk of miscarriage. *Am J Reprod Immunol* (2004) 52(5):312–6. doi: 10.1111/j.1600-0897.2004.00227.x

30. Sun J, Teng D, Li C, Peng S, Mao J, Wang W, et al. Association between iodine intake and thyroid autoantibodies: a cross-sectional study of 7073 early pregnant women in an iodine-adequate region. *J Endocrinol Invest* (2020) 43(1):43–51. doi: 10.1007/s40618-019-01070-1

31. Adu-Gyamfi EA, Wang YX, Ding YB. The interplay between thyroid hormones and the placenta: a comprehensive review†. *Biol Reprod* (2020) 102(1):8–17. doi: 10.1093/biolre/ioz182

32. Karakosta P, Alegakis D, Georgiou V, Roumeliotaki T, Fthenou E, Vassilaki M, et al. Thyroid dysfunction and autoantibodies in early pregnancy are associated with increased risk of gestational diabetes and adverse birth outcomes. *J Clin Endocrinol Metab* (2012) 97(12):4464–72. doi: 10.1210/jc.2012-2540

33. Nogues P, Dos Santos E, Couturier-Tarrade A, Berveiller P, Arnould L, Lamy E, et al. Maternal obesity influences placental nutrient transport, inflammatory status, and morphology in human term placenta. *J Clin Endocrinol Metab* (2021) 106(4):e1880–96. doi: 10.1210/clinem/dgaa660

34. Alavi A, Adabi K, Nekuie S, Jahromi EK, Solati M, Sobhani A, et al. Thyroid dysfunction and autoantibodies association with hypertensive disorders during pregnancy. *J Pregnancy* (2012) 2012:742695. doi: 10.1155/2012/742695

35. Naruse K, Tsunemi T, Kawahara N, Kobayashi H. Preliminary evidence of a paternal-maternal genetic conflict on the placenta: Link between imprinting disorder and multi-generational hypertensive disorders. *Placenta* (2019) 84:69–73. doi: 10.1016/j.placenta.2019.02.009

36. Goldstein JA, Gallagher K, Beck C, Kumar R, Gernand AD. Maternal-fetal inflammation in the placenta and the developmental origins of health and disease. *Front Immunol* (2020) 11:531543. doi: 10.3389/fimmu.2020.531543

37. Harding AT, Goff MA, Froggatt HM, Lim JK, Heaton NS. GPER1 is required to protect fetal health from maternal inflammation. *Science* (2021) 371(6526):271–6. doi: 10.1126/science.aba9001

38. Freedman AA, Hogue CJ, Marsit CJ, Rajakumar A, Smith AK, Goldenberg RL, et al. Associations between the features of gross placental morphology and birthweight. *Pediatr Dev Pathol* (2019) 22(3):194–204. doi: 10.1177/1093526618789310

39. Eriksson JG, Kajantie E, Thornburg KL, Osmond C, Barker DJ. Mother's body size and placental size predict coronary heart disease in men. *Eur Heart J* (2011) 32(18):2297–303. doi: 10.1093/eurheartj/ehr147

40. Kajantie E, Thornburg KL, Eriksson JG, Osmond C, Barker DJ. In preeclampsia, the placenta grows slowly along its minor axis. *Int J Dev Biol* (2010) 54(2-3):469–73. doi: 10.1387/ijdb.082833ek

41. Salafia CM, Maas E, Thorp JM, Eucker B, Pezzullo JC, Savitz DA. Measures of placental growth in relation to birth weight and gestational age. *Am J Epidemiol* (2005) 162(10):991–8. doi: 10.1093/aje/kwi305

42. Silva JF, Vidigal PN, Galvão DD, Boeloni JN, Nunes PP, Ocarino NM, et al. Fetal growth restriction in hypothyroidism is associated with changes in proliferative activity, apoptosis and vascularisation of the placenta. *Reprod Fertil Dev* (2012) 24(7):923–31. doi: 10.1071/RD11219

43. Yampolsky M, Salafia CM, Shlakhter O, Haas D, Eucker B, Thorp J. Modeling the variability of shapes of a human placenta. *Placenta* (2008) 29(9):790–7. doi: 10.1016/j.placenta.2008.06.005

44. Stewart-Akers AM, Krasnow JS, Brekosky J, Deloia JA. Endometrial leukocytes are altered numerically and functionally in women with implantation defects. *Am J Reprod Immunol* (1998) 39(1):1–11. doi: 10.1111/j.1600-0897.1998.tb00326.x

45. Kim NY, Cho HJ, Kim HY, Yang KM, Ahn HK, Thornton S, et al. Thyroid autoimmunity and its association with cellular and humoral immunity in women with reproductive failures. *Am J Reprod Immunol* (2011) 65(1):78–87. doi: 10.1111/j.1600-0897.2010.00911.x

46. Vasilopoulou E, Loubière LS, Lash GE, Ohizua O, McCabe CJ, Franklyn JA, et al. Triiodothyronine regulates angiogenic growth factor and cytokine secretion by isolated human decidual cells in a cell-type specific and gestational age-dependent manner. *Hum Reprod* (2014) 29(6):1161–72. doi: 10.1093/humrep/deu046

47. Wen Y, Cheng M, Qin L, Xu W. TNFα-induced abnormal activation of TNFR/NF-κB/FTH1 in endometrium is involved in the pathogenesis of early spontaneous abortion. *J Cell Mol Med* (2022) 26(10):2947–58. doi: 10.1111/jcmm.17308

48. Fakhr Y, Koshti S, Habibyan YB, Webster K, Hemmings DG. Tumor necrosis factor-α Induces a preeclamptic-like phenotype in placental villi via sphingosine kinase 1 activation. *Int J Mol Sci* (2022) 23(7):3750. doi: 10.3390/ijms23073750

49. Ma Y, Ye Y, Zhang J, Ruan CC, Gao PJ. Immune imbalance is associated with the development of preeclampsia. *Med (Baltimore)* (2019) 98(14):e15080. doi: 10.1097/MD.0000000000015080

50. Dela Justina V, Gonçalves JS, de Freitas RA, Fonseca AD, Volpato GT, Tostes RC, et al. Increased O-linked N-acetylglucosamine modification of NF-κB and augmented cytokine production in the placentas from hyperglycemic rats. *Inflammation* (2017) 40(5):1773–81. doi: 10.1007/s10753-017-0620-7

51. Haider S, Knöfler M. Human tumour necrosis factor: physiological and pathological roles in placenta and endometrium. *Placenta* (2009) 30(2):111–23. doi: 10.1016/j.placenta.2008.10.012

52. Otun HA, Lash GE, Innes BA, Bulmer JN, Naruse K, Hannon T, et al. Effect of tumour necrosis factor-α in combination with interferon-γ on first trimester extravillous trophoblast invasion. *J Reprod Immunol* (2011) 88(1):1–11. doi: 10.1016/j.jri.2010.10.003

53. Chistiakov DA, Killingsworth MC, Myasoedova VA, Orekhov AN, Bobryshev YV. CD68/macrosialin: not just a histochemical marker. *Lab Invest* (2017) 97(1):4–13. doi: 10.1038/labinvest.2016.116

54. Kim EN, Yoon BH, Jeon EJ, Lee JB, Hong JS, Lee JY, et al. Placental deposition of C-reactive protein is a common feature of human pregnancy. *Placenta* (2015) 36(6):704–7. doi: 10.1016/j.placenta.2015.03.006

55. Li C, Zhou J, Huang Z, Pan X, Leung W, Chen L, et al. The clinical value and variation of antithyroid antibodies during pregnancy. *Dis Markers* (2020) 2020:8871951. doi: 10.1155/2020/8871951

56. Peoc'h K, Puy V, Fournier T. Haem oxygenases play a pivotal role in placental physiology and pathology. *Hum Reprod Update* (2020) 26(5):634–49. doi: 10.1093/humupd/dmaa014

57. Siwetz M, Blaschitz A, El-Heliebi A, Hiden U, Desoye G, Huppertz B, et al. TNF-α alters the inflammatory secretion profile of human first trimester placenta. *Lab Invest* (2016) 96(4):428–38. doi: 10.1038/labinvest.2015.159

58. Yu N, Wu JL, Xiao J, Fan L, Chen SH, Li W. HIF-1α regulates angiogenesis via Notch1/STAT3/ETBR pathway in trophoblastic cells. *Cell Cycle* (2019) 18(24):3502–12. doi: 10.1080/15384101.2019.1689481

59. Bastida-Ruiz D, Yart L, Wuillemin C, Ribaux P, Morris N, Epiney M, et al. The fine-tuning of endoplasmic reticulum stress response and autophagy activation during trophoblast syncytialization. *Cell Death Dis* (2019) 10(9):651. doi: 10.1038/s41419-019-1905-6

60. Fradet S, Pierredon S, Ribaux P, Epiney M, Shin Ya K, Irion O, et al. Involvement of membrane GRP78 in trophoblastic cell fusion. *PloS One* (2012) 7(8):e40596. doi: 10.1371/journal.pone.0040596

61. Bastida-Ruiz D, Wuillemin C, Pederencino A, Yaron M, Martinez de Tejada B, Pizzo SV, et al. Activated α2-macroglobulin binding to cell surface GRP78 induces trophoblastic cell fusion. *Sci Rep* (2020) 10(1):9666. doi: 10.1038/s41598-020-66554-0

62. Khong TY, Mooney EE, Ariel I, Balmus NC, Boyd TK, Brundler MA, et al. Sampling and definitions of placental lesions: amsterdam placental workshop group consensus statement. *Arch Pathol Lab Med* (2016) 140(7):698–713. doi: 10.5858/arpa.2015-0225-CC

63. Di Girolamo R, Liberati M, Silvi C, D'Antonio F. Levothyroxine supplementation in euthyroid pregnant women with positive autoantibodies: A systematic review and meta-analysis. *Front Endocrinol (Lausanne)* (2022) 13:759064. doi: 10.3389/fendo.2022.759064

64. Habibi N, Labrinidis A, Leemaqz SY, Jankovic-Karasoulos T, McCullough D, Grieger JA, et al. Effect of selenium and iodine on oxidative stress in the first trimester human placenta explants. *Nutrients* (2021) 13(3):800. doi: 10.3390/nu13030800

65. Wang JQ, Hu YB, Liang CM, Xia X, Li ZJ, Gao H, et al. Aluminum and magnesium status during pregnancy and placenta oxidative stress and inflammatory mRNA expression: China Ma'anshan birth cohort study. *Environ Geochem Health* (2020) 42(11):3887–98. doi: 10.1007/s10653-020-00619-x

66. Wang JQ, Hu YB, Gao H, Sheng J, Huang K, Zhang YW, et al. Sex-specific difference in placental inflammatory transcriptional biomarkers of maternal phthalate exposure: a prospective cohort study. *J Expo Sci Environ Epidemiol* (2020) 30(5):835–44. doi: 10.1038/s41370-020-0200-z

frontiers | Frontiers in Endocrinology

TYPE Review
PUBLISHED 03 October 2023
DOI 10.3389/fendo.2023.1256877

Check for updates

OPEN ACCESS

EDITED BY
Laurent M. Sachs,
Muséum National d'Histoire Naturelle, France

REVIEWED BY
Heike Heuer,
Essen University Hospital, Germany
Mary E. Gilbert,
United States Environmental Protection Agency (EPA), United States

*CORRESPONDENCE
Frédéric Flamant
Frederic.flamant@ens-lyon.fr

RECEIVED 11 July 2023
ACCEPTED 18 September 2023
PUBLISHED 03 October 2023

CITATION
Richard S, Ren J and Flamant F (2023) Thyroid hormone action during GABAergic neuron maturation: The quest for mechanisms. *Front. Endocrinol.* 14:1256877. doi: 10.3389/fendo.2023.1256877

COPYRIGHT
© 2023 Richard, Ren and Flamant. This is an open-access article distributed under the terms of the Creative Commons Attribution License (CC BY). The use, distribution or reproduction in other forums is permitted, provided the original author(s) and the copyright owner(s) are credited and that the original publication in this journal is cited, in accordance with accepted academic practice. No use, distribution or reproduction is permitted which does not comply with these terms.

Thyroid hormone action during GABAergic neuron maturation: The quest for mechanisms

Sabine Richard, Juan Ren and Frédéric Flamant*

Institut de Génomique Fonctionnelle de Lyon, UMR5242, Ecole Normale Supérieure de Lyon, Centre National de la Recherche Scientifique, Université Claude Bernard-Lyon 1, USC1370 Institut National de Recherche pour l'Agriculture, l'Alimentation et l'Environnement, Lyon, France

Thyroid hormone (TH) signaling plays a major role in mammalian brain development. Data obtained in the past years in animal models have pinpointed GABAergic neurons as a major target of TH signaling during development, which opens up new perspectives to further investigate the mechanisms by which TH affects brain development. The aim of the present review is to gather the available information about the involvement of TH in the maturation of GABAergic neurons. After giving an overview of the kinds of neurological disorders that may arise from disruption of TH signaling during brain development in humans, we will take a historical perspective to show how rodent models of hypothyroidism have gradually pointed to GABAergic neurons as a main target of TH signaling during brain development. The third part of this review underscores the challenges that are encountered when conducting gene expression studies to investigate the molecular mechanisms that are at play downstream of TH receptors during brain development. Unravelling the mechanisms of action of TH in the developing brain should help make progress in the prevention and treatment of several neurological disorders, including autism and epilepsy.

KEYWORDS

brain development, parvalbumin interneurons, thyroid hormone receptors, animal models, hypothyroidism, neurological disorders

1 Introduction

Thyroid hormone (TH) signaling plays a major role in mammalian brain development (1). Any alteration in TH economy during brain development – be it TH synthesis, TH transport or activity of TH receptors (TRs) – is likely to induce long-lasting and irreversible defects, ranging from mild intellectual disability to profound physical and mental impairments. This has been known for a long time, but the precise underlying mechanisms are still unknown. Data obtained in the past years in animal models have pinpointed the GABAergic system as a major target of TH signaling during development (2, 3). GABAergic neurons, which use GABA (gamma-aminobutyric acid) as a neurotransmitter, are the chief inhibitory neurons in the vertebrate central nervous

system. Alteration in the development of the GABAergic system is known to be associated with neurological disorders such as intellectual disability, autism spectrum disorder (ASD), and epilepsy (4). On the other hand, thyroid dysfunction is often associated with some of these neurological disorders, such as anxiety and seizure susceptibility (5, 6). Wiens and Trudeau (7) have previously reviewed *in vitro* and *in vivo* evidence in rodents, indicating that alterations in TH signaling may affect the GABAergic system in several ways: GABA synthesis and metabolism, GABA release and reuptake, GABA receptor expression and function, etc. However, the molecular and cellular mechanisms by which TH impacts GABAergic neurons are unknown. The aim of the present review is to gather the available information about the direct involvement of TH in GABAergic neuron maturation.

TH (either its most active form T3: 3,3',5-triiodo-L-thyronine, or its less active precursor T4: thyroxine) binds to nuclear receptors, which are transcription factors regulating gene expression. Two genes (*THRA* and *THRB* in humans, *Thra* and *Thrb* in rodents) encode the TRα1, TRβ1 and TRβ2 nuclear receptors. While TRα1 is present at all developmental stages in many cell types and in all the rodent brain areas, TRβ1 mRNA appears later and TRβ2 is restricted to few brain areas (8). However, alternate splicing of *Thra* mRNA also generates the TRα2 mRNA, which encodes a non-receptor protein. Notably, in the brain, TRα2 is more abundant than TRα1 (9). Knowing that direct measurement of TR protein concentrations is difficult, due to poor antibody specificity and very low abundance of TR proteins, the respective abundance of the different TR isotypes in the different cell types remains unclear. In humans, old studies of TH binding suggest that TRβ1 is the predominant receptor in the human fetal brain (10).

More convincingly than TR expression patterns, both human and mouse genetics clearly demonstrate that TRα1 mediates crucial, significant actions of TH on early brain development, while TRβ1 and TRβ2 appear to be necessary for more specific and discreet steps of brain development (11–14). Patients who bear mutations in *THRA* are very likely to present significant neurological disorders such as epilepsy, motor incoordination or impaired cognitive function (15, 16). *THRB* mutations alter the regulation of the hypothalamo-pituitary-thyroid axis, increasing the circulating level of TH, which may in turn alter neurodevelopment. Neurocognitive impairment has been frequently associated with mutations in *THRB*, but the consequences on brain function appear to be less dramatic than those induced by *THRA* mutations (17, 18).

In the present paper, we will retrace how rodent models have helped uncover the critical role of TH/TR signaling in the differentiation of GABAergic neurons. Deciphering the network of TH/TR target genes in GABAergic neurons during brain development appears as a promising way of generating novel approaches to alleviate various neurodevelopmental disorders associated with GABAergic dysfunction, including epilepsy and ASD. Moreover, identifying TH target genes in GABAergic neurons during brain development is likely to contribute to a more general understanding of TH action in the brain.

2 Disruption of TH signaling during development induces a wide array of neurological disorders, including GABAergic dysfunction

Disruption of TH signaling may arise from very different causes affecting various aspects of TH molecular landscape (19). In mammals, TH is synthesized in the thyroid gland from tyrosine and iodine. In the blood and cerebrospinal fluid, TH is partly bound to distributor proteins, such as transthyretin, thyroxine-binding globulin, albumin and lipoproteins (20). The main source of TH for the fetus is from the mother throughout gestation, since even when the fetal thyroid starts to synthesize TH, the maternal TH remains the main source of circulating fetal TH (21). Transfer of maternal TH to the fetal brain involves crossing the placental and blood-brain barriers. TH entry into the brain is facilitated by specific transmembrane transporters, with monocarboxylate transporter 8 (Mct8) and organic anion transporter polypeptide 1c1 (Oatp1c1) playing a prominent role in TH brain transport in rodents (1). Around 80% of the T3 that is present in the brain derives from local deiodination of T4, mediated by type 2 iodothyronine deiodinase (Dio2), while the rest originates from the circulation (22). Deiodinase 3 (Dio3) degrades T4 and T3 into inactive metabolites and is thus the major physiological TH inactivator (23). As a consequence of the multiplicity of molecular actors involved from maternal TH synthesis to regulation of the expression of TH target genes, a wide variety of causes may affect thyroid hormone economy in the fetal brain (24): iodine deficiency, insufficient TH synthesis by the thyroid gland, problems in blood and cerebrospinal fluid transport of TH, abnormalities in the placental barrier, defects in membrane transport proteins, altered enzymatic activity of deiodinases, defects in cytosolic TH binding proteins, and last but not least, defects in TH receptor activity. The consequences of such defects have been previously described in the specialized literature. From this array of causes, TH deficiency during fetal and postnatal development may cause diverse kinds of neurological impairment (1). As a matter of example, we have chosen to mention here three emblematic diseases linked to poor TH signaling during development, one linked to a lack of hormone, the second to a deficit in TH membrane transporters and the third to a deficit in TH receptors.

- Congenital hypothyroidism, defined in humans as partial or complete TH deficiency at birth, can start early during development and represents the major cause of preventable intellectual disability in the world. If not detected and treated early, congenital hypothyroidism can have devastating effects on neurocognitive function. The clinical spectrum goes from mere developmental delay to persistent intellectual disability, hearing and speech impairment, psychomotor impairment, with the most severe condition being historically known as cretinism (25, 26). A major factor influencing the degree of severity

of the symptoms is the time at which TH deficiency occurs, relative to brain developmental steps. In children with normal thyroid function born to hypothyroid mothers, TH starts to be synthesized shortly before birth, which allows partial recuperation after the initial developmental delay. In hypothyroid children born to euthyroid mothers, the maternal TH contribution during the latter part of gestation also provides partial compensation for the inadequate fetal TH supply. By contrast, hypothyroidism that stems *in utero* and that extends throughout childhood has more severe consequences (27). Newborn screening, accompanied by T4 replacement therapy, has been efficiently implemented for decades in several countries, but most newborns worldwide remain away from such protocols of screening and treatment (28). Moreover, even under T4 treatment, significant impairment in clinical and cognitive scores may persist in children with congenital hypothyroidism (29).

- Allan-Herndon-Dudley syndrome is a rare X-linked disease that affects human males with mutations in the *Slc16a2* gene encoding Mct8, which is critically needed for TH to enter the human brain. Allan-Herndon-Dudley patients have a shortened life expectancy and present with physical and intellectual disability, speech deficits and severe neurological abnormalities, including, in some cases, epilepsy (30–33). Histopathological analyses have revealed that hypomyelination is the most salient feature of the brains of Allan-Herndon-Dudley patients. Notably, at the level of the cerebral cortex, López-Espíndola et al. (34) have shown that this syndrome is associated with a reduction in the numbers of parvalbumin (PV)-expressing neurons, a category of GABAergic interneurons which play pivotal roles in cortical development and function. In addition, Allan-Herndon-Dudley patients' cerebellum displays abnormal differentiation of Purkinje cells, which are GABAergic projection neurons (34).
- Resistance to thyroid hormone receptor alpha (RTHα) is another rare disease due to mutations in *THRA*, the gene coding for TRα1. The clinical features of patients with RTHα are quite heterogeneous. Delayed milestones in the development of motor and speech abilities are the most common neurological symptoms (15). Notably, among the 40 reported cases to date, three had epilepsy (35–37), which significantly outweighs the incidence of epilepsy in the general population [4-10 per 1,000 people (38)]. Moreover, it has been suggested that the proportion of *THRA* mutations was higher in ASD patients than in the general population. Testing this possibility, Kalikiri and colleagues (39) made the astonishing discovery of seven novel *THRA* mutations, all likely to be pathological, in a small cohort of 30 patients with ASD in India. This adds to another case of ASD with a *THRA* mutation, which was previously discovered in Canada (40).

The variety of neurological symptoms associated with TH signaling defects is explained by the fact that TH influences a wide panel of cellular processes in the developing brain, such as neurogenesis, neuronal migration, neuronal and glial cell differentiation, myelination and synaptogenesis (1). Accordingly, many genes have been found to be under direct or indirect regulation by TH (41), and deciphering the precise mechanisms underlying TH action will necessarily involve isolating direct from indirect effects.

3 Rodent models point to the GABAergic system as a major target of TH/TR signaling during development

The timing of neurodevelopmental stages differs significantly between humans and rodents, rodent early post-natal stages roughly corresponding to the end of the second trimester of human pregnancy (24). However, as major steps in brain development are conserved between humans and rodents, our understanding of the role of TH in the developing brain has greatly benefited from rodent studies. Seminal work undertaken to decipher the actions of TH in the developing brain involved rat models of congenital hypothyroidism. In the past decades, genetic tools have allowed to develop mouse models precisely designed to dissect the effects of TH in specific cells of the brain. The following sections will focus on these models and their contribution to our understanding of the role of TH in GABAergic neuron development.

3.2 Rat models of congenital hypothyroidism show defects in GABAergic neuron maturation

The morphological consequences of congenital hypothyroidism have been extensively studied and include alterations in cortical lamination, high density of hippocampal neurons, poor differentiation of the gray-white matter boundary and delayed cerebellar development (1). The following paragraphs will focus on the effects of developmental hypothyroidism on GABAergic neurons.

3.1.1 Cerebellum

The relative simplicity of the microanatomy of the cerebellar cortex, as well as its strong TH signaling dependency, make it an excellent model to study the neurodevelopmental function of TH. The proliferation and migration of granule cells, which represent the vast majority of the neuronal population in the cerebellum, are stimulated by contacts with a monolayer of GABAergic projection neurons, called Purkinje cells. Congenital hypothyroidism dramatically affects the morphological maturation of Purkinje cells. The growth, dendrite arborization and dendrite spine number of Purkinje cells are markedly decreased in hypothyroid rats (42–44). The cerebellum also contains GABAergic interneurons, called basket, stellate and Golgi cells. Early studies of rat cerebellum have shown that congenital hypothyroidism delayed the postnatal increase in GABA receptor density (45), and lowered the final number of basket cells (42). More recently,

Manzano et al. (46) have reported that hypothyroid rats at postnatal day (PND) 16 exhibited a decreased number of Golgi cells, as well as a delayed disappearance of the precursors of cerebellar GABAergic interneurons. Moreover, they found that on PND8, the proliferation of GABAergic interneuron precursors in cerebellar white matter was reduced in hypothyroid rats. Thus, several components of the GABAergic system are impaired in the hypothyroid rat cerebellum.

3.1.2 Cortex and hippocampus

In 1996, Berbel et al. (47) were the first to describe the impact of severe congenital hypothyroidism on a subset of cortical GABAergic inhibitory neurons expressing the calcium-binding protein parvalbumin (PV). They described a striking reduction in PV-positive terminals in the neocortex of adult hypothyroid rats (47). Ten years later, Gilbert et al. (48) further showed that moderate degrees of TH insufficiency during development were sufficient to induce a significant reduction of PV fiber staining and PV cell body count in rat cortex and hippocampus at PND23. By contrast, hypothyroid rats have been shown to exhibit an increased density of calretinin neurons, another GABAergic interneuron subtype, in the dentate gyrus of the hippocampus (48). These effects were in part irreversible, since returning to a euthyroid state in adulthood only allowed partial recovery (48, 49). By means of cross-fostering and hormonal replacement studies, Gilbert et al. (48) also emphasized that the developmental window over which TH insufficiency occurred was determinant, the first postnatal weeks appearing as the most critical stages for TH influence on PV expression in the cortex and hippocampus. However, TH insufficiency that spanned the prenatal and postnatal period produced more profound deficits in PV staining than postnatal insufficiency alone. Of note, adult-onset hypothyroidism did not appear to impact the expression of PV in the cortex and hippocampus (48). Last but not least, the number of GABAergic neurons in the cortex and hippocampus was not altered by congenital hypothyroidism, indicating that the decrease in PV staining resulted from an alteration in phenotypic expression of PV, rather than neuronal loss (48). This was later confirmed by showing that hypothyroid rats did not differ from controls in the number of cells that expressed a GABA-synthesizing enzyme, GAD67 [glutamic acid decarboxylase 67 aka GAD1; (50)]. Intriguingly though, the expression of another GAD isotype, GAD65 (aka GAD2), was significantly reduced in both neuronal somata and processes in the hippocampus of the same hypothyroid rats (50). In a separate study, it was also found that the protein levels of GAD67 were lower in the medial prefrontal cortex of hypothyroid, compared to control, rats (51). In rats, but not in mice (52), a defect in neuronal migration causes heterotopia, i.e. the accumulation of gray matter in the corpus callosum (53). Of note, a few GABAergic neurons have been identified within the heterotopia, even though they constitute a minority of the heterotopic cells.

Electrophysiology studies of the dentate gyrus of the hippocampus in adult rats that were hypothyroid during development, have revealed that alterations in GABAergic interneuron populations were associated with functional deficits in inhibitory synaptic transmission (48, 54). Accordingly, in the hippocampus of hypothyroid rats at PND15, there was a near 80% reduction in KCC2 protein, a neuron-specific K^+/Cl^- cotransporter that is a key player in determining the response of excitatory neurons to GABAergic neurotransmission (50).

3.2 Genetically-modified mouse models shed light on the molecular mechanisms underlying TH action on developing GABAergic neurons

Mutations of proteins of the TH signaling pathway, notably TRs and TH transporters, often cause defects in GABAergic neuron differentiation in the cerebellum, cortex, hippocampus and other brain regions (Table 1).

In several instances, it was found that mutant mice expressing a *Thra* or *Thrb* knock-in mutation exhibited stronger phenotypes than mice in which *Thra* or *Thrb* had been knocked out. This results from a number of reasons, notably that (12)some of the knock-in mutated alleles encoding for TRs exert dominant-negative activity: they prevent the normal function of intact TRs that are still present in cells. Therefore, some germline *Thra* knock-in mutations have particularly drastic effects on brain development, even in heterozygous mice (55). Indeed, dominant-negative receptors constitutively interact with corepressor proteins, and thus permanently repress the expression of TR target genes, whether TH is present or not. Moreover, it has been observed that *Thra* knock-in mutations, encoding for dominant-negative forms of TRα1, do not only affect the transcription of TRα1 target genes, but also induce a repression of known TRβ1 target genes, thus strengthening the impact on the resulting phenotype (56). However, the main explanation for the mild neurological consequences of KOs is that getting rid of TRs does not only eliminate TH-induced activation of gene expression, but also eliminates the transcriptional repression mediated by unliganded or mutant receptors (12, 57).

3.2.1 Cerebellum

Mice with a dominant-negative *Thrb* allele exhibit severe neurological deficiencies, notably a marked impairment in balance and coordination, and profound defects in cerebellar development, notably in the number and arborization of cerebellar Purkinje cells (58, 59). By contrast, no reduction in Purkinje cell number was found in *Thrb* KO mice, which appeared to exhibit normal neurological development, with the exception of a loss of auditory function (60, 61).

In the cerebellum of TRα1 KO mice, there was no apparent defect in granule cell migration, nor in Purkinje cell morphology (12), but further analyses revealed a reduced number of GABAergic interneuron precursors between PND4 and PND10, a reduced rate of proliferation of GABAergic interneuron precursors in the white matter at PND6 as well as a reduced expression of a GABAergic transporter (GAT-1) at PND11 (46).

The development of the cerebellum was also found to be significantly impaired in *Dio3*$^{-/-}$ mice, in which the intracellular TH content is increased (62). Notably, *Dio3*$^{-/-}$ mice exhibited accelerated expansion of the molecular layer, which contains the

TABLE 1 Mouse models with gene mutations that are cited in the present paper.

Protein	Protein function	Type of mutation	Floxed	Mouse Genome Informatics reference*	Alias	GABAergic phenotype
Type 2 deiodinase	Conversion of T4 into T3	KO		$Dio2^{tm1Acb}$	*Dio2 KO*	Weak
Type 3 deiodinase	Conversion of T4 and T3 into inactive metabolites	KO		$Dio3^{tm1Stg}$	*Dio3 KO*	Weak
Oatp1c1	TH transporters	KO	Yes	$Slco1c1^{tm1Arte}$	*Oatp1c1fl*	No
Mct8		KO		$Slc16a2^{tm1a(KOMP)Wtsi}$	*Mct8 KO*	No
		KO		$Slc16a2^{tm1Dgen}$	*Mct8 KO*	No
		KO		No MGI reference. See Wirth et al. *J. Neurosci.*, July 29, 2009, 29(30):9439 –9449	*Mct8-*	No
		KO		$Slc16a2^{tm1.1Sref}$	*Mct8 KO*	Yes
		KO	Yes	$Slc16a2^{tm1c(KOMP)Wtsi}$	*Mct8fl*	Yes
		Missense KI (P253L)		$Slc16a2^{em2Agfz}$	*P253L*	Yes
TRα1	Nuclear receptor of T3	Frameshift KI		$Thra^{em1Ffla}$ to $Thra^{em4Ffla}$	$Thra^{S1,S2,L1,L2}$	Yes
		Frameshift KI	Yes	$Thra^{em6Ffla}$	$Thra^{Slox}$	Yes
		KO		$Thra^{tm1Ven}$	$TR\alpha1^{KO}$	No
		KO		$Thra^{tm2Jas}$	$TR\alpha^{0}$	No
		KO		$Thra^{tm1Jas}$	*TRα-*	No
		Missense KI (L400R)	Yes	$Thra^{tm1Ffla}$	$Thra^{AMI}$	Yes
		Missense KI (R384C)		$Thra^{tm3Ven}$	$TR\alpha1^{m}$	Yes
TRβ1 TRβ2	Nuclear receptors of T3	KO		$Thrb^{tm1Df}$	*Thrb KO-*	No

* https://www.informatics.jax.org/

All these models were used to analyze the function of thyroid hormone in mouse brain development, sometimes in combination with one another.

dendritic tree of Purkinje cells. However, the number of Purkinje cells did not differ between *Dio3*$^{-/-}$ and control mice. Notably, the expansion of the molecular layer follows a normal timing in *Dio3*$^{-/-}$ *TRα1*$^{-/-}$ double KO (DKO) mice, indicating a role for TRα1 in mediating the action of TH on Purkinje cell maturation.

In knock-in mice expressing $TR\alpha1^{R384C}$, which are characterized by a 10-fold reduction in the affinity of TRα1 to TH, there was an overall delay in the development of the cerebellum. Cerebellar Purkinje cells showed a delayed, but otherwise normal, arborization (2). At PND9, the expression of PV, calbindin and calretinin was lower in mice expressing $TR\alpha1^{R384C}$ than in control mice, but these differences were normalized a few days later (63). By PND21, the structure of the cerebellum was similar in mice expressing $TR\alpha1^{R384C}$ and in control littermates. Notwithstanding, adult mice expressing $TR\alpha1^{R384C}$ showed reduced motor performance on the Rotarod. T3 treatment during PND10-PND35 resulted in complete normalization of their locomotor behavior as adults. By contrast, T3 treatment in adults did not improve performance (2), indicating the existence of a specific time window for the action of TH/TRα1 signaling on brain development.

A series of mouse models mimicking human *THRA* mutations resulted in various degrees of alteration of the molecular functions of TRα1 (64). However, these mice exhibited little defects in cerebellar histology, the most notable defect being a slight reduction in the density of PV-expressing GABAergic interneurons in the molecular layer. The mild phenotype of these mice with frameshifts produced by genome editing contrasts with the severity of the phenotype of previously used *Thra* knock-in mice. Further investigations have revealed that the elimination of alternate splicing in these knock-in mice increased the expression level of the mutated TRα1 receptor and the severity of the phenotype (64).

In mice lacking both TH transporters, Mct8 and Oatp1c1 (*Mct8/Oatp1c1* DKO mice), TH signaling in the brain is significantly reduced and the arborization of the dendritic tree of Purkinje cells is significantly delayed, due a defect in intraneuronal transport of TH (65).

Finally, Amano et al. (66) have reported transient postnatal cerebellar defects, including alterations in granule cell migration and in Purkinje cell electrophysiological properties, in a mouse model of hypothyroidism, *Duoxa*$^{-/-}$ KO mice, which lack a dual

oxidase that is essential for thyroid hormone synthesis. In particular, despite the fact that cerebellar histology returned to normal on postnatal day 25, motor coordination was still impaired at that age in *Duoxa*$^{-/-}$ mice, suggesting irreversible behavioral defects in these mice.

3.2.2 Cerebral cortex

In 2008, Wallis et al. (63) provided a detailed histological study of different subtypes of cortical GABAergic interneurons in knock-in mice expressing TRα1^{R384C}. Consistent with what had previously been described in hypothyroid rats, they found a developmental delay in the appearance of PV immunoreactive neurons in these mutant mice. An electrophysiological investigation of the PND19-PND21 cortex of mouse pups expressing TRα1^{R384C} revealed a 10-fold reduction in fast spiking neurons compared to controls. This was in line with the results of the immunohistochemical study, since many cortical PV immunoreactive cells are fast spiking neurons. At adult stages though, the density in PV neurons did not significantly differ between mutant and control mice (63, 67).

PV-expressing neurons were not the only GAABAergic neuron subtype found to be impacted by impaired TH signaling. Indeed, in mice expressing TRα1^{R384C}, the density of calretinin-positive neurons in the cortex was significantly increased in adult mutant mice, compared to control mice. Regarding calbindin immunoreactivity, the authors described different results depending on the cortical layers under study: while mutant mice exhibited a lower density of calbindin-positive cells in layers II-III, there were no significant differences between mutant and control mice in layers IV-VI. The population of cortical somatostatin-positive neurons did not differ between mutant and control mice. Moreover, the total number of GABAergic cells in the cortex, as assessed by GAD67 immunoreactivity, did not differ significantly between mutant and control mice, indicating that the proliferation and migration of cortical GABAergic neuron precursors was unaffected by the mutation. As a whole, these results indicated that impaired TH/TRα1 signaling impacted the maturation of several populations of cortical GABAergic neurons, but the effects differed depending on the subtype of GABAergic neuron under study (63).

In an attempt to rescue the expression of PV in young mice expressing TRα1^{R384C}, Wallis et al. (63) treated mutant mouse pups with TH between PND11 and PND13, but this failed to induce the expression of PV in the short term. By contrast, PV expression was restored in PND14 mice expressing TRα1^{R384C} that were exposed to high levels of TH from around birth. This suggests that TH/TRα1 signaling does not directly regulate PV expression, but rather influences the cell maturation process in a broader way.

Blocking TH entry into the brain also severely compromises the differentiation of cortical GABAergic interneurons. Indeed, Mayerl et al. (65) have recorded significantly reduced PV and Gad67 immunoreactivity (Gad67 being used as a marker of all GABAergic interneurons) in the somatosensory cortex of 12-day old and adult *Mct8/Oatp1c1* DKO mice, indicating that these defects were not transient, but permanent. In addition, they observed in the somatosensory cortex of adult, but not 12-day old, mice, a significant increase in the density of calretinin neurons. These results are congruent with those obtained in mice expressing TRα1^{R384C}, in which the affinity of TRα1 for TH is significantly reduced (63). In agreement with the previous results, in *Mct8/Dio2* DKO mice, PV expression in cortical neurons was also found to be significantly reduced until adulthood (67). Moreover, several classes of GABAergic interneurons were found to be affected in mice expressing a mutated Mct8 transporter (P253L) mimicking a mutation found in human patients: in the cortex of these mice at adult stage, a decreased density of PV-, calbindin- and GAD65/67-positive neurons, as well as an increased density of calretinin-positive neurons, were reported (68).

3.2.3 Hippocampus

TRα1$^{-/-}$ mice showed reduced PV perisomatic terminals on hippocampal CA1 pyramidal neurons, compared to controls (69). These structural defects were associated with poor performance in hippocampal-dependent behavioral tasks.

Likewise, in adult mice expressing TRα1^{R384C} dominant negative receptor, the number of PV-positive cell somata and the density of PV-positive terminals in the CA1 region of the hippocampus were found to be significantly reduced, compared to control mice (2). Fast-spiking PV-expressing interneurons are involved in the generation of rhythmic network oscillations in the gamma frequency range, which play an important role in higher processes in the brain, such as learning, memory, cognition and perception (70, 71). Extracellular field recordings from the stratum pyramidale in hippocampal slices (63) showed that the gamma oscillation frequency (20–80 Hz) was significantly lower in mutant mice expressing TRα1^{R384C}, compared to controls, which was congruent with the reduced number of PV-expressing neurons (63). Moreover, hippocampal pyramidal neurons from mice expressing TRα1^{R384C} showed hypoexcitablility, compared to those of control mice (72). The notable impairments in the maturation of GABAergic neurons in knock-in mice expressing TRα1^{R384C} led the authors to suspect that these mice might be more susceptible to epilepsy than control mice. Unexpectedly, they were found to present a marked resistance to pentylenetetrazole-induced seizures, compared to control mice (72). Accordingly, pentylenetetrazole induced a significant increase in neuronal activity in the hippocampus of control mice, but not of mice expressing TRα1^{R384C}. This phenotype was likely due to altered chloride homeostasis in principal neurons of mutant mice. In normal mouse neurodevelopment, GABAergic transmission is excitatory at early postnatal stages. During the second and third weeks of life, changes in the expression of chloride channels in principal neurons lead GABAergic transmission to switch from excitatory to inhibitory (73). Since Hadjab-Lallemend and colleagues (72) have found that mice expressing TRα1^{R384C} exhibited an imbalance in chloride channel subtypes in principal neurons, it is suspected that in these mice GABAergic transmission is maintained in an immature state, *i.e.* excitatory, until adulthood. Exposure to high levels of TH during both embryonic and postnatal developmental periods combined but not in adulthood, allowed to normalize the seizure behavior observed in these mutant mice (72).

The brain defects observed in mice expressing TRα1^{R384C} were also accompanied by significant changes in hippocampal-dependent behavior, indicative of increased anxiety and impaired memory (2). Interestingly, most of these behavioral defects, together with the structural defects in the hippocampus, could be reversed by exogenous administration of a high dose of TH for 12 days in adulthood. By contrast, the anxiety and memory defects observed in adulthood could not be prevented by an early TH treatment (between PND10 and PND35) (2). The latter results on mice expressing TRα1^{R384C} are at odds with the clinical observation that many of the defects induced by altered TH signaling on brain development are irreversible unless they are treated early in life. They underscore the complexity of TH action in the brain, and the necessity to get a better knowledge of the timely action of TH in different brain regions.

Intriguingly, a short-term treatment of knock-in mice expressing TRα1^{R384C} with a GABA receptor antagonist (pentylenetetrazol) rescued their memory performance, and this was accompanied by histological and electrophysiological changes reflecting an increase in the local excitatory drive in the CA1 region of the hippocampus (74).

In mice expressing a mutated Mct8 transporter (P253L), histological analysis of the hippocampus revealed defects in GABAergic interneuron populations that were similar to those previously described in the cortex: decreased density of PV-, calbindin- and GAD65/67-positive neurons, as well as increased density of calretinin-positive neurons (68).

3.2.4 Hypothalamus

Mittag et al. (75, 76) have described a population of PV-expressing neurons in the mouse anterior hypothalamus, which requires prenatal signaling *via* both TRα1 and TRβ isoforms for proper development. These neurons are involved in the central autonomic control of blood pressure and heart rate, and are also temperature-sensitive. As hypothyroidism in humans is associated with bradycardia (77), it is conceivable that these effects are mediated by PV-expressing hypothalamic neurons. However, to our knowledge, there is no evidence that this population of PV-expressing neurons is GABAergic, as Laing et al. (78) have recently reported that anterior hypothalamic PV-expressing neurons in mice are glutamatergic.

3.3 Conditional mutant mouse models targeting specific cell types point to a direct effect of TH/TR signaling in developing GABAergic neurons

Rodent models of hypothyroidism as well as classical knock-in and KO mouse lines, as reviewed in the preceding paragraphs, have shed light on the complex influence of thyroid hormone on brain development, with GABAergic neurons appearing as particularly sensitive to impaired TH signaling. The advent of conditional mutagenesis, allowing to alter TH signaling in specific cell types, has allowed to get more insight into the brain cell types in which TH has a direct action.

Thra^{AMI} allele encodes for a dominant-negative version of TRα1 (TRα1^{L400R}), which is expressed only in cells where Cre recombinase is present (55). Ubiquitous expression of TRα1^{L400R} was shown to induce a severe phenotype, leading to death around the 3rd or 4th week of life (55). The same level of severity was observed when TRα1^{L400R} was expressed exclusively in brain cells (79). A detailed histological analysis of the cerebellum in these mice has revealed profound alterations in neuronal and glial differentiation, which were reminiscent of congenital hypothyroidism, including a strong reduction in the size and density of Purkinje cell arborization, a delay in GABAergic interneuron maturation, a delay in the migration of granule cell progenitors and abnormal Bergmann glia maturation (80). Crossing *Thra^{AMI}* mice with mice expressing Cre in specific cerebellar cell types allowed to carry out a genetic dissection of the effects of TH in the developing cerebellum (81). The principal targets of TH in the cerebellum proved to be Purkinje cells, GABAergic interneurons, oligodendrocyte precursor cells and Bergmann glia (79, 82). Strikingly, the migration of granule cell precursors was altered when TH signaling was blocked specifically in Bergmann glia, or in Purkinje cells and GABAergic interneurons, but not in the least when TH signaling was blocked in granule cells themselves. Similar observations have been made in mice expressing a dominant-negative TRβ receptor in cerebellar Purkinje cells. Indeed, these mutant mice exhibited delayed Purkinje cell dendrite arborization, as well as delayed granule cell migration (83). Collectively, these results indicate that the defect in radial migration of granule cell precursors, which is a typical hallmark of the hypothyroid cerebellum, is not a cell-autonomous consequence of the lack of TH signaling, but rather results from an alteration of granule cell precursor environment (79).

Mice expressing a mutated dominant negative TRα1 receptor in all GABAergic neurons (either TRα1^{L400R} or TRα1^{E395fs401X}) were found to present epileptic seizures as early as 11 days of age (3). At two weeks of age, the maturation of GABAergic neurons of different types (PV-, somatostatin-, NPY- or calretinin-expressing cells) appeared to be severely impaired, in the cerebellum as well as in the cortex, hippocampus and striatum. In particular, the density of PV-expressing neurons was drastically reduced in all these brain areas. Most of these mice died before the end of the 4th week of life. The mice that survived until adulthood exhibited signs of hyperactivity and the defects in GABAergic neurons were still present. Notably, there was no normalization of PV expression over time (3). This was the first demonstration that TH signaling has a cell-autonomous effect influencing the maturation of GABAergic neurons, and that this developmental effect has lifelong consequences.

Mice expressing a dominant-negative TRβ receptor in cerebellar Purkinje cells were found to exhibit significant impairment in altered long-term synaptic plasticity at parallel fiber–Purkinje cell synapses in adulthood, even though there was no abnormality in the morphology or basal properties of these synapses at this age (84). These results stress the importance of TH action during neural development in establishing proper cerebellar function in adulthood, even if cerebellar morphology appears to be normal.

Conditional mutagenesis was also used to abolish TH transporter expression specifically in progenitors of PV interneurons [*Mct8 fl/fl; Oatp1c1 fl/fl; Nkx2.1Cre* mice (85)]. This induced a reduction in the density of PV+ interneurons, as well as an increase in the density of calretinin-positive neurons in the somatosensory cortex of 12-day old pups. These results clearly point to PV-expressing neurons as direct targets of TH signaling during development. However, cell numbers normalized in the adult conditional KO mice, whereas these changes were sustained at later time points when the same transporters were knocked out ubiquitously (*Mct8/Oatp1c1* DKO mice), indicating that the influence of TH on PV neuron maturation relies not only on cell-autonomous effects, but also on TH signaling in other cell types (85). As Sonic hedgehog (Shh) signaling pathway in the medial ganglionic eminence is known to play a key role in determining the fate of PV neuron progenitors (86), the level of activation of this pathway was assessed in ubiquitous *Mct8/Oatp1c1* DKO mice and in conditional *Mct8 fl/fl; Oatp1c1 fl/fl; Nkx2.1Cre* mice. At early stages of brain development, *i.e.* E12.5, it was found that Shh signaling was significantly reduced in the medial ganglionic eminence of *Mct8/Oatp1c1* DKO mice, but not in conditional *Mct8 fl/fl; Oatp1c1 fl/fl; Nkx2.1Cre* mice. In other words, Shh pathway in PV neuron progenitors was impacted when TH transporters were knocked out ubiquitously, but not when they were knocked out specifically in PV neuron progenitors. This indicates that non-cell autonomous mechanisms must relay the influence of TH on Shh signaling pathway in PV neuron progenitors of the medial ganglionic eminence (85).

As a conclusion, the current understanding is that what was initially found in the cerebellum also holds true in the rest of the brain: TH acts directly on a limited number of cell types, notably GABAergic neurons, but its influence propagates to other cell types through intercellular communication, notably *via* neurotrophins (79, 82).

4 Challenges in identifying TR target genes in developing GABAergic neurons

4.1 Identification of TR target genes in developing GABAergic neurons in rodents

Since RNA-seq has advantageously replaced microarray analysis, a growing number of datasets of gene expression linked to TH signaling has accumulated [reviews in (87) and (41)]. These results are theoretically suitable for identifying genes which are putative TR target genes in GABAergic neurons and identifying the molecular mechanisms that lead from TH stimulation to neuronal maturation. However, this remains a difficult task. To start with, although early studies have shown that a few genes, notably *Hr* and *Klf9*, are T3-responsive in many cell types (88, 89), more recent studies have mainly demonstrated that the repertoire of TH-responsive genes widely varies across cell types and brain areas (41). Thus, it finally appears that the overlap between sets of TR target genes in different types of cells might be limited. As regards developing GABAergic neurons, this implies that TH might not play the same role in cortical fast-spiking parvalbumin neurons, striatal medium spiny neurons or cerebellar Purkinje cells, to mention a few.

In spite of continuous advances in gene expression analysis techniques, identifying true TR target genes in developing GABAergic neurons remains challenging, for a number of reasons. One major issue is to handle the extreme cellular heterogeneity of the brain. As GABAergic neurons represent a minority of the cell population in most brain areas, the response to TH in GABAergic neurons is often masked by the response to TH in other cell types. The striatum is a favorable exception, as it is mainly populated by GABAergic medium spiny neurons (3, 90). For brain areas where GABAergic neurons are less abundant, RNA sequencing can be advantageously coupled to cell sorting in order to analyze gene expression levels in a specific cell type.

Several criteria should be fulfilled for a gene to be considered as a direct TR target gene. First, if one considers that TRs are essentially transcription activators, their target genes are expected to be down-regulated in the brain of hypothyroid mice or in the brain of mice carrying mutations that impair TH signaling (74, 91–93). Gene expression analyses in a variety of mouse models with impaired thyroid hormone signaling have confirmed that TR KO mice have an attenuated phenotype compared to hypothyroid mice, which is in agreement with a potent role of unliganded TRs in the repression of gene expression (13).

Second, when comparing gene expression levels between different conditions in a given brain region, one must take into account that cell composition may differ between conditions. In the analyses of mixed cell populations, like the whole cortex, whole striatum (3) or primary neuronal cell cultures prepared from fetal cortex (94) or from post-natal cerebellum (95), a decrease in the abundance of a GABAergic neuron-specific mRNA caused by hypothyroidism or by a genetic mutation is not sufficient to conclude that TH directly regulates the transcription of this gene within GABAergic neurons. An alternative explanation is that the long-term alteration of TH signaling has modified the composition of the cell population in hypothyroid/mutant mice, and that GABAergic neurons are under-represented in the brain area under study, when compared to control mice. A way to circumvent this problem is to analyze gene expression levels a few hours after treating mice with TH, and combine these results with those obtained in hypothyroid and mutant mouse groups. Considering genes that are upregulated shortly after TH treatment and downregulated in mice with impaired TH signaling tightens the analysis around potential TR target genes, while avoiding secondary effects due to tissue reorganization.

A third difficulty in determining the direct influence of TH/TR signaling on the transcription of a given gene in GABAergic neurons is to rule out effects that are downstream of TH signaling. Indeed, in many genetically modified animals as well as in models of pharmacologically-induced hypothyroidism, general growth and development are significantly affected, so that it is likely that there are additional factors, secondary to TH signaling disruption, that contribute to the neurological status and

neuroanatomical integrity. Thus, changes in gene expression that are recorded in GABAergic neurons may be secondary to an extracellular event, such as induction of neurotrophin secretion by T3 by neighboring cells (96). Primary cell cultures constitute a way to reduce interactions between neighboring cell types (94, 95). One of the most powerful methods to investigate what is going on in a specific cell type *in vivo* relies on Cre/loxP recombination, which allows the mutation of specific genes in specific cell types. This approach was used to study gene expression in the striatum of $Thra^{AMI/gn}$ mice, in which the expression of the dominant-negative $TR\alpha1^{L400R}$ mutant receptor selectively abrogates response to TH in GABAergic neurons. As a whole, the putative direct TR target genes identified in that study did not highlight a specific pathway, but rather illustrated that TH signaling in GABAergic neurons is likely to affect a wide variety of functions such as cellular interactions, axon pathfinding or electrical and synaptic activity of the cell (3).

Finally, the cell-autonomous response of gene expression, as identified by RNA sequencing data from cell type-specific mutant mouse models, is not a full demonstration for a TR-mediated transactivation. Indeed, the effect of TH on a given gene can also be secondary to an intracellular event. For example, it can result from the TH-induced upregulation of a transcription activator. Although a time-course analysis following short-term TH treatment helps to recognize genuine TR target genes, one of the best current indications for a direct transcriptional activation relies on chromatin analysis. In the striatum, the expression of a tagged TRα1 expressed only in GABAergic neurons has allowed to address the occupancy of chromatin at a genome-wide scale. This has led to the conclusion that, although thousands of genomic sites are occupied by TRα1, the number of genes that are transcriptionally activated by the ligand-activated receptor is surprisingly small (3). Atac-seq analysis may be used to identify TH-induced changes in chromatin compaction, which indirectly inform of TR occupancy. One of the main advantages of this technique is that it can be efficiently implemented even when starting with small cell numbers (97).

Up to now, the analysis of TR target genes has failed to provide a unified picture of the influence of TH in GABAergic neurons. However, it is clear that many genes identified as TH-responsive in primary cultures of cortical neurons are related to the radial migration and terminal differentiation of cortical GABAergic interneurons (94). Gene expression analyses have also provided interesting working hypotheses, some of which have been tested in *in vitro* systems. Thus, it has been shown that a crosstalk between the signaling pathways mediated by TH on the one hand, and by αvβ3 integrin on the other hand, seems to play an important role in postnatal dendritic arborization of Purkinje cells (98). Another notable example is the demonstration that an up-regulation of *Klf9* by TH is a key event in the postnatal loss of the regenerative capacity that Purkinje cells display after axotomy (99).

When analyzing genome-wide datasets, a special attention has often been paid to the *Pvalb* gene, which encodes PV. Indeed, histological analyses have consistently shown a reduction in PV expression in rodent models with altered TH signaling (see section 3 in the present review). In a microarray analysis conducted in the cortex and striatum of 21-day-old hypothyroid mouse pups, *Pvalb* came out as one of the most strongly downregulated genes (13). Even subclinical hypothyroidism was shown to induce a large fold decrease in *Pvalb* mRNA expression in 14-day-old rats (100). Moreover, *Pvalb* mRNA levels in the cortex and striatum were significantly lower in $TR\alpha1^{-/-}$ and $TR\alpha1^{-/-}$ $TR\beta1^{-/-}$ mouse pups than in control mice. By contrast, *Pvalb* mRNA levels were not affected in $TR\beta1^{-/-}$ mice, suggesting a predominant implication of TRα1 in mediating the effects of TH on PV expression (13). Finally, in $Thra^{E403X/E403X}$ mice, which express the first *Thra* mutation that was discovered in a patient, RNA-sequencing analysis has shown that genes such as *Flywch2*, *Pvalb*, and *Syt2*, which are preferentially expressed in PV-expressing neurons, were downregulated compared to control mice (93). As a conclusion, *Pvalb* expression is significantly reduced in mouse models with altered TH signaling, but up to now there is no convincing evidence that *Pvalb* is a direct target gene of TRs.

4.2 Insights from gene expression studies in the human brain

Even if the rodent brain is widely used as a model to decipher what is going on in the human brain, the brains of rodents and primates differ in several ways and studies in the human brain, when available, are extremely valuable to help translating the rodent data to the clinic. Notably, in the primate cortex, GABAergic neurons account for about 20% of the total neuron population, whereas in rodents, this percentage is about 15%. This difference is mainly due to an increase in the calretinin-expressing interneuron population. It is thought that the increased interneuron population is related to the increased associative functions and connectivity of the primate cortex, compared to the rodent cortex (101). Another major difference between the mouse and human brains relates to TH transporters in the blood-brain-barrier: in mice, both Mct8 and Oatp1c1 play a role in TH entry into the brain, whereas Oatp1c1 is not present in the human blood-brain-barrier. This explains why disruption of the *Mct8* gene in mice does not result in neurological impairment, while it has severe consequences in humans (101, 102).

Datamining in single cell RNA-seq studies was performed for the human fetal cortex at gestational weeks 16–18, equivalent to mid gestation in rodents (103). Although a similar analysis has not been performed in mice, it seems that the expression pattern of the main components of TH signaling is not the same in human and rodents. In particular, some cells of the human GABAergic lineage express *THRB* at this early stage, whereas it appears that *Thrb* expression is induced at later stages in the mouse brain (8). More precisely in humans, *THRB* expression is predominant in the subpopulation of GABAergic neuron progenitors migrating from the caudal ganglionic eminence and in calretinin-expressing interneurons that derive from these progenitors. This raises the interesting possibility that *THRB* mutations selectively alter calretinin-expressing GABAergic interneurons in the human cortex. Moreover, *SLC16A2* (encoding Mct8 transporter) and *THRA* show widespread expression in most human cortical cell types.

5 Concluding considerations

GABAergic neurons, and notably PV-expressing neurons, are a main target of TH signaling during brain development. Although the precise instrumental role of TH in these neurons remains elusive, a widely accepted working hypothesis considers that TH promotes the transition from the embryonic to adult pattern of gene expression in the brain (94, 104). For example, TH is involved in triggering the loss of axon regenerative capacity in Purkinje cells (99), such loss of axon regenerative capacity being a hallmark of brain maturation in rodents (105). At a wider scale, it is tempting to speculate that TH is involved in the regulation of critical periods of heightened plasticity in the brain (106). In agreement with such hypothesis, blocking TR signaling specifically in GABAergic neurons was found to significantly impair the development of perineuronal nets, which constitute a specialized extracellular matrix enwrapping mature PV-expressing neurons (3). Thus, TH signaling might trigger the setting-up of perineuronal nets, which stabilizes neuronal networks after taking into account the input from environmental stimuli (107). Such mechanisms are critical for proper brain development.

GABAergic neurons are fundamental for maintaining the balance between excitation and inhibition throughout the brain (108). In particular, PV-expressing neurons play key roles in the coordination of neuronal networks and associated oscillations (70). Thus, as impaired TH signaling during brain development significantly affects GABAergic neurons in general, and PV-expressing neurons in particular, this may account for many of the neurological disorders seen in patients with impaired TH signaling. Indeed, as was previously mentioned, studies that were carried out in in the last ten years have revealed that patients with *THRA* mutations display a high risk of epilepsy and ASD (Section 2 of the present review).

Besides being highly sensitive to altered TH signaling, PV-expressing neurons appear as an important node in many neurodevelopmental disorders, including ASD and epilepsy. ASD is a multifactorial neurodevelopmental disorder that encompasses a complex and heterogeneous set of traits. One unifying explanation for the complexity of ASD may lie in the disruption of the balance between excitatory and inhibitory circuits during critical periods of development (109), which echoes our current understanding of TH action in GABAergic circuits. Moreover, post-mortem studies of the cerebral cortex of ASD patients have revealed that the number of PV-expressing interneurons was decreased, and that *Pvalb* was the most strongly downregulated gene, compared to control patients (110, 111). Finally, Berbel and collaborators (112) have highlighted that brain morphological changes observed in mouse models of developmental hypothyroidism, such as alterations in cortical lamination, high neuronal density in several hippocampal layers, poor differentiation of the gray-white matter boundary or neuronal heterotopias, resembled the brain lesions of children with autism. The same authors noted that a large number of genes that have been found to be TH-regulated at the transcriptional level in rodent cerebral cortex have also been found to be mutated in ASD patients (112, 113).

As for ASD, epilepsy encompasses a group of multifactorial diseases, suggesting that diverse genetic or environmental insults may impair common pathways, leading in the end to symptoms of epilepsy. Again, PV-expressing neurons might be at the crossroads of these common pathways. Indeed, impaired development or function of PV-expressing interneurons has been associated with some genetic forms of epilepsy in humans (114). As a consequence, PV-expressing neurons have been identified as a critical target of therapeutic approaches in epilepsy (115).

Collectively, the convergence of symptoms between hypothyroid, epileptic and ASD patients suggests that common pathways involving PV-expressing neurons might underlie these pathologies of brain development. Such convergence might partly be linked to comorbidities that contribute independently to the overt pathology, but in any case, improving our understanding of the role of TH in the development of the GABAergic system, notably in PV-expressing neurons, should help make progress in the prevention and treatment of several neurological disorders. In addition, deciphering the network of TH target genes in the brain may help detect pharmacological or chemical agents that are likely to disrupt TH signaling, and give an insight on subtle neurological insults that may result from exposure to such TH system-disrupting chemicals (116). However, there is still a long way to go before we understand the precise molecular mechanisms underlying TH action in the brain. Notably, the huge diversity of GABAergic neurons (117) makes it difficult to depict a unified view of the mechanisms of action of TH in these neurons. It is hoped that the advent of single-cell RNA sequencing (118) and of spatio-temporal transcriptomics (119) will help untangling the role of TH signaling in each GABAergic neuron subtype, in each brain region, at all developmental stages.

Author contributions

FF: Writing – original draft, Writing – review and editing. SR: Writing – original draft, Writing – review and editing. JR: Writing – review and editing.

Funding

JR was supported by grants of the China Scholarship Council and ENS de Lyon, within the framework of the PROSFER program (Program of Sino-French Education for Research). Research in our group is funded by the European Union's Horizon 2020 research and innovation program, under grant agreement no. 825753 (ERGO) and by the French Agence Nationale de la Recherche (Hypothyro project, ANR 22-CE14-0026-01).

Conflict of interest

The authors declare that the research was conducted in the absence of any commercial or financial relationships that could be construed as a potential conflict of interest.

The author(s) declared that they were an editorial board member of Frontiers, at the time of submission. This had no impact on the peer review process and the final decision.

Publisher's note

All claims expressed in this article are solely those of the authors and do not necessarily represent those of their affiliated organizations, or those of the publisher, the editors and the reviewers. Any product that may be evaluated in this article, or claim that may be made by its manufacturer, is not guaranteed or endorsed by the publisher.

References

1. Bernal J. Thyroid hormones in brain development and function. In: Feingold KR, Anawalt B, Boyce A, Chrousos G, de Herder WW, Dhatariya K, editors. *Endotext*. South Dartmouth (MA: MDText.com, Inc (2015). p. 1–62.

2. Venero C, Guadaño-Ferraz A, Herrero AI, Nordström K, Manzano J, de Escobar GM, et al. Anxiety, memory impairment, and locomotor dysfunction caused by a mutant thyroid hormone receptor alpha1 can be ameliorated by T3 treatment. *Genes Dev* (2005) 19(18):2152–63. doi: 10.1101/gad.346105

3. Richard S, Guyot R, Rey-Millet M, Prieux M, Markossian S, Aubert D, et al. A pivotal genetic program controlled by thyroid hormone during the maturation of GABAergic neurons. *iScience* (2020) 23(3):100899. doi: 10.1016/j.isci.2020.100899

4. Braat S, Kooy RF. The GABAA receptor as a therapeutic target for neurodevelopmental disorders. *Neuron* (2015) 86(5):1119–30. doi: 10.1016/j.neuron.2015.03.042

5. Sait Gönen M, Kisakol G, Savas Cilli A, Dikbas O, Gungor K, Inal A, et al. Assessment of anxiety in subclinical thyroid disorders. *Endocr J* (2004) 51(3):311–5. doi: 10.1507/endocrj.51.311

6. Andersen SL, Laurberg P, Wu CS, Olsen J. Maternal thyroid dysfunction and risk of seizure in the child: a Danish nationwide cohort study. *J Pregnancy* (2013) 2013:636705. doi: 10.1155/2013/636705

7. Wiens SC, Trudeau VL. Thyroid hormone and gamma-aminobutyric acid (GABA) interactions in neuroendocrine systems. *Comp Biochem Physiol A Mol Integr Physiol* (2006) 144(3):332–44. doi: 10.1016/j.cbpa.2006.01.033

8. Bradley DJ, Towle HC, Scott Young IIIW. Spatial and temporal expression of α- and β-thyroid hormone receptor mRNAs, including the β2 subtype, in the developing mammalian nervous system. *J Neurosci* (1992) 12(6):2288–302. doi: 10.1523/JNEUROSCI.12-06-02288.1992

9. Minakhina S, Bansal S, Zhang A, Brotherton M, Janodia R, De Oliveira V, et al. A direct comparison of thyroid hormone receptor protein levels in mice provides unexpected insights into thyroid hormone action. *Thyroid* (2020) 30(8):1193–204. doi: 10.1089/thy.2019.0763

10. Bernal J, Pekonen F. Ontogenesis of the nuclear 3, 5, 3'-triiodothyronine receptor in the human fetal brain. *Endocrinology* (1984) 114(2):677–9. doi: 10.1210/endo-114-2-677

11. Itoh Y, Esaki T, Kaneshige M, Suzuki H, Cook M, Sokoloff L, et al. Brain glucose utilization in mice with a targeted mutation in the thyroid hormone α or β receptor gene. *Proc Natl Acad Sci U S A* (2001) 98(17):9913–8. doi: 10.1073/pnas.171319498

12. Morte B, Manzano J, Scanlan T, Vennström B, Bernal J. Deletion of the thyroid hormone receptor α1 prevents the structural alterations of the cerebellum induced by hypothyroidism. *Proc Natl Acad Sci* (2002) 99(6):3985–9. doi: 10.1073/pnas.062413299

13. Gil-Ibañez P, Morte B, Bernal J. Role of thyroid hormone receptor subtypes alpha and beta on gene expression in the cerebral cortex and striatum of postnatal mice. *Endocrinology* (2013) 154(5):1940–7. doi: 10.1210/en.2012-2189

14. Flamant F, Gauthier K, Richard S. Genetic investigation of thyroid hormone receptor function in the developing and adult brain. *Curr Top Dev Biol* (2017) 125:303–35. doi: 10.1016/bs.ctdb.2017.01.001

15. Erbas IM, Demir K. The clinical spectrum of resistance to thyroid hormone alpha in children and adults. *J Clin Res Pediatr Endocrinol* (2021) 13(1):1–14. doi: 10.4274/jcrpe.galenos.2020.2019.0190

16. Moran C, Chatterjee K. Resistance to thyroid hormone due to defective thyroid receptor alpha. *Best Pract Res Clin Endocrinol Metab* (2015) 29(4):647–57. doi: 10.1016/j.beem.2015.07.007

17. Ferrara AM, Onigata K, Ercan O, Woodhead H, Weiss RE, Refetoff S. Homozygous thyroid hormone receptor beta-gene mutations in resistance to thyroid hormone: three new cases and review of the literature. *J Clin Endocrinol Metab* (2012) 97(4):1328–36. doi: 10.1210/jc.2011-2642

18. Concolino P, Costella A, Paragliola RM. Mutational landscape of resistance to thyroid hormone beta (RTHβ). *Mol Diagnosis Ther* (2019) 23:353–68. doi: 10.1007/s40291-019-00399-w

19. Krude H, Kuhnen P, Biebermann H. Treatment of congenital thyroid dysfunction: Achievements and challenges. *Best Pract Res Clin Endocrinol Metab* (2015) 29(3):399–413. doi: 10.1016/j.beem.2015.04.004

20. Alshehri B, D'Souza DG, Lee JY, Petratos S, Richardson SJ. The diversity of mechanisms influenced by transthyretin in neurobiology: development, disease and endocrine disruption. *J Neuroendocrinol* (2015) 27(5):303–23. doi: 10.1111/jne.12271

21. Barez-Lopez S, Obregon MJ, Bernal J, Guadano-Ferraz A. Thyroid hormone economy in the perinatal mouse brain: implications for cerebral cortex development. *Cereb Cortex* (2018) 28(5):1783–93. doi: 10.1093/cercor/bhx088

22. Crantz FR, Silva JE, Larsen PR. An analysis of the sources and quantity of 3,5,3′-triiodothyronine specifically bound to nuclear receptors in rat cerebral cortex and cerebellum. *Endocrinology* (1982) 110(2):367–75. doi: 10.1210/endo-110-2-367

23. Luongo C, Trivisano L, Alfano F, Salvatore D. Type 3 deiodinase and consumptive hypothyroidism: a common mechanism for a rare disease. *Front Endocrinol (Lausanne)* (2013) 4:115. doi: 10.3389/fendo.2013.00115

24. Richard S, Flamant F. Regulation of T3 availability in the developing brain: the mouse genetics contribution. *Front Endocrinol (Lausanne)* (2018) 9:265. doi: 10.3389/fendo.2018.00265

25. Hulse A. Congenital hypothyroidism and neurological development. *J Child Psychol Psychiat* (1983) 24(4):629–35. doi: 10.1111/j.1469-7610.1983.tb00139.x

26. Prezioso G, Giannini C, Chiarelli F. Effect of thyroid hormones on neurons and neurodevelopment. *Horm Res Paediatr* (2018) 90(2):73–81. doi: 10.1159/000492129

27. Gilbert ME, Rovet J, Chen Z, Koibuchi N. Developmental thyroid hormone disruption: prevalence, environmental contaminants and neurodevelopmental consequences. *Neurotoxicology* (2012) 33(4):842–52. doi: 10.1016/j.neuro.2011.11.005

28. Kopel J. A global perspective on newborn congenital hypothyroidism screening. *Proc (Bayl Univ Med Cent)* (2020) 33(1):137–9. doi: 10.1080/08998280.2019.1668715

29. Persani L. Rescue of neurological development in congenital hypothyrodism: we should leave no stone unturned. *J Clin Endocrinol Metab* (2021) 106(12):e5267–e5269. doi: 10.1210/clinem/dgab487

30. Schwartz CE, May MM, Carpenter NJ, Rogers RC, Martin J, Bialer MG, et al. Allan-Herndon-Dudley syndrome and the monocarboxylate transporter 8 (MCT8) gene. *Am J Hum Genet* (2005) 77(1):41–53. doi: 10.1086/431313

31. Remerand G, Boespflug-Tanguy O, Tonduti D, Touraine R, Rodriguez D, Curie A, et al. Expanding the phenotypic spectrum of Allan-Herndon-Dudley syndrome in patients with SLC16A2 mutations. *Dev Med Child Neurol* (2019) 61(12):1439–47. doi: 10.1111/dmcn.14332

32. Grijota-Martinez C, Barez-Lopez S, Gomez-Andres D, Guadano-Ferraz A. MCT8 deficiency: the road to therapies for a rare disease. *Front Neurosci* (2020) 14:380. doi: 10.3389/fnins.2020.00380

33. Groeneweg S, van Geest FS, Abaci A, Alcantud A, Ambegaonkar GP, Armour CM, et al. Disease characteristics of MCT8 deficiency: an international, retrospective, multicentre cohort study. *Lancet Diabetes Endocrinol* (2020) 8(7):594–605. doi: 10.1016/S2213-8587(20)30153-4

34. López-Espíndola D, Morales-Bastos C, Grijota-Martinez C, Liao XH, Lev D, Sugo E, et al. Mutations of the thyroid hormone transporter MCT8 cause prenatal brain damage and persistent hypomyelination. *J Clin Endocrinol Metab* (2014) 99(12):E2799–804. doi: 10.1210/jc.2014-2162

35. Moran C, Schoenmakers N, Agostini M, Schoenmakers E, Offiah A, Kydd A, et al. An adult female with resistance to thyroid hormone mediated by defective thyroid hormone receptor alpha. *J Clin Endocrinol Metab* (2013) 98(11):4254–61. doi: 10.1210/jc.2013-2215

36. van Gucht AL, Meima ME, Zwaveling-Soonawala N, Visser WE, Fliers E, Wennink JM, et al. Resistance to thyroid hormone alpha in an 18-month-old girl: clinical, therapeutic, and molecular characteristics. *Thyroid* (2016) 26(3):338–46. doi: 10.1089/thy.2015.0463

37. Le Maire A, Bouhours-Nouet N, Soamalala J, Mirebeau-Prunier D, Paloni M, Guee L, et al. Two novel cases of resistance to thyroid hormone due to THRA mutation. *Thyroid* (2020) 30(8):1217–21. doi: 10.1089/thy.2019.0602

38. World Health Organization. *Epilepsy 2023* (2023). Available at: https://www.who.int/news-room/fact-sheets/detail/epilepsy.

39. Kalikiri MK, Mamidala MP, Rao AN, Rajesh V. Analysis and functional characterization of sequence variations in ligand binding domain of thyroid hormone receptors in autism spectrum disorder (ASD) patients. *Autism Res* (2017) 10(12):1919–28. doi: 10.1002/aur.1838

40. Yuen RKC, Thiruvahindrapuram B, Merico D, Walker S, Tammimies K, Hoang N, et al. Whole-genome sequencing of quartet families with autism spectrum disorder. *Nat Med* (2015) 21:185. doi: 10.1038/nm.3792

41. Zekri Y, Guyot R, Flamant F. An atlas of thyroid hormone receptors' Target genes in mouse tissues. *Int J Mol Sci* (2022) 23(19):1444. doi: 10.3390/ijms231911444

42. Nicholson JL, Altman J. The effects of early hypo- and hyperthyroidism on the development of rat cerebellar cortex. I. Cell proliferation and differentiation. *Brain Res* (1972) 44:13–23. doi: 10.1016/0006-8993(72)90362-9

43. Koibuchi N, Chin WW. Thyroid hormone action and brain development. *Trends Endocrinol Metab* (2000) 11(4):123–8. doi: 10.1016/S1043-2760(00)00238-1

44. Li JQ, Wang X, Yan YQ, Wang KW, Qin DK, Xin ZF, et al. The effects on fetal brain development in the rat of a severely iodine deficient diet derived from an endemic area: observations on the first generation. *Neuropathol Appl Neurobiol* (1986) 12 (3):261–76. doi: 10.1111/j.1365-2990.1986.tb00139.x

45. Patel AJ, Smith RM, Kingsbury AE, Hunt A, Balázs R. Effects of thyroid state on brain development: muscarinic acetylcholine and GABA receptors. *Brain Res* (1980) 198:389–402. doi: 10.1016/0006-8993(80)90752-0

46. Manzano J, Cuadrado M, Morte B, Bernal J. Influence of thyroid hormone and thyroid hormone receptors in the generation of cerebellar gamma-aminobutyric acid-ergic interneurons from precursor cells. *Endocrinology* (2007) 148(12):5746–51. doi: 10.1210/en.2007-0567

47. Berbel P, Marco P, Cerezo JR, DeFelipe J. Distribution of parvalbumin immunoreactivity in the neocortex of hypothyroid adult rats. *Neurosci Lett* (1996) 204:65–8. doi: 10.1016/0304-3940(96)12318-1

48. Gilbert ME, Sui L, Walker MJ, Anderson W, Thomas S, Smoller SN, et al. Thyroid hormone insufficiency during brain development reduces parvalbumin immunoreactivity and inhibitory function in the hippocampus. *Endocrinology* (2007) 148(1):92–102. doi: 10.1210/en.2006-0164

49. Shiraki A, Akane H, Ohishi T, Wang L, Morita R, Suzuki K, et al. Similar distribution changes of GABAergic interneuron subpopulations in contrast to the different impact on neurogenesis between developmental and adult-stage hypothyroidism in the hippocampal dentate gyrus in rats. *Arch Toxicol* (2012) 86 (10):1559–69. doi: 10.1007/s00204-012-0846-y

50. Sawano E, Takahashi M, Negishi T, Tashiro T. Thyroid hormone-dependent development of the GABAergic pre- and post-synaptic components in the rat hippocampus. *Int J Dev Neurosci* (2013) 31(8):751–61. doi: 10.1016/j.ijdevneu.2013.09.007

51. Cunha Menezes E, Rabelo Santos P, Costa Goes T, Barboza Carvalho VC, Teixeira-Silva F, Stevens HE, et al. Effects of a rat model of gestational hypothyroidism on forebrain dopaminergic, GABAergic, and serotonergic systems and related behaviors. *Behav Brain Res* (2019) 366:77–87. doi: 10.1016/j.bbr.2019.03.027

52. Ramhøj L, Guyot R, Svingen T, Kortenkamp A, Flamant F, Axelstad M. Is periventricular heterotopia a useful endpoint for developmental thyroid hormone system disruption in mouse toxicity studies? *Regul Toxicol Pharmacol* (2023), 105445. doi: 10.1016/j.yrtph.2023.105445

53. Goodman JH, Gilbert ME. Modest thyroid hormone insufficiency during development induces a cellular malformation in the corpus callosum: a model of cortical dysplasia. *Endocrinology* (2007) 148(6):2593–7. doi: 10.1210/en.2006-1276

54. Friauf E, Wenz M, Oberhofer M, Nothwang HG, Balakrishnan V, Knipper M, et al. Hypothyroidism impairs chloride homeostasis and onset of inhibitory neurotransmission in developing auditory brainstem and hippocampal neurons. *Eur J Neurosci* (2008) 28(12):2371–80. doi: 10.1111/j.1460-9568.2008.06528.x

55. Quignodon L, Vincent S, Winter H, Samarut J, Flamant F. A point mutation in the activation function 2 domain of thyroid hormone receptor alpha1 expressed after CRE-mediated recombination partially recapitulates hypothyroidism. *Mol Endocrinol* (2007) 21(10):2350–60. doi: 10.1210/me.2007-0176

56. Tinnikov A, Nordström K, Thorén P, Kindblom JM, Malin S, Rozell B, et al. Retardation of post-natal development caused by a negatively acting thyroid hormone receptor α1. *EMBO J* (2002) 21(19):5079–87. doi: 10.1093/emboj/cdf523

57. Flamant FDR, Poguet A-L, Plateroti M, Chassande O, Gauthier K, Streichenberger N, et al. Congenital hypothyroid Pax8–/– mutant mice can be rescued by inactivating the TRα Gene. *Mol Endocrinol* (2002) 16(1):24–32. doi: 10.1210/mend.16.1.0766

58. Hashimoto K, Curty FH, Borges PP, Lee CE, Abel ED, Elmquist JK, et al. An unliganded thyroid hormone receptor causes severe neurological dysfunction. *Proc Natl Acad Sci* (2001) 98(7):3998–4003. doi: 10.1073/pnas.051454698

59. Portella AC, Carvalho F, Faustino L, Wondisford FE, Ortiga-Carvalho TM, Gomes FC. Thyroid hormone receptor beta mutation causes severe impairment of cerebellar development. *Mol Cell Neurosci* (2010) 44(1):68–77. doi: 10.1016/j.mcn.2010.02.004

60. Forrest D, Erway LC, Ng L, Altschuler R, Curran T. Thyroid hormone receptor β is essential for development of auditory function. *Nat Genet* (1996) 13:354–7. doi: 10.1038/ng0796-354

61. Sandhofer C, Schwartz HL, Mariash CN, Forrest D, Oppenheimer JH. Beta isoforms are not essential for thyroid hormone-dependent acceleration of PCP-2 and myelin basic protein gene expression in the developing brains of neonatal mice. *Mol Cell Endocrinol* (1998) 137:109–15. doi: 10.1016/S0303-7207(98)00005-7

62. Peeters RP, Hernandez A, Ng L, Ma M, Sharlin DS, Pandey M, et al. Cerebellar abnormalities in mice lacking type 3 deiodinase and partial reversal of phenotype by deletion of thyroid hormone receptor alpha1. *Endocrinology* (2013) 154(1):550–61. doi: 10.1210/en.2012-1738

63. Wallis K, Sjögren M, van Hogerlinden M, Silberberg G, Fisahn A, Nordström K, et al. Locomotor deficiencies and aberrant development of subtype-specific GABAergic interneurons caused by an unliganded thyroid hormone receptor α1. *J Neurosci* (2008) 28(8):1904–15. doi: 10.1523/JNEUROSCI.5163-07.2008

64. Markossian S, Guyot R, Richard S, Teixeira M, Aguilera N, Bouchet M, et al. CRISPR/cas9 editing of the mouse Thra gene produces models with variable resistance to thyroid hormone. *Thyroid* (2018) 28(1):139–50. doi: 10.1089/thy.2017.0389

65. Mayerl S, Muller J, Bauer R, Richert S, Kassmann CM, Darras VM, et al. Transporters MCT8 and OATP1C1 maintain murine brain thyroid hormone homeostasis. *J Clin Invest* (2014) 124(5):1987–99. doi: 10.1172/JCI70324

66. Amano I, Takatsuru Y, Toya S, Aijima A, Iwasaki T, Grasberger H, et al. Aberrant cerebellar development in mice lacking dual oxidase maturation factors. *Thyroid* (2016) 26(5):741–52. doi: 10.1089/thy.2015.0034

67. Barez-Lopez S, Grijota-Martinez C, Auso E, Fernandez-de Frutos M, Montero-Pedrazuela A, Guadano-Ferraz A. Adult mice lacking Mct8 and Dio2 proteins present alterations in peripheral thyroid hormone levels and severe brain and motor skill impairments. *Thyroid* (2019) 29(11):1669–82. doi: 10.1089/thy.2019.0068

68. Valcárcel-Hernández V, Guillén-Yunta M, Bueno-Arribas M, Montero-Pedrazuela A, Grijota-Martínez C, Markossian S, et al. A CRISPR/Cas9-engineered avatar mouse model of monocarboxylate transporter 8 deficiency displays distinct neurological alterations. *Neurobiol Dis* (2022) 174:105896. doi: 10.1016/j.nbd.2022.105896

69. Guadaño-Ferraz A, Benavides-Piccione R, Venero C, Lancha C, Vennström B, Sandi C, et al. Lack of thyroid hormone receptor alpha1 is associated with selective alterations in behavior and hippocampal circuits. *Mol Psychiatry* (2003) 8(1):30–8. doi: 10.1038/sj.mp.4001196

70. Hu H, Gan J, Jonas P. Interneurons. Fast-spiking, parvalbumin(+) GABAergic interneurons: from cellular design to microcircuit function. *Science* (2014) 345 (6196):1255263. doi: 10.1126/science.1255263

71. Kriener B, Hu H, Vervaeke K. Parvalbumin interneuron dendrites enhance gamma oscillations. *Cell Rep* (2022) 39(11):110948. doi: 10.1016/j.celrep.2022.110948

72. Hadjab-Lallemend S, Wallis K, van Hogerlinden M, Dudazy S, Nordstrom K, Vennstrom B, et al. A mutant thyroid hormone receptor alpha1 alters hippocampal circuitry and reduces seizure susceptibility in mice. *Neuropharmacology* (2010) 58 (7):1130–9. doi: 10.1016/j.neuropharm.2010.02.005

73. Ben-Ari Y. The GABA excitatory/inhibitory developmental sequence: a personal journey. *Neuroscience* (2014) 279:187–219. doi: 10.1016/j.neuroscience.2014.08.001

74. Wang Y, Fisahn A, Sinha I, Nguyen DP, Sterzenbach U, Lallemend F, et al. Hippocampal transcriptome profile of persistent memory rescue in a mouse model of THRA1 mutation-mediated resistance to thyroid hormone. *Sci Rep* (2016) 6:18617. doi: 10.1038/srep18617

75. Mittag J, Lyons DJ, Sallstrom J, Vujovic M, Dudazy-Gralla S, Warner A, et al. Thyroid hormone is required for hypothalamic neurons regulating cardiovascular functions. *J Clin Invest* (2013) 123(1):509–16. doi: 10.1172/JCI65252

76. Harder L, Dudazy-Gralla S, Muller-Fielitz H, Hjerling Leffler J, Vennstrom B, Heuer H, et al. Maternal thyroid hormone is required for parvalbumin neurone development in the anterior hypothalamic area. *J Neuroendocrinol* (2018) 30(3): e12573. doi: 10.1111/jne.12573

77. Kim KH, Lee J, Ahn CH, Yu HW, Choi JY, Lee HY, et al. Association between thyroid function and heart rate monitored by wearable devices in patients with hypothyroidism. *Endocrinol Metab (Seoul)* (2021) 36(5):1121–30. doi: 10.3803/EnM.2021.1216

78. Laing BT, Anderson MS, Bonaventura J, Jayan A, Sarsfield S, Gajendiran A, et al. Anterior hypothalamic parvalbumin neurons are glutamatergic and promote escape behavior. *Curr Biol* (2023) 33(15):3215–28 e7. doi: 10.1016/j.cub.2023.06.070

79. Fauquier T, Chatonnet F, Picou F, Richard S, Fossat N, Aguilera N, et al. Purkinje cells and Bergmann glia are primary targets of the TRalpha1 thyroid hormone receptor during mouse cerebellum postnatal development. *Development* (2014) 141(1):166–75. doi: 10.1242/dev.103226

80. Fauquier T, Romero E, Picou F, Chatonnet F, Nguyen X-N, Quignodon L, et al. Severe impairment of cerebellum development in mice expressing a dominant-negative mutation inactivating thyroid hormone receptor alpha1 isoform. *Dev Biol* (2011) 356 (2):350–8. doi: 10.1016/j.ydbio.2011.05.657

81. Picou F, Fauquier T, Chatonnet F, Richard S, Flamant F. Deciphering direct and indirect influence of thyroid hormone with mouse genetics. *Mol Endocrinol* (2014) 28 (4):429–41. doi: 10.1210/me.2013-1414

82. Picou F, Fauquier T, Chatonnet F, Flamant F. A bimodal influence of thyroid hormone on cerebellum oligodendrocyte differentiation. *Mol Endocrinol* (2012) 26 (4):608–18. doi: 10.1210/me.2011-1316

83. Yu L, Shimokawa N, Iwasaki T, Xu M, Lesmana R, Koibuchi N, et al. Aberrant cerebellar development of transgenic mice expressing dominant-negative thyroid hormone receptor in cerebellar Purkinje cells. *Endocrinology* (2015) 156(4):1565–76. doi: 10.1210/en.2014-1079

84. Ninomiya A, Amano I, Kokubo M, Takatsuru Y, Ishii S, Hirai H, et al. Long-term depression-inductive stimulation causes long-term potentiation in mouse Purkinje cells with a mutant thyroid hormone receptor. *Proc Natl Acad Sci U S A* (2022) 119(45): e2210645119. doi: 10.1073/pnas.2210645119

85. Mayerl S, Chen J, Salveridou E, Boelen A, Darras VM, Heuer H. Thyroid hormone transporter deficiency in mice impacts multiple stages of GABAergic

interneuron development. *Cereb Cortex* (2022) 32(2):329–41. doi: 10.1093/cercor/bhab211

86. Xu Q, Guo L, Moore H, Waclaw RR, Campbell K, Anderson SA. Sonic hedgehog signaling confers ventral telencephalic progenitors with distinct cortical interneuron fates. *Neuron* (2010) 65(3):328–40. doi: 10.1016/j.neuron.2010.01.004

87. Chatonnet F, Flamant F, Morte B. A temporary compendium of thyroid hormone target genes in brain. *Biochim Biophys Acta* (2015) 1849(2):122–9. doi: 10.1016/j.bbagrm.2014.05.023

88. Thompson CC. Thyroid hormone-responsive genes in developing cerebellum include a novel synaptotagmin and a *hairless* homolog. *J Neurosci* (1996) 16(24):7832–40. doi: 10.1523/JNEUROSCI.16-24-07832.1996

89. Denver RJ, Ouellet L, Furling D, Kobayashi A, Fujii-Kuriyama Y, Puymirat J. Basic transcription element-binding protein (BTEB) is a thyroid hormone-regulated gene in the developing central nervous system. Evidence for a role in neurite outgrowth. *J Biol Chem* (1999) 274(33):23128–34. doi: 10.1074/jbc.274.33.23128

90. Diez D, Grijota-Martinez C, Morreale de Escobar G, Bernal J, Morte B, Pinchera A, et al. Thyroid hormone action in the adult brain: gene expression profiling of the effects of single and multiple doses of Triiodo-l-thyronine in the rat striatum. *Endocrinology* (2008) 149(8):3989–4000. doi: 10.1210/en.2008-0350

91. Morte B, Ceballos A, Diez D, Grijota-Martínez C, Dumitrescu AM, Di Cosmo C, et al. Thyroid hormone-regulated mouse cerebral cortex genes are differentially dependent on the source of the hormone: a study in monocarboxylate transporter-8- and deiodinase-2-deficient mice. *Endocrinology* (2010) 151(5):2381–7. doi: 10.1210/en.2009-0944

92. Poguet AL, Legrand C, Feng X, Yen PM, Meltzer P, Samarut J, et al. Microarray analysis of knockout mice identifies cyclin D2 as a possible mediator for the action of thyroid hormone during the postnatal development of the cerebellum. *Dev Biol* (2003) 254(2):188–99. doi: 10.1016/S0012-1606(02)00039-8

93. Fang Y, Dang P, Liang Y, Zhao D, Wang R, Xi Y, et al. Histological, functional and transcriptomic alterations in the juvenile hippocampus in a mouse model of thyroid hormone resistance. *Eur Thyroid J* (2022) 11(2). doi: 10.1530/ETJ-21-0097

94. Gil-Ibañez P, García-García F, Dopazo J, Bernal J, Morte B. Global transcriptome analysis of primary cerebrocortical cells: identification of genes regulated by triiodothyronine in specific cell types. *Cereb Cortex* (2017) 27(1):706–17. doi: 10.1093/cercor/bhv273

95. Chatonnet F, Guyot R, Picou F, Bondesson M, Flamant F. Genome-wide search reveals the existence of a limited number of thyroid hormone receptor alpha target genes in cerebellar neurons. *PloS One* (2012) 7(5):e30703. doi: 10.1371/journal.pone.0030703

96. Neveu I, Arenas E. Neurotrophins promote the survival and development of neurons of the cerebellum of hypothyroid rats in vivo. *J Cell Biol* (1996) 133(3):631–46. doi: 10.1083/jcb.133.3.631

97. Aramaki M, Wu X, Liu H, Liu Y, Cho YW, Song M, et al. Transcriptional control of cone photoreceptor diversity by a thyroid hormone receptor. *Proc Natl Acad Sci U S A* (2022) 119(49):e2209884119. doi: 10.1073/pnas.2209884119

98. Ariyani W, Miyazaki W, Amano I, Koibuchi N. Involvement of integrin alphavbeta3 in thyroid hormone-induced dendritogenesis. *Front Endocrinol (Lausanne)* (2022) 13:938596. doi: 10.3389/fendo.2022.938596

99. Avci HX, Lebrun C, Wehrle R, Doulazmi M, Chatonnet F, Morel MP, et al. Thyroid hormone triggers the developmental loss of axonal regenerative capacity via thyroid hormone receptor alpha1 and kruppel-like factor 9 in Purkinje cells. *Proc Natl Acad Sci U S A* (2012) 109(35):14206–11. doi: 10.1073/pnas.1119853109

100. Royland JE, Parker JS, Gilbert ME. A genomic analysis of subclinical hypothyroidism in hippocampus and neocortex of the developing rat brain. *J Neuroendocrinol* (2008) 20(12):1319–38. doi: 10.1111/j.1365-2826.2008.01793.x

101. Bernal J, Morte B, Diez D. Thyroid hormone regulators in human cerebral cortex development. *J Endocrinol* (2022) 255(3):R27–36. doi: 10.1530/JOE-22-0189

102. Wirth EK, Roth S, Blechschmidt C, Holter SM, Becker L, Racz I, et al. Neuronal 3',3,5-triiodothyronine (T3) uptake and behavioral phenotype of mice deficient in Mct8, the neuronal T3 transporter mutated in Allan-Herndon-Dudley syndrome. *J Neurosci* (2009) 29(30):9439–49. doi: 10.1523/JNEUROSCI.6055-08.2009

103. Diez D, Morte B, Bernal J. Single-cell transcriptome profiling of thyroid hormone effectors in the human fetal neocortex: expression of SLCO1C1, DIO2, and THRB in specific cell types. *Thyroid* (2021) 31(10):1577–88. doi: 10.1089/thy.2021.0057

104. Ren J, Flamant F. Thyroid hormone as a temporal switch in mouse development. *Eur Thyroid J* (2023) 12(2). doi: 10.1530/ETJ-22-0225

105. Lear BP, Moore DL. Moving CNS axon growth and regeneration research into human model systems. *Front Neurosci* (2023) 17:1198041. doi: 10.3389/fnins.2023.1198041

106. Batista G, Hensch TK. Critical period regulation by thyroid hormones: potential mechanisms and sex-specific aspects. *Front Mol Neurosci* (2019) 12:77. doi: 10.3389/fnmol.2019.00077

107. Reh RK, Dias BG, Nelson CA 3rd, Kaufer D, Werker JF, Kolb B, et al. Critical period regulation across multiple timescales. *Proc Natl Acad Sci U S A* (2020) 117 (38):23242–51. doi: 10.1073/pnas.1820836117

108. Tao HW, Li YT, Zhang LI. Formation of excitation-inhibition balance: inhibition listens and changes its tune. *Trends Neurosci* (2014) 37(10):528–30. doi: 10.1016/j.tins.2014.09.001

109. Gogolla N, Leblanc JJ, Quast KB, Sudhof TC, Fagiolini M, Hensch TK. Common circuit defect of excitatory-inhibitory balance in mouse models of autism. *J Neurodev Disord* (2009) 1(2):172–81. doi: 10.1007/s11689-009-9023-x

110. Hashemi E, Ariza J, Rogers H, Noctor SC, Martinez-Cerdeno V. The number of parvalbumin-expressing interneurons is decreased in the prefrontal cortex in autism. *Cereb Cortex* (2017) 27(3):1931–43. doi: 10.1093/cercor/bhw021

111. Schwede M, Nagpal S, Gandal MJ, Parikshak NN, Mirnics K, Geschwind DH, et al. Strong correlation of downregulated genes related to synaptic transmission and mitochondria in post-mortem autism cerebral cortex. *J Neurodev Disord* (2018) 10 (1):18. doi: 10.1186/s11689-018-9237-x

112. Berbel P, Navarro D, Roman GC. An evo-devo approach to thyroid hormones in cerebral and cerebellar cortical development: etiological implications for autism. *Front Endocrinol (Lausanne)* (2014) 5:146. doi: 10.3389/fendo.2014.00146

113. Navarro D, Alvarado M, Navarrete F, Giner M, Obregon MJ, Manzanares J, et al. Gestational and early postnatal hypothyroidism alters VGluT1 and VGAT bouton distribution in the neocortex and hippocampus, and behavior in rats. *Front Neuroanat* (2015) 9(9). doi: 10.3389/fnana.2015.00009

114. Jiang X, Lachance M, Rossignol E. Involvement of cortical fast-spiking parvalbumin-positive basket cells in epilepsy. *Prog Brain Res* (2016) 226:81–126. doi: 10.1016/bs.pbr.2016.04.012

115. Godoy LD, Prizon T, Rossignoli MT, Leite JP, Liberato JL. Parvalbumin role in epilepsy and psychiatric comorbidities: from mechanism to intervention. *Front Integr Neurosci* (2022) 16:765324. doi: 10.3389/fnint.2022.765324

116. Holbech H, Matthiessen P, Hansen M, Schuurmann G, Knapen D, Reuver M, et al. ERGO: breaking down the wall between human health and environmental testing of endocrine disrupters. *Int J Mol Sci* (2020) 21(8):2954. doi: 10.3390/ijms21082954

117. Gouwens NW, Sorensen SA, Baftizadeh F, Budzillo A, Lee BR, Jarsky T, et al. Integrated morphoelectric and transcriptomic classification of cortical GABAergic cells. *Cell* (2020) 183(4):935–53 e19. doi: 10.1016/j.cell.2020.09.057

118. Sreenivasan VKA, Dore R, Resch J, Maier J, Dietrich C, Henck J, et al. Single-cell RNA-based phenotyping reveals a pivotal role of thyroid hormone receptor alpha for hypothalamic development. *Development* (2023) 150(3). doi: 10.1242/dev.201228

119. Sampath Kumar A, Tian L, Bolondi A, Aragonés Hernández A, Stickels R, Kretzmer H, et al. Spatiotemporal transcriptomic maps of whole mouse embryos at the onset of organogenesis. *Nat Genet* (2023) 55:1546–718. doi: 10.1038/s41588-023-01435-6

frontiers | Frontiers in Endocrinology

TYPE Systematic Review
PUBLISHED 10 October 2023
DOI 10.3389/fendo.2023.1230932

Check for updates

OPEN ACCESS

EDITED BY
Laurent M Sachs,
Muséum National d'Histoire Naturelle, France

REVIEWED BY
Krzysztof Cezary Lewandowski,
Medical University of Lodz, Poland
Paraskevi Xekouki,
University of Crete, Greece

*CORRESPONDENCE
Esmaeil Mehraeen
es.mehraeen@gmail.com
Soudabeh Yarmohammadi
yarmohammadisoudabeh@gmail.com

RECEIVED 08 June 2023
ACCEPTED 25 September 2023
PUBLISHED 10 October 2023

CITATION
SeyedAlinaghi S, Yarmohammadi S, Dashti M, Ghasemzadeh A, Siami H, Molla A, Mahrokhi S, Qaderi K, Arjmand G, Parikhani SN, Amrollah MF, Mirghaderi P, Mehraeen E and Dadras O (2023) The relationship of hip fracture and thyroid disorders: a systematic review. *Front. Endocrinol.* 14:1230932. doi: 10.3389/fendo.2023.1230932

COPYRIGHT
© 2023 SeyedAlinaghi, Yarmohammadi, Dashti, Ghasemzadeh, Siami, Molla, Mahrokhi, Qaderi, Arjmand, Parikhani, Amrollah, Mirghaderi, Mehraeen and Dadras. This is an open-access article distributed under the terms of the Creative Commons Attribution License (CC BY). The use, distribution or reproduction in other forums is permitted, provided the original author(s) and the copyright owner(s) are credited and that the original publication in this journal is cited, in accordance with accepted academic practice. No use, distribution or reproduction is permitted which does not comply with these terms.

The relationship of hip fracture and thyroid disorders: a systematic review

SeyedAhmad SeyedAlinaghi[1], Soudabeh Yarmohammadi[2*], Mohsen Dashti[3], Afsaneh Ghasemzadeh[3], Haleh Siami[4], Ayoob Molla[5], Sona Mahrokhi[1], Kowsar Qaderi[6], Ghazal Arjmand[7], Sahar Nooralioghli Parikhani[8], Masoomeh Fathi Amrollah[1], Peyman Mirghaderi[9], Esmaeil Mehraeen[10*] and Omid Dadras[11]

[1]Iranian Research Center for HIV/AIDS, Iranian Institute for Reduction of High-Risk Behaviors, Tehran University of Medical Sciences, Tehran, Iran, [2]Trauma Research Center, Kashan University of Medical Sciences, Kashan, Iran, [3]Department of Radiology, Tabriz University of Medical Sciences, Tabriz, Iran, [4]School of Medicine, Islamic Azad University of Medical Sciences, Tehran, Iran, [5]School of Medicine, Bushehr University of Medical Sciences, Bushehr, Iran, [6]Department of Midwifery, School of Nursing and Midwifery, Kermanshah University of Medical Sciences, Kermanshah, Iran, [7]School of Medicine, Shahid Beheshti University of Medical Sciences, Tehran, Iran, [8]School of Medicine, Tehran University of Medical Sciences, Tehran, Iran, [9]Students' Scientific Research Center (SSRC), Tehran University of Medical Sciences, Tehran, Iran, [10]Department of Health Information Technology, Khalkhal University of Medical Sciences, Khalkhal, Iran, [11]Bergen Addiction Research, Department of Addiction Medicine, Haukland University Hospital, Bergen, Norway

Introduction: Bone density regulation is considered one of the systems affected by thyroid hormones, leading to low bone density that can result in pathologic fractures, including hip fractures. This review aimed to update clinicians and researchers about the current data regarding the relationship between hip fractures and thyroid disorders.

Methods: English papers were thoroughly searched in four main online databases of Scopus, Web of Science, PubMed, and Embase. Data extraction was done following two steps of screening/selection using distinct inclusion/exclusion criteria. This study used the Preferred Reporting Items for Systematic Reviews and Meta-Analysis (PRISMA) checklist and the Newcastle-Ottawa Scale (NOS) as bias assessment.

Results: In total, 19 articles were included in the research. The risk of hip fractures in women with differentiated thyroid cancer (DTC) is higher than hip fractures caused by osteoporosis. Men with hyperthyroidism and subclinical hyperthyroidism are at higher risk for hip fracture. Also, a decrease in serum thyroid stimulating hormone (TSH) may be associated with an increased risk of hip fracture.

Conclusion: Reaching a consensus conclusion regarding the association between subclinical thyroid dysfunction and hip fracture is not feasible due to the heterogenicity of evidence; however, there may be a higher risk of fracture in individuals with subclinical hyperthyroidism.

KEYWORDS

hip fracture, thyroid disease, thyroid disorder, thyroid dysfunction, thyroid

10.3389/fendo.2023.1230932

Introduction

Regulating metabolism and cell adjustment are just examples of what thyroid hormones do in the human body. Changes in these hormone levels occur in hypothyroidism, hyperthyroidism, subclinical hypothyroidism, and subclinical hyperthyroidism (1). Hypothyroidism is a common endocrine disorder caused by autoimmune thyroiditis (Hashimoto thyroiditis), iodine deficiency, or following surgery or radioiodine therapy (2). Hyperthyroidism is defined by elevated circulating free thyroid hormones, and overt hyperthyroidism is recognized as a low bone density or osteoporosis risk factor in older women. However, the relationship between biochemically defined subclinical hypothyroidism or hyperthyroidism and fracture risk is unknown. Still, in patients with subclinical hyperthyroidism, studies have shown that minor changes in thyroid hormone and/or thyroid stimulating hormone (TSH) levels can worsen bone mineral density (BMD) (3).

The bone remodeling cycle is what we call a continuous process of bone formation and bone resorption throughout the lifetime, and apart from local factors from osteoblasts and osteoclasts, the bone remodeling process is regulated by systemic factors such as calcitonin, parathyroid hormone (PTH), vitamin D3, estrogen, thyroid hormones, glucocorticoids, and growth hormones (4). T3 hormone increases bone formation through TRα receptors on osteoblasts and osteoclasts, but it can also increase osteoclast formation and the resorption process (5). Additionally, TSH action on the TSHR found in both osteoblasts and osteoclasts can also affect the bone remodeling cycle like T3 (6).

Changes in these hormone levels greatly affect bone metabolism and density and can lead to a decreased bone mineral density (BMD) that presents as osteoporosis. About 30–40% of osteoporosis patients are at great risk of osteoporotic bone fractures with a high mortality risk. The most frequent osteoporotic fractures are vertebral, distal radius, and hip fractures. Vertebral and hip fractures are considered life-threatening pathologies in the elderly (3). Hip fractures are a significant and incapacitating condition that disproportionately affects older women (7–15). While the epidemiology of hip fractures varies across countries, it is estimated that approximately 18% of women and 6% of men globally will be affected by this condition. Although the age-standardized incidence rate has decreased in many nations, the aging population generates a much greater impact (7–15). Therefore, the number of hip fractures globally is expected to swell from 1.26 million in 1990 to 4.5 million by the year 2050. The financial burden associated with this ailment is colossal since it requires long hospital stays and subsequent rehabilitation. Additionally, hip fracture is correlated with other adverse effects such as disability, depression, and cardiovascular diseases, which further exacerbates societal costs (7–15).

This review aimed to update clinicians and researchers about the current evidence regarding the relationship between hip fractures and thyroid disorders.

Methods

According to the Preferred Reporting Items for Systematic Reviews and Meta-Analysis (PRISMA), this systematic review was carried out (16). The Newcastle-Ottawa Scale (NOS) quality assessment tool was used to evaluate methodological quality.

Data sources

Systematic searches were conducted in Embase, PubMed, Scopus, and Web of Science databases without time limitation. Manual checks were made for any additional studies bibliography of relevant studies.

The following keywords were used in combination:

A: "Hip fracture" OR "Trochanteric fracture" OR "Intertrochanteric fracture" OR "Sub trochanteric fracture" OR "Femoral fracture" [Title/Abstract]

B: "Thyroid disease" OR "Thyroid disorder" OR "Thyroid dysfunction" [Title/Abstract]

C: [A] AND [B]

Study selection

In two stages of screening and selection, publications of interest were included. First, titles and abstracts were evaluated, and relevant publications were chosen for the second stage. This step involved reading through the complete text of these papers. Studies were selected for analysis using the following inclusion and exclusion criteria:

1. Studies that addressed hip fractures and thyroid disorders.
2. Original articles.
3. English studies.

Exclusion criteria:

1. A systematic review, meta-analysis, qualitative studies, case report, and letter to the editor.
2. Articles that do not have full text, or in a language other than English.

Data extraction

For data extraction, the records were divided among four impartial assessors to retrieve the following details: study type, nation, first author, publication year, target population, comparison, and data on bone metabolism, including biochemical parameters, parameters of bone damage, and fracture data.

Quality assessment and risk evaluation

The study's methodological quality was assessed using the NOS. It focused on three areas, including participant selection (0-4 points), comparability of study groups (0-2 points), and ascertainment of exposure (0-3 points), containing eight questions with a total score of nine. Finally, based on the total number of stars received, each study was assigned one of three grades: excellent, fair, or poor. When a study received 3 or 4 stars in the selection domain, 1 or 2 stars in the comparability domain, and 2 or 3 stars in the outcome/exposure domain, it was considered to have "excellent" quality. In the selection domain, "fair" was used for 2 stars, in the comparability domain for 1 or 2 stars, and in the outcome/exposure domain for 2 or 3 stars. "Poor" was used when the selection domain, comparability domain, or outcome/exposure domain received 0 stars, 1 star, or no stars, respectively (Table 1). Also, this review study complies with the PRISMA checklist to increase soundness and reliability (35).

Results

Among 839 records identified by the search, nineteen studies were included in this review (Figure 1). Table 2 provides an overview of the included studies and the extracted data. A total of 15 cohorts and 4 cross-sectional studies reported the data of 229,294 males and 2,838,789 females.

Thyroid cancer

Women with differentiated thyroid cancer (DTC) showed significant changes in Fracture Risk Assessment Tool (FRAX), with a higher increase in the probability of hip fracture than of major osteoporotic fracture (TSH [n.v. 0.3~4.2 mIU/L]: 0.66 ± 1.22 (0.16)) (18). Also, women with a history of hyperthyroidism and thyroid cancer had their first fracture earlier ($P<0.01$) than women without thyroid disease (28), but there were no significant differences between women with thyroid disease and women without thyroid disease in the number or type of fractures (28).

Hyperthyroidism

Low serum TSH levels (0.1 mU/L) as an indicator of hyperthyroidism in women older than 65 were correlated with higher new hip fractures (20). Males with hyperthyroidism (TSH <0.10 mIU/L) (3, 21) and subclinical hyperthyroidism (17) are at increased risk for hip fracture. Interestingly, thyrotoxicosis, without the aid of other risk factors such as hypogonadism, particularly in

TABLE 1 Newcastle-Ottawa Scale (NOS) bias risk assessment of the study.

The first author (reference)	Selection (out of 4)	Comparability (out of 2)	Exposure/Outcome (out of 3)	Total (Out of 9)
Polovina et al. (17)	2	2	2	6
Vera et al. (18)	2	2	2	6
Lee et al. (19)	2	2	2	6
Bauer et al. (20)	3	2	2	7
Cauley et al. (21)	3	2	3	8
Gallagher et al. (22)	2	1	2	5
Polovina et al. (23)	2	2	2	6
Abrahamsen et al. (24)	3	2	2	7
Nguyen et al. (25)	3	1	2	6
Ahmad et al. (26)	2	2	2	6
Siru et al. (27)	3	2	3	8
Solomon et al. (28)	2	2	2	6
Svare et al. (29)	4	2	3	9
Waring et al. (30)	4	2	2	8
G. P. Leese (31)	4	1	2	7
Jennifer S. Lee (3)	4	2	2	8
Bo Abrahamsen (32)	4	2	2	8
L.J Melton III (33)	3	1	3	7
Margaret C. Garin (34)	4	2	3	9

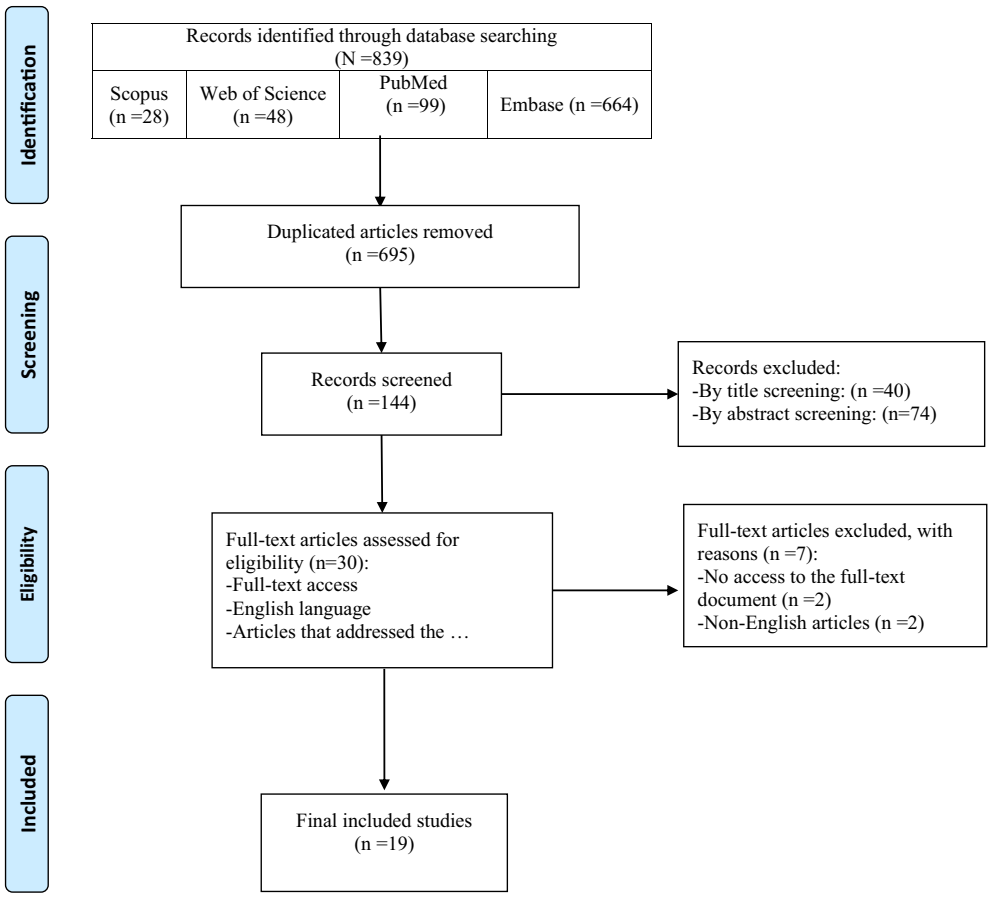

FIGURE 1
PRISMA 2020 flow diagram of the study retrieval process.

men receiving gonadotropin-releasing hormone (GnRH) agonist therapy for prostate cancer, were responsible for the 5-fold increased hip fracture risk in males and 2.1-fold in females (22). Whether treatment of the subclinical syndrome reduces this risk remains unknown (3).

Euthyroid

In euthyroid older men, TSH and FT4 were not associated with Bone Turnover Markers (BTMs) or hip fracture incidence (27). Lower TSH levels in the euthyroid range were related to lower BMD and weaker femoral structure in elderly women but not men (19). Another study on older men reported that although neither TSH nor FT4 was associated with bone loss, lower serum TSH may be associated with an increased risk of hip fractures (relative hazard [RH] 1.31 per SD decrease in TSH, 95% CI 1.01 – 1.71) (30).

Thyroid hormone therapy

Women taking thyroid hormone for various thyroid disorders do not appear to have an enhanced prevalence of hip, vertebral, or forearm fractures (28). In another study, excessive thyroxine dosing was significantly but slightly associated with an increased risk of hip fracture (HR= 1.09; 95% CI: 1.04 to 1.15) (32).

Hypothyroidism

In hypothyroid people, low-energy trauma more likely occurred (71%) compared to 32% of euthyroid subjects (P<0.001) (26). Patients with hypothyroidism presenting with fractures are more likely females with low-energy trauma (26). TSH was a predictive factor for fractures in women with subclinical hypothyroidism (23, 24). No statistically significant relation was found between baseline TSH and subsequent fracture risk, but the data suggest a weak positive association with hip fracture risk among women with both low and high TSH (29–32).

Other outcomes

Lower BMD and FRAX scores for hip and osteoporotic fractures were associated with TPO-Ab in euthyroid postmenopausal women (23). The relative risk of any fractures for patients with thyroidectomy versus their controls was increased 1.5-fold (95% CI, 0.7–3.2) (25). There is a little but statistically

TABLE 2 Description of the findings reported in eligible studies.

ID	The first author (reference)	Country	Study type	Study population (n=) Female (), Male()	Age Mean ± SD	Type of thyroid disorder	Thyroid disorder symptoms	Sites of fracture	Hip fracture rate Mean ± SD/Percent	Hip fracture symptoms	Relationship between thyroid disorders and hip fracture in Female/Male (Yes or No)	History of thyroid disorder	Relationship between thyroid disorder and hip fracture Adj HR/CI	Other risk factors for fracture	Drug used
1	Polovina et al. (17)	Serbia	Cross-sectional	Case: Female (27) Control: Female (51)	58.85 ± 7.83	autoimmune thyroid disease or toxic goiter	NR	Vertebral and hip fracture FRAX score	Hip fracture risk in the group with subclinical hyperthyroidism was 1.33 ± 3.92 *vs* controls 0.50 ± 0.46 (p = 0.022).	NR	Yes	None	-0.208 (-0.413, 0.004)	previous fractures, smoking status, alcohol consumption, parental fractures, MBI, fat mass, diabetes mellitus, and the onset of menopause	no steroid therapy longer than 6 months
2	Vera et al. (18)	Italy	Cohort	Case: Female (74) Control: Female (120)	51.9 ± 12.0	differentiated thyroid cancer (DTC)	NR	hip fracture and major osteoporotic fracture (MOF)	FRAX hip fracture: Baseline; 1.2 ± 2.0/0.6, Second evaluation; 1.9 ± 3.2/1.1 FRAX hip fracture in fracture pts: baseline; 3.5 ± 3.8/1.9, second evaluation; 4.6 ± 3.9/2.9	NR	Yes In DTC women, significant changes in FRAX were found, with a higher increase in the probability of hip fracture than of MOF.	NR	NR	Menopausal status, BMI, smoking status, Disease-free for DTC recurrence, diseases involving bone, Calcium/ vitamin D supplementation, Anti-resorptive therapy	levothyroxine
3	Lee et al. (19)	Korea	Cross-sectional	Female (674) Male (343)	71.6 ± 4.7	euthyroidism	NR	hip fracture, vertebral fracture, and non-vertebral fracture	Female (4.5 ± 3.6) Male (2.1 ± 1.7)	NR	Female (Yes) Male (No) Lower TSH levels in the euthyroid range are related to lower bone mineral density BMD and weaker femoral structure in elderly women.	NR	NR	Menopausal status, BMI, smoking status, Drinking status, and hormone replacement	NR
4	Bauer et al. (20)	USA	Cohort	Female (1209)	Hip: Fracture (75.3 ± 6 5.6), No-fracture (71.7 ± 6 5.3) Vertebral: Fracture (73.2 ± 6 5.6), No-fracture (71.3 ± 6 5.0) Any non-spine: Fracture (72.8 ± 6 5.4), No-fracture (71.6 ± 6 5.2)	Hyperthyroidism	NR	hip fracture, vertebral fracture, and any non-spine fracture	2.0 ± 6 2.5	NR	Yes Women older than 65 with low serum TSH levels, indicating physiologic hyperthyroidism, are at increased risk for new hip and vertebral fractures. Use of thyroid hormone itself does not increase the risk for fracture if TSH levels are normal.	Previous hyperthyroidism or Graves disease,	relative hazard 3.6 (1.0–12.9)	Weight, history of hyperthyroidism, use of thyroid hormones, and use of oral estrogen	NR
5	Cauley et al. (21)	USA	Cohort	5994 Males No hip fracture (5698) Hip fracture (178)	Hip fracture (77.81 ± 6.08) No hip fracture (73.48 ± 5.81)	Hyperthyroidism	NR	Hip fracture	7 (3.93)	NR	Yes	NR	2.86 (1.32, 6.20)	demographic, lifestyle (alcohol consumption (average number of drinks per week), smoking, and dietary intake), personal and family medical history, functional status, anthropometric,	NR

(Continued)

10.3389/fendo.2023.1230932

TABLE 2 Continued

ID	The first author (reference)	Country	Study type	Study population (n=) Female (), Male()	Age Mean ± SD	Type of thyroid disorder	Thyroid disorder symptoms	Sites of fracture	Hip fracture rate Mean ± SD/Percent	Hip fracture symptoms	Relationship between thyroid disorders and hip fracture in Female/Male (Yes or No)	History of thyroid disorder	Relationship between thyroid disorder and hip fracture Adj HR/CI	Other risk factors for fracture	Drug used
														cognitive, visual, and neuromuscular function	
6	Gallagher et al. (22)	USA	Cohort	Male (2) Female (11)	Median (78)	Thyrotoxicosis	NR	Hip fracture	NR	NR	Yes	NR	Male: 5.0 (0.6- 18.0) Female: 2.1 (1.04-3.7) Total: 2.3 (1.2-3.9)	cortisone therapy, radiotherapy to the pelvis, diabetes, rheumatoid arthritis, hemiplegia, hyperthyroidism, malabsorption syndrome, and gastric surgery	NR
7	Polovina et al. (23)	Serbia	Cross-sectional	Female (189)	Euthyroid: TPOAb- (60.46 ± 6.53), TPOAb+ (61.13 ± 7.10) Subclinical hyperthyroid: TPOAb- (59.63 ± 6.42), TPOAb+ (58.41 ± 7.72)	Autoimmune thyroid disease	NR	hip fracture and major osteoporotic fracture	TPOAb-: 1.06 ± 2.11 TPOAb+: 1.00 ± 1.18	NR	Yes Lower bone mineral density and FRAX scores for hip and osteoporotic fractures were associated with the presence of TPOAb in euthyroid postmenopausal women	None	T-score: 0.350 (0.189-0.651) FRAX: 2.053 (1.336-4.325)	BMI, fat mass, menopausal status, smoking status, diabetes mellitus, parental fractures, previous fractures, vitamin D level TSH was a better predictive factor for fractures in women with subclinical hypothyroidism	NR
8	Abrahamsen et al. (24)	Denmark	Cohort	Elevated TSH: Male (2386), Female (6027) Normal TSH: Male (99738), Female (122400)	Elevated TSH (54.3) Normal TSH: 50.2	Hypothyroidism	NR	hip fracture and major osteoporotic fracture	Female: 18-49, 0.21 (0.06–0.53); 50-74, 3.6 (2.8–4.5) Male: 18-49, 0.5 (0.1–1.3); 50-74, 2.9 (1.7–4.5)	NR	Yes	None	Baseline TSH value >4 mIU/L: All, 0.90 (0.80–1.02); Female, 0.94 (0.82–1.08); Male, 0.70 (0.51–0.97) Thyroxine prescription: All, 0.93(0.76–1.15); Female, 0.99 (0.79–1.24); Male, 0.60 (0.33–1.11) subsequent 6-month periods with low TSH >4 mIU/L: All, 0.99 (0.95–1.03); Female, 0.99 (0.95-1.03); Male, 0.96 (0.87–1.07) subsequent 6-month periods with low TSH< 0.3 mIU/L: All, 1.09 (1.04–1.15); Female, 1.10 (1.03–1.16); Male, 1.08 (0.93–1.25)	Previous fracture, history of comorbid conditions, and using medication such as Prednisolone or Osteoporosis medications	Thyroxine and subsequent 6-month periods with low TSH
9	Nguyen et al. (25)	USA	Cohort	Male (136)	Median age (43)	thyroidectomy	NR	thoracic or lumbar vertebra, proximal humerus, distal forearm, pelvis, or proximal femur fracture	NR	NR	Yes	Thyroid adenoma, goiter, and hyperthyroidism	the relative risk of any fractures for thyroidectomies patients Versus their controls was increased 1.5-fold (95% CI, 0.7–3.2).	Age at thyroidectomy, Extent of surgery, Extent of surgery, hyper/hypothyroidism, thyroid replacement, smoking status, ethanol use, and obesity	NR
10	Ahmad et al. (26)	Pakistan	Cohort	Hypothyroid: Female (27), male (8) Euthyroid:	Median ± IQR Hypothyroid (60 ± 29)	hypothyroidism	NR	Proximal Femur, Proximal Humerus,	29%	NR	Low-energy trauma more likely occurred in hypothyroid (71%)	NR	NR	NR	NR

(Continued)

10.3389/fendo.2023.1230932

TABLE 2 Continued

ID	The first author (reference)	Country	Study type	Study population (n=) Female (), Male()	Age Mean ± SD	Type of thyroid disorder	Thyroid disorder symptoms	Sites of fracture	Hip fracture rate Mean ± SD/Percent	Hip fracture symptoms	Relationship between thyroid disorders and hip fracture in Female/Male (Yes or No)	History of thyroid disorder	Relationship between thyroid disorder and hip fracture Adj HR/CI	Other risk factors for fracture	Drug used
				Female (395), Male (917)	Euthyroid (42 ± 32)			and Distal Radius and/ or Elbow			compared to 32% of euthyroid subjects (P < 0.001).				
11	Siru et al. (27)	Australia	Cohort	Euthyroid: male (3117) Subclinical hypothyroidism: male (135) Subclinical hyperthyroidism: Male (86)	Euthyroid: 76.71 ± 3.47 Subclinical hypothyroidism: 77.78 ± 3.89 Subclinical hyperthyroidism: 77.27 ± 4.01	subclinical hyper - and hypothyroidism	NR	Hip fracture	NR	NR	No In euthyroid older men, TSH and FT4 were not associated with BTMs or incident hip fracture.	NR	Subclinical hypothyroidism: 1.50 (0.73 -3.07) Subclinical hyperthyroidism: 1.62 (0.71 -3.69)	BMI, WHR, smoking status, alcohol use, vigorous activity, hypertension, dyslipidemia, diabetes, CVD, cancer, frailty, creatinine status, and vitamin D status	
12	Solomon et al. (28)	USA	Cross-sectional	Female (300)	73 ± 12	Goiter, thyroid cancer, hypothyroidism, hyperthyroidism, thyroid nodules	NR	Hip fracture, spine fracture, forearm fracture	10.8%	NR	Yes	Women with a history of Hyperthyroidism and thyroid cancer had their first fracture earlier (p < 0.01) than women without thyroid disease.	there were no significant differences between women with thyroid disease and women without thyroid disease groups in the number or type of fractures.	Weight and height, smoking status, Menstrual/obstetrical status	Thyroxine women taking thyroid hormone for a variety of thyroid disorders do not appear to have an enhanced prevalence of hip, vertebral, or forearm fractures, but women with a history of hyperthyroidism may have a the propensity for their fractures to occur earlier in life
13	Svare et al. (29)	Norway	Cohort	Female (16610) Male (8595)	NR	Hyperthyroidism and Hypothyroidism	NR	ulnar and radial forearm fractures and hip fracture	NR	NR	No statistically significant relation between baseline TSH and subsequent fracture risk, but the data suggest a weak positive association with hip fracture risk among women with both low and high TSH	None	Female: TSH <0.5 (1.30 (0.87–1.94)), TSH>3.5 (1.19 (0.93–1.52)), TSH >4.0 and TPOAb-negative (1.87 (1.11–3.16)), TSH >4.0 and TPOAb-positive (1.75 (1.24–2.46)) Male: TSH <0.5 (0.99 (0.40–2.43)), TSH>3.5 0.64 (0.37–1.09	BMI, smoking status, and Recreational physical activity	NR
14	Waring et al. (30)	USA	Cohort	Male (1817)	Nonspine fracture: Yes (75.4 ± 6.4), No (73.6 ± 5.9) Hip fracture: yes (78.1 ± 6.1), No (73.6± 5.8)	Subclinical hyper/ hypothyroidism	NR	Nonspine fracture and Hip fracture	Subclinical hyperthyroid: 1 ± 4.8 Subclinical hypothyroid: 4 ± 6.5	NR	There was no association between TSH or FT4 and bone loss, and fracture risk did not Differ	high thyroid or Graves' disease or low thyroid	Subclinical hyperthyroid: 0.63 (0.15–2.69) Subclinical hypothyroid: 0.75 (0.40–1.41) although neither TSH nor FT4 is associated with bone loss, lower	BMI, health status, physical activity status, smoking status, alcohol consumption, Oral corticosteroid use Participants who experienced hip fractures had a significantly lower BMI	NR

(Continued)

10.3389/fendo.2023.1230932

TABLE 2 Continued

ID	The first author (reference)	Country	Study type	Study population (n=) Female (), Male()	Age Mean ± SD	Type of thyroid disorder	Thyroid disorder symptoms	Sites of fracture	Hip fracture rate Mean ± SD/Percent	Hip fracture symptoms	Relationship between thyroid disorders and hip fracture in Female/Male (Yes or No)	History of thyroid disorder	Relationship between thyroid disorder and hip fracture Adj HR/CI	Other risk factors for fracture	Drug used
											r significantly by thyroid function category		serum TSH may be associated with an increased risk of hip fractures in older men	(p<0.001), lower physical activity score (p=0.01), were more likely to report a history of "high thyroid" or "Graves' disease" (p=0.05), and consumed, on average, more alcoholic drinks per week (p<0.001) than those without hip fractures.	
15	G. P. Leese (31)	Scotland	cohort	female (1062) male (118)	NR	hypothyroid	NR	Hip/neck of femur	NR	NR	No There was no increase in risk for overall fracture, or fractured neck of femur in those on thyroxine with suppressed or normal TSH.	NR	There was no excess of fractures in patients on L-thyroxine even if the TSH is suppressed.	NR	L-thyroxine
16	Jennifer S. Lee (3)	USA	cohort	female (2270) male (1408)	72.8 ± 5.6	Subclinical hyperthyroidism or hypothyroidism	NR	NR	NR	NR	YES for men NO for women Older men with subclinical hyperthyroidism or hypothyroidism are at increased risk for hip fracture. Whether treatment of the subclinical syndrome reduces this risk is unknown.	NR	Men with subclinical hypothyroidism had a multivariable-adjusted HR of 2.31 (95% CI, 1.25-4.27); those with subclinical hyperthyroidism, 3.27 (0.99-11.30)./There was no association between subclinical thyroid dysfunction and hip fracture in women.	Thyroid function/BMI/ Age/Sex/Alcohol use/Cigarette smoking/Thiazide use/Diabetes mellitus/Age at menopause/ Estrogen use/Calcium supplement intake/Physical activity/Frailty status/ Antithyroid or corticosteroid medication/Thyroid hormone medication/Antiosteoporosis medication	Thyroid hormone medication/ Antithyroid or corticosteroid medication
17	Bo Abrahamsen (32)	Denmark	cohort	female (129029) male (102326)	62.4	thyrotoxicosis	NR	Hip/spine/ forearm/ humerus	4.3% for thyrotoxicosis/ 1.5% for euthyroid	NR	No Elevated baseline TSH was not associated with an increased risk of hip fracture (HR 0.90; 95% CI, 0.80 to 1.02) or major osteoporotic fractures (HR 0.97; 95% CI, 0.90 to 1.05), nor was subsequent thyroxine prescription predictive of increased risk of fractures.	96% euthyroid/ 4% thyrotoxicosis	Low TSH was significantly more associated with major osteoporotic fractures than normal TSH. patients who present with an elevated TSH, the long-term risk of hip and other osteoporotic fractures is strongly related to the cumulative duration of periods with low TSH—likely from excessive replacement.	Age/chronic comorbid conditions/Fracture history/ recent Prednisolone use/ Osteoporosis medications use/	**Yes** excessive thyroxine dosing —was significantly associated with an increased risk of both hip fracture (HR 1.09; 95% CI, 1.04 to 1.15) and major osteoporotic fracture (HR 1.10; 95% CI, 1.06 to 1.14)

(Continued)

10.3389/fendo.2023.1230932

10.3389/fendo.2023.1230932

TABLE 2 Continued

ID	The first author (reference)	Country	Study type	Study population (n=) Female (), Male()	Age Mean ± SD	Type of thyroid disorder	Thyroid disorder symptoms	Sites of fracture	Hip fracture rate Mean ± SD/Percent	Hip fracture symptoms	Relationship between thyroid disorders and hip fracture in Female/Male (Yes or No)	History of thyroid disorder	Relationship between thyroid disorder and hip fracture Adj HR/CI	Other risk factors for fracture	Drug used
18	LJ Melton III (33)	USA	Cohort	630 female	42.5 ± 13.25	Thyroidectomy	NR	Vertebra/ pelvis/rib/ hip forearm	NR	NR	Yes	13.5% hyperthyroid/ 0.47% hypothyroid/ 60.5% euthyroid with adenoma/ 2.69% euthyroid with goiter/ 7.46% with malignancy	There is a little but statistically significant rise in the risk of hip fractures (95% CI 1.01–1.8)	age/ hyperparathyroidism/ osteogenesis imperfecta/ peptic ulcer disease/ gastrectomy/malabsorption syndrome/ chronic obstructive lung disease/ renal failure/ rheumatoid arthritis/ hemiplegia/hemiparesis/ parkinsonism/multiple myeloma	NR
19	Margaret C. Garin (34)	USA	cohort	female (2765) Male (2171)	65 years and older	Subclinical hyperthyroidism and hypothyroidism	NR	NR	NR	NR	NR	13.7% hypothyroid/ 84.6% euthyroid/ 1.6% hyperthyroid	There was no association between subclinical hypothyroidism or subclinical hyperthyroidism and hip fracture risk.	Age/BMI/Activity level/Ever-smoker/Alcohol use/Estrogen use/Corticosteroid use/Thiazide use/ no association was found between subclinical hyperthyroidism and incident hip fracture in either sex	NR

significant rise in the risk of hip fractures among thyroidectomized patients (33).

Since some studies focused on women, results may be influenced by involutional osteoporosis (25). Osteoporosis was identified in 90% of hypothyroid subjects who underwent a DEXA scan (26).

Other risk factors for hip fracture

Risk factors for hip fracture reported to be age (3, 32), sex (3), previous fractures (21, 23, 24, 32), smoking status (3, 17–19, 21, 23, 28–31), alcohol consumption (3, 17, 19, 21, 25, 30), parental fractures (17, 23), body mass index (BMI) (3, 17–19, 21, 23, 28–30), fat mass and weight (17, 20, 23, 25), menopausal status (3, 17–19, 23), disease-free for DTC recurrence, diseases involving bone anti-resorptive therapy (18), vitamin D level (23), calcium/vitamin D supplementation (3, 18), hormone replacement and use of oral estrogen (3, 19, 20), history of hyperthyroidism (3, 20, 22, 25), use of thyroid hormones (3, 20, 25, 32) were among factors related to hip fracture.

Medical history (21, 24, 30, 32), cognitive, visual, and neuromuscular function (21), diabetes mellitus (3, 17, 22, 23), rheumatoid arthritis, hemiplegia, malabsorption syndrome, and gastric surgery, radiotherapy to the pelvis (22), and using medication such as Prednisolone or Osteoporosis medications (3, 22, 24, 30, 32) were among factors correlated with hip fracture. Also, thiazide use, frailty status (3), age at thyroidectomy, extent of surgery (3, 25), menstrual/obstetrical status (28), and physical activity status (3, 29, 30) were related to hip fracture.

Discussion

We have conducted a systematic literature review to investigate the potential association between thyroid dysfunction and hip fracture outcome. Results indicate that the association of subclinical hypo- and hyperthyroidism with increased risk of hip fracture is still unclear since there is inevitable heterogenicity in the methodology of the studies. Studies were different regarding sample size, follow-up duration, comorbidities, history of previous fracture, history of medication (background therapies), thyroid pathogenesis (thyroid cancer, Goiter, thyroid nodule, autoimmune thyroid disease, etc.), severity of disease, number of events or traumas that occurred, and menopause status in women.

The systematic review and meta-analysis of seven population-based cohorts reported that participants with subclinical hypo- and hyperthyroidism, particularly among those with TSH levels of less than 0.10 mIU/L, compared with euthyroid participants had higher hazard ratios for hip and non-spine fracture but without statistical differences ($P>0.05$) (36). In like manner, all articles mentioned TSH levels of lower than 0.10 mIU/L as a cut off value, however, various articles have reached diffrenet results regarding the association between subclinical thyroid disorders and fractures. A similar meta-analysis study by Zhu et al. investigated 17 prospective cohorts, including 313,557 individuals, and found that subclinical

hyperthyroidism contributes to a significantly increased risk of hip, spine, and non-spine fractures by calculating relative risks; however, subclinical hypothyroidism was not associated with risk of any fracture (37). Additionally, in line with our findings, they concluded that age, cutoff value, and follow-up duration might play an important role in BMD, leading to higher fracture risk. Fang et al. evaluated sex-related differences between subclinical thyroid dysfunction and fractures. They demonstrated no significant sex-related differences. Unlike previous studies, they have argued that there is a greater risk of any fracture in men than in women with follow-ups of fewer than ten years; however, the risk of hip fracture was higher in women than men without a significant difference (38).

Mortenson et al., while focusing on the association of different medications with the risk of hip fracture, investigated the impact of thyroid hormone as one of the medications on hip fragility. They reported that patients who were overtreated or undertreated with exogenous thyroid hormone had a significantly higher risk of hip fracture (39). On the contrary, some studies hold up the view that endogenous subclinical hyperthyroidism has more effect on BMD than exogenous (40, 41). Also, Wirth et al. found that excluding all exogenous thyroid hormone recipients and limiting the analysis to individuals with endogenous subclinical hyperthyroidism showed an increased risk from 1.38 to 2.16 for hip fracture (36). A similar work by Ku et al. has demonstrated that TSH suppression therapy after thyroidectomy in postmenopausal women significantly decreased hip, lumbar spine, and femoral neck BMD; conversely, in premenopausal women, significantly increased lumbar spine and femoral neck BMD. Additionally, the case and control groups had no significant difference in men.

Different hypothetical mechanisms have been proposed to illustrate the relationship between thyroid hormone and BMD. First, osteoclasts have receptors for thyroid hormones which can directly influence its function, and since high thyroid hormone results in lower TSH hormone; therefore, besides the direct effect of thyroid hormone, it has an indirect impact on bone turnover and bone loss by regulating TSH (42, 43). Secondly, individuals with subclinical hyperthyroidism seem to have lower thigh muscle strength, possibly leading to increased fall-related fractures (44, 45). Thirdly, unlike osteoclasts, osteoblasts have receptors for both thyroid and estrogen hormones, indicating that these hormones play a crucial role in bone formation. As a result, subclinical hyperthyroidism and low estrogen levels, especially in postmenopausal women, are associated with osteoporosis and an increased risk of fractures (46, 47). Likewise, hypothyrodism has negative impacts on bone health, including reducing bone remodeling, provoking falls, reducing the osteoblast activity and decelerating secondary bone mineralization (5, 48). Notably, there is a possibility that hypothyroid patients who are already on treatment with thyroxine supplements were in fact iatrogenic hyperthyroid (26). Consequently, thyroid hormones profoundly impact BMD (39); however, individuals' age might have a more important role due to the severity of osteoporosis, the number of traumas or fallings, and the previous history of fractures considerably increasing in elderlies (44). Moreover, many studies do not distinguish between underlying pathogenesis, such as thyroid cancers, thyroid tumors, goiter, thyroid nodules, autoimmune thyroid disease, etc. These conditions affect bone turnover in various ways, possibly responsible for confounding results of included studies and previous reviews.

Limitation

Different approaches and methodologies were applied in the included studies, resulting in significant heterogenicity. For instance, different follow-up duration, a wide variety of statistical analysis reports (hazard ratio, relative risk ratio, odds ratio, etc.), and the absence of clear control cases limited our interpretation. Additionally, there is an increase in the upper physiological TSH reference range with age (e.g. 97.5 percentile from 4.32 mUI/l at the age of 20-30 to 5.23 mUI/l around the age 80 and 5.71 mUI/l around age of 90). Thus, some older individuals (i.e. with an increased risk of fracture) may be misclassified as having subclinical hypothyroidism, while their TSH may be indeed within their age-specific reference range. Plus, considering the conditions in which the thyroid hormones are evaluated is very important. For instance, assessing hormone levels right after the fracture is not recommended since fractures can be one of the triggers of acute stress and a contributing factor to the change in TSH levels. Furthermore, selection bias may be present despite our efforts not to set a strict and narrow inclusion criterion. Nevertheless, it is essential to study the available literature to reach a consistent conclusion and recognize the gaps that still need to be addressed.

The main strength of this study is that, in contrast to recent studies to find a positive trend for the impacts of subclinical thyroid dysfunction on hip fracture, our study tried to avoid biases and report reliable evidence in this matter. In this regard, we did not exclude studies due to heterogeneity or contradicted results. For future studies, we recommend that studies share their data in valid and authorized data banks to help big data scientists perform more detailed stratified analysis.

Conclusion

Reaching a consensus conclusion is not feasible regarding the association between subclinical thyroid dysfunction and hip fracture due to the heterogenicity of evidence, but we believe that confirming thyroid dsyfunction as a validated risk factor for hip fracture is yet to come. More studies with clear control selection are required to shed light on this matter which adjusts all possible potential confounders such as sex, age, endogenous or exogenous thyroid hormone, follow-up duration, age-adjusted cutoff values, body weight, cigarette smoking, previous fracture, and the epidemic of falls.

Data availability statement

The raw data supporting the conclusions of this article will be made available by the authors, without undue reservation.

Author contributions

(1) The conception and design of the study: EM, SS (2) Acquisition of data: SY, MD, AG (3) Analysis and interpretation of data: HS, AM (4) Drafting the article: EM, SM, KQ, GA, SP, MA, PM (5) Revising it critically for important intellectual content: SS, SY, OD (6) Final approval of the version to be submitted: SS, EM, OD. All authors contributed to the article and approved the submitted version.

Acknowledgments

The present study was conducted in collaboration with Khalkhal University of Medical Sciences, Tehran University of Medical Sciences, and Kashan University of Medical Sciences.

Conflict of interest

The authors declare that the research was conducted in the absence of any commercial or financial relationships that could be construed as a potential conflict of interest.

Publisher's note

All claims expressed in this article are solely those of the authors and do not necessarily represent those of their affiliated organizations, or those of the publisher, the editors and the reviewers. Any product that may be evaluated in this article, or claim that may be made by its manufacturer, is not guaranteed or endorsed by the publisher.

References

1. Apostu D, Lucaciu O, Oltean-Dan D, Mureşan A-D, Moisescu-Pop C, Maxim A, et al. The influence of thyroid pathology on osteoporosis and fracture risk: A review. *Diagnostics* (2020) 10(3):149. doi: 10.3390/diagnostics10030149

2. de Gouveia Dal Pino EM, Kowal G. Particle acceleration by magnetic reconnection. *Magnetic Fields Diffuse Media* (2015), 373–98. doi: 10.1007/978-3-662-44625-6_13

3. Lee JS, Bůžková P, Fink HA, Vu J, Carbone L, Chen Z, et al. Subclinical thyroid dysfunction and incident hip fracture in older adults. *Arch Internal Med* (2010) 170 (21):1876–83. doi: 10.1001/archinternmed.2010.424

4. Siddiqui JA, Partridge NC. Physiological bone remodeling: systemic regulation and growth factor involvement. *Physiology* (2016) 31(3):233–45. doi: 10.1152/physiol.00061.2014

5. Bassett JD, Williams GR. Role of thyroid hormones in skeletal development and bone maintenance. *Endocrine Rev* (2016) 37(2):135–87. doi: 10.1210/er.2015-1106

6. Baliram R, Latif R, Zaidi M, Davies T. Expanding the role of thyroid-stimulating hormone in skeletal physiology. *Front Endocrinol* (2017) 8:252. doi: 10.3389/fendo.2017.00252

7. Veronese N, Maggi S. Epidemiology and social costs of hip fracture. *Injury* (2018) 49(8):1458–60. doi: 10.1016/j.injury.2018.04.015

8. Soleimani M, Barkhordari S, Mardani F, Shaarbafchizadeh N, Naghavi-Al-Hosseini F. Rationing access to total hip and total knee replacement in the Islamic Republic of Iran to reduce unnecessary costs: policy brief. *East Mediterr Health J* (2020) 26(11):1396–402. doi: 10.26719/emhj.20.109

9. Soleimani M, Babagoli M, Baghdadi S, Mirghaderi P, Fallah Y, Sheikhvatan M, et al. Return to work following primary total hip arthroplasty: a systematic review and meta-analysis. *J Orthop Surg Res* (2023) 18(1):95. doi: 10.1186/s13018-023-03578-y

10. Moharrami A, Mirghaderi SP, Marzban S, Moazen-Jamshidi SMM, Shakoor D, Mortazavi SMJ. Total Hip Arthroplasty via direct anterior approach for osteonecrosis; comparison with primary hip osteoarthritis in a mid term follow up. *J Clin Orthop Trauma* (2022) 34:102042. doi: 10.1016/j.jcot.2022.102042

11. Hoveidaei AH, Nakhostin-Ansari A, Hosseini-Asl SH, Khonji MS, Razavi SE, Darijani SR, et al. Increasing burden of hip osteoarthritis in the Middle East and North Africa (MENA): an epidemiological analysis from 1990 to 2019. *Arch Orthop Trauma Surg* (2023) 143(6):3563–73. doi: 10.1007/s00402-022-04582-3

12. Fard SB, Jamshidi SMMM, Hoveidaei AH, Razzaghof M, Mortazavi SMJ. Nonunion following valgus subtrochanteric osteotomy for neglected femoral neck fracture: A case report. *Int J Surg Case Rep* (2023) 103:107905. doi: 10.1016/j.ijscr.2023.107905

13. Ebrahimpour A, Sadighi M, Hoveidaei AH, Chehrassan M, Minaei R, Vahedi H, et al. Surgical treatment for bisphosphonate-related atypical femoral fracture: A systematic review. *Arch Bone Jt Surg* (2021) 9(3):283–96. doi: 10.22038/abjs.2020.52698.2608

14. Ebrahimpour A, Chehrassan M, Hoveidaei AH, Jafari Kafiabadi M, Sadighi M, Manafi Rasi A, et al. Surgical management of extremity fractures in COVID-19 patients. *J Orthop Spine Trauma* (2022) 7(4):127–33. doi: 10.18502/jost.v7i4.8858

15. Beheshti Fard S, Moharrami A, Mirghaderi SP, Mortazavi SMJ. Broken pin removal from hip joint using arthroscopic grasper – A technical note and review of literature. *Injury* (2022) 53(11):3853–7. doi: 10.1016/j.injury.2022.08.054

16. Moher D, Shamseer L, Clarke M, Ghersi D, Liberati A, Petticrew M, et al. Preferred reporting items for systematic review and meta-analysis protocols (PRISMA-P) 2015 statement. *Syst Rev* (2015) 4(1):1–9. doi: 10.1186/2046-4053-4-1

17. Polovina S, Micić D, Miljić D, Milić N, Micić D, Popović V. The fracture risk assessment tool (FRAX® score) in subclinical hyperthyroidism. *Vojnosanit Pregl* (2015) 72(6):510–6. doi: 10.2298/VSP1506510P

18. Vera L, Gay S, Campomenosi C, Paolino S, Pera G, Monti E, et al. Ten-year estimated risk of bone fracture in women with differentiated thyroid cancer under TSH-suppressive levothyroxine therapy. *Endokrynol Pol* (2016) 67(4):350–8. doi: 10.5603/EP.a2016.0046

19. Lee SJ, Kim KM, Lee EY, Song MK, Kang DR, Kim HC, et al. Low normal TSH levels are associated with impaired BMD and hip geometry in the elderly. *Aging Dis* (2016) 7(6):734. doi: 10.14336/AD.2016.0325

20. Bauer DC, Ettinger B, Nevitt MC, Stone KLGroup SoOFR. Risk for fracture in women with low serum levels of thyroid-stimulating hormone. *Ann Internal Med* (2001) 134(7):561–8. doi: 10.7326/0003-4819-134-7-200104030-00009

21. Cauley JA, Cawthon PM, Peters KE, Cummings SR, Ensrud KE, Bauer DC, et al. Risk factors for hip fracture in older men: the osteoporotic fractures in men study (MrOS). *J Bone Mineral Res* (2016) 31(10):1810–9. doi: 10.1002/jbmr.2836

22. Gallagher JC, Melton L, Riggs BL. Examination of prevalence rates of possible risk factors in a population with a fracture of the proximal femur. *Clin Orthop Relat Res* (1980) 153:158–65. doi: 10.1097/00003086-198011000-00021

23. Polovina SP, Miljic D, Zivojinovic S, Milic N, Micic D, Brkic VP. The impact of thyroid autoimmunity (TPOAb) on bone density and fracture risk in postmenopausal women. *Hormones (Athens)* (2017) 16(1):54–61. doi: 10.14310/horm.2002.1719

24. Abrahamsen B, Jørgensen HL, Laulund AS, Nybo M, Bauer DC, Brix TH, et al. The excess risk of major osteoporotic fractures in hypothyroidism is driven by cumulative hyperthyroid as opposed to hypothyroid time: An observational register-based time-resolved cohort analysis. *J Bone Mineral Res* (2015) 30(5):898–905. doi: 10.1002/jbmr.2416

25. Nguyen TT, Heath IIIH, Bryant SC, O'Fallon WM, Melton LJ III. Fractures after thyroidectomy in men: A population-based cohort study. *J Bone Mineral Res* (1997) 12 (7):1092–9. doi: 10.1359/jbmr.1997.12.7.1092

26. Ahmad T, Muhammad ZA, Nadeem S. Is hypothyroidism associated with outcomes in fracture patients? Data from a trauma registry. *J Surg Res* (2021) 268:527–31. doi: 10.1016/j.jss.2021.07.036

27. Siru R, Alfonso H, Chubb SP, Golledge J, Flicker L, Yeap BB. Subclinical thyroid dysfunction and circulating thyroid hormones are not associated with bone turnover markers or incident hip fracture in older men. *Clin Endocrinol* (2018) 89(1):93–9. doi: 10.1111/cen.13615

28. Solomon Bl, Wartofsky L, Burman K. Prevalence of fractures in postmenopausal women with thyroid disease. *Thyroid* (1993) 3(1):17–23. doi: 10.1089/thy.1993.3.17

29. Svare A, Nilsen TIL, Åsvold BO, Forsmo S, Schei B, Bjøro T, et al. Does thyroid function influence fracture risk? Prospective data from the HUNT2 study, Norway. *Eur J Endocrinol* (2013) 169(6):845–52. doi: 10.1530/EJE-13-0546

30. Waring AC, Harrison S, Fink HA, Samuels MH, Cawthon PM, Zmuda JM, et al. A prospective study of thyroid function, bone loss, and fractures in older men: the MrOS study. *J Bone Mineral Res* (2013) 28(3):472–9. doi: 10.1002/jbmr.1774

31. Leese G, Jung R, Guthrie C, Waugh N, Browning M. Morbidity in patients on L-thyroxine: a comparison of those with a normal TSH to those with a suppressed TSH. *Clin Endocrinol* (1992) 37(6):500–3. doi: 10.1111/j.1365-2265.1992.tb01480.x

32. Abrahamsen B, Jørgensen HL, Laulund AS, Nybo M, Brix TH, Hegedüs L. Low serum thyrotropin level and duration of suppression as a predictor of major osteoporotic fractures—the OPENTHYRO register cohort. *J Bone Mineral Res* (2014) 29(9):2040–50. doi: 10.1002/jbmr.2244

33. Melton IIIL, Ardila E, Crowson C, O'Fallon W, Khosla S. Fractures following thyroidectomy in women: a population-based cohort study. *Bone* (2000) 27(5):695–700. doi: 10.1016/S8756-3282(00)00379-3

34. Garin MC, Arnold AM, Lee JS, Robbins J, Cappola AR. Subclinical thyroid dysfunction and hip fracture and bone mineral density in older adults: the cardiovascular health study. *J Clin Endocrinol Metab* (2014) 99(8):2657–64. doi: 10.1210/jc.2014-1051

35. da Maia TF, de Camargo BG, Pereira ME, de Oliveira CS, Guiloski IC. Increased risk of fractures and use of proton pump inhibitors in menopausal women: A systematic review and meta-analysis. *Int J Environ Res Public Health* (2022) 19 (20):13501. doi: 10.3390/ijerph192013501

36. Wirth CD, Blum MR, da Costa BR, Baumgartner C, Collet T-H, Medici M, et al. Subclinical thyroid dysfunction and the risk for fractures: a systematic review and meta-analysis. *Ann Internal Med* (2014) 161(3):189–99. doi: 10.7326/M14-0125

37. Zhu H, Zhang J, Wang J, Zhao X, Gu M. Association of subclinical thyroid dysfunction with bone mineral density and fracture: a meta-analysis of prospective cohort studies. *Endocrine* (2020) 67:685–98. doi: 10.1007/s12020-019-02110-9

38. Fang H, Zhao R, Cui S, Wan W. Sex differences in major cardiovascular outcomes and fractures in patients with subclinical thyroid dysfunction: a systematic review and meta-analysis. *Aging (Albany NY).* (2022) 14(20):8448. doi: 10.18632/aging.204352

39. Mortensen SJ, Mohamadi A, Wright CL, Chan JJ, Weaver MJ, von Keudell A, et al. Medications as a risk factor for fragility hip fractures: a systematic review and meta-analysis. *Calcified Tissue Int* (2020) 107:1–9. doi: 10.1007/s00223-020-00688-1

40. Yan Z, Huang H, Li J, Wang J. Relationship between subclinical thyroid dysfunction and the risk of fracture: a meta-analysis of prospective cohort studies. *Osteoporosis Int* (2016) 27:115–25. doi: 10.1007/s00198-015-3221-z

41. Belaya ZE, Melnichenko GA, Rozhinskaya LY, Fadeev VV, Alekseeva TM, Dorofeeva OK, et al. Subclinical hyperthyroidism of variable etiology and its influence on bone in postmenopausal women. *Hormones (Athens)* (2007) 6 (1):62–70.

42. Cooper DS, Biondi B. Subclinical thyroid disease. *Lancet* (2012) 379(9821):1142–54. doi: 10.1016/S0140-6736(11)60276-6

43. Baliram R, Sun L, Cao J, Li J, Latif R, Huber AK, et al. Hyperthyroid-associated osteoporosis is exacerbated by the loss of TSH signaling. *J Clin Invest* (2012) 122 (10):3737–41. doi: 10.1172/JCI63948

44. Morrison A, Fan T, Sen SS, Weisenfluh L. Epidemiology of falls and osteoporotic fractures: a systematic review. *Clinicoecon outcomes Res* (2012) 5:9–18.

45. Brennan MD, Powell C, Kaufman KR, Sun PC, Bahn RS, Nair KS. The impact of overt and subclinical hyperthyroidism on skeletal muscle. *Thyroid* (2006) 16(4):375–80. doi: 10.1089/thy.2006.16.375

46. Van der Eerden B, Gevers E, Löwik C, Karperien M, Wit J. Expression of estrogen receptor α and β in the epiphyseal plate of the rat. *Bone* (2002) 30(3):478–85. doi: 10.1016/S8756-3282(01)00703-7

47. Robson H, Siebler T, Stevens DA, Shalet SM, Williams GR. Thyroid hormone acts directly on growth plate chondrocytes to promote hypertrophic differentiation and inhibit clonal expansion and cell proliferation. *Endocrinology* (2000) 141(10):3887–97. doi: 10.1210/endo.141.10.7733

48. Bassett JD, Williams GR. The molecular actions of thyroid hormone in bone. *Trends Endocrinol Metab* (2003) 14(8):356–64. doi: 10.1016/S1043-2760(03)00144-9

frontiers | Frontiers in Endocrinology

TYPE Review
PUBLISHED 07 March 2024
DOI 10.3389/fendo.2024.1347802

Check for updates

OPEN ACCESS

EDITED BY
Marco António Campinho,
University of Algarve, Portugal

REVIEWED BY
Samantha J. Richardson,
RMIT University, Australia
Fernanda Marques,
University of Minho, Portugal

*CORRESPONDENCE
Sylvie Remaud
sremaud@mnhn.fr

†These authors have contributed equally to this work

RECEIVED 01 December 2023
ACCEPTED 08 February 2024
PUBLISHED 07 March 2024

CITATION
Valcárcel-Hernández V, Mayerl S, Guadaño-Ferraz A and Remaud S (2024) Thyroid hormone action in adult neurogliogenic niches: the known and unknown. *Front. Endocrinol.* 15:1347802. doi: 10.3389/fendo.2024.1347802

COPYRIGHT
© 2024 Valcárcel-Hernández, Mayerl, Guadaño-Ferraz and Remaud. This is an open-access article distributed under the terms of the Creative Commons Attribution License (CC BY). The use, distribution or reproduction in other forums is permitted, provided the original author(s) and the copyright owner(s) are credited and that the original publication in this journal is cited, in accordance with accepted academic practice. No use, distribution or reproduction is permitted which does not comply with these terms.

Thyroid hormone action in adult neurogliogenic niches: the known and unknown

Victor Valcárcel-Hernández[1†], Steffen Mayerl[2†], Ana Guadaño-Ferraz[3] and Sylvie Remaud[1*]

[1]Laboratory Molecular Physiology and Adaptation, CNRS UMR 7221, Department Adaptations of Life, Muséum National d'Histoire Naturelle, Paris, France, [2]Department of Endocrinology, Diabetes and Metabolism, University Hospital Essen, University Duisburg-Essen, Essen, Germany, [3]Department of Neurological Diseases and Aging, Instituto de Investigaciones Biomédicas Sols-Morreale, Consejo Superior de Investigaciones Científicas (CSIC)-Universidad Autónoma de Madrid (UAM), Madrid, Spain

Over the last decades, thyroid hormones (THs) signaling has been established as a key signaling cue for the proper maintenance of brain functions in adult mammals, including humans. One of the most fascinating roles of THs in the mature mammalian brain is their ability to regulate adult neurogliogenic processes. In this respect, THs control the generation of new neuronal and glial progenitors from neural stem cells (NSCs) as well as their final differentiation and maturation programs. In this review, we summarize current knowledge on the cellular organization of adult rodent neurogliogenic niches encompassing well-established niches in the subventricular zone (SVZ) lining the lateral ventricles, the hippocampal subgranular zone (SGZ), and the hypothalamus, but also less characterized niches in the striatum and the cerebral cortex. We then discuss critical questions regarding how THs availability is regulated in the respective niches in rodents and larger mammals as well as how modulating THs availability in those niches interferes with lineage decision and progression at the molecular, cellular, and functional levels. Based on those alterations, we explore the novel therapeutic avenues aiming at harnessing THs regulatory influences on neurogliogenic output to stimulate repair processes by influencing the generation of either new neurons (i.e. Alzheimer's, Parkinson's diseases), oligodendrocytes (multiple sclerosis) or both (stroke). Finally, we point out future challenges, which will shape research in this exciting field in the upcoming years.

KEYWORDS

thyroid hormones, adult, adult neurogenesis, adult oligodendrogenesis, SVZ: subventricular zone, SGZ: subgranular zone of the hippocampus

Introduction

Adult neurogliogenesis is a process strictly regulated in all mammals, including humans. In particular, neurogenesis occurs throughout the lifespan in specific and restricted areas of the brain. The subventricular zone (SVZ) lining the lateral ventricles (1, 2) and the subgranular zone (SGZ) in the hippocampus (3, 4) are the two main niches in which adult generation of new neural cells has been extensively described in physiological and pathological conditions. However, several other brain areas have also been identified as emerging sites of newly generated neurons and glial cells in adult mammals, although the origin of progenitors underlying this process remains controversial. Such niches include the hypothalamus (5, 6), striatum (2, 7–9), and cerebral cortex (10, 11), among others, such as the amygdala (12, 13). However, even though neurogliogenesis has already been extensively studied, mechanisms underlying the generation of new neural cells in the adult are not completely disentangled up to date.

Among the potential players controlling these processes, thyroid hormones (THs), T_3 (3,5,3'-triiodothyronine) and T_4 (thyroxine) arise as top candidates. The role of THs on adult neurogliogenesis has been well established in mammals, and especially in rodents, for some time now (14–16), with various aspects ranging from the control of cell proliferation (17–21), determination and differentiation (18–22), to cell death (18, 23).

However, mechanisms underlying TH-dependent neurogliogenic processes are only emerging in the two main neurogenic niches (SVZ and SGZ), but further research is needed to assess TH action in other emerging adult neurogliogenic niches. We hypothesize that a dynamic interaction between TH signaling regulators tightly modulates intracellular TH action, thus regulating neural stem cell (NSC) behavior (i.e., proliferation and neuron/glia determination) and progenitor differentiation. Cell-specific THs availability in the brain is finely tuned by (i) THs supply to cerebral tissues carried out by TH-distributor proteins such as transthyretin (TTR) (24) and ii) transmembrane TH-transporters (THTs) (25). Moreover, TH action in the brain is regulated by iii) a balance between TH-activating deiodinases (mainly type 2 deiodinase, or DIO2, in the brain, that locally converts T_4 to T_3) and inactivating deiodinases (mainly type 3 deiodinase or DIO3) (26). Finally, to translate the THs signal into changes in gene expression, iv) the presence of ligand (T_3)-dependent nuclear receptors (TR) (27) such as TRα1, TRβ1 or TRβ2, is the main way for THs action.

Besides the obvious interest in understanding the molecular and cellular aspects of adult neurogliogenic processes and their interactions with THs, it is also important to note that the generation of new neural cells in the adult brain has major functional impacts on health and disease, and a better knowledge of these TH-dependent mechanisms could lead to new therapeutic avenues. Hence, in this review, we describe the features of the known, and lesser-known neurogliogenic niches in the adult rodent brain, as well as the multiple roles of THs in regulating neurogliogenic processes in both health and disease. Finally, given the lack of knowledge on several aspects addressed in this review, we point out several future challenges, trying to pinpoint the most significant knowledge gaps, that will most likely drive further research.

Thyroid hormone action in the SVZ

SVZ-NSCs, also known as B1 cells, are astrocytic-type cells (28, 29) generated during embryonic development. After this embryonic period, "pre-B" cells enter quiescence until adulthood, where they can be reactivated (30, 31), especially following a brain injury (1, 32, 33). A fine regulation between quiescent and proliferative NSCs is required to preserve the NSC pool within the SVZ niche (30, 31, 34, 35). Elegant real-time imaging experiments demonstrated that B1 cells generate actively proliferating Transient Amplifying Progenitors (C cells or TAP) by asymmetric division (36, 37). TAPs can divide symmetrically up to three times before generating neuroblasts (A cells), characterized by their limited proliferative capacity and the expression of the specific marker doublecortin (DCX+) (37). DCX+ neuroblasts migrate towards the olfactory bulbs (OB) along a tangential migration pathway, the Rostral Migratory Stream (RMS) (38). In the OB, neuroblasts migrate radially and differentiate into distinct populations of GABAergic (expressing calbindin and calretinin) and dopaminergic (expressing tyrosine hydroxylase) interneurons (39–41) that integrate into pre-existing interneuron networks (41–43). These newly generated olfactory neurons play a role in the olfactory function of rodents, particularly in the discrimination and memorization of odors, which are crucial for the animal's adaptation to its environment (for mating and offspring care) (43–46).

Glial cells, including astrocytes and oligodendrocyte precursors (OPCs, identifiable by the oligodendroglia lineage marker OLIG2), are also derived from a subpopulation of SVZ B1 cells (2, 47–49). OPCs derived from SVZ-NSCs migrate towards white matter tracts in proximity to the lateral ventricles (i.e., corpus callosum, striatum) where they differentiate into mature myelinating oligodendrocytes (2, 21, 50–52). Interestingly, SVZ-OPCs never produce glial cells located in OBs (53, 54). Functional studies of oligodendrocytes derived from SVZ-NSCs are limited. SVZ-OPCs are capable of successfully repairing damaged demyelinated lesions in the corpus callosum and striatum, close to the lateral ventricle (21, 51, 52). Thus, SVZ-OPCs constitute an endogenous source of myelin-enhancing oligodendrocytes in the adult mammalian brain. It is of particular relevance to stimulate this endogenous production of SVZ-OPCs in order to improve functional myelin recovery, by promoting (i) the generation of OPCs from SVZ-NSCs, (ii) the migration of these OPCs to the injury sites and (iii) the differentiation of these OPCs into mature myelinating oligodendrocytes. This question is of particular interest given that postmortem brain studies in patients who died of multiple sclerosis (MS) have shown that SVZ-derived OPCs also migrate to lesions located in the corpus callosum (50). Thus, the recruitment of newly generated OPCs in adults is conserved between humans and rodents.

The role of THs in the biology of SVZ-NSCs has been investigated mainly by Remaud's group over the past two decades in the young adult mouse (Figure 1). We first determined the expression pattern of several regulators of THs action (i.e, TRs, THTs, TH-distributor proteins, deiodinases) within the adult mammalian SVZ to identify the cell types that preferentially

respond to THs. By immunohistochemistry, we demonstrated that only the TRα1 isoform is expressed in SVZ cells, and not TRβ (18, 55) and that TRα1 is found especially in neuroblasts (55) but not in OLIG2+ OPC (21) (Figure 1). Interestingly, we found that TRα1 (considered as a neuronal determinant) and EGFR (a TH-target gene involved in glial determination) are asymmetrically segregated during NSC/progenitor division, suggesting that one daughter cell inheriting TRα1 will become a neuroblast whereas EGFR+ sister cells will be determined toward an oligodendroglial fate (21) (Figure 1). Regarding the expression of key THTs, monocarboxylate transporter 8 (MCT8), and organic anion-transporting polypeptide 1C1 (OATP1C1) are mainly detected in committed neuronal cells (56) (Figure 1). Altogether, these data suggest that TH signaling is more active in SVZ-derived neuronal cells whereas oligodendroglial cells do not seem to harbor the arsenal of regulators that would allow them to respond to THs signaling. Accordingly, OLIG2+ and SOX10+ OPCs express high levels of DIO3 (Figure 1), the THs-inactivating enzyme that is not expressed in neuronally committed SVZ-cells (21), showing that OPCs are protected from the effects of THs not only by the expression of DIO3 but also by the absence of TRα1 expression. Moreover, Vancamp et al. (2019) reported that, although mRNAs for the TH-distributor protein *Ttr* were detected in SVZ, especially in NSCs and neuroblasts, by RTqPCR, they did not detect the TTR protein using immunohistochemistry (57). This strongly suggests that TTR-mediated THs supply could be a key factor favoring neuronal specification (57). However, the detection of *Ttr* transcripts *versus* the failure to detect TTR protein by immunohistochemistry requires further investigation to better determine the action of *Ttr* within SVZ cells. As the intracellular action of THs can be regulated at multiple levels in the targeted SVZ cells, depending on the expression of THTs, deiodinases, TH-distributor proteins or receptors, two factors that modulate the intracellular response to TH should be given a more careful consideration. First, the expression of the TRα2 isoform should be better investigated in future studies concerning the cellular and molecular responses to THs signaling, as its putative dominant-negative role (without T_3 affinity) may counteract the intracellular action of THs. Indeed, TRα2 is highly expressed in the brain, notably in adult SVZ cells as we demonstrated by RTqPCR following FACS-dissected murine SVZs (56). Second, to gain an overview of the regulation of T_3 availability in the various SVZ cell types, it is crucial to define the role and the expression pattern at the protein level of DIO2 that remains unexplored yet.

We established that fine tuning of intracellular T_3 ligand availability in the different SVZ cell types governs neuron/glia fate orientation of adult murine NSCs. In particular, we demonstrated that hypothyroidism, induced by PTU (6-n-propyl-2-thiouracil) treatment, reduced the number of mitotically active cells in adult mice, by arresting NSCs and progenitors during the S phase (18). A similar phenotype was found in Trα$^{0/0}$ mice (18), lacking all isoforms encoded by the *Thra* locus (58). Moreover, a decreased apoptosis was observed in the SVZ of PTU-induced hypothyroid mice (18, 23). A T_3 intraperitoneal injection restored proliferation and apoptosis to levels similar to the control group, demonstrating that T_3 is required for progenitor proliferation within the adult SVZ. Furthermore, adult PTU-induced hypothyroid mice also showed a reduction in the number of migrating neuroblasts along the RMS (18), thus negatively impacting the generation of new olfactory interneurons. In line with these findings, we showed that TH signaling acts as a

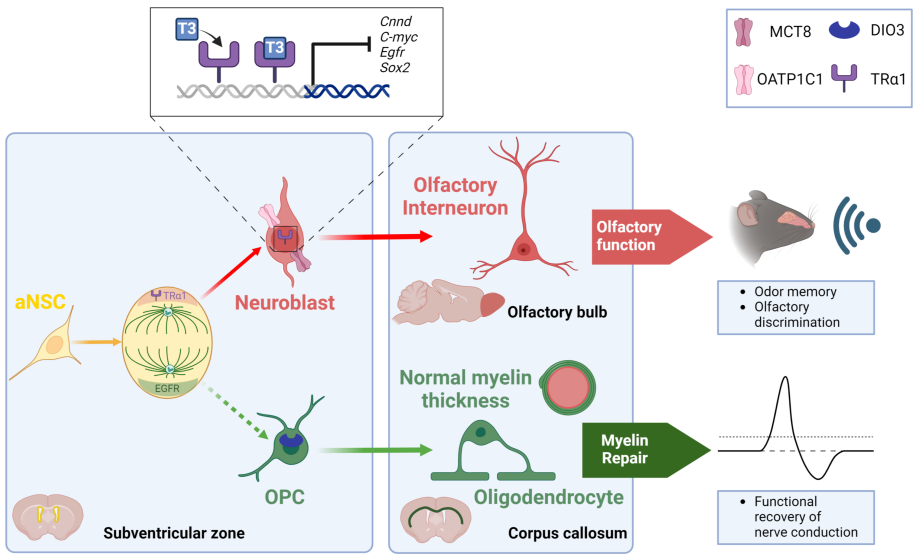

FIGURE 1
TH signaling modulates the neuronal *versus* glial fate decision within the SVZ niche of the adult mouse. During NSC division, an asymmetric segregation of a neural determination factor (TRα1) and a glial determination marker (EGFR) is observed. Moreover, T_3 through its receptor TRα1, drives NSC commitment preferentially towards a neuroblast via downregulating various genes involved in glial determination (*Egfr*), cell cycle progression (*c-Myc*, *Cnnd1*) and NSC pluripotency (*Sox2*). Neuroblasts generate olfactory interneurons in the olfactory bulbs that participate in olfactory behavior that is strongly affected when THs action is impaired. A lack of T_3 favors the generation of new SVZ-derived OPCs. These SVZ-OPCs can repair myelin in the corpus callosum and restore normal nerve conduction after a demyelinating insult using the cuprizone mouse model.

neurogenic switch by promoting the commitment of NSCs and progenitors preferentially to a neuronal fate (21, 55). TRα1 overexpression using an *in vivo* non-viral gene transfer method (58, 59) increased neuroblast generation in the most dorsal part of the SVZ. We have shown that T_3 - *via* its receptor TRα1 - promoted neuronal determination through transcriptional repression of (i) *Sox2*, a key gene involved in NSC pluripotency (55) and (ii) crucial genes involved in regulating cell cycle progression such as *Ccnd1* and *c-Myc* (18, 59). Furthermore, we also showed in 2017 that T_3 promoted neuronal fate at the expense of oligodendroglial fate, notably through modulation of cell metabolism (15). In particular, mitochondrial respiration and fission are more active in neuronal precursors, compared to the situation in oligodendroglial precursors.

While T_3 favors a neuronal fate, a TH-free window in contrast promoted the generation of new OPCs derived from adult murine SVZ-NSCs (15, 21). We reported *in vivo*, by immuno histochemistry, that SVZ-OPCs are protected from the T_3-mediated pro-neurogenic effects *via* (i) a high expression of DIO3 (21) (ii) a lack of TRα1 expression and (iii) an absence of two key THTs, MCT8 and OATP1C1 (18, 21). In contrast, neuroblasts express TRα1 but not DIO3, suggesting that TH signaling is active in neuronal cells. Moreover, a transient reduction of *Dio3* expression (by *in vivo* non-viral transfection using a DNA plasmid expressing a shRNA directed against mRNA encoding *Dio3*) induced a significant decline in the number of SVZ-OPCs, illustrating the importance of this "T_3-free window" in SVZ-oligodendrogenesis. While a transient lack of T_3 is required for SVZ-OPC specification, T_3 is also well known for accelerating OPC exit from the cell cycle and committing them to differentiation *via* TRα1, in cooperation with another nuclear receptor, RXRϒ (60, 61). Furthermore, we have recently shown that adult mice deficient for the TH-distributor protein TTR - exhibiting low levels of T_3 and T_4 in the CSF (62) - increased the generation of new SVZ-derived OPCs at the expense of the production of new neuroblasts (57). Thus, the neuron/glia balance is shifted once again in favor of oligodendrogenesis in the context of central hypothyroidism. Similarly, our latest work revealed increased SVZ-OPC production in the absence of MCT8 and OATP1C transporters using the *Mct8*$^{-/-}$, *Oatp1c1*$^{-/-}$ double knockout dKO mice (56). In turn, the production of mature neuroblasts is diminished and associated with a migration defect.

What is the functional relevance of the T_3-dependent regulation of the neuron-glia balance? As mentioned previously, T_3 preferentially drives NSC fate towards neuroblasts. In various pharmacological and genetic backgrounds, that reflect a central hypothyroidism, we have shown that reduced SVZ-neurogenesis is associated with impaired olfactory behavior in adult mice, and in particular with a reduced short-term olfactory memory (56) (Figure 1). We also examined the functionality of the "T_3-free window" in a well-established model of demyelination using cuprizone, a gliotoxin that induces death of mature oligodendrocytes (63) predominantly distributed in the corpus callosum for a six-week cuprizone treatment period (21). Transient hypothyroidism was then applied to mice during the demyelination phase, a phase during which new SVZ-OPCs are reported to proliferate, thus promoting myelin repair (64). In that context, we have shown that these mice efficiently repaired demyelinating lesions in the corpus callosum, especially just above the ventricles. Indeed, waves of remyelination originating in the dorsal part of the SVZ are puzzlingly observed. Unexpectedly, quantification of myelin thickness by electron microscopy revealed that myelin sheath at remyelination sites is of normal thickness around the axons of the corpus callosum (21). Furthermore, electrophysiological experiments were performed by measuring compound action potentials (CAPs) in coronal corpus callosum slices one week after endogenous remyelination (64). We highlighted that such hypothyroidism, applied during demyelination, enabled a functional recovery of nerve conduction (21) (Figure 1). Similarly, TTR null mice also displayed an increase in oligodendrogenesis during development (65) as well as a thicker myelin sheath in the corpus callosum following cuprizone withdrawal (66). Thus, SVZ-derived OPCs constitute an endogenous source of glial progenitors capable of functionally repairing a demyelinated lesion localized in the corpus callosum, close to the lateral ventricles as it has been also demonstrated by other works (51, 52). However, how a TH-deficient environment contributes to restoring a myelin sheath of normal thickness is still an unresolved question.

Our findings on TH action on SVZ-NSCs led to TH signaling being considered as a potential key signal for stem cell-based regenerative medicine (67). The regenerative potential of THs has been well documented in fish, maintaining a large adult pool of NSCs (68, 69). In contrast, in mammals, which exhibit a neonatal THs peak [for review, see (70)], CNS regenerative capacities are drastically diminished after this THs peak. The adult SVZ niche, which remains sensitive to THs throughout life, provides a potential source of neural cells that can be mobilized in pathophysiological conditions requiring the supply of new neurons (as seen in Alzheimer's) or oligodendroglial cells (as observed in MS), or both (as in the case of stroke). Here, we focus on the contribution of THs in repairing demyelinating lesions that are characteristic of MS, a chronic inflammatory disease that affects the entire CNS (brain and spinal cord). It is the first cause of motor disability in young adults. In addition, the worldwide incidence of this disease has been unexpectedly increasing over the last twenty years (71) and therefore represents a major public health issue. MS is associated with multiple demyelinating lesions (plaques), inflammatory cells, loss of oligodendrocytes, and decreased axon density (72). A burning question is to understand how to mobilize the cell type that favor remyelination. OPCs, which account for 5% to 8% of adult CNS cells, and the myelin-forming oligodendrocytes derived from them, are obvious targets for promoting myelin repair [for review, see (73)]. One approach to boosting myelin recovery is to enhance the pool of oligodendrocyte progenitors. Two endogenous sources can be mobilized for MS patients: (i) newly-generated adult OPCs from NSCs, as discussed above, and (ii) parenchyma-resident OPCs (pOPCs), generated during development and which persist in the adult brain. Thus, the SVZ represents an attractive endogenous

source of OPCs. Postmortem examination of brains from individuals diagnosed with MS revealed efficient recruitment of SVZ-derived OPCs to sites of injury in the corpus callosum (50). The rodent model of cuprizone-induced demyelination, as mentioned above, has been used to assess the effect of THs on remyelination. Franco et al. (2008) showed that T_3 injections during the recovery/remyelination period - following 2 weeks of cuprizone-based demyelination - induced an increase in OLIG2+ oligodendroglial cells exiting the cell cycle in the SVZ along with increased detection of TRα1 and TRβ in SVZ cells by immunohistochemistry. An increased number of mature oligodendrocytes expressing hallmark markers (O4, MBP, PLP, CC1) was observed in the corpus callosum (74). Similarly, an MRI analysis also showed that T_3 injections in mice, during the recovery weeks after cuprizone treatment, enhanced remyelination in the corpus callosum (75). In these two studies, however, the origin of the remyelinating cells (SVZ-derived OPCs or pOPCs) was not clearly stated. Since then, work several groups including ours (21, 51, 52), has shown - using cell tracing experiments - that adult murine SVZ OPCs were able to migrate to myelin damage induced in the corpus callosum and then differentiate into mature myelinating oligodendrocytes. Our protocol - based on a transient hypothyroidism window applied during the demyelination phase followed by T_4/T_3 pulses during recovery - allows to restore a myelin sheath of similar thickness to that of the euthyroid control group. In contrast, pOPCs did not respond to this transient hypothyroidism, unlike newly generated OPCs, showing that these two OPC subpopulations respond differentially to THs signaling. The underlying challenge would be deciphering the molecular mechanisms that regulate the differential response to THs of SVZ OPCs (complete remyelination) and pOPCs (incomplete remyelination), in order to better understand the mechanisms responsible for functional myelin repair.

Future challenges:

- What is the function of some regulators (i.e., DIO2, TTR, TRα2) in the physiology of adult SVZ-NSCs? In particular, the role of TTR as a TH-distributor protein in the CSF and/or a function independent of THs should be better deciphered. Furthermore, the function of the TRα2 isoform would deserve more in-depth consideration since TRα2 is highly expressed in adult SVZ cells and may act as a dominant-negative regulator (with no affinity for T_3) countering intracellular THs effects.
- How do THs differentially regulate the response of SVZ-derived OPCs *versus* resident OPCs following a demyelinating lesion?
- Non-genomic effects, that do not require an interaction between T_3 and its TR, are not yet known on NSC proliferation and determination within the SVZ niche and should be assessed in further studies

Thyroid hormone action in the SGZ

Adult hippocampal neurogenesis is a highly orchestrated process that continuously generates new granule cell neurons throughout life. To this end, the SGZ of the dentate gyrus harbors radial glia-like NSCs that express markers like GFAP or Nestin as shown in rodents (14, 76, 77). Though they can also differentiate into astrocytes, NSCs mainly divide asymmetrically thereby giving rise to rapidly proliferating TAPs that are also referred to as type 2 progenitors (76, 78). Based on their expression profile, this population is further sub-divided into Nestin positive, type 2a progenitors, which then develop into DCX positive, type 2b progenitors (14, 76). Subsequently, these cells form into neuroblasts, which exhibit a reduced proliferative capacity, eventually exit from the cell cycle, and differentiate into immature granule cell neurons (76). Both neuroblasts and immature neurons continue to express DCX but can be distinguished by the presence of the calcium-binding protein calretinin in immature neurons (79). The sequential progression through these distinct stages is a rapid process and in mice, new immature neurons are derived from NSCs within three days (79). The final steps encompassing short-distance migration, maturation, and functional integration of new neurons into the existing granule cell network take 4-6 weeks in rodents (76). This continuous generation of new neurons significantly contributes to the high plasticity of the adult hippocampus. Several studies have demonstrated a critical role for adult hippocampal neurogenesis in cognitive flexibility and more specifically in learning and memory processes, in emotional regulation, anxiety, and spatial navigation (78, 80, 81). Although much better characterized in the rodent brain, observations in humans that demonstrated the presence of DCX+ cells and detected new neurons in the hippocampus strongly argue for the existence of adult hippocampal neurogenesis also in humans (77, 78).

THs constitute an important extrinsic signaling cue for adult hippocampal neurogenesis and components of the TH signaling pathway were identified at all stages of the program in mice. Transcript analyses on isolated neurogenic populations revealed the expression of the THs transporting amino acid transporters *Lat1* and *Lat2* in SGZ-NSCs and type 2 progenitors (19) (Figure 2). *In vitro* and *in vivo* studies highlighted the presence of TRβ isoforms in Nestin positive as well as in proliferating, BrdU positive hippocampal progenitors whereas TRα1 was mainly detected in DCX+ neuroblasts and granule cell neurons (82, 83). Likewise, we demonstrated that the latter two populations are equipped with the highly specific THT MCT8 while mature granule neurons further express MCT10, LAT2, and DIO3 (19). *Oatp1c1* promoter activity was detected in subsets of all progenitor and neuronal populations though the causes and consequences of this heterogeneity remain to be investigated (84). Together, the expression patterns of TH signaling components suggest that progenitor and mature neuronal populations within the adult hippocampal neurogenic lineage possess the ability to directly sense and integrate the TH signal.

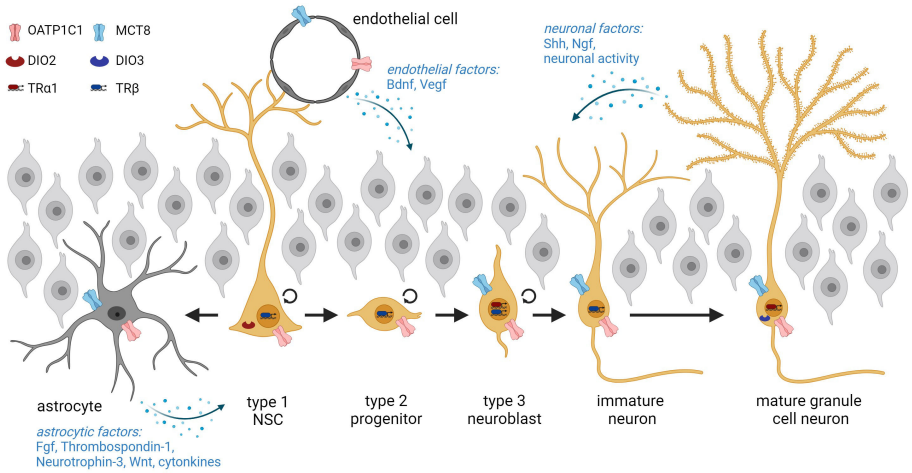

FIGURE 2
Overview of adult hippocampal neurogenesis starting from NSCs in the subgranular zone and progression through the different stages. NSCs are in intimate contact with the endothelium and can either generate type 2 progenitors or differentiate terminally into astrocytes. The cellular expression of THs transporters and deiodinases within adult hippocampal lineage cells is depicted. Neurogenesis is further regulated by extrinsic factors derived from astrocytes, endothelial cells, and neurons. Graphic was created with Biorender.

A wealth of experimental studies has addressed the consequences of manipulated THs availability on neurogenesis in the adult SGZ and demonstrated THs-induced effects predominantly during the later stages of the neurogenic program (14, 19, 20, 82, 83, 85, 86). Adult-onset hypothyroidism led to decreased precursor cell survival and a reduced number of DCX positive progenitor cells in rodents (20, 22, 83, 85, 87, 88). These observations, however, were made in animals in which experimental interventions caused a strong decrease in circulating THs levels. Low-dose PTU treatment induced adult-onset hypothyroxinemia (subclinical hypothyroidism) in rats that did not result in similar alterations in SGZ neurogenesis indicating that most likely the extent of THs insufficiency is critical (89). T_3-induced, adult-onset hyperthyroidism conversely accelerated progenitor differentiation in mice (22). Along this line, the level of TRα1 correlates inversely with the total number of DCX positive cells. TRα1 null (TRα1$^{-/-}$) mice harbor elevated numbers of DCX positive cells, while the same cell population is reduced in TRα2$^{-/-}$ mice, which overexpress TRα1 6-fold as both isoforms are derived from the same gene through alternative splicing (82). Rather than to the absence of the non-TH-binding TRα2 isoform in the latter model, the reduction in DCX positive cells has been attributed to the increased concentration of TRα1 that in light of limited cellular T_3 availability generates a condition comparable to local hypothyroidism. Together, these findings point to a negative impact of the TRα1 aporeceptor on lineage progression. Our studies further showed that absence of MCT8 either globally or specifically in the adult neurogenic lineages using a tamoxifen-inducible form of Cre recombinase expressed under the Nestin promoter (Nestin-CreERT2) diminished the differentiation to immature neurons and the formation of new granule cell neurons (19). Mechanistically, this has been linked to a delayed cell cycle exit through decreased expression of the cell cycle inhibitor p27Kip1 in DCX positive cells *in vivo*. Similarly, the global absence of OATP1C1 impaired progenitor differentiation and program progression, but whether this reflects a lineage-intrinsic function remains elusive (84). This is but one example for the future challenge to identify the lineage-autonomous impacts of TH signaling components. Likewise, the question as to which pathways mediate TH effects on hippocampal neurogenesis *in vivo* awaits further investigation.

In contrast to the well-established action in later stages, the potential impact of THs on early progenitor populations in the adult SGZ remains controversial. While adult-onset hypothyroidism in rats exposed to PTU or methimazole (MMI) did not result in altered BrdU incorporation into cycling progenitors, their number was reduced in adult-onset thyroidectomized rats, an effect that was rescued by THs administration to the drinking water (20, 83, 85). Moreover, the global absence of TRβ in mice stimulated progenitor proliferation and BrdU incorporation in the SGZ indicating a regulatory function of THs/TRβ in NSC activation and progenitor proliferation (90). It has been suggested that unliganded TRβ exerts a repressive function on NSC turn-over, which would be lifted upon T_3 binding (67). This scenario, however, requires the uptake of THs into SVZ-NSCs through a yet unidentified pathway. Recent hippocampal single cell and single nuclei RNA sequencing studies advanced this idea and highlighted the presence of *Oatp1c1* transcripts in NSCs in line with *in vivo Oatp1c1* promoter activity studies (84, 91–93). Interestingly, these sequencing studies also detected *Dio2* transcript expression in murine SGZ-NSCs. Although further work is still needed, it is a fascinating idea that NSCs are equipped with the machinery to take up T_4 and generate T_3 in a cell-autonomous manner, as has been proposed to take place in radial glial cells in the prenatal human cerebral cortex (94). At the same time, super-resolution microscopy revealed that hippocampal NSC processes contact intimately the blood-brain barrier (BBB) and are capable of directly accessing blood-born substances (95). In this

context, NSCs were shown to take up BBB-impermeable substances in an otherwise unimpeded BBB environment stressing how privileged this access is. It is thus tempting to hypothesize that NSCs directly take up T_4 from the circulation via up-regulation of OATP1C1 in the activated state, and convert it locally to T_3, which in turn stimulates NSC turn-over. The T_4-dependency of such a scenario may explain the apparent lack of effect in T_3-induced hyperthyroidism (22). Moreover, due to their slow cell cycle kinetics and high degree of quiescent NSCs, the consequences of altered THs signaling on NSC activation may be mild and may only become obvious after a longer time interval than is usually assessed in adult-onset hypothyroid models (96). Such a regulatory influence on NSC activation may further explain the preservation of NSC numbers with age as seen in *Mct8* knockout (KO) and *Mct8/Oatp1c1* dKO mice potentially associated with their reduced T_4 serum levels and different degrees of central THs deficit (84, 97). Though acting through a different pathway, THs feature a similar function on the regulation of NSC maintenance and activity in the SVZ (16).

Importantly, modulating the thyroidal state in adult rodents also affects hippocampus-related behaviors that depend on proper SGZ neurogenesis such as spatial memory or the regulation of anxiety and mood (80, 81). Adult-onset hyperthyroidism compromised learning and memory function and increased anxiety in rats and mice (98, 99). Likewise, hypothyroidism in adult rodents either by thyroidectomy or administration of PTU or MMI as well as a low iodine diet resulted in an anxiety-depression-like state as well as impaired learning and spatial memory performance (20, 100–103). Why adult-onset hypo- and hyperthyroidism culminate in similar behavior impairments remains elusive. Though the underlying molecular pathways certainly differ, these observations suggest a gatekeeper function of balanced THs signaling for hippocampal functions. Anxiety-depression-like behaviors were further observed in TRα1 mutant mice, in which THs binding affinity is reduced 10-fold, and in global *Mct8* KO mice (84, 104). Whether the behavioral changes in the latter genetically modified models are solely the consequence of a perturbed adult hippocampal neurogenic program or if developmental alterations contribute to it, remains elusive. Definite answers require the detailed analysis of inducible KO models that lack TH signaling components specifically in adult NSCs and, consequently, their progeny.

In addition to these lineage-intrinsic mechanisms, adult hippocampal neurogenesis is under the control of non-cell-autonomous signaling cues derived from the stem cell niche. Within the mammalian SGZ, the niche encompasses astrocytes, BBB endothelial cells, microglia, and granule cell neurons as prominent cell types (105). Several lines of evidence suggest that an altered astrocytic response can mediate parts of the effects of modulated THs levels on the adult neurogenic program. First, astrocytes express DIO2 (106) and are thus central in regulating brain T_3 availability and action (106–108). Second, astrocyte-specific deletion of *Dio2* in mice results in an increased anxiety-depression-like phenotype and thus in a pathological condition that has been associated with impaired hippocampal neurogenesis before (109–111). Though BrdU incorporation was not affected in this mouse model, a detailed characterization of the neurogenic stages is still pending. Third, astrocytes secrete TH-regulated factors like Fibroblast growth factors, Thrombospondin-1, Neurotrophin-3, or WNT ligands that in turn influence the neurogenic program (14, 112, 113) (Figure 2). RNA sequencing studies on cultured astrocytes exposed to T_3 revealed alterations in WNT signaling components with a direct up-regulation of *Wnt7a*, which is a known regulator of SGZ progenitor proliferation, differentiation, and dendritic arborization (113, 114). Astrocytes and microglia further release cytokines that are involved in progenitor proliferation and survival (78). Similarly, TH-regulated signals derived from the vasculature like BDNF or VEGF, neuronal factors such as SHH and NGF, and neuronal activity converge on the progression of hippocampal precursors through the neurogenic program (17, 112, 115–117) (Figure 2). Yet, we have just begun to decipher the non-cell-autonomous mechanisms in niche cells by which THs influence progression through the adult hippocampal program. Inducible and conditional KO approaches will certainly broaden this exciting field of research in the future.

Whether adult hippocampal neurogenesis occurs in humans is still under debate (105, 118, 119). A growing number of studies demonstrates the presence of DCX+ cells in the human SGZ though the question as to the comparability of the molecular signature between rodent and human neuroblast markers has been raised following the detection of DCX in neurons (120). Single cell and single nuclear sequencing studies on human hippocampal tissue are still sparse and often do not depict NSCs and neurogenic populations while a neurogenic trajectory can be clearly delineated in the macaque brain (120–123). Until the existence of adult human hippocampal neurogenesis is unequivocally demonstrated and a marker repertoire established, it is very difficult to pinpoint both the expression of THs signaling components and TH-regulatory effects on adult human hippocampal neurogenesis.

Despite these difficulties, a wealth of clinical data evidences a link between an altered thyroidal state and affected hippocampus-related cognitive functions in humans. Hypothyroidism in adulthood results in anxiety, depression, specific spatial and associative memory impairments, and dementia as well as a decreased hippocampal volume (14, 16, 109, 124–126). T_4 supplementation is able to improve cognitive perturbations in sub-clinically, but not overt hypothyroid subjects in tests addressing hippocampal functions (126). Interestingly, adult-onset hyperthyroidism culminates in cognitive impairments, anxiety, and depression (14, 109, 127). In sum, the pathological alterations seen in humans align with changes in experimental animals with abnormal thyroidal states that have been linked to impairments in adult hippocampal neurogenesis.

Future challenges:

- What are the lineage-autonomous effects of THs within the adult hippocampal neurogenic program? In particular, is there a role for THs in the regulation of NSC physiology?

- Do TH action in stem cell niche cells contribute to regulating adult hippocampal neurogenesis in a non-cell-autonomous manner?
- Do THs contribute to the regulation of adult hippocampal neurogenesis in humans?

Thyroid hormone action outside canonical neurogenic niches

TH and neurogliogenesis in the hypothalamus

Neurogenesis in the hypothalamus was first reported two decades ago (6, 128) and has been stated to occur in different areas within the hypothalamus with important functions in metabolism, feeding, and sexual behavior. First, it has been demonstrated to occur in ependymal cells lining the third ventricle and more widely also in tanycytes (129). Moreover, hypothalamic DCX+ neuroblasts have been described in rodents, sheep, and humans, although with slight variations in distribution patterns, but mainly in the arcuate nucleus (129–133) with progenitor cells also producing a variable percentage of astrocytes (131). As for adult hypothalamic oligodendrogenesis, its existence had not been proven in rodents until very recently when it was unequivocally shown that the median eminence of the hypothalamus can give rise to new OPCs (5, 134).

Implications of hypothalamic neurogenesis are wide, and rank from repair after tissular lesions to influence on sexual behavior and weight control (135). As for adult hypothalamic oligodendrogenesis, in rodents it is associated with the regulation of energy balance and hypothalamic leptin sensitivity (5).

Interestingly, the hypothalamus is known to be a strongly THs regulated brain area in mammals. From early studies reporting the expression of DIO2 mostly in the median eminence (136), evidence has accumulated reporting the expression of the different TH regulators in the rodent brain. In particular, deiodinases (107, 137, 138) and THTs (139) are detected in high abundance in ependymal cells lining the third ventricle and in tanycytes, with the latter expressing DIO2, OATP1C1, and MCT8, suggesting that TH action is important in this cell type (107, 138, 139). Moreover, this strong expression of various TH regulators, including DIO2 and DIO3, THTs such as MCT8, and receptors TRα and TRβ has also been reported in the human hypothalamus (140, 141).

Neurogenesis in the adult rodent hypothalamus has been also demonstrated to be controlled by growth factors (GFs) such as FGF2 (129), BDNF (130), and in a wider fashion by insulin-like growth factor 1 (IGF1) (Figure 3). While the first GF acts mostly on ependymal cells, the latter can act also on tanycytes (142) which could be considered a mostly IGF1-responsive cell population. Interestingly, apart from the aforementioned link between FGF2, BDNF, and THs, IGF1 has also been reported to have a strong interplay with THs (143) (Figure 3). Indeed, depletion of TH-availability regulators such as DIO3 or MCT8 and OATP1C1 induces increased or reduced IGF1 dynamics, respectively, in different tissues including the brain (97, 144). Altogether, GFs influence further supports a potential effect of THs on hypothalamic neurogenesis. Furthermore, mechanisms underlying hypothalamic oligodendrogenesis have not been described until very recently. However, genes consistent with the genomic footprint of hypothalamic OPCs include *MYC* and genes involved in the notch pathway (145). Interestingly, both are known to be TH-regulated within the adult mammalian SVZ and the postnatal cerebral cortex, respectively (18, 113), suggesting that THs may

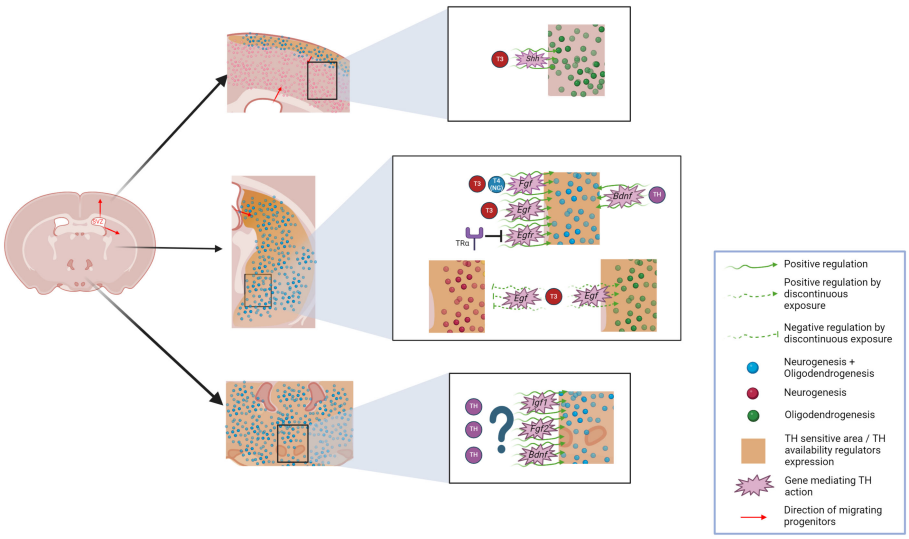

FIGURE 3
Overview of potential THs-effects on adult neurogliogenesis occurring on emerging niches including the hypothalamus, striatum and cerebral cortex. Generation of neurons and glia in the adult mammal brain is depicted for these niches and THs-influenced areas are highlighted. Potential genes mediating this THs-effect are also included. Graphic was created with Biorender.

regulate hypothalamic oligodendrogenesis in a similar way to the situation in the SVZ and other parts of the brain.

Upon considering the important hypothalamic functions regarding regulation of energy balance and metabolism, as well as sexual behavior, and their potential association with THs, understanding the link between THs and hypothalamic neurogliogenesis could be crucial to better understand several pathophysiological processes. Regarding weight regulation, mediated by hypothalamic neurogenesis, a better understanding of THs' role in modulating hypothalamic neurogliogenesis may be a significant advance in the prevention of pathological weight gain or loss and metabolic dysfunction usually associated with thyroid-related disorders (146–148). Furthermore, considering the common clinical implications of hypothalamic demyelination in fatigue and weight dysregulation associated to MS, enhancing hypothalamic remyelination in this region could also improve the quality of life of MS patients (149).

With all this in mind, both in physiological and pathophysiological contexts, THs appear as actors to be studied in depth in the hypothalamus, not only with the aim of understanding their role but also to potentially manipulate them to impact neurogliogenesis and thus lead to therapeutic outcomes.

Future challenges:

- What is the ontogeny of oligodendroglial progenitors in the median eminence?
- Does hypothyroidism and/or other changes in TH availability alter neurogliogenesis in the hypothalamus?
- Would it be possible to manipulate TH availability or TH downstream effectors expression at the cellular level to regulate neurogliogenesis as a therapeutic approach for different pathological conditions, while avoiding the side effects derived from excessive TH signaling?

TH and neurogliogenesis in the striatum

Although neurogenesis in the adult basal ganglia, particularly in the striatum, was already suspected towards the end of the past century, and later stated in rodents (150, 151) it was not until, 2014 that Ernst and colleagues demonstrated it in humans (7), by using C14 retro-tracing. In the meantime, adult oligodendrogenesis in this area was also demonstrated (2, 50, 152).

Neurogenic potential in the striatum tends to be overlooked, however, high DCX expression levels in the striatum have been reported both by transcriptomic and protein analysis, as shown previously for other neurogenic niches such as the hippocampus (153, 154). Neural progenitors in the striatum originate mainly in the SVZ. SVZ cells exhibit great heterogeneity and are able to migrate to several areas, including the classical migration to the olfactory bulbs, but also to the cerebral cortex, amygdala, or the striatum (8, 155). Moreover, studies in rodents have demonstrated active adult gliogenesis in the striatum, independent from SVZ input (156). Cell fate determination of neural progenitors is dependent on a plethora of factors and has been proven to be modulable in several ways (130, 151, 156), however, THs have never been proposed as one of those ways for striatal neuro-gliogenesis.

Adult striatal neurogliogenesis is not only interesting from a cellular ontology point of view but also has potential translatable implications to pathology. Of particular relevance are two pathological contexts, ischemic/stroke insults and neurodegenerative diseases. First, brain ischemia damages CNS tissues and in response, induces neurogenesis, oligodendrogenesis, and angiogenesis together with astrogliosis (157) to enhance brain repair. After an ischemic insult, the SVZ has been demonstrated to produce neuronal and oligodendroglial precursor cells that migrate into the striatal tissue using blood vessels as guidance and scaffold (158–161) in a process modulable by GFs (162, 163). These newly generated neurons have the ability to fully integrate and generate functional synaptic contacts within striatal neuronal networks (164) although this mechanism has been observed to be weaker in primates than in rodents (165). As for post-ischemic striatal oligodendrogenesis, it involves local pOPCs and SVZ progenitors that are recruited to the lesioned area, where they are able to exert neuroprotective effects and effectively generate myelin, although myelin has been reported thinner when produced by pOPCs (51, 161).

As for neurodegenerative diseases, Huntington's disease (HD) outcome is strongly linked to the extent of striatal neurogenesis, as reviewed by Jurkowsky and colleagues (135). First reports in HD subjects reported reduced, if not depleted neurogenesis (7) However, later reports in animal models of the disease, particularly in rodents, and in human HD samples have reported increased adult striatal neurogenesis in concurrency of HD (166–168). This process has commonly been linked to an increase in the arrival of SVZ-derived progenitors to the striatum (168). However, it has also been reported to be closely related with local striatal astrocytes gaining neurogenic function (167), with neurogenesis from both origins potentially acting as a recovery mechanism for the cell loss associated to the disease, even in humans.

It is worth noting that the striatum is also strongly influenced by THs. Expression of some TH-availability regulators was first reported in the striatum more than 40 years ago, with evidence of striatal DIO2 and DIO3 activity among the highest in the rodent brain (169). However, we had to wait until the present century to unravel the local expression of THTs, such as MCT8 and OATP1C1, both in mice, non-human primates, and humans, with a particularly high expression of OATP1C1 (170–172). Indeed, our recent work described the expression of both transporters in striatal motor neuron circuitry, as well as in pericytes in the primate striatum, implying the importance of THs in this area (172). Moreover, in rats, thyroidectomy and subsequent depletion of THs in the striatal area have been demonstrated to induce a number of transcriptomic changes (173). After THs depletion, T_3 administration to hypothyroid rats proved that THs modulate several genetic pathways, including genes involved in neurogliogenesis, such as *Egr1*, involved in maintaining NSC proliferation or *Klf9*, crucial to oligodendroglial cells differentiation (174, 175).

However, cellular mechanisms underlying THs regulation of neurogliogenesis within the striatum are not established yet. This regulation, even if it has not yet been established, likely occurs in relation to the GABAergic system. It has been demonstrated that a majority of the generated neurons in the adult striatum are GABAergic interneurons (7, 150, 176). Control of GABAergic system homeostasis is one of the hallmarks of THs action, and THs depletion or deficient signaling, mainly exerted through TRα have been proven to reduce the number of GABAergic cells (104, 177, 178). This reinforces the idea of an important effect for THs in striatal neurogenesis.

Although the molecular mechanism for this potential control has not been reported, among the different substances able to control adult striatal neurogenesis, GFs have been demonstrated to be crucial and stand out as potential THs downstream effectors. EGF, FGF and BDNF have been reported to increase the generation of new cells to different extents, including neurogenesis and oligodendrogenesis, both in health and disease (151, 152, 162, 179–182) (Figure 3).

Interestingly, all those molecules have been demonstrated to be dependent on TH signaling, with effects reported from both T_3 and T_4 (55, 116, 183–185). These data back up the hypothesis that local and temporal control of TH availability is crucial to neurogliogenesis, and so are the components involved in this control. It is interesting to observe that, given the importance of both GFs to striatal neurogliogenesis, they have been reported to be regulated also by different controllers of TH availability, such as deiodinases and THTs, whose depletion is able to change the expression of both GFs, through TH signaling (97, 144).

Once the putative effect of THs in adult striatal neurogliogenesis has been defined, it is necessary to understand its potential in a pathophysiological context. Aside from the aforementioned potential GFs-mediated influence in pathologies such as ischemia and HD, that remains speculative, there are reports in the literature of THs' influence in the striatum affecting pathophysiological contexts. Interestingly, an increase in the vulnerability of striatal medium spiny neurons to HD has also been reported in deficient TH signaling, which would point to an important effect of THs in this process (186).

Although knowledge of THs influence on striatal neurogliogenesis is scarce, there is growing evidence that suggests that THs should not be overlooked as actors in the process. Further studies should be pursued in the matter, as being able to control the process of neurogliogenesis using THs regulation may be a great step forward in the managing of different pathological conditions.

Future challenges:

- What is the ontogeny of the local progenitors present in the striatum that do not belong to SVZ derived cells?
- Does hypothyroidism and/or other changes in TH availability alter neurogliogenesis in the striatum?
- Would it be possible to manipulate striatal TH signaling as a therapeutic approach for different pathological conditions?
- Would THs manipulation induce deleterious side-effects that overcome the potential positive effects of regulating striatal neurogliogenesis?

TH and neurogliogenesis in the cerebral cortex

For some time now, growing evidence highlights that not only cortical oligodendrogenesis but also neurogenesis occurs after embryogenesis, notably through adulthood in the mammalian brain, with important implications in disease states. Adult cortical oligodendrogenesis has been observed in rodents and humans, in physiological and pathophysiological states (2, 8, 50, 187).

In normal conditions, adult cortical neurogenesis, particularly in humans, remains controversial. After years of a fixed paradigm of non-existent cortical neurogenesis, in, 1999, Gould and colleagues claimed the discovery of newly generated neurons in the macaque cortex, originating from ectopic migration of SVZ-derived progenitors (188). However, this discovery was rejected shortly afterward by Kornack and colleagues (189), although other groups obtained similar data using different monkey species (12). Gould's data were confirmed also by the successful generation of neurospheres from human cortical progenitor cells (190). However, C14 studies both in healthy samples and in cortical stroke-affected individuals contrast the apparent presence of pluripotent progenitors, as they described that most of the newly generated cells do not express neuronal markers (165, 191).

In rodents, the strongest indicator of adult cortical neurogenesis is the electron microscopic detection of newly generated [3H] thymidine cortical neurons in rodent brains (169). Later, they were further supported by the finding of proliferating progenitors in the murine cerebral cortex that were directed towards a neuronal fate (positive for DCX and/or the neuronal markers NeuN and Hu) (11) after a provoked insult in deep layers of the cerebral cortex.

These newly generated cells were able to establish connections with other regions, including the hypothalamus and spinal cord (192). Later, it was demonstrated that neurogenic progenitors included not only ectopic SVZ progenitors but also a local pool of cells ubiquitously residing in the adult rodent cerebral cortex, producing mainly glial cells but retaining the ability to produce new neurons (150, 193). Among the different layers of the cerebral cortex, layer I has been suggested to harbor the highest neurogenic potential, given its importance during development and in early postnatal weeks both in primates and in rodents (10, 194) (Figure 3). This neurogenic activity has been demonstrated in adulthood after ischemic insult, with new neurons being generated in layer I and integrated into inner cortical layers (195).

Cortical oligodendrogenesis has been assessed in other pathological contexts, including demyelinating diseases and especially MS. Its potential to repair demyelinating lesions has been investigated in murine models, and the existence of the process in the human MS context has also been demonstrated (50, 196) (Figure 3). In this context, it is of great importance to

understand the mechanisms underlying this process, and again,THs arise as a key candidate to regulate these processes.

As was thoroughly reviewed by Wang and colleagues (197), MCT8 and OATP1C1 have been consistently detected in the cerebral cortex of different species, including rodents, non-human-primates and humans, through all stages of development. This study has for the first time precisely reported the cellular location of both transporters. Aside from the classically described expression in blood vessels, the authors have shown neuronal expression of both transporters, especially in layer I of the cerebral cortex (197) (Figure 3). In particular, OATP1C1 was strongly detected in pyramidal neurons. As DIO2 has not been demonstrated to colocalize in these neurons (138), the presence of the transporter could indicate either increased importance of T_4 or, as the authors suggest, the ability of these neurons to accumulate T_4 and release it when necessary to other surrounding cell types. Interestingly, the authors described the expression of OATP1C1 in Corpora amylacea. These globular structures, equally located in cortical layer I, have been described to also express the TH-distributor protein TTR (198), suggesting a function in the storage/buffering and/or delivery of T_4 in layer I upon local need.

Despite the various lines of evidence on adult cortical neurogliogenesis and the control of TH availability occurring locally in different cortical areas, the role of THs in cortical neurogliogenesis remains to be clarified.

Future challenges:

- Are THs a factor in cortical neurogliogenesis regulation?
- Is this regulation linked to parenchymal or cell-by-cell intracellular THs levels?
- Is this cell-by-cell regulation being carried out by progenitors present at the niches, as if the maintenance of neurogliogenic potential depends on paracrine-like TH signaling inside the niche?
- Would it be possible to manipulate TH availability or TH downstream effectors expression to regulate neurogliogenesis at the cellular level, to avoid the side effects derived from excessive TH signaling?

Conclusion

Since the seminal discovery of neurogliogenic niches in the adult mammalian brain, enormous progress has been made in understanding the role of adult-generated neurons and glial cells in health and disease. In this review, we have highlighted THs as a key factor that controls neurogliogenic fate decisions and lineage progression at multiple levels. To that end, we have summarized existing knowledge on the precise spatiotemporal regulation of TH availability in progenitor and mature cells. Yet, many questions as to the cell-specific role of THs and TH signaling regulators as well as the functional outcome of altered TH availability are still unanswered. Future research employing new model systems and advanced methodology is needed to close those gaps. Likewise, past investigations have mainly focused on the "classical" neurogliogenic niches in the SVZ and SGZ, while the putative role of TH signaling in emerging niches in the hypothalamus, striatum, and cerebral cortex is still largely elusive. By pointing out critical open questions we aspired to spark future studies to fill in the blanks. The expected answers will help to fully harness THs' potential to shift the fate of progenitor cells and thus foster regenerative processes in pathological conditions when new neurons and/or new oligodendrocytes are urgently needed.

Author contributions

VV-H: Conceptualization, Writing – original draft, Writing – review & editing. SM: Conceptualization, Writing – original draft, Writing – review & editing. AG-F: Conceptualization, Writing – original draft, Writing – review & editing. SR: Conceptualization, Writing – original draft, Writing – review & editing.

Funding

The author(s) declare financial support was received for the research, authorship, and/or publication of this article. SM was supported by a grant of the Deutsche Forschungsgemeinschaft (CRC/TR 296;P19). This study was supported by grants from the Spanish Ministry of Research and Innovation MCIN/AEI/10., 13039/501100011033, and by "ERDF A way of making Europe" (Grants No. SAF2017-86342-R and PID2020-113139RB-I00 to AG. SR was supported by the Centre National de la Recherche Scientifique, the Muséum National d'Histoire Naturelle and The EU H2020 contract Thyrage (grant, 666869) "ARSEP grant (Cashemire)".

Conflict of interest

The authors declare that the research was conducted in the absence of any commercial or financial relationships that could be construed as a potential conflict of interest.

Publisher's note

All claims expressed in this article are solely those of the authors and do not necessarily represent those of their affiliated organizations, or those of the publisher, the editors and the reviewers. Any product that may be evaluated in this article, or claim that may be made by its manufacturer, is not guaranteed or endorsed by the publisher.

References

1. Doetsch F, Caillé I, Lim DA, García-Verdugo JM, Alvarez-Buylla A. Subventricular zone astrocytes are neural stem cells in the adult mammalian brain. *Cell*. (1999) 97:703–16. doi: 10.1016/S0092-8674(00)80783-7

2. Menn B, Garcia-Verdugo JM, Yaschine C, Gonzalez-Perez O, Rowitch D, Alvarez-Buylla A. Origin of oligodendrocytes in the subventricular zone of the adult brain. *J Neurosci*. (2006) 26:7907–18. doi: 10.1523/JNEUROSCI.1299-06.2006

3. Bonaguidi MA, Song J, Ming GL, Song H. A unifying hypothesis on mammalian neural stem cell properties in the adult hippocampus. *Curr Opin Neurobiology*. (2012) 22:754–61. doi: 10.1016/j.conb.2012.03.013

4. Flor-García M, Terreros-Roncal J, Moreno-Jiménez EP, Ávila J, Rábano A, Llorens-Martín M. Unraveling human adult hippocampal neurogenesis. *Nat Protoc*. (2020) 15:668–93. doi: 10.1038/s41596-019-0267-y

5. Buller S, Kohnke S, Hansford R, Shimizu T, Richardson WD, Blouet C. Median eminence myelin continuously turns over in adult mice. *Mol Metab*. (2023) 69:101690. doi: 10.1016/j.molmet.2023.101690

6. Evans J, Sumners C, Moore J, Huentelman MJ, Deng J, Gelband CH, et al. Characterization of mitotic neurons derived from adult rat hypothalamus and brain stem. *J Neurophysiol*. (2002) 87:1076–85. doi: 10.1152/jn.00088.2001

7. Ernst A, Alkass K, Bernard S, Salehpour M, Perl S, Tisdale J, et al. Neurogenesis in the striatum of the adult human brain. *Cell*. (2014) 156:1072–83. doi: 10.1016/j.cell.2014.01.044

8. Suzuki SO, Goldman JE. Multiple cell populations in the early postnatal subventricular zone take distinct migratory pathways: A dynamic study of glial and neuronal progenitor migration. *J Neurosci*. (2003) 23:4240–50. doi: 10.1523/JNEUROSCI.23-10-04240.2003

9. Zhao M, Momma S, Delfani K, Carlen M, Cassidy RM, Johansson CB, et al. Evidence for neurogenesis in the adult mammalian substantia nigra. *Proc Natl Acad Sci U S A*. (2003) 100:7925–30. doi: 10.1073/pnas.1131955100

10. Costa MR, Kessaris N, Richardson WD, Götz M, Hedin-Pereira C. The marginal zone/layer I as a novel niche for neurogenesis and gliogenesis in developing cerebral cortex. *J Neurosci*. (2007) 27:11376–88. doi: 10.1523/JNEUROSCI.2418-07.2007

11. Magavi SS, Leavitt BR, Macklis JD. Induction of neurogenesis in the neocortex of adult mice. *Nature*. (2000) 405:951–5. doi: 10.1038/35016083

12. Bernier PJ, Bedard A, Vinet J, Levesque M, Parent A. Newly generated neurons in the amygdala and adjoining cortex of adult primates. *Proc Natl Acad Sci U S A*. (2002) 99:11464–9. doi: 10.1073/pnas.172403999

13. Jhaveri DJ, Tedoldi A, Hunt S, Sullivan R, Watts NR, Power JM, et al. Evidence for newly generated interneurons in the basolateral amygdala of adult mice. *Mol Psychiatry*. (2018) 23:521–32. doi: 10.1038/mp.2017.134

14. Fanibunda SE, Desouza LA, Kapoor R, Vaidya RA, Vaidya VA. Thyroid hormone regulation of adult neurogenesis. In: *Vitamins and Hormones*, *1st ed*. Elsevier Inc (2018). 211–251 p. doi: 10.1016/bs.vh.2017.04.006

15. Gothié JD, Demeneix B, Remaud S. Comparative approaches to understanding thyroid hormone regulation of neurogenesis. *Mol Cell Endocrinol*. (2017) 459:104–15. doi: 10.1016/j.mce.2017.05.020

16. Remaud S, Gothié Jd, Morvan-dubois G, Demeneix BA. Thyroid hormone signaling and adult neurogenesis in mammals. *Front Endocrinol (Lausanne)*. (2014) 5:1–7. doi: 10.3389/fendo.2014.00062

17. Desouza LA, Sathanoori M, Kapoor R, Rajadhyaksha N, Gonzalez LE, Kottmann AH, et al. Thyroid hormone regulates the expression of the sonic hedgehog signaling pathway in the embryonic and adult Mammalian brain. *Endocrinology*. (2011) 152:1989–2000. doi: 10.1210/en.2010-1396

18. Lemkine GF, Raji A, Alfama G, Turque N, Hassani Z, Alegria-Prévot O, et al. Adult neural stem cell cycling in *vivo* requires thyroid hormone and its alpha receptor. *FASEB J*. (2005) 19:1–17. doi: 10.1096/fj.04-2916fje

19. Mayerl S, Heuer H, ffrench-Constant C. Hippocampal neurogenesis requires cell-autonomous thyroid hormone signaling. *Stem Cell Rep*. (2020) 14:845–60. doi: 10.1016/j.stemcr.2020.03.014

20. Montero-Pedrazuela A, Venero C, Lavado-Autric R, Fernández-Lamo I, García-Verdugo JM, Bernal J, et al. Modulation of adult hippocampal neurogenesis by thyroid hormones: Implications in depressive-like behavior. *Mol Psychiatry*. (2006) 11:361–71. doi: 10.1038/sj.mp.4001802

21. Remaud S, Ortiz FC, Perret-Jeanneret M, Aigrot MS, Gothié JD, Fekete C, et al. Transient hypothyroidism favors oligodendrocyte generation providing functional remyelination in the adult mouse brain. *Elife*. (2017) 6:1–20. doi: 10.7554/eLife.29996

22. Kapoor R, Desouza L a, Nanavaty IN, Kernie SG, Vaidya V a. Thyroid hormone accelerates the differentiation of adult hippocampal progenitors. *J Neuroendocrinol*. (2012) 24:1259–71. doi: 10.1111/j.1365-2826.2012.02329.x

23. Richardson SJ, Lemkine GF, Alfama G, Hassani Z, Demeneix BA. Cell division and apoptosis in the adult neural stem cell niche are differentially affected in transthyretin null mice. *Neurosci Lett*. (2007) 421:234–8. doi: 10.1016/j.neulet.2007.05.040

24. Rabah SA, Gowan IL, Pagnin M, Osman N, Richardson SJ. Thyroid hormone distributor proteins during development in vertebrates. *Front Endocrinol (Lausanne)*. (2019) 10:506. doi: 10.3389/fendo.2019.00506

25. Bernal J, Guadaño-Ferraz A, Morte B. Thyroid hormone transporters—functions and clinical implications. *Nat Rev Endocrinol*. (2015) 11:406. doi: 10.1038/nrendo.2015.66

26. Bianco AC, Kim BW. Deiodinases: implications of the local control of thyroid hormone action. *J Clin Invest*. (2006) 116:2571–9. doi: 10.1172/JCI29812

27. Bernal J. Thyroid hormone receptors in brain development and function. *Nat Clin Pract Endocrinol Metab*. (2007) 3:249–59. doi: 10.1038/ncpendmet0424

28. Doetsch F, García-Verdugo JM, Alvarez-Buylla A. Cellular composition and three-dimensional organization of the subventricular germinal zone in the adult mammalian brain. *J Neurosci*. (1997) 17:5046. doi: 10.1523/JNEUROSCI.17-13-05046.1997

29. Kriegstein A, Alvarez-Buylla A. The glial nature of embryonic and adult neural stem cells. *Annu Rev Neurosci*. (2009) 32:149–84. doi: 10.1146/annurev.neuro.051508.135600

30. Furutachi S, Miya H, Watanabe T, Kawai H, Yamasaki N, Harada Y, et al. Slowly dividing neural progenitors are an embryonic origin of adult neural stem cells. *Nat Neurosci*. (2015) 18:657–65. doi: 10.1038/nn.3989

31. Fuentealba LC, Rompani SB, Parraguez JI, Obernier K, Romero R, Cepko CL, et al. Embryonic origin of postnatal neural stem cells. *Cell*. (2015) 161:1644–55. doi: 10.1016/j.cell.2015.05.041

32. Morshead CM, Reynolds BA, Craig CG, McBurney MW, Staines WA, Morassutti D, et al. Neural stem cells in the adult mammalian forebrain: A relatively quiescent subpopulation of subependymal cells. *Neuron*. (1994) 13:1071–82. doi: 10.1016/0896-6273(94)90046-9

33. Codega P, Silva-Vargas V, Paul A, Maldonado-Soto AR, DeLeo AM, Pastrana E, et al. Prospective identification and purification of quiescent adult neural stem cells from their *in vivo* niche. *Neuron*. (2014) 82:545–59. doi: 10.1016/j.neuron.2014.02.039

34. Kippin TE, Martens DJ, van der Kooy D. p21 loss compromises the relative quiescence of forebrain stem cell proliferation leading to exhaustion of their proliferation capacity. *Genes Dev*. (2005) 19:756–67. doi: 10.1101/gad.1272305

35. Mich JK, Signer RAJ, Nakada D, Pineda A, Burgess RJ, Vue TY, et al. Prospective identification of functionally distinct stem cells and neurosphere-initiating cells in adult mouse forebrain. *Elife*. (2014) 3:e02669. doi: 10.7554/eLife.02669

36. Ortega F, Gascón S, Masserdotti G, Deshpande A, Simon C, Fischer J, et al. Oligodendrogliogenic and neurogenic adult subependymal zone neural stem cells constitute distinct lineages and exhibit differential responsiveness to Wnt signalling. *Nat Cell Biol*. (2013) 15:602–13. doi: 10.1038/ncb2736

37. Ponti G, Obernier K, Guinto C, Jose L, Bonfanti L, Alvarez-Buylla A. Cell cycle and lineage progression of neural progenitors in the ventricular-subventricular zones of adult mice. *Proc Natl Acad Sci U S A*. (2013) 110:E1045-54. doi: 10.1073/pnas.1219563110

38. Doetsch F, Alvarez-Buylla A. Network of tangential pathways for neuronal migration in adult mammalian brain (subventricular zonesubependymal layerneurogenesis). *Proc Natl Acad Sci U S A*. (1996) 93:14895-900. doi: 10.1073/pnas.93.25.14895

39. Lepousez G, Valley MT, Lledo PM. The impact of adult neurogenesis on olfactory bulb circuits and computations. *Annu Rev Physiol*. (2013) 75:339–63. doi: 10.1146/annurev-physiol-030212-183731

40. Lois C, Alvarez-Buylla A. Proliferating subventricular zone cells in the adult mammalian forebrain can differentiate into neurons and glia. *Proc Natl Acad Sci U S A*. (1993) 90:2074–7. doi: 10.1073/pnas.90.5.2074

41. Lois C, Alvarez-Buylla A. Long-distance neuronal migration in the adult mammalian brain. *Science*. (1994) 264:1145–8. doi: 10.1126/science.8178174

42. Imayoshi I, Sakamoto M, Ohtsuka T, Takao K, Miyakawa T, Yamaguchi M, et al. Roles of continuous neurogenesis in the structural and functional integrity of the adult forebrain. *Nat Neurosci*. (2008) 11:1153–61. doi: 10.1038/nn.2185

43. Lledo PM, Merkle FT, Alvarez-Buylla A. Origin and function of olfactory bulb interneuron diversity. *Trends Neurosci*. (2008) 31:392–400. doi: 10.1016/j.tins.2008.05.006

44. Ming GL, Song H. Adult neurogenesis in the mammalian brain: significant answers and significant questions. *Neuron*. (2011) 70:687–702. doi: 10.1016/j.neuron.2011.05.001

45. Rochefort C, Gheusi G, Vincent JD, Lledo PM. Enriched odor exposure increases the number of newborn neurons in the adult olfactory bulb and improves odor memory. *J Neurosci*. (2002) 22:2679–89. doi: 10.1523/JNEUROSCI.22-07-02679.2002

46. Enwere E, Shingo T, Gregg C, Fujikawa H, Ohta S, Weiss S. Aging results in reduced epidermal growth factor receptor signaling, diminished olfactory neurogenesis, and deficits in fine olfactory discrimination. *J Neurosci*. (2004) 24:8354–65. doi: 10.1523/JNEUROSCI.2751-04.2004

47. Figueres-Oñate M, Sánchez-Villalón M, Sánchez-González R, López-Mascaraque L. Lineage tracing and cell potential of postnatal single progenitor cells in vivo. *Stem Cell Rep*. (2019) 13:700–12. doi: 10.1016/j.stemcr.2019.08.010

48. Capilla-Gonzalez V, Cebrian-Silla A, Guerrero-Cazares H, Garcia-Verdugo JM, Quinones-Hinojosa A. The generation of oligodendroglial cells is preserved in the rostral migratory stream during aging. *Front Cell Neurosci*. (2013) 7:147. doi: 10.3389/fncel.2013.00147

49. Gonzalez-Perez O, Alvarez-Buylla A. Oligodendrogenesis in the subventricular zone and the role of epidermal growth factor. *Brain Res Rev*. (2011) 67:147–56. doi: 10.1016/j.brainresrev.2011.01.001

50. Nait-Oumesmar B, Picard-Riera N, Kerninon C, Decker L, Seilhean D, Höglinger GU, et al. Activation of the subventricular zone in multiple sclerosis: Evidence for early glial progenitors. *Proc Natl Acad Sci U S A*. (2007) 104:4694–9. doi: 10.1073/pnas.0606835104

51. Xing YL, Röth PT, Stratton JAS, Chuang BHA, Danne J, Ellis SL, et al. Adult neural precursor cells from the subventricular zone contribute significantly to oligodendrocyte regeneration and remyelination. *J Neurosci*. (2014) 34:14128–46. doi: 10.1523/JNEUROSCI.3491-13.2014

52. Brousse B, Magalon K, Durbec P, Cayre M. Region and dynamic specificities of adult neural stem cells and oligodendrocyte precursors in myelin regeneration in the mouse brain. *Biol Open*. (2015) 4:980–92. doi: 10.1242/bio.012773

53. Figueres-Oñate M, López-Mascaraque L. Adult olfactory bulb interneuron phenotypes identified by targeting embryonic and postnatal neural progenitors. *Front Neurosci*. (2016) 10:194. doi: 10.3389/fnins.2016.00194

54. Spassky N, Heydon K, Mangatal A, Jankovski A, Olivier C, Queraud-Lesaux F, et al. Sonic hedgehog-dependent emergence of oligodendrocytes in the telencephalon: evidence for a source of oligodendrocytes in the olfactory bulb that is independent of PDGFRalpha signaling. *Development*. (2001) 128:4993–5004. doi: 10.1242/dev.128.24.4993

55. López-Juárez A, Remaud S, Hassani Z, Jolivet P, Pierre Simons J, Sontag T, et al. Thyroid hormone signaling acts as a neurogenic switch by repressing Sox2 in the adult neural stem cell niche. *Cell Stem Cell*. (2012) 10:531–43. doi: 10.1016/j.stem.2012.04.008

56. Luongo C, Butruille L, Sébillot A, Le Blay K, Schwaninger M, Heuer H, et al. Absence of both thyroid hormone transporters MCT8 and OATP1C1 impairs neural stem cell fate in the adult mouse subventricular zone. *Stem Cell Rep*. (2021) 16:337–53. doi: 10.1016/j.stemcr.2020.12.009

57. Vancamp P, Gothié JD, Luongo C, Sébillot A, Le Blay K, Butruille L, et al. Gender-specific effects of transthyretin on neural stem cell fate in the subventricular zone of the adult mouse. *Sci Rep*. (2019) 9:1–14. doi: 10.1038/s41598-019-56156-w

58. Remaud S, López-Juárez SA, Bolcato-Bellemin AL, Neuberg P, Stock F, Bonnet ME, et al. Inhibition of sox2 expression in the adult neural stem cell niche *in vivo* by monocationic-based siRNA delivery. *Mol Ther Nucleic Acids*. (2013) 2:e89. doi: 10.1038/mtna.2013.8

59. Hassani Z, François JC, Alfama G, Dubois GM, Paris M, Giovannangeli C, et al. A hybrid CMV-H1 construct improves efficiency of PEI-delivered shRNA in the mouse brain. *Nucleic Acids Res*. (2007) 35:e65. doi: 10.1093/nar/gkm152

60. Durand B, Raff M. A cell-intrinsic timer that operates during oligodendrocyte development. *BioEssays*. (2000) 22:64–71. doi: 10.1002/(SICI)1521-1878(200001)22:1<64::AID-BIES11>3.0.CO;2-Q

61. Billon N, Jolicoeur C, Tokumoto Y, Vennström B, Raff M. Normal timing of oligodendrocyte development depends on thyroid hormone receptor alpha 1 (TRα1). *EMBO J*. (2002) 21:6452–6460–6460. doi: 10.1093/emboj/cdf662

62. Palha JA, Fernandes R, de Escobar GM, Episkopou V, Gottesman M, Saraiva MJ. Transthyretin regulates thyroid hormone levels in the choroid plexus, but not in the brain parenchyma: study in a transthyretin-null mouse model. *Endocrinology*. (2000) 141:3267–72. doi: 10.1210/endo.141.9.7659

63. Ludwin SK. Central nervous system demyelination and remyelination in the mouse: an ultrastructural study of cuprizone toxicity. *Lab Invest*. (1978) 39:597–612.

64. Picard-Riera N, Nait-Oumesmar B, Baron-Van Evercooren A. Endogenous adult neural stem cells: limits and potential to repair the injured central nervous system. *J Neurosci Res*. (2004) 76:223–31. doi: 10.1002/jnr.20040

65. Alshehri B, Pagnin M, Lee JY, Petratos S, Richardson SJ. The role of transthyretin in oligodendrocyte development. *Sci Rep*. (2020) 10:4189. doi: 10.1038/s41598-020-60699-8

66. Pagnin M, Dekiwadia C, Petratos S, Richardson SJ. Enhanced re-myelination in transthyretin null mice following cuprizone mediated demyelination. *Neurosci Lett*. (2022) 766:136287. doi: 10.1016/j.neulet.2021.136287

67. Vancamp P, Demeneix BA, Remaud S. Monocarboxylate transporter 8 deficiency: delayed or permanent hypomyelination? *Front Endocrinol (Lausanne)*. (2020) 11. doi: 10.3389/fendo.2020.00283

68. Grandel H, Kaslin J, Ganz J, Wenzel I, Brand M. Neural stem cells and neurogenesis in the adult zebrafish brain: origin, proliferation dynamics, migration and cell fate. *Dev Biol*. (2006) 295:263–77. doi: 10.1016/j.ydbio.2006.03.040

69. Bhumika S, Darras VM. Role of thyroid hormones in different aspects of nervous system regeneration in vertebrates. *Gen Comp Endocrinol*. (2014) 203:86–94. doi: 10.1016/j.ygcen.2014.03.017

70. Gothié JD, Vancamp P, Demeneix B, Remaud S. Thyroid hormone regulation of neural stem cell fate : From development to ageing. *Acta physiologica*. (2020) :1–24. doi: 10.1111/apha.13316

71. Dilokthornsakul P, Valuck RJ, Nair KV, Corboy JR, Allen RR, Campbell JD. Multiple sclerosis prevalence in the United States commercially insured population. *Neurology*. (2016) 86:1014–21. doi: 10.1212/WNL.0000000000002469

72. Haider L, Zrzavy T, Hametner S, Höftberger R, Bagnato F, Grabner G, et al. The topograpy of demyelination and neurodegeneration in the multiple sclerosis brain. *Brain*. (2016) 139:807–15. doi: 10.1093/brain/awv398

73. Lubetzki C, Zalc B, Williams A, Stadelmann C, Stankoff B. Remyelination in multiple sclerosis: from basic science to clinical translation. *Lancet Neurol*. (2020) 19:678–88. doi: 10.1016/S1474-4422(20)30140-X

74. Franco PG, Silvestroff L, Soto EF, Pasquini JM. Thyroid hormones promote differentiation of oligodendrocyte progenitor cells and improve remyelination after cuprizone-induced demyelination. *Exp Neurol*. (2008) 212:458–67. doi: 10.1016/j.expneurol.2008.04.039

75. Jeannin E, Robyr D, Desvergne B. Transcriptional regulatory patterns of the myelin basic protein and Malic enzyme genes by the thyroid hormone receptors alpha1 and beta1. *J Biol Chem*. (1998) 273:24239–48. doi: 10.1074/jbc.273.37.24239

76. Kempermann G, Song H, Gage FH. Neurogenesis in the adult hippocampus. *Cold Spring Harb Perspect Biol*. (2015) 7:a018812. doi: 10.1101/cshperspect.a018812

77. Kozareva DA, Cryan JF, Nolan YM. Born this way: Hippocampal neurogenesis across the lifespan. *Aging Cell*. (2019) 18:e13007. doi: 10.1111/acel.13007

78. Cope EC, Gould E. Adult neurogenesis, glia, and the extracellular matrix. *Cell Stem Cell*. (2019) 24:690–705. doi: 10.1016/j.stem.2019.03.023

79. Kempermann G, Jessberger S, Steiner B, Kronenberg G. Milestones of neuronal development in the adult hippocampus. *Trends Neurosci*. (2004) 27:447–52. doi: 10.1016/j.tins.2004.05.013

80. Cameron HA, Glover LR. Adult neurogenesis: Beyond learning and memory. *Annu Rev Psychol*. (2015) 66:53–81. doi: 10.1146/annurev-psych-010814-015006

81. Anacker C, Hen R. Adult hippocampal neurogenesis and cognitive flexibility — linking memory and mood. *Nat Rev Neurosci*. (2017) 18:335–46. doi: 10.1038/nrn.2017.45

82. Kapoor R, van Hogerlinden M, Wallis K, Ghosh H, Nordstrom K, Vennstrom B, et al. Unliganded thyroid hormone receptor alpha1 impairs adult hippocampal neurogenesis. *FASEB J*. (2010) 24:4793–805. doi: 10.1096/fj.10-161802

83. Desouza LA, Ladiwala U, Daniel SM, Agashe S, Vaidya RA, Vaidya VA. Thyroid hormone regulates hippocampal neurogenesis in the adult rat brain. *Mol Cell Neurosci*. (2005) 29:414–26. doi: 10.1016/j.mcn.2005.03.010

84. Mayerl S, Martin AA, Bauer R, Schwaninger M, Heuer H, Ffrench-Constant C. Distinct actions of the thyroid hormone transporters mcT8 and oatp1c1 in murine adult hippocampal neurogenesis. *Cells*. (2022) 11:1–15. doi: 10.3390/cells11030524

85. Ambrogini P, Cuppini R, Ferri P, Mancini C, Ciaroni S, Voci A, et al. Thyroid hormones affect neurogenesis in the dentate gyrus of adult rat. *Neuroendocrinology*. (2005) 81:244–53. doi: 10.1159/000087648

86. Kapri D, Fanibunda SE, Vaidya VA. Thyroid hormone regulation of adult hippocampal neurogenesis: Putative molecular and cellular mechanisms. *Vitam Horm*. (2022) 118:1–33. doi: 10.1016/bs.vh.2021.10.001

87. Nam SM, Kim JW, Yoo DY, Jung HY, Chung JY, Kim DW, et al. Hypothyroidism increases cyclooxygenase-2 levels and pro-inflammatory response and decreases cell proliferation and neuroblast differentiation in the hippocampus. *Mol Med Rep*. (2018) 17:5782–8. doi: 10.3892/mmr

88. Sánchez-Huerta K, García-Martínez Y, Vergara P, Segovia J, Pacheco-Rosado J. Thyroid hormones are essential to preserve non-proliferative cells of adult neurogenesis of the dentate gyrus. *Mol Cell Neurosci*. (2016) 76:1–10. doi: 10.1016/j.mcn.2016.08.001

89. Gilbert ME, Goodman JH, Gomez J, Johnstone AFM, Ramos RL. Adult hippocampal neurogenesis is impaired by transient and moderate developmental thyroid hormone disruption. *Neurotoxicology*. (2017) 59:9–21. doi: 10.1016/j.neuro.2016.12.009

90. Kapoor R, Ghosh H, Nordstrom K, Vennstrom B, Vaidya VA. Loss of thyroid hormone receptor β is associated with increased progenitor proliferation and NeuroD positive cell number in the adult hippocampus. *Neurosci Lett*. (2011) 487:199–203. doi: 10.1016/j.neulet.2010.10.022

91. Shin J, Berg DA, Zhu Y, Shin JY, Song J, Bonaguidi MA, et al. Single-cell RNA-seq with waterfall reveals molecular cascades underlying adult neurogenesis. *Cell Stem Cell*. (2015) 17:360–72. doi: 10.1016/j.stem.2015.07.013

92. Hochgerner H, Zeisel A, Lönnerberg P, Linnarsson S. Conserved properties of dentate gyrus neurogenesis across postnatal development revealed by single-cell RNA sequencing. *Nat Neurosci*. (2018) 21:290–9. doi: 10.1038/s41593-017-0056-2

93. Habib N, Li Y, Heidenreich M, Swiech L, Avraham-Davidi I, Trombetta JJ, et al. Div-Seq: Single-nucleus RNA-Seq reveals dynamics of rare adult newborn neurons. *Science*. (2016) 353:925–8. doi: 10.1126/science.aad7038

94. López-Espíndola D, García-Aldea Á, Gómez de la Riva I, Rodríguez-García AM, Salvatore D, Visser TJ, et al. Thyroid hormone availability in the human fetal brain: novel entry pathways and role of radial glia. *Brain Struct Funct*. (2019) 224:2103–19. doi: 10.1007/s00429-019-01896-8

95. Licht T, Sasson E, Bell B, Grunewald M, Kumar S, Kreisel T, et al. Hippocampal neural stem cells facilitate access from circulation via apical cytoplasmic processes. *Elife*. (2020) 9. doi: 10.7554/eLife.52134

96. Urbán N, Blomfield IM, Guillemot F. Quiescence of adult mammalian neural stem cells: A highly regulated rest. *Neuron*. (2019) 104:834–48. doi: 10.1016/j.neuron.2019.09.026

97. Mayerl S, Müller J, Bauer R, Richert S, Kassmann CM, Darras VM, et al. Transporters MCT8 and OATP1C1 maintain murine brain thyroid hormone homeostasis. *J Clin Invest*. (2014) 124:1987–99. doi: 10.1172/JCI70324

98. Taşkın E, Artis AS, Bitiktas S, Dolu N, Liman N, Süer C. Experimentally induced hyperthyroidism disrupts hippocampal long-term potentiation in adult rats. *Neuroendocrinology*. (2011) 94:218–27. doi: 10.1159/000328513

99. Zhu W, Wu F, Li J, Meng L, Zhang W, Zhang H, et al. Impaired learning and memory generated by hyperthyroidism is rescued by restoration of AMPA and NMDA receptors function. *Neurobiol Dis*. (2022) 171:105807. doi: 10.1016/j.nbd.2022.105807

100. Niedowicz DM, Wang WX, Price DA, Nelson PT. Modulating thyroid hormone levels in adult mice: impact on behavior and compensatory brain changes. *J Thyroid Res*. (2021) 2021:9960188. doi: 10.1155/2021/9960188

101. Chamas L, Seugnet I, Poirier R, Clerget-Froidevaux MS, Enderlin V. A fine regulation of the hippocampal thyroid signalling protects hypothyroid mice against glial cell activation. *Int J Mol Sci*. (2022) 23(19):11938. doi: 10.3390/ijms231911938

102. Chaalal A, Poirier R, Blum D, Gillet B, Le Blanc P, Basquin M, et al. PTU-induced hypothyroidism in rats leads to several early neuropathological signs of Alzheimer's disease in the hippocampus and spatial memory impairments. *Hippocampus*. (2014) 24:1381–93. doi: 10.1002/hipo.22319

103. Alzoubi KH, Gerges NZ, Aleisa AM, Alkadhi KA. Levothyroxin restores hypothyroidism-induced impairment of hippocampus-dependent learning and memory: Behavioral, electrophysiological, and molecular studies. *Hippocampus*. (2009) 19:66–78. doi: 10.1002/hipo.20476

104. Venero C, Guadaño-Ferraz A, Herrero AI, Nordström K, Manzano J, De Escobar GM, et al. Anxiety, memory impairment, and locomotor dysfunction caused by a mutant thyroid hormone receptor ??1 can be ameliorated by T3 treatment. *Genes Dev*. (2005) 19:2152–63. doi: 10.1101/gad.346105

105. Boldrini M, Fulmore CA, Tartt AN, Simeon LR, Pavlova I, Poposka V, et al. Human hippocampal neurogenesis persists throughout aging. *Cell Stem Cell*. (2018) 22:589–599.e5. doi: 10.1016/j.stem.2018.03.015

106. Guadaño-Ferraz A, Obregón MJ, St Germain DL, Bernal J, Obregon MJ, StGermain DL. The type 2 iodothyronine deiodinase is expressed primarily in glial cells in the neonatal rat brain. *Proc Natl Acad Sci U S A*. (1997) 94:10391–6. doi: 10.1073/pnas.94.19.10391

107. Guadaño-Ferraz A, Escámez MJ, Rausell E, Bernal J. Expression of type 2 iodothyronine deiodinase in hypothyroid rat brain indicates an important role of thyroid hormone in the development of specific primary sensory systems. *J Neurosci*. (1999) 19:3430–9. doi: 10.1523/JNEUROSCI.19-09-03430.1999

108. Morte B, Bernal J. Thyroid hormone action: Astrocyte-neuron communication. *Front Endocrinol (Lausanne)*. (2014) 5. doi: 10.3389/fendo.2014.00082

109. Ittermann T, Völzke H, Baumeister SE, Appel K, Grabe HJ. Diagnosed thyroid disorders are associated with depression and anxiety. *Soc Psychiatry Psychiatr Epidemiol*. (2015) 50:1417–25. doi: 10.1007/s00127-015-1043-0

110. Gomes-Leal W. Adult hippocampal neurogenesis and affective disorders: New neurons for psychic well-being. *Front Neurosci*. (2021) 15:594448. doi: 10.3389/fnins.2021.594448

111. Bocco BMLC, Werneck-de-Castro JP, Oliveira KC, Fernandes GW, Fonseca TL, Nascimento BPP, et al. Type 2 deiodinase disruption in astrocytes results in anxiety-depressive-like behavior in male mice. *Endocrinol*. (2016) 157:3682–95. doi: 10.1210/en.2016-1272

112. Bonafina A, Paratcha G, Ledda F. Deciphering new players in the neurogenic adult hippocampal niche. *Front Cell Dev Biol*. (2020) 8:548. doi: 10.3389/fcell.2020.00548

113. Morte B, Gil-Ibáñez P, Bernal J. Regulation of gene expression by thyroid hormone in primary astrocytes: Factors influencing the genomic response. *Endocrinology*. (2018) 159:2083–92. doi: 10.1210/en.2017-03084

114. Arredondo SB, Valenzuela-Bezanilla D, Mardones MD, Varela-Nallar L. Role of wnt signaling in adult hippocampal neurogenesis in health and disease. *Front Cell Dev Biol*. (2020) 8:860. doi: 10.3389/fcell.2020.00860

115. Eu WZ, Chen YJ, Chen WT, Wu KY, Tsai CY, Cheng SJ, et al. The effect of nerve growth factor on supporting spatial memory depends upon hippocampal cholinergic innervation. *Transl Psychiatry*. (2021) 11:162. doi: 10.1038/s41398-021-01280-3

116. Giordano T, Pan JB, Casuto D, Watanabe S, Arneric SP. Thyroid hormone regulation of NGF, NT-3 and BDNF RNA in the adult rat brain. *Mol Brain Res*. (1992) 16:239–45. doi: 10.1016/0169-328X(92)90231-Y

117. Gonzalez-Reyes LE, Chiang CC, Zhang M, Johnson J, Arrillaga-Tamez M, Couturier NH, et al. Sonic Hedgehog is expressed by hilar mossy cells and regulates cellular survival and neurogenesis in the adult hippocampus. *Sci Rep*. (2019) 9:17402. doi: 10.1038/s41598-019-53192-4

118. Moreno-Jiménez EP, Flor-García M, Terreros-Roncal J, Rábano A, Cafini F, Pallas-Bazarra N, et al. Adult hippocampal neurogenesis is abundant in neurologically healthy subjects and drops sharply in patients with Alzheimer's disease. *Nat Med*. (2019) 25:554–60. doi: 10.1038/s41591-019-0375-9

119. Sorrells SF, Paredes MF, Cebrian-Silla A, Sandoval K, Qi D, Kelley KW, et al. Human hippocampal neurogenesis drops sharply in children to undetectable levels in adults. *Nature*. (2018) 555:377–81. doi: 10.1038/nature25975

120. Franjic D, Skarica M, Ma S, Arellano JI, Tebbenkamp ATN, Choi J, et al. Transcriptomic taxonomy and neurogenic trajectories of adult human, macaque, and pig hippocampal and entorhinal cells. *Neuron*. (2022) 110:452–469.e14. doi: 10.1016/j.neuron.2021.10.036

121. Ayhan F, Kulkarni A, Berto S, Sivaprakasam K, Douglas C, Lega BC, et al. Resolving cellular and molecular diversity along the hippocampal anterior-to-posterior axis in humans. *Neuron*. (2021) 109:2091–2105.e6. doi: 10.1016/j.neuron.2021.05.003

122. Tran MN, Maynard KR, Spangler A, Huuki LA, Montgomery KD, Sadashivaiah V, et al. Single-nucleus transcriptome analysis reveals cell-type-specific molecular signatures across reward circuitry in the human brain. *Neuron*. (2021) 109:3088–103. doi: 10.1016/j.neuron.2021.09.001

123. Zhang H, Li J, Ren J, Sun S, Ma S, Zhang W, et al. Single-nucleus transcriptomic landscape of primate hippocampal aging. *Protein Cell*. (2021) 12:695–716. doi: 10.1007/s13238-021-00852-9

124. Ittermann T, Wittfeld K, Nauck M, Bülow R, Hosten N, Völzke H, et al. High thyrotropin is associated with reduced hippocampal volume in a population-based study from Germany. *Thyroid*. (2018) 28:1434–42. doi: 10.1089/thy.2017.0561

125. Cooke GE, Mullally S, Correia N, O'Mara SM, Gibney J. Hippocampal volume is decreased in adults with hypothyroidism. *Thyroid®*. (2013) 24:433–40. doi: 10.1089/thy.2013.0058

126. Correia N, Mullally S, Cooke G, Tun TK, Phelan N, Feeney J, et al. Evidence for a specific defect in hippocampal memory in overt and subclinical hypothyroidism. *J Clin Endocrinol Metab*. (2009) 94:3789–97. doi: 10.1210/jc.2008-2702

127. Hage MP, Azar ST. The link between thyroid function and depression. *J Thyroid Res*. (2012) 2012:590648. doi: 10.1155/2012/590648

128. Markakis EA, Palmer TD, Randolph-Moore L, Rakic P, Gage FH. Novel neuronal phenotypes from neural progenitor cells. *J Neurosci*. (2004) 24:2886–97. doi: 10.1523/JNEUROSCI.4161-03.2004

129. Xu Y, Tamamaki N, Noda T, Kimura K, Itokazu Y, Matsumoto N, et al. Neurogenesis in the ependymal layer of the adult rat 3rd ventricle. *Exp Neurol*. (2005) 192:251–64. doi: 10.1016/j.expneurol.2004.12.021

130. Pencea V, Bingaman KD, Wiegand SJ, Luskin MB. Infusion of brain-derived neurotrophic factor into the lateral ventricle of the adult rat leads to new neurons in the parenchyma of the striatum, septum, thalamus, and hypothalamus. *J Neurosci*. (2001) 21:6706–17. doi: 10.1523/JNEUROSCI.21-17-06706.2001

131. Mohr MA, Sisk CL. Pubertally born neurons and glia are functionally integrated into limbic and hypothalamic circuits of the male Syrian hamster. *Proc Natl Acad Sci U S A*. (2013) 110:4792–7. doi: 10.1073/pnas.1219443110

132. Haan N, Goodman T, Najdi-Samiei A, Stratford CM, Rice R, El Agha E, et al. Fgf10-expressing tanycytes add new neurons to the appetite/energy-balance regulating centers of the postnatal and adult hypothalamus. *J Neurosci*. (2013) 33:6170–80. doi: 10.1523/JNEUROSCI.2437-12.2013

133. Batailler M, Droguerre M, Baroncini M, Fontaine C, Prevot V, Migaud M. DCX-expressing cells in the vicinity of the hypothalamic neurogenic niche: a comparative study between mouse, sheep, and human tissues. *J Comp Neurol*. (2014) 522:1966–85. doi: 10.1002/cne.23514

134. Zilkha-Falb R, Kaushansky N, Ben-Nun A. The median eminence, A new oligodendrogenic niche in the adult mouse brain. *Stem Cell Rep*. (2020) 14:1076–92. doi: 10.1016/j.stemcr.2020.04.005

135. Jurkowski MP, Bettio L K, Woo E, Patten A, Yau SY, Gil-Mohapel J. Beyond the hippocampus and the SVZ: Adult neurogenesis throughout the brain. *Front Cell Neurosci*. (2020) 14:576444. doi: 10.3389/fncel.2020.576444

136. Riskind PN, Kolodny JM, Reed Larsen P. The regional hypothalamic distribution of type II 5′-monodeiodinase in euthyroid and hypothyroid rats. *Brain Res*. (1987) 420:194–8. doi: 10.1016/0006-8993(87)90260-5

137. Tu HM, Legradi G, Bartha T, Salvatore D, Lechan RM, Larsen PR. Regional expression of the type 3 iodothyronine deiodinase messenger ribonucleic acid in the rat central nervous system and its regulation by thyroid hormone*. *Endocrinology*. (1999) 140:784–90. doi: 10.1210/endo.140.2.6486

138. Tu HM, Kim SW, Salvatore D, Bartha T, Legradi G, Larsen PR, et al. Regional distribution of type 2 thyroxine deiodinase messenger ribonucleic acid in rat hypothalamus and pituitary and its regulation by thyroid hormone. *Endocrinology*. (1997) 138:3359–68. doi: 10.1210/endo.138.8.5318

139. Roberts LM, Woodford K, Zhou M, Black DS, Haggerty JE, Tate EH, et al. Expression of the thyroid hormone transporters monocarboxylate transporter-8 (SLC16A2) and organic ion transporter-14 (SLCO1C1) at the blood-brain barrier. *Endocrinology*. (2008) 149:6251–61. doi: 10.1210/en.2008-0378

140. Alkemade A, Vuijst CL, Unmehopa UA, Bakker O, Vennström B, Wiersinga WM, et al. Thyroid hormone receptor expression in the human hypothalamus and anterior pituitary. *J Clin Endocrinol Metab*. (2005) 90:904–12. doi: 10.1210/jc.2004-0474

141. Alkemade A, Friesema EC, Unmehopa UA, Fabriek BO, Kuiper GG, Leonard JL, et al. Neuroanatomical pathways for thyroid hormone feedback in the human hypothalamus. *J Clin Endocrinol Metab*. (2005) 90:4322–34. doi: 10.1210/jc.2004-2567

142. Pérez-Martín M, Cifuentes M, Grondona JM, López-Avalos MD, Gómez-Pinedo U, García-Verdugo JM, et al. IGF-I stimulates neurogenesis in the hypothalamus of adult rats. *Eur J Neurosci*. (2010) 31:1533–48. doi: 10.1111/j.1460-9568.2010.07220.x

143. Smith TJ. Insulin-like growth factor pathway and the thyroid. *Front Endocrinol (Lausanne)*. (2021) 12:653627. doi: 10.3389/fendo.2021.653627

144. Martinez ME, Hernandez A. The type 3 deiodinase is a critical modulator of thyroid hormone sensitivity in the fetal brain. *Front Neurosci*. (2021) 15:1–15. doi: 10.3389/fnins.2021.703730

145. Zhou X, Lu Y, Zhao F, Dong J, Ma W, Zhong S, et al. Deciphering the spatial-temporal transcriptional landscape of human hypothalamus development. *Cell Stem Cell*. (2022) 29:328–343.e5. doi: 10.1016/j.stem.2021.11.009

146. Di Cosmo C. La resistenza e le altre sindromi da ridotta sensibilità agli ormoni tiroidei. *L'Endocrinologo*. (2022) 23:20–6. doi: 10.1007/s40619-021-01008-x

147. Masnada S, Sarret C, Antonello CE, Fadilah A, Krude H, Mura E, et al. Movement disorders in MCT8 deficiency/Allan-Herndon-Dudley Syndrome. *Mol Genet Metab*. (2022) 135:109–13. doi: 10.1016/j.ymgme.2021.12.003

148. Morreale de Escobar G, Pastor R, Obregon MJ, Escobar del Rey F. Effects of maternal hypothyroidism on the weight and thyroid hormone content of rat embryonic tissues, before and after onset of fetal thyroid function. *Endocrinology*. (1985) 117:1890–900. doi: 10.1210/endo-117-5-1890

149. Burfeind KG, Yadav V, Marks DL. Hypothalamic dysfunction and multiple sclerosis: Implications for fatigue and weight dysregulation. *Curr Neurol Neurosci Rep*. (2016) 16:98. doi: 10.1007/s11910-016-0700-3

150. Dayer AG, Cleaver KM, Abouantoun T, Cameron HA. New GABAergic interneurons in the adult neocortex and striatum are generated from different precursors. *J Cell Biol*. (2005) 168:415–27. doi: 10.1083/jcb.200407053

151. Kuhn HG, Winkler J, Kempermann G, Thal LJ, Gage FH. Epidermal growth factor and fibroblast growth factor-2 have different effects on neural progenitors in the adult rat brain. *J Neurosci*. (1997) 17:5820–9. doi: 10.1523/JNEUROSCI.17-15-05820.1997

152. Gonzalez-Perez O, Romero-Rodriguez R, Soriano-Navarro M, Garcia-Verdugo JM, Alvarez-Buylla A. Epidermal growth factor induces the progeny of subventricular zone type B cells to migrate and differentiate into oligodendrocytes. *Stem Cells*. (2009) 27:2032–43. doi: 10.1002/stem.119

153. Kang HJ, Kawasawa YI, Cheng F, Zhu Y, Xu X, Li M, et al. Spatio-temporal transcriptome of the human brain. *Nature*. (2011) 478:483–9. doi: 10.1038/nature10523

154. Tong J, Furukawa Y, Sherwin A, Hornykiewicz O, Kish SJ. Heterogeneous intrastriatal pattern of proteins regulating axon growth in normal adult human brain. *Neurobiol Dis*. (2011) 41:458–68. doi: 10.1016/j.nbd.2010.10.017

155. Shapiro LA, Ng K, Zhou QY, Ribak CE. Subventricular zone-derived, newly generated neurons populate several olfactory and limbic forebrain regions. *Epilepsy Behav*. (2009) 14 Suppl 1:74–80. doi: 10.1016/j.yebeh.2008.09.011

156. Mao L, Wang JQ. Gliogenesis in the striatum of the adult rat: alteration in neural progenitor population after psychostimulant exposure. *Dev Brain Res*. (2001) 130:41–51. doi: 10.1016/S0165-3806(01)00195-X

157. Zhang ZG, Chopp M. Neurorestorative therapies for stroke: underlying mechanisms and translation to the clinic. *Lancet Neurol*. (2009) 8:491–500. doi: 10.1016/S1474-4422(09)70061-4

158. Arvidsson A, Collin T, Kirik D, Kokaia Z, Lindvall O. Neuronal replacement from endogenous precursors in the adult brain after stroke. *Nat Med*. (2002) 8:963–70. doi: 10.1038/nm747

159. Hayakawa K, Seo JH, Pham LDD, Miyamoto N, Som AT, Guo S, et al. Cerebral endothelial derived vascular endothelial growth factor promotes the migration but not the proliferation of oligodendrocyte precursor cells in vitro. *Neurosci Lett*. (2012) 513:42–6. doi: 10.1016/j.neulet.2012.02.004

160. Kojima T, Hirota Y, Ema M, Takahashi S, Miyoshi I, Okano H, et al. Subventricular zone-derived neural progenitor cells migrate along a blood vessel scaffold toward the post-stroke striatum. *Stem Cells*. (2010) 28:545–54. doi: 10.1002/stem.306

161. Zhang R, Chopp M, Zhang ZG. Oligodendrogenesis after cerebral ischemia. *Front Cell Neurosci*. (2013) 7:1–7. doi: 10.3389/fncel.2013.00201

162. Yoshikawa G, Momiyama T, Oya S, Takai K, Tanaka Ji, Higashiyama S, et al. Induction of striatal neurogenesis and generation of region-specific functional mature neurons after ischemia by growth factors. *Lab Invest J Neurosurg*. (2010) 113:835–50. doi: 10.3171/2010.2.JNS09989

163. Zhu W, Cheng S, Xu G, Ma M, Zhou Z, Liu D, et al. Intranasal nerve growth factor enhances striatal neurogenesis in adult rats with focal cerebral ischemia. *Drug Deliv*. (2011) 18:338–43. doi: 10.3109/10717544.2011.557785

164. Hou SW, Wang YQ, Xu M, Shen DH, Wang JJ, Huang F, et al. Functional integration of newly generated neurons into striatum after cerebral ischemia in the adult rat brain. *Stroke*. (2008) 39:2837–44. doi: 10.1161/STROKEAHA.107.510982

165. Tonchev AB, Yamashima T, Sawamoto K, Okano H. Enhanced proliferation of progenitor cells in the subventricular zone and limited neuronal production in the striatum and neocortex of adult macaque monkeys after global cerebral ischemia. *J Neurosci Res*. (2005) 81:776–88. doi: 10.1002/jnr.20604

166. Curtis MA, Penney EB, Pearson AG, van Roon-Mom WMC, Butterworth NJ, Dragunow M, et al. Increased cell proliferation and neurogenesis in the adult human Huntington's disease brain. *Proc Natl Acad Sci U S A*. (2003) 100:9023–7. doi: 10.1073/pnas.1532244100

167. Nato G, Caramello A, Trova S, Avataneo V, Rolando C, Taylor V, et al. Striatal astrocytes produce neuroblasts in an excitotoxic model of Huntington's disease. *Development*. (2015) 142:840–5. doi: 10.1242/dev.116657

168. Tattersfield AS, Croon RJ, Liu YW, Kells AP, Faull RLM, Connor B. Neurogenesis in the striatum of the quinolinic acid lesion model of Huntington's disease. *Neuroscience*. (2004) 127:319–32. doi: 10.1016/j.neuroscience.2004.04.061

169. Kaplan MS. Neurogenesis in the 3-month-old rat visual cortex. *J Comp Neurol*. (1981) 195:323–38. doi: 10.1002/cne.901950211

170. Heuer H, Maier MK, Iden S, Mittag J, Friesema ECH, Visser TJ. The monocarboxylate transporter 8 linked to human psychomotor retardation is highly expressed in thyroid hormone-sensitive neuron populations. *Endocrinology* (2005) 146:1701–6. doi: 10.1210/en.2004-1179

171. Pizzagalli F, Hagenbuch B, Stieger B, Klenk U, Folkers G, Meier PJ. Identification of a novel human organic anion transporting polypeptide as a high affinity thyroxine transporter. *Mol Endocrinol*. (2002) 16:2283–96. doi: 10.1210/me.2001-0309

172. Wang T, Wang Y, Montero-Pedrazuela A, Prensa L, Guadaño-Ferraz A, Rausell E. Thyroid hormone transporters MCT8 and OATP1C1 are expressed in projection neurons and interneurons of basal ganglia and motor thalamus in the adult human and macaque brains. *Int J Mol Sci*. (2023) 24:1–33. doi: 10.20944/preprints202304.0602.v1

173. Diez D, Grijota-Martinez C, Agretti P, De Marco G, Tonacchera M, Pinchera A, et al. Thyroid hormone action in the adult brain: Gene expression profiling of the effects of single and multiple doses of triiodo-l-thyronine in the rat striatum. *Endocrinol*. (2008) 149:3989–4000. doi: 10.1210/en.2008-0350

174. Cera AA, Cacci E, Toselli C, Cardarelli S, Bernardi A, Gioia R, et al. Egr-1 maintains NSC proliferation and its overexpression counteracts cell cycle exit triggered by the withdrawal of epidermal growth factor. *Dev Neurosci*. (2018) 40:223–33. doi: 10.1159/000489699

175. Bernhardt C, Sock E, Fröb F, Hillgärtner S, Nemer M, Wegner M. KLF9 and KLF13 transcription factors boost myelin gene expression in oligodendrocytes as partners of SOX10 and MYRF. *Nucleic Acids Res*. (2022) 50:11509–28. doi: 10.1093/nar/gkac953

176. Inta D, Alfonso J, von Engelhardt J, Kreuzberg MM, Meyer AH, van Hooft JA, et al. Neurogenesis and widespread forebrain migration of distinct GABAergic neurons from the postnatal subventricular zone. *Proc Natl Acad Sci U S A*. (2008) 105:20994–9. doi: 10.1073/pnas.0807059105

177. Gilbert ME, Sui L, Walker MJ, Anderson W, Thomas S, Smoller SN, et al. Thyroid hormone insufficiency during brain development reduces parvalbumin immunoreactivity and inhibitory function in the hippocampus. *Endocrinology*. (2007) 148:92–102. doi: 10.1210/en.2006-0164

178. Wallis K, Sjögren M, van Hogerlinden M, Silberberg G, Fisahn A, Nordström K, et al. Locomotor deficiencies and aberrant development of subtype-specific GABAergic interneurons caused by an unliganded thyroid hormone receptor alpha1. *J Neurosci*. (2008) 28:1904–15. doi: 10.1523/JNEUROSCI.5163-07.2008

179. Aguirre A, Dupree JL, Mangin JM, Gallo V. A functional role for EGFR signaling in myelination and remyelination. *Nat Neurosci*. (2007) 10:990–1002. doi: 10.1038/nn1938

180. Miyamoto N, Maki T, Shindo A, Liang AC, Maeda M, Egawa N, et al. Astrocytes Promote Oligodendrogenesis after White Matter Damage *via* Brain-Derived Neurotrophic Factor. *J Neurosci*. (2015) 35:14002–8. doi: 10.1523/JNEUROSCI.1592-15.2015

181. Francis JS, Olariu A, McPhee SW, Leone P. Novel role for aspartoacylase in regulation of BDNF and timing of postnatal oligodendrogenesis. *J Neurosci Res*. (2006) 84:151–69. doi: 10.1002/jnr.20866

182. Cho SR, Benraiss A, Chmielnicki E, Samdani A, Economides A, Goldman SA. Induction of neostriatal neurogenesis slows disease progression in a transgenic murine model of Huntington disease. *J Clin Invest*. (2007) 117:2889–902. doi: 10.1172/JCI31778

183. Gomes FC, Maia CG, de Menezes JR, Neto VM. Cerebellar astrocytes treated by thyroid hormone modulate neuronal proliferation. *Glia*. (1999) 25:247–55.

184. Gilbert ME, Lasley SM. Developmental thyroid hormone insufficiency and brain development: A role for brain-derived neurotrophic factor (BDNF)? *Neuroscience*. (2013) 239:253–70. doi: 10.1016/j.neuroscience.2012.11.022

185. Davis PJ, Goglia F, Leonard JL. Nongenomic actions of thyroid hormone. *Nat Rev Endocrinol*. (2016) 12:111–21. doi: 10.1038/nrendo.2015.205

186. Francelle L, Galvan L, Gaillard MC, Guillermier M, Houitte D, Bonvento G, et al. Loss of the thyroid hormone-binding protein Crym renders striatal neurons more vulnerable to mutant huntingtin in Huntington's disease. *Hum Mol Genet*. (2015) 24:1563–73. doi: 10.1093/hmg/ddu571

187. Hughes EG, Orthmann-Murphy JL, Langseth AJ, Bergles DE. Myelin remodeling through experience-dependent oligodendrogenesis in the adult somatosensory cortex. *Nat Neurosci*. (2018) 21:696–706. doi: 10.1038/s41593-018-0121-5

188. Gould E, Reeves AJ, Graziano MSA, Gross CG. Neurogenesis in the neocortex of adult primates. *Sci (1979)*. (1999) 286:548–52. doi: 10.1126/science.286.5439.548

189. Kornack DR, Rakic P. Cell proliferation without neurogenesis in adult primate neocortex. *Sci (1979)*. (2001) 294:2127–30. doi: 10.1126/science.1065467

190. Arsenijevic Y, Villemure JG, Brunet JF, Bloch JJ, Déglon N, Kostic C, et al. Isolation of multipotent neural precursors residing in the cortex of the adult human brain. *Exp Neurol*. (2001) 170:48–62. doi: 10.1006/exnr.2001.7691

191. Bhardwaj RD, Curtis MA, Spalding KL, Buchholz BA, Fink D, Björk-Eriksson T, et al. Neocortical neurogenesis in humans is restricted to development. *Proc Natl Acad Sci U S A*. (2006) 103:12564–8. doi: 10.1073/pnas.0605177103

192. Chen J, Magavi SSP, Macklis JD. Neurogenesis of corticospinal motor neurons extending spinal projections in adult mice. *Proc Natl Acad Sci U S A*. (2004) 101:16357–62. doi: 10.1073/pnas.0406795101

193. Tamura Y, Kataoka Y, Cui Y, Takamori Y, Watanabe Y, Yamada H. Multi-directional differentiation of doublecortin- and NG2-immunopositive progenitor cells in the adult rat neocortex in *vivo*. *Eur J Neurosci*. (2007) 25:3489–98. doi: 10.1111/j.1460-9568.2007.05617.x

194. Zecevic N, Rakic P. Development of layer I neurons in the primate cerebral cortex. *J Neurosci*. (2001) 21:5607–19. doi: 10.1523/JNEUROSCI.21-15-05607.2001

195. Ohira K, Furuta T, Hioki H, Nakamura KC, Kuramoto E, Tanaka Y, et al. Ischemia-induced neurogenesis of neocortical layer 1 progenitor cells. *Nat Neurosci*. (2010) 13:173–9. doi: 10.1038/nn.2473

196. Clemente D, Ortega MC, Arenzana FJ, de Castro F. FGF-2 and Anosmin-1 are selectively expressed in different types of multiple sclerosis lesions. *J Neurosci*. (2011) 31:14899–909. doi: 10.1523/JNEUROSCI.1158-11.2011

197. Wang Y, Wang T, Montero-pedrazuela A, Guadaño-ferraz A, Rausell E. Thyroid hormone transporters MCT8 and OATP1C1 are expressed in pyramidal neurons and interneurons in the adult motor cortex of human and macaque brain. *Int J Mol Sci*. (2023) 24:3207. doi: 10.3390/ijms24043207

198. Sousa L, Coelho T, Taipa R. CNS involvement in hereditary transthyretin amyloidosis. *Neurology*. (2021) 97:1111 LP – 1119. doi: 10.1212/WNL.0000000000012965

frontiers | Frontiers in Endocrinology

TYPE Original Research
PUBLISHED 11 March 2024
DOI 10.3389/fendo.2024.1360188

Check for updates

OPEN ACCESS

EDITED BY
Douglas Forrest,
National Institutes of Health (NIH),
United States

REVIEWED BY
David Sharlin,
Minnesota State University, United States
Hong Liu,
National Institute of Diabetes and Digestive and Kidney Diseases (NIH), United States

*CORRESPONDENCE
Laurent M. Sachs
laurent.sachs@mnhn.fr

†These authors share last authorship

RECEIVED 22 December 2023
ACCEPTED 15 February 2024
PUBLISHED 11 March 2024

CITATION
Tribondeau A, Du Pasquier D, Benchouaia M, Blugeon C, Buisine N and Sachs LM (2024) Overlapping action of T_3 and T_4 during *Xenopus laevis* development. *Front. Endocrinol.* 15:1360188. doi: 10.3389/fendo.2024.1360188

COPYRIGHT
© 2024 Tribondeau, Du Pasquier, Benchouaia, Blugeon, Buisine and Sachs. This is an open-access article distributed under the terms of the Creative Commons Attribution License (CC BY). The use, distribution or reproduction in other forums is permitted, provided the original author(s) and the copyright owner(s) are credited and that the original publication in this journal is cited, in accordance with accepted academic practice. No use, distribution or reproduction is permitted which does not comply with these terms.

Overlapping action of T_3 and T_4 during *Xenopus laevis* development

Alicia Tribondeau[1], David Du Pasquier[2], Médine Benchouaia[3], Corinne Blugeon[3], Nicolas Buisine[1†] and Laurent M. Sachs[1*†]

[1]Unité Mixte de Recherche 7221, Département Adaptation du Vivant, Centre National de la Recherche Scientifique, Muséum National d'Histoire Naturelle, Alliance Sorbonne Universités, Paris, France, [2]Watchfrog Laboratory, Evry-Courcouronnes, France, [3]Genomique ENS, Institut de Biologie de l'ENS (IBENS), Département de Biologie, École Normale Supérieure, Centre National de la Recherche Scientifique (CNRS), Institut National de la Santé et de la Recherche Médicale (INSERM), Universités Paris Sciences & Lettres (PSL), Paris, France

Thyroid hormones are involved in many biological processes such as neurogenesis, metabolism, and development. However, compounds called endocrine disruptors can alter thyroid hormone signaling and induce unwanted effects on human and ecosystems health. Regulatory tests have been developed to detect these compounds but need to be significantly improved by proposing novel endpoints and key events. The *Xenopus* Eleutheroembryonic Thyroid Assay (XETA, OECD test guideline no. 248) is one such test. It is based on *Xenopus laevis* tadpoles, a particularly sensitive model system for studying the physiology and disruption of thyroid hormone signaling: amphibian metamorphosis is a spectacular (thus easy to monitor) life cycle transition governed by thyroid hormones. With a long-term objective of providing novel molecular markers under XETA settings, we propose first to describe the differential effects of thyroid hormones on gene expression, which, surprisingly, are not known. After thyroid hormones exposure (T_3 or T_4), whole tadpole RNAs were subjected to transcriptomic analysis. By using standard approaches coupled to system biology, we found similar effects of the two thyroid hormones. They impact the cell cycle and promote the expression of genes involves in cell proliferation. At the level of the whole tadpole, the immune system is also a prime target of thyroid hormone action.

KEYWORDS

thyroid hormones, *Xenopus laevis*, transcriptomic, *Xenopus* Eleutheroembryonic Thyroid Assay, cell proliferation

Introduction

Multicellular organisms evolved complex communication systems to coordinate developmental programs. One such neuroendocrine system, the hypothalamic–pituitary–thyroid (HPT) axis, is a central player in orchestrating body morphogenesis and homeostasis. The axis is composed of brain thyrotropin-releasing hormone (TRH) neurons, pituitary thyrotropes producing thyroid-stimulating hormone (TSH), and the thyroid gland (1). TRH acts *via* its receptor expressed by the pituitary thyrotropes to stimulate the synthesis of pituitary TSH. Following its release, TSH binds its receptor expressed on the thyroid gland to induce the production and release of thyroid hormones (THs) in the bloodstream, mainly thyroxine (T_4) and to a lesser extent triiodothyronine (T_3). T_4, often considered to be the precursor for T_3, is converted to T_3 by mono-deiodinases (DIO) at target tissues. Both THs act by binding to ligand-activated transcription factors (thyroid hormone receptors; TR) belonging to the nuclear receptor family (2). THs' main action is then through regulating gene transcription (3). Finally, THs negatively feedback on the hypothalamic TRH neurons and thyrotropes to maintain proper TH levels.

THs play key roles in vertebrate growth, metabolism, and development by controlling cell proliferation, differentiation, migration, and homeostasis. Disruption of THs signaling increase the risk of adverse effects such as cognitive deficits and metabolic diseases/disorders. Thus, perturbations of the TH axis are of "high concern", especially given the adverse effects caused by anthropogenic and natural chemicals (4). The concern is amplified due to the many gaps in the understanding of the link between potential endocrine disruptor compounds (EDCs), the mode of action of their adverse effects, and the numerous disruption mechanisms (5).

Xenopus laevis is an ideal model organism to test thyroid axis disruption *in vivo* as THs orchestrate tadpole metamorphosis (6), but most of all, THs actions and mode of actions are highly conserved across vertebrates. Indeed, the conservation during vertebrate evolution of the mechanisms underlying these major biological processes regulated by THs is striking from fish and amphibian metamorphoses to egg hatching in sauropsids and birth in mammals (1). In particular for *X. laevis*, early larval stage [7 days post-fertilization at 21°C, Nieuwkoop–Faber stage 45 (7)] are suitable for *in vivo* screening, as at this stage, tadpoles possess all the elements of TH signaling (TRs, DIOs, and transporters) and are competent to respond to TH agonist and antagonist treatment. The model also benefits from the prolific reproduction with more than 1,000 embryos per clutch, the small size of tadpoles at this stage (5 mm at NF45) nicely fitting into multiple well plates and allowing the use of small amounts of test chemicals, and finally, a developmental window where action of TH agonist and antagonist translate into clear phenotypes, as exemplified by nervous system defects resulting from alterations in the balance of neuron versus glial cell population (8). Last but not the least, a *Xenopus*-based assay has been validated by OECD, the Organization for Economic Co-operation and Development: The *Xenopus* Eleutheroembryonic Thyroid Assay (XETA) test guideline no. 248 is a mid-throughput and short-term/fast assay to measure the response of tadpoles (stage NF 45) to potential thyroid active chemicals. The test exploits the transgenic line of *X. laevis, Tg(thibz:eGFP)*, which expresses GFP under the control of a 850-bp regulatory region of the TH/bZIP gene, encoding a leucine zipper transcription factor highly sensitive to TH regulation (9). However, in the absence of complete knowledge on the effect of TH disruption at this developmental window, the test is used to identify thyroid active chemicals but not to demonstrate any potential adverse effects.

In order to fill this gap, we subjected tadpoles to the conventional XETA procedure, but instead of measuring changes in GFP fluorescence, we characterized transcriptome changes by high throughput sequencing of RNA (RNA-seq technology). Transcriptome analysis was chosen because it provides a global and unbiased view of the messenger RNA molecules produced from virtually every gene and specific changes according to cell types, the biological and environmental state of the cells at the time of measurement. This strategy is therefore particularly well suited to monitor THs-induced biological responses because they mainly act through nuclear receptors, in which the transcription factor activity can deeply alter the transcriptome of target cells. Another advantage is that XETA treatment duration is 3 days, thereby providing a relatively late readout of the action of THs, well suited to infer novel end points. In this work, we focus on treatments with agonists, T_3 and T_4, the two main natural hormones. This choice is justified by 1) the low level of circulating THs at stage NF45, offering a unique *in vivo* situation to measure agonist effects, and 2) the potential difference in the bioavailability of both T_3 and T_4 at target cells due to variation in transport, deiodination, and TR binding. Importantly, the transcriptome analysis was realized on RNA extracted from whole tadpole. Despite the difficulties inherent to any measurement on a whole animal, the long-term goal is to identify and provide novel molecular markers of TH signaling alterations readily transferable into novel endpoints for the XETA test guideline. In this context, and given the current need to screen thousands of chemicals, working with whole embryos (i.e., no tissue dissection) is a strategic advantage.

The present work is a proof of principle where we measured transcriptome alterations following treatment with THs. To our knowledge, such broad measure of TH effects has not been described previously. Our results show a strong transcriptional reprogramming for genes involved in all aspects of cell division, with a potential connection to the immune system.

Materials and methods

Solutions preparation

T_3 and T_4 stock solutions at 6.51 g L^{-1} and 0.8 g L^{-1} were prepared following the protocol of the OECD test guideline no. 248 (*Xenopus* Eleutheroembryo Thyroid Assay) with 3,3′,5-Triiodo-L-thyronine (Sigma: T6397) and L-Thyroxine (Sigma: T2501) powders and ultrapure water. Then, stock solutions were diluted in Evian water to obtain exposure solution at 3.25 µg L^{-1} for T_3 and 70 µg L^{-1} for T_4 containing 0.01% of DMSO (Sigma: D8418). The

concentration of T_3 corresponds to the plasma concentration of this hormone during metamorphosis of *X. laevis* and is known to induce morphological changes and modulation of TH target genes in premetamorphic tadpoles (10). The concentration of T_4 was chosen to give the same fluorescence induction in XETA as that of T_3 (data not shown). pHs were always between 6.5 and 8.5 as recommended by the XETA protocol. Exposure solutions were stored at 4°C between daily medium renewal and placed at 21°C 3 h before medium renewal.

Exposure and sample collection

Adult *Xenopus* wild type and transgenic strains were kept in the facilities of Watchfrog (license number: C 91 228 109). The work was conducted in strict accordance with governmental legislations. All procedures involving animal experimentation were approved by the French Ministry of Research under the DAP number APAFIS No. 36464-20220214115229365 v4. Exposure was done following the OECD XETA test guideline. A total of 10 *X. laevis* THb/ZIP-GFP transgenic line tadpoles at stage NF45 (7) were placed in to a six-well plate with 8 mL of exposure solution. Tadpoles were exposed to control (Evian water and 0.01% DMSO), T_3 or T_4 treatments in the dark, at 21°C. The media were renewed every day. After 3 days of exposure, the 10 tadpoles were pooled in a single tube (i.e., 10 tadpoles per treatment) and snap frozen (dry ice and ethanol, 99%). Samples were stored at −75°C. Experiments were repeated three times to obtain three biological replicates.

RNA extraction and purification

RNA extractions were done in two steps. First, a stainless-steel ball (INOX AISI 304 grade 100 AFBMA) and 500 µL RNAble (Eurobio ref: GEXEXT00-0U) were added in each sample and lysed with tissue lyser II apparatus (QIAGEN, Courtaboeuf, France) at 30 Hz for 1 min. Tubes were transferred on ice, and 100 µL of chloroform was added, homogenized vigorously by hand and put on ice for 5 min. Samples were then centrifugated 12,000 *g* at 4°C during 15 min. Next, 175 µL of AquaPhenol (Q-Biogene: AquaPH01) and 100 µL of chloroform were added to 350 µL of supernatant. Following centrifugation, 12,000 *g* at 4°C during 15 min, 250 µL of supernatant was recovered and mixed with 200 µL of ethanol 70%, 10 s on a vortex. The mix was deposited on purification columns (RNeasy Mini Kit, Qiagen: 74104). RNAs were purified according to the manufacturer's instructions and eluted with 14 µL of RNAse-free water. RNA concentration was measured with nanodrop, and RNA quality was assayed using the Agilent Bioanalyser with standard procedure (Agilent RNA 6000 Nano, Agilent: 5067-1511).

RNA sequencing and data processing

Library preparation and Illumina sequencing were performed at the Ecole Normale Supérieure Genomique ENS core facility (Paris, France). Messenger (polyA+) RNAs were purified from 1,000 ng of total RNA using oligo(dT). Libraries were performed using the strand-specific RNA-Seq library preparation stranded mRNA Prep, ligation kit (Illumina) and were multiplexed by five on nine flowcells. A 75-bp read sequencing was performed on a NextSeq 500 (Illumina). A mean of 65 ± 23 million passing Illumina quality filter reads was obtained for each of the nine samples (Supplementary Table S1). Quality control of sequencing was checked with FASTQC, and all banks were good quality with a PHRED score > 34. The first 13 bp of all reads were clipped to remove sequencing adaptors that remain and mapped on the *X. laevis* genome v9.2 using BOWTIE 0.12.3 (11) with the following parameters: "-5 15 -l 50 -n 1 -m 1". Data were transformed into BED format with awk script, and redundant reads were removed by using the SORT and UNIQ UNIX commands. Mapping efficiency was higher than 55% and down to approximately 10% after removal of redundancy, resulting in ≥5 million non-redundant reads mapped. Read count table was computed using INSECTBED v2.25 from the BEDTOOLS toolkit. Differential analysis was performed with DESeq v1.10.1 in parametric mode (estimateDispersions parameters: method=pooled, fitType=parametric), and only genes with pval ≤ 0.05 and $|\log2FC| \geq 0.95$ were considered as differentially expressed.

Gene Ontology

Gene Ontology analysis was performed with gProfiler (12). METASCAPE software (13) was used to highlight biological processes in a physical protein–protein interaction network context.

Biological networks

The network construction is based on KEGG pathways database (Kyoto Encyclopedia of Genes and Genomes database) (14) with JEPETTO cytoscape plugin. All pathways that contain at least one DE gene were merged to form a single network. The resulting network is visualized with CYTOSCAPE v3.8.2 software (15) and layout were computed with "edge weighted spring-embedded" algorithm then adjusted by hand to improve the visualization. Functional categories of KEGG pathways are very diverse (signaling pathway, metabolic pathway…), and the reconstructed network should be referenced as a network of biological pathways where nodes represent gene products and edges are functional interactions between them. Hubs are defined as nodes highly connected (degree ≥ 20).

Results

T_3 and T_4 massively regulate a limited number of biological processes

At the end of the differential analysis, 1,828 genes are differentially expressed (DE) following treatment with T_3 (1,184 upregulated and 644 downregulated) and 2,108 with T_4 (1,385 upregulated and 723 downregulated) (Supplementary Tables S2, S3,

10.3389/fendo.2024.1360188

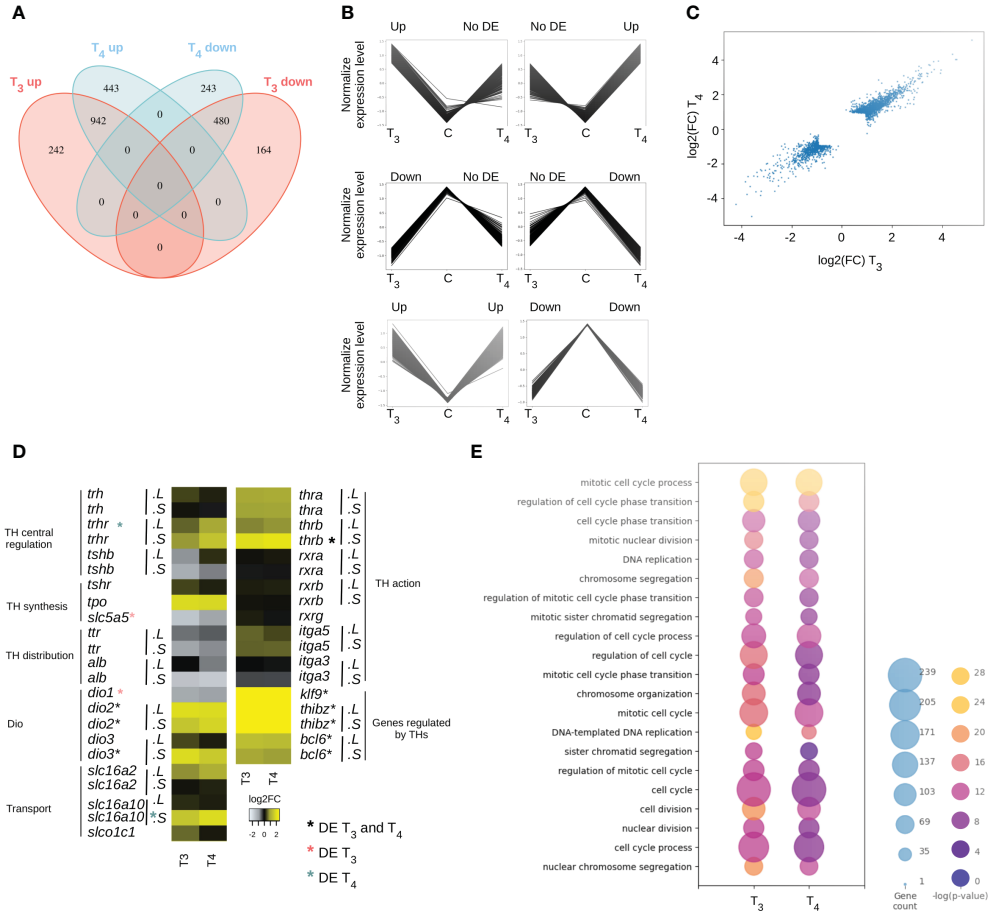

FIGURE 1
T_3 and T_4 treatment induce similar biological responses. **(A)** Differentially expressed (DE) genes up- and downregulated with T_3 (red) and T_4 (blue). **(B)** Type of regulation for each DE gene. **(C)** Rate of genes expression level between T_3 and T_4 condition. **(D)** Expression level of thyroid signaling related genes. ".L" and ".S": genes located on long or short chromosome, respectively. *DE genes with both T_3 and T_4. *DE genes with T_3. *DE genes with T_4. pval ≤ 0.05. **(E)** Biological processes involved in T_3 and T_4 responses.

respectively). The two treatments have 1,422 DE genes in common (Figure 1A). The expression of 406 genes is specifically regulated with T_3 but not T_4 (242 upregulated and 164 downregulated) and, conversely, 686 genes with T_4 but not T3 (443 upregulated and 243 downregulated). Overall, two-thirds of the differentially expressed (DE) genes are upregulated following TH treatments. In all cases, the two hormones induce similar responses, either up- or downregulation, as illustrated by the missing synexpression groups displaying opposite regulation following T_3 and T_4 treatments (Figure 1B). Furthermore, all genes DE for only one of the two hormones still display expression changes albeit not significant (Figure 1B), resulting in a good correlation between T_3 and T_4 treatment (Figure 1C).

The slight differences observed between T_3 and T_4 effects can have at least three non-mutually exclusive origins. First, the two hormones have different sets of target genes. Second, they can act on the expression of genes involved in thyroid signaling leading to the modification of TH synthesis, of the biological availability of the hormone in target organs, or of its action. Third, their potency to change gene expression might be different, thus resulting in slightly different regulation kinetics and overlapping but distinct sets of target genes. Overall, all steps of TH signaling are affected by treatment with T_3 or T_4 (Figure 1D), where gene responses correlate well even though they do not reach statistical significance with both (see above). At the level of the central regulation of TH synthesis, T_3 and T_4 not only increase significantly the expression of the thyrotropin receptor (*rtrh*) but also decrease the expression of the β subunit of the thyroid-stimulating hormone (*tshb*), with a stronger effect for T_3 than for T_4. At the level of the thyroid gland, both hormones induce an increase in thyroid peroxidase (*tpo*) expression and a significant decrease in the sodium/iodide symporter (*slc5a5*, NIS). For the transport of THs in the blood, a decrease in the expression is observed for transthyretin (*ttr*) and the gene coding for albumin (*alb*). THs also act on the expression of genes involved in the import/export of THs in the cell. The expression of monocarboxylate transporter 8 (*slc16a2*, MCT8) and monocarboxylate transporter 10 (*slc16a10*, MCT10) increases and that of solute carrier organic anion transporter family member 1C1 (*slco1c1*, OATP1c1) increases slightly only under the effect of T_3. Deiodinases are all significantly regulated by T_3 or T_4. The expression of type 1 deiodinase (*dio1*) decreases slightly, that of

the two genes encoding type 2 deiodinase (*dio2*) increases and only that of the S form of type 3 deiodinase (*dio3*) increases. Finally, at the level of TH action in target cells, T_3 and T_4 increase the expression of the two forms of nuclear receptors (*thra* and *thrb*) and have no effect on their heterodimerization partners (*rxra, rxrb*, and *rxrg*). They also have a weak effect on the expression of the two genes whose products are at the origin of the formation of the membrane receptor (*itga3* and *itga5*). All these observations show that signaling is impacted with both promoting (*trhr*, *tpo*, *alb-like-2*, *dio2*, *thra*, and *thrb*) and limiting effects (*tshb*, *slc5a5*, *ttr*, *alb*, and *dio3*). However, genes known for their TH-modulated expression are well significantly upregulated during T_3 and T_4 treatments (*klf9*, *thbzip*, and *bcl6*), with very similar variations for the two hormones (Figure 1D).

Next, we carried out gene ontology analysis to highlight the biological functions targeted by T_3 and T_4 treatment and their specific action, if any. By taking all the genes expressed (but not necessarily DE) as a reference, the lists of genes DE under the effect of T_3 or T_4 are respectively enriched in genes corresponding to 87 and 68 GO terms (Supplementary Tables S4, S5, respectively). All T_4 GO terms are found with T_3, resulting in 19 terms specific to T_3 (Supplementary Table S6). Overall, the GO terms are mainly related to the cell cycle and DNA replication (Figure 1E). GO terms only found with T_3 are related to meiotic processes, G2/M and G1/S phase transition and nuclear division. Then, the same analysis was performed with genes only DE with T_3 and with T_4, and no GO terms were significantly enriched.

Hubs within the biological network are T_3 and T_4 target genes

We next modeled TH response in term of network biology. This integrative approach nicely provides a global and cross-pathway description of their functional impact and help understand the nature of interactions and relations between T_3 and T_4 DE genes. Our network coalesced 160 KEGG signaling pathways including at least one DE gene (Supplementary Table S7) and is composed of a set of nodes (genes) and a set of undirected connections (edges) representing functional interaction between nodes. The network consists of 16,645 edges and 3,767 nodes (Figure 2A). As often the case, only a fraction of DE genes is found in the network: 234 DE genes following treatment with T_3 and 277 DE genes following treatment with T_4. This roughly corresponds to approximately a quarter of all DE genes. The KEGG pathways containing the most DE genes are "metabolic pathways" (55), "cell cycle" (39), and "pathways in cancer" (33) (Figure 2B, Supplementary Table S7).

Structural analysis of networks is commonly used to predict the dynamical properties of biological networks (16). We first focus on one such metric, the degree centrality, corresponding to the number of edges at each node. Most nodes are poorly connected within the network (i.e., low degree). Higher-degree nodes, called hubs, are topologically important and have a strong structural role, which translates into a strong biological importance. This phenomenon, called the centrality–lethality rule, simply refers to the fact that attacking (e.g., knocking down) hubs deeply destabilizes biological networks and results in strong phenotypic alterations. Our network includes 408 hubs (nodes with at least 20 edges), of which 30 are regulated by T_3 and 31 by T_4 (Figure 2C). The variation in expression for these DE hubs is very similar between the two hormones. There are 26 common hubs between the two treatment conditions (Figure 2C): *casp3*, *ccna2*, *ccnb1*, *cdk1*, *cdk2*, *cdkn1a*, *e2f1*, *fn1*, *lig1*, *mcm2*, *mcm4*, *mcm5*, *mcm6*, *mcm7*, *plk1*, *pola1*, *pole*, *prkcd*, *psme3*, *ptpn6*, *rpa2*, *rpa3*, *skp2*, *snrpg*, *traf3*, and *zbtb16*. The majority of them display strong responses and are most often upregulated (log2FC up to 2.23). Many encode for cyclin-dependent kinases (*cdk*), a family of protein kinases with important roles in the control of cell division, while other hubs relate to cell division, such as the components of the minichromosome maintenance protein complex (mcm 2, 4, 5, 6, and 7). This complex forms a DNA helicase essential for genome DNA replication. Several components of the DNA replication machinery, the DNA polymerases subunits *pold1*, *pola1*, and *pole*, are also found in the list of DE hubs. Five hubs are downregulated: *notch1*, *sf3a1*, *fn1*, *prkcd*, and *ptpn6* (Figure 2C). *notch1* encodes for a receptor in Notch signaling pathway (NOTCH1, Notch Receptor 1). *sf3a1* encodes for a subunit of the splicing factor complex (SF3A1, splicing factor 3a subunit 1). *prkcd* encodes for a protein kinase C, tumor suppressor, or positive regulator of cell cycle progression. *ptpn6* codes for a protein tyrosine phosphatase. Ontology analysis of DE hubs shows that they are involved not only in mitotic cell cycle phase transition and DNA replication but also in anatomical structure homeostasis and activation of the pre-replicative complex (Figure 2D).

T_3 and T_4 differentially expressed genes form specific subnetworks

Another important feature emerging from of our analysis of molecular networks is a set of "chains" of DE genes, where interacting nodes (as defined in pathways) are collectively DE. As such, chains are *de facto* hot spots of TH action within the network. We could identify six subnetworks with more than two T_3 and T_4 DE genes connected to each other (Figure 3A). The largest subnetwork is a giant component of 81 nodes, while the other five are much smaller (size between 2 and 10 nodes). There are also seven pairs of nodes regulated by both T_3 and T_4 (Figure 3A). Strikingly, of a total of 35 DE hubs, 31 are presently located in the giant component and the remaining four (SF3A1, SNRPG, FN1, and TBP) are located in smaller chains (Figure 2C).

Of the 317 T_3 and T_4 DE genes found in the entire network, 81 are found in the largest subnetwork, the vast majority of which respond to both T_3 and T_4. The transcriptional response of other nodes is relatively similar after treatment with each TH, although it fails to reach statistical significance with one or the other hormone (12 genes for T_3 and 21 for T_4). For a large part, genes belonging to this subnetwork relate to cell cycle, DNA replication, and DNA damage response (Figure 3B). More than half are involved in mitotic cell cycle (43 out of 81) and cell cycle (58 out of 81). This subnetwork also concentrates 18 upregulated genes coding for protein involved in DNA damage response (BRCA1, CASP3,

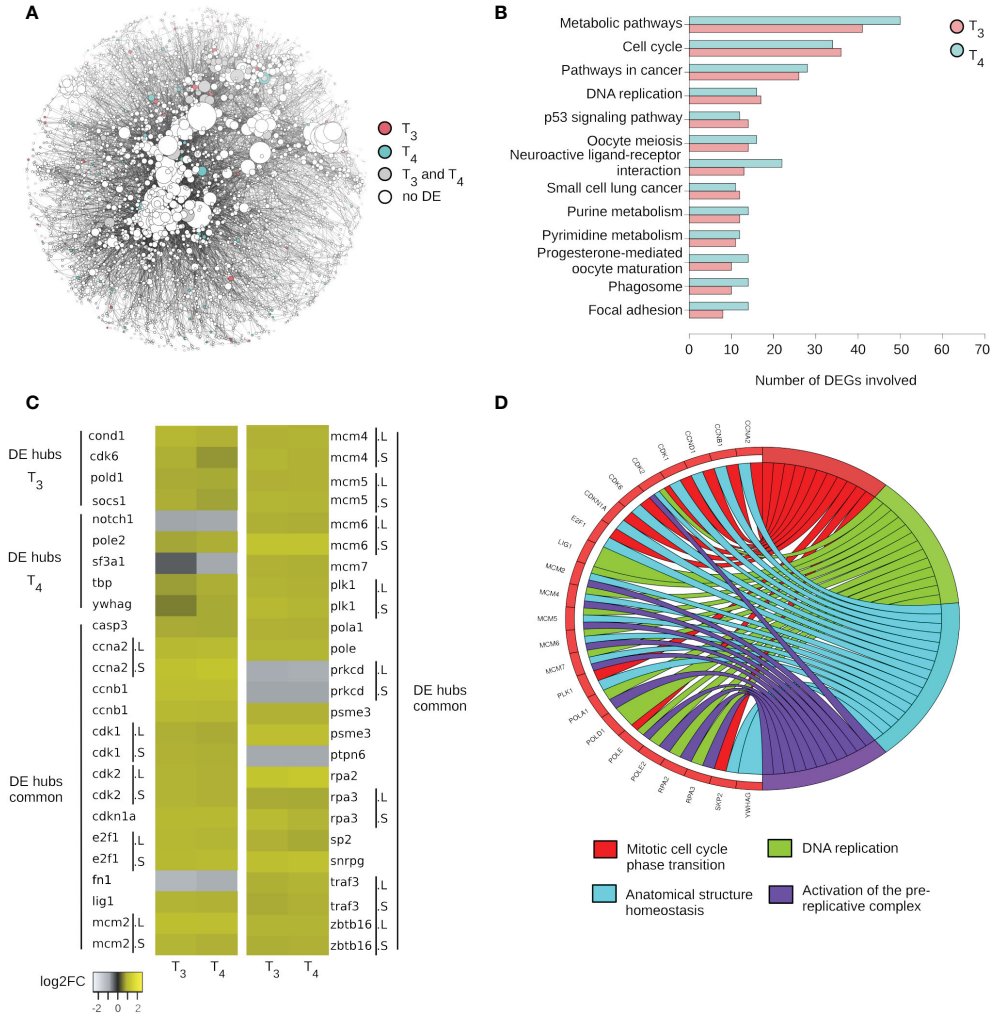

FIGURE 2
T_3 and T_4 impact same pathways and most of DE hubs. **(A)** Network of gene (products) interactions. **(B)** The first 10 KEGG pathways containing most of DE genes in both conditions. **(C)** Expression level of DE hubs. ".L" and ".S": genes located on long or short chromosome, respectively. **(D)** Biological processes impacted by DE hubs and deducted from a protein–protein interaction analysis.

CCNB1, CCNB2, CCNB3, CCND1, CCND2, CCNE2, CDC25C, CDK1, CDK2, CDK6, CDKN1A, CHEK1, CHEK2, E2F1, RAD51, and RPA2). It is possible to distinguish another subset with four genes (GDF5, ACVR2B, INHBC, and INHBA) involved in TGF-beta signaling pathway. In this subnetwork, the number of downregulated genes is more limited (nine out of 81). They are coding for the proteins BLNK, PTPN6, PRKCD, FABP1, PPARG, INHBC, XIAP, LMNA, and ALOX12B). Two of them have already been sited because they are hubs (PTPN6 and PRKCD). We note that they belong to a chain with BLNK, a protein playing critical role in B-cell development.

Other chains are much smaller. The longest is composed of 10 nodes (F13B, JAM3, FGA, and CDH5 are upregulated, and GP1BB, GP9, FGB, GP1BA, FGG, and ITGAM are downregulated), linked to platelets and blood coagulation (Figure 3C). The next chain is very small, only four nodes (FN1, MMP9, THBS2, and THBS3) are involved in cell-to-cell and cell-to-matrix interactions (Figure 3C), two of which (the hub FN1 and THBS3) are being downregulated. The fourth subnetwork is composed of the ephrins EFNA5 and EFNA2, and the ephrin receptor EPHA5, all upregulated by THs (Figure 3C). The fifth and last chain composed of more than two nodes includes the upregulated genes coding for TBP, POLR2C, and TAF4B involved in transcription.

There are also seven pairs (chains of length 2) of DE genes. Three pairs are involved in immune system functions: the gene coding for the Toll-like Receptor 2 (TLR2), a crucial mediator of innate immunity activation, is linked to SFTPA1, a surfactant protein involved in the defense against pathogen, both upregulated; the downregulated genes CYBA (phagocyte oxidase complex) and the catalytic subunit NOX1; and IRF3 (upregulated) and MAVS (downregulated), important mediators of innate immune response and interferon signaling. Two other pairs are involved in the nervous system: GRIK2 and GRID2 encoding subunits of the glutamate ionotropic receptor, and ARSA and GAL3ST1 involved neuron myelination. The last two pairs are involved in RNA splicing and recycling endosomes, respectively: the

10.3389/fendo.2024.1360188

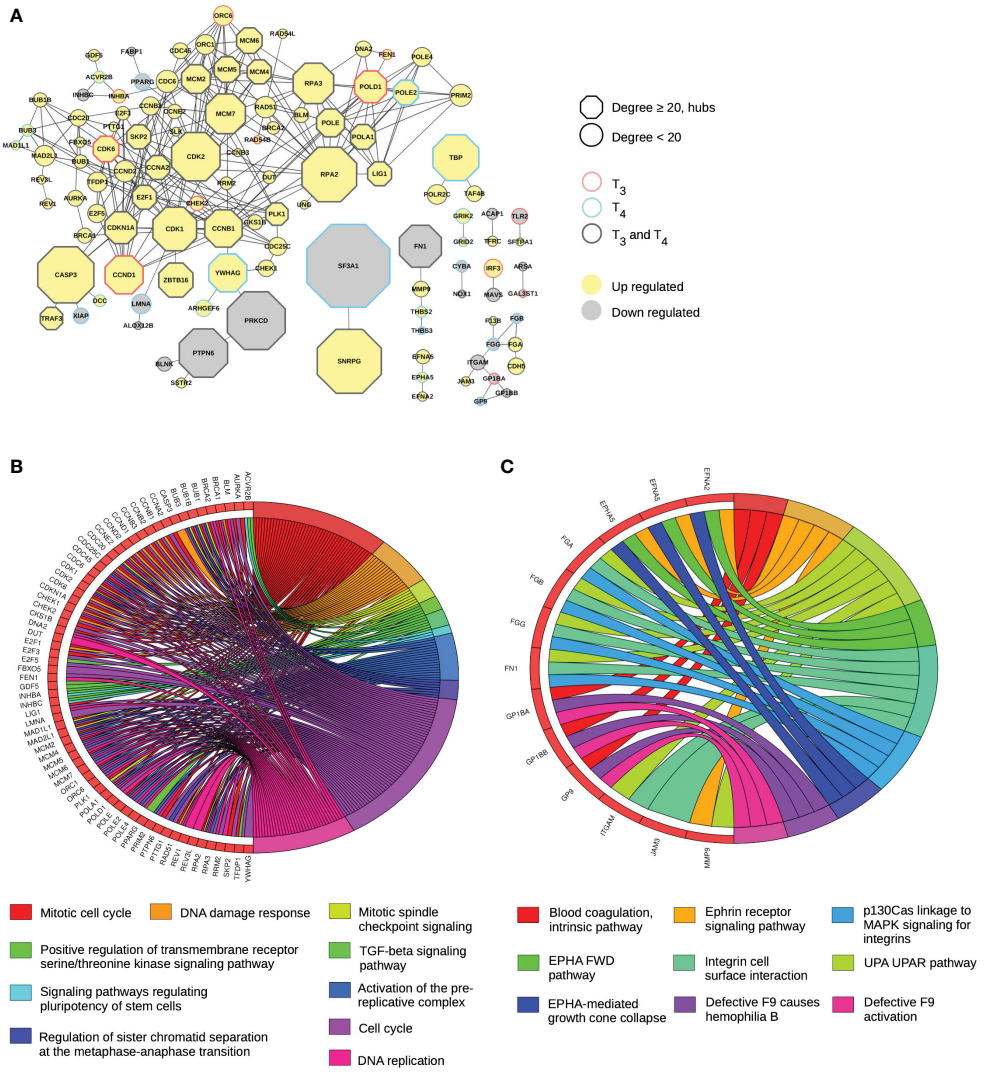

FIGURE 3
T_3 and T_4 responses concentrate in same subnetworks. **(A)** Subnetworks of gene (products) regulated by T_3 and T_4. **(B)** Principal biological processes impacted by the huge subnetwork and deducted from a protein–protein interaction analysis. **(C)** Principal biological processes impacted by small subnetworks and deducted from a protein–protein interaction analysis.

hubs SF3A1 (downregulated) and SNRPG (upregulated), followed by ACAP1 (upregulated) and TFRC (downregulated).

Discussion

Aside from the well-known diversity of TH actions during amphibian metamorphosis (6), early larval development is also a TH-sensitive period commonly used to test thyroid endocrine disruption. Unfortunately, the effects of TH agonists and TH antagonists at this developmental window are only partly described, and available data are very scarce. Our work, based on endocrinology, RNA-seq, and system biology, is a first attempt to elucidate the transcriptional action of both T_3 and T_4 in early *X. laevis* larvae. We show that at the level of whole embryos, T_3 and T_4 treatments lead to changes in the mRNA levels of components of the TH signaling pathway and a strong transcriptional reprogramming of cell division.

THs regulate the cell cycle machinery

In *Xenopus*, THs are known to induce cell proliferation during metamorphosis. During intestinal remodeling, adult intestinal stem cells multiply and differentiate into adult epithelial system, while the larval epithelium degenerates (17). Furthermore, transcriptome analysis of intestinal cells from premetamorphic wild-type versus *TRα*-knockout tadpoles treated with or without T_3 showed strong enrichment with cell-cycle-related genes (18). Similar results were obtained in other tissues such as hindlimbs, which appear during metamorphosis (19), and brain, which is deeply remodeled through neural cell proliferation in ventricular and subventricular zones

(20). THs are also important mediators of cell proliferation in mammals (21) for cells as diverse as rat pituitary GH-producing cells, which proliferate in response to T_3 by shortening G1 phase (22), hepatocytes (23), intestinal epithelial cells (24), cardiomyocytes (25), and skin cells (26).

Here, we show that T_3 and T_4 actions induce the expression of many genes involved in cell proliferation, and to this regard, our results are similar to the TH-induced transcriptome reprogramming typically found at metamorphosis in specific tissues (18–20). A significant fraction of them is located in the largest subnetwork, which is involved in most of the biological processes related to cell division: "induction of cell cycle", "control of cell cycle progression", "DNA replication", "activation of the pre-replicative complex", and "DNA repair and sister chromatin separation".

A set of DE genes is well known for its major role in cell cycle: transcription factors E2F 1, 3, and 5 (all upregulated) mediate cell proliferation (27), while CDC6, CDC45, CDC25C, and CDC20 are cell division cycle proteins involved in the initiation of DNA replication. The control of cell cycle progression is also ensured by cyclin-dependent kinases (28), such as CDK1, which modulates the centrosome cycle and mitotic onset, promotes G2-M transition, and regulates G1 progress and G1-S transition. The CDK2 kinase triggers the duplication of centrosomes and DNA, promotes the E2F transcriptional program and the initiation of DNA synthesis at the G1-S transition, modulates G2 progression, and controls the timing of entry into mitosis by controlling the subsequent activation of the cyclin B/CDK1 complex. CDKN1A, the cyclin-dependent kinase inhibitor 1A, is involved in TP53-mediated inhibition of cellular proliferation in response to DNA damage. CDK6, the cyclin-dependent kinase 6, is important for cell cycle G1 phase progression and transition to S phase. Cyclin A2 (ccna2) controls the cell cycle at the G1/S (start) and G2/M (mitosis) transitions by acting through the formation of specific serine/threonine protein kinase holoenzyme complexes with the cyclin-dependent protein kinases CDK1 or CDK2 (ccne1). Cyclin B1 (ccnb1) and B2 (ccnb2) are involved in the control of the G2/M (mitosis) transition, and cyclin E2 (ccne2) is a regulator of the late G1 and early S phase. Cyclin D1 (ccnd1, CDK4) is a regulatory subunit of the CDK4–CDK6 complex. Interestingly, cyclin D1 expression is known to increase following T_3 treatment (22, 23).

Most of the components of the Minichromosome Maintenance Complex (MCM) are also DE (mcm2, mcm4, mcm5, mcm6, and mcm7) (29). Only mcm3 is missing, indicating that the vast majority of them is regulated by THs and further supports their role in promoting cell cycle. This complex forms a replicative helicase essential for DNA replication initiation and elongation. ORC1 and ORC6 are both components of the origin recognition complex (ORC) that binds origins of replication and are required to assemble the pre-replication complex necessary at DNA replication initiation (30). Several DNA polymerase coding genes (pola1, pold1, pole, pole2, and pole4) are DE (31). Actors of DNA repair (32) also increase: RAD51, which plays an important role in homologous strand exchange, a key step in DNA repair through homologous recombination; RAD54B, involved in DNA repair and mitotic recombination; the two BRCA DNA repair associated (BRCA1 and BRCA2) that play a central role in DNA repair by facilitating cellular responses to DNA damage; and CHECK1, a serine/threonine-protein kinase, which is required for checkpoint-mediated cell cycle arrest and activation of DNA repair in response to the presence of DNA damage or un-replicated DNA. CHECK1 is a component of the G2/M checkpoint, phosphorylating and inactivating CDC25C, required for cell cycle arrest in response to DNA damage.

Finally, the expression of genes involved in spindle assembly is also induced: the BUB1 mitotic checkpoint serine/threonine kinase, an essential component of the spindle-assembly checkpoint signaling needed for appropriate chromosome alignment (33), and the Aurora kinase A (AURKA), a mitotic serine/threonine kinase that contributes to the regulation of cell cycle progression *via* its association with the centrosome and the spindle microtubules during mitosis. AURKA has a critical role in various mitotic events including the establishment of mitotic spindle, centrosome duplication, centrosome separation and maturation, chromosomal alignment, spindle assembly checkpoint, and cytokinesis. Overall, TH action during early larval period will target mainly biological processes linked to cell proliferation with its increase.

TH disruption: potential implications for tadpole development

Our results can help in understanding the potential effects of TH signaling disruption during amphibian larval development. Does the increase in cell proliferation cause an adverse effect? The beginning of the larval period is not well known. Organogenesis is generally complete, and the animal grows slowly. For brain development, it was shown that this period is marked by a low level of neurogenesis due to a dramatic lengthening of the average cell cycle with quiescence progenitor cells poised for reactivation at metamorphosis (34, 35). Obviously, THs (and TR) play a causative role in anuran metamorphosis. However, TR is expressed during the entire larval period, well before metamorphosis, and the rise in THs. Depending upon the presence and absence of TH, TRs can act as both activators and repressors of TH-inducible genes, respectively, TRs have dual functions in frog development (36). As a reminder, TRs function initially as repressors of TH-inducible genes at tadpole stages to prevent premature metamorphosis. Later, TRs act as transcriptional activators of the same genes and activate the metamorphic process. The important point is that the function of unliganded TR before metamorphosis ensures a proper period of tadpole growth. This essential function is also highlighted by TR knockout showing that TRs have a role in the timing of the development with the formation of most adult organs/tissues merely requiring the derepression of TR target genes, while larval tissue degeneration requires liganded TR (37). Even though metamorphosis can be induced precociously by exogenous THs, such treatment does not replicate natural metamorphosis. The potential explanations for this discrepancy are the involvement of other hormones such as glucocorticoids (38) and/or the required signal level for metamorphosis that need to be well controlled over the entire period of the tadpole transformation and need to be

adapted to each tissue (39). Thus, inadequate level of THs or agonist will lead to improper TH response gene expression, improper developmental rates, and finally adverse effects. Indeed, THs and EDCs can induce changes in the balance of neuron versus glial cell population by modifying the proportion of cell dividing (8). It is well known that this phenomenon drives to nervous system defect and pathologies (40).

If the effect of THs on cell proliferation is the most obvious, our results provide other avenues for identifying potential adverse effects. First, we found a decrease in mRNA level coding for NOTCH1 (Notch receptor 1), one of the only five hubs in our network downregulated. This receptor in Notch signaling pathway is involved in the development of numerous cell and tissue types across species by regulating interactions between physically adjacent cells (41). Since, NOTCH1 participates in organ formation, tissue function, and repair, disruption of its signaling may cause pathological consequences (42). Two downregulated hubs are present in the large subnetwork including the factors involved in the cell cycle. These two genes code for PRKCD and PTPN6. *prkcd* encodes for protein kinase C delta, a negative regulator of cell cycle progression or positive regulator of cell proliferation. This may look contradictory, but PRKCD in normal condition prevents cell cycle progression (43). The decrease in its expression is therefore consistent with the increase in pro-cell division factors observed in our study. However, in stressful conditions, PRKCD can lose its gatekeeper function at cell cycle checkpoints to stimulate essential cell proliferation. The second downregulated hub, *ptpn6*, codes for a protein tyrosine phosphatase involved in growth, differentiation, the mitotic cycle, and oncogenic transformation (44). The protein is expressed primarily in hematopoietic and epithelial cells, downregulating pathways that promote cell proliferation (45). The downregulation of *ptpn6* in our model agrees with this function. Interestingly, PTPN6 also acts as a negative regulator of receptors involved in immune responses (B-cell antigen receptor, T-cell antigen receptor, and natural killer cell-activating receptor) and cytokine receptors (46). The PTPN6's role in signaling of the innate and adaptive immune system correlates with its link in our network with another downregulated gene, BLNK and PRKCD, forming a chain of proteins coded by downregulated genes. BLNK, the B-cell linker protein, is involved in B-cell development and its activation (47).

The link of our study with the hematopoietic cells is strengthened by several other observations. First, the subnetwork including F13B, GP1BB, GP9, JAM3, FGB, GP1BA, FGG, FGA, ITGAM, and CDH5 is involved in platelet function and blood clotting (48). Second, in the subnetwork composed of the four nodes (FN1, MMP9, THBS2, and THBS3), *fn1* is one of the downregulated hubs and encodes fibronectin involved in cell adhesion and migration processes like embryogenesis, blood coagulation, host defense, and metastasis (49). There are also THBS2 and THBS3 that belong to the thrombospondin family with anti-angiogenic property (50). Third, the Toll-like receptor 2 (TLR2) is downregulated. TLR2 has a crucial role in pathogen recognition and activation of innate immunity (51). TLR2 is linked to SFTPA1 that is upregulated. SFTPA1 is a surfactant protein important in the defense against pathogen in lungs (52). Finally, the last duo of DE genes includes IRF3 (upregulated) and MAVS (downregulated), where IRF3 (interferon regulatory factor 3) plays an important role in the innate immune response against viruses (53) and MAVS (mitochondrial antiviral signaling protein) is a protein required for activation of transcription factors, which modulate expression of IFN-beta and also contributes to antiviral innate immunity (54). Globally, our results suggest that TH treatment might affect hematopoiesis or hematopoietic function that can lead in part to reduced blood coagulation and reduced immune response.

XETA provides a read out of endocrine response mechanisms, but is not designed to detect adverse effects. Whole transcriptome studies have the potential to fill this gap and provide candidate thyroid-responsive biomarkers and end/points. They are, in turn, the building blocks that link together molecular initiating events to the sequence of key events leading to relevant adverse outcomes, at the organism or population level. In this work, we describe the typical TH response in an experimental setting compliant with XETA. As such, we provide the reference data onto which the impact of EDCs can be fully addressed.

In conclusion, early exposure to THs or EDCs acting as agonist might disrupt proper larval development through increase in cell proliferation and decrease in animal capacity to provide immune response.

Data availability statement

The data presented in the study are deposited in the Sequence Read Archive repository, accession number PRJNA1044078.

Ethics statement

The animal study was approved by Comité d'éthique de génopole en expérimentation animale CEEA51. The study was conducted in accordance with the local legislation and institutional requirements.

Author contributions

AT: Data curation, Investigation, Methodology, Validation, Writing – original draft, Writing – review & editing. DDP: Methodology, Writing – review & editing. MB: Investigation, Writing – review & editing. CB: Investigation, Writing – review & editing. NB: Conceptualization, Investigation, Methodology, Supervision, Writing – review & editing. LS: Conceptualization, Funding acquisition, Project administration, Supervision, Writing – original draft, Writing – review & editing.

Funding

The author(s) declare that financial support was received for the research, authorship, and/or publication of this article. This work in funded from the European Union's Horizon 2020 research and

innovation program, under grant agreement No. 825753 (ERGO). The Genomique ENS core facility was supported by the France Génomique national infrastructure, funded as part of the "Investissements d'Avenir" program managed by the Agence Nationale de la Recherche (contract ANR-10-INBS-0009).

Acknowledgments

We thank T. Lecuyer and N. Loire at Watchfrog for their teaching of Xenopus Eleutheroembryonic Thyroid Assay protocol.

Conflict of interest

The authors declare that the research was conducted in the absence of any commercial or financial relationships that could be construed as a potential conflict of interest.

The author(s) declared that they were an editorial board member of Frontiers, at the time of submission. This had no impact on the peer review process and the final decision.

Publisher's note

All claims expressed in this article are solely those of the authors and do not necessarily represent those of their affiliated organizations, or those of the publisher, the editors and the reviewers. Any product that may be evaluated in this article, or claim that may be made by its manufacturer, is not guaranteed or endorsed by the publisher.

Supplementary material

The Supplementary Material for this article can be found online at: https://www.frontiersin.org/articles/10.3389/fendo.2024.1360188/full#supplementary-material

SUPPLEMENTARY TABLE 1
Number of sequencing reads and mapping statistics.

SUPPLEMENTARY TABLE 2
Differential expressed genes with T_3 treatment (pval ≤ 0.05).

SUPPLEMENTARY TABLE 3
Differential expressed genes with T_4 treatment (pval ≤ 0.05).

SUPPLEMENTARY TABLE 4
Biological processes involved with T_3.

SUPPLEMENTARY TABLE 5
Biological processes involved with T_4.

SUPPLEMENTARY TABLE 6
Biological processes only involved with T_3.

SUPPLEMENTARY TABLE 7
KEGG pathways containing at least one DE gene.

References

1. Rousseau K, Dufour S, Sachs LM. Interdependence of thyroid and corticosteroid signaling in vertebrate developmental transitions. *Front Ecol Evol*. (2021) 9:735487. doi: 10.3389/fevo.2021.735487

2. Grimaldi A, Buisine N, Miller T, Shi Y-B, Sachs LM. Mechanisms of thyroid hormone receptor action during development: Lessons from amphibian studies. *Biochim Biophys Acta BBA - Gen Subj*. (2013) 1830:3882–92. doi: 10.1016/j.bbagen.2012.04.020

3. Flamant F, Cheng S-Y, Hollenberg AN, Moeller LC, Samarut J, Wondisford FE, et al. Thyroid hormone signaling pathways: time for a more precise nomenclature. *Endocrinology*. (2017) 158:2052–7. doi: 10.1210/en.2017-00250

4. Gilbert ME, Rovet J, Chen Z, Koibuchi N. Developmental thyroid hormone disruption: Prevalence, environmental contaminants and neurodevelopmental consequences. *NeuroToxicology*. (2012) 33:842–52. doi: 10.1016/j.neuro.2011.11.005

5. La Merrill MA, Vandenberg LN, Smith MT, Goodson W, Browne P, Patisaul HB, et al. Consensus on the key characteristics of endocrine-disrupting chemicals as a basis for hazard identification. *Nat Rev Endocrinol*. (2020) 16:45–57. doi: 10.1038/s41574-019-0273-8

6. Shi Y. *Amphibian Metamorphosis: From Morphology to Molecular Biology* (1999). Available online at: https://www.semanticscholar.org/paper/Amphibian-Metamorphosis%3A-From-Morphology-to-Biology-Shi/ccebe21acb092642bb9437909832dfde5ffcaf3e (Accessed December 21, 2022).

7. Nieuwkoop PD, Faber JHubrecht laboratorium. *Normal table of Xenopus laevis (Daudin): a systematical and chronological survey of the development from the fertilized egg till the end of metamorphosis*. Facsim, editor. New York London: Garland (1994).

8. Fini J-B, Mughal BB, Le Mével S, Leemans M, Lettmann M, Spirhanzlova P, et al. Human amniotic fluid contaminants alter thyroid hormone signalling and early brain development in Xenopus embryos. *Sci Rep*. (2017) 7:43786. doi: 10.1038/srep43786

9. Mughal BB, Fini J-B, Demeneix BA. Thyroid-disrupting chemicals and brain development: an update. *Endocr Connect*. (2018) 7:R160–86. doi: 10.1530/EC-18-0029

10. Leloup J, Buscaglia M. La triiodothyroinine: hormone de la metamorphose des amphibiens. *C R Acad Sci*. (1977) 284:2261–3.

11. Langmead B, Trapnell C, Pop M, Salzberg SL. Ultrafast and memory-efficient alignment of short DNA sequences to the human genome. *Genome Biol*. (2009) 10:R25. doi: 10.1186/gb-2009-10-3-r25

12. Raudvere U, Kolberg L, Kuzmin I, Arak T, Adler P, Peterson H, et al. g:Profiler: a web server for functional enrichment analysis and conversions of gene lists, (2019 update). *Nucleic Acids Res*. (2019) 47:W191–8. doi: 10.1093/nar/gkz369

13. Zhou Y, Zhou B, Pache L, Chang M, Khodabakhshi AH, Tanaseichuk O, et al. Metascape provides a biologist-oriented resource for the analysis of systems-level datasets. *Nat Commun*. (2019) 10:1523. doi: 10.1038/s41467-019-09234-6

14. Kanehisa M, Goto S. KEGG: kyoto encyclopedia of genes and genomes. *Nucleic Acids Res*. (2000) 28:27–30. doi: 10.1093/nar/28.1.27

15. Shannon P, Markiel A, Ozier O, Baliga NS, Wang JT, Ramage D, et al. Cytoscape: A software environment for integrated models of biomolecular interaction networks. *Genome Res*. (2003) 13:2498–504. doi: 10.1101/gr.1239303

16. Charitou T, Bryan K, Lynn DJ. Using biological networks to integrate, visualize and analyze genomics data. *Genet Sel Evol*. (2016) 48:27. doi: 10.1186/s12711-016-0205-1

17. Sun G, Roediger J, Shi Y-B. Thyroid hormone regulation of adult intestinal stem cells: Implications on intestinal development and homeostasis. *Rev Endocr Metab Disord*. (2016) 17:559–69. doi: 10.1007/s11154-016-9380-1

18. Tanizaki Y, Shibata Y, Zhang H, Shi Y-B. Analysis of thyroid hormone receptor α-knockout tadpoles reveals that the activation of cell cycle program is involved in thyroid hormone-induced larval epithelial cell death and adult intestinal stem cell development during xenopus tropicalis metamorphosis. *Thyroid*. (2021) 31:128–42. doi: 10.1089/thy.2020.0022

19. Tanizaki Y, Shibata Y, Zhang H, Shi Y-B. Thyroid hormone receptor α Controls the hind limb metamorphosis by regulating cell proliferation and wnt signaling pathways in xenopus tropicalis. *Int J Mol Sci*. (2022) 23:1223. doi: 10.3390/ijms23031223

20. Wen L, He C, Sifuentes CJ, Denver RJ. Thyroid hormone receptor alpha is required for thyroid hormone-dependent neural cell proliferation during tadpole metamorphosis. *Front Endocrinol*. (2019) 10:396. doi: 10.3389/fendo.2019.00396

21. Pascual A, Aranda A. Thyroid hormone receptors, cell growth and differentiation. *Biochim Biophys Acta BBA - Gen Subj*. (2013) 1830:3908–16. doi: 10.1016/j.bbagen.2012.03.012

22. Barrera-Hernandez G, Park KS, Dace A, Zhan Q, Cheng S. Thyroid hormone-induced cell proliferation in GC cells is mediated by changes in G1 cyclin/cyclin-dependent kinase levels and activity. *Endocrinology*. (1999) 140:5267–74. doi: 10.1210/endo.140.11.7145

23. Hönes GS, Kerp H, Hoppe C, Kowalczyk M, Zwanziger D, Baba HA, et al. Canonical thyroid hormone receptor β Action stimulates hepatocyte proliferation in male mice. *Endocrinology*. (2022) 163:bqac003. doi: 10.1210/endocr/bqac003

24. Giolito MV, Plateroti M. Thyroid hormone signaling in the intestinal stem cells and their niche. *Cell Mol Life Sci*. (2022) 79:476. doi: 10.1007/s00018-022-04503-y

25. Chattergoon NN. Thyroid hormone signaling and consequences for cardiac development. *J Endocrinol*. (2019) 242:T145–60. doi: 10.1530/JOE-18-0704

26. Contreras-Jurado C, García-Serrano L, Gómez-Ferrería M, Costa C, Paramio JM, Aranda A. The thyroid hormone receptors as modulators of skin proliferation and inflammation*. *J Biol Chem*. (2011) 286:24079–88. doi: 10.1074/jbc.M111.218487

27. DeGregori J, Johnson DG. Distinct and overlapping roles for E2F family members in transcription, proliferation and apoptosis. *Curr Mol Med*. (2006) 6:739–48. doi: 10.2174/1566524010606070739

28. Malumbres M, Barbacid M. Mammalian cyclin-dependent kinases. *Trends Biochem Sci*. (2005) 30:630–41. doi: 10.1016/j.tibs.2005.09.005

29. Ishimi Y. Regulation of MCM2-7 function. *Genes Genet Syst*. (2018) 93:125–33. doi: 10.1266/ggs.18-00026

30. Bell SP. The origin recognition complex: from simple origins to complex functions. *Genes Dev*. (2002) 16:659–72. doi: 10.1101/gad.969602

31. Hoitsma NM, Whitaker AM, Schaich MA, Smith MR, Fairlamb MS, Freudenthal BD. Structure and function relationships in mammalian DNA polymerases. *Cell Mol Life Sci*. (2020) 77:35–59. doi: 10.1007/s00018-019-03368-y

32. Cortez D. Replication-coupled DNA repair. *Mol Cell*. (2019) 74:866–76. doi: 10.1016/j.molcel.2019.04.027

33. Pavin N, Tolić IM. Mechanobiology of the mitotic spindle. *Dev Cell*. (2021) 56:192–201. doi: 10.1016/j.devcel.2020.11.003

34. Thuret R, Auger H, Papalopulu N. Analysis of neural progenitors from embryogenesis to juvenile adult in Xenopus laevis reveals biphasic neurogenesis and continuous lengthening of the cell cycle. *Biol Open*. (2015) 4:1772–81. doi: 10.1242/bio.013391

35. Moreno N, González A. Pattern of Neurogenesis and Identification of Neuronal Progenitor Subtypes during Pallial Development in Xenopus laevis. *Front Neuroanat*. (2017) 11:24. doi: 10.3389/fnana.2017.00024

36. Sachs LM, Damjanovski S, Jones PL, Li Q, Amano T, Ueda S, et al. Dual functions of thyroid hormone receptors during Xenopus development. *Comp Biochem Physiol B Biochem Mol Biol*. (2000) 126:199–211. doi: 10.1016/S0305-0491(00)00198-X

37. Shi Y-B. Life without thyroid hormone receptor. *Endocrinology*. (2021) 162:bqab028. doi: 10.1210/endocr/bqab028

38. Sachs LM, Buchholz DR. Insufficiency of thyroid hormone in frog metamorphosis and the role of glucocorticoids. *Front Endocrinol*. (2019) 10:287. doi: 10.3389/fendo.2019.00287

39. Frieden E, Just JJ. Hormonal responses in amphibian metamorphosis. In: Litwack G, editor. *Biochemical Actions of Hormones*. New York, NY: Academic Press (1970). p. 1–52. doi: 10.1016/B978-0-12-452801-7.50006-7

40. Demeneix BA. Evidence for prenatal exposure to thyroid disruptors and adverse effects on brain development. *Eur Thyroid J*. (2019) 8:283–92. doi: 10.1159/000504668

41. Artavanis-Tsakonas S, Rand MD, Lake RJ. Notch signaling: cell fate control and signal integration in development. *Science*. (1999) 284:770–6. doi: 10.1126/science.284.5415.770

42. Zhou B, Lin W, Long Y, Yang Y, Zhang H, Wu K, et al. Notch signaling pathway: architecture, disease, and therapeutics. *Signal Transduct Target Ther*. (2022) 7:1–33. doi: 10.1038/s41392-022-00934-y

43. Jackson DN, Foster DA. The enigmatic protein kinase Cδ: complex roles in cell proliferation and survival. *FASEB J*. (2004) 18:627–36. doi: 10.1096/fj.03-0979rev

44. Neel BG, Gu H, Pao L. The 'Shp'ing news: SH2 domain-containing tyrosine phosphatases in cell signaling. *Trends Biochem Sci*. (2003) 28:284–93. doi: 10.1016/S0968-0004(03)00091-4

45. Rodríguez-Ubreva FJ, Cariaga-Martinez AE, Cortés MA, Romero-De Pablos M, Ropero S, López-Ruiz P, et al. Knockdown of protein tyrosine phosphatase SHP-1 inhibits G1/S progression in prostate cancer cells through the regulation of components of the cell-cycle machinery. *Oncogene*. (2010) 29:345–55. doi: 10.1038/onc.2009.329

46. Penafuerte C, Perez-Quintero LA, Vinette V, Hatzihristidis T, Tremblay ML. Mining the Complex Family of Protein Tyrosine Phosphatases for Checkpoint Regulators in Immunity. In: Yoshimura A, editor. Emerging Concepts Targeting Immune Checkpoints in Cancer and Autoimmunity *Current Topics in Microbiology and Immunology*. Springer International Publishing, Cham (2017). p. 191–214. doi: 10.1007/82_2017_68

47. Pappu R, Cheng AM, Li B, Gong Q, Chiu C, Griffin N, et al. Requirement for B cell linker protein (BLNK) in B cell development. *Science*. (1999) 286:1949–54. doi: 10.1126/science.286.5446.1949

48. Sang Y, Roest M, de Laat B, de Groot PG, Huskens D. Interplay between platelets and coagulation. *Blood Rev*. (2021) 46:100733. doi: 10.1016/j.blre.2020.100733

49. Pankov R, Yamada KM. Fibronectin at a glance. *J Cell Sci*. (2002) 115:3861–3. doi: 10.1242/jcs.00059

50. Good DJ, Polverini PJ, Rastinejad F, Le Beau MM, Lemons RS, Frazier WA, et al. A tumor suppressor-dependent inhibitor of angiogenesis is immunologically and functionally indistinguishable from a fragment of thrombospondin. *Proc Natl Acad Sci*. (1990) 87:6624–8. doi: 10.1073/pnas.87.17.6624

51. Yu L, Wang L, Chen S. Endogenous toll-like receptor ligands and their biological significance. *J Cell Mol Med*. (2010) 14:2592–603. doi: 10.1111/j.1582-4934.2010.01127.x

52. Floros J, Tsotakos N. Differential regulation of human surfactant protein A genes, SFTPA1 and SFTPA2, and their corresponding variants. *Front Immunol*. (2021) 12:766719. doi: 10.3389/fimmu.2021.766719

53. Hamrashdi MAL, Brady G. Regulation of IRF3 activation in human antiviral signaling pathways. *Biochem Pharmacol*. (2022) 200:115026. doi: 10.1016/j.bcp.2022.115026

54. Ren Z, Ding T, Zuo Z, Xu Z, Deng J, Wei Z. Regulation of MAVS expression and signaling function in the antiviral innate immune response. *Front Immunol*. (2020) 11:1030. doi: 10.3389/fimmu.2020.01030

Frontiers in Endocrinology

Explores the endocrine system to find new therapies for key health issues

The second most-cited endocrinology and metabolism journal, which advances our understanding of the endocrine system. It uncovers new therapies for prevalent health issues such as obesity, diabetes, reproduction, and aging.

Discover the latest Research Topics

See more →

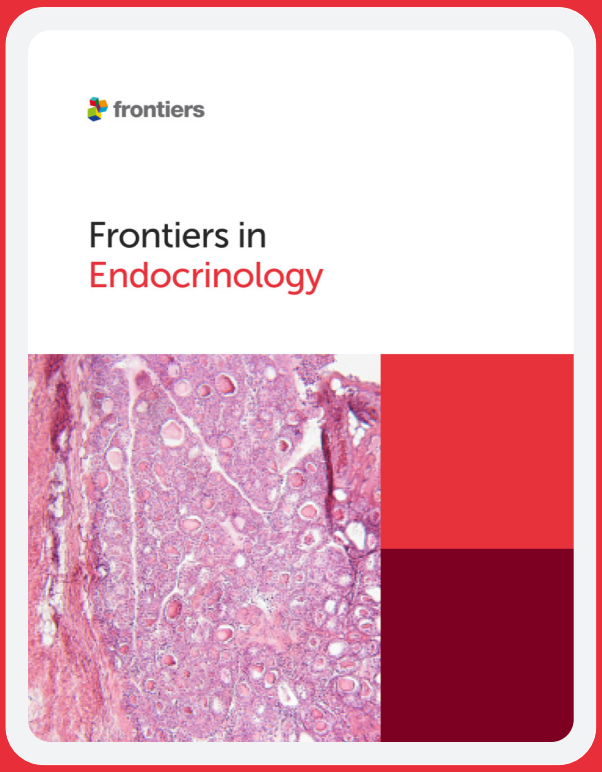

Frontiers

Avenue du Tribunal-Fédéral 34
1005 Lausanne, Switzerland
frontiersin.org

Contact us

+41 (0)21 510 17 00
frontiersin.org/about/contact